

# **MicroRNA involvement in colorectal cancer cell metabolism**

by

**Ayla Orang**

*Thesis*

*Submitted to Flinders University*

*for the degree of*

**Doctor of Philosophy**

College of Medicine and Public Health

January 2020

---

# Table of Contents

---

<b>Table of Contents</b> .....	<b>ii</b>
<b>List of Figures</b> .....	<b>viii</b>
<b>List of Tables</b> .....	<b>xii</b>
<b>List of Abbreviations</b> .....	<b>xiii</b>
<b>Summary</b> .....	<b>xvi</b>
<b>Declaration</b> .....	<b>xviii</b>
<b>Publications and Presentations</b> .....	<b>xix</b>
Peer-reviewed Publications.....	xix
Poster Presentations .....	xix
Oral presentations .....	xix
Awards .....	xx
<b>Acknowledgements</b> .....	<b>xxi</b>
<b>Chapter 1. Literature Review</b> .....	<b>22</b>
1.1 Introduction.....	22
1.2 miRNAs and their biogenesis .....	22
1.3 Colorectal Cancer (CRC) .....	23
1.4.1 Epidemiology of colorectal cancer.....	24
1.4.2 Diagnosis and treatment of CRC.....	24
1.4.3 Genetic and epigenetic events in colorectal cancer development .....	25
1.4.4 CRC and metabolic issues .....	26
1.4.5 Risk factors in colorectal cancer development.....	26
1.4 Metabolic reprogramming .....	27
1.5 Inter-connection between aerobic glycolysis and mitochondria.....	29
1.6 Hypoxia and glycolysis.....	30
1.7 Metabolic consequences of miRNA associations with driver mutations and transformation .....	36

## TABLE OF CONTENTS

1.7.1 KRAS proto-oncogene .....	38
1.7.2 MYC proto-oncogene .....	39
1.7.3 PI3K / AKT pathway .....	42
1.7.4 Mechanistic Target of Rapamycin Kinase (mTOR) .....	45
1.7.5 Tumour Protein p53 (TP53) .....	46
1.7.6 Sirtuins .....	49
1.8 Towards future applications for disrupting cancer cell glycolysis .....	58
1.9 Metformin .....	59
1.9.1 Origin and history .....	59
1.9.2 Anti-cancer effects of metformin .....	59
1.9.3 Mechanism of action of metformin .....	61
1.9.4 Effect of Metformin and CRC cells .....	64
1.9.5 Metformin and miRNAs .....	66
1.10 Challenges of metformin in cancer .....	68
1.11 Aims and hypotheses .....	69
<b>Chapter 2. Materials and Methods .....</b>	<b>71</b>
2.1 Cell culture .....	71
2.2 Mycoplasma testing .....	72
2.3 mRNA and miRNA expression analysis .....	73
2.3.1 RNA extraction .....	73
2.3.2 RNA quantification and quality analysis .....	74
2.3.3 Primer Design .....	74
2.3.4 DNase treatment, cDNA synthesis and Real-time PCR .....	75
2.4 Protein extraction, quantification, separation and detection .....	76
2.4.1 Protein extraction .....	76
2.4.2 Protein quantitation .....	76
2.5 Cell transfection with small inhibitory RNAs (siRNAs) and miRNA oligonucleotide duplexes (mimics) .....	78

## TABLE OF CONTENTS

2.6 Metformin treatment.....	78
2.7 Cell proliferation and cell death assays.....	79
2.7.1 Real-time cell growth analysis.....	79
2.7.2 Crystal violet assay.....	79
2.7.3 Apoptosis assay.....	79
2.8 Metabolic assays.....	80
2.8.1 Lactate assay.....	80
2.8.2 ATP assay.....	80
2.8.3 XTT assay.....	81
2.8.4 Measurement of oxygen consumption rate (OCR).....	81
2.8.5 Measurement of Extracellular Acidification Rate (ECAR).....	82
2.9 Transcriptome and small RNA sequencing.....	82
2.10 Statistical methods.....	83
2.11 Bioinformatics analyses.....	83
2.11.1 Differential expression analysis.....	83
2.11.2 microRNA target analysis.....	83
2.11.3 Network construction and analysis.....	84
2.11.4 Pathway and gene ontology analysis and subnetwork construction.....	84
2.12 High throughput screening and high content imaging.....	84
2.12.1 miRNA mimic transfections.....	84
2.12.2 Metformin treatment of functional screen plates.....	85
2.12.3 Cell staining and high content imaging.....	85
2.12.4 Primary screen data analysis.....	86
2.12.5 Validation screen.....	87
2.13 miRNA target validation.....	87
2.14 Reagents and equipment used for experiments.....	88
<b>Chapter 3. Characterising metformin responses in CRC cells.....</b>	<b>94</b>
3.1 Introduction and aims.....	94

## TABLE OF CONTENTS

3.2 Results .....	94
3.2.1 Consequences of glycolysis inhibition in CRC cells .....	94
3.2.2 Metformin has a dose-dependent effect on CRC cell viability .....	99
3.2.3 p53 and Kras mutational status do not affect the anti-proliferative effect of metformin.....	101
3.2.4 Low concentrations of metformin have no pro-apoptotic effect on CRC cells .....	102
3.2.5 <i>TP53</i> and <i>KRAS</i> mutational status do not affect the pro-apoptotic effect of metformin.....	104
3.2.6 Metformin treatment results in reduced ATP synthesis in a dose-dependent manner in CRC cells .....	104
3.2.7 Effect of metformin on mitochondrial oxidoreductase activity of the colorectal cancer cells.....	107
3.2.8 Effect of metformin on the metabolic profile of CRC cells .....	109
3.2.9 Effect of metformin on PI3K/AKT pathway .....	111
3.3 Discussion.....	113
<b>Chapter 4. Metformin associated changes in miRNA and transcriptome profiles of CRC .....</b>	<b>117</b>
4.1 Introduction.....	117
4.2 Results .....	118
4.2.1 Identification of differentially expressed mRNAs with metformin treatment	118
4.2.2 Identification of differentially expressed miRNAs with metformin treatment .....	119
4.2.3 miRNA target prediction and integrative network construction .....	120
4.2.4 Integrative Protein- protein interaction (PPI) and miRNA- mRNA network	121
4.2.5 Enrichment analysis of GO-terms .....	122
4.2.6 Global pathway regulation in response to metformin treatment of CRC cells .....	126

## TABLE OF CONTENTS

4.2.7 Identification of hub genes, key miRNAs and potential molecular mechanisms of metformin .....	128
4.2.8 Expression of putative miRNA-gene pairs within PI3K-Akt pathway following metformin treatment of HCT116 cells.....	129
4.2.9 Validation of anti-correlation between expression levels of miRNAs and potential target mRNAs within PI3K-Akt pathway.....	132
4.2.10 Proliferation of colorectal cancer cells following transfection with miR-132-3p, miR-2110 and miR-590-3p mimics .....	134
4.2.11 Expression of PIK3R3 protein levels in CRC cells following transfection with miR-132-3p, miR-2110 mimics .....	136
4.2.12 Validation of <i>PIK3R3</i> as a direct target of miR-2110 .....	138
4.2.13 Confirmation of <i>PIK3R3</i> as a gene that influence proliferation .....	139
4.2.14 Confirmation of the role of miR-2110 – PIK3R3 pair in the regulation of CRC cell proliferation.....	141
4.2.15 Effect of miR-132-3p and miR-2110 on PI3K/Akt/ mTOR pathway.....	143
4.2.16 Expression of potential miRNA-gene pairs within MAPK pathway following metformin treatment of HCT116 cells.....	145
4.2.17 Validation of anti-correlation between expression levels of miRNAs and putative target genes within MAPK pathway.....	147
4.2.18 Proliferation of colorectal cancer cells associated with miR-222-3p and miR-589-3p overexpression.....	148
4.2.19 Expression of <i>STMN1</i> in CRC cells following transfection with miR-222-3p or miR-589-3p mimics .....	150
4.2.20 Validation of <i>STMN1</i> as a direct target of miR-222-3p and miR-589-3p.....	151
4.2.21 Confirmation of the role of <i>STMN1</i> in regulating CRC cell proliferation....	153
4.2.22 The biological relevance of <i>STMN1</i> suppression by miR-222-3p and miR-589-3p in CRC cells.....	155
4.3 Discussion.....	159
<b>Chapter 5. Functional High-throughput screening identifies miRNAs that enhance the anti-cancer properties of metformin.....</b>	<b>164</b>

## TABLE OF CONTENTS

5.1 Introduction.....	164
5.2 Results .....	165
5.2.1 Primary High Throughput Screening.....	165
5.2.2 Secondary High Throughput Screening .....	169
5.2.3 Real-time Proliferation Validation of secondary screen hits .....	173
5.2.4 Changes in glycolytic characteristics of HCT116 cells associated with metformin sensitizing miRNAs.....	176
5.2.5 Changes in respiration characteristics of HCT116 cells associated with metformin sensitizing miRNAs.....	183
5.2.6 Proliferation of colorectal cancer cells associated with metformin sensitizing miRNA mimics' transfection.....	192
5.2.7 Apoptosis of colorectal cancer cells associated with metformin-sensitizing miRNA mimic transfections .....	198
5.3 Discussion.....	205
<b>Chapter 6. General conclusions .....</b>	<b>212</b>
6.1 Thesis summary .....	212
6.2 The Warburg effect and interpretations of an established concept .....	212
6.3 Anti-neoplastic effects of metformin on colorectal cells.....	214
6.4 Comprehensive transcriptome and miRNA profile analysis of metformin treatment in CRC cells to uncover regulatory mechanisms .....	217
6.5 miR-132-3p and miR-2110 mediate the anti-cancer activity of metformin by inhibiting PIK3R3 expression and the PI3K/Akt pathway .....	220
6.6 miR-222-3p and miR-589-3p mediate the anti-proliferative activity of metformin by targeting STMN1.....	222
6.7 Functional screening identifies miRNAs that modulate the sensitivity of CRC cells to metformin.....	226
6.8 Systems biology approach for metformin-associated networks .....	231
<b>Appendices .....</b>	<b>233</b>
<b>References.....</b>	<b>264</b>

# List of Figures

---

FIGURE 1-1. MIRNA BIOGENESIS PATHWAY.....	23
FIGURE 1-2. MIRNAS TARGETING GLYCOLYTIC AND MITOCHONDRIAL ENZYMES. ....	37
FIGURE 1-3. INTERCONNECTIONS BETWEEN THE GLYCOLYTIC DRIVERS AND SUPPRESSORS AND THE ROLE OF MIRNAS IN THESE NETWORKS.....	50
FIGURE 1-4. OVERVIEW OF PROPOSED MECHANISM OF ACTION OF METFORMIN.....	64
FIGURE 3-1: PROLIFERATION OF HCT116 CELLS 65 HOURS POST-TRANSFECTION WITH LDHA OR PKM2 siRNA. ....	95
FIGURE 3-2: METABOLIC CHANGES ASSOCIATED WITH D- GLUCOSE AND OLIGOMYCIN TREATMENT OF HCT116 CELLS. ....	96
FIGURE 3-3: BIO-ENERGETIC ANALYSIS OF HCT116 CELLS TRANSFECTED WITH LDHA OR PKM2 siRNA.....	98
FIGURE 3-4: VIABILITY OF DIFFERENT COLORECTAL CANCER CELLS AFTER 72 H OF 2.5 MM, 5 MM AND 10 MM METFORMIN TREATMENT. ....	100
FIGURE 3-5: PROLIFERATION CURVES FOR HCT116 CELLS TREATED WITH 0, 2.5, 5 AND 10 MM METFORMIN, 24 H POST CELL SEEDING. ....	101
FIGURE 3-6: PROLIFERATION OF HCT116 <i>TP53</i> NULL AND HKE-3 ( <i>KRAS</i> COMPLEMENTED) CELLS AFTER 72 H OF 2.5 MM, 5 MM AND 10 MM METFORMIN TREATMENT. ....	102
FIGURE 3-7: APOPTOSIS OF HCT116, RKO, DLD-1, SW480, HT29 AND CACO2 CELLS AFTER 72 H OF 2.5 MM, 5 MM AND 10 MM METFORMIN TREATMENT. ....	103
FIGURE 3-8: APOPTOSIS OF HCT116 <i>TP53</i> NULL AND HKE-3 ( <i>KRAS</i> COMPLEMENTED) CELLS AFTER 72 H OF 2.5 MM, 5 MM AND 10 MM METFORMIN TREATMENT. ....	104
FIGURE 3-9: ATP SYNTHESIS OF CRC CELLS AFTER 72 H OF 2.5 MM, 5 MM AND 10 MM METFORMIN TREATMENT. ....	107
FIGURE 3-10: MITOCHONDRIAL OXIDOREDUCTASE ACTIVITY OF CRC CELL PANEL 72 HOURS POST-TREATMENT WITH 2.5 MM, 5 MM AND 10 MM METFORMIN.....	109
FIGURE 3-11: THE EFFECT OF METFORMIN ON METABOLIC CHARACTERISTICS OF HCT116 CELLS WAS TESTED. ....	110
FIGURE 3-12: CHANGES IN mTORC1, p70S6K AND AMPK PHOSPHORYLATION OF HCT116 CELLS ASSOCIATED WITH 2.5, 5 AND 10 MM METFORMIN TREATMENT. ....	112
FIGURE 4-1: VOLCANO PLOT FOR TRANSCRIPTOME PROFILING OF HCT116 CELLS TREATED WITH 2.5 MM METFORMIN.....	119
FIGURE 4-2: VOLCANO PLOT FOR SMALL RNA SEQUENCING OF HCT116 CELLS TREATED WITH 2.5 MM METFORMIN.....	120
FIGURE 4-3: THE MIRNA-BASED NETWORK AFFECTED BY METFORMIN TREATMENT OF COLORECTAL CANCER CELLS. ....	122
FIGURE 4-4: METFORMIN ASSOCIATED CHANGES IN BIOLOGICAL PROCESSES IN HCT116 CELLS. ....	124
FIGURE 4-5: METFORMIN ASSOCIATED CHANGES IN MOLECULAR FUNCTIONS IN HCT116 CELLS. ....	125
FIGURE 4-6: METFORMIN ASSOCIATED CHANGES IN CELLULAR COMPARTMENTS IN HCT116 CELLS. ....	126
FIGURE 4-7: OVERREPRESENTED KEGG PATHWAYS FOR DE GENES ASSOCIATED WITH METFORMIN TREATMENT OF HCT116 CELLS. ....	127
FIGURE 4-8. QUANTITATIVE REAL-TIME PCR ANALYSIS OF mRNA LEVELS IN HCT116 CELLS FOR GENES IDENTIFIED IN PI3K-AKT SIGNALLING PATHWAY AS BEING INFLUENCED BY 2.5 MM METFORMIN TREATMENT. ....	130

## LIST OF FIGURES

FIGURE 4-9: QUANTITATIVE REAL-TIME PCR ANALYSIS OF MIRNA LEVELS IN HCT116 CELLS FOR MIRNAS IDENTIFIED IN PI3K-AKT SIGNALLING PATHWAY AS BEING AFFECTED BY 2.5 mM METFORMIN TREATMENT. ....	131
FIGURE 4-10: PUTATIVE TARGET GENE EXPRESSION IN HCT116 CELLS AFTER TRANSFECTION WITH CORRESPONDING PREDICTED MIRNA.....	133
FIGURE 4-11: PROLIFERATION OF HCT116 CELLS 96 HOURS POST-TRANSFECTION WITH MIR-132-3P, MIR-2110 AND MIR-590-3P. ....	134
FIGURE 4-12: PROLIFERATION OF DIFFERENT COLORECTAL CANCER CELLS 96 HOURS POST-TRANSFECTION WITH MIR-132-3P. ....	135
FIGURE 4-13: PROLIFERATION OF DIFFERENT COLORECTAL CANCER CELLS 96 HOURS POST-TRANSFECTION WITH MIR-2110. ....	136
FIGURE 4-14: TARGET GENE PROTEIN LEVELS IN HCT116 CELLS AFTER TRANSFECTION WITH MIR-132-3P, MIR-2110.....	137
FIGURE 4-15: <i>PIK3R3</i> EXPRESSION CHANGES IN HCT116 CELLS AFTER CO-TRANSFECTION WITH MIR-2110 AND SPECIFIC TARGET PROTECTORS. ....	139
FIGURE 4-16: PROLIFERATION OF DIFFERENT COLORECTAL CANCER CELLS 96 HOURS AFTER TRANSFECTION WITH <i>PIK3R3</i> siRNA. ....	140
FIGURE 4-17: PROLIFERATION OF HCT116 CELLS 72 HOURS POST-TRANSFECTION WITH <i>PIK3R3</i> TARGET PROTECTORS AND MIR-2110 MIMICS COMPARED WITH MIR-2110 MIMICS AND NEGATIVE CONTROL MIMICS.....	143
FIGURE 4-18: ALTERATION IN P70 S6 KINASE PHOSPHORYLATION LEVELS OF HCT116 CELLS AFTER TRANSFECTION WITH MIR-132-3P, MIR-2110 MIMICS OR <i>PIK3R3</i> siRNA COMPARED TO NC. ....	144
FIGURE 4-19: QUANTITATIVE REAL-TIME PCR RESULTS FOR SELECTED DIFFERENTIALLY EXPRESSED GENES ASSOCIATED WITH METFORMIN TREATMENT OF CRC CELLS WITHIN MAPK PATHWAY. ....	146
FIGURE 4-20: QUANTITATIVE REAL-TIME PCR RESULTS FOR SELECTED DIFFERENTIALLY EXPRESSED MIRNAS ASSOCIATED WITH METFORMIN TREATMENT OF CRC CELLS WITHIN MAPK PATHWAY. ....	147
FIGURE 4-21: SELECTED GENE EXPRESSION CHANGES IN HCT116 CELLS 96 HOURS POST-TRANSFECTION WITH CORRESPONDING MIRNA MIMICS. ....	148
FIGURE 4-22: PROLIFERATION OF DIFFERENT COLORECTAL CANCER CELLS 96 HOURS POST-TRANSFECTION WITH MIR-222-3P. ....	149
FIGURE 4-23: PROLIFERATION OF DIFFERENT COLORECTAL CANCER CELLS 96 HOURS POST-TRANSFECTION WITH MIR-589-3P. ....	150
FIGURE 4-24: TARGET GENE PROTEIN LEVELS IN HCT116 CELLS AFTER TRANSFECTION WITH MIR-222-3P, MIR-589.....	151
FIGURE 4-25: <i>STMN1</i> EXPRESSION CHANGES IN HCT116 CELLS AFTER CO-TRANSFECTION WITH MIR-222-3P OR MIR-589-3P AND SPECIFIC TARGET PROTECTORS.....	153
FIGURE 4-26: PROLIFERATION OF DIFFERENT COLORECTAL CANCER CELLS 96 HOURS AFTER TRANSFECTION WITH <i>STMN1</i> siRNA. ....	154
FIGURE 4-27: PROLIFERATION OF HCT116 CELLS 72 HOURS POST-TRANSFECTION WITH <i>STMN1</i> TARGET PROTECTORS AND MIR-222-3P MIMICS COMPARED WITH MIR-2110 MIMICS AND NEGATIVE CONTROL MIMICS.....	156
FIGURE 4-28: PROLIFERATION OF HCT116 CELLS 72 HOURS POST-TRANSFECTION WITH <i>STMN1</i> TARGET PROTECTORS AND MIR-589-3P MIMICS COMPARED WITH MIR-2110 MIMICS AND NEGATIVE CONTROL MIMICS.....	158
FIGURE 5-1: SCHEMATIC OF HIGH-THROUGHPUT SENSITIZATION SCREEN OF MIRNA MIMICS FOR CRC CELL RESPONSE TO METFORMIN TREATMENT. ....	166
FIGURE 5-2: PAIRWISE CORRELATION BETWEEN THE TWO INDEPENDENT REPLICATES OF THE SCREENING.....	167
FIGURE 5-3: SUMMARY OF SCREEN RESULTS IN HCT116 CELLS. ....	167
FIGURE 5-4: SCATTER PLOT REPRESENTATION OF THE METFORMIN SENSITIZATION SCREEN WITH A MIRNA MIMICS LIBRARY. ....	168
FIGURE 5-5: PAIRWISE CORRELATION BETWEEN THE THREE INDEPENDENT REPLICATES OF THE SECONDARY FUNCTIONAL SCREEN. ...	170

## LIST OF FIGURES

FIGURE 5-6: VIABILITY OF HCT116 CELLS TRANSFECTED WITH MIRNA MIMICS HAVING STRONG SYNERGETIC EFFECT WITH 2.5 MM METFORMIN TREATMENT. ....	171
FIGURE 5-7: VIABILITY OF HCT116 CELLS TRANSFECTED WITH MIRNA MIMICS HAVING STRONG SYNERGETIC EFFECT WITH 2.5 MM METFORMIN TREATMENT. ....	173
FIGURE 5-8: PROLIFERATION OF HCT116 96 H POST- MIRNA MIMIC TRANSFECTION AND METFORMIN TREATMENT.....	176
FIGURE 5-9: AGILENT SEAHORSE XF GLYCOLYSIS STRESS TEST PROFILE OF THE KEY PARAMETERS OF GLYCOLYTIC FUNCTION. ..	176
FIGURE 5-10: CHANGES IN GLYCOLYSIS ASSOCIATED WITH MIRNA MIMIC TRANSFECTIONS IN COMBINATION WITH METFORMIN TREATMENT OF HCT116 CELLS.....	178
FIGURE 5-11: CHANGES IN MAXIMUM GLYCOLYTIC CAPACITY OF HCT116 CELLS ASSOCIATED WITH MIRNA MIMIC TRANSFECTIONS IN COMBINATION WITH METFORMIN TREATMENT. ....	180
FIGURE 5-12: CHANGES IN THE GLYCOLYTIC RESERVE OF HCT116 CELLS ASSOCIATED WITH MIRNA MIMIC TRANSFECTIONS IN COMBINATION WITH METFORMIN TREATMENT. ....	182
FIGURE 5-13: AGILENT SEAHORSE XF MITOCHONDRIAL STRESS TEST PROFILE OF THE KEY PARAMETERS OF RESPIRATION.....	183
FIGURE 5-14: CHANGES IN THE RESERVED RESPIRATORY CAPACITY OF HCT116 CELLS ASSOCIATED WITH MIRNA MIMIC TRANSFECTIONS IN COMBINATION WITH METFORMIN TREATMENT. ....	185
FIGURE 5-15: CHANGES IN COUPLING EFFICIENCY OF HCT116 CELLS ASSOCIATED WITH MIRNA MIMIC TRANSFECTIONS IN COMBINATION WITH METFORMIN TREATMENT. ....	186
FIGURE 5-16: CHANGES IN BASAL RESPIRATION OF HCT116 CELLS ASSOCIATED WITH MIRNA MIMIC TRANSFECTIONS IN COMBINATION WITH METFORMIN TREATMENT. ....	188
FIGURE 5-17: CHANGES IN MAXIMAL RESPIRATORY CAPACITY OF HCT116 CELLS ASSOCIATED WITH MIRNA MIMIC TRANSFECTIONS IN COMBINATION WITH METFORMIN TREATMENT. ....	190
FIGURE 5-18: CHANGES IN ATP SYNTHESIS OF HCT116 CELLS ASSOCIATED WITH MIRNA MIMIC TRANSFECTIONS IN COMBINATION WITH METFORMIN TREATMENT. ....	191
FIGURE 5-19: PROLIFERATION OF CRC CELL LINES AFTER TRANSFECTION WITH MIR-18B-5P MIRNAS AND TREATMENT WITH METFORMIN OR CONTROL MEDIUM FOR 96 HOURS.....	193
FIGURE 5-20: PROLIFERATION OF CRC CELL LINES AFTER TRANSFECTION WITH MIR-145-3P MIRNAS AND TREATMENT WITH METFORMIN OR CONTROL MEDIUM FOR 96 HOURS.....	194
FIGURE 5-21: PROLIFERATION OF CRC CELLS AFTER TRANSFECTION WITH MIR-1181 AND TREATMENT WITH METFORMIN OR CONTROL MEDIUM FOR 96 HOURS.....	195
FIGURE 5-22: PROLIFERATION OF CRC CELLS AFTER TRANSFECTION WITH MIR-376B-5P AND TREATMENT WITH METFORMIN OR CONTROL MEDIUM FOR 96 HOURS.....	196
FIGURE 5-23: PROLIFERATION OF CRC CELLS AFTER TRANSFECTION WITH MIR-676-3P AND TREATMENT WITH METFORMIN OR CONTROL MEDIUM FOR 96 HOURS.....	197
FIGURE 5-24: PROLIFERATION OF CRC CELLS AFTER TRANSFECTION WITH MIR-718 AND TREATMENT WITH METFORMIN OR CONTROL MEDIUM FOR 96 HOURS. ....	198
FIGURE 5-25: APOPTOSIS OF CRC CELL LINES AFTER TRANSFECTION WITH MIR-18B-5P AND TREATMENT WITH METFORMIN OR CONTROL MEDIUM FOR 96 HOURS.....	199

## LIST OF FIGURES

FIGURE 5-26: APOPTOSIS OF CRC CELL LINES AFTER TRANSFECTION WITH miR-145-3P AND TREATMENT WITH METFORMIN OR CONTROL MEDIUM FOR 96 HOURS.....	200
FIGURE 5-27: APOPTOSIS OF CRC CELL LINES AFTER TRANSFECTION WITH miR-1181 AND TREATMENT WITH METFORMIN OR CONTROL MEDIUM FOR 96 HOURS.....	201
FIGURE 5-28: APOPTOSIS OF CRC CELL LINES AFTER TRANSFECTION WITH miR-376B-5P AND TREATMENT WITH METFORMIN OR CONTROL MEDIUM FOR 96 HOURS.....	202
FIGURE 5-29: APOPTOSIS OF CRC CELL LINES AFTER TRANSFECTION WITH miR-676-3P AND TREATMENT WITH METFORMIN OR CONTROL MEDIUM FOR 96 HOURS.....	203
FIGURE 5-30: APOPTOSIS OF CRC CELL LINES AFTER TRANSFECTION WITH miR-718 AND TREATMENT WITH METFORMIN OR CONTROL MEDIUM FOR 96 HOURS. ....	204
FIGURE 5-31: THE miRNA-BASED NETWORK: METFORMIN TREATMENT-REGULATED miRNAs INTEGRATED WITH METFORMIN SENSITIZING miRNAs AND THEIR PUTATIVE TARGET GENES. ....	208
FIGURE 6-1: PROPOSED MOLECULAR MODEL FOR MECHANISM OF ACTION OF METFORMIN IN CRC CELLS. ....	226

# List of Tables

---

TABLE 1-1. SUMMARY OF MIRNAS DIRECTLY TARGETING GLYCOLYTIC ENZYMES AND TRANSPORTERS.....	28
TABLE 1-2. SUMMARY OF ASSOCIATIONS BETWEEN MIRNAS AND HYPOXIA.....	34
TABLE 1-3. SUMMARY OF MIRNAS REGULATED BY THE TRANSCRIPTION FACTOR MYC.....	41
TABLE 1-4. SUMMARY OF MIRNAS REGULATED BY THE TRANSCRIPTION FACTOR P53.....	48
TABLE 1-5. SUMMARY OF MIRNAS TARGETING METABOLISM-RELATED ONCOGENES AND TUMOUR SUPPRESSORS.....	53
TABLE 1-6. SUMMARY OF STUDIES ON THE EFFECT OF METFORMIN IN CANCER PREVENTION.....	60
TABLE 1-7. SUMMARY OF IN VITRO STUDIES ON THE ANTI-CANCER EFFECTS OF METFORMIN IN CRC CELL LINES.....	65
TABLE 1-8. SUMMARY OF STUDIES ON THE METFORMIN ASSOCIATED CHANGES IN MIRNA EXPRESSION LEVELS.....	66
TABLE 2-1. COLON CANCER CELL LINES CLASSIFIED BY DRIVER MUTATIONS.....	71
TABLE 2-2. MASTER MIX COMPOSITION FOR MYCOPLASMA TESTING OF CRC CELL LINES.....	72
TABLE 2-3. OPERETTA HIGH-CONTENT IMAGING SETTINGS.....	86
TABLE 2-4. CHEMICALS AND REAGENTS.....	88
TABLE 2-5: EQUIPMENT AND SOFTWARE.....	89
TABLE 2-6: PRIMERS AND OLIGONUCLEOTIDES.....	90
TABLE 2-7: ANTIBODIES.....	93
TABLE 2-8: BUFFERS AND SOLUTIONS.....	93
TABLE 4-1: ENRICHED KEGG PATHWAYS OVERREPRESENTED WITH METFORMIN TREATMENT OF HCT116.....	128
TABLE 4-2: MIRNA-TARGET GENE PAIRS IDENTIFIED WITHIN PI3K-AKT PATHWAY.....	129
TABLE 4-3: TARGETSCAN PREDICTED BINDING SITES FOR MIR-2110 IN THE 3'-UTR OF <i>PIK3R3</i> .....	138
TABLE 4-4: MIRNA-TARGET GENE PAIRS IDENTIFIED WITHIN MAPK PATHWAY.....	145
TABLE 4-5: TARGETSCAN PREDICTED BINDING SITES FOR MIR-222-3P AND MIR-589-3P IN THE 3'-UTR OF <i>STMN1</i> .....	152

# List of Abbreviations

---

2HG: 2-hydroxyglutarate  
AGO: argonaute  
ALDO: aldolase  
AMPK: AMP-activated protein kinase  
APC: adenomatous polyposis coli  
C/EBP $\beta$ : CCAAT-enhancer-binding protein  $\beta$   
CDC20: cell division cycle 20  
COX: cytochrome c oxidase complex  
CUL2: cullin 2  
DNMT1: DNA (cytosine-5)-methyltransferase 1  
dsmiRNA: double-stranded miRNA  
EMT: epithelial to mesenchymal transition  
ENO1: enolase 1  
EphA1: erythropoietin-producing hepatoma receptor A1  
ERK: extracellular-signal-regulated kinase  
EZH2: enhancer of zeste homolog 2  
FIH-1: factor inhibiting HIF-1  
FOXO: forkhead box O  
GAPDH: glyceraldehyde-3- phosphate dehydrogenase  
GDH: glutamate dehydrogenase 1  
GLS: glutaminase  
GLS: hypoxia-inducible factor-1  
GLUTS: glucose transporters  
GPD1L: glycerol-3-phosphate dehydrogenase 1 like  
HDAC: histone deacetylase  
Her2/Neu: human epidermal growth factor receptor 2  
HK2: hexokinase 2  
HNF3 $\beta$ : hepatocyte nuclear factor 3-beta  
HRE: hypoxia response element  
IDH: isocitrate dehydrogenase  
IGF2: insulin-like factor 2  
ISCU: iron-sulfur cluster scaffold

## LIST OF ABBREVIATIONS

ITC: isothiocyanate  
KLF15: Kruppel-like factor 15  
LDHA: lactate dehydrogenase A  
MAGI2: membrane-associated guanylate kinase inverted 2  
MAX: MYC associated factor X  
MCT: monocarboxylate transporters  
MDH: malate dehydrogenase  
miRNA: microRNA  
mitomiRs: mitochondria-related miRNAs  
MMP-2: metalloproteinase-2  
MnSOD: Mn Superoxide Dismutase  
mTOR: mechanistic target of rapamycin  
NOX: NADPH oxidase  
OXPHOS: oxidative phosphorylation  
PARP-1: poly(ADP-ribose) polymerase 1  
PDH: pyruvate dehydrogenase  
PDK1: pyruvate dehydrogenase kinase  
PEPCK: phosphoenolpyruvate carboxykinase 2  
PET: positron emission tomography  
PFK1: 6-phosphofructo-1-kinase  
PGC1 $\alpha$ : PPAR $\gamma$  coactivator 1 $\alpha$   
PGK1: phosphoglycerate kinase 1  
PGM: phosphoglycerate mutase  
PHD: prolyl-4-hydroxylase  
PKM2: pyruvate kinase  
PPP2R1B: protein phosphatase 2 scaffold subunit Abeta  
pre-miRNA: precursor miRNA  
pri-miRNA: primary miRNA  
PTEN: phosphatase and tensin homolog  
RIP1: receptor-interacting protein 1  
RISC: RNA-induced silencing complex  
ROS: reactive oxygen species  
SCO2/1: synthesis of cytochrome c oxidase 2/1  
SDH: succinate dehydrogenase

## LIST OF ABBREVIATIONS

SG: stress granule

SIRT: sirtuin

STAT3: signal transducer and activator of transcription 3

TCA: tricarboxylic acid

TGF- $\beta$ : transforming growth factor beta 1

TIGAR: TP53-induced glycolysis and apoptosis regulator

TLK: transketolase

TP53INP1: tumour protein P53 inducible nuclear protein 1

TPI: triose-phosphate isomerase

TSC: tuberous sclerosis proteins

USP28: ubiquitin specific peptidase 28

VEGFA: Vascular endothelial growth factor A

VHL: promyelocytic leukemia protein

VHL: Von Hippel-Lindau

# Summary

---

Colorectal Cancer (CRC) is the third most common cancer worldwide and second in Australia, affecting both males and females almost equally. Despite all the progress in cancer diagnosis and treatment, CRC still represents the second highest number of cancer deaths in Australia and the five-year survival rate for this cancer is about 65%. It is a disease that most frequently originates from mutations in the different proto-oncogenes such as *KRAS* and tumour suppressors such as *TP53*.

miRNAs are small non-coding RNAs that are transcribed from intergenic or intragenic regions. Metabolic reprogramming involves pathways that rely upon microRNA regulation. MicroRNAs ensure post-transcriptional buffering of adaptive metabolic responses. Therefore, dysregulated microRNAs can impact energy flux in cancer cells and, thus, have potential as therapeutic modalities to disrupt cancer metabolism.

Metformin is a biguanide that was discovered in the late 1950s and is the first-line therapy for type 2 diabetes. In diabetic patients, it inhibits hepatic glucose production, by reducing cellular concentrations of ATP and then mimicking a fasting condition. In 2005, a 23% reduction in the incidence of any cancer in type 2 diabetic patients treated with metformin was reported and in recent years, results from retrospective epidemiological and *in vitro* studies have supported the rationale of designing clinical trials using metformin as an adjuvant in chemotherapy for cancer patients.

Although glycolysis accounts for the main energy production pathway for CRC cells, here we showed that they retain the ability to switch between glycolysis and OXPHOS when one is inhibited or less active. Also, metformin had a dose-dependent effect on CRC cell viability and ATP production and HCT116 cells were the most responsive cell line in terms of metformin's role on suppressing Complex 1, with *TP53* and *KRAS* mutation status having little effect on these characteristics. Metformin also exerted its anti-cancer activity through targeting the mTOR signalling pathway, inducing a metabolic stress and compensatory increase in CRC cell glycolysis.

Full transcriptome and small RNA next generation sequencing were performed for CRC cells treated with metformin. Potential protein-protein interactions, within specific biological pathways that are affected by metformin treatment, were extracted from differentially expressed mRNAs and miRNAs and used to build system networks. Metformin treatment

## SUMMARY

resulted in downregulation of some pro-proliferative and upregulation of some anti-proliferative miRNAs.

Pathway analysis predicted that PI3K-Akt and MAPK signalling pathways are the pathways most significantly impacted following metformin treatment

Investigation of potential miRNA-gene pairs revealed that metformin upregulates miR-2110 and miR-132-3p to target *PIK3R3* and, consequently, regulate CRC cell proliferation and the PI3K-Akt signalling pathway. Also, metformin upregulated miR-222-3p and miR-589-3p, which directly target *STMN1* to inhibit CRC cell proliferation. Overall, these data will contribute to the growing knowledge of metformin responses and the role of miRNAs in CRC signalling pathways.

In addition, unbiased high throughput functional screens of a synthetic miRNA library, in combination with metformin treatment, were used to identify additional miRNAs that impact the metformin response. Experimental validation of selected hits identified eight miRNAs that sensitize CRC cells to the anti-proliferative effect of metformin. Among those sensitizing miRNAs, miR-676-3p had a pro-apoptotic function in combination with metformin. Investigation of the combined effect of miRNAs and metformin on CRC cell metabolism identified miR-376b-3p regulating both CRC glycolytic and respiration parameters, while miR-676-3p, miR-18b-5p and miR-145-3p affected glycolysis only and miR-1181 and miR-718 regulated CRC respiration. Identification of miRNAs that sensitize CRC cells to metformin, and their potential transcript targets, are early steps in the design of innovative therapeutic strategies.

## DECLARATION

# Declaration

---

I certify that this thesis does not incorporate without acknowledgment any material previously submitted for a degree or diploma in any university; and that to the best of my knowledge and belief it does not contain any material previously published or written by another person except where due reference is made in the text.

Full Name: Ayla Orang

Date: 27 July 2019

# Publications and Presentations

---

## Peer-reviewed Publications

Orang AV, Peterson J, McKinnon RA, Michael MZ. 2019. Micromanaging aerobic respiration and glycolysis in cancer cells. *Molecular metabolism*. 23:98-126

## Poster Presentations

Orang AV, McKinnon RA, Peterson J, Sykes PJ, Michael MZ. Functional microRNA-mRNA interactions in colorectal cancer cell response to metformin. Keystone, Gastrointestinal Control of Metabolism. Copenhagen, Denmark, May 2017.

Orang AV, McKinnon RA, Peterson J, Sykes PJ, Michael MZ. Integrative analysis of miRNA and mRNA expression profiles in colorectal cancer cell response to metformin. Combio2017. Adelaide Convention Centre, Adelaide, Australia, May 2017.

Orang AV, McKinnon RA, Peterson J, Michael MZ. Harnessing miRNAs to enhance the therapeutic effect of metformin on colorectal cancer cells. combio2018, Sydney Convention Centre, Sydney, Australia, September 2018.

## Oral presentations

Orang AV, McKinnon RA, Peterson J, Sykes PJ, Michael MZ. Functional microRNA-mRNA interactions in colorectal cancer cell response to metformin. ASMR SA Division: Annual Scientific Meeting, Adelaide, Australia, June 2017.

Orang AV, McKinnon RA, Peterson J, Sykes PJ, Michael MZ. Integrative analysis of miRNA and mRNA expression profiles in colorectal cancer cell response to metformin. Cancer in SA Translational Research Meeting, SAHMRI, Adelaide, Australia, May 2017.

Orang AV, McKinnon RA, Peterson J, Sykes PJ, Michael MZ. Harnessing miRNAs to enhance the therapeutic effect of metformin on colorectal cancer cells. Epigenetics Consortium of SA meeting (EpiCSA), Adelaide, Australia, October 2017.

## PUBLICATIONS AND PRESENTATIONS

### Awards

Three Minute Thesis University Final Winner - Flinders University, Australia; September 2017

ASBMB Poster Prize - Combio2018, Sydney, Australia; October 2018

Runner-up Poster Prize - Cancer Research Afternoon, Flinders Centre for Innovation in Cancer, Flinders University, Australia; September 2018

# Acknowledgements

---

First and foremost, I would like to sincerely thank my principal supervisor Associate Professor Michael Michael for noticing my potential, giving me the opportunity to become a part of his research laboratory and passing on his expert knowledge in the field of miRNAs. I also extend thanks to my co-supervisors Professor Ross McKinnon and Associate Professor Janni Petersen for their advice and helpful perspectives throughout my PhD and during the final production of this thesis.

My laboratory colleagues also deserve thanks for the support they provided over my PhD, and I am particularly grateful to Saira Ali and Marie Lowe for their help and support. I would also like to thank Dr Darling Rojas-Canales, Kym McNicholas and Annette Mazzone for their helpful conversations.

I would like to thank Dr Amanda Aloia from the Cell Screen SA Facility who assisted me with various aspects of this work especially in performing the high throughput functional screen. I also thank Professor Senji Shirasawa (Fukuoka University, Fukuoka, Japan) for the kind donation of HKe-3 cell line.

Also, thanks to Flinders Genomics Facility for doing the RNA and small RNA sequencing, Dr Shashikanth Marri for performing the sequencing analyses and Professor Rebecca Robker from the Robinson Institute for kindly allowing me to use the Seahorse BioAnalyzer.

Personally, I would like to thank my parents and siblings, extended family and friends for their love and support through my PhD journey. Finally, but most importantly, this work is dedicated to my husband, Reza, who has been a constant source of support and encouragement during the challenges of PhD research. I am truly thankful for having you in my life.

# Chapter 1. Literature Review

---

It is acknowledged that this chapter (in particular, Sections 1.1-1.8) is based on the following review article that I published in the journal *Molecular Metabolism*:

Orang AV, Peterson J, McKinnon RA, Michael MZ. 2019. Micromanaging aerobic respiration and glycolysis in cancer cells. *Molecular Metabolism*. 23:98-126

## 1.1 Introduction

In the 1920s, Otto Warburg reported for the first time that while cells under normal conditions utilize glucose to derive 70% of required ATP through mitochondrial oxidative phosphorylation (OXPHOS), cancer cells metabolize glucose by glycolysis even in the presence of adequate oxygen supply [1, 2]. Since then, aerobic glycolysis has been regarded as a hallmark of cancer that provides bioenergetic, biosynthetic and redox balance advantages for cancer cells [3].

Although Warburg's seminal studies resulted in a misinterpretation that irreversible inactivation of mitochondrial respiration is the primary and sole cause of aerobic glycolysis in cancer cells, later it was reported that impaired respiration is inadequate to explain the metabolic shift [4]. The study of cancer cell glycolysis continues to surprise, revealing further associations between a metabolic switch in cancer cells, mutations in mitochondrial metabolic enzymes and altered mitochondrial function [5, 6]. In addition, discoveries that associate oncogene and tumour suppressor gene dysfunction with metabolic reprogramming suggest that both environmental and genetic factors underlie the metabolic heterogeneity of tumours [7, 8]. Moreover, in light of numerous microRNA-related studies, it is now important to consider the roles of these small non-coding RNAs in fine-tuning gene expression at different stages of tumorigenesis. Accumulating evidence supports the involvement of miRNAs in modulating cancer cell metabolism by directly and indirectly regulating genes associated with aerobic glycolysis [9].

## 1.2 miRNAs and their biogenesis

microRNAs (miRNAs) are small non-coding RNAs that canonically play a major role in post-transcriptional gene repression. Themselves the products of RNA polymerase II or III dependent transcription, primary (pri)-miRNA transcripts are 5'-7-methylguanosine capped, spliced and 3'-polyadenylated and may give rise to one or more mature miRNAs. Some miRNAs may also derive from processed intronic sequences [10]. In the nucleus, pri-miRNAs are subjected to cleavage by

Drosha releasing precursor (pre)-miRNA hairpin structures. Pre-miRNAs are then transported to the cytoplasm where cleavage by Dicer results in a 19–24 nucleotide double-stranded miRNA of which one strand, the mature miRNA, is transferred to the Argonaute (AGO) component of the RNA-induced silencing complex (RISC). AGO acts as a RISC effector protein modulating mRNA stability and translation (Figure 1-1) [11, 12].

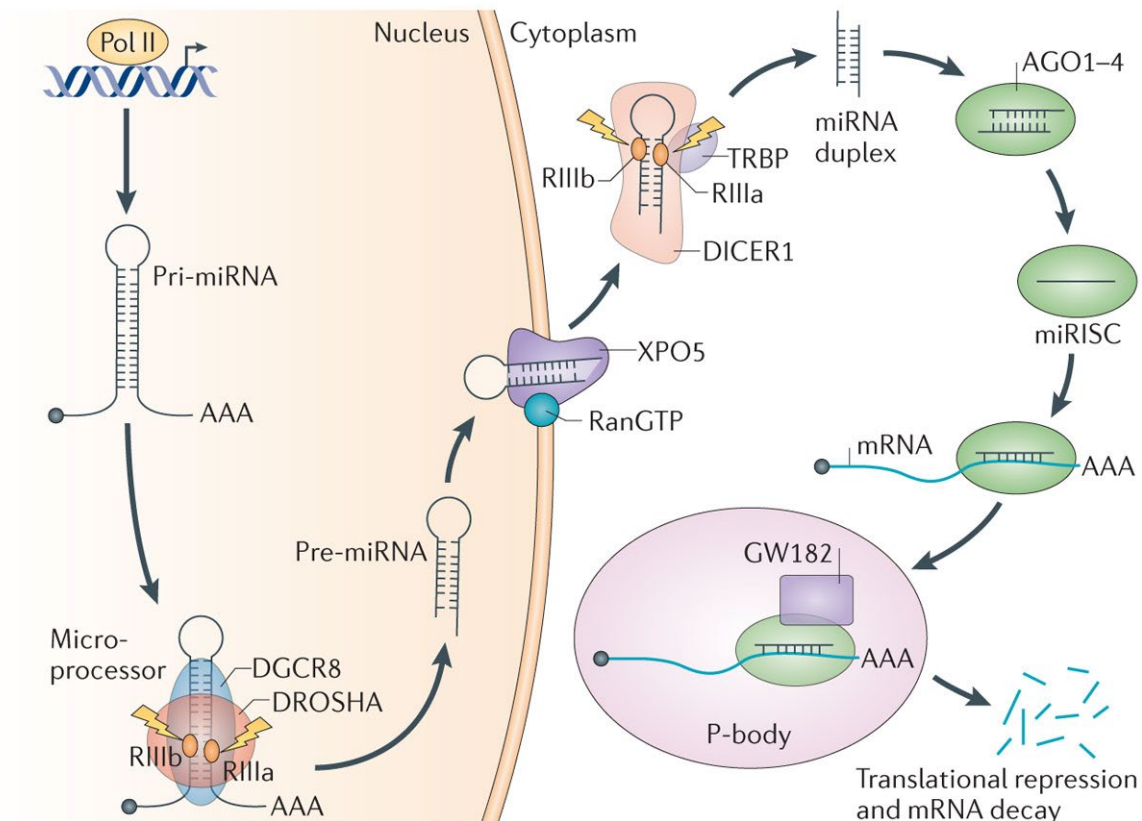


**Figure 1-1. miRNA biogenesis pathway.**

Primary miRNAs (pri-miRNAs) are transcribed by RNA polymerase II followed by a cleavage by microprocessor including DROSHA and DGCR8 which produces precursor miRNAs (pre-miRNAs). Pre-miRNAs are then exported from the nucleus to the cytoplasm by exportin 5 (XPO5) where further processing occurs by DICER1 ribonuclease to produce double stranded mature miRNAs. The guide strand is then loaded into miRNA-induced silencing complex (miRISC), which contains DICER1 and Argonaute (AGO) proteins and helps in binding to the target mRNA and miRNA-mediated gene suppression [13].

### 1.3 Colorectal Cancer (CRC)

Colorectal cancer (CRC), also known as bowel cancer, includes cancers of the colon, the rectosigmoid junction and the rectum [14, 15]. Majority of CRC cases occur due to old age and

lifestyle factors, with only a small number of cases having underlying genetic disorders [16]. Beside genetic events, epigenetic factors are also responsible for CRC tumorigenesis [17-20].

### 1.4.1 Epidemiology of colorectal cancer

Worldwide, CRC is the third most common cancer diagnosed and the third leading cause of all cancer deaths which represents 9.4% of all incidents of cancer in men and 10.1% in women [21]. The geographical distribution of CRC demonstrates variations with the highest incidence rate in Australia, New Zealand, Canada, the United States, and parts of Europe and the lowest risks include China, India, and parts of Africa and South America [21]. CRC mortality accounts for 600,000 deaths recorded in 2008 worldwide, making it the fourth most common cause of cancer related death [15].

In Australia, CRC is the third most commonly diagnosed cancer and is estimated to remain the third most prevalent cancer in 2019. According to Cancer Council Australia, in 2015, 15604 new cases were diagnosed. 9% of all cancer deaths were caused by CRC, which represents the second highest number of cancer deaths in Australia, with a five year survival rate of 69% [22]. According to AIHW, while CRC incidence projections indicate that the number of new CRC cases per year may stabilise by 2020, it will remain among the most common cancers diagnosed [14]. CRC is mainly sporadic with approximately 5% of patients associated with highly penetrant inherited mutations [23, 24].

### 1.4.2 Diagnosis and treatment of CRC

According to the National Health and Medical Research Council (NHMRC) guidelines, in asymptomatic patients aged 50 and over, CRC may be detected through faecal occult blood tests (FOBT) at least every two years. Also, sigmoidoscopy may also be considered for patients at low risk for every 5 years from the age of 50. Those with moderate risk of CRC, the diagnosis guideline offers colonoscopy every 5 years from the age 50 or sigmoidoscopy plus double contrast barium enema with FOBT in intervening years. Investigation of genetic background and annual or 2 yearly colonoscopy from the age 25 is offered for patients at high risk [25].

Treatment strategies are refined depending on the CRC stages [26]. Surgical resection with curative intent is the strategy applied for early stages of CRCs. While surgical excision is the preferred option for localised tumours, in patients with diagnosed lymph node metastasis, adjuvant chemotherapy may be employed after surgical resection [27]. Metastatic CRC patients may be treated with chemotherapeutic agents. While there is a 67% five-year survival rate for detected and

treated CRC patients, the median survival rate falls to approximately six months with metastatic CRC [28].

### 1.4.3 Genetic and epigenetic events in colorectal cancer development

CRC is mostly sporadic however, approximately 5% of patients carry inherited mutations [24]. CRC has a multifaceted aetiology and its progression requires multiple changes in genetic, environmental, and inflammatory factors, resulting in the loss-of-function of tumour suppressor genes and gain-of-function of oncogenes [29, 30]. CRC development involves a multi-step path where it originates with benign adenomatous polyps on the inner wall of the colon and rectum and progressively develops into advanced adenoma and carcinoma, invasive carcinoma and eventually distant metastases that account for the most advanced stage of development [31]. Chromosomal instability (CIN), microsatellite instability (MSI) and CpG island methylation phenotype (CIMP) are main factors involved in CRC [32].

Germ line mutations of the adenomatosis polyposis coli (*APC*) tumour suppressor gene present as one of the most common driver mutations for familial adenomatous polyposis (FAP) [33]. Also, germline mutations in DNA mismatch repair genes result in hereditary non-polyposis colorectal cancer (HNPCC) or Lynch syndrome [34-36]. Also, germ line mutations in *APC* gene and in several other genes predispose to hereditary-type CRC and are involved in onset and development of CRC [37-39]; these mutations lead to changes in gene expression and promote transformation of the normal mucosa. The remaining CRC cases are sporadic which occurs with accumulation of somatic genetic and epigenetic changes[24].

Epigenetics are defined as mechanisms by which the structure of the chromatin and level of gene expression are modified without changes in the DNA sequence. These modifications mainly include methylation, acetylation and hydroxylation of histones and modification of histone-like proteins [40]. Internal and external factors can induce epigenetic modifications and may have similar effects to pathogenic mutations. The involvement of epigenetic change in carcinogenesis, including CRC onset and development, has been shown in numerous studies [41]. Aberrant expression of miRNA profiles has also been shown in CRC, with increased levels of some miRNAs with oncogenic potential, and decreased levels of other miRNAs with tumour suppressor roles [42-44].

#### 1.4.4 CRC and metabolic issues

Changes in metabolic profile are associated with CRC, which include perturbations in the macromolecule biosynthesis and pentose-phosphate pathways, as well as glycolytic, gluconeogenic, and tricarboxylic acid and oxidative phosphorylation intermediates [45].

Metabolites from different samples acquired from serum, urine, stool, and tissue, represent the downstream functional products of gene expression and protein synthesis and include environmental exposures and microbial metabolism, and, consequently can affect CRC progression [46].

In CRC tissue samples, 31 differential metabolites were compared with adjacent mucosal levels to identify an almost 70% increase in cellular glucose [47]. Similarly, Qiu et al., reported 15 altered metabolites in matched CRC surgical specimens in China and USA, which were then used to develop a predictive tool for recurrence and survival of CRC patients after treatment [48]. Studies of Brown et al., also identified 8 metabolites including 2-aminoadipate, betaine aldehyde, N-methyl diethanolamine, alpha-hydroxyisovalerate, oxidized Cysteine-Glycine dipeptide, deoxycholate, 7-ketodeoxycholate, sorbitol, and asparagine that were discriminatory between CRC and adjacent mucosa [45]. Changes in the metabolic profiles of colon polyps are mainly due to the specific mutations that result in higher rates of proliferation, invasion and cell survival. These changes include the Warburg effect, *APC/KRAS/BRAF* gene mutations and MSI status [49-51]. Therefore, metabolic fingerprints could be specific markers that can distinguish adjacent mucosa from CRC and may reveal stages of pathogenesis and response to preventive strategies [52] [53].

#### 1.4.5 Risk factors in colorectal cancer development

Since the majority of the CRC incidences arise from an accumulation of sporadic mutations and epigenetic alterations, advanced age is considered to be one of the most important risk factors for CRC [16, 17, 30, 54]. Familial history of CRC is another risk factor, even in the absence of the known syndromes [55]. Diet, obesity, physical activity levels, smoking, alcohol consumption and exposure to UV light are lifestyle and environmental factors that modify CRC risk. [16, 30, 56].

A number of epidemiological studies have shown the association of type 2 diabetes with higher risk of CRC development [57, 58]. This was attributed to elevated insulin, due to insulin resistance and hyperinsulinaemia, which is observed in type 2 diabetic patients since insulin is an important colonic epithelial growth factor and is a potential mitogen [59, 60]. Insulin-like growth factor 1 was also shown to promote CRC carcinogenesis by enhancing cell proliferation and suppressing cell death [60]. Hyperglycaemia, observed in diabetic patients, is another factor

that contributes to CRC development and progression through regulation of reactive oxygen species and effectiveness of the immune system [61].

#### 1.4 Metabolic reprogramming

Proliferating cells and, indeed, cancer cells require constant cell division. In order to maintain this, there is an urgent need to provide a consistent energy source, macromolecular biosynthesis, and controlled redox status. Therefore, to optimise proliferation, growth and survival, cancer cells redirect their metabolic pathways and alter the production and consumption of numerous metabolites [62, 63].

To support cancer cell proliferation, glycolysis provides the precursors for major macromolecules including the carbohydrates, proteins, lipids, and nucleic acids needed to produce a new cell. Therefore, aerobic glycolysis imbues cancer cells with ribose, amino acids and fatty acids [64, 65]. The upregulation of glycolysis is mostly due to the increased expression of enzymes and transporters involved in glucose uptake, lactate production, and lactate secretion. These proteins include glucose transporters (GLUT1-4), hexokinase 2 (HK2), glyceraldehyde-3-phosphate dehydrogenase (GAPDH), 6-phosphofructo-1-kinase (PFK1), aldolase (ALDO), triose-phosphate isomerase (TPI), phosphoglycerate kinase 1 (PGK1), phosphoglycerate mutase (PGM), enolase 1 (ENO1), pyruvate kinase (PKM2), lactate dehydrogenase (LDHA) and monocarboxylate transporters (MCTs).

There is substantial evidence regarding the importance of aberrant expression of oncomiRs and tumour suppressor miRNAs targeting key players in aerobic glycolysis to give proliferation, growth, and invasion advantages to cancer cells (Figure 1-1). Such changes in miRNA activity reflect a mechanism by which cancer cells bypass checkpoints that determine thresholds of biosynthetic enzyme activities.

In addition to miRNAs directly targeting genes involved in cancer cell glycolysis, summarized in Table 1-1, several indirect mechanisms have been reported for miRNA-mediated regulation of glycolytic genes. Horie et al. [66] showed that forced expression of miR-133 decreases *GLUT4* expression by directly targeting Kruppel-like factor 15 (*KLF15*) in cardiomyocytes. *KLF15* is a transcription factor required for *GLUT4* transcription. Also, miR-155 was reported to upregulate HK2 through signal transducer and activator of transcription 3 (STAT3) activation, as well as through miR-143 repression by targeting CCAAT-enhancer-binding protein  $\beta$  (*C/EBP $\beta$* ). Moreover, miR-143 was found to target HK2 directly, linking inflammatory miR-155-related

signalling with cancer-associated changes in metabolism [67, 68]. PKM is one of the rate limiting enzymes in glycolysis. While PKM1 expression was shown to be active in normal cells, cancer cells switch *PKM1* to the tumour-associated PKM2. Also, some miRNAs were reported to regulate polypyrimidine tract-binding protein 1 (PTB-1), which processes *PKM* transcripts and is involved in PKM1 to PKM2 conversion in tumour cells. These miRNAs, including miR-1, miR-124, miR-133b, miR-137 and miR-340 were shown to directly inhibit cancer cell proliferation and may also explain the repressed PTB-1 expression associated with tumour progression *in vivo* [69-73].

Although several decades have passed since the first report on cancer metabolism, with many studies since, a definitive mechanism underpinning the Warburg metabolic shift has remained obscure. Moreover, how individually disrupted metabolic pathways converge to coordinate a global metabolic shift and facilitate the tumour phenotype remains to be fully elucidated.

**Table 1-1. Summary of miRNAs directly targeting glycolytic enzymes and transporters.**

Gene	miRNAs	Diseases	References
<b>GLUT1</b>	miR-495, miR-1291, miR-130b, miR-199a, miR-138, miR-150, miR-532, miR-301a, miR-19a/b, miR-22, miR-132, miR-218, miR-340, miR-541	Renal Cell Carcinoma, Glioma, Breast Cancer, Prostate Cancer, Bladder Cancer, Oral Squamous Cell Carcinoma, Glioblastoma Multiforme	[74-82]
<b>GLUT2</b>	miR-143	-	[83]
<b>GLUT3</b>	miR-195, miR-106a	Bladder Cancer, Glioblastoma	[84, 85]
<b>GLUT4</b>	miR-223, miR-93, miR-150, miR-192, miR-106b	Cardiomyocytes, Polycystic Ovary Syndrome, Diabetes Mellitus	[86-89]
<b>HK1</b>	miR-138	Head and neck squamous cell carcinoma	[90]
<b>HK2</b>	miR-34a, miR-143, miR-125a/b, miR-497, miR-181b/c, miR-98, miR-4458, miR-199a	Colorectal Cancer, Head and Neck Squamous Cell Carcinoma, Breast Cancer, Lung Cancer, Glioblastoma, Hepatocellular Carcinoma, Chronic Lymphocytic Leukaemia, Primary keratinocytes, Osteocarcinoma, Prostate Cancer, Gastric Cancer	[67, 90-102]
<b>GPI</b>	miR-34a, miR-302b, miR-17, miR-200 family	Colorectal Cancer, Primordial Germ Cells, Breast Cancer	[91, 103, 104]
<b>PFK</b>	miR-520, miR-320a, miR-106b, miR-26b, miR-206	Hepatocellular Carcinoma, Lung Adenocarcinoma, Renal Cell Carcinoma, Osteosarcoma, Breast Cancer	[105-110]
<b>ALDOA</b>	miR-34c, miR-122, miR-15a, miR-16-1	Emphysematous Lung, Hepatocellular Carcinoma, Leukaemia, Lung Cancer	[111-114]
<b>GAPDH</b>	miR-644a	Prostate Cancer	[115]
<b>TPI1</b>	miR-15a, miR-16-1, miR-107, miR-195	Leukaemia, Renal Cell Carcinoma, Lung Cancer, Bladder Cancer	[112, 114, 116, 117]
<b>PGK1</b>	miR-107, miR-29a, miR-1256, miR-17-92 cluster	Renal Cell Carcinoma, Prostate Cancer, Lung Cancer, Pancreatic Cancer, Squamous Cell Lung Carcinoma	[116, 118-120]
<b>PGM</b>	Let-7g, miR-29a, miR-33b, miR-21	Primary Human Hepatocytes, Lung Cancer, Renal Cell Carcinoma	[109, 119, 121, 122]
<b>ENO1</b>	miR-17-92 cluster, miR-29a	Lung Cancer	[119, 120]
<b>PKM2</b>	miR-34a, miR-122, miR-133a/b, miR-326, miR-99a, miR-128	Colorectal Cancer, Hepatocellular Carcinoma, Squamous Cell Carcinoma of Tongue, Glioblastoma, Type 2 Diabetes, Prostate Cancer	[91, 123-126]
<b>LDHA</b>	miR-375, miR-24, miR-23a, miR-210, miR-30a, miR-34a/c, miR-374a, miR-383, miR-4524a/b, miR-369, miR-410, miR-590	Maxillary Sinus Squamous Cell Carcinoma, Acute Myocardial Ischemia, Breast Cancer, Colorectal Cancer, Hypoxia-Induced Cardiomyocytes Dysfunction, Ovarian Cancer, Cervical Cancer, Gestational Diabetes Mellitus, Type2 Diabetes	[127-137]

<b>MCTs</b>	miR-29a/b, miR-124, miR-376a-5p, miR-495	Pancreatic $\beta$ Cells, Medulloblastomas, Type2 Diabetes	[138-140]
-------------	--	--	-----------

## 1.5 Inter-connection between aerobic glycolysis and mitochondria

Whilst glycolysis accounts for the generation of almost two thirds of the ATP required for tumour cells, in most cancer cells mitochondria are still functional and generate the remaining energy requirements [141]. Mitochondria also contribute to pivotal roles in controlling anaplerotic and cataplerotic pathways within cancer cells. Indeed, several roles for mitochondria in carcinogenesis, other than ATP production for cellular demands, have been established [142]. As a result, functions including hypoxia resistance, apoptosis escape, reactive oxygen species (ROS) control, and bio-synthetic contributions are attributed to mitochondria. Mutations in mitochondrial TCA cycle genes, encoded by nuclear DNA, were found in various types of cancers. Mutational inactivation of these enzymes contributed to a metabolic shift through direct adaptation to decreased OXPHOS or, alternatively, by epigenetic modification caused by cytosolic and mitochondrial accumulation of oncometabolites such as 2-hydroxyglutarate (2HG) [143-147].

Studies of miRNA localization from nucleus to mitochondria have led to the discovery of mitochondria-related miRNAs (mitomiRs). A considerable body of literature demonstrated the miRNA contributions to every aspect of mitochondrial metabolism, respiration and dynamics [148]. Additionally, ROS generated within mitochondria were found to be strictly regulated by several miRNAs (reviewed in [149]). miRNAs that regulate tricarboxylic acid (TCA) cycle transcripts include miR-183, miR-210 and miR-734a, which target isocitrate dehydrogenase (*IDH*), succinate dehydrogenase (*SDH*), and malate dehydrogenase (*MDH*), respectively [150-152] (Figure 1-1). Moreover, several electron transport chain components are reportedly regulated by miRNAs. For instance, miR-338 and miR-181c downregulate cytochrome c oxidase complex COX4 and COX1, respectively. Hypoxically regulated miR-210 represses iron-sulphur cluster scaffold (*ISCU*) and *COX10* translation [153-155]. Glutaminase (GLS) is a rate-limiting enzyme in glutamine metabolism which converts glutamine to glutamate. An increasing number of reports revealed cooperation of c-Myc and p53 with several miRNAs such as miR-23a/b, miR-125b, miR-30 and miR-504 in modulating GLS activity [156]. Based on these reports, it is clear that miRNAs target both nuclear mRNAs and mitochondrial mRNAs. Moreover, the Crabtree effect, originally identified in fermenting yeast, enables some cancer cells to switch between glycolysis and OXPHOS in spite of functional mitochondria and also challenges the “purely glycolytic cancer cell” paradigm. The Crabtree effect is considered to be a short-term and reversible mechanism and

an adaptive response of mitochondria to the heterogeneous microenvironment of cancer cells [157]. Hence, there is still a need to fully determine whether changes in mitochondrial functionality, mediated by several miRNAs, contribute to cellular transformation. Otherwise it may be considered a secondary phenomenon, which arises from changes in cell glycolysis and/or other signalling pathways also regulated by miRNAs.

## 1.6 Hypoxia and glycolysis

Hypoxia is a common feature in proliferating solid tumours. In normal cells, hypoxia leads to cellular adaptation, or p53-dependent apoptosis and cell death. However, cancer cells acquire mutations in p53 and other genes, along with changes in their metabolic pathways in order to survive and even proliferate under hypoxic stress. A key mediator of responses to hypoxia is hypoxia-inducible factor-1 (HIF-1), a transcription factor that plays a pivotal role in responding to decreased oxygen levels, initiating hypoxia-related processes such as OXPHOS repression and induced glycolysis [158].

Although prolyl-4-hydroxylase (PHD) and factor inhibiting HIF-1 (FIH-1; also known as HIF1AN) dependent regulation of HIF-1 is primarily thought to be the sole mechanism of HIF-1 regulation [159] it is now clear that hypoxia influences miRNA biogenesis and these miRNAs can regulate *HIF-1a* and *HIF-1 $\beta$*  expression [160]. HIF-1 $\alpha$  is also regulated at the DNA, RNA, protein and DNA binding levels [161]. Translational regulation of HIF-1 $\alpha$  could also be a consequence of activating the mechanistic target of rapamycin (mTOR) signalling pathway in cancer cells. Many miRNAs, such as miR-99a, were shown to repress *HIF-1a* expression by targeting mTOR [125]. The abnormal activation of HIF-1 under normoxia could alternatively be a result of changes in cancer-associated genes. Such tumourigenic mutations include loss of function in tumour suppressors such as P53, phosphatase and tensin homolog (PTEN) [162], Von Hippel-Lindau (VHL) [163], LKB1 [164], promyelocytic leukemia protein (PML) [165] and tuberous sclerosis proteins (TSC1/TSC2) [166] along with mutational activation of oncogenes such as *Ras* [167], *V-Src* [168], phosphoinositide 3-kinase (*PI3K*) [169] and human epidermal growth factor receptor 2 (*Her2/Neu*) [170]. PKM2 was also reported to enhance *HIF-1* transcription, through binding to its promoter, and promote HIF-1 stabilization by inhibiting PHD interactions [171]. Mitochondria also act as both targets and effectors of HIF-1 activation [149]. To adapt to a hypoxic microenvironment and acquire lethal cancer characteristics, HIF-1 activation leads to a range of physiological responses [172]. At the transcriptional level, HIF-1 $\alpha$  activates a variety of genes following translocation into the nucleus, dimerization with HIF-1 $\beta$  and

binding to hypoxia response elements (HREs) upstream of target genes. Besides HRE-dependent responses, HIF-1 $\alpha$  interacts with other signal transduction pathways including Notch [173], Wnt [174] and c-Myc [175].

Activated HIF-1 is directly and indirectly associated with increased expression of virtually all glycolytic transporters and enzymes [172]. Moreover, HIF-1 affects mitochondria through various mechanisms and stimulates glycolysis indirectly by suppressing mitochondrial oxidative metabolism which enables HIF-1 to function as a switch between glycolysis and OXPHOS [176]. HIF-1 represses mitochondrial pyruvate dehydrogenase (PDH) activity [158], which is a gate-keeping enzyme feeding the TCA cycle by converting pyruvate to acetyl-CoA. HIF-1 suppresses PDH expression by actively upregulating pyruvate dehydrogenase kinase (PDK1), a PDH suppressor [177]. By such regulation, pyruvate is converted to lactate, cytosolic NADH is re-oxidized and glycolysis is continued. As a consequence, PDH suppression by activated HIF-1 protects cells from increased ROS generated within mitochondria [178]. In addition, HIF-1 regulates mitochondrial function in response to oxygen by mediating a subunit switch in COX4. HIF-1 induces COX4I2 subunit expression under hypoxic conditions, while the normoxic COX4I1 subunit is downregulated through HIF-1-mediated activation of LON, a mitochondrial protease. This subunit switch optimises the efficiency of respiration in response to hypoxia by influencing H<sub>2</sub>O<sub>2</sub> levels in an oxygen-dependent manner [176]. Zhao et al. [179] showed that HIF-1 $\alpha$  upregulates TKT and TKTL2, two transketolase enzymes of the pentose phosphate pathway, to elevate the ribose production required for nucleic acid anabolic pathways.

Thus far, no mutations within the *HIF-1* genes have been associated with its activation or related regulation of glucose metabolism, however aberrant HIF1 activity has proved to be important in the initiation and maintenance of some tumours [161].

Hypoxia is a significant mediator of miRNA biosynthesis, at both the transcriptional and post-transcriptional levels [180]. A recently identified subset of miRNAs are known as “hypoxia regulated miRNAs” (also termed hypoxiamiRs or HRMs). Hypoxia regulates hypoxiamiRs in either a HIF-1 dependent or independent manner [181]. First reported by Kulshreshtha et al. [160], hypoxia is capable of upregulating miRNA expression (Figure 1-2 and Table 1-2). Among these hypoxia-inducible miRNAs, miR-210 and miR-26 were found to have dynamic recruitment of HIF-1 to their promoters. Upon activation, HIF-1 $\alpha$  translocates to the nucleus and targets HREs of downstream genes, including miRNA encoding genes. Interestingly, hypoxia is also associated with miRNA downregulation. In that regard, the miR-17~92 cluster was downregulated by hypoxia in p53 wild type cells [182]. Similarly, Lei et al. [183] reported miR-20b upregulation in

HIF1-knockdown cells. Other hypoxia-suppressed miRNAs are listed in Table 1-2. Nevertheless, contrasting reports, with miRNAs such as miR-26 and miR-19, demonstrate that hypoxia-dependent regulation of miRNAs is cell type and microenvironment dependent [160, 184]. Among downregulated hypoxiamiRs, HIF-1 was shown to downregulate miR-17 and miR-199a [185, 186]. HIF-1 also regulates miRNA expression indirectly by mediating the expression of other transcription factors, examples being activation of miR-10b by HIF-1-dependent *TWIST1* expression and regulation of miR-20a/b through vascular endothelial growth factor A (VEGFA) targeting by HIF-1 [187, 188]. Beside miRNAs directly regulated by hypoxia, it is evident that hypoxia is post-transcriptionally involved in the regulation of hypoxiamiR biogenesis, processing and function in both a HIF-dependent and independent manner. It was shown that hypoxia accelerates Ago2 assembly to RISC and its translocation to stress granules by upregulating Ago2 prolyl-hydroxylation and increasing its endonuclease activity [189]. Moreover, HIF-1 regulates expression of the prolyl 4-hydroxylase, alpha polypeptide I (P4HA1) by regulating miR-124 expression [190]. In fact, stress granule formation increased in a hypoxia-dependent manner. Nonetheless, ADP-ribosylation of Ago2 in response to oxidative stress is another mechanism that eventually leads to relief of miRNA-mediated repression. Interestingly, it was reported that some miRNA maturation that is not dependent on Dicer activity [191], might be processed by the endonuclease activity of Ago2, the levels of which are induced by hypoxia. Accordingly, Dicer was found to be downregulated by hypoxia, while miR-451 was upregulated [192, 193].

*HIF-1a* may be directly targeted by miRNAs in various diseases, including cancer (Table 1-2). Besides direct translational repression, some miRNAs inhibit other factors that modulate HIF-1 expression and stability. As FIH-1 inhibits the transcriptional activation of *HIF-1a*; miRNAs that suppress FIH-1, such as miR-31, miR-135b and miR-184, result in *HIF-1* activation [191, 194, 195]. FIH-1 was also shown to regulate cell metabolism through reducing glycogen and attenuating AKT signalling [196]. miR-92-1 suppresses HIF-1 degradation by targeting *pVHL* [197]. miR-206 targets the HIF-1/FHL-1 pathway on pulmonary artery smooth muscle cells to promote hypertension [198]. Increased expression of miR-21 was shown to increase *HIF-1a* and *VEGF* expression in prostate cancer possibly through a PTEN-dependent pathway [199]. miR-107 downregulates mRNA and protein levels of *HIF-1 $\beta$*  in endothelial progenitor cells while overexpression of *HIF-1 $\beta$*  also blocks the effects of miR-107 [200, 201]. miR-185 targets *HIF-2a* transcripts and, thus, indirectly moderates HIF-1 expression and stability [202].

Feedback loops have been reported in the miRNA regulation of *HIF-1*. miR-210 forms a positive feedback loop with HIF-1 where hypoxia-induced miR-210 further induces HIF-1 $\alpha$  protein

stability [203]. Kelly et al. [203] showed that miR-210 targets glycerol-3-phosphate dehydrogenase 1 like (*GPD1L*), a HIF-1 regulator, and overexpression of miR-210 results in decreased HIF-1 proline hydroxylation and increased accumulation during hypoxia. What's more, HIF-1 directly induces miR-210 expression, which then causes synthesis of cytochrome c oxidase 2/1 (SCO2/1) protein activation and enhanced TCA cycle function [204]. Hypoxia was shown to induce C/EBP levels, which in turn increases PU1 activation and binding to the miR-424 promoter to induce its expression. Upregulated miR-424 inhibits cullin 2 (CUL2) and leads to HIF-1 stabilization and nuclear translocation [205]. Overexpression of miR-494 and miR-21 significantly increases Akt phosphorylation and subsequently induces HIF-1 activity [199, 206]. Recent evidence that the activities of non-coding RNAs, including oncogenic miR-21, can be manipulated by small molecules suggests that such processes may be druggable [207].

As a predominant oncomiR, the miR-17~92 cluster has been heavily investigated for its association with hypoxia. Bertozzi et al. [208] showed that miR-17-5p reduced HIF-1 $\alpha$  at low camptothecin exposure. miR-17 and miR-20a also target the 3'UTR of *HIF-1* and *HIF-2* in primary human macrophages [209]. All members of this cluster were shown to directly target HIF-1 in lung cancer [120]. miR-17 and miR-20a were downregulated by HIF-1 through a transcriptional and HIF-1 $\beta$ -independent manner and by downregulating *c-Myc* expression [185]. miR-20a is a hypoxia-responsive miRNA that targets *HIF-1* in breast cancer, lung adenocarcinoma, colorectal cancer and endometriotic stromal cells [120, 187, 209-211]. In the paralogous miR-106a~363 cluster, miR-20b is known to target HIF-1 in hepatocellular carcinoma (HCC) and breast cancer cells [212, 213]. Also, chromatin immunoprecipitation analyses revealed that miR-20b prevents HIF-1 binding to the *VEGF* promoter and, thus, modulates *VEGFA* expression [212].

Aberrant expression of miRNAs, which can result from hypoxia encountered during tumour progression, may play a critical role in HIF-1 regulation and altered downstream effects (Figure 2). Interestingly, some miRNAs that target HIF-1 were also reported to be modulated by hypoxia in both a HIF-dependent and independent manner. However, some anomalies regarding hypoxiamiRs and miRNAs that regulate HIF-1 still exist. For instance, Bartoszewska et al. [214] showed that *HIF-1* is a direct target of miR-429 in HUVEC cells and is induced during hypoxia. However, Sun et al. [206] showed that overexpression of miR-429 increases *HIF-1a* expression, under both hypoxia and normoxia, and couldn't find a miR-429 target sequence in the 3'UTR of *HIF-1a* in liver cells. These inconsistencies likely depend on cellular context and experimental conditions. Moreover, as HIF is mainly post-translationally regulated, miRNA activity may be largely redundant in some systems. Table 1-2 summarizes the associations between hypoxia and

miRNAs in different cancers. It has been proposed [141] that the observed Warburg effect is entirely attributable to the *in vivo* tumour hypoxia and is, in fact, a manifestation of the Pasteur Effect.

**Table 1-2. Summary of associations between miRNAs and hypoxia.**

miRNA	Disease/Cell line	Regulation of HIF/mechanism	Regulation of miRNA by Hypoxia	References
<b>miR-17-92 cluster</b>	Lung Cancer, Cervical Adenocarcinoma, Inflammation, Colon Cancer, Breast Cancer, Hepatocarcinoma	Downregulation/ targeting <i>HIF-1a</i> and <i>HIF-2</i>	Downregulation	[120, 183, 185, 208, 209, 212, 215]
<b>miR-15b</b>	Hemophilia, Nasopharyngeal Carcinoma	Downregulation/ targeting <i>HIF-2</i>	Downregulation	[215, 216]
<b>miR-16</b>	Nasopharyngeal Carcinoma	NA	Downregulation	[215]
<b>miR-19a</b>	Oral Squamous Cell Carcinoma, Human Atherosclerotic Lesions	NA	Downregulation/Upregulation	[184, 217]
<b>miR-20a/b</b>	Nasopharyngeal Carcinoma, Lung Cancer	Downregulation/ targeting <i>HIF-1a</i> and <i>HIF-2a</i>	Downregulation	[120, 215]
<b>miR-21</b>	Breast Cancer, Prostate Cancer	Upregulation	Upregulation	[160, 199, 218]
<b>miR-22</b>	Clear Cell Renal Cell Carcinoma, Colorectal Cancer, Heart muscle, Oral Squamous Cell Carcinoma	Downregulation/ targeting <i>HIF-1a</i>	Upregulated/Downregulated	[181, 184, 219, 220]
<b>miR-23a/b</b>	Colorectal Cancer, Breast Cancer	NA	Upregulated	[160, 221]
<b>miR-24</b>	Colorectal Cancer, Breast Cancer	NA	Upregulated	[221]
<b>miR-26a/b</b>	Nasopharyngeal Carcinoma, Colorectal Cancer, Breast Cancer	NA	Upregulated/Downregulated	[215, 221]
<b>miR-27a/b</b>	Heart Muscle, Colorectal Cancer, Breast Cancer	NA	Upregulated	[181, 221]
<b>miR-30b/d/e</b>	Oral Squamous Cell Carcinoma, Colorectal Cancer, Breast Cancer, Nasopharyngeal Carcinoma	NA	Downregulation/Upregulated	[184, 215]
<b>miR-29b</b>	Oral Squamous Cell Carcinoma	NA	Downregulated	[184, 221]
<b>miR-31</b>	Colorectal Cancer, Human Corneal Epithelial Keratinocytes, Oral Squamous Cell Carcinoma	Upregulation / targeting <i>FIH1</i>	Upregulated	[184, 194, 196, 222, 223]
<b>miR-33a</b>	Melanoma	Downregulation/ targeting <i>HIF-1a</i>	NA	[224]
<b>miR-93</b>	Colorectal Cancer, Breast Cancer	NA	Upregulation	[160]
<b>miR-99a</b>	Type 2 Diabetes	Downregulation/ targeting <i>HIF-1a</i>	NA	[125]
<b>miR-101</b>	Oral Squamous Cell Carcinoma	NA	Downregulation	[184]
<b>miR-103</b>	Colorectal Cancer, Breast Cancer	NA	Upregulated	[160]

CHAPTER 1

<b>miR-106b</b>	Colorectal Cancer, Breast Cancer	NA	Upregulated	[160]
<b>miR-107</b>	Ischaemic Heart Disease, Colorectal Cancer, Colorectal Cancer, Breast Cancer	Downregulation/ targeting <i>HIF-1<math>\beta</math></i>	Upregulation	[160, 200, 201]
<b>miR-122a</b>	Oral Squamous Cell Carcinoma	NA	Downregulation	[184]
<b>miR-125b</b>	Colorectal Cancer, Breast Cancer	NA	Upregulated	[160]
<b>miR-128</b>	Prostate Cancer	Downregulation/ targeting <i>HIF-1<math>\alpha</math></i>	NA	[126]
<b>miR-135b</b>	Prostate Cancer, Breast Cancer	Upregulation/ targeting <i>FIH-1</i>	NA	[191, 225]
<b>miR-138</b>	Clear Cell Renal Cell Carcinoma, Ovarian Cancer	Downregulation / targeting <i>HIF-1<math>\alpha</math></i>	NA	[226, 227]
<b>miR-141</b>	Oral Squamous Cell Carcinoma	NA	Downregulation	[160]
<b>miR-155</b>	Cervical Adenocarcinoma, Nasopharyngeal Carcinoma	Downregulation/ targeting <i>HIF-1<math>\alpha</math></i>	Upregulation	[208, 215]
<b>miR-181a/b/c</b>	Colorectal Cancer, Breast Cancer, Nasopharyngeal Carcinoma, Heart Muscle	NA	Upregulated/Downregulated	[160, 181, 215]
<b>miR-184</b>	Glioma	Upregulation/ targeting <i>FIH-1</i>	NA	[195]
<b>miR-186</b>	Oral Squamous Cell Carcinoma, Gastric Cancer	Downregulating/ targeting <i>HIF-1<math>\alpha</math></i>	Downregulation	[184, 228]
<b>miR-192</b>	Colorectal Cancer, Breast Cancer	NA	Upregulated	[160]
<b>miR-195</b>	Hypoxic Chondrocytes, Colorectal Cancer, Breast Cancer	Downregulation/ targeting <i>HIF-1<math>\alpha</math></i>	Upregulation	[160, 229]
<b>miR-197</b>	Oral Squamous Cell Carcinoma	NA	Downregulation	[184]
<b>miR-199a/b</b>	Ovarian Cancer, Sickle Cell Disease, Lung Cancer exposed to arsenic, Heart muscle	Downregulation/ targeting <i>HIF-1<math>\alpha</math></i> and <i>HIF-2<math>\alpha</math></i>	Downregulation	[181, 186, 230, 231]
<b>miR-204</b>	Pulmonary Arterial Hypertension	Downregulation/ targeting <i>HIF-1<math>\alpha</math></i>	NA	[232]
<b>miR-206</b>	Pulmonary Arterial Hypertension	Downregulation/ targeting <i>HIF-1<math>\alpha</math></i>	NA	[198]
<b>miR-210</b>	Cervical Cancer, Head and Neck Paragangliomas, Hypotriploid Human Kidney Cell Line, Ischemia, Breast Cancer, Nasopharyngeal Carcinoma, Oral Squamous Cell Carcinoma, Heart Muscle, Colorectal Cancer, Breast Cancer	NA	Upregulation	[160, 181, 184, 203, 215, 233-235]
<b>miR-213</b>	Colorectal Cancer, Breast Cancer	NA	Upregulation	[160]
<b>miR-361</b>	Umbilical Vein Endothelial Cells (HUVEC)	Downregulation/ targeting <i>HIF-1<math>\alpha</math></i>	Downregulation	[236]

<b>miR-374</b>	Oral Squamous Cell Carcinoma, Breast Cancer	Upregulation/ targeting <i>TXNIP</i>	Downregulation	[184, 237]
<b>miR-422b</b>	Oral Squamous Cell Carcinoma	NA	Downregulation	[184]
<b>miR-424</b>	Ovarian Cancer, Oral Squamous Cell Carcinoma	Upregulation/ targeting <i>CUL2</i>	Downregulation	[183, 184, 205]
<b>miR-429</b>	Human Endothelial Cells	Downregulation/ targeting <i>HIF-1a</i>	Upregulation	[214]
<b>miR-494</b>	Lung Cancer	NA	NA	[206]
<b>miR-519c</b>	Hepatic Cancer	Downregulation/ targeting <i>HIF-1a</i>	NA	[238]
<b>miR-565</b>	Oral Squamous Cell Carcinoma	NA	Downregulation	[184]

## 1.7 Metabolic consequences of miRNA associations with driver mutations and transformation

While oncoproteins and tumour suppressor proteins are well-known for their roles in regulating cellular processes such as cell proliferation, they are also capable of affecting cancer cell metabolism. Activation of certain oncogenic signals is important for stimulating glycolysis. Various mutations in different oncogenes and tumour suppressors show that cancer cells alter metabolism to adapt to their microenvironment [239]. These fundamental genes include oncogenes such as *KRAS*, *MYC*, *AKT* and *MTOR*, along with their inhibitors (*PTEN* and *TSC1/2*) and activator (*EGFR*). They also include tumour suppressor genes such as *TP53*, along with its negative regulator murine double mutant 2 (*MDM2*) and metabolic effector TP53-induced glycolysis and apoptosis regulator (*TIGAR*). Sirtuins are further regulatory molecules that can act both as oncogenes and tumour suppressors and will be discussed later. Accumulating evidence highlights the association of miRNAs with oncogenes and tumour suppressors. Some cancer associated genes, such as *HIF1*, *MYC* and *TP53*, regulate both the expression and functions of some miRNAs and are regulated by miRNAs. Table 1-5 and Figure 1-2 summarize recent findings on miRNA-mediated regulation of oncogenes and tumour suppressors.

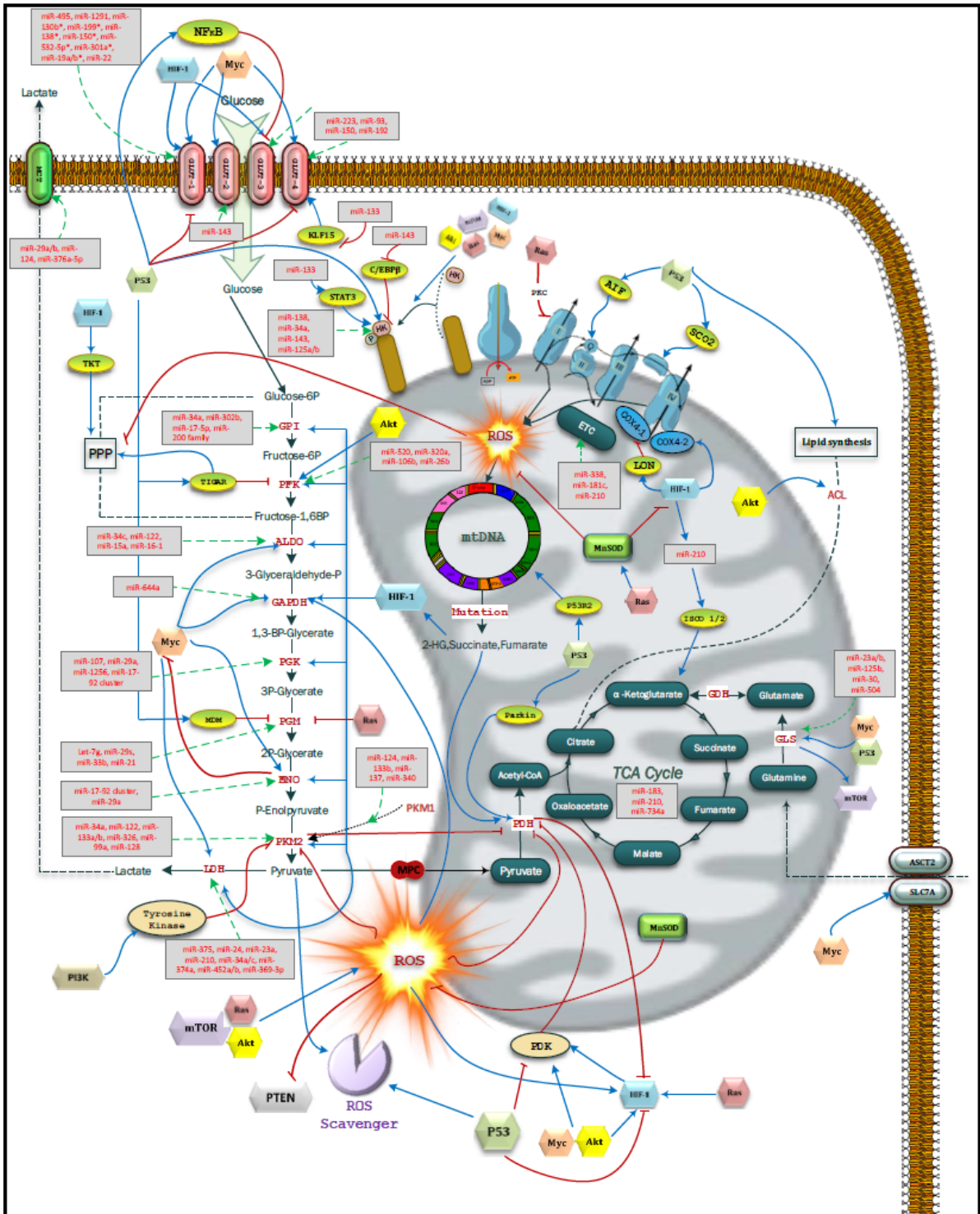


Figure 1-2. miRNAs targeting glycolytic and mitochondrial enzymes.

### 1.7.1 KRAS proto-oncogene

The *KRAS* oncogene features as an early mutation in up to 45% of colorectal tumours, notable because it can drive many hallmarks of cancer [240]. *KRAS*-mediated transformation is linked with mitochondrial respiratory dysfunction and elevated NADPH oxidase (NOX)-mediated ROS generation [241, 242]. Wang et al. [243] postulated that oncogenic KRAS influences complex I activity in the electron transport chain, most likely by downregulating complex I assembly factor protein (NDUFAF1) and, as a consequence, induces mitochondrial dysfunction. However, additional oncogenic signals and/or loss of tumour suppressors, including dysregulated miRNAs, are required for tumourigenesis.

Unsurprisingly, *KRAS* is a target of multiple miRNAs, including let-7, miR-96, miR-134 and miR-143 (Summarized in Table 1-5). These miRNAs affect cancer cell metabolism, cell cycle arrest, apoptosis, cell migration and invasion, especially by modulating RAS/MAPK signalling (Figure 1-2)

*KRAS* is frequently mutated in human neoplasia including pancreatic, colorectal and lung cancer. The oncogenic *KRAS*<sup>G12V</sup> variant, which leads to higher KRAS activity, was reported to be the most frequent mutation. However, despite low *KRAS* mutation frequency in glioblastoma and breast cancer cells, activation of the wild-type KRAS pathway is common in these cancers. Also, sequence variants in the *KRAS* 3'UTR (rs712) were found in gastric cancer, colorectal cancer, papillary thyroid cancer, breast cancer and non-small cell lung cancer, which disrupt let-7 binding site and subsequent miRNA-mediated downregulation [244-248].

The expression of some miRNAs such as let-7, miR-126, miR-200c, miR-193b and miR-4689 was found to be lower in *KRAS* mutant cells, as compared to tumours expressing wild-type *KRAS* [248-252], confirming the context dependent activity of miRNAs, even in regulating *KRAS* itself. Kopp et al. [249] reported that in breast cancer cells harbouring the *KRAS*<sup>G13D</sup> mutation, miR-200c targets *KRAS* transcripts and inhibits proliferation and cell cycle progression, while in *KRAS* wild type cells miR-200c affects proliferation through other targets. Despite different miR-126 expression levels in *KRAS* mutant and wild type colon cancer cells, Hara et al. [250] showed that over-expression of miR-126 does not alter *KRAS* expression and function. In contrast, Jiao et al. [253] showed *KRAS* regulation by miR-126 in pancreatic cancer. Such variations suggest that the activity of some miRNAs is subjected to changes through both transcriptional and post-transcriptional processes during tumourigenesis. Examples are erythropoietin-producing hepatoma receptor A1 (EphA1) upregulating let-7 in multiple myeloma [254], EVI1 suppressing

miR-96 in pancreatic ductal adenocarcinoma [255], KLF4 downregulating miR-134 in glioblastoma [256] and MYC associated factor X (MAX) inhibiting miR-193a in breast cancer [257]. Therefore, coordinated suppression of miRNAs, as is found in various cancers, would not only influence oncogenic *KRAS* activity but may also influence other genes involved in *KRAS*-related signalling to cooperatively initiate tumourigenesis, including genes in metabolic pathways.

### 1.7.2 MYC proto-oncogene

Overexpression of the *c-MYC* proto-oncoprotein plays pivotal roles in sustaining the transformed phenotype of most cancer cells [258]. The discovery that LDHA is among 20 putative targets of *c-MYC* provided evidence that *c-MYC* directly regulates glycolysis. Since then, other glycolytic genes including *GLUTs*, *GAPDH*, *PGK*, *HK2*, *ENO1*, *PGM*, *PKM2* and *MCTs* are also reportedly induced by *c-MYC* [259].

Along with its role in glycolysis, *c-MYC* was found to regulate mitochondrial biogenesis, respiration and function [260]. Upregulation of some nuclear genes that encode proteins for mitochondrial function, mitochondrial DNA replication and transcription of mitochondrial DNA are known to be direct consequences of *c-MYC* overexpression [261]. *c-MYC* also contributes to mitochondrial biogenesis and gives rise to the synthesis of acetyl-CoA and fatty acid biosynthesis required for cancer cell proliferation. In parallel, *c-MYC* upregulates the glutamine catabolism required for biosynthetic processes by inducing *GLS* and the glutamine transporters, *ASCT2* and *SLC7A25* [262, 263]. Overall, while *c-MYC* enhances glycolysis and consequently depletes pyruvate required for mitochondrial OXPHOS, it also confers the ability for cancer cells to utilize non-glucose substrates and maintain mitochondrial respiration to support cancer cell proliferation and progression.

*c-MYC* cooperates with HIF-1, or acts independently, to regulate glycolysis and OXPHOS [264]. In normal cells, MYC enhances glycolytic flux to OXPHOS. However, in cancer cells, *c-MYC* cooperates with HIF-1 and *PKM2* to upregulate glycolysis and provide adequate metabolic intermediates for biomass synthesis [265]. While upregulation of HIF-1-mediated glycolysis was observed under hypoxic conditions, *c-MYC* regulates glycolytic genes independently under normal oxygen tension. In addition, while HIF-1 upregulates *PDK1* under hypoxia, *c-MYC* cooperates with HIF-1 to further upregulate *PDK1* and, thus, amplifies the hypoxic response. Therefore, under normoxia, *c-MYC* enhances glycolysis but it cooperates with HIF-1 to upregulate *PDK1* and reduce mitochondrial respiration under hypoxic conditions [266]. Intriguingly, elevated *ENO1* was

shown to form a negative feedback loop with activated c-MYC. c-MYC-induced ENO1 increases the expression of MBP1, a transcription factor, and suppresses *c-MYC* expression [267].

c-MYC both regulates miRNA expression and is, in turn, controlled by them (Table 1-3 and Table 1-5). Several miRNAs have been shown to modulate *c-MYC* expression by different mechanisms (Figure 1-2). Let-7a, miR-22, miR-33b, miR-34a, miR-130a, miR-145 and miR-155 were found to suppress *c-MYC* after binding with canonical target sequences in the *c-MYC* 3'UTR [268-275]. miR-24 binds to a seedless, but highly complementary, sequence while miR-18-5p and miR-774 bind to the protein coding region of *c-MYC* mRNA [270, 276, 277]. Some other miRNAs, such as miR-363-3p act more indirectly. In HCC, miR-363-3p destabilizes c-MYC through targeting USP28, a ubiquitin protease of MYC, and promoting the degradation of pre-existing c-MYC protein [278]. Several reports indicate a coordinated and reciprocal relationship between c-MYC and miRNA expression levels. For instance, Liao et al. [277] showed a negative feedback and auto-regulatory role for c-MYC levels, as monitored by miR-185-3p. They confirmed that miR-185-3p is a genuine transcriptional target of c-MYC but also that miR-185-3p inhibits *c-MYC* translation by targeting the coding region of *c-MYC* transcripts.

c-MYC activates or represses a variety of genes, including miRNA genes, mainly through interactions with different complexes and proteins. c-MYC suppresses *MIR122* gene transcription in liver tumours through association with a conserved promoter region upstream of the *MIR122* gene. It also downregulates hepatocyte nuclear factor 3-beta (HNF3 $\beta$ ), which normally activates miR-122 and enhances its stability [279, 280].

miR-122 was reported to suppress *c-MYC* expression indirectly by targeting *E2F1* and *TFDP2* (E2F dimerization partner 2) mRNA [281]. In addition, feedback regulation was reported for miR-17-5p/c-MYC/E2F in some cancers, including breast and prostate [282]. Nadiminty et al. [283] reported a LIN28/let-7/c-MYC loop that plays an important role in some cancers. Relief of c-MYC repression occurs when LIN28, a highly conserved RNA-binding factor, binds let-7 precursors and inhibits miRNA maturation [284]. There is a direct relationship between c-MYC, its dimerization partner, MAX, and the expression of some miRNAs such as let-7a and miR-22 [274, 285]. c-MYC can also transcriptionally activate some miRNAs, including the miR-17-92 cluster, through interaction with MAX protein at the polycistronic promoter region [282, 286]. Ting et al. [274] showed that increased miR-22 limits the amount of MAX protein available for c-MYC binding by directly targeting it and, therefore, affects the expression of downstream targets of the c-MYC/MAX complex. In contrast, interaction of c-MYC with MIZ-1 represses expression of some c-MYC target genes through displacement of p300 co-activator protein [287]. There is

also a miRNA/c-MYC negative feedback loop in HCC with miR-148a-5p directly targeting *c-MYC* and, as previously mentioned, miR-363-3p indirectly destabilizing c-MYC by targeting ubiquitin specific peptidase 28 (USP28) [278]. Other miRNAs that are repressed transcriptionally and post-transcriptionally by c-MYC are summarized in Table 1-3.

The activation of c-MYC alone is unable to transform cells. Therefore, there is cooperation between oncogenic partners, such as RAS, and inactivation of tumour suppressors such as p53 in c-MYC dependent tumour development [288-290]. Hence, along with passive adaptation of tumour cells, oncogenic mutations and transcriptional controls, such as the reciprocal association of c-MYC with several miRNAs, enhance the ability of cancer cells to consume non-glucose substrates and fuel mitochondria. This may explain the inefficiency of drugs which only target glycolysis and add another layer of complexity to therapeutic strategies.

**Table 1-3. Summary of miRNAs regulated by the transcription factor MYC.**

miRNA	Regulation	Disease/cells	References
miR-2b	Upregulation	Drosophila S2 Cells	[291]
miR-277	Upregulation	Drosophila S2 Cells	[291]
miR-92	Upregulation	Neuroblastoma, Burkitt Lymphoma	[282, 292]
miR-106a	Upregulation	Neuroblastoma, Burkitt Lymphoma	[282, 292]
Let-7a/c	Up/Downregulation	Neuroblastoma, Burkitt Lymphoma, Breast Cancer, Prostate cancer	[283, 284, 292, 293]
miR-17	Upregulation	Neuroblastoma, Burkitt Lymphoma	[282, 292]
miR-93	Upregulation	Neuroblastoma	[292]
miR-99	Upregulation	Neuroblastoma	[292]
miR-221	Upregulation	Neuroblastoma	[292]
miR-18	Upregulation	Burkitt Lymphoma	[282]
miR-19	Upregulation	Burkitt Lymphoma	[282]
miR-20	Upregulation	Burkitt Lymphoma	[282]
miR-15a	Downregulation	Lymphoma	[294]
miR-16	Downregulation	Lymphoma	[294]
miR-22	Downregulation	Lymphoma	[294]
miR-23a/b	Downregulation	Lymphoma, Prostate Cancer	[156]
miR-26a/b	Downregulation	Lymphoma, Burkitt Lymphoma, Prostate Cancer	[294-296]
miR-29	Downregulation	Lymphoma, lung Adenocarcinoma	[294, 297]
miR-34	Downregulation	Lymphoma	[294]
miR-146a	Downregulation	Lymphoma	[294]
miR-150	Downregulation	Lymphoma	[294]
miR-195	Downregulation	Lymphoma	[294]
miR-141	Upregulation	Embryonic Stem Cells, Nasopharyngeal Carcinoma	[298, 299]
miR-200	Upregulation	Embryonic Stem Cells	[298]

<b>miR-429</b>	Upregulation	Embryonic Stem Cells	[298]
<b>miR-9</b>	Upregulation	Breast Cancer	[300, 301]
<b>miR-185</b>	Upregulation	Non-small Cell Lung Cancer	[277]
<b>miR-122</b>	Downregulation	Hepatocellular Carcinoma	[279-281]

### 1.7.3 PI3K / AKT pathway

The PI3K intracellular signalling pathway plays a critical role in cell apoptosis, proliferation and protein synthesis. Its role in regulation of glucose uptake and metabolism is equally definitive. PI3K dysregulation was reported in several human cancers and several drugs targeting this pathway are currently in clinical trials [302]. Activation of PI3K leads to an upregulation of downstream effectors such as AKT and mTOR.

The evolutionarily conserved serine/threonine kinase, AKT, was reported to be one of the most prevalent and constitutively activated onco-proteins in malignant cells [303, 304]. AKT is an important activity-dependent stimulus for cancer cell metabolism, influencing glycolysis by both direct and indirect mechanisms. AKT plays a central role in the regulation of cellular energy metabolism and glucose homeostasis. It stimulates ATP generation by accelerating both glycolytic and oxidative metabolism with a concomitant increase in oxygen consumption to preserve energy. AKT activation results in ROS generation and, therefore, contributes to tumourigenesis by inducing mutations and facilitating tumour-promoting signalling pathways and inducing mutations [305]. Elevated, AKT-mediated, glycolysis plays a major role in proliferation and survival of transformed cells. AKT increases glucose uptake, directly, by increasing the expression and plasma membrane translocation of glucose transporters (GLUT1, GLUT2, and GLUT4) [306]. It also maintains MMP and promotes the association of HK2 with the mitochondrial outer membrane by mediating HK2 phosphorylation and inhibiting glucose-6 phosphate dissociation from the mitochondrial membrane [307]. This may enhance enzymatic efficiency of the kinase, promote metabolic coupling between glycolysis and OXPHOS, increase ATP synthesis through OXPHOS and decrease susceptibility to apoptosis [305]. Indirectly, AKT activates PFK1 phosphorylation and activation by inducing PFK2 and releases forkhead box O1 (FOXO)-mediated repression of glycolysis. AKT also activates mTORC1 indirectly through phosphorylating and, thus, inactivating TSC2, an mTOR inhibitor [308-310]. The ability of AKT to increase glucose uptake and glycolysis in tumour cells may also require cooperation from other cancer-associated proteins, such as c-MYC and HIF-1. Although AKT-transformed cells show elevated levels of amino acid and lipid transporters that are linked to cell growth, constitutive activation of AKT renders cells dependent

on an extracellular glucose supply for survival [305]. Together these findings demonstrate the coordinated regulation of glycolysis and OXPHOS by oncogenic AKT.

AKT, which is described as “Warburg’s kinase”, provides selective advantages to tumour cells by increasing both glycolysis and OXPHOS [311]. Several miRNAs were reported to modulate *AKT* expression directly by targeting *AKT* mRNA, and protein phosphorylation and/or indirectly regulating its upstream stimuli, such as EGFR and its upstream repressors, such as PTEN (Figure 1-2).

While some miRNAs, such as miR-637 in glioma, miR-302a and miR-29b in prostate cancer and miR-143 in bladder cancer, directly bind the *AKT* 3’UTR and inhibit its translation, some other miRNAs, reduce AKT phosphorylation without affecting total AKT levels. For instance, miR-126 reduces AKT phosphorylation by inhibiting by phosphatidylinositol 3-kinase regulatory subunit beta (p85 $\beta$ ) [312-316] (Table 1-5).

Other proteins and regulatory factors also contribute to regulating AKT activation in different cell types and conditions. For instance, the over-expression of Rictor, a target of miR-34a and mTORC2 component, causes activation of AKT in glioma stem cells [317]. Rictor activation results in mTORC2 activation and consequently, AKT is further activated by mTORC2 mediated phosphorylation [318]. In breast cancer cells miR-205, which is often downregulated in cancer, targets *HER3* receptor transcripts and suppresses the activation of AKT [319]. Protein phosphatase 2 scaffold subunit A $\beta$  (PPP2R1B) is another intermediate in AKT signal transduction, directly interacting with AKT, and is a target of miR-200c in esophageal cancer cells [320]. Al-Khalaf and Aboussekhra [321] showed that miR-141 and miR-146b-5p target an RNA binding protein, AUF1, which has an important role in PI3K/AKT/mTOR pathway regulation. AUF1 binds to and stabilizes *PDK1* mRNA and promotes AKT phosphorylation and activation. AUF1 was also reported to negatively regulate PTEN phosphatase and activate PI3K [322, 323]. Additionally, some *AKT*-targeting miRNAs were shown to regulate drug sensitivity in cancer cells, such as miR-29b and miR-200c that influence chemotherapy responses in prostate and esophageal cancers, respectively [314, 320].

However, the miRNAs that regulate AKT signalling do not act to fully repress AKT and its mediators. Rather, they fine tune expression in a context-specific manner. Therefore, it is likely that *AKT* is not exclusively regulated by specific miRNAs and further, it is not surprising that some miRNAs, such as miR-153 which targets both *PTEN* and *AKT* [324, 325], play complex pleiotropic roles in regulating PI3K/AKT signalling.

Although a number of studies have reported *EGFR* gene amplification in some cancers, post-transcriptional modulation remains a significant cause of *EGFR* overexpression in cancer cells (Table 1-5). For instance, miR-7 was found to regulate expression of multiple effectors of the *EGFR* signalling pathway, as well as directly targeting *EGFR* mRNA. Zhou and Hu et al. [326] showed that miR-7 overexpression in epithelial ovarian carcinoma (EOC) cells results in reduced expression of *EGFR* without any changes in *EGFR* phosphorylation. A feedback loop between miR-7 and *EGFR* was reported [326, 327], as increased *EGFR* activity results in extracellular-signal-regulated kinase (ERK)-mediated degradation of *YAN*, which is a miR-7 repressor. Further, miR-7 binds to the *YAN* 3'UTR and represses its expression [328].

*PTEN* has a central role in cell cycle progression. Although mutational loss of *PTEN* was reported in some cancers, epigenetic factors, including miRNAs, also regulate *PTEN* expression [329] (Table 1-5). Due to the unusually long 3'UTR of *PTEN*, it contains binding sites for many miRNAs, which can reduce its mRNA levels (including miR-32, miR-29, miR-26a/b, miR-217, miR-486, miR-193a, miR-519d) [330-338] or *PTEN* translation without affecting its mRNA levels (miR-93, miR-214, miR-221, miR-494, miR-21) [339-345].

Furthermore, miR-185 in HCC and miR-26a in low-grade glioma alter *PTEN* promoter methylation and play a subordinate role in *PTEN* gene regulation by targeting DNA (cytosine-5)-methyltransferase 1 (*DNMT1*) and enhancer of zeste homolog 2 histone methyltransferase (*EZH2*) [331, 346]. Therefore, along with direct regulation of *PTEN* by the aforementioned miRNAs, several miRNAs regulate *PTEN* through indirect mechanisms. Examples include *PTEN* repression via miR-101 and miR-1 both targeting the *PTEN* activator, membrane-associated guanylate kinase inverted 2 (*MAGI-2*); as well as *PTEN* induction following the miR-185 targeting of *PTEN* silencer, *DNMT1* [346-348].

High glucose was shown to affect some *PTEN* targeting miRNAs, such as stimulating miR-21 levels in renal cancer or lowering miR-32 levels in HCC, depending on the physiological status of the cells, which results in *AKT* activation or suppression, respectively [349, 350].

*PTEN* dephosphorylates *PIP3*, generated by *PI3K*, to inhibit *AKT* activation. Suppression of *PTEN*, through miRNA-mediated mechanisms, enhances *AKT* phosphorylation and signalling and supports cell proliferation and survival [351]. *PTEN* inhibition also results in cystic vestibular schwannoma development and cancer cell invasion via induced metalloproteinase-2 (*MMP-2*) [352]. Transforming growth factor beta 1 (*TGF-β*) mediated *AKT* activation is another consequence of reduced *PTEN* activity [338, 353]. Decreased *PTEN* expression was also shown

to impair p53-dependent responses in cancer cells [335]. Moreover, some miRNAs were shown to induce drug- and radio-resistance by inhibiting *PTEN*. For instance, miR-21 induces daunorubicin resistance in leukemia, miR-214 induces cisplatin resistance in ovarian cancer cells and miR-221 induces TRAIL- and radio-resistance in glioma cells by inhibiting *PTEN* [337, 342, 354]. Breast cancer metastases in the brain also display increased aggression due to suppression of *PTEN* by astrocyte exosomal miRNAs [355].

#### 1.7.4 Mechanistic Target of Rapamycin Kinase (mTOR)

Mechanistic target of rapamycin (mTOR), also known as mammalian target of rapamycin, consists of two divergent complexes: complex 1 (mTORC1) and (mTORC2). mTORC1 acts as a metabolic hub, integrating extracellular stimuli with nutrient availability and cellular energy to coordinate responses. mTORC1 is mainly involved in cellular proliferation, translation and metabolic programming while mTORC2 regulates cell survival, cytoskeletal organization and degradation of newly synthesized polypeptides [356, 357].

mTOR is stimulated by loss of function of some inhibitors including LKB1, PML, *PTEN*, and *TSC1/2* or activation of some oncogenes such as *AKT* and *RAS* [164, 165, 311, 358]. Activated mTOR, in turn, dramatically enhances the translational machinery and ribosome biogenesis, increases cell growth in response to mitogens, growth factors and hormones, and upregulates some transcription factors [359]. It also activates several glycolytic enzymes such as *GLUT1*, *LDHA*, *PKM2* and *HK2* [360-362]. The connection between hypoxia and mTOR is of particular interest. Although it has been shown that mTOR is able to induce *HIF-1* translation, mTOR activity is reduced in hypoxia, likely through negative feedback [363, 364]. Hypoxia-mediated inhibition of mTOR could be through activation of tuberous sclerosis protein (*TSC1/2*) via *AMPK*, *REDD1* or *BNIP3* activation [166, 358, 365, 366]. However, there is also evidence that hypoxia-mediated inhibition of mTOR is more prevalent in normal cells compared with cancer cells [367]. Therefore, it may be concluded that mutations in the mTOR signalling pathway account for the reduced hypoxia-mediated mTOR inhibition. It was discovered that mTOR, along with p53, spares the available serine for glutathione synthesis by stimulation of *PKM2* protein synthesis, which links glycolysis to anabolic pathways [368]. Moreover, mTOR suppresses autophagy and mitophagy and, therefore, produces ROS. AMP-activated protein kinase (*AMPK*), an mTOR inhibitor, plays a vital role in metabolic flux and regulates *GLUT4* expression, mitochondrial biogenesis and fatty acid oxidation. Complex interaction between mTOR, *AKT* and *AMPK* to regulate *GLUT4* translation has also been shown [369]. Activated *AKT* phosphorylates and inhibits AS160 Rab GTPase activating protein in the cytoplasm leading to increased translocation of the insulin-

responsive glucose transporter, GLUT4 to the membrane [370]. Also, ADP and ATP play a critical role in the stability of AKT phosphorylation at residues T308 and S473 and, therefore, act as on/off switches as ATP binds to these phosphorylated sites and protects them against phosphatases. Consequently, AMPK regulates AKT phosphorylation by responding to the equilibrium of the adenylate pool [369, 371]. On the other hand, Kumar et al., [372] reported that *FRic<sup>-/-</sup>* murine fat cells, with ablated Rictor, showed impaired insulin-stimulated GLUT4 translocation to the plasma membrane and decreased glucose transport.

Given the integral role that mTOR plays in oxygen and nutrient sensing it is notable that several miRNAs may directly or indirectly influence mTOR activity. Increased expression of MTOR coexists with downregulation of several miRNAs in various types of cancer (Table 1-5 and Figure 1-2). Examples include miR-99a/b, miR-100 and miR-199b in cancers, including endometrial cancer, esophageal squamous cell carcinoma and bladder cancer [373-376]. miR-99 and miR-100 were also reported to be endogenous inhibitors of mTOR protein abundance [377]. miR-7 was found to target *MTOR* directly and form a negative feedback loop by also directly repressing EGFR and thus results in pleiotropic inhibition of protein translation [378, 379]. Chen et al. and Lin and Shao et al. [380, 381] reported a significant inhibition of mTOR expression, at both RNA and protein levels, by miR-101. Also, miR-373 and miR-520c were reported to reduce *MTOR* mRNA and protein levels and increase MMP9, which consequently results in the increased migration and invasion capability of cancer cells [382]. A negative regulator of mTOR is TSC1/2 complex. miR-451 was found to target TSC1 and stimulate the stemness phenotype of myeloma cells through activation of the PI3K/AKT/mTOR pathway [383, 384]. These findings further highlight the role of mTOR, situated at the crossroads of cancer-related signalling pathways. They show the interplay between components of signalling cascades and miRNAs, with practical implications for cancer therapy.

### 1.7.5 Tumour Protein p53 (TP53)

p53 is a transcription factor and tumour suppressor that plays critical roles in controlling cell cycle progression through DNA damage response and apoptosis, which has been shown to regulate both glycolysis and OXPHOS [239]. In general, p53 inhibits glycolysis transcriptionally by suppressing *GLUT1*, *GLUT3*, and *PGM* expression. Therefore, loss of p53 function in many cancers contributes to either glycolysis or the pentose phosphate pathway (PPP) [204, 385]. Mutated p53 was shown to reduce oxygen consumption and mitochondrial respiration. First, diminished p53 activity reduces OXPHOS by eliminating its suppression of SCO2, a protein essential for COX assembly and mitochondrial respiration [386]. Moreover, p53 may affect

mtDNA by regulating the expression of ribonucleotide reductase subunit p53R2 and, ultimately, regulating mitochondrial oxidative respiration [387]. P53R2 plays important roles in both the biogenesis of mitochondria and mtDNA maintenance [388]. Although p53 induces oxidative stress by its pro-apoptotic function, it can also adversely impact redox maintenance [389]. Anti-oxidant roles of p53 include upregulation of GLS2 and subsequent increase in glutathione as well as enhanced stability of NRF2, an important antioxidant transcription factor, under oxidative stress [390, 391]. Other p53 functions that regulate metabolism include induced *PTEN* expression, which inhibits the PI3K pathway and glycolysis, cooperation with the OCT1 transcription factor to modulate the balance between glycolysis and OXPHOS and reduced fatty acid oxidation in response to metabolic flux [392-394].

The identification of several miRNAs that target p53 implies complex regulation and may explain the development of malignancies in cells with wild-type p53, where miRNA-mediated repression of *TP53* and its transactivational genes, such as *CDKN1A*, *BBC3*, *DNM1L* and *BAX*, is sufficient to cause tumourigenesis [395, 396]. p53 both regulates, and is regulated by, miRNAs. Many of these miRNAs were shown to directly target *TP53* in different systems (summarized in Table 1-5). It is becoming clear that most of these miRNAs represent conservative regulation of p53 activity, targeting multiple components of the p53 pathway. Also, the functional overlap between these miRNAs indicates the potential for cumulative miRNA dysregulation influencing the p53 network during tumourigenesis. p53 suppresses glucose transporters and glycolytic enzymes by enhancing TIGAR [397]. TIGAR is best characterised by its negative regulation of fructose-2, 6-bisphosphatase. Eventually, TIGAR directs glucose to PPP and enhances NADPH production [398]. miR-144 targets TIGAR and modulates autophagy, apoptosis and metastasis in lung cancer cells [399]. In order to survive, cancer cells can also render p53 inactive by point mutation or through degradation induced by the E3 ubiquitin ligase, (MDM2) [400, 401]. Aside from gene mutations, promoter (de)methylation and proteolytic degradation, *MDM2* is regulated by miRNAs. miRNAs such as miR-605 and miR-660 directly target *MDM2* and modulate MDM:p53 interaction, aiding rapid stabilization and accumulation of p53. On the other hand, p53 transactivates the expression of the miR-605 host gene *PRKG1* through binding to its promoter region, which results in a positive feedback loop and increased p53 activity [402, 403]. Other miRNAs that suppress *MDM2* include miR-509-5p in HCC and cervical cancer, miR-29b in non-small cell lung cancer (NSCLC), miR-143/145 in head and neck squamous cell carcinoma (HNSCC), miR-192, miR-215, miR-194 and miR-339-5p in renal cell adenocarcinoma, breast cancer and colorectal cancer [404-407] (Figure 1-2).

## CHAPTER 1

In addition to the aforementioned functions of p53 in regulating cell metabolism, miRNA biosynthesis also involves p53-signalling components. p53 interacts with the Drosha complex and accelerates the processing of targeted primary miRNA sequences to precursor miRNA fragments [408]. Specific miRNAs are also transcriptionally regulated by p53 [404, 409, 410] (Table 1-4). Most of these p53-responsive miRNAs are involved in both positive and negative feedback loops. For instance, members of the miR-34 family are induced through p53 binding to their promoter in response to stress and, in turn, *TP53* mRNA has been validated as a direct target of miR-34 [411, 412]. miR-605 and miR-509-5p/MDM2/p53 are examples of positive feedback loops where p53 induces miRNA synthesis and miR-509-5p and miR-605 target *MDM2* to increase p53 protein levels [402, 404]. miR-17-5p/TP53INP1/p53 is another regulatory feedback loop. miR-17-5p targets TP53INP1 mRNA transcript which encodes a p53-induced nuclear protein and also is a direct target of p53; so, miR-17-5p functions as a mediator in a regulatory loop in colon and cervical cancer[410]. Other miRNAs that target tumour protein P53 inducible nuclear protein 1 (*TP53INP1*) include miR-130b in hepatocarcinoma, miR-155 in pancreatic cells and miR-125b in endometrial carcinoma [413-415]. Therefore, both regulation of the p53 network by miRNAs, and p53 induction of miRNA levels, are tightly coordinated to enable response to stimuli.

These findings show that the p53 network is more complex than previously envisioned and suggest that additional regulatory layers, incorporating miRNAs, provide derepression of *TP53* enabling it to accumulate rapidly in response to cell stress. The aforementioned functions establish a new driver of the Warburg effect and demonstrate that p53 may act as a "brake" on glycolysis and neoplastic cell proliferation.

**Table 1-4. Summary of miRNAs regulated by the transcription factor p53.**

miRNA	Regulation	Disease/cells	References
<b>Let-7a/b</b>	Downregulation	Colorectal Cancer	[416]
<b>miR-17</b>	Downregulation	Colorectal Cancer	[182]
<b>miR-20a</b>	Downregulation	Colorectal Cancer	[182]
<b>miR-29</b>	Upregulation	Colorectal Cancer	[417]
<b>miR-200c</b>	Upregulation	Mammary Gland, Colorectal Cancer	[418, 419]
<b>miR-183</b>	Upregulation	Mammary Gland	[418]
<b>miR-34a/b/c</b>	Upregulation	Colorectal Cancer, Non-Small Cell Lung Cancers, Ovary Clear Cell Carcinoma, Osteosarcoma, Pancreatic Cancer, Prostate Cancer, Ovarian Carcinoma	[411, 420-424]
<b>miR-605</b>	Upregulation	Breast Cancer, Lung Carcinoma	[425]
<b>miR-145</b>	Upregulation	Breas Cancer, Colorectal Cancer	[290]

## CHAPTER 1

<b>miR-192</b>	Upregulation	Colorectal Cancer, Multiple Myeloma, Ovary Clear Cell Carcinoma, Osteosarcoma	[407, 419, 421, 426]
<b>miR-194</b>	Upregulation	Multiple Myeloma, Colorectal Cancer	[407, 426]
<b>miR-215</b>	Upregulation	Colorectal Cancer, Multiple Myeloma, Ovary Clear Cell Carcinoma, Osteosarcoma	[407, 419, 421, 426]
<b>miR-141</b>	Upregulation	Colorectal Cancer	[419]
<b>miR-519d</b>	Upregulation	Hepatocellular Carcinoma	[335]
<b>miR-107</b>	Upregulation	Colorectal Cancer	[200, 427]
<b>miR-509</b>	Upregulation	Cervical Cancer, Hepatocellular Carcinoma	[404]

### 1.7.6 Sirtuins

Sirtuins are a conserved family of NAD<sup>+</sup>-dependent deacetylases. Advances in sirtuin biology have identified multiple targets for the seven mammalian sirtuins (SIRT1-7) and, recently, their participation in tumorigenesis and regulation of cancer cell metabolism [428].

SIRT1 is a nuclear protein that shuttles between the nucleus and cytoplasm, especially when insulin signalling is inhibited [429]. SIRT1 modulates several cellular pathways by deacetylating a subset of nuclear and cytosolic targets. AMPK and SIRT1 cooperate in the induction of gluconeogenesis, glycolysis and lipid catabolism, mitochondrial biogenesis and respiration by phosphorylation and then deacetylation of PPARgamma coactivator 1alpha (PGC1 $\alpha$ ) and FOXO transcription factors [430-433]. A homeostatic and negative feedback loop has been reported among SIRT1, p53, FOXO3A and FOXO1. During energy stress FOXO3A binds to p53 promoter, repressing SIRT1 expression, and in turn SIRT1 inhibits p53 activity by excessive deacetylation and also through FOXO3A activation [434-436]. In addition, SIRT1 is involved in the oxidative response, working together with HIF-1, p53 and Myc [437].

SIRT6 is another member of the sirtuin nuclear histone deacetylase (HDAC) family, which exerts both nuclear ADP-ribosyltransferase activity and deacetyltransferase activity with roles in epigenetic regulation of genomic stability, cellular metabolism, stress response, aging and cancer [438-441]. Yin and Gao et al. [442] showed that neuronal SIRT6 overexpression significantly suppresses insulin-like factor 2 (IGF2) activity and other proteins such as AKT and mTOR at the chromatin level. SIRT6 activation results in inhibition of HIF-1, glycolysis and respiration, as well as induction of homologous and non-homologous DNA repair. The latter function of SIRT6 occurs through ADP-ribosylation of poly(ADP-Ribose) polymerase 1 (PARP-1) [443, 444]. SIRT6 regulates *HIF-1* and *c-Myc* expression, at the transcriptional level, through chromatin deacetylation

and also regulates HIF-1 stability through an unknown mechanism [445]. Mostoslavsky et al. [446] reported a novel role for SIRT6 in glucose homeostasis in mice. Accordingly, subsequent studies confirmed its vital role in direct and indirect regulation of glucose uptake and metabolism. Nevertheless, SIRT6 was found to transcriptionally regulate some c-Myc targets involved in ribosomal biogenesis and glutamine utilization, rather than those involved in regulating cancer cell glycolysis [447]. In contrast to SIRT6 that acts independently, SIRT1 cooperates with c-Myc to suppress p53 activity and increase c-Myc- induced *LDHA* expression [445]. SIRT7 is a nucleolar sirtuin member that activates transcription by binding to RNA polymerase [448, 449]. Vakhrusheva et al. [450] reported a p53 hyperacetylation state in SIRT7 knockout mice, which results in increased apoptosis and decreased resistance to oxidative stress.

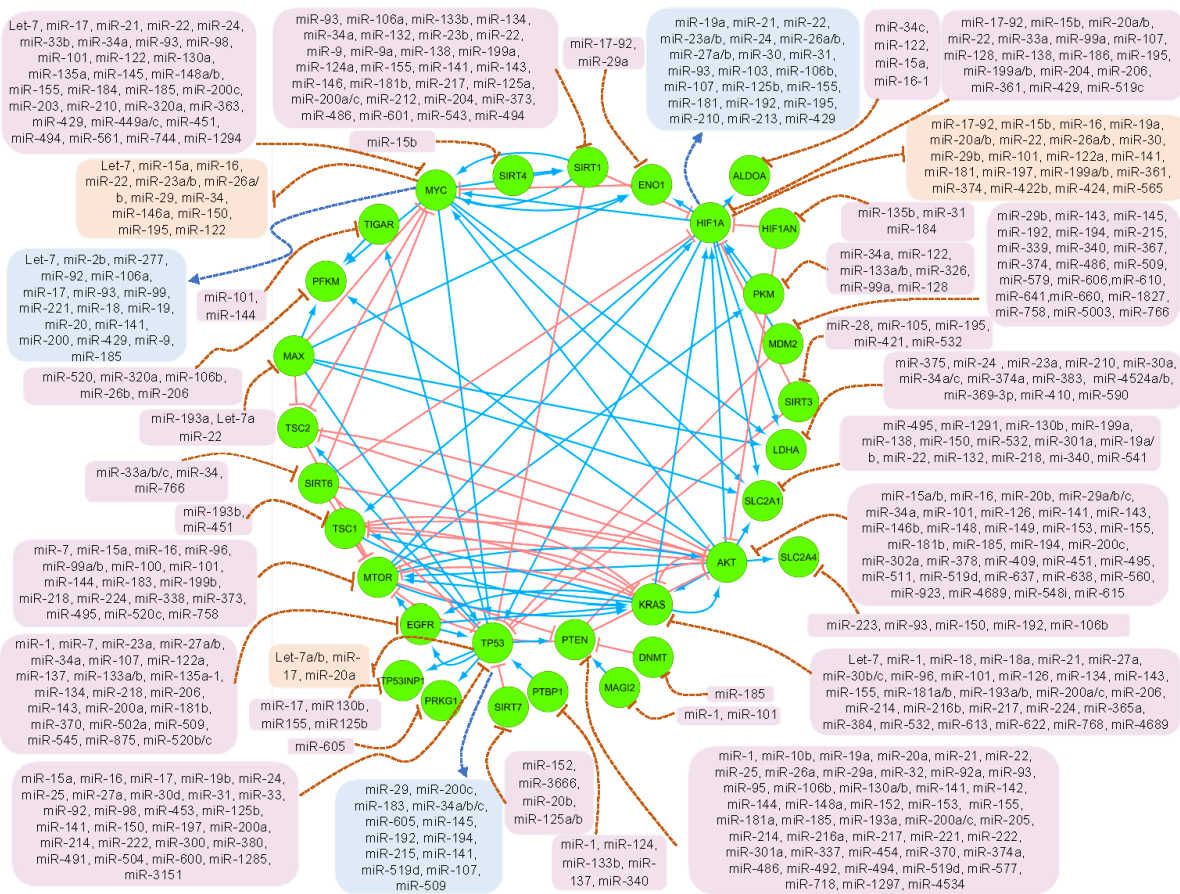


**Figure 1-3. Interconnections between the glycolytic drivers and suppressors and the role of miRNAs in these networks.**

Protein-protein interactions identified using String V10.0. Interconnections between the drivers and suppressors of glycolysis, and the role of miRNAs in these networks. Protein-protein interactions identified using String V10.0. Solid blue lines indicate protein activation while solid red lines indicate protein inhibition. Dotted blue and red lines represent transcription factor-mediated activation or inhibition of the miRNAs, respectively. miRNAs in pink boxes repress gene expression, while those in orange and blue boxes indicate miRNAs that are inhibited or activated

by the transcription factors, respectively. Specific miRNAs present in both the pink boxes and either the orange or blue boxes, may represent feedback loops in particular cellular contexts.

The miRNA-mediated regulation of nuclear sirtuins, with an emphasis on SIRT1 and SIRT6, has highlighted their roles in glycolysis. SIRT1 has been the most extensively studied member in this context. miR-34a was the first discovered *SIRT1* targeting miRNA. miR-34 is a p53-related miRNA that most importantly regulates cell cycle. miR-34 downregulates *SIRT1* expression by directly binding to its 3'UTR and indirectly through targeting nicotinamide phosphoribosyltransferase (NAMPT), the rate limiting enzyme in NAD<sup>+</sup> biosynthesis [451-453]. Xu et al. [454] reported *SIRT1* targeting by miR-22, which modulates the retinoblastoma signalling pathway. miR-204 targets *SIRT1* in osteocarcinoma cells and inhibits epithelial-mesenchymal transition (EMT) of the cancer cells [455]. Similarly, miR-200c has been reported to form a negative feedback loop with SIRT1, attenuating epithelial to mesenchymal transition (EMT) in breast cancer cells [456]. Likewise, miR-181a and miR-9 regulate *SIRT1* and impact insulin signalling, glucose homeostasis and cell apoptosis [457-459]. miR-143, miR-93 and miR-217 lead to decreased glucose uptake, downregulated microsomal glutathione S-transferase 1 and inhibited angiogenesis, respectively, by targeting *SIRT1* [460-462]. Several other miRNAs that modulate *SIRT1* expression and activation include miR-9, miR-34c, miR-132, miR-135, miR-146, miR-181b, miR-195, miR-199 and miR-499 [463-467] (Figure 1-2).

Post-transcriptional regulation of *SIRT6* by miR-33a/b plays a vital role in regulation of cholesterol and lipid metabolism via acetylation of its targets [442, 468-470]. Sharma et al. [471] reported a negative feedback loop between SIRT6 and miR-766 in dermal fibroblasts. *SIRT7* expression is elevated in highly metabolic and proliferative cells and was reported to be a target of miR-125a/b inducing G1 cell cycle arrest [472].

SIRT2 is predominantly cytosolic but it also shuttles to the nucleus and is mainly enriched in the brain [473]. SIRT2 was reported to deacetylate histone H3, p300, FOXO1, FOXO3A, adenomatous polyposis coli (APC), cell division cycle 20 (CDC20), p65, PGM, phosphoenolpyruvate carboxykinase 2 (PEPCK) and receptor-interacting protein 1 (RIP1) and, therefore, regulates cell cycle, genome integrity, energy homeostasis, gluconeogenesis, glycolysis, oxidative stress modulation, cell growth and death [474-480]. miR-339 was shown to target SIRT2, increasing NF- $\kappa$ B and FOXO1 acetylation in neuroblastoma cells [481]. Moreover, *in silico* analysis revealed a longevity associated SNP of *SIRT2* within the binding site of three miRNAs (called miRSNPs). Therefore, miR-3170, miR-92a-1-5p and, more importantly, miR-615-5p were

predicted to target *SIRT2* resulting in reduction in *SIRT2* expression [482]. Li and Dai et al. [333] showed that *SIRT2* is downregulated in glioma. *SIRT2* acts as a tumour suppressor and inhibits glioma growth by targeting miR-21 expression through deacetylating p65 and blocking p65 binding to the miR-21 promoter. Regulation of miR-21 activity is particularly important as this miRNA displays significant oncogenic activity [483].

Three mitochondrial sirtuins are *SIRT3*, *SIRT4* and *SIRT5*. *SIRT3* is the major mitochondrial sirtuin, which promotes ATP production by regulating TCA cycle enzymes such as acetyl COA synthetase, IDH2, glutamate dehydrogenase 1 (GDH) and SDH during energy stress. GDH upregulation leads to an induction in glutamine metabolism which consequently produces more ATP and releases insulin [484-487]. It also upregulates Mn superoxide dismutase (MnSOD), downregulates ROS, HIF-1 and p53 and activates FOXO3A to modulate redox homeostasis and maintain mitochondrial membrane potential [488-492]. *SIRT3*-mediated regulation of OXPHOS components has been shown. The targets include components of complex I, II, III and V such as NDUFA11/S8, SDHA/B and ATP5A1/B1/F1 [488, 493, 494]. Altogether, *SIRT3* is capable of reversing the Warburg effect toward mitochondrial predominance and ATP synthesis. *SIRT4* is another mitochondrial sirtuin which seems to function as a tumour suppressor by downregulating GDH through ADP-ribosylation activity and consequently suppressing glutamine utilization and the flow of amino acids into the TCA cycle [484]. Nasrin et al. [495] showed that reduced *SIRT4* results in increased fatty acid oxidation and mitochondrial metabolism. They also demonstrated an increase in *SIRT1* expression levels. miR-193 mediated suppression of *SIRT3* leads to impaired energy metabolism and ATP synthesis in myocardium [496]. miR-23a was also shown to target *PGC1* and thereby indirectly modulate *SIRT3* expression [497]. Moreover, upregulation of miR-28-5p, resulting from oxidative stress, directly targets *SIRT3* [498]. Liang et al. [499] reported SNPs in the miR-105 and miR-532 binding sites in the *SIRT3* 3'UTR that are associated with ovarian cancer treatment responses. In addition, Slaby et al. [500] reported three miRNAs that are regulated by natural agents called isothiocyanates in colorectal cancer (CRC) cells. *In silico* analysis also revealed CRC-related SNPs within the 3'UTR of genes, including *SIRT5*, may influence binding of these isothiocyanate-regulated miRNAs.

Collectively, SIRT's play important roles in a wide range of metabolic pathways and interact with many transcriptional regulators. miRNAs targeting SIRT's (summarized in Table 1-5) may modulate SIRT-related signal transduction and downstream effectors, providing insight into novel therapeutic strategies.

## CHAPTER 1

**Table 1-5. Summary of miRNAs targeting metabolism-related oncogenes and tumour suppressors.**

miRNAs	Gene	Disease	Reference
Let-7	<i>KRAS, MYC</i>	Breast Cancer, Colorectal Cancer, Lung Cancer, Glioma, Malignant Mesothelioma, Oropharyngeal Squamous Cell Carcinoma, Pancreatic Ductal Adenocarcinoma, Gastric Cancer, Prostate Cancer, Burkitt Lymphoma, Malignant Bronchial Epithelial Cell, Pulmonary Hypertension	[248, 254, 273, 283, 285, 501-508]
miR-1	<i>KRAS, EGFR, PTEN</i>	Nasopharyngeal Carcinoma, Head and Neck Squamous Cell Carcinoma, Cardiovascular Disease	[347, 509-511]
miR-100	<i>mTOR</i>	Esophageal Squamous Cell Carcinoma, Bladder Cancer, Endometrioid Endometrial Carcinoma, Breast Cancer	[374-376, 512]
miR-101	<i>KRAS, MYC, AKT, mTOR, TIGAR</i>	Hepatocellular Carcinoma, Osteosarcoma, Clear Cell Renal Cell Carcinoma, Prostate Cancer	[380, 381, 513-515]
miR-105	<i>SIRT3</i>	Ovarian Cancer	[499]
miR-106a/b	<i>SIRT1, PTEN</i>	Pituitary Tumour, Breast Cancer	[516-518]
miR-107	<i>EGFR</i>	Non-Small Cell Lung Cancer	[519]
miR-10b	<i>PTEN</i>	Breast Cancer	[520]
miR-122/a	<i>MYC, EGFR</i>	Hepatocellular Carcinoma, Inflammatory Bowel Disease	[281, 521]
miR-124a	<i>SIRT1</i>	Neuropathic Pain	[522]
miR-125a/b	<i>SIRT1, SIRT7, TP53</i>	Hepatocellular Carcinoma, Age-Related Cataract, Multiple Myeloma, Non-Small Cell Lung Cancer, Colorectal Cancer, Neuroblastoma, Cataract	[472, 523-528]
miR-126	<i>KRAS, AKT</i>	Pancreatic Cancer, Squamous Tongue Cell Carcinoma, Glioma, Colorectal Cancer	[253, 312, 529, 530]
miR-1285	<i>TP53</i>	Neuroblastoma, Hepatoblastoma	[531]
miR-1294	<i>MYC</i>	Esophageal Squamous Cell Carcinoma	[532]
miR-1297	<i>PTEN</i>	Breast Cancer	[533]
miR-130a/b	<i>MYC, PTEN</i>	Osteocarcinoma, Bladder Carcinoma, Non-small Cell Lung Cancer	[272, 534-536]
miR-132	<i>SIRT1</i>	Glioma, Type2 Diabetes Mellitus, Gastric Cancer, Colitis	[537-540]
miR-133a/b	<i>EGFR, SIRT1</i>	Pancreatic Cancer, Ovarian Cancer, Hepatocellular Carcinoma	[541, 542]
miR-134	<i>KRAS, EGFR</i>	Renal Cell Carcinoma, Glioblastoma, Non-Small Cell Lung Cancer, Colorectal Cancer	[256, 543-545]
miR-135a/a-1	<i>MYC, EGFR</i>	Renal Cell Carcinoma, Prostate Cancer	[546, 547]
miR-137	<i>EGFR</i>	Glioblastoma Multiforme, Thyroid Cancer	[548, 549]
miR-138	<i>SIRT1</i>	Diabetic Vascular Smooth Muscle Cells, Intervertebral Disc Degeneration, Pancreatic Cancer, Osteocarcinoma	[550-553]
miR-141	<i>PTEN, AKT, TP53, SIRT1</i>	Esophageal Cancer, Osteosarcoma, Multiple Myeloma, Pluripotent Stem Cells, Glioma, HB infection	[321, 525, 554-557]
miR-142	<i>PTEN</i>	Cutaneous Squamous Cell Carcinoma	[558]
miR-143	<i>KRAS, EGFR, AKT, MDM2, SIRT1</i>	Colorectal Cancer, Non-Small Cell Lung Cancer, Bladder Cancer, Head and Neck Squamous Cell Carcinoma, Pancreatic Cancer	[315, 406, 460, 559-563]
miR-144	<i>PTEN, mTOR, TIGAR</i>	Pancreatic Neuroendocrine Tumour, Preeclampsia, Salivary Adenoid Carcinoma, Renal Cell Carcinoma, Inflammation of Microglia, Lung Cancer	[399, 564-567]
miR-145	<i>MYC, MDM2, SIRT1</i>	Non-Small Cell Lung Cancer, Esophageal Squamous Cell Carcinoma, Ovarian Cancer, Oral Squamous Cell Carcinomas, Glioblastoma, Head and Neck Squamous Cell Carcinoma, Pancreatic Cancer	[275, 406, 460, 568-570]
miR-146b	<i>AKT</i>	Osteosarcoma	[321]

## CHAPTER 1

miR-148a/b	<i>PTEN, AKT, MYC</i>	Osteosarcoma, Renal Cell Carcinoma, Hepatocellular Carcinoma	[2, 278, 571, 572]
miR-149	<i>AKT</i>	Hepatocellular Carcinoma, Neuroblastoma, Glioblastoma Multiforme	[573-575]
miR-150	<i>TP53</i>	Lung Cancer	[576]
miR-152	<i>PTEN, SIRT7</i>	Hepatic Insulin Resistance, Human Dental Pulp Stem Cells	[577, 578]
miR-153	<i>PTEN, AKT</i>	Prostate Cancer, Lung Cancer	[324, 325]
miR-155	<i>KRAS, MYC, PTEN, AKT, SIRT5, SIRT1</i>	Gastric Carcinoma, hepatocellular Carcinoma, Waldenström Macroglobulinemia, Leukemia, Colorectal Cancer, Neuropathic Pain	[269, 350, 500, 522, 579-581]
miR-15a/b,miR-16	<i>TP53, mTOR, AKT, SIRT4</i>	Multiple Myeloma, Glioma, Ischemia, Dermal Fibroblasts	[525, 582-585]
miR-17	<i>MYC, TP53</i>	Neuroblastoma, Cervical Cancer	[410, 586]
miR-18/a	<i>KRAS</i>	Human Squamous Carcinoma, Colorectal Cancer, Liver Cancer, Ovarian Cancer	[587, 588]
miR-181a/b/d	<i>PTEN, KRAS, EGFR, AKT, SIRT1</i>	Colorectal Cancer, Osteosarcoma, Oral Squamous Cell Carcinoma, Glioma, Cutaneous Squamous Cell Carcinoma, Acute Myeloid Leukemia, Glioblastoma Multiforme, Hepatic Stellate Cells, Non-Alcoholic Fatty Liver Diseases	[589, 590] [591-597]
miR-1827	<i>MDM2</i>	Colorectal Cancer	[598]
miR-183	<i>mTOR</i>	Neuropathic Pain	[599]
miR-184	<i>MYC</i>	Non-Small Cell Lung Cancer, Nasopharyngeal Carcinoma	[600, 601]
miR-185	<i>MYC, PTEN, AKT</i>	Colorectal Cancer, Breast Cancer, Hepatocellular Carcinoma, Idiopathic Pulmonary Fibrosis, Non-Small Cell Lung Cancer	[277, 346, 602-604]
miR-192	<i>MDM2</i>	Colorectal Cancer, Multiple Myeloma	[407, 426]
miR-193a/b	<i>PTEN, KRAS, TSC1/2</i>	Renal Cell Carcinoma, Colon Cancer, Breast Cancer, Pancreatic Ductal Adenocarcinoma, Cutaneous Squamous Cell Carcinoma, Amyotrophic Lateral Sclerosis	[251, 257, 605-608]
miR-194	<i>AKT, MDM2</i>	Gall Bladder Cancer, Multiple Myeloma	[407, 426, 609]
miR-195	<i>SIRT3</i>	Myocardium	[496]
miR-197	<i>TP53</i>	Non-Small Cell Lung Cancer	[610]
miR-199a/b	<i>SIRT1, mTOR</i>	Pluripotent Stem Cells, Hyperglycemia-Induced Pancreatic $\beta$ -Cell Loss, Endometrioid Endometrial Carcinoma	[374, 611, 612]
miR-19a/b	<i>PTEN, TP53</i>	Bladder Cancer, Osteosarcoma, Myeloma, Liver Cancer, Breast Cancer	[613-616]
miR-200a/c	<i>EGFR, TP53, KRAS, PTEN, SIRT1, MYC, AKT</i>	Bladder Cancer, Breast Cancer, Multiple Myeloma, Nasopharyngeal Carcinoma, Colorectal Cancer, Hepatic Stellate Cell, Pluripotent Stem Cell, Lung Adenocarcinoma, Renal Cell Carcinoma, Ovarian Cancer, Esophageal Cancers	[320, 383, 525, 617-626]
miR-203	<i>MYC</i>	Cutaneous Squamous Cell Carcinoma	[627]
miR-204	<i>SIRT1</i>	Osteosarcoma, Spermatogonial Stem Cell, Hepatocellular Carcinoma	[455, 628, 629]
miR-205	<i>PTEN</i>	Ovarian Cancer	[630]
miR-206	<i>KRAS, EGFR</i>	Gastric Cancer, Pancreatic Ductal Adenocarcinoma, Oral Squamous Cell Carcinoma, Head and Neck Squamous Cell Carcinoma	[510, 631-633]
miR-20a/b	<i>PTEN, AKT, SIRT7</i>	Coronary Artery Disease, Diabetic Retinopathy, Diabetic Nephropathy	[634-636]
miR-21	<i>KRAS, MYC, PTEN</i>	Lung Cancer, Breast Cancer, Diabetic Kidney Disease, Colorectal Cancer, Hepatocellular Carcinoma, Leukemia, Vestibular Schwannomas, Glioblastoma, Bladder Cancer, Radio-resistance Lung Cancer	[345, 354, 505, 613, 637-642],
miR-210	<i>MYC</i>	Colorectal Cancer, Glioblastoma, Cervical Cancer, Breast Cancer	[643]
miR-212	<i>SIRT1</i>	Prostate Cancer	[644]
miR-214	<i>KRAS, PTEN, TP53</i>	Non-small Cell Lung Cancer, Ovarian Cancer, Breast Cancer, Ovarian Cancer Stem Cells	[340, 645-648]
miR-215	<i>MDM2</i>	Colorectal Cancer, Multiple Myeloma	[407, 426]
miR-216a/b	<i>PTEN, KRAS</i>	Acute Pancreatitis, Kidney Disorders, Ovarian Cancer, Nasopharyngeal Carcinoma	[338, 649-651]

## CHAPTER 1

miR-217	<b><i>KRAS, PTEN, SIRT1</i></b>	Pancreatic Ductal Adenocarcinoma, Lung Cancer, Kidney Disorders, Podocyte Injury, Ageing	[338, 461, 652-654]
miR-218	<b><i>EGFR, mTOR</i></b>	Non-Small Cell Lung Cancer, Prostate Cancer	[655, 656]
miR-22	<b><i>MYC, PTEN, SIRT1</i></b>	Leukemia, Clear Cell Renal Cell Carcinoma, Glioblastoma, Ischemia-Reperfusion Injury	[274, 657-661]
miR-221	<b><i>PTEN</i></b>	Radiosensitive Cancer Cells, Glioblastoma	[342, 662]
miR-222	<b><i>PTEN, TP53</i></b>	Radiosensitive Cancer Cells, Oral Squamous Cell Carcinoma	[395, 662]
miR-224	<b><i>KRAS, mTOR</i></b>	Colorectal Cancer, Gastric Cancer	[663, 664]
miR-23a/b	<b><i>EGFR, SIRT5, SIRT1</i></b>	Coronary Artery Disease, Colorectal Cancer, Diabetic Retinopathy	[500, 665, 666]
miR-24	<b><i>MYC, TP53</i></b>	Leukemia, Embryonic Stem Cells, Hepatocellular Carcinoma	[276, 667, 668]
miR-25	<b><i>PTEN, TP53</i></b>	Diabetic Nephropathy, Multiple Myeloma, Non-Small Cell Lung Cancer, Colorectal Cancer	[525, 669, 670]
miR-26a	<b><i>PTEN</i></b>	Glioblastoma	[331]
miR-27a/b	<b><i>KRAS, TP53, EGFR, SIRT5</i></b>	Esophageal Squamous Cells Carcinoma, Colorectal Cancer, Renal Cell Carcinoma, Non-Small Cell Lung Cancer	[500, 547, 671-673]
miR-28	<b><i>SIRT3</i></b>	Primary human tenocytes	[498],
miR-29a/b/c	<b><i>PTEN, AKT, MDM2</i></b>	Colorectal Cancer, Gastric Cancer, Prostate Cancer, Breast Cancer, Non-Small Cell Lung Cancer	[314, 337, 405, 674-677]
miR-300	<b><i>TP53</i></b>	Lung Cancer, Colorectal Cancer	[678, 679]
miR-301a	<b><i>PTEN</i></b>	Pancreatic Cancer, Malignant Melanoma	[680, 681]
miR-302a	<b><i>AKT</i></b>	Prostate Cancer	[313]
miR-30b/c/d	<b><i>KRAS, TP53</i></b>	Colorectal Cancer, Breast Cancer, Non-Small Cell Lung Cancer, Multiple Myeloma, Cardiac Disease	[396, 670, 682-684]
miR-31	<b><i>TP53</i></b>	Breast Cancer	[685]
miR-3151	<b><i>TP53</i></b>	Malignant Melanoma	[686]
miR-32	<b><i>PTEN</i></b>	Hepatocellular Carcinoma	[336]
miR-320a	<b><i>MYC</i></b>	Hepatocellular Carcinoma	[687]
miR-33	<b><i>TP53</i></b>	Hematopoietic Stem Cells	[688]
miR-337	<b><i>PTEN</i></b>	Endometrial Carcinoma	[689]
miR-338	<b><i>mTOR</i></b>	Colon Cancer	[690]
miR-339	<b><i>MDM2, SIRT2</i></b>	Breast Cancer, Neuroblastoma	[481, 691]
miR-33a/b/c	<b><i>SIRT6, MYC</i></b>	Liver Cancer, Osteosarcoma	[268, 468]
miR-340	<b><i>MDM2</i></b>	Prostate Cancer	[692]
miR-34a	<b><i>MYC, EGFR, AKT, SIRT6, SIRT1</i></b>	Hepatocellular Carcinoma, Prostate Cancer, Renal Cell Carcinoma, Non-Small Cell Lung Cancer, Glioma, Colorectal Cancer, Non-Alcoholic Fatty Liver Diseases, Pancreatic Cancer	[271, 289, 317, 460, 693-697]
miR-363	<b><i>MYC</i></b>	Prostate Cancer, Hepatocellular Carcinoma	[278, 698]
miR-365a	<b><i>KRAS</i></b>	Cutaneous Squamous Cell Carcinoma	[606]
miR-3666	<b><i>SIRT7</i></b>	Breast Cancer	[699]
miR-367	<b><i>MDM2</i></b>	Hepatocellular Carcinoma	[700]
miR-370	<b><i>EGFR, PTEN</i></b>	Gastric Cancer, Colorectal Cancer, Gastric Cancer	[545, 701, 702]
miR-373	<b><i>mTOR, SIRT1</i></b>	Fibrosarcoma	[382]
miR-374/a	<b><i>MDM2, PTEN</i></b>	Bladder Cancer, Breast Cancer	[703, 704]
miR-377	<b><i>SIRT1</i></b>	Obesity	[705]
miR-378	<b><i>AKT</i></b>	Breast Cancer	[706]
miR-380	<b><i>TP53</i></b>	Neuroblastoma	[707]
miR-384	<b><i>KRAS</i></b>	Colorectal Cancer	[708]

## CHAPTER 1

miR-409	<b>AKT</b>	Breast Cancer	[709]
miR-421	<b>SIRT3</b>	Non-Alcoholic Fatty Liver Disease	[710]
miR-429	<b>MYC</b>	Gastric Cancer, Breast Cancer	[619, 711]
miR-449a/c	<b>MYC</b>	Glioblastoma, Gastric Carcinoma, Osteosarcoma, Prostate Cancer	[712-714]
miR-451	<b>MYC, AKT</b>	Docetaxel-Resistant Lung Adenocarcinoma, Dilated Cardiomyopathy, Bladder Cancer, Non-Small Cell Lung Cancer, Glioblastoma	[715-720]
miR-451	<b>TSC1/2</b>	Multiple Myeloma, Hypertrophic Cardiomyopathy	[384, 721]
miR-453	<b>TP53</b>	Lung Cancer	[722]
miR-4534	<b>PTEN</b>	Prostate Cancer	[723]
miR-454	<b>PTEN</b>	Non-Small Cell Lung Cancer	[724]
miR-4689	<b>KRAS, AKT</b>	Colorectal Cancer,	[252]
miR-486	<b>PTEN, MDM2, SIRT1</b>	Cardiac Myocytes, Lung Cancer, Erythroleukemia	[332, 725, 726]
miR-491	<b>TP53</b>	Pancreatic Cancer	[727]
miR-492	<b>PTEN</b>	Hepatic Cancer	[728]
miR-494	<b>MYC, PTEN, SIRT1</b>	Epithelial Ovarian Cancer, Cardiac Disease, Myeloid-Derived Suppressor Cells, Cervical Cancer, Gastric Carcinoma, Pancreatic Cancer	[343, 353, 729-733]
miR-495	<b>AKT, mTOR</b>	Prostate Cancer	[734],
miR-496	<b>mTOR</b>	Ageing	[735]
miR-5003	<b>MDM2</b>	Breast Cancer	[736]
miR-502a	<b>EGFR</b>	Colorectal Cancer	[737]
miR-504	<b>TP53</b>	Non-Small Cell Lung Cancer, Colorectal Cancer, Multiple Myeloma, Abdominal Aortic Aneurysm	[409, 670, 738]
miR-509	<b>EGFR, MDM2</b>	Tongue Squamous Cell Carcinoma, Cervical Cancer, Hepatocellular Carcinoma, Prostate Cancer	[404, 739, 740]
miR-511	<b>AKT</b>	Prostate Cancer	[741]
miR-519d	<b>PTENAKT</b>	Hepatocellular Carcinoma	[335]
miR-520 b/c/e	<b>EGFR, mTOR, SIRT1</b>	Gastric Cancer, Fibrosarcoma	[382, 742]
miR-532	<b>KRAS, SIRT3</b>	Lung Adenocarcinoma, Ovarian Cancer	[499, 743]
miR-543	<b>SIRT1</b>	Hypertension, Gastric Cancer	[744, 745]
miR-545	<b>EGFR</b>	Colorectal Cancer	[746]
miR-548i	<b>AKT</b>	Non-Small Cell Lung Cancer	[747]
miR-561	<b>MYC</b>	Gastric Cancer	[748]
miR-577	<b>PTEN</b>	Glioblastoma	[332]
miR-579	<b>MDM2</b>	Melanoma	[749]
miR-600	<b>TP53</b>	Colorectal Cancer	[750]
miR-601	<b>SIRT1</b>	Pancreatic Cancer	[751]
miR-606	<b>MDM2</b>	Breast Cancer, Lung Cancer, Colorectal Cancer	[402]
miR-610	<b>MDM2</b>	Glioma	[752]
miR-613	<b>KRAS</b>	Ovarian Cancer	[753]
miR-615	<b>AKT</b>	Pancreatic Ductal Adenocarcinoma	[754]
miR-622	<b>KRAS</b>	Lung Cancer, Colorectal Cancer	[755, 756]
miR-637	<b>AKT</b>	Glioma	[316]
miR-638	<b>AKT</b>	Lung Cancer	[757]
miR-641	<b>MDM2</b>	Lung Cancer	[758]

## CHAPTER 1

miR-650	<b><i>AKT</i></b>	Rheumatoid Arthritis	[759]
miR-660	<b><i>MDM2</i></b>	Lung Cancer	[403]
miR-7	<b><i>EGFR, mTOR</i></b>	Ovarian Cancer, Glioblastoma, Lung Cancer, Breast Cancer, Hepatocellular Carcinoma, Gastric Cancer	[326-328, 378, 379, 760, 761]
miR-718	<b><i>PTEN</i></b>	Kaposi's Sarcoma, Inflammation	[341, 762]
miR-744	<b><i>MYC</i></b>	Hepatocellular Carcinoma	[270]
miR-758	<b><i>mTOR, MDM2</i></b>	Hepatocellular Carcinoma	[763]
miR-766	<b><i>MDM2, SIRT6</i></b>	Breast Cancer, Dermal Fibroblast	[764], [471]
miR-768	<b><i>KRAS</i></b>	Lung Cancer	[765]
miR-875	<b><i>EGFR</i></b>	Prostate Cancer	[766]
miR-9/a	<b><i>SIRT1PTEN</i></b>	Hepatic Stellate Cells, Non-Alcoholic Fatty Liver Disease, Acute Myeloid Leukemia, Colorectal Cancer, Nasopharyngeal Carcinoma, Non-Small Cell Lung Cancer	[767-772]
miR-92	<b><i>TP53</i></b>	Multiple Myeloma, Pluripotent Stem Cells	[525, 555],
miR-923	<b><i>AKT</i></b>	Lung Cancer	[757]
miR-93	<b><i>MYC, PTEN, SIRT1</i></b>	Colon Cancer, Ovarian Cancer, Myocardial Ischemia/Reperfusion(I/R) Injury, Breast Cancer, Ageing	[773], [339, 462, 518, 774]
miR-95	<b><i>PTEN</i></b>	Radioresistance Lung Cancer	[638]
miR-96	<b><i>KRAS, mTOR</i></b>	Pancreatic Ductal Adenocarcinoma, Pancreatic Cancer, Colorectal Cancer, Myocardial Hypertrophy	[255, 684, 775-777]
miR-98	<b><i>MYC, TP53</i></b>	Breast Cancer, Lung Cancer	[505, 722]
miR-99a/b	<b><i>mTOR</i></b>	Breast Cancer, Esophageal Squamous Cell Carcinoma, Cervical Cancer, Endometrioid Endometrial Carcinoma	[373, 374, 376]

## 1.8 Towards future applications for disrupting cancer cell glycolysis

Colorectal cancer (CRC) remains as one of the leading causes of cancer-related death worldwide. Early diagnosis and treatment of the disease as well as accurate staging are key factors in improved survival outcomes [14, 15]. CRC has a multifaceted etiology and both genetic and epigenetic alterations are responsible for CRC tumorigenesis [17-20]. CRC is associated with changes in metabolomics enriched in macromolecule biosynthesis and energy producing pathway to provide building blocks and energy for continuous proliferation of neoplastic cells [45].

Metabolomics provides a new exciting platform to explore potential anti-cancer drugs. A universally observed phenotype of malignant cells is their propensity to import glucose and secrete lactate, even in the presence of oxygen. The characterization of aerobic glycolysis has led to dramatic advances in tumour imaging. Positron emission tomography (PET) scans, widely used for cancer diagnosis, exploit the ability of cancer cells to sequester excessive glucose from the blood stream. Ever since aerobic glycolysis was found to be a characteristic of tumour cells and was accepted as a hallmark of cancer, it has been proposed that suppressing aerobic glycolysis would be a promising strategy to treat cancer. As a consequence, several studies have reported the use of glycolytic enzyme inhibitors. For instance, lonidamine as a HK2 inhibitor, PEP analogues as PKM inhibitors, as well as FX-11 and panepoxydone as LDHA inhibitors, have been considered potential therapeutic agents (reviewed in [778] and [779]). However, as glycolysis is also a vital metabolic pathway in normal cells, inhibition of aerobic glycolysis remains challenging when identifying potential cancer-specific targets. Although a definitive explanation for Warburg's observations is overdue, the control of this process by oncogenes and tumour suppressors, coupled with epigenetic factors including microRNAs, provides additional insight. So far, ample evidence supports associations between the metabolic shift in cancer cells and oncogene activation or inactivation of tumour suppressors. The elusive nature of metabolic rewiring and branching in cancer cells, along with influences upon other signalling pathways, raise concerns as to whether targeting a single component of this complex circuit will be sufficient to eradicate cancer cells with minimal side effects. Despite several reports of the involvement of miRNA-mediated gene regulation, there is still much to learn about how miRNAs contribute to the Warburg effect. Development of new miRNA-mediated strategies, that target metabolic pathways rather than single components, have the potential to enhance future cancer treatment. Systems biology approaches that iteratively couple massively parallel gene expression analytical technologies with high throughput functional screens, may identify additional miRNAs or miRNA-targets with

promise for cancer diagnosis, prognosis and drug development. Polymorphisms in the miRNA binding sites of oncogenes are known to influence cancer predisposition and therapeutic response, which may further inform target selection [247, 780]. Conversely, acquired somatic mutations in miRNA-binding sites may also lead to the reduced efficacy of miRNA-based therapies. Similarly, the demands of other tissues, such as the highly glucose-dependent nature of brain and retina, will necessitate tissue-specific delivery of anti-glycolysis miRNAs in a therapeutic context where administration already presents challenges. Regardless, multi-faceted solutions are required to provide hope for cancer patients who currently have limited options.

## 1.9 Metformin

### 1.9.1 Origin and history

Biguanides have been used since the 17th century, as a component of the *Galega officinalis* extract, for treatment of the excessive volume of urination associated with the development of Diabetes mellitus [781]. Later in 1922, Werner and Bellow synthesized biguanides (metformin and phenformin), which were effective and safer than traditional botanicals [782] for treating type 2 diabetes. In 1977, as a result of increased lactic acidosis and cardiac related deaths, phenformin was removed from the market in the United States, while it continued to be cautiously used by endocrinologists in France and Scotland [783]. In 1998, a randomized, multicentre clinical trial of 3867 patients over 10 years, carried out by UK Prospective Diabetes Study Group, showed the survival benefits of metformin in patients with diabetes and cardiovascular diseases [784]. Since then, metformin has had an excellent safety profile in its 20 years of post-market surveillance and has been widely used in clinical practice as a first line therapy for diabetes in over 120 million people [785]. In addition to the glucose lowering effect, metformin has been shown to reduce the risks of myocardial infarction and to treat diseases such as non-alcoholic fatty liver disease and cancer [786-789].

### 1.9.2 Anti-cancer effects of metformin

In 2005, in a case-controlled study on almost 12000 T2DM patients conducted by Evans et al [790], metformin showed a reduction effect on the risk of cancer. Since then, epidemiological and retrospective studies and meta-analyses have demonstrated a lower incidence of tumour development in patients with T2DM treated with metformin, compared with those on alternative treatments, highlighting an association between metformin and tumorigenesis. Table 1.6 summarizes the studies on the association of metformin and cancer prevention.

**Table 1-6. Summary of studies on the effect of metformin in cancer prevention.**

Study design	Year	Outcomes	Reference
Case-controlled study on 11876 T2DM patients	2005	Metformin reduced the risk of cancer in patients with diabetes.	[790]
Population-based retrospective cohort study on 10309 T2DM patients	2006	Metformin treated group had a lower cancer-associated mortality rate compared with that of the sulfonylurea or insulin treated group.	[791]
Case-controlled study of 4085 T2DM patients	2009	The tumour incidence of patients with diabetes treated with metformin was lower than that in the control group.	[792]
Case-controlled study of 973 patients with pancreatic adenocarcinoma	2009	Metformin was associated with a reduced risk of pancreatic cancer in patients with diabetes.	[793]
Retrospective cohort study on 62809 T2DM patients	2009	Metformin was associated with the lowest risk of solid tumour genesis compared with insulin or sulfonylurea treatment while insulin treatment increased the risk of colorectal and pancreatic cancer. However, metformin therapy did not reduce the risk of breast or prostate cancer.	[794]
Case-controlled study on 2529 T2DM patients who received neoadjuvant chemotherapy for early-stage breast cancer	2009	Diabetic patients with breast cancer treated with metformin and neoadjuvant chemotherapy had a higher pathological complete response rate compared with those untreated with metformin.	[795]
Population-based case-controlled study on 1001 cases of prostate cancer and 942 controls	2009	Metformin treatment was associated with a decreased prostate cancer risk.	[796]
Case-controlled study of 465 patients with HCC, 618 cases with liver cirrhosis and 490 controls with no liver disease	2010	Treatment with metformin significantly reduced the risk of developing HCC compared with sulphonylurea and insulin therapy.	[797]
Case-controlled study on 610 HCC patients compared with 618 matched cirrhotic patients and 1696 controls	2010	Metformin reduced the risk of HCC in diabetic patients with chronic liver disease.	[798]
Prospectively- followed cohort study on 1353 patients with T2DM	2010	Metformin-treated patients exhibit a reduced cancer mortality compared with that of the controls.	[799]
Systematic review and meta-analysis of epidemiologic studies	2010	Diabetic patients taking metformin had a reduced tumour risk (particularly, pancreatic cancer and HCC, but not colon, breast or prostate cancer) compared to those on alternative treatments.	[800]
Nested case-controlled analysis of 22621 female patients with T2DM	2010	Patients with diabetes treated with metformin for more than 5 years had a decreased risk of breast cancer.	[801]
Clinical trial of 23 patients	2010	Treatment with metformin was associated with a lower risk of colorectal carcinogenesis.	[802]
Nested case-controlled analysis on 63049 incident users of oral hypoglycemic agent (OHA), in which 739 cases of prostate cancer were matched to 7359 controls	2011	Metformin treatment did not decrease the risk of prostate cancer in patients with diabetes.	[803]
Retrospective study of 233 consecutive cases of prostate cancer patients with coexisting T2DM	2011	Metformin treatment improved the overall survival of prostate cancer patients with diabetes.	[804]
Retrospective study of 302 patients with diabetes and pancreatic cancer	2012	Metformin treatment increased the survival time in pancreatic cancer patients with diabetes.	[805]
Systematic review and meta-analysis of 21195 T2DM patients	2012	Metformin treatment may reduce the risk of cancer incidence and mortality.	[806]
Cohort study and a nested case-controlled analysis on 115578 T2DM patients treated with metformin	2013	Metformin treatment was not associated with the incidence of colorectal cancer in patients with T2DM.	[807]
Population-based case-controlled study on 2088 patients with primary CRC and 9060 controls	2014	Long-term metformin treatment had a protective effect of CRC in T2DM female patients.	[808]

## Chapter 1

Case controlled study on 2682 patients with T2DM and 5364 in the control group	2015	Metformin use was associated with a reduced risk of developing CRC among T2DM patients.	[809]
Case controlled study on T2DM patients, 286106 untreated and 193369 were treated with metformin	2015	Metformin treatment was associated with a decreased risk of ovarian cancer.	[810]
Case controlled on T2DM patients, 824 untreated and 917 treated with metformin	2016	Metformin use was associated with a decreased risk of kidney cancer in patients with T2DM.	[811]
Case controlled on T2DM patients, 119 untreated and 1273 treated with metformin	2016	Metformin reduced the risk of oral cancer, especially when the cumulative duration was more than 21.5 months.	[812]
Cohort study of 32 patients with a history of bladder cancer compared with 33 patients with bladder cancer recurrence (placebo group)	2016	Although metformin delayed tumour recurrence, it had no considerable inhibitory effect on the recurrence rate of bladder cancer.	[813]
Case controlled on T2DM patients, 16217 untreated and 287971 treated with metformin	2016	Metformin significantly reduced gastric cancer risk, especially when the cumulative duration was more than approximately 2 years.	[814]
Systematic review and meta-analysis of 8726 patients	2017	Metformin treatment was associated with a reduced risk of colorectal adenoma, especially in high-risk populations consisting of patients with diabetes mellitus or a history of colorectal neoplasia (CRN).	[815]
Case controlled on T2DM patients, 15414 untreated and 280159 treated with metformin	2017	Metformin use reduced the risk of lung cancer in patients with T2DM.	[816]
Systematic review and meta-analysis	2017	Metformin reduced all-cause mortality and diseases of ageing independent of its effect on T2DM.	[817]
Cohort study of 47351 patients with T2DM	2018	Metformin had an effect on chemoprevention of colorectal cancer.	[818]
Retrospective cohort study on 128453 metformin users and 128453 non-users	2018	Metformin was associated with the prevention of thyroid cancer development with no effect on the early phase of treatment.	[819]
propensity score-matched retrospective cohort of 84434 veterans newly prescribed metformin or a sulfonylurea as monotherapy	2018	Metformin had no association with prevention of most cancers except liver cancer.	[820]
Cohort study of 2353 newly onset T2DM patients grouped into 722 nonusers of antidiabetic medication 374 on metformin monotherapy, 653 on sulfonylurea monotherapy, 302 on metformin and sulfonylurea combination therapy, and 302 on other medication therapies	2019	Metformin or sulfonylurea treatment was associated with lower risk of cancer incidence in a cohort of newly onset T2DM patients.	[821]

### 1.9.3 Mechanism of action of metformin

The anti-proliferative and anti-metabolic effects of metformin have been shown in different types of cancer including breast, prostate, lung, liver, ovarian and colon [822-827]. Metformin is a weak base which results in its cationic charge at physiological pH levels. Metformin circulates in both free and bound forms and the half-life of the drug is about 90 minutes [828]. In the intestine, metformin concentration can peak at 10 mM [784, 829]. The intestinal uptake of metformin is

mediated by the plasma membrane monoamine transporter (PMAT, encoded by gene SLC29A4) [830]. However, there are scarce in-vivo and clinical data regarding the role of PMAT in the pharmacokinetics of metformin. Organic cationic transporters (OCT3 and OCT1, encoded by gene SLC22A3 and SLC22A1, respectively) are also responsible for intestinal and hepatic uptake and transfer of metformin from the interstitial fluid [831, 832]. Beside PMAT and OCT transporters, human multidrug and toxin extrusion 1 (MATE1, encoded by the gene SLC47A1) and MATE2-K (gene SLC47A2) are also responsible for metformin uptake [833-836]. Interestingly, normal epithelial cell lines respond to a lesser extent to the anti-proliferative effect of metformin compared with cancer cell lines, which highlights the cancer specificity of this drug [837].

In 2000, two independent groups discovered the suppression of mitochondrial respiratory chain complex I as the main action of metformin [785, 838] thereby reducing the conversion of glucose to  $\alpha$ -ketoglutarate in the TCA cycle and subsequently increasing glutamine metabolism. Later, in 2001, Zhou et al [839] reported that metformin activates AMP activated protein kinase (AMPK) by inhibiting complex 1 of the mitochondrial respiratory chain, thus increasing the cellular AMP/ATP ratio. However, later it was shown that the metabolic effect of metformin is preserved in liver-specific AMPK-deficient mice which confirmed complex I and not AMPK as the main target. Targeting of complex I results in a decrease in NADH oxidation and the proton-driven synthesis of ATP from ADP and inorganic phosphate, which ultimately induces the AMP/ATP ratio and inhibition of hepatic gluconeogenesis and lipogenesis through AMPK-dependent and AMPK-independent pathways [838]. The activation of the upstream liver kinase B1 (LKB1) is necessary for the AMPK-dependent pathway [840]. Therefore, the effect of metformin on cellular and molecular function could be divided into two: the AMPK dependent and independent categories.

### **1.9.3.1 AMPK-dependent effects of metformin**

Once activated, AMPK, an intracellular energy sensor, restores cellular energy levels by its anti-anabolic and pro-catabolic activities. These activities result in suppressed cell mitosis and cell proliferation [841-843]. Metformin also enhances the p53-p21 axis and AMPK-dependent pathway and downregulates Cyclin D1 levels, thereby inducing G1 arrest in breast cancer cells [844]. Activated AMPK also suppresses IGF-1-induced activation of AKT/TSC1/mTOR by phosphorylating insulin receptor substrate-1 [845-848]. Other AMPK-dependent effects of metformin include inhibition of DNA synthesis, induction of G0/G1 arrest, cell apoptosis and suppression of multi-drug resistant 1 gene activation [849-852]. AMPK activation also results in

enhanced levels of phosphorylated IRS-1, suppressing IGF-1 induced activation of the mTOR pathway [827, 847, 848], (Figure 1-4).

mTOR, as described above, is also a master regulator of cellular energy homeostasis and metformin has been shown to suppress mTOR activities in different types of cancers [850, 851, 853-856]. AMPK is a major suppressor of mTOR by phosphorylating and activating TSC2 and, consequently, RHEB GTPase inhibition. Also, active AMPK inhibits mTORC1 by direct phosphorylation of Raptor [857, 858]. However, beside AMPK-dependent inhibition of mTOR, there are some independent pathways that are described in the following section.

### **1.9.3.2 AMPK-independent effects of metformin**

In contrast to the AMPK-dependent effects of metformin, AMPK suppression did not block the anti-proliferative and anti-cell cycle progression effects of metformin, which suggested some AMPK-independent functions for metformin [837, 859]. DNA damage response 1 (REDD1) inhibits mTOR and was shown to mediate the anti-cell cycle progression effects of metformin [860]. Inhibition of tumour necrosis factor alpha (TNF $\alpha$ ) is another AMPK-independent function of metformin, which consequently leads to the repression of chronic inflammatory responses and cancer progression [861, 862]. Metformin can also inhibit mTOR activity through the reduction of IGF-1 levels and activation of Rag GTPase. Sahra et al [860] also showed that metformin mediated mTOR inhibition can be exerted via a p53- dependent manner and REDD1 induction. Furthermore, metformin exerts an insulin sensitizing effect and inhibits the growth, proliferation, invasion and clonogenic capacity of cancer cells; this is through reducing the circulating levels of IGF-1 and suppressing the androgen-mediated up-regulation of IGF-1R. Nevertheless, this beneficial effect of metformin has not yet proved to be totally AMPK-independent [847, 863, 864], (Figure 1-4).

Other pathways that are involved in the anti-tumour effects of metformin may also include MAPK-related signalling pathways that regulate cell growth, differentiation, proliferation, apoptosis and migration [865-868]. Metformin showed a pro-apoptotic function through activating the JNK/p38 MAPK pathway and upregulating DNA damage-inducible gene 153 (GADD153) expression [869]. Metformin also inhibits the Her2 pathway through downregulation of HER2 oncoprotein via an AMPK-independent inhibition of mTOR activity [870, 871].

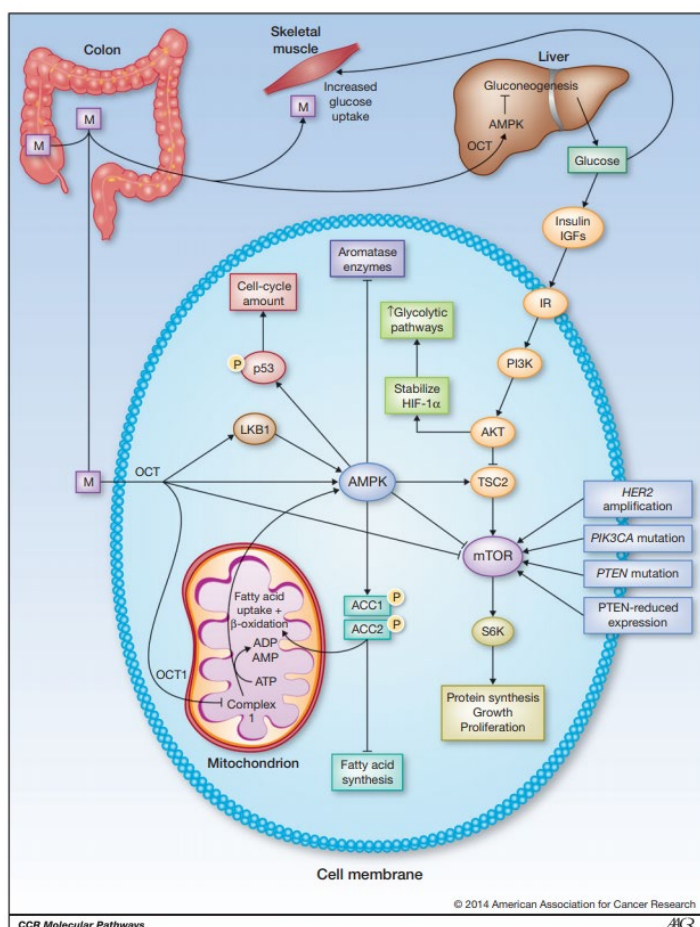


**Figure 1-4. Overview of proposed mechanism of action of metformin.**

Metformin (M) is absorbed through gut and can act via systemic processes following uptake in liver and cell level molecular pathways [872].

#### 1.9.4 Effect of Metformin and CRC cells

Several epidemiological studies confirmed metformin as an anti-cancer agent in colorectal cancer, reporting reduced colorectal cancer mortality or incidence among patients with T2DM treated with standard clinical doses of metformin [794, 873-875] (Table 1-6). Although most of these studies

were retrospective, possibly bearing selection biases, there is extensive *in vitro* and *in vivo* evidence supporting the anti-oncogenic capabilities of metformin in colorectal cancer. Table 1-7 summarises recent *in vitro* studies on the anti-oncogenic effect of metformin on CRC cells.

Murine models have also been used to evaluate the anti-oncogenic effects of metformin on colorectal cancer. Buzzai et al [876] showed that in HCT116 p53 +/+ and p53 -/- xenografts, metformin selectively suppressed p53 knockout colon cancer growth. In Wister rats with dextran sulphate sodium-induced colon cancer, the combination of metformin with vitamin D significantly reduced the number of aberrant crypt foci (ACF) and suppressed colon tumour growth through the AMPK/mTOR pathway [877]. Likewise, in mice with colon cancer and fed a high-energy diet, metformin resulted in increased apoptosis through AMPK activation and SDP-ribose polymerase (PARP) cleavage [826].

**Table 1-7. Summary of *in vitro* studies on the anti-cancer effects of metformin in CRC cell lines.**

Doses	Cell lines	Effects of metformin	References
20 mM	HCT116	Metformin suppressed CRC cell growth and migration with no effects on the cell apoptosis	[878]
5 mM	HCT116 and p53 KO HCT116	Metformin resulted in moderate radiation protection of CRC cells. p53 status did not affect the ability of metformin to inhibit mitochondrial function and AMPK activation.	[859]
0.02-10 mM	HCT116	Metformin caused a significant dose- and time-dependent decrease in mitochondrial function and reduced the tumour size and hypoxia levels in mice carrying HCT116 tumours.	[879]
10 mM	HCT116	Metformin activated AMPK and p53 in a time-dependent manner and subsequent MDMX phosphorylation.	[880]
10 mM	chemotherapy-resistant HCT116 and HT29	Metformin reduced cell proliferation and migration in chemotherapy-resistant CRC cells.	[881]
1-5 mM	HCT116 and p53 KO HCT116	Metformin upregulated miR-34a levels in p53 wild type HCT116 cells but not in p53 KO HCT116 cells and increased the susceptibility of p53 wild type cells to oxidative stress.	[882]
2-10 mM	Caco-2, HCT116, HT29 and SW1116	Metformin suppressed cell proliferation and induced glucose uptake and lactate production.	[883]
1 mM	SW1116, HT-29 and Caco2	Metformin had an anti-growth effect when combined with 10 mM 2-DG.	[884]
	HT29 and HCT116	Metformin sensitized HT29 cell line to oxaliplatin, while it did not show synergy in HCT116 or in combination with 5-FU in both the cell lines	[885]
60 μM	HCT116 and HT29	Metformin decreased cell viability, increased the early and late apoptosis, and induced the expression of the pro-apoptotic gene BAX. It also increased PTEN mRNA levels, decreased FASN mRNA abundance in a time-dependent manner and suppressed CSC formation under hyperinsulinemic condition.	[886]
2.5–10 mM	HCT116 and p53 KO HCT116	Metformin-induced clonogenic cell death, radio-sensitization, delayed repair of DNA damage and cell cycle arrest was higher in p53 KO cells.	[887]
2 mM	HCT116 and p53 KO HCT116	Metformin decreased AMPK- dependent manner in p53 wild type cells with no significant stimulation of glucose consumption or lactate production in cells lacking p53.	[876]
8-10 mM	HCT116 and Caco2	Metformin reduced cell viability and inflammatory response and induced apoptosis and oxidative stress.	[888]

<b>5-40 mM</b>	LoVo and HT29	Metformin inhibited cell growth in a time and dose dependent manner. 40 mM metformin treatment decreased PKM2 protein level and HK activity and increased IDH protein level and PDH activity.	[889]
<b>10-20 mM</b>	COLO205	Metformin reduced cell viability, increased AMPK activation and decreased the phosphorylated mTOR protein levels	[890]
<b>5 mM</b>	Hypoxic SW620	Metformin increased AMPK activation and also suppressed mTOR and AKT activation and accumulation of HIF-1.	[891]
<b>5 mM</b>	SW480	Metformin decreased proliferation in a dose and time dependent manner and suppressed cell cycle progressed and telomerase activity.	[892]
<b>2.5-20 mM</b>	HT-29	Metformin suppressed cell proliferation, activated AMPK and reduced levels of phospho-S6K and general protein synthesis.	[893]

### 1.9.5 Metformin and miRNAs

Numerous studies have linked the anti-tumour effect of metformin to the regulation of oncogenic and tumour suppressor miRNAs. In general, metformin upregulates DICER1 which was shown to be AMPK-dependent in diabetic humans and mice, as well as cultured cancer cells [894, 895]. Some of these studies are summarized in Table 1-8. All this evidence has drawn attention to the roles of miRNAs in cancer initiation and progression. This also highlights novel target therapies that can reverse or re-introduce oncogenic and tumour suppressor miRNAs in the context of cancer cells. While a number of limitations need to be addressed for miRNA replacement therapy, development of specific and effective delivery systems may help in translation of such miRNA-based therapies into applications for cancer and other diseases. For instance, miR-143 and miR-145 are of potential utility as miRNA-based therapies in CRC. Downregulation of both miRNAs was shown in gastric and colon cancers. Validated targets for these miRNAs includes oncogenes such as *FLN1*, *STAT1*, *YES*, *ERK5* and *MYC*. Karimi et al., investigated the therapeutic potentials of both miRNAs in CRC and showed decreased tumour growth in xenograft model [896]. In addition, a phase I study utilized TargomiRs loaded with miR-16 based mimics in patients with malignant pleural mesothelioma and showed a well-tolerated dose of TargomiRs with early signs of anti-tumour activity [897]. Therefore, replacing miRNA function may provide a therapeutic benefit.

**Table 1-8. Summary of studies on the metformin associated changes in miRNA expression levels.**

Doses	Cell lines/ tissues	Upregulated miRNAs	Downregulated miRNAs	Effects of metformin	Reference
<b>1 mM</b>	MCF-7	Let-7a, miR-32 and miR-96	miR-183	decreased mammosphere formation	[898]
<b>0.5 mM</b>	MCF-7, BT-474 and SUM-159	miR-33a	NA	downregulated c-Myc and IRS-2	[895]
<b>1-10 mM</b>	MKN1, MKN45, and MKN74,	miR-21, miR-361-5p, miR-26b and let-7f	miR-1826, miR-1260, miR-1280	decreased cell proliferation, cyclin D1 and Cdk2/4 levels, suppressed cell cycle progression, and EGFR and IGF-1R levels	[899]

## Chapter 1

	xenograft model				
<b>20 mM</b>	AsPC-1, AsPC-1-GTR, MiaPaCa-2, and MiaPaCa-2-GTR	let-7a/b, miR-26a, miR-101 and miR-200b/c	NA	downregulated EZH2, OCT4, NOTCH1 and EpCAM expression and decreased pancreatosphere growth	[900]
<b>5 mM</b>	Panc1 and SW1990	miR-26a, miR-192, let-7c	NA	downregulated HMGA1 expression, decreased cell proliferation and migration and induced apoptosis	[901]
<b>10 mM</b>	A549 and NCI-H358	NA	miR-222	upregulated p27, p57, PTEN and decreased cell proliferation	[902]
<b>5-10 mM</b>	T.T, KYSE30 and KYSE70	17 miRNAs	45 miRNAs	decreased cell proliferation, angiogenesis, and downregulated cyclin D1, EGFR and IGF-1R levels	[903]
<b>1-5 mM</b>	PC3	10 miRNAs	12 miRNAs	decreased proliferation	[904]
<b>5 mM</b>	Vcap	miR-30a, miR-143 and miR-196b	NA	downregulated SOX4 expression, and decreased cell proliferation, migration and invasion	[905]
<b>10 mM</b>	786-o	miR-26	NA	downregulated BCL-2 and Cyclin D1 expression and decreased cell proliferation	[906]
<b>1-5 mM</b>	MCF-7, A549, MDA-MB-231, SKOV3, HCT116, p53 KO HCT116	miR-34a	NA	downregulated SIRT1 expression and increased susceptibility of cancer cell to oxidative stress	[882]
<b>10 mM</b>	MCF-7, MDA-MB, BT-549 and HCC70	miR-193a/b	NA	decreased fatty acid synthesis and induced apoptosis	[907]
<b>10 mM</b>	Huh7	33 miRNAs	18 miRNAs	decreased cell proliferation and downregulated cyclin D1, Cdk4 and cyclin E expression	[908]
<b>20-40 mM</b>	HCCC-9810, RBE, SSP25 and Hucct1	miR-124, miR-182, miR-27b and let-7b	miR-221 and miR-181a	downregulated cyclin and cyclin dependent kinase proteins and decreased cell proliferation	[909]
<b>0.5 mM</b>	Panc02	miR-34a	NA	downregulated Notch and tumour sphere formation	[910]
<b>20 mM</b>	Panc1	miR-221	NA	Upregulated p27 and G1 phase arrest	[911]
<b>10-40 mM</b>	MDA-MB-231, MDA-MB-468, and MCF-7	miR-26a	NA	decreased cell proliferation and reduced PTEN, E2F3, BCL2 and EZH2, DLC1 expression	[912]
<b>5-10 mM</b>	PK1, PK9, Panc1 and xenograft model	19 miRNAs	19 miRNAs	decreased cells proliferation, downregulated cyclin D1 and Cdk4 protein levels and phosphorylation of EGFR and IGF-1R	[913]
<b>2.5 μM</b>	HepG2	miR-23a	NA	Induced apoptosis and downregulated FOXA1	[914]
<b>20 mM</b>	MCF-7	NA	miR-27a	upregulated AMPKα2 expression, reduced cell proliferation and induced cell apoptosis	[915]
<b>25-125 mM</b>	FaDu	NA	miR-21-5p	inhibited cell proliferation and upregulated PDCD4	[916]

## Chapter 1

<b>1.25-20 mM</b>	KB	miR-26a		inhibited proliferation, induced apoptosis and downregulated of MCL-1 expression	[917]
<b>1-10 mM</b>	CAKI-1 and CAKI-2	NA	miR-21	increased PTEN expression	[918]
<b>2 mM</b>	MCF-7 and ARK2	let-7	NA	inhibited cell growth and invasion and AKT2 activity	[919]
<b>5-20 mM</b>	MDA-MB-231, BT549, MCF-7, and T-47-D	miR-200c	NA	inhibited cell growth, migration, and invasion induced apoptosis and downregulated AKT2 expression	[920]
<b>0.5 mM</b>	SUM159PT, MCF-7, BT-474, BT-549, mouse breast cancer xenografts and in sera from breast cancer patients	NA	miR-21	enhanced expression of critical upstream activators of the AMPK, calcium-binding protein 39-like and Sestrin-1, leading to AMPK activation and inhibition of mTOR	[921]
<b>1-10 mM</b>	HuTu80	17 miRNAs	33 miRNAs	inhibited proliferation, induced cell cycle arrest in the G0/G1 and reduced expression and phosphorylated of EGFR and ROR2	[922]
<b>0.2- 5 mM</b>	769-P and A498	miR-34a	NA	induced cell cycle arrest	[923]
<b>1-10 mM</b>	GF- $\beta$ -induced SW480 and HCT116	miR-200a, miR-200c and miR-429	miR-34a	bidirectional regulation of the [SNAIL/miR-34]:[ZEB/miR-200] system in the EMT process to inhibit EMT in general increase proportion of E/M hybrid cells in the total population	[924]
<b>10 mM</b>	PANC-1 and BxPC-3	miR-199a-5p, miR-140-5p and miR-152-3p	NA	downregulated DNA-binding activity of NF- $\kappa$ B, TGF $\alpha$ , IKK $\beta$ , ERBB2 and VEGF expression and suppressed angiogenesis and growth	[925]

### 1.10 Challenges of metformin in cancer

Although, the main mechanism of action of metformin has been well-studied in diabetes, there are still some challenges associated with chronic metformin treatment for cancer. There are some discrepancies regarding the adequacy of the applicable systemic doses of metformin to induce a metabolic stress in cancer cells. Furthermore, the heterogeneity of cancer cells with multiple driver mutations make it even more complex to investigate the amount of metformin accumulation in the cells and to predict the cancer cells response to metformin [926]. It was shown that metformin treatment leads to an auto-resistance response in cancer cell, through depolarizing the mitochondrial membrane and, therefore, limiting the accumulation of the drug [838]. Chronic mTOR inhibition occurred by metformin treatment, was also shown to result in blockade of negative feedback loop and drug resistance through IGF-R signalling pathway. IRS-1 is an activator of AKT/ S6K pathway and is a downstream effector of IGF-IR. S6K was also proved

to be a suppressor of IRS-1. Therefore, inhibition of mTOR located upstream of S6K pathway leads to an undesired relieving of this negative feedback loop and, thus, limits drug responsiveness and increases cell survival [927]. Zhou et al., [928] showed the heritability of the glycaemic response to metformin and that the response could be polymorphic and intrinsic to the genetic variation of the individuals.

Recently, development of high throughput technologies in genomics, transcriptomics, proteomics, metabolomics and epigenomics provides the means to comprehensively study the effects and pharmacology of metformin [929]. This will contribute to the characterization of metformin, with a view to enhancing the efficiency of pharmaceutical research [930]. A better understanding of metformin's pharmacokinetics and pharmacodynamics, and its direct and indirect anti-cancer target pathways, may lead to optimal evaluation of this agent.

### 1.11 Aims and hypotheses

As shown in this chapter, CRC development is associated with epigenetic modifications, including changes in miRNAs, along with changes in metabolic processes. Due to the Warburg effect, CRC cells rely on glycolysis for continued growth and proliferation. Although a definitive explanation for this metabolic switch is overdue, the control of this process by oncogenes and tumour suppressors, coupled with epigenetic factors including microRNAs is still elusive. Therefore, this study aimed to investigate the cellular and metabolic outcomes of glycolysis inhibition in CRC cells. It was hypothesized that CRC cells rely on glycolysis for continuous cell growth and proliferation.

Also, as discussed in this chapter, metabolic inhibition of cancer cells requires multi-targeting strategies and therefore, combinations of miRNAs with chemotherapeutic drugs may be feasible in minimizing the possible side effects and maximizing the efficacy in tumour regression. Metformin has shown a range of anti-cancer properties in different types of cancer, including CRC, mainly through inhibiting mitochondrial respiration and inducing a metabolic stress. While the anti-cancer roles of metformin have been shown in various studies, there is still a need to investigate microRNA-mediated gene regulation in metformin-associated signalling networks. This study, therefore, aimed to study the changes in transcriptome and miRNA profiles of CRC cells treated with metformin to investigate the affected signalling networks and, in particular, the roles of miRNAs in the context of the anti-cancer effects of metformin. It was hypothesised that *modification of miRNA activity may contribute to the anti-proliferative effect of metformin in colorectal cancer.*

**Aim 1.**

To determine the cellular and metabolic consequences of inhibiting glycolysis and respiration in CRC cells; and to confirm the anti-cancer properties of metformin in CRC cells. (Described in Chapter 3)

**Aim 2.**

To determine the effect of metformin on the transcriptome and miRNA profiles of CRC cells, and specifically to investigate the effect of metformin treatment on metabolic and cancer-related pathways and the role of miRNAs in this context. (Described in Chapter 4)

**Aim 3.**

To identify miRNAs with the ability to sensitize CRC cells to the anti-proliferative properties of metformin and investigate their role in regulating CRC cellular metabolism (Described in Chapter 5).

# Chapter 2. Materials and Methods

## 2.1 Cell culture

A number of CRC lines with different mutations were used for this study. HCT116 colorectal carcinoma cell line (ATCC, Manassas, VA, USA) is an adherent cell line which is derived from the epithelium of a 48-year old male's ascending colon. The isogenic HCT116 p53<sup>-/-</sup> cell line (Peter MacCallum Cancer Centre, Melbourne, Australia) is identical to HCT116 with wild type p53 except for targeted modification of the p53 gene. RKO (ATCC, Manassas, VA, USA) is a poorly differentiated colon carcinoma cell line [931]. SW480 is a metastatic colorectal carcinoma cell line (ATCC, Manassas, VA, USA) and was established from a primary colon adenocarcinoma from a 50 year old Caucasian male [932]. DLD1 is derived from human colorectal adenocarcinoma and is shown to have diploid karyotype [933]. HT-29 is derived from a 44 year old Caucasian female [934]. These cell lines were maintained in Dulbecco's Modified Eagle's Medium, DMEM, (Invitrogen, Life Technologies, California, USA) containing 10% Foetal Bovine Serum (FBS) (Bovogen Biologicals, VIC, Australia) and buffered with bicarbonate. For special treatments and assays the concentration of D-Glucose, Glutamine, Phenol Red and FBS varied. Cells were cultured at 37°C and 5% CO<sub>2</sub> with less than 75% confluence and no added antibiotics were required. The mutational status of the above-mentioned colon cancer cells was summarized in Table 2.1.

**Table 2-1. Colon cancer cell lines classified by driver mutations.**

Cell line	KRAS	BRAF	PIK3CA	PTEN	TP53
HCT116	G13D/+	+/+	H1047R/+	+/+	+/+
RKO	+/+	V600E/+	H1047R/+	+/+	+/+
SW480	G12V/+	+/+	+/+	+/+	R273H:P309S
DLD_1	G13D	+/+	E545K:D549N	+/+	S241F/+
HT-29	+/+	V600E/+	P449T/+	+/+	R273H/+

Cells were sub-cultured (passaged) approximately twice per week. Medium was aspirated and discarded and the cells rinsed with 1 x phosphate buffered saline, PBS, (Sigma-Aldrich, St Louis, MO, USA) to remove traces of FBS which naturally contains trypsin inhibitor. PBS was aspirated and the adherent cells were dissociated using 0.25 % (w/v) trypsin (Invitrogen, Life Technologies, California, USA) at 37°C for 5 minutes. The enzymatic action of the trypsin was stopped by adding same volume of complete growth medium to the detached cells. A split ratio of 1:5 to 1:8 or a

seeding density of  $3 \times 10^4$  viable cells/cm<sup>2</sup> to  $5 \times 10^4$  viable cells/cm<sup>2</sup> is used when subculturing the cells. Cells were discarded after a maximum of 20 passages.

Cells were stored by adding approximately  $10^7$  cells in 200  $\mu$ L complete medium and 200  $\mu$ L cryopreservation mix containing cold medium, FBS and Dimethyl sulfoxide, DMSO, (Sigma-Aldrich, St Louis, MO, USA) with the ratio of 5:3:1, respectively. The cells were frozen slowly by placing in a container with isopropanol. The frozen cryovials stored at -80°C freezer for short term storage or liquid nitrogen for long term storage.

## 2.2 Mycoplasma testing

Cells were shown by routine testing to be mycoplasma free. To prepare samples for mycoplasma testing cells growing in T-75 flask were trypsinized, neutralised and 200ul of the cell suspension added to 1ml sterile saline. The tube was centrifuged at 6500rpm for 5 minutes at room temperature. The supernatant was aspirated off and the pellet was re-suspended in 90  $\mu$ L of 0.05 M NaOH. To lyse the cells and extract the DNA the suspension was heated at 98°C for 10 minutes and let it to cool followed by addition of 10  $\mu$ L 1 M Tris, pH 7.5 (Sigma-Aldrich, St Louis, MO, USA). 1 in 10 dilution of sample was made. To amplify the extracted DNA with mycoplasma genus-specific primer sets (GPO-1 and MGSO) as well as HRAG-1 primer set as an internal control [935]. The master mix composition for PCR is listed in Table 2.2. 2  $\mu$ L of DNA sample added to 23  $\mu$ L of the prepared master mix and PCR program was set to 1 cycle denaturation of 94°C for 10 minutes, 50 cycles of annealing including 94°C for 30 seconds, 53°C for 1 minute and 72°C for 1 minute and 1 cycle elongation of 72°C for 5 minutes.

**Table 2-2. Master mix composition for mycoplasma testing of CRC cell lines.**

Reagent	$\mu$ L/ well
10 x PCR buffer	2.5
50 mM MgCl <sub>2</sub>	1.0
100 ng/ $\mu$ L GPO-1 primer	1.0
100 ng/ $\mu$ L MGSO primer	1.0
10 mM dNTPs	0.5
100 ng/ $\mu$ L HRAG forward primer	0.5
100 ng/ $\mu$ L HRAG reverse primer	0.5
10 u/ $\mu$ L Platinum Taq polymerase	0.2
H <sub>2</sub> O	15.38
Total	23.0

1% agarose gel was made by dissolving 1.5 gr Agarose (AppliChem, Darmstadt, Germany) in 75ml 1x TAE buffer (Table 2-8) and 7.5  $\mu$ L Gel Rel (Biotium, California, USA) added to detect the bands. The sample was run for approximately 1 hour and imaged on ChemiDoc™ Imaging Systems (BioRad, California, USA). The DNA ladder used in the mycoplasma testing was 100 bp (Promega, Madison, WI, USA).

## 2.3 mRNA and miRNA expression analysis

### 2.3.1 RNA extraction

Cells were grown in 24-well plate and the RNAs were extracted by adding 400  $\mu$ L/well TRIzol RNA Isolation Reagent (Sigma-Aldrich, St Louis, MO, USA) directly to the cells. Cells were lysed by scraping and pipetting up and down several times. Cells harvested from two wells pooled together in a 1.5 ml Eppendorf tube. Total RNA was extracted according to the manufacturer's instructions, as detailed below.

Homogenised samples were incubated for 5 min at room temperature to permit complete dissociation of the nucleoprotein complex. 80  $\mu$ L chloroform (Chem-supply, Gillman, SA, Australia) was added, the tube was shaken vigorously by hand for 15 seconds, incubated at room temperature for approximately 3 minutes and then centrifuged at  $12,000 \times g$  for 15 min at  $4^{\circ}\text{C}$ . This process separates the sample into three phases: the lower red phenol-chloroform phase, an interphase, and a clear upper aqueous phase. The aqueous phase of the mixture, which contains RNA, was removed carefully, avoiding any withdrawal of the interphase or organic layer and was transferred into a new Eppendorf tube.

200  $\mu$ L of 100% isopropanol (Chem-supply, Gillman, SA, Australia) was added to the aqueous phase to precipitate the RNA. The sample was incubated at room temperature for about 10 min, followed by a centrifugation at  $12,000 \times g$  for 20 min at  $4^{\circ}\text{C}$ . Supernatant was then removed carefully and the pellet was washed by adding 500  $\mu$ L of chilled 75% ethanol (Chem-supply, Gillman, SA, Australia). The sample was vortexed briefly, then centrifuged at  $7,500 \times g$  for 5 min at  $4^{\circ}\text{C}$ . The ethanol wash was then aspirated and the remaining RNA pellet air-dried on ice for approximately 10 min. The RNA pellet was then resuspended in 20 – 40  $\mu$ L of RNase-free water, ready for quantitation.

### 2.3.2 RNA quantification and quality analysis

To quantify the RNA Nanodrop-8000 spectrophotometer (Nanodrop Technologies, Wilmington, DE, USA) was used. The pedestals were first blanked with 1  $\mu$ L RNase-free water, then wiped and loaded with 1  $\mu$ L of each sample to obtain RNA quantity and absorbance at 230, 260 and 280 nm. The 260/280 ratio was used as a measure of purity where ratio of  $\sim$ 2.0 was generally accepted. The 260/230 ratio was also used as a secondary measure of nucleic acid purity where acceptable values were commonly in the range of 2.0-2.2. RNA was then stored at  $-80^{\circ}\text{C}$ .

The RNA integrity was also assessed using an RNA 6000 Nano Kit run on an Agilent 2100 bioanalyzer (Agilent Technologies, California, USA). Each RNA chip contains an interconnected set of microchannels for RNA fragments separation based on their size. The bioanalyzer separate RNA fragments by means of micro-fluidics and capillary electrophoresis. The quantitative range of the bioanalyzer for mRNA assay is 25-500 ng/ $\mu$ L. Samples were diluted using RNase-free water. To prepare the gel-dye mix 225  $\mu$ L of gel matrix was added into a spin filter and centrifuged at 1,500 g for 10 minutes at room temperature. 65  $\mu$ L of and 1  $\mu$ L of dye concentrate from RNA 6000 Nano Kit aliquoted into a 0.5 mL RNase-free microcentrifuge tubes and centrifuged at 13,000g from 10 min at room temperature. Meantime, diluted samples were heated for 2 minutes on a heating block set to  $70^{\circ}\text{C}$ . A new RNA chip was set up on the chip priming station and the gel-dye mix, RNA marker, ladder and samples were loaded into the chip according to the manufacturer's instruction. The chip was vortexed in the IKA vortexer (Agilent Technologies, California, USA) for 1 minute at 2,400 rpm and then was ran in the Agilent 2100 Bioanalyzer instrument. The RNA Integrity Number (RIN) more than 7 was selected as good quality RNAs.

### 2.3.3 Primer Design

To quantify the RNA expression levels for extracted RNAs, primer pairs were designed to target desired mRNAs using online PCR primer tool, Primer-BLAST, NCBI. For efficient amplification in real-time PCR, forward and reverse primers were designed so that the PCR product size is less than 150 base pairs (bp). The annealing temperature ( $T_m$ ) was set to a minimum of  $57^{\circ}\text{C}$  and a maximum of  $63^{\circ}\text{C}$  with a maximum difference of  $3^{\circ}\text{C}$  in the  $T_m$  of the forward and reverse primer pairs. The recommended primers were checked to end with a C or G residue.

To ensure maximum product stability the GC content was set around 50-60%. To increase the sensitivity of the primers to a specific splice variant, primers were designed to span an exon-intron junction on target mRNA so that one half hybridizes to the 3' end of one exon and the other half

to the 5' end of the adjacent exon. The primer sets were then checked in Oligo Calc for potential hairpin formation and self-dimerization. Details of forward and reverse primers, spanning each gene region, are shown in Table 2-6.

### 2.3.4 DNase treatment, cDNA synthesis and Real-time PCR

To remove any genomic DNA contamination the RQ1 RNase free DNase kit (Promega, Wisconsin, USA) was used. 22.5  $\mu\text{L}$  of each RNA sample (0.1  $\mu\text{g}/\mu\text{L}$ ) was treated with 2 units DNase I in 1x DNase buffer and incubated at 37°C for 20 minutes. The DNase I enzyme was then deactivated by adding 2.5  $\mu\text{L}$  DNase deactivation slurry from the Ambion DNA-free™ Kit (Invitrogen, Life Technologies, California, USA) and precipitated by a centrifugation at 10000 g for 1.5 minute.

For cDNA synthesis, 1  $\mu\text{L}$  (100 ng) of Random Hexamer primers (Invitrogen, Life Technologies, California, USA) was added to 10  $\mu\text{L}$  total DNase treated RNA (1  $\mu\text{g}$ ) and incubated at 70°C for 5 min followed by a 5 min incubation on ice. 14  $\mu\text{L}$  Master mix containing 5  $\mu\text{L}$  RT buffer, 1.25  $\mu\text{L}$  dNTP mix (Promega, WI, USA), 6.75  $\mu\text{L}$  RNase-free water and 200 units/ rxn of M-MLV Reverse Transcriptase (Promega, WI, USA) added to make a 25  $\mu\text{L}$  reaction. Following a 10 min incubation at room temperature, reverse transcription was carried out in the Programmable Thermal Controller 100 (PTC100) (MJ Research, Quebec, Canada) with a 50 min hold at 50°C, followed by a 15 min hold at 70°C. The resulting cDNA was then diluted 1:3 using sterile water for use in real-time RT-PCR.

Real-time RT-PCR reaction mix was prepared by adding 2  $\mu\text{L}$  diluted cDNA to 18  $\mu\text{L}$  master mix containing 2  $\mu\text{L}$  of 3  $\mu\text{M}$  gene specific forward primer (Table 2-6), 2  $\mu\text{L}$  of  $\mu\text{M}$  gene specific reverse primer, 10  $\mu\text{L}$  Power SYBR green quantitative real-time RT-PCR master mix (Invitrogen, Life Technologies, California, USA) and 4  $\mu\text{L}$  RNase –free water. PCR reactions were in triplicates and performed in the Qiagen Rotorgene Q real-time PCR cycler (Qiagen, Limburg, Netherlands). Cycling consisted of 95 °C hold for 10 minutes, 90 °C for 15 seconds for denaturation and 60 °C for 1 minute for annealing and extension. Transcript levels were normalised relative to levels of endogenous control *B2M* or *ACTB* mRNA (Table 2-6), depending on the treatments. Mean normalised expression levels were calculated based on Cq values using Qgene [936]. To calculate the amplification efficiency of each primer set, a standard curve was generated using Cts from samples prepared by serial dilution of cDNA synthesised from RNAs extracted from HCT116 cells.

## 2.4 Protein extraction, quantification, separation and detection

### 2.4.1 Protein extraction

Radioimmunoprecipitation assay buffer (RIPA buffer) was used to lyse cells (Table 2-8). 1 Complete mini protease inhibitor cocktail tablet and 1 phosphatase inhibitor cocktail tablet (Roche Applied Science, Mannheim, Germany) was dissolved in 1.5 mL and 1 mL distilled water, respectively. 750  $\mu$ L of the protease inhibitor solution and 500  $\mu$ L of phosphatase inhibitor solution added to 3750  $\mu$ L of RIPA buffer. Cells were washed in 1  $\times$  PBS after media removal, and 600  $\mu$ L lysis buffer mix per  $8 \times 10^6$  cells was added directly and scraped the cells to extract the protein and homogenise the protein extracts. Protein extracts were stored at  $-20^{\circ}\text{C}$ .

### 2.4.2 Protein quantitation

To determine the protein concentration of extracted protein solutions prior to polyacrylamide gel electrophoresis, a fluorescence-based quantitation kit called EZQ<sup>®</sup> Protein Quantitation Kit was used. Ovalbumin 2 mg/mL (BioRad, California, USA) was used as a standard protein and different concentrations of ovalbumin (0.02 mg/mL- 2mg/mL) were prepared in RIPA buffer to generate the standard curve for protein quantification. 1  $\mu$ L of the standards as well as the samples were spotted on an assay paper in triplicates. The paper was allowed to dry before washing with 40 mL 100% methanol for 5 minutes. Subsequently, the assay paper was dried on low heat, and 35 mL of the EZQ protein quantitation reagent was added to stain the proteins and incubated on an orbital shaker for 30 minutes at room temperature. The paper was then rinsed 3 times for 2 min in 40 mL washing buffer containing 10% methanol and 7% acetic acid. The fluorescence from the protein-spotted assay paper was then detected using SYPRO RUBY protocol in ChemiDoc<sup>™</sup> Imaging Systems (BioRad, California, USA) and the data were analysed using Carestream Molecular Imaging Software (Bruker, Connecticut, USA) and Image Lab<sup>™</sup> Software (BioRad, California, USA). A standard curve was created by plotting the corrected fluorescence values of the standards versus the corresponding protein mass and the protein concentration of the samples was calculated from the standard curve.

#### 2.4.2.1 Acrylamide SDS-PAGE gel casting

1.5 mm thick SDS-PAGE gels were prepared. 10% gel solution made by mixing 2 mL resolving buffer (Table 2-8), 75  $\mu$ L 10% SDS pH 7.2, 2.92 mL H<sub>2</sub>O, 2.5 mL 30% Acrylamide-Bis (BioRad, California, USA), 37.5  $\mu$ L 10% Ammonium Persulfate, APS, (Sigma-Aldrich, St Louis, MO, USA) and 6  $\mu$ L Tetramethylethylenediamine, TEMED, (BioRad, California, USA). 6 mL of the mix poured into the gel assembly and was left to set for 30 minutes. Stacking gel solution was made by

adding 260  $\mu\text{L}$  of 0.5 M Tris-HCl pH 6.8 (Table 2-8), 600  $\mu\text{L}$  of 30% Acrylamide, 37.5  $\mu\text{L}$  10% SDS pH 7.2, 2.92 mL H<sub>2</sub>O, 19  $\mu\text{L}$  10% APS and 6  $\mu\text{L}$  TEMED. Approximately 3 mL stacking gel mix was added on top of the separation gel mix within the slides, placed the combs in and incubated at room temperature for 30 minutes before taking out the comb and loading the protein samples.

#### 2.4.2.2 Protein separation by gel electrophoresis

Loading dye was prepared in 3:1 ratio of 3 $\times$  SDS loading dye (Table 2-8) and 1M DTT, respectively. 25-45 ng of each protein sample was used, in a total volume of 20  $\mu\text{L}$  containing 5  $\mu\text{L}$  4  $\times$  SDS loading dye mix (Table 2-8), protein samples and RIPA buffer and were boiled on heating block for 3 minutes. The vertical electrophoresis cell was set up with a precast acrylamide SDS-PAGE gel and filled with 1 $\times$  SDS running buffer (Table 2-8). Samples, as well as a protein marker, were loaded into the gel wells and the gel was run at constant 150V for approximately 1 hour. Gel was carefully removed from the apparatus and if the precast gel was used, the gel was imaged using ChemiDoc™ Imaging Systems (BioRad, California, USA) and stain-free gel protocol.

#### 2.4.2.3 Electrophoretic Transfer

To elute proteins from the gel and transfer them to a 0.2  $\mu\text{M}$  polyvinylidene difluoride membrane (LF-PVDF) (BioRad, California, USA) a semi-dry transfer system, Trans-blot Turbo Transfer System (BioRad, California, USA), was used. A PVDF membrane was soaked in methanol and two transfer stacks were soaked in transfer buffer (BioRad, California, USA), (Table 2-8) for 3 minutes. The gel and membrane were then sandwiched between the transfer stacks and transferred at constant current of 1.3 A for 7 minutes. At the end, the gel and the membrane were imaged using ChemiDoc™ Imaging Systems (BioRad, California, USA) and stain-free gel protocol. In case of self-cast gels, the membrane was stained using 1  $\times$  Ponceau S stain solution (Table 2-8) for 2 minutes, rinsed with H<sub>2</sub>O and scanned using Epson Perfection 4990 Photo Scanner (Epson America, California, USA).

#### 2.4.2.4 Protein detection with antibodies

After transfer, membrane was blocked using 5% skim milk in 1 $\times$  TBS with 1 or 0% Tween-20 (Sigma-Aldrich, St Louis, MO, USA) prior to an overnight incubation at 4°C with desired primary antibody (Table 2-7). Primary antibody dilutions were made based on the manufacturer's data sheet. After overnight incubation, membrane was washed four times in 1 $\times$  TBS-T and incubated with secondary horseradish peroxidase-conjugated goat anti-rabbit IgG for 1 hour at the desired dilution. After four more washes with 1 $\times$  TBS-T, the enhanced chemiluminescence (ECL) assay

was used (5 min dark incubation with 0.5 mL of ECL substrate and 0.5 mL of enhancer) to visualise bands using ChemiDoc™ Imaging Systems (BioRad, California, USA). The protein band intensities were normalized to total protein using Image Lab™ Software (BioRad, California, USA) and AlphaEaseFC™ Software (Alpha Innotech, California, USA) for precast and cast gels, respectively. Reference protein levels (ACTIN 1 and GAPDH) were used as endogenous controls.

## 2.5 Cell transfection with small inhibitory RNAs (siRNAs) and miRNA oligonucleotide duplexes (mimics)

The cells were reverse-transfected with mimics or siRNAs while seeding into 6-, 24- or 96-well plates. The final concentration of mimics and siRNAs were 25 nM and cell seeding density was  $2.0 \times 10^5$ ,  $1.5 \times 10^4$  and  $5.0 \times 10^3$  cells per well for 6-, 24- and 96-well plates, respectively. The transfection was done by a lipid-based Lipofectamine™ 2000 Transfection Reagent (Invitrogen, Life Technologies, California, USA) that forms liposome and transfers RNA into the cells. For miRNA mimics, siRNAs and transfection reagent dilution during the process of transfection, Opti-MEM reduced serum medium (Invitrogen, Life Technologies, California, USA) was used and the transfection was carried out according to the manufacturer's protocol.

Briefly, adherent cell lines were detached by trypsin, centrifuged at 1,200 rpm, resuspended at complete medium and a small aliquot was removed for cell counting using a haemocytometer. Diluted transfection reagent was incubated for 5 min, then combined with diluted siRNA/miRNA mimic and incubated for a further 15 min. 500  $\mu$ L, 100  $\mu$ L and 50  $\mu$ L of siRNA/miRNA mimic and transfection reagent mix was added to each well of 6-, 24- and 96-well plate. 1,500  $\mu$ L, 500  $\mu$ L and 100  $\mu$ L cell dilution added to the siRNA/miRNA mimic-Lipofectamine mix in the wells. The plates were incubated for about 30 min at room temperature prior to incubation at 37°C within the humidified incubator.

## 2.6 Metformin treatment

Metformin hydrochloride (Sigma-Aldrich, Missouri, USA) was dissolved in sterile water to make the 1 M stock solution and stored at -20°C. The stock solution was then further diluted freshly in appropriate cell culture medium. Cells were cultured in appropriate well-plates and cell densities for 24 hours and subsequently treated with 0 mM, 2.5 mM, 5 mM or 10 mM metformin hydrochloride in, at least, triplicates for 72 hours.

## 2.7 Cell proliferation and cell death assays

### 2.7.1 Real-time cell growth analysis

Cell proliferation was measured using the IncuCyte Live-cell Analysis System (Essen BioScience, Michigan, USA), which performs live content imaging through acquiring, analysing and quantifying images from living cells over time. For different experiments, cells were seeded at different cell densities and in different cell culture plates. The proliferation of the cells was tracked every 2 h and the data were presented as the percentage of the cell confluency over time.

Proliferation validation experiments were performed using xCELLigence RCTA platform (ACEA Biosciences, California, USA). Cells were seeded in E-plates (ACEA Biosciences, California, USA) and cell proliferation was assayed as measures of cell index inferred by changes in electrical conductivity of cell media. Prior to readings, the cell indices were adjusted to zero by adding 50  $\mu\text{L}$  of media with 10% FBS.

### 2.7.2 Crystal violet assay

Crystal violet is an assay to obtain quantitative information about the relative density of the cells adhering to the culture plate by staining DNA. 10 $\times$  Crystal violet solution was made by dissolving 1 g Crystal violet (Sigma-Aldrich, Missouri, USA) in 500 mL 10% buffered-formalin (Orion Labs, California, USA). The Crystal violet was further diluted in buffered-formalin. To perform the assay for cells grown in 96-well plates, culture medium was removed from the wells carefully and the plate was washed twice with 150  $\mu\text{L}$  1 $\times$ PBS. 50  $\mu\text{L}$  1 $\times$  Crystal violet solution was added to each well and incubated at room temperature for 10 minutes. The plate was then washed two times by immersion in a large beaker and drained upside down on paper towel. To solubilize the crystal violet stained DNA, 100  $\mu\text{L}$  1% SDS solution was added to the stain and the plate was agitated on orbital shaker until a uniform colour was achieved. To quantify the total DNA content of the cells the absorbance at 570 nm was measured using an EnSight Multimode Plate Reader (Perkin Elmer, Ohio, USA).

### 2.7.3 Apoptosis assay

Cell apoptosis was measured by Caspase-Glo<sup>®</sup> 3/7 Assay kit (Promega, Madison, WI, USA). The Caspase-Glo<sup>®</sup> 3/7 Assay is a luminescent assay that measures caspase-3 and -7 activities of the cells. The assay provides a proluminescent caspase-3/7 substrate, which is cleaved to release aminoluciferin, a substrate of luciferase used in the production of a luminescent signal. To perform this assay, cells were grown in 384-well plates with the required transfections and/or treatment.

## CHAPTER 2

The Caspase-Glo® 3/7 Buffer and lyophilized Caspase-GloR 3/7 Substrate was equilibrated to room temperature before use and then mixed by swirling or inverting the contents until the substrate is thoroughly dissolved in buffer. The medium was aspirated from the wells leaving 25 µL of the medium. 12 µL combined substrate and buffer were added to the cells. The plate was foil-covered, placed on a shaker for 1 minute, pulse spun and incubated at room temperature for 30 minutes. Following 30 minutes incubation, the luminescence was measured using an EnSight Multimode Plate Reader. 3 replicates of each group were tested and the data were normalised to cell number acquired from crystal violet viability assay.

### 2.8 Metabolic assays

#### 2.8.1 Lactate assay

To quantify lactate release, an enzymatic reaction (demonstrated below) was performed using L-lactate dehydrogenase enzyme (LDH) and Nicotinamide adenine dinucleotide (NAD<sup>+</sup>). To allow the reaction to run to the complete oxidation of lactate molecules, hydrazine was used to react with pyruvate. The increased absorbance at 340 nm is due to NADH formation and is proportional to the lactate originally present.  $\text{Pyruvate} + \text{NADH} \leftrightarrow \text{Lactate} + \text{NAD}^+$

Cells were seeded into a 96-well plate with appropriate cell densities, transfection and metformin treatment. Medium was transferred from the wells into 1.5 mL Eppendorf microtubes. The samples were either stored at -80°C or proceeded to lactate assay immediately after transfer. To perform the assay, 250 µL reaction mix containing 81.97 µL Glycine buffer containing 0.6 M glycine and 0.5 M hydrazine (pH 9.2) (Sigma-Aldrich, Missouri, USA), 4.098 µL LDH (Sigma-Aldrich, Missouri, USA), 2.47 µL NAD (Sigma-Aldrich, Missouri, USA) and 161 µL H<sub>2</sub>O added to 10-20 µL of medium, mixed briefly and incubated at 37°C for 15 minutes. The absorbance read at 340 nm was performed using a VERSAmax Absorbance Microplate Reader. To generate a standard curve, a serial dilution of lactate standard (1 M) and lactate assay were done. For background correction, a sample of intact medium, at the same volume as the samples, was tested in triplicate. All samples were tested in triplicate and the data were applied to a standard curve and normalised to the cell number acquired by crystal violet assay (Section 2.7.3).

#### 2.8.2 ATP assay

HCT116, DLD-1, RKO, SW480 and HT-29 cells were seeded in 96 well-plates at a seeding density of  $3 \times 10^4$ ,  $3 \times 10^4$ ,  $2 \times 10^4$ ,  $3 \times 10^4$ ,  $4 \times 10^4$  cells/mL, respectively. The cells were incubated at 37°C

## CHAPTER 2

and 5% CO<sub>2</sub> for 24 hours before treating the cells with 2.5 mM, 5 mM and 10 mM metformin and continued incubation for another 72 hours. After 96 hours post-seeding, dATP standards made at 0.1 – 50 μM using 1 x ATP reaction buffer from the ATP Determination Kit (Molecular Probes, Life Technologies, California, USA). Cells were gently washed with 1 x PBS and 50 μL Cell Culture Lysis Reagent (Promega, Madison, WI, USA) added to the cells and were shaken for 15 minutes. The reaction mix per sample was composed of 89 μL H<sub>2</sub>O, 5 μL of 20X reaction buffer, 5 μL of 10 mM Luciferin and 0.025 μL of 5 mg/L Luciferase. 10 μL of cell lysate was transferred into a white opaque 96 well-plate and 100 μL reaction mix was added to the lysate and incubated at room temperature for 10 minutes at dark. The luminescence was then read using EnSight Multimode Plate Reader. Standard curve was generated using standard dATP values and the concentration of ATP was calculated for each sample.

### 2.8.3 XTT assay

XTT (Molecular Probes, Life Technologies, California, USA) is a tetrazolium-based compound and is sensitive to cellular redox potential (mainly mitochondrial oxidoreductase activity). Cells with active mitochondrial respiration convert the water-soluble XTT compound to an orange coloured formazan product. HCT116, DLD-1, RKO, SW480 and HT-29 Cells were seeded in 96 well-plate at a seeding density of  $3 \times 10^4$ ,  $3 \times 10^4$ ,  $2 \times 10^4$ ,  $3 \times 10^4$ ,  $4 \times 10^4$  cells/mL, respectively. The cells were incubated at 37°C and 5% CO<sub>2</sub> for 24 hours before treating the cells with 2.5 mM, 5 mM or 10 mM metformin and continuing incubation for another 72 hours. Then 50 μL of supernatant media was aspirated from the wells with 100 μL remaining media and 25 μL XTT reaction mix was added to the cells and incubated for 2 hours at 37°C and 5% CO<sub>2</sub>. XTT reaction mix was composed of 0.0625 μL of PMS (3 mg/mL in PBS) and 25 μL of XTT solution (1 mg/mL in PBS) The XTT absorbance was then read at 450 nM using EnSight Multimode Plate Reader.

### 2.8.4 Measurement of oxygen consumption rate (OCR)

OCR was measured using a Seahorse XFe96 Extracellular Flux Analyzer (Agilent Technologies, California, USA) according to the manufacturer's protocol. Cells were seeded in a Seahorse XFe 96 well plate (Agilent Technologies, California, USA) using normal growth medium at a density of  $3 \times 10^4$  and reverse transfected with 25 nM miRNA mimics using Lipofectamine 2000 transfection reagent and incubated at 37°C and 5% CO<sub>2</sub> for 24 hours followed by a media change and metformin treatment. 3 days after incubation, the assay was performed in XF minimal basal medium (Agilent Technologies, California, USA) supplemented with 10 mM D-glucose (Sigma-Aldrich, Missouri, USA), 1 mM sodium pyruvate (Invitrogen, Life Technologies, California, USA)

and 2 mM glutamine (Invitrogen, Life Technologies, California, USA) and adjusted pH at 7.4. The sensor cartridge was hydrated overnight by adding 200  $\mu\text{L}$ /well of Seahorse XF Calibrant (Agilent Technologies, California, USA) and incubating overnight at 37°C in a humidified atmosphere without CO<sub>2</sub>. On the day of the assay, cells were washed twice and pre-incubated in basal medium at 37°C and 0% CO<sub>2</sub> for 1 hour. Oligomycin A (1  $\mu\text{M}$ ), FCCP (0.6  $\mu\text{M}$ ) and rotenone/Antimycin A (1  $\mu\text{M}$ ) were added into the corresponding ports and the cartridge was loaded to the XFe96 Extracellular Flux Analyzer to perform the calibration and then to evaluate the mitochondrial respiratory capacity. Crystal violet assay (described in 2.7.3) was then performed and the data normalised to the DNA content present in each well.

### 2.8.5 Measurement of Extracellular Acidification Rate (ECAR)

Similar to OCR, ECAR measurements were acquired using a Seahorse XFe96 Extracellular Flux Analyzer. Accordingly, the basal medium was supplemented with 2 mM Glutamine with adjusted pH 7.4. Cells were washed twice with the medium and incubated for 1 hour in non-CO<sub>2</sub> incubator. 25  $\mu\text{L}$ /well of 10 mM Glucose, 1 $\mu\text{M}$  Oligomycin and 50 mM 2-DG were loaded into the ports and the cartridge was loaded into the analyser. The ECAR measurements were normalised to DNA content of the corresponding well, acquired by crystal violet assay (described in 2.7.3).

## 2.9 Transcriptome and small RNA sequencing

To study the effect of metformin on gene expression, transcriptome and small RNA sequencing were performed for RNA samples from HCT116 cells treated with 2.5 mM metformin for 3 days and compared to untreated control RNA. To perform Next Generation Sequencing (NGS), the quality of RNA samples was analysed using an Agilent 2100 Bioanalyzer system (section 2.3.2). RNA qualities with RNA integrity number (RIN)  $\geq 0.9$  were proceeded with library preparation. Following RNA preparation, the generation of libraries, including adapter ligation and PCR amplification and sequencing were performed at the Flinders Genomics Facility (Flinders University, Adelaide, Australia) using TruSeq Stranded Total RNA and small RNA Sample Preparation Kits (Illumina Inc., California, USA) for RNA and small RNA sequencing, respectively. Subsequently, it should be mentioned that ribosomal RNA (rRNA) depletion was performed for RNA sequencing prior to library preparation. The paired-end 100 bp sequencing was performed using the Illumina NextSeq sequencing platform (Illumina Inc., California, USA) and approximately 30-40 and 10-20 million reads were generated per sample for RNA and small RNA sequencing, respectively.

## 2.10 Statistical methods

GraphPad Prism software (version 6) (GraphPad Software Inc, California, USA) was used for statistical analyses and the data were presented as mean  $\pm$  standard deviation (SD) for a minimum of three biological replicates. Parametric unpaired Student's t-test was used to compare two groups and p value  $\leq 0.05$  considered as significant.

## 2.11 Bioinformatics analyses

### 2.11.1 Differential expression analysis

The primary data analyses for transcriptome and small RNA sequencing were performed by the Flinders Genomics Facility bioinformatician, Dr. Shashikanth Marri. For data preparation, quality check and analysis, the data were trimmed for adaptors using FASTX-toolkit followed by quality analysis of the reads using FASTQ and assembly, mapping and alignment of reads to Ensembl human genome (Grch38.p5\_v24) or miRbase 20.1 using STAR [937] and SAMtool [938]. Aligned reads were then converted to raw counts using HTseq [939] and differential expression analysis performed using DESeq2 [940]. The differentially expressed miRNAs and mRNAs were refined using the following criteria: raw counts  $\geq 50$ , adjusted p value  $\leq 0.05$  and  $-1 \geq \log_2$  Fold change  $\geq 1$ .

### 2.11.2 microRNA target analysis

To predict miRNA targets and collate previously validated targets, seven online resources were used. miRTarBase (release 7.0) [941] and miRecord (release 2013) [942] contain validated miRNA targets and those targets that were validated with strong evidence (reporter assays) were selected. To collect the predicted targets, TargetScan (release 7.1) [943], miRmap (release 1.1) [944], miRDB (release 6.0) [945], DIANA-microTCD (release 5.0) [946] and miRanda (release 3.3a) [947] were used. Relatively strict thresholds were selected in an attempt to reduce the number of false positive targets. In TargetScan, targets with a context score smaller or equal to -0.15 were retained. In DIANA-microTCD, targets with miTG scores greater or equal to 0.85 were selected. Predicted targets from miRDB with a score greater or equal to 80 were also kept. For miRanda and miRmap a cut-off threshold of miRSV score  $\leq -1.2$  and mirmap score  $\geq 90$  were applied, respectively. Finally, differentially expressed miRNA-target mRNA pairs were extracted only if there was an anti-correlation between metformin induced miRNA and mRNA levels (if miRNA was downregulated the mRNA should be upregulated and vice versa) and the pairs were common to at least 2 databases.

### 2.11.3 Network construction and analysis

Protein-protein interaction (PPI) networks were constructed using NetworkAnalyst online tool (Release 3.0) and extracted as a zero-ordered network from IMEx Interaction, which is a literature-curated comprehensive data from InnateDB ([948]. The PPI network was visualised and the expression values were incorporated into the network using Cytoscape software (version 3.4.0) [949]. The PPI network was then analyzed by network analyser, a plug-in of Cytoscape, and the topological properties of the network were assessed [950]. An important central parameter (degree) was considered for screening of the nodes. Genes with degree  $\geq 1$  were then selected and the network interaction file was extracted from Cytoscape. Selected miRNA-gene pairs (section 2.3.2) were added into the interaction files and then visualised using Cytoscape.

### 2.11.4 Pathway and gene ontology analysis and subnetwork construction

ClueGo (version 2.3.3), a Cytoscape plug-in was used to extract the non-redundant KEGG (version 305) pathways and GO terms (Biological Processes, Molecular Functions and Cellular Compartments) in functionally organized networks representing the connection between the pathways or GO terms based on the similarity of their linked genes [951]. At least 3 genes per term and 4 percent attribution in the term were considered. The terms were grouped based on the kappa scores, which is a robust measurement of the agreement occurring by chance. For network connectivity, kappa score was set at 0.04. GO term fusion was applied and cut-off for term p value was 0.05. For GO analysis, the experimental evidences were selected which include Inferred from Experiment (EXP), Inferred from Direct Assay (IDA), Inferred from Physical Interaction (IPI), Inferred from Mutant Phenotype (IMP), Inferred from Genetic Interaction (IGI) and Inferred from Expression Pattern (IEP).

Pathway with the lowest term p value and the leading pathway with the lowest group p value were selected and sub-networks were constructed using Cytoscape. To map the gene-miRNA pairs into the selected KEGG pathways, pathways were retrieved from the Wikipathways and PathVisio software was used to visualize the genes and incorporate miRNAs into the pathways [952, 953].

## 2.12 High throughput screening and high content imaging

### 2.12.1 miRNA mimic transfections

HCT116 cells were maintained as described at section 2.1. Cells were maintained at  $< 75\%$  confluence and tested for mycoplasma. The cells were transfected in 384-well plate format with 25 nM final concentration of Dharmacon Human miRIDIAN miRNA Mimic Library 19.0 + 21.0

Supplement (Dharmacon, Horizon Discovery Group, Cambridge, UK) using the Cell Explorer platform (Perkin Elmer, Massachusetts, USA), comprising a Janus Liquid Handler Workstation and BioTek Microplate Washer and Dispenser (Perkin Elmer, Massachusetts, USA). siRNA targeting PLK1 gene and scrambled negative control (Invitrogen, Life Technologies, California, USA) used as a positive and negative death control Table 2-6. Transfection was performed with DharmaFECT 2 Transfection Reagent (Dharmacon, Horizon Discovery Group, Cambridge, UK) in Opti-MEM I Reduced Serum Media (Invitrogen, Life Technologies, California, USA), using volumes of 0.05 and 8  $\mu\text{L}/\text{well}$ , respectively. The screen was performed in duplicates: two replicates for miRNA mimic transfected and metformin treated plates (A, B) and two for miRNA mimic transfected and non-treated plates (C, D). Firstly, 32  $\mu\text{L}/\text{well}$  Dharmafect 2 in Opti-MEM I was dispensed into A plate using BioTek and incubated for 5 minutes at room temperature. Using the Janus workstation, 8  $\mu\text{L}$  of each miRNA mimic (625 nM) was dispensed from library plates into the corresponding A plates and then 10  $\mu\text{L}$  aliquoted to each of B, C, and D plates. Using the BioTek dispenser, 5  $\mu\text{L}/\text{well}$  Opti-MEM I dispensed into A, B, C and D plates and plates were then incubated at room temperature for 20 minutes. Meantime, control siRNAs were dispensed into A plate and then distributed into B, C and D plates. Cells were counted and seeded at 900 cells/well (35  $\mu\text{L}$ ) using the BioTek dispenser and incubated at room temperature for 30 minutes before incubating them at 37°C and 5% CO<sub>2</sub> for 24 hours. After 24 hours incubation, the media was changed for plates C and D and metformin treatment was performed form plates A and B, aspirating 25  $\mu\text{L}/\text{well}$  of media and dispensing 25  $\mu\text{L}/\text{well}$  of media or 5 mM metformin using the BioTek dispenser. Plates were then incubated at 37°C and 5% CO<sub>2</sub> for 72 hours.

### 2.12.2 Metformin treatment of functional screen plates

After 24 hours incubation, the medium was changed for plates C and D and metformin treatment was performed for plates A and B at the final concentration of 2.5 mM, aspirating 25  $\mu\text{L}/\text{well}$  of media and dispensing 25  $\mu\text{L}/\text{well}$  of media/5 mM metformin using the BioTek dispenser. Plates were then incubated at 37°C and 5% CO<sub>2</sub> for 72 hours.

### 2.12.3 Cell staining and high content imaging

Treatment-induced changes in cell number and cell morphology were investigated using the Operetta high-content imaging system (Perkin Elmer Life Sciences, Boston, MA, USA), along with Harmony software (Perkin Elmer Life Sciences, Boston, MA, USA ) and PhenoLOGIC machine learning, according to a method recently described by Massey [954]. Briefly, after 96 hours post-transfection and treatment, cells were labelled with final concentrations: 0.5 mM Calcein-AM/well and 2 mM Hoechst 33342 /well, by adding 50  $\mu\text{L}$  of 2 x final concentration of dyes in 1X PBS

and incubating for 15 min at room temperature. Subsequently, 50  $\mu\text{L}$  of the dyes and the media were removed by automated aspiration and the cells were fixed by adding 50  $\mu\text{L}$  of 5% (*v/v*) formaldehyde in PBS and incubating for 20 minutes at room temperature. Cells were washed twice with PBS and stored in 50  $\mu\text{L}$  PBS at 4°C. Cells were then imaged with an Operetta high-content imaging system using a 20 $\times$  long working distance objective. Typically, 3 fields per well were imaged. Image acquisition settings were described in Table 2-3.

**Table 2-3. Operetta high-content imaging settings.**

Channel	Transmission%	Time (ms)	Height ( $\mu\text{m}$ )
Brightfield	75	50	5
Hoechst 33342	60	40	22
Calcein-AM	6	25	22

#### 2.12.4 Primary screen data analysis

The dynamic range was calculated between the positive and negative control using  $Z'$  factor [955]. The  $Z'$ -factor is defined in terms of four parameters: the mean ( $\mu$ ) and standard deviations ( $\sigma$ ) of both the positive ( $p$ ) and negative ( $n$ ) controls (Equation 2-1).

**Equation 2-1.  $Z'$  Factor calculation.**

$$Z' \text{ Factor} = \frac{3(\sigma_p - \sigma_n)}{|\mu_p - \mu_n|}$$

The values calculated for  $Z'$  factor, for each screen plate, were binned in the following manner and the analyses were done only if the  $Z'$  factor was “excellent” or “good” where 0.5-1 indicates excellent, 0.3-0.5 indicates good, 0-0.3 was acceptable and there was too much overlap between the controls if  $Z'$  factor was less than 0.

Raw values for each replicate were normalised to the average of the negative control raw values for the same plate, the normalised values for duplicates were averaged to get the final normalised value per treatment and to classify the hits, the fold change ratios of averaged normalised values, for samples relative to negative controls, were calculated. The standard thresholds and binning nomenclature for average normalised viability scores were defined as: LC (low cell count) for fold change ratios less than 0.5, CV2 (moderate cell viability) for values between 0.5 and 0.8, CV1 (no change in viability) for values between 0.8 and 1.15 and HI (increased viability) for values more than 1.15.

For hit identification, the control versus drug bin was defined by calculating the percent ratio of metformin treated groups versus un-treated cohorts and the % ratios more than 30 were selected as the preliminary hits. To stratify the hits into priority outcome groups according to set cut-offs for each bin, the following criteria were set:

Among control/drug bins greater than 30%, the hits were selected if: 1) the average raw counts for the selected miRNA were more than 30, either in metformin treated or untreated HCT116 cells (the information was acquired from small RNA sequencing data). 2) miRNAs were from the same miRNA cluster or family. 3) miRNAs were shown to be up or downregulated by metformin treatment according to the literature (Summarized in Table 1.8). 4) miRNAs were involved in pathways, biological processes, cellular compartments or molecular functions. miRNA Pathway Dictionary Database (miRPathDB) was used to perform the pathway and gene ontology analyses (<https://mpd.bioinf.uni-sb.de/>) and selected those terms and pathways with strong evidence and FDR adjusted p value <0.05) [956].

### 2.12.5 Validation screen

To confirm the reproducibility of the primary screen configuration, the lead screen hits were rescreened under the same conditions as described in 2.14.1, 2.14.2 and 2.14.3. To confirm the hits, the coefficient of drug interaction was calculated for each miRNA mimic as described in [957]. The CDI values were classified as: 1)  $CDI \leq 0.7$  strong synergistic effect with metformin treatment, 2)  $0.7 < CDI \leq 1$  synergistic effect with metformin, 3)  $1 < CDI \leq 1.1$  additive effect with metformin, 4)  $CDI > 1.1$  antagonistic effect with metformin.

## 2.13 miRNA target validation

For predicted miRNA-mRNA target pair validation, miScript Target Protectors (Qiagen, Limburg, Netherlands) were used. The target protectors are modified single-stranded RNAs that interfere with the miRNA binding sites on the 3'UTR of the predicted targets, while having no effect on the other targets of the same miRNAs. In 24 well-plates, HCT116 cells were co-transfected with miRNA mimics and also the corresponding target protector/s designed for the specific genes or with a negative control target protector. The Qiagen online algorithm was used to design target protectors. The miRNA-mRNA pairs and the sequence of designed target protectors are listed in Table 2-6. The concentration of target protectors and miRNA mimics were 500 nM and 25 nM, respectively. The cells were seeded at a cell density of  $2.4 \times 10^4$  cells/mL, the media changed 24 hours post transfection and RNA was harvested 48 hours post-transfection using Trizol (2.3.1) for real-time RT-PCR.

## 2.14 Reagents and equipment used for experiments

Table 2-4. Chemicals and reagents

Reagent	Supplier
Acetone	Chem-supply, Gillman, SA, Australia
Acryamide-Bis	BioRad, Helcules, California, USA
Ammonium persulfate (APS)	Sigma–Aldrich, St Louis, MO, USA
Buffered Formalin (10%)	Orion Labs, California, USA
Chloroform	Chem-supply, Gillman, SA, Australia
Complete Mini Phosphatase Inhibitor Cocktail Tablets	Roche, Basel, Switzerland
Complete Mini Protease Inhibitor Cocktail Tablets	Roche, Basel, Switzerland
Crystal Violet	Sigma–Aldrich, St Louis, MO, USA
DharmaFECT 2 Transfection Reagent	Dharmacon, Horizon Discovery Group, Cambridge, UK
Dimethyl sulfoxide	Sigma–Aldrich, St Louis, MO, USA
DL-Dithiothreitol	Sigma–Aldrich, St Louis, MO, USA
DNA ladders (100 bp)	Promega, Madison, WI, USA
DNA loading dye	New England Biolabs, Ipswich, MA, USA
DNase buffer	Promega, Madison, WI, USA
DNase inactivation slurry	Ambion, Foster City, CA, USA
dNTP mix	Promega, Madison, WI, USA
Dulbecco's Modified Eagle Medium	Invitrogen, Newcastle, NSW, Australia
Enhanced chemiluminescence reagents	SuperSignal West Pico, Rockford, IL, USA
E-plate 16	Roche, Basel, Switzerland
Ethanol	Chem-supply, Gillman, SA, Australia
EZQ Protein Quantitation kit	Invitrogen, Newcastle, NSW, Australia
Fast SYBR Green Master Mix	Applied Biosystems, Foster City, CA, USA
Foetal bovine serum	Bovogen Biologicals, Essendon, VIC, Australia
Formaldehyde	Chem-supply, Gillman, SA, Australia
Glycine	Sigma–Aldrich, St Louis, MO, USA
Human miRIDIAN miRNA Mimic Library 19.0 + 21.0 Supplement	Dharmacon, Horizon Discovery Group, Cambridge, UK
Hydrochloric acid	Chem-supply, Gillman, SA, Australia
Immobilon transfer polyvinylidene difluoride membrane	BioRad, Helcules, California, USA
Isopropanol	Chem-supply, Gillman, SA, Australia
Lipofectamine 2000 Transfection Reagent	Invitrogen, Newcastle, NSW, Australia
Metformin hydrochloride	Sigma–Aldrich, St Louis, MO, USA
M-MLV Reverse Transcriptase, Rnase H minus, Point mutant	Promega, Madison, WI, USA
N,N,N',N'-Tetramethylethylenediamine (TEMED)	BioRad, Helcules, California, USA
Opti-MEM Reduced Serum Medium	Invitrogen, Newcastle, NSW, Australia
Ovalbumin (2mg/ml)	BioRad, Helcules, California, USA
Phosphate Buffer Saline	Sigma–Aldrich, St Louis, MO, USA
Platinum Taq Polymerase	Invitrogen, Newcastle, NSW, Australia

## CHAPTER 2

Pre-stained protein markers (broad range 10 – 230 kDa)	New England Biolabs, Ipswich, MA, USA
PVDF membrane	BioRad, Hercules, California, USA
Random Hexamer	Invitrogen, Newcastle, NSW, Australia
RQ1 RNase-Free DNase	Promega, Madison, WI, USA
Skim milk powder	Fonterra, Mt Waverley, VIC, Australia
Sodium chloride	Chem-supply, Gillman, SA, Australia
Sodium dodecyl sulfate	Sigma–Aldrich, St Louis, MO, USA
TaqMan MicroRNA Reverse Transcription Kit	Applied Biosystems, Foster City, CA, USA
Triton X-100	Sigma–Aldrich, St Louis, MO, USA
Trizma Base	Sigma–Aldrich, St Louis, MO, USA
Trizma HCl	Sigma–Aldrich, St Louis, MO, USA
TRIzol Reagent	Sigma–Aldrich, St Louis, MO, USA
TrypLE Express (trypsin)	Invitrogen, Newcastle, NSW, Australia
Tween-20	Sigma–Aldrich, St Louis, MO, USA
Whatman filter paper	Whatman, Maidstone, Kent, UK

**Table 2-5: Equipment and software**

<b>Equipment</b>	<b>Supplier</b>
Agilent 2100 Bioanalyzer	Agilent Technologies, Santa Clara, CA, USA
Allegra X-22 R centrifuge	Beckman Coulter, Brea, CA, USA
Axiovert 25 light microscope	Ziess, Jena, Germany
BioTek Microplate Washer	Perkin Elmer, Massachusetts, USA
ChemiDoc Image System	Bio-Rad, Hercules, CA, USA
CO2 water jacketed cell incubator	Forma Scientific, Marietta, OH, USA
Cytoscape software (version 3.4.0)	National Institute of General Medical Sciences, MSC, USA
Dry block heater	Thermoline L+M, Sydney, NSW, Australia
Ensign Multimode Plate Reader	Perkin Elmer, Ohio, USA
Epson Perfection 4990 Scanner	Epson America, California, USA
Gel tank blotting system	Bio-Rad, Hercules, CA, USA
GeneAmp PCR system 9700 thermal cycler	Applied Biosystems, Foster City, CA, USA
IKA vortexer	Agilent Technologies, Santa Clara, CA, USA
Illumina Nextseq sequencing platform	Illumina Inc., California, USA
IncuCyte Live Cell Image Analysis System	Essen Bioscience
JANUS Liquid Handler Workstations	Perkin Elmer, Massachusetts, USA
Microcentrifuge 5424	Eppendorf, Hamburg, Germany
Nanodrop-8000	Nanodrop Technologies, Wilmington, DE, USA
Operetta high-content imaging system	Perkin Elmer, Massachusetts, USA
Power-Pac Basic	Bio-Rad, Hercules, CA, USA
Programmable Thermal Controller	MJ Research, Waltham, MA, USA
Rocking platform	Ratek, Boronia, VIC, USA
Rotorgene Q	Qiagen, Valencia, CA, USA
Tempette Junior TE-85 water bath	Techne, Staffordshire, UK
Turbo Semi-wet Transfer System	Bio-Rad, Hercules, CA, USA

CHAPTER 2

Ultra-low temperature freezer (-80°C)	Thermo Scientific Revco, Waltham, MA, USA
Weigh scales	Shimadzu, Kyoto, Japan
xCELLigence RTCA DP instrument	Roche, Basel, Switzerland

**Table 2-6: Primers and oligonucleotides**

Assay	Assay ID	Supplier
Random primer 6	S1230S (5' d(N <sub>6</sub> ) 3' [N=A,C,G,T])	New England Biolabs, Ipswich, MA, USA
<b>Taqman assays:</b>	<b>Assay ID</b>	<b>Supplier</b>
hsa-miR-106b-5p	000442	Applied Biosystems, Foster City, CA, USA
hsa-miR-132-3p	000457	
hsa-miR-149-5p	002255	
hsa-miR-185-5p	002271	
hsa-miR-195-5p	000494	
hsa-miR-2110	121216_mat	
hsa-miR-222-3p	002276	
hsa-miR-345-5p	002186	
hsa-miR-34a-5p	000426	
hsa-miR-374a-5p	002125	
hsa-miR-429	001024	
hsa-miR-589-3p	001543	
hsa-miR-590-3p	002677	
hsa-miR-7-1-3p	001338	
hsa-miR-766-3p	001986	
hsa-miR-92a-1-5p	002137	
hsa-miR-16	000391	
RNU6B	001093	
<b>miRNA oligonucleotide duplexes:</b>	<b>Sequences</b>	<b>Supplier</b>
hsa-miR-1181 antisense	5' GCUCGGGUGGGCGGCGACGGUU 3'	GenePharma, Shanghai, China
hsa-miR-1181 sense	5' CCGUCGCCGCCACCCGAGCCG 3'	
hsa-miR-132-3p antisense	5' ACCAUGGCUGUAGACUGUUAUU 3'	
hsa-miR-132-3p sense	5' UACAGUCUACAGCCCAUGGUCG 3'	
hsa-miR-145-3p antisense	5' AACAGUAUUUCCAGGAAUCCUU 3'	
hsa-miR-145-3p sense	5' GGAUUCUGGAAAUAUCUGUUCU 3'	
hsa-miR-149-5p antisense	5' GAGUGAAGACACGGAGCCAGAUU 3'	
hsa-miR-149-5p sense	5' UCUGGCCUCCGUGUCUUCACUCCC 3'	
hsa-miR-18b-5p antisense	5' AACUGCACUAGAUGCACCUUAUU 3'	
hsa-miR-18b-5p sense	5' UAAGGUGCAUCUAGUGCAGUUAG 3'	
hsa-miR-2110 antisense	5' CUCAGCGGCCGUUCCCAAUU 3'	
hsa-miR-2110 sense	5' UUGGGGAAACGGCCGUGAGUG 3'	
hsa-miR-222-3p antisense	5' CCAGUAGCCAGAUGUAGCUUU 3'	
hsa-miR-222-3p sense	5' AGCUACAUCUGGCUACUGGGU 3'	
hsa-miR-3187-3p antisense	5' GCGCAGCCCCAUGGCCAAUU 3'	
hsa-miR-3187-3p sense	5' UUGGCCAUGGGGCGCGCGG 3'	
hsa-miR-345-5p antisense	5' GCCCUGGACUAGGAGUCAGCUU 3'	
hsa-miR-345-5p sense	5' GCUGACUCCUAGUCCAGGGCUC 3'	
hsa-miR-3687 antisense	5' GUCGCACGAACGCCUGUCCGGGUU3'	
hsa-miR-3687 sense	5' CCCGACAGGCGUUCGUGCGACGU 3'	
hsa-miR-374a-5p antisense	5' CUUAUCAGGUUGUAUUUAAAUU 3'	
hsa-miR-374a-5p sense	5' UUAUAAUACAACCUGAUAAGUG 3'	
hsa-miR-376b-5p antisense	5' ACAUAGAAGGAUAUCCACGUU 3'	

CHAPTER 2

hsa-miR-376b-5p sense	5' CGUGGAUAUUCUUCUAUGUUU 3'	
hsa-miR-449c-5p antisense	5' AGCCGCUAGCAAUACACUGCCUAUU 3'	
hsa-miR-449c-5p sense	5' UAGGCAGUGUAUUGCUAGCGGCUGU 3'	
hsa-miR-548v antisense	5' GUGCAAAAAGUAACUGUAGCUUU 3'	
hsa-miR-548v sense	5' AGCUACAGUUACUUUUGCACCA 3'	
hsa-miR-589-3p antisense	5' UGGGAACCGCAUUUGUUCUGAUU 3'	
hsa-miR-589-3p sense	5' UCAGAACAAAUGCCGGUCCAGU 3'	
hsa-miR-590-3p antisense	5' UAGCUUAUACAUAUUUUUAUU 3'	
hsa-miR-590-3p sense	5' UAAUUUUUAUGUAUAAGCUAGU 3'	
hsa-miR-655-5p antisense	5' ACAUAACACGGUAUACCCUUU 3'	
hsa-miR-655-5p sense	5' AGAGGUUAUCCGUGUUAUGUUC 3'	
hsa-miR-676-3p antisense	5' CUCAACAACCUUAGGACAGUU 3'	
hsa-miR-676-3p sense	5' CUGUCCUAAGGUUGUUGAGUU 3'	
hsa-miR-718 antisense	5' ACGCCCGGCGGGGCGGAAGUU 3'	
hsa-miR-718 sense	5' CUUCCGCCCGCCGGGCGUCG 3'	
hsa-miR-92a-1-5p antisense	5' CAUUGCAACCGAUCCCAACCUUU 3'	
hsa-miR-92a-1-5p sense	5' AGGUUGGGAUCGGUUGCAAUGCU 3'	
hsa-miR-99a-3p antisense	5' GACCCAUAAGAAGCGAGCUUGUU 3'	
hsa-miR-99a-3p sense	5' CAAGCUCGCUUCUAUGGGUCUG 3'	
NC mimic antisense	5' ACGUGACACGUUCGGAGAATT 3'	
NC mimic sense	5' UUCUCCGAACGUGUCACGUTT 3'	
<b>Gene specific primers</b>	<b>Sequences</b>	<b>Supplier</b>
ACTNB Forward	5' TTGCCGACAGGATGCAGAAG 3'	Sigma–Aldrich, St Louis, MO, USA
ACTNB Reverse	5' GCCGATCCACACGGAGTACT 3'	
B2M Forward	5' GCCGTGTGAACCATGTGACTTT 3'	GeneWorks Thebarton, South Australia
B2M Reverse	5' CCAAATGCGGCATCTTCAAA 3'	
CDKN1A Forward	5' AGACACTGGCCCTCAAATC 3'	Integrated DNA Technologies, Iowa, USA
CDKN1A Reverse	5' GTCTGACTCCTTGTTCCGCT 3'	
EFNA4 Forward	5' ATTACAGCGCTTACACCCCTT 3'	
EFNA4 Reverse	5' ATGGGCTGACTCAGACTTCC 3'	
GADD45A Forward	5' CAAGGGGCTGAGTGAGTTCAA 3'	
GADD45A Reverse	5' TCCITCCTGCATGGTTCTTTGTA 3'	
GAPDH Forward	5' TGCACCACCAACTGCTTAGC 3'	GeneWorks Thebarton, South Australia
GAPDH Reverse	5' GGCATGGACTGTGGTCATGAG 3'	
GPO1	5' ACTCCTACGGGAGGCAGCAGTA 3'	
HRAG-1 Forward	5' AGGAATTTAACTCACAACTGC 3'	
HRAG-1 Reverse	5' GCCATGAAGAGCAGTGAATTA 3'	
LAMC1 Forward	5' AAGACTGAACAGCAGACCGC 3'	Integrated DNA Technologies, Iowa, USA
LAMC1 Reverse	5' ATCCCGTCCCTTCTTTGCAG 3'	
LDHA Forward	5' AGCCCGATTCCGTTACCT 3'	
LDHA Reverse	5' CACCAGCAACATTCAATCCA 3'	

CHAPTER 2

<b>MECOM forward</b>	5' AGCAACGTCGAATCAAGACC 3'	GeneWorks Thebarton, South Australia
<b>MECOM Reverse</b>	5' AGCTTCAAGTGGGTCTAGTTAGTT 3'	
<b>MGSO</b>	5' TGCACCATCTGTCACTCTGTAAACCTC 3'	
<b>MKNK2 Forward</b>	5' CTGGTCCGAGCTACCTCACG 3'	Integrated DNA Technologies, Iowa, USA
<b>MKNK2 Reverse</b>	5' ATTTGATTGGGGGACGGGTG 3'	
<b>MYB Forward</b>	5' GTCGGAAGGTGCAACAGGAA 3'	
<b>MYB Reverse</b>	5' CAGGGAGTTGAGCTGTAGGC 3'	
<b>PDGFA Forward</b>	5' ACTGGATTCTGTCCGGGTG 3'	
<b>PDGFA Reverse</b>	5' TACAGCGAGGAGGTGTGGTT 3'	
<b>PIK3R3 Forward</b>	5' CTGTGCTCTGTGGCCGAT 3'	
<b>PIK3R3 Reverse</b>	5' TGGAGCACTAGCTCCTCAGA 3'	
<b>PKM2 Forward</b>	5' ATTATTTGAGGAACTCCGCCGCT 3'	GeneWorks Thebarton, South Australia
<b>PKM2 Reverse</b>	5' ATTCCGGGTACACAGCAATGATGG 3'	
<b>RRAS Forward</b>	5' TGTCTGACTACGACCCCACT 3'	
<b>RRAS Reverse</b>	5' GTACTGCTCTCTCATGGCCC 3'	Integrated DNA Technologies, Iowa, USA
<b>STMN1 Forward</b>	5' TTGTTTGGATGCCTCAGCCC 3'	
<b>STMN1 Reverse</b>	5' TGCCCCACCTGTAACGTAGA 3'	
<b>THBS1 Forwards</b>	5' CATGATCGCCGAGTGCAAGA 3'	
<b>THBS1 Reverse</b>	5' ACACCAGGAAGTTGGCGTTG 3'	
<b>TNFRS1A Forward</b>	5' CTGGAGCTGTTGGTGGGAATA 3'	
<b>TNFRS1A Reverse</b>	5' CTTTGTGGCACTTGGTACAGC 3'	
<b>VEGFA Forward</b>	5' GTGCATTGGAGCCTTGCCTTG 3'	
<b>VEGFA Reverse</b>	5' ACTCGATCTCATCAGGGTACTC 3'	
<b>miScript target protectors:</b>	<b>Seed sequence (and location on 3'UTR)</b>	<b>Supplier</b>
<b>PIK3R3</b>	Site 1: TTCCCAA (nucleotides 1041-1048)	Qiagen, Valencia, CA, USA
	Site 2: TTCCCAA (nucleotides 1937-1944)	
	Site 3: TTCCCAA (nucleotides 3467-3474)	
<b>STMN1</b>	Site 1: ATGTAGC (nucleotides 219-225)	
	Site 2: TGTTCTG (nucleotides 703-709)	
<b>negative control miScript target protector</b>	# MTP000002	
<b>Silencing siRNAs</b>	<b>Sequence</b>	<b>Supplier</b>
<b>PIK3R3_8 FlexiTube siRNA</b>	5' CAGGGCTGTAGTATTCAGTAA 3'	Qiagen, Valencia, CA, USA
<b>Negative control siRNA</b>	# SI03650325	
<b>Silencer™ Select Pre-Designed PLK1 human siRNA 2</b>	5' CAACCAAAGUCGAAUAUGATT 3' 5' UCAUAUUCGACUUUGGUUGCC 3'	Ambion, Foster City, CA, USA
<b>Negative control siRNA</b>	# 4390843	
<b>STMN1 siRNA</b>	5' GUGCGGAAGAACAAAGAAUTT 3' 5' AUUCUUUGUUCUCCGCACTT 3'	GenePharma, Shanghai, China
<b>NC siRNA</b>	5' UUCUCCGAACGUGUCACGUTT 3' 5' ACGUGACACGUUCGGAGAATT 3'	
<b>LDHA siRNA smartpool</b>	5' AAAGTCTTCTGATGTCATA 3' 5' TAAGGGTCTTTACGGAATA 3' 5' GGCAAAGACTATAATGTAA 3' 5' GGAGAAAGCCCGTCTTAATT 3'	Dharmacon, Horizon Discovery Group, Cambridge, UK
<b>PKM2 siRNA Smartpool</b>	5' TTGTTTGGATGCCTCGTTC 3' 5' TGGAGCTGTTGGTGGGAAT 3' 5' GGAGCACTAGCTCCTCAGA 3' 5' AGGGAGTTGAGCTGTAGGC 3'	
<b>Negative control siRNA Smartpool</b>	# D-001810-10	

## CHAPTER 2

**Table 2-7: Antibodies**

Antibody	Dilution	Supplier
p70 S6 Kinase	1:1000	Cell Signaling Technology, Danvers, MA, USA
Phospho-p70 S6 Kinase (Thr389)	1:500	Cell Signaling Technology, Danvers, MA, USA
$\alpha$ -Actinin Antibody	1:1000	Cell Signaling Technology, Danvers, MA, USA
AMPK $\alpha$ 1/2	1:500	Abcam, Cambridge, MA, USA
phospho-AMPK $\alpha$ (Thr172)	1:2000	Sigma–Aldrich, St Louis, MO, USA
STMN1	1:10000	Abcam, Cambridge, MA, USA
PIK3R3	1:1000	Cell Signaling Technology, Danvers, MA, USA
LDHA	1:1000	Cell Signaling Technology, Danvers, MA, USA
PKM2	1:1000	Cell Signaling Technology, Danvers, MA, USA

**Table 2-8: Buffers and solutions**

Buffer/ solution	Formula
<b>RIPA buffer</b>	10 mM Tris/HCl pH 7.4, 150 mM NaCl, 1mM EGTA, 1% Triton X-100, 1% deoxycholate, 0.1% SDS, 1 mM DDT. For 50 mM: 0.5 mL 1M Tris/HCl, 6.25 mL 1.2 M NaCl, 1 mL 50 mM EGTA, 0.5 mL Triton X-100, 5 mL 10% deoxycolate, 0.5 mL 10% SDS, 50 $\mu$ L 1M DTT, water to 50 mL.
<b>Resolving buffer</b>	For 15 mL: 4 mL 1.5 M Tris/HCl pH 8.8, 150 $\mu$ L 10% SDS, 5 mL Acrylamide, 75 $\mu$ L 10% APS, 12 $\mu$ L TEMED, water to 15 mL.
<b>Stacking buffer</b>	For 7.5 mL: 525 $\mu$ L 0.5 M Tris/HCl pH 6.8, 75 $\mu$ L 10% SDS, 1.2 mL Acrylamide, 38 $\mu$ L 10% APS, 12 $\mu$ L TEMED, water to 7.5 mL.
<b>5<math>\times</math> SDS Running buffer</b>	125 mM Tris Base, 1 M Glycine, 0.5% SDS. For 500 mL: 7.57 g Tris/HCl, 37.5 g Glycine, 25 mL of 10% SDS, water to 500 mL.
<b>Western Transfer buffer</b>	For 1 L: 200 mL of 5x BioRad Transfer buffer, 600 mL 100% ethanol, water to 1 L.
<b>10<math>\times</math> TBS</b>	0.2 M Tris Base, 1.37 M NaCl. For 500 mL: 12.1 g Tris Base, 40 g NaCl, water to 500 mL. pH adjusted to 7.6 using conc. HCl.
<b>1<math>\times</math> TBS-T</b>	1 $\times$ TBS, 0.1% Tween-20 For 500 mL: 50 mL 10 $\times$ TBS, 5 mL 10 $\times$ Tween-20, water to 500 mL.

# Chapter 3. Characterising metformin responses in CRC cells

---

## 3.1 Introduction and aims

As a tumour trait and to adapt to the hypoxic environment, continuously proliferating cancer cells switch to glycolysis to meet their energetic and biosynthetic demands. Therefore, interfering with aerobic glycolysis using targeted drugs, such as glycolytic enzyme inhibitors, could be therapeutically beneficial [778, 958]. However, the role of mitochondrial respiration has been undervalued in cancer biology and a clear insight into the adaptation of tumour cell mitochondria, upon glycolysis inhibition, is needed. On the other hand, drugs that serve as therapeutic agents by targeting mitochondrial activity confirm the reliance on mitochondrial activity in tumorigenesis and the necessity of multi-target interventions to target cancer metabolism.

Metformin is a biguanide that has been shown to have several anti-cancer properties [792]. At an organismal level, metformin treatment reduces insulin levels, which is a mitogen for cancer cells [849]. At the molecular level, metformin inhibits mitochondrial complex I of the electron transport chain and, thereby, reduces ATP production. A decreased ATP : AMP ratio results in AMPK activation which inhibits mTOR complex 1 [852]. As outlined in Chapter 1, mTOR regulates p70S6K and 4E-BP phosphorylation as two main downstream effectors [359], (Figure 1-4).

In the present chapter, the necessity for a high glycolytic rate in the tumour phenotype and the link between this phenomenon and alterations in mitochondrial metabolism is explored. Therefore, the aim of this chapter was to investigate the metabolic changes associated with inhibiting glycolysis in CRC cells and then to study the cellular and metabolic consequences of treating CRC cells with metformin.

## 3.2 Results

### 3.2.1 Consequences of glycolysis inhibition in CRC cells

HCT116 cells were transfected with LDHA and PKM2 siRNAs and proliferation measurements were taken using the IncuCyte Live Cell Analysis system every two hours. Confluency measurements showed about 10% higher proliferation in LDHA and PKM2 siRNA transfected cells compared with the negative control siRNA 65 hours post-transfection (Figure 3-1). The

knockdown efficiencies of LDHA and PKM2 siRNAs were 96 and 83 % at mRNA levels and 99 and 98% at protein levels, respectively (Appendix 1)

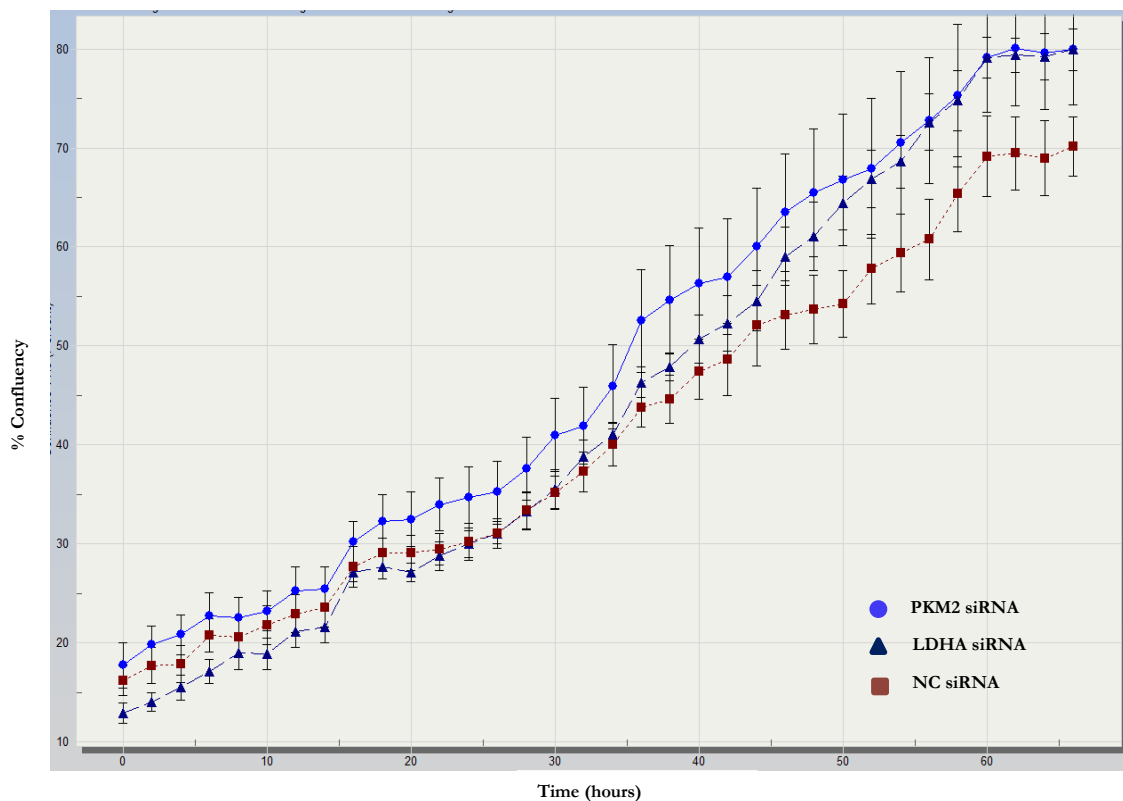


**Figure 3-1: Proliferation of HCT116 cells 65 hours post-transfection with LDHA or PKM2 siRNA.**

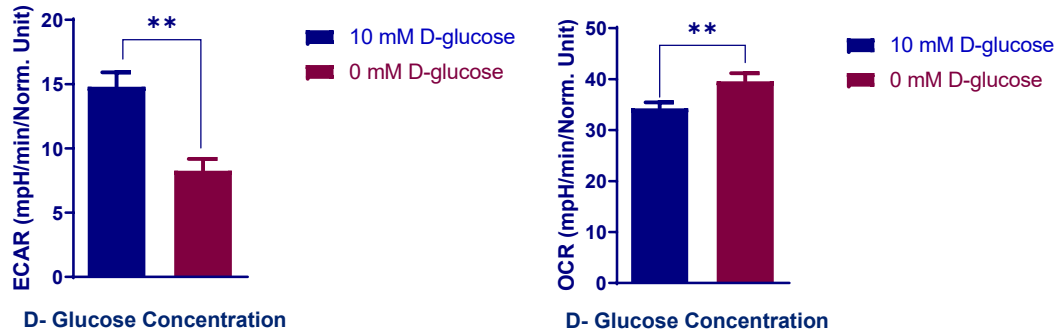
The % confluency measurements were obtained using IncuCyte Live Cell Analysis System. Light blue line with circular markers and dark blue line with triangle markers indicate LDHA and PKM2 siRNA transfected HCT116 cells while red line with square markers indicates negative control siRNA transfected cells. The mean  $\pm$  SEM of three cell culture replicates, at each 2 hour time interval, is shown.

To investigate the glycolytic and mitochondrial activity of HCT116 cells, extracellular acidification rate (ECAR), which is associated with the production of lactic acid, and oxygen consumption rate (OCR), as a measure of mitochondrial respiration rate, were acquired using a Seahorse XFe96 Extracellular Flux Analyzer.

HCT116 cells showed about 15% increased mitochondrial respiration ( $P = 0.0095$ ) when glycolysis was inhibited by removing D-glucose from the media compared with 10 mM D-glucose treated cells ( $P = 0.0015$ , Figure 3-2A). Also, when oxidative phosphorylation was inhibited by 1  $\mu$ M

oligomycin treatment ( $P < 0.0001$ ), HCT116 cells had a greater glycolytic rate as indicated by a 50% increase in ECAR levels, p value 0.0004 (Figure 3-2B).

(A)



(B)

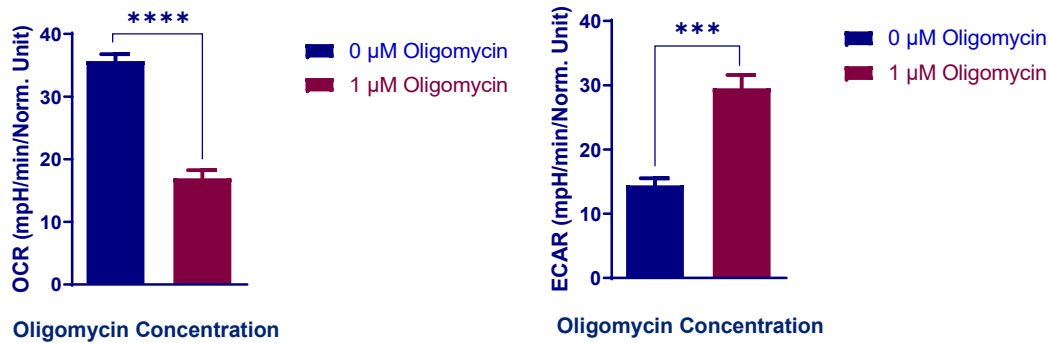


**Figure 3-2: Metabolic changes associated with D- glucose and oligomycin treatment of HCT116 cells.**

Real-time ECAR and OCR measurement in HCT116 cells treated with 10 mM D- glucose (A) and 1  $\mu$ M oligomycin (B) for 30 min compared with cells in control medium as a measure of glycolytic and mitochondrial activity of the cells, respectively. Results are expressed as mean  $\pm$  SD of 3 culture replicates and statistical significance is indicated with asterisks (\*\*  $P \leq 0.01$ , \*\*\*  $P \leq 0.001$ , \*\*\*\*  $P \leq 0.0001$ ).

To gain some understanding of the dependency of tumour cell growth on the glycolytic phenotype and the adaptation of mitochondrial metabolism upon glycolysis inhibition, the effect of blocking glucose to lactate conversion by LDHA or PKM2 RNA interference was explored. The results showed that suppressing aerobic lactate production, as confirmed by a decrease in glycolysis by 16% and 32% in LDHA and PKM2 siRNA transfected HCT116 cells, respectively ( $P < 0.05$  and 0.01, respectively, Figure 3-3a), directly impacts mitochondrial respiration. HCT116 cells with decreased LDHA and PKM2 activities demonstrated an increase in basal respiration, (by 38% and

## CHAPTER 3

123% with LDHA and PKM2 siRNA transfection, respectively) and maximal respiration (by 38% and 194% with LDHA and PKM2 siRNA transfection, respectively) and ATP synthesis (by 45% and 124% with LDHA and PKM2 siRNA transfection, respectively) (Figure 3-3b). Altogether, these data suggest that although CRC cells, in accordance with the Warburg effect, represent hyperactivated glycolysis for fast proliferation and growth, they retain the ability to switch to mitochondrial activity once glycolysis is suppressed, which imbues cancer cells with more efficient energy production and proliferation rates.

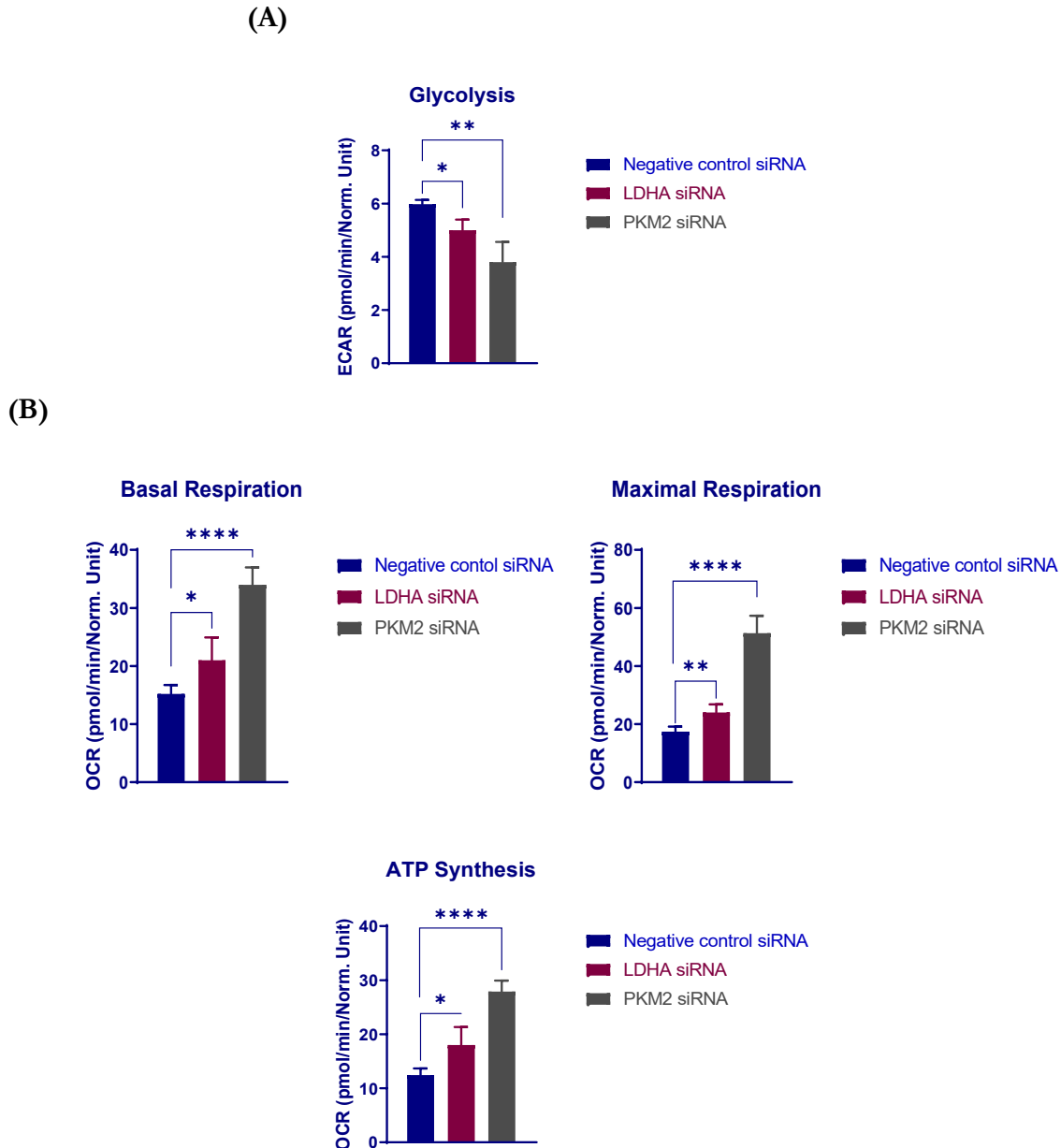


**Figure 3-3: Bio-energetic analysis of HCT116 cells transfected with LDHA or PKM2 siRNA.**

ECAR measurements for monitoring glycolysis in LDHA or PKM2 siRNA transfected cells (A) and OCR measurement for representing maximal and basal respiration and ATP turnover (B). Results are expressed as mean  $\pm$  SD independent culture replicates ( $n \geq 3$ ). The data are compared with negative control siRNA transfected HCT116 cells and the statistical significance is indicated with asterisks (\*  $P \leq 0.05$ , \*\*  $P \leq 0.01$ , \*\*\*\*  $P \leq 0.0001$ ). Glycolysis: [(maximum rate measurement before oligomycin injection) – (last rate before glucose injection)], basal respiration: [(last rate measurement before oligomycin injection) – (non-mitochondrial respiration rate)], maximal respiration: [(maximum rate after FCCP injection) – (non-mitochondrial respiration)] and ATP synthesis [(last rate measurement before oligomycin injection) – (minimum rate after oligomycin injection)].

### 3.2.2 Metformin has a dose-dependent effect on CRC cell viability

Since HCT116 cells showed an increase in proliferation when the mitochondrial activity of the cells was elevated, metformin treatment was performed to suppress mitochondrial respiration and replicate the results observed with oligomycin treatment. To this end, the effect of increasing doses of metformin treatment on CRC cell proliferation was tested. Treatment of a panel of CRC cell lines including HCT116, RKO, DLD-1, SW480, Caco2 and HT29 cells with increasing concentrations of metformin led to a dose-dependent decrease in cell viability over a period of 72 hours treatment. Viability measures using crystal violet dye, which binds to DNA and protein of the cells [959], showed that by 72 hours there is a dose-dependent reduction in cell growth with metformin treatment compared with the untreated control cells (Figure 3-4). Treatment of colorectal cancer cells revealed HCT116 cells to be the most susceptible and dose-dependent to the anti-proliferative effects of metformin. This was shown as 19%, 48% and 66 % reductions in cell viability with 2.5, 5 and 10 mM metformin treatments, respectively, compared to the untreated control cells ( $P \leq 0.0001$ ) (Figure 3-4).

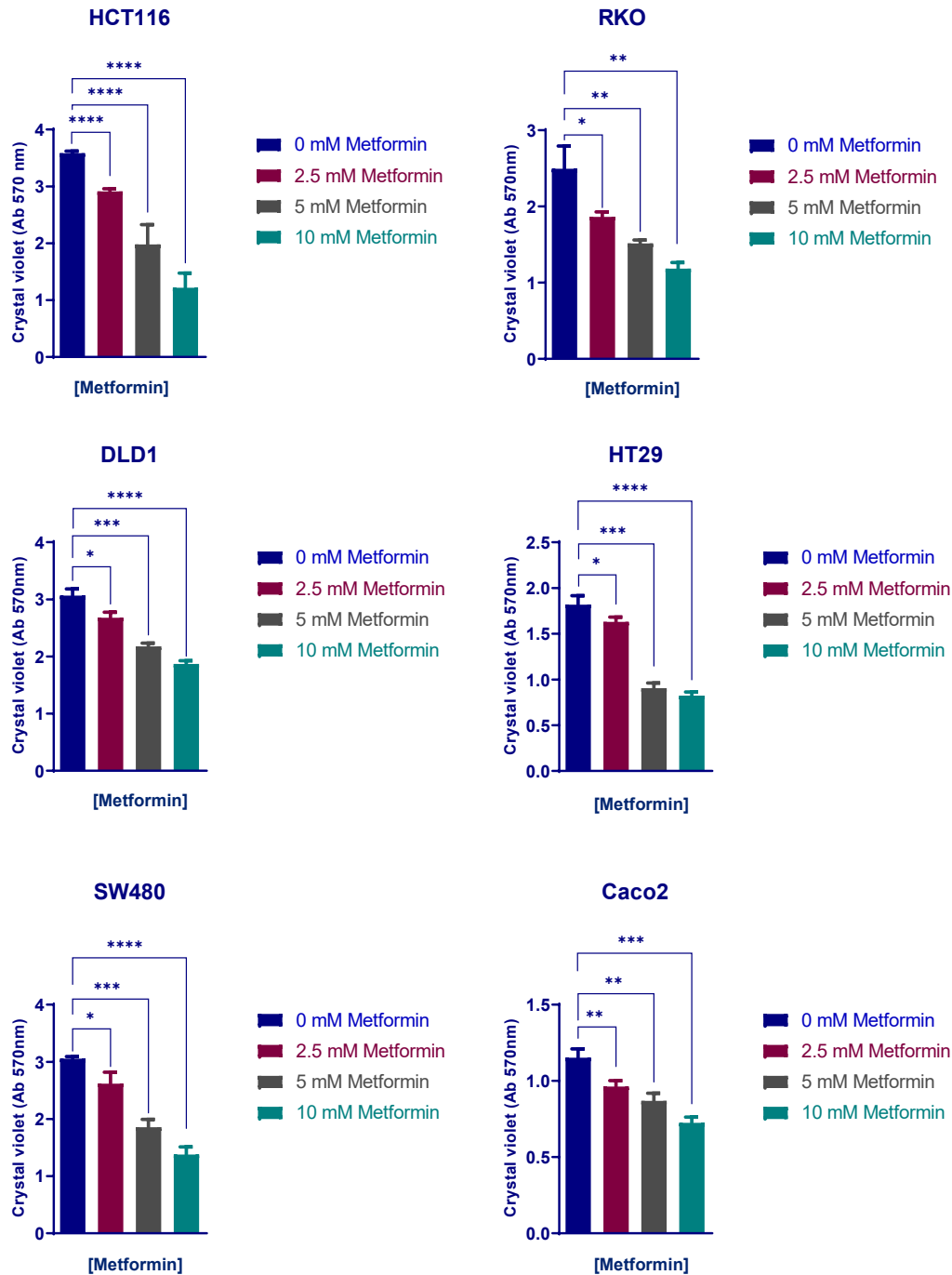


**Figure 3-4: Viability of different colorectal cancer cells after 72 h of 2.5 mM, 5 mM and 10 mM metformin treatment.**

Crystal violet absorbance measurements in HCT116, RKO, DLD-1, SW480, Caco2 and HT29 cells treated with increasing doses of metformin, compared with cells in control medium. Results are expressed as mean  $\pm$  SD of at least 3 replicates and statistical significance is indicated with asterisks (\*  $P \leq 0.05$ , \*\*  $P \leq 0.01$ , \*\*\*  $P \leq 0.001$ , \*\*\*\*  $P \leq 0.0001$ ).

The effect of metformin treatment on HCT116 cell proliferation was confirmed using the IncuCyte real-time live cell imaging instrument over a period of 72 hours after treatment (Figure 3-5). Collectively, these results confirm the anti-proliferative effect of metformin on CRC cells in a dose-dependant manner.

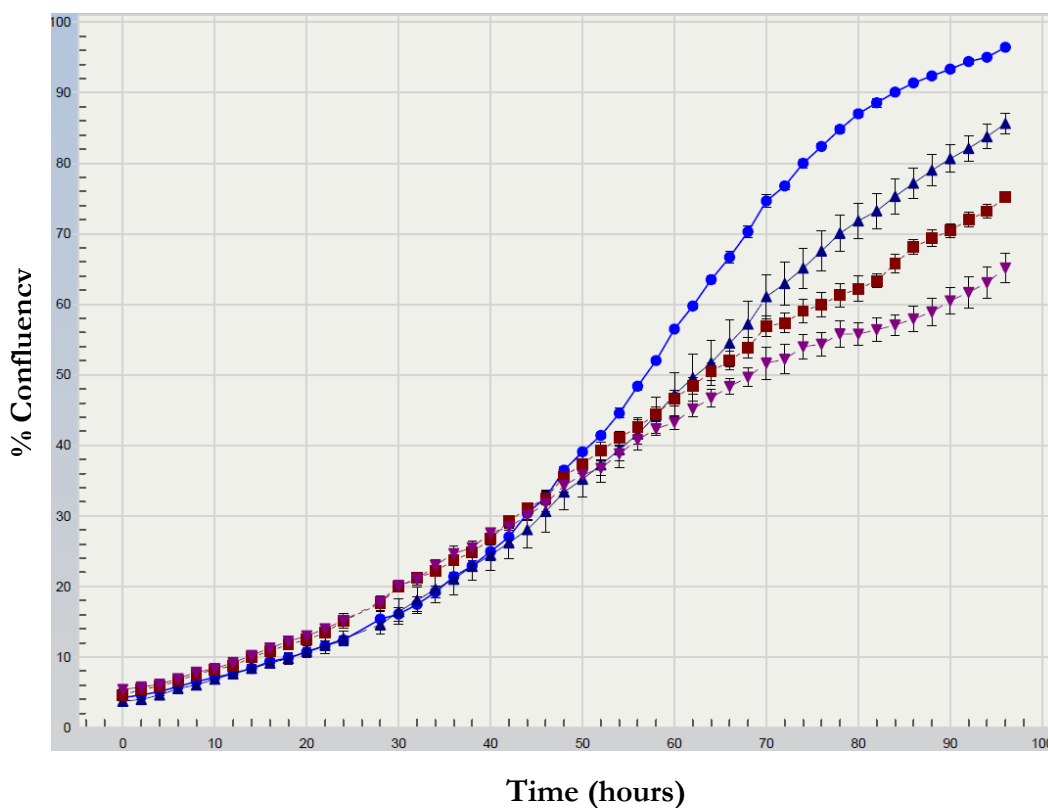


**Figure 3-5: Proliferation curves for HCT116 cells treated with 0, 2.5, 5 and 10 mM metformin, 24 h post cell seeding.**

The % confluency measurements for HCT116 cells treated with metformin and control medium were obtained using the IncuCyte Live Cell Analysis System. Metformin treatment was performed 24 hours post-cell seeding. The mean  $\pm$  SEM of three cell culture replicates, at 2 hour time intervals, is shown.

### 3.2.3 p53 and Kras mutational status do not affect the anti-proliferative effect of metformin

To test the effect of two major driver mutations (in *TP53* and *KRAS*) on the CRC cellular responses to metformin, two isogenic cell lines derived from HCT116 cells bearing *TP53* null (HCT116 p53 -/-) and mutant *KRAS* (HCT116 Kras +/-) status were tested. The viability of these cell lines was assessed using crystal violet assay following a 72 hour treatment and compared to

standard HCT116 cell response (as in Figure 3-6). As shown in Figure 3-6, *TP53* and *KRAS* status do not have significant effects on the cell response to the anti-proliferative effect of metformin.

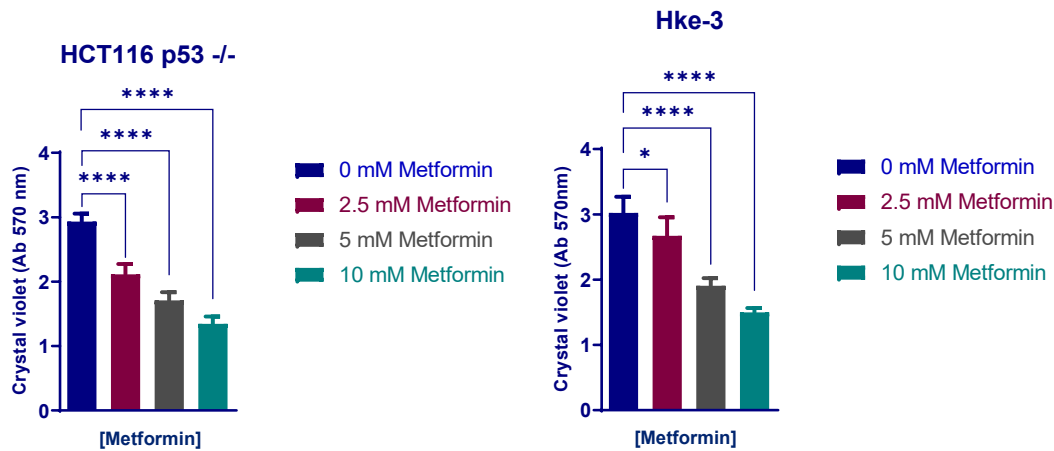


**Figure 3-6: Proliferation of HCT116 *TP53* null and Hke-3 (*KRAS* complemented) cells after 72 h of 2.5 mM, 5 mM and 10 mM metformin treatment.**

End point crystal violet staining representing viability of isogenic CRC cells 72 h post-metformin treatment. Results are expressed as mean  $\pm$  SD of at least 3 replicates and the statistical significance is indicated with asterisks (\*  $P \leq 0.05$ , \*\*\*\*  $P \leq 0.0001$ ).

### 3.2.4 Low concentrations of metformin have no pro-apoptotic effect on CRC cells

Effects of 2.5 mM, 5 mM and 10 mM metformin treatment on caspase 3/7 activity as a measure of apoptosis in HCT116, RKO, DLD-1, SW480, Caco2 and HT29 cells were explored. The caspase 3/7 activity was measured after 72 hours metformin treatment and data were normalised to the cell count (Figure 3-7). While 2.5 mM metformin treatment of CRC cells did not lead to a significant change in caspase 3/7 activity, 10 mM metformin treatment showed a significant pro-apoptotic role in all CRC cells tested with greater than two-fold increase evident in SW480, RKO and HCT116 cells compared to untreated control cells ( $P < 0.05$ ). There was an enhancement in caspase activity associated with 5 mM metformin treatment of SW480 and RKO cells (45 and 65 %, respectively,  $P < 0.05$ ).

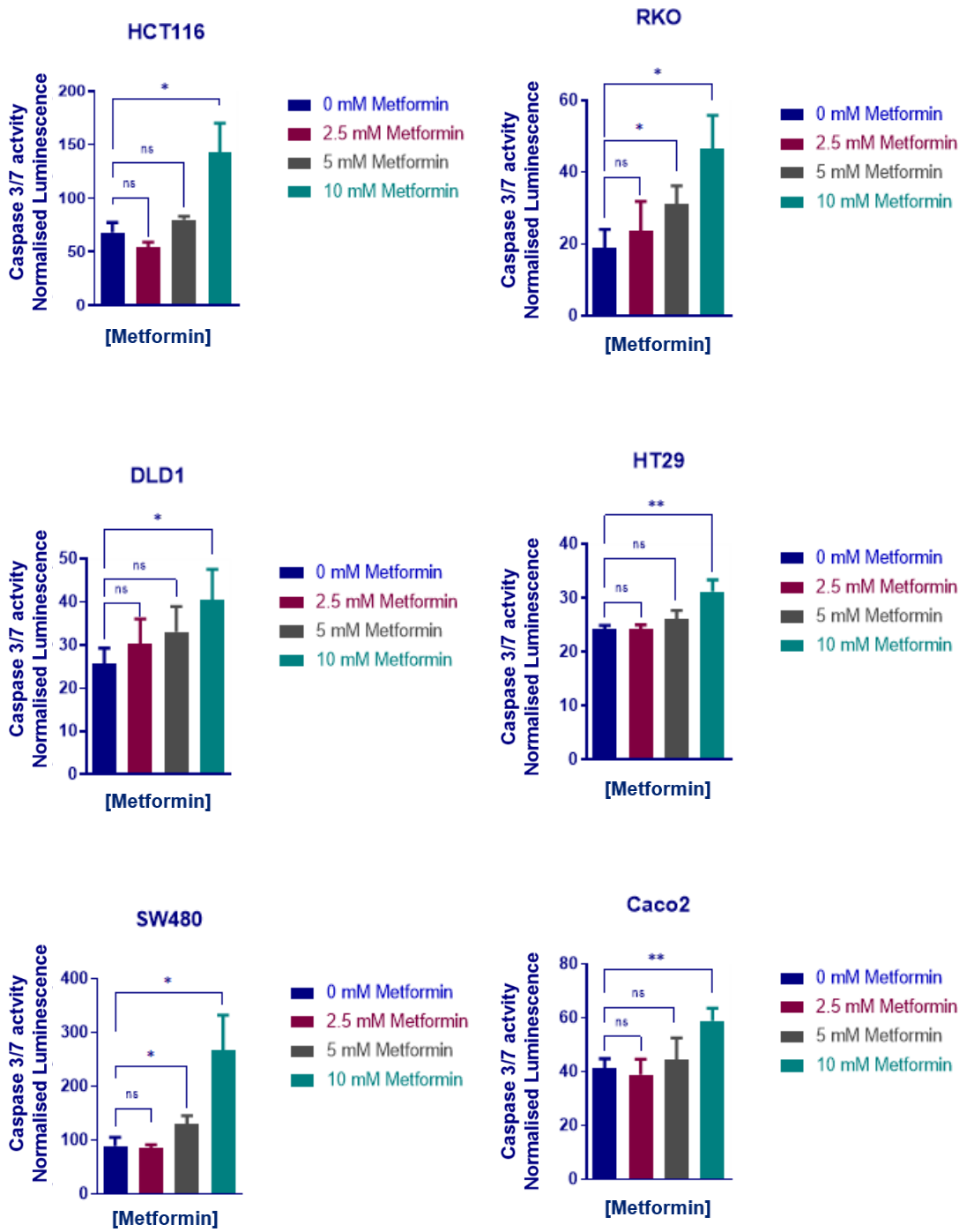
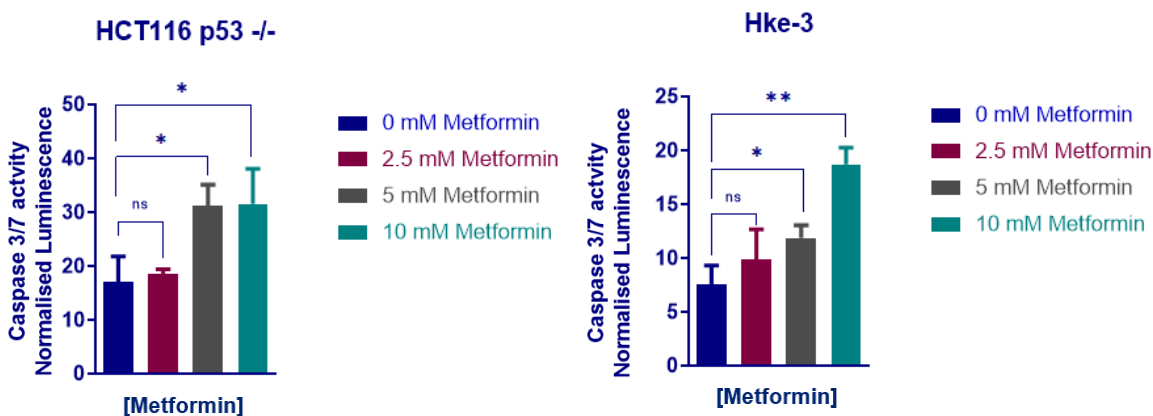


Figure 3-7: Apoptosis of HCT116, RKO, DLD-1, SW480, HT29 and Caco2 cells after 72 h of 2.5 mM, 5 mM and 10 mM metformin treatment.

Caspase 3/7 activity-related luminescence in HCT116, DLD-1, RKO, Caco2, SW480 and HT29 cells treated with increasing doses of metformin, compared with cells in control medium. Results are expressed as mean  $\pm$  SD of at least 3 replicates and statistical significance is indicated with asterisks (ns  $P > 0.05$ , \*  $P \leq 0.05$ , \*\*  $P \leq 0.01$ ).

### 3.2.5 *TP53* and *KRAS* mutational status do not affect the pro-apoptotic effect of metformin

To test the effect of driver mutations on the CRC cells' pro-apoptotic response to metformin, caspase 3/7 activity was quantified in *TP53* KO and *KRAS* complemented isogenic cell lines. As shown in Figure 3-8 and compared to HCT116 cells with wild type p53 and mutant *KRAS* (Figure 3-7), the p53 knock out isogenic cell line showed a further 65% induction in apoptosis at 5 mM metformin treatment. ( $P < 0.05$ ). In addition, in Hke-3 cells, there was about 38% enhanced effect on apoptosis at both 5 mM and 10 mM metformin compared to mutant *KRAS* HCT116 cells ( $P < 0.05$  and  $< 0.01$ , respectively). Therefore, these data suggest that although there was no significant change in the pro-apoptotic effect of metformin at 2.5 mM concentration, compared to the modified isogenic cell lines, wild-type p53 and overactive *KRAS* confer resilience to the pro-apoptotic role of metformin at higher concentrations.



**Figure 3-8: Apoptosis of HCT116 *TP53* null and Hke-3 (*KRAS* complemented) cells after 72 h of 2.5 mM, 5 mM and 10 mM metformin treatment.**

Caspase 3/7 activity measurements in HCT116 p53 -/- and HKe-3 cells treated with increasing doses of metformin, compared with cells in control medium. Results are expressed as mean  $\pm$  SD of at least 3 replicates and the statistical significance is indicated with asterisks (ns  $P > 0.05$ , \*  $P \leq 0.05$ , \*\*  $P \leq 0.01$ ).

### 3.2.6 Metformin treatment results in reduced ATP synthesis in a dose-dependent manner in CRC cells

Treatment of HCT116, RKO, DLD-1, SW480, HT29 and Caco2 CRC cells with increasing concentrations of metformin led to decreased ATP synthesis over a period of 72 hours treatment compared with the untreated control cells (Figure 3-9). ATP measures using a luciferase-based

## CHAPTER 3

assay showed that ATP turnover was susceptible to 5 mM and 10 mM metformin treatment in all 6 CRC cell lines and 2.5 mM metformin treatment resulted in a significant reduction in ATP levels in HCT116, DLD-1, HT29 and SW480 cells with RKO and SW480 cells having the most significant effect with 10 mM metformin treatment ( $P < 0.0001$ ). Comparing *TP53* and *KRAS* knock out isogenic cells derived from and compared to HCT116 cells, it can be concluded that the suppressing role of metformin on ATP synthesis is independent of *TP53* and *KRAS* status.

CHAPTER 3

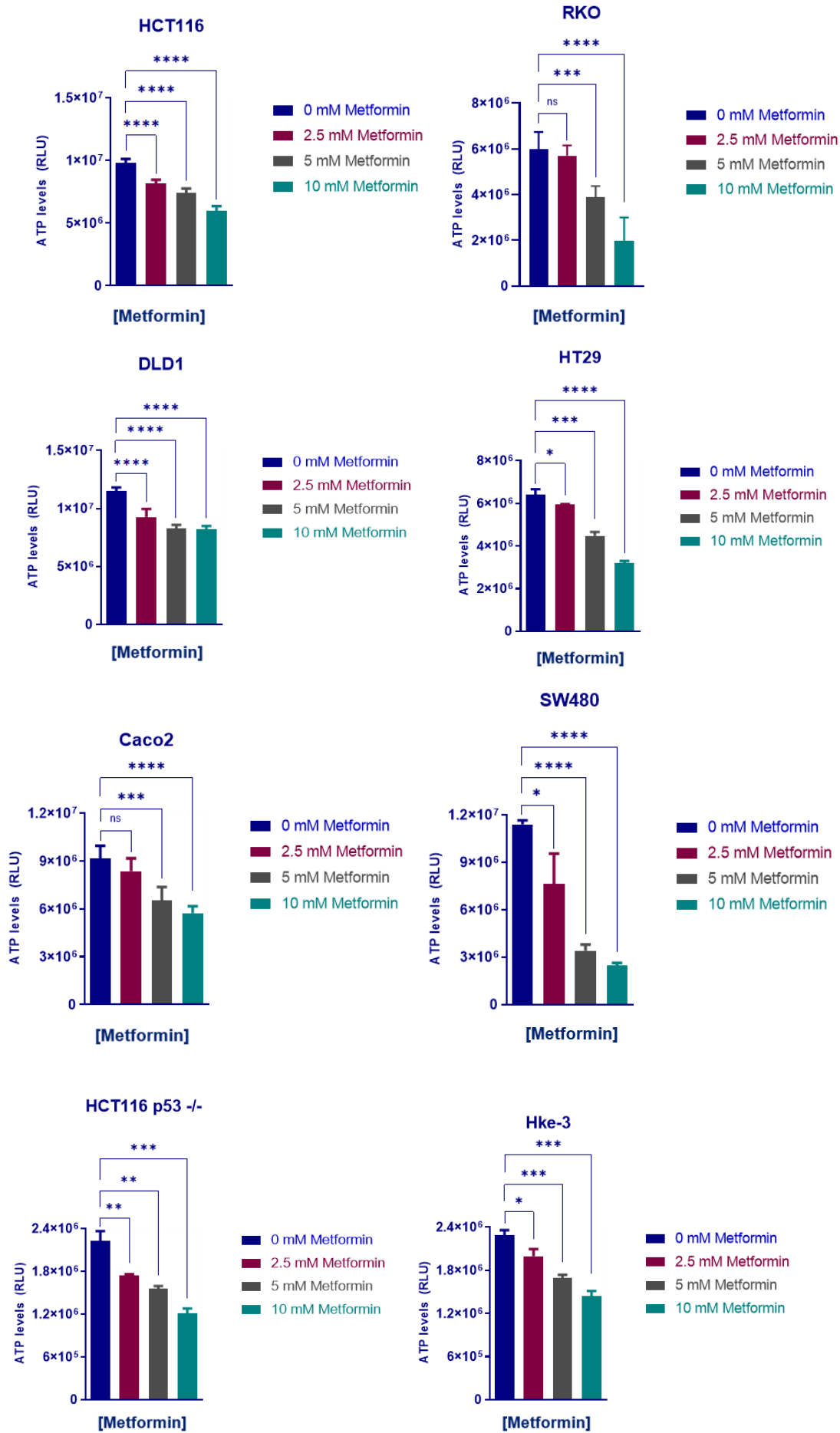


**Figure 3-9: ATP synthesis of CRC cells after 72 h of 2.5 mM, 5 mM and 10 mM metformin treatment.**

ATP measurements were performed using luciferase-base assay in HCT116, RKO, DLD-1, SW480, HT29 and Caco2 cells as well as p53-null and wild type *KRAS* isogenic cells treated with increasing doses of metformin, compared with cells in control medium. Results are expressed as mean  $\pm$  SD of at least 3 replicates and the statistical significance is indicated with asterisks (ns  $P > 0.05$ , \*  $P \leq 0.05$ , \*\*  $P \leq 0.01$ , \*\*\*  $P \leq 0.001$ , \*\*\*\*  $P \leq 0.0001$ ).

### 3.2.7 Effect of metformin on mitochondrial oxidoreductase activity of the colorectal cancer cells

Mitochondrial complex I oxidoreductase activity was assessed measuring the reduction rate of XTT (2,3-bis-(2-methoxy-4-nitro-5-sulphophenyl)-2H-tetrazolium-5-carboxanilide) by NADH produced in mitochondria. Among the CRC cell panel treated with increasing doses of metformin, HCT116 cells showed the highest dose-dependent susceptibility to the effect of metformin, having about 40 % reduction in mitochondrial activity at 10 mM metformin treatment. Also, RKO and HT-29 showed a slight reduction in oxidoreductase activity at high concentrations of metformin treatment. On the other hand, SW480 and DLD-1 showed no susceptibility to any concentrations of metformin. Compared to wild type p53 and activated *KRAS* proto-oncogene in HCT116, p53-null and wild type *KRAS* isogenic cell lines showed slightly less response to the anti-complex I role of metformin. By overlaying XTT assay results with ATP turnover changes associated with metformin treatment of the CRC cell panel, it was reasoned that HCT116 cells that showed a dose-dependent susceptibility to metformin treatment could provide the perfect model to study the targets and metabolic consequences of metformin.

CHAPTER 3

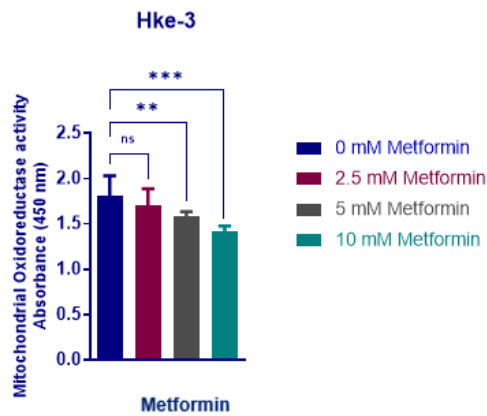
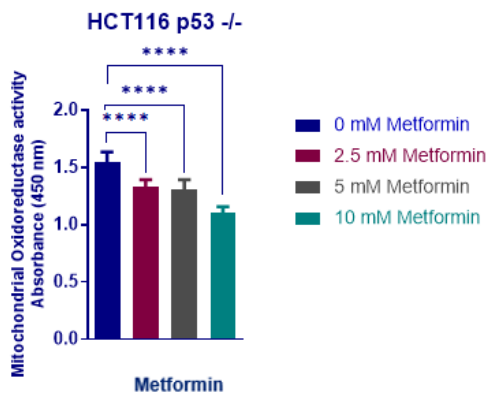
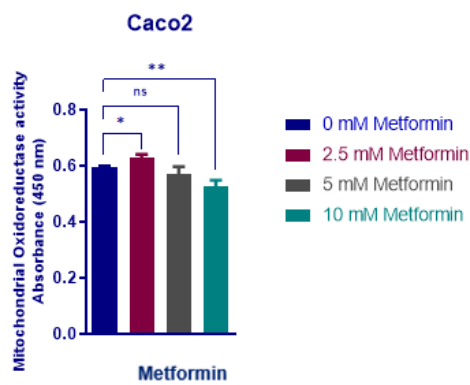
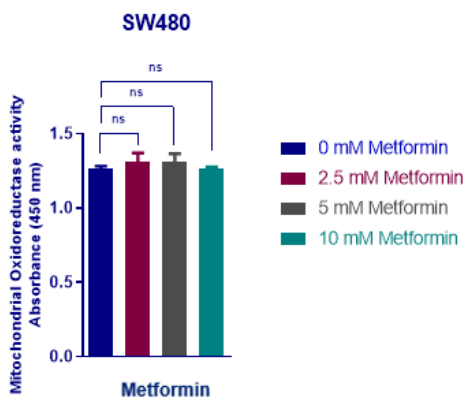
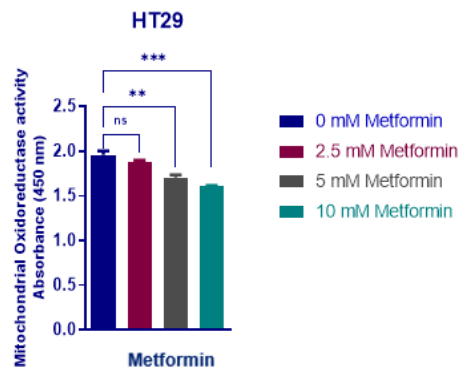
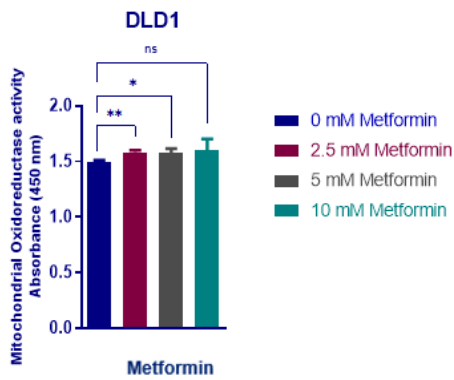
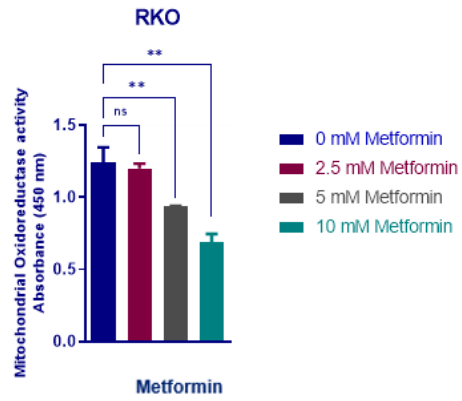
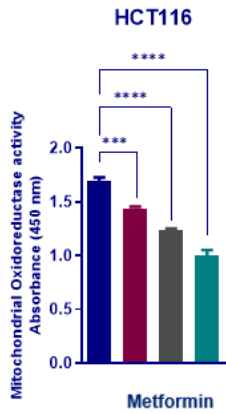


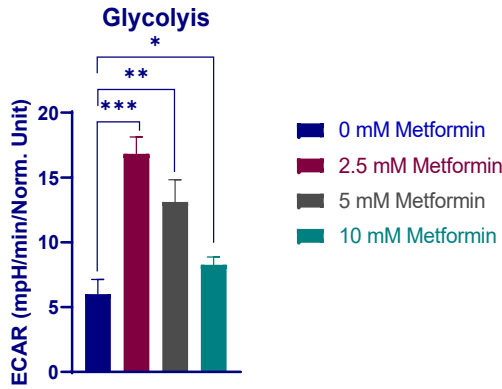
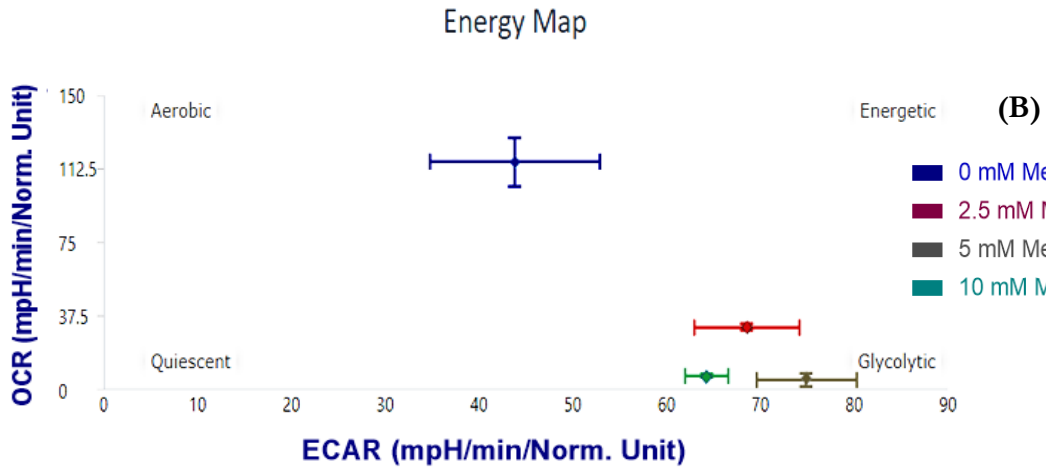
**Figure 3-10: Mitochondrial oxidoreductase activity of CRC cell panel 72 hours post-treatment with 2.5 mM, 5 mM and 10 mM metformin.**

The reduction rate of XTT by complex I activity was measured in CRC cells treated with metformin and compared with cells in control medium. Results are expressed as mean  $\pm$  SD of at least 3 replicates and the statistical significance is indicated with asterisks (ns  $P > 0.05$ , \*  $P \leq 0.05$ , \*\*  $P \leq 0.01$ , \*\*\*  $P \leq 0.001$ , \*\*\*\*  $P \leq 0.0001$ ).

**3.2.8 Effect of metformin on the metabolic profile of CRC cells**

The effect of metformin on metabolic characteristics of HCT116 cells was tested. As shown in an energy map (Figure 3-11A), metformin treatment resulted in a dramatic reduction in OCR levels, as reflected in basal and maximal respiration (Figure 3-11C). In addition, although there was a positive correlation between metformin doses and acidification rate in HCT116 cells (Figure 3-11A), the part of acidification that accounts for glycolysis showed a threshold effect at 2.5 mM metformin. In addition, metformin appeared to have a dose-dependent suppression effect on glycolytic capacity (Figure 3-11B).

(A)



(C)

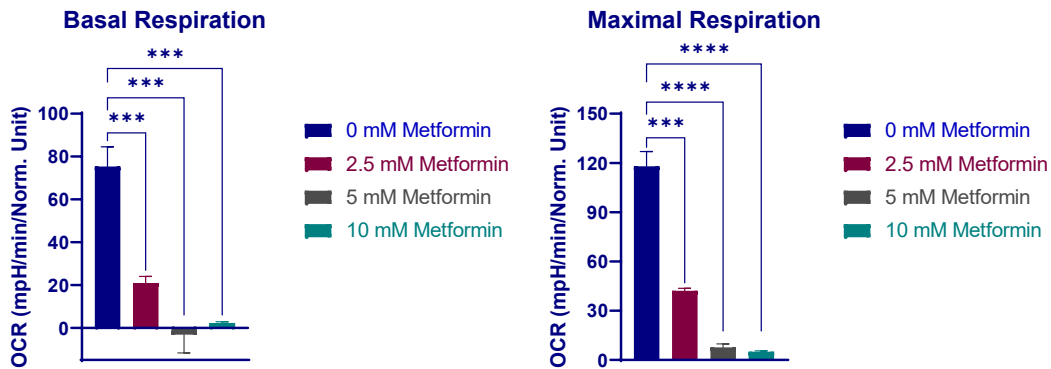


**Figure 3-11: The effect of metformin on metabolic characteristics of HCT116 cells was tested.**

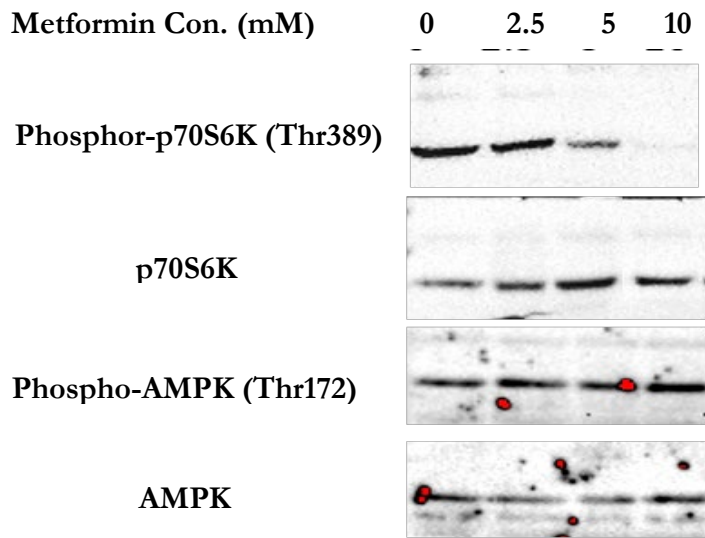
Energy map (A), glycolytic characteristics (B) and oxidative phosphorylation characteristics (C) of HCT116 cells treated with 2.5, 5 and 10 mM metformin for 72 hours are shown. ECAR and OCR measurements were taken using Seahorse XFe96 Extracellular Flux Analyzer. Results are

expressed as mean  $\pm$  SD of at least 3 replicates and the statistical significance is indicated with asterisks (ns  $P > 0.05$ , \*  $P \leq 0.05$ , \*\*  $P \leq 0.01$ , \*\*\*  $P \leq 0.001$ , \*\*\*\*  $P \leq 0.0001$ ). Glycolysis: [(maximum rate measurement before oligomycin injection) – (last rate before glucose injection)], Glycolytic Capacity: [(maximum rate measurement after oligomycin injection) – (last rate before glucose injection)], basal respiration: [(last rate measurement before oligomycin injection) – (non-mitochondrial respiration rate)], maximal respiration: [(maximum rate after FCCP injection) – (non-mitochondrial respiration)].

### 3.2.9 Effect of metformin on PI3K/AKT pathway

The inhibition of mTOR signalling following AMPK activation is considered to be a major consequence of metformin treatment in cancer cells [960]. To confirm the effect of metformin treatment on the PI3K-mTOR signalling pathway, AMPK, mTOR and P70S6K protein activity were selected for further investigation. Detected by immunoblot and normalised to total protein, metformin treatment resulted in elevated AMPK activity as shown by increased normalised phospho-AMPK (Thr172) signals (Figure 3-12a). Also, normalised phospho-mTORC1 (Ser24448) showed a dose-dependent decrease in levels, following metformin treatment of HCT116 cells, as measured by specific AlphaLISA assay (Figure 3-12b). As the downstream effector of the signalling pathway, inhibition of mTORC1 by metformin resulted in a decreased p70S6K activity as shown by diminished phospho-p70 S6K (Thr389) (Figure 3-12a). Together, these results support the proposed mechanism of action of metformin in HCT116 cells by modulating the mTOR signalling pathway.

(A)



(B)

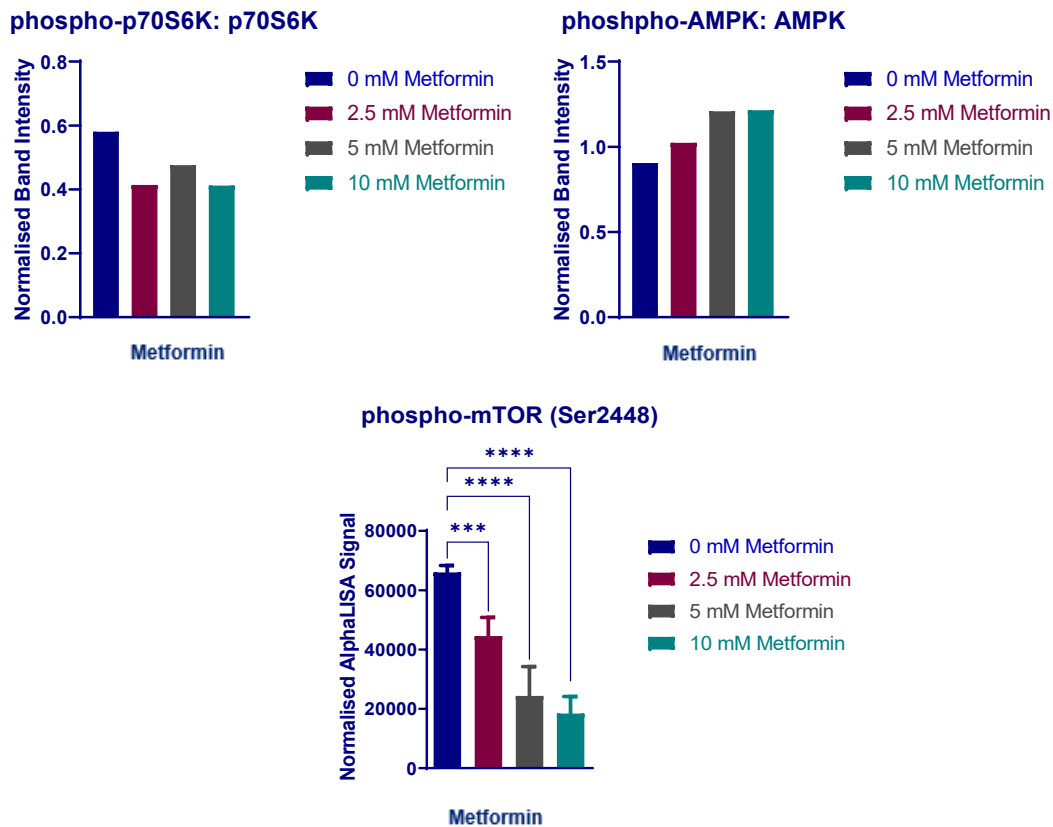


**Figure 3-12: Changes in mTORC1, p70S6K and AMPK phosphorylation of HCT116 cells associated with 2.5, 5 and 10 mM metformin treatment.**

Total p70S6K, phospho-p70S6K (Thr389), total AMPK and phospho-AMPK (Thr172) protein levels in cells treated with metformin compared with cells in control medium, as measured by Western blot image analysis and densitometry results of the total protein: phospho-protein ratio (A). Normalised AlphaLISA measures (B) for phospho-mTORC1 (Ser2448) protein levels in cells

treated with metformin and compared with cells in control medium shown as mean  $\pm$  SD of at least 3 replicates and normalised to the cell count. The statistical significance is indicated with asterisk (\*\*\*)  $P \leq 0.001$ , \*\*\*\*  $P \leq 0.0001$ ).

### 3.3 Discussion

In this chapter, the metabolic and biological characteristics of CRC cells were examined to develop a model for further investigations. Proliferating cells, and indeed cancer cells, require continuous cell division. In order to maintain this, there is an urgent need to provide a consistent energy source, macromolecular biosynthesis, and controlled redox status. Therefore, to optimise proliferation, growth and survival, cancer cells redirect their metabolic pathways and alter the production and consumption of numerous metabolites [62, 63]. In the 1920s, Otto Warburg's study compared glycolysis in cancer and normal cells in both air and nitrogen, to simulate normal and low oxygen abundance, and presented a major advance in understanding cancer metabolism. He demonstrated that both normal and cancer cells have a higher rate of glycolysis in hypoxia, while only cancer cells exhibit upregulated glycolysis in normoxia [961]. Nevertheless, based on the "Pasteur effect", in normal cells glycolysis is indirectly suppressed due, in part, to the presence of oxygen. As cancer cells rapidly use glucose to generate lactate through glycolysis, even in an oxygen-rich environment, this metabolic phenomenon became known as "aerobic glycolysis". Subsequently, aerobic glycolysis has been described as a universal metabolic hallmark of diverse tumour types [962]. LDHA overexpression was shown to be upregulated in different cancer types [963]. Accordingly, several studies have shown the feasibility of drugs that target glycolytic enzymes to inhibit cancer cell growth. Kim et al. [964], showed that an LDHA inhibitor (PSTMB), results in reduced LDHA activity and lactate production and inhibited cell growth of lung, breast, liver, colon and kidney cancer and melanoma. Glycolysis was shown to be augmented in tamoxifen resistant breast cancer cells, as shown in increased PKM2 and LDHA protein levels, and therefore, LDHA inhibition by oxamate treatment resulted in decreased cancer cell growth and increased cell apoptosis [965]. Similarly, several other studies, showed that pharmacological and genetic inhibition of LDHA reduces the cancer cell growth by inhibiting aerobic glycolysis [135, 958, 966-970]. PKM2 inhibitors also had suppressive effects on cancer cell growth. PKM2 is specifically enriched in continuously proliferating cancer cells and is a rate-limiting enzyme in glycolysis [971]. The high expression and lower catalytic enzyme activity of PKM2 are essential for the metabolic shift in cancer cells, to suppress ROS and promote tumour growth. Therefore, PKM2 may serve as a target for anti-cancer drugs [265, 972]. PKM2 inhibition resulted in decreased glycolytic activity of several cancer types and suppressed tumorigenesis [973-975]. For instance, TLN-232 is a PKM2

inhibitor and in a phase II clinical trial was shown to have anti-cancer properties in metastatic renal cells [976]

In this chapter, the metabolic characteristics of CRC cells were studied. Despite, active glycolysis in CRC cells, as shown by decreased extracellular acidification rates in glucose deprived cells (Figure 3-2), surprisingly, CRC cells transfected with the glycolytic enzyme siRNAs (LDHA or PKM2) showed a slightly higher proliferation rate compared with the control group (Figure 3-1).

Since the ratio of glycolysis to respiration was significantly elevated, Warburg originally hypothesized that cells undergoing aerobic glycolysis have impaired mitochondrial activity and reduced respiration; therefore, aerobic glycolysis is an essential adaptation to compensate for the lack of ATP generated through oxidative phosphorylation (OXPHOS) [1]. However, a twist in Warburg's concept has emerged with the findings that some cancer cells retain their mitochondrial function and consume oxygen similar to normal cells [977, 978]. Accordingly, as shown in Figure 3-11, HCT116 CRC cells, have active glycolysis and oxidative phosphorylation. Therefore, inhibition of either glycolysis or oxidative phosphorylation by glucose deprivation or oligomycin treatment, resulted in a concomitant increase in glycolysis or oxidative phosphorylation, respectively, to compensate for the energy loss (Figure 3-2). The results observed with glycolysis inhibition in LDHA and PKM2 siRNA transfected cells confirmed the simultaneous increase in mitochondrial activity as was shown by greater basal and maximal respiration and ATP synthesis (Figure 3-3). Collectively, these results emphasize the necessity of multi-target interventions for preventing CRC growth.

Metformin is an anti-diabetic drug with pleiotropic effects on cancer metabolism. Most of these effects have been traced to the mitochondrial oxidative phosphorylation chain (4-20). In this Chapter, metformin was used to target the mitochondrial respiration in CRC cells. In view of that, metformin treatment resulted in a marked decrease in basal and maximal respiration of HCT116 CRC cells. This decrease in oxidative phosphorylation was accompanied by an increase in glycolysis (Figure 3-11) and confirms the results observed with oligomycin treatment (Figure 3-2). Furthermore, the biological outcomes of metformin treatment were also investigated to characterize and develop a model for the following studies. In previous studies on CRC cells, metformin-associated decreases in cell proliferation, cell migration, cell cycle progression, hypoxia and inflammatory responses, as well as increases in apoptosis, susceptibility of the cells to oxidative stress or oxaliplatin, and moderate radiation protection, were reported [859, 876, 879-889]. Accordingly, metformin treatment of a panel of CRC cell lines bearing different driver mutations (Table 2-1) resulted in a dose-dependent decrease in cell viability and ATP turnover, with *TP53*

and *KRAS* mutational status having little to no significant effect on the response (Figure 3-4, Figure 3-6 and Figure 3-9). Despite consistent literature on the anti-proliferative effect of metformin, there are contradictions regarding the cytotoxicity of metformin. While some studies showed a pro-apoptotic effect of metformin in some cells [876, 878, 886], the protective effect of metformin against apoptosis is also reported and is mainly related to the stimulation of autophagy [851, 979, 980]. What's more, the effect of metformin on cell death seems to be dose and context dependent. In this present Chapter, the pro-apoptotic function of metformin was significant only in high concentration treatments (10 mM, Figure 3-7). The disparate effects on cell apoptosis may be explained by the different effects of moderate and excessive activation of autophagy which leads to decreased or stimulated cell death, respectively [851, 979]. However, the effect of metformin induced activation of autophagy through the AMPK pathway needs further investigation. Also, the effect of metformin on the activity of oxidative phosphorylation was tested. Although metformin had a dose-dependent inhibitory effect on ATP synthesis in all CRC cell lines, contrary to expectations, only HCT116 cells showed the same pattern of metformin effect on complex I oxidoreductase activity and there was not a significant change in complex I activity in other cell lines. Also, *TP53* and *KRAS* mutational status seemed to have no dramatic change on this effect (Figure 3-9 and Figure 3-10). Although it is difficult to explain this result, it might be related to the multi targeting nature of metformin and that there might be targets within glycolysis or an uncoupling effect that could possibly reduce ATP synthesis through glycolysis or uncouple nutrient oxidation from ATP production. It is worth mentioning that according to El-Mir et al., and Foretz et al., only high concentrations of metformin treatment (~ 5 mM) resulted in complex I inhibition in intact hepatocytes, leading to an increase in AMP/ATP ratio. Therefore, these studies dispute the relevance of complex I inhibition in the metformin-mediated response and emphasize AMPK- independent pathways [785, 981].

This chapter demonstrated the anti-proliferative effect of metformin examined in different colon cancer cell lines with different MSI status and driver mutations including *KRAS*, *BRAF*, *PIK3CA* and *TP53*. Also, the effect of *TP53* and *KRAS* mutational status on the function of metformin was tested. Overall, this chapter provided evidence to support the concept that metformin exerts a dose-dependent role in CRC cell proliferation and viability and it has overlapping biological functions in different colon cancer cells. Among the cell lines tested, HCT116 appears to be the most responsive cell line to the different anti-cancer effects of metformin, including reduced viability and suppressed mitochondrial activity. Also, activated *KRAS* or loss of p53 does not protect colon cancer cells from the anti-cancer properties of metformin. Finally, these effects may be explained by the targeting of mitochondrial respiration observed by dramatically reduced OCRs,

## CHAPTER 3

activated AMPK through increased phosphorylation and finally, suppressed mTOR and p70S6K by reduced phosphorylation levels (Figure 3-11 and Figure 3-12).

# Chapter 4. Metformin associated changes in miRNA and transcriptome profiles of CRC

---

## 4.1 Introduction

In this chapter, the anticancer characteristics of metformin was explored focusing on its effects on signalling pathways that occur through a direct modulation of associated genes and miRNAs.

As shown in Chapter 3, metformin, has proven to have anti-cancer properties in CRC cell lines through targeting metabolic reprogramming of cancer cells. Potential mechanisms of action of metformin on cancer cells are mainly associated with activation of AMPK, inhibition of the mTOR pathway, regulating inflammatory responses and promoting cell death in cancer stem cells [839, 982-985]. The anti-cancer effects of metformin on CRC cells have previously been shown by reducing the spontaneous intestinal polyp growth in *ApcMin/+* mice and sensitization of CRC cells to some chemotherapeutic agents [986] which has led to clinical trials evaluating the combinatorial effect of metformin with standard chemotherapeutics [987].

However, various targeting molecules have been found to be associated with metformin which highlights the pleiotropic nature of this drug in exerting anti-cancer properties through simultaneously targeting numerous pathways during tumorigenesis and tumour progression. Therefore, the molecular mechanism and crosstalk between signalling pathways contributing to the anti-cancer effects of metformin in CRC cells remain relatively elusive.

On the other hand, growing evidence confirms several miRNA modulations to be associated with the anti-cancer mechanisms of action for metformin. Accordingly, metformin treatment resulted in aberrant expression of miRNAs in hepatocellular carcinoma, pancreatic cancer, oesophageal squamous cancer, gastric cancer, lung cancer and prostate cancer [899, 901, 903, 904, 908].

Combined, a functional interplay involving specific modulations in miRNA expression levels takes place along with the changes in the expression levels of other genes. Hence, the implications of the interplay between miRNAs and target genes, within specific metabolic and signalling pathways, requires further investigation.

Based on the results obtained in Chapter 3, to be able to manipulate the system easily, HCT116 colorectal cancer cell line was used. The aim was to simulate the conditions that occur *in vivo* where a proliferating colorectal tumour or a metastasis encounters a reduction in available nutrients during its continuous growth. For this aim, 2.5 mM was chosen as the final concentration of metformin that results in an anti-proliferative effect but not yet a cytotoxic effect.

The aim of this chapter was to obtain a comprehensive snapshot of the changes associated with metformin treatment of HCT116 cells, through transcriptome and small RNA sequencing analyses, and characterize metformin response pathways and regulatory elements in a systematic manner.

## 4.2 Results

### 4.2.1 Identification of differentially expressed mRNAs with metformin treatment

In order to obtain a list of protein-coding genes that are differentially expressed in HCT116 cells in response to 2.5 mM metformin treatment, HCT116 cell were treated with 2.5 mM metformin for 72 hours and following RNA extraction and quality check, libraries were prepared by adaptor ligation and PCR amplification. After ribosomal RNA (rRNA) depletion, a paired-end 100 bp sequencing was performed to generate approximately 30 million reads per sample. Differential expression analysis was then performed for the transcriptome sequencing data. The differentially expressed (DE) protein-coding genes are selected using the criteria:  $p \text{ value} \leq 0.05$ ,  $|\text{Log}_2\text{Foldchange}| \geq 1$ . Out of 13512 identified protein-coding genes, 1221 genes were significantly, differentially expressed with a total of 554 upregulated and 667 downregulated genes (Figure 4-1, Appendix 2).

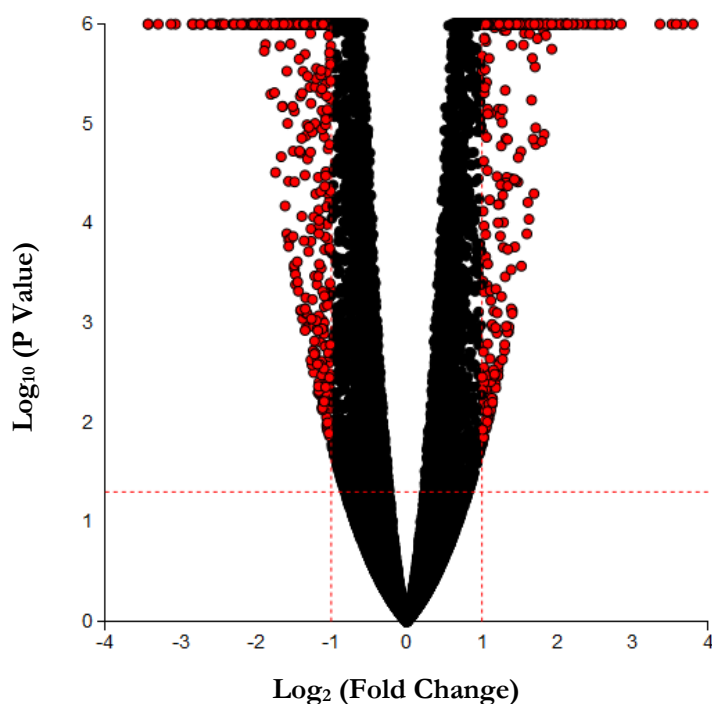


**Figure 4-1: Volcano plot for transcriptome profiling of HCT116 cells treated with 2.5 mM metformin.**

Protein-coding genes that were identified in RNA sequencing are shown. Red dots represent differentially expressed genes and black are the ones with no significant changes. Adviata iPathway Guide tool was used to generate the plot. Y axis represents  $-\log_{10}(\text{p value})$  and x axis represents  $\log_2$  fold change. Differentially expressed mRNAs identified with the cut-offs of  $P \leq 0.05$  and  $1 \leq \text{Log}_2 \text{ fold change} \leq -1$ .

#### 4.2.2 Identification of differentially expressed miRNAs with metformin treatment

To elucidate the altered miRNA profiles resulting from 2.5 mM metformin treatment of HCT116 colorectal cancer cells, similar to transcriptome sequencing, RNA samples were prepared, and the qualities were checked before generating libraries and small RNA sequencing which resulted in approximately 10 million reads per sample. Differential expression analysis was then performed for small RNA sequencing data taking into account  $p \text{ value} \leq 0.05$  and  $|\text{Log}_2\text{Foldchange}| \geq 1$  thresholds. Out of 540 identified miRNAs, 104 miRNAs were differentially expressed with 63 and 41 miRNAs being upregulated and downregulated, respectively (Figure 4-2, Appendix 3).

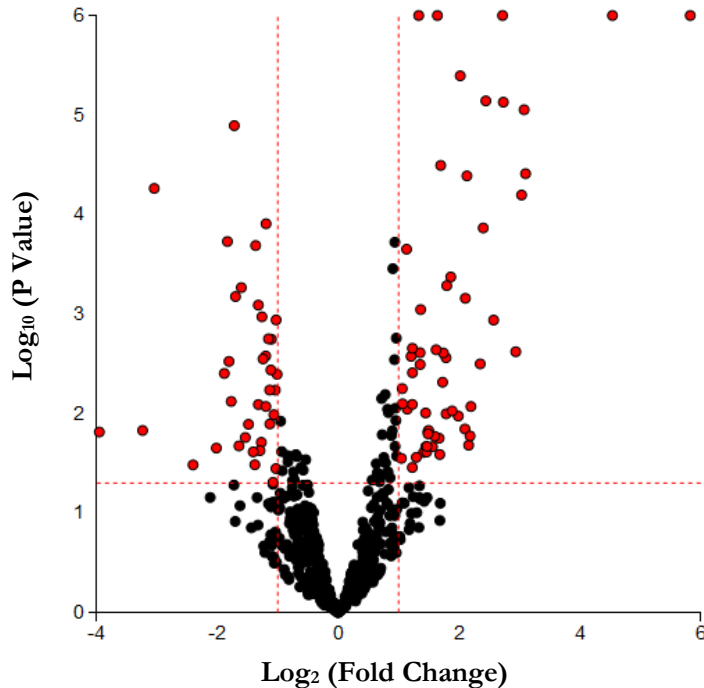


**Figure 4-2: Volcano plot for small RNA sequencing of HCT116 cells treated with 2.5 mM metformin.**

miRNAs that were identified in small RNA sequencing are shown. Red dots represent differentially expressed miRNAs and black are the ones with no significant change in the expression levels. Adviaata iPathway Guide web tool was used to generate the plot. Y axis represents  $-\log_{10}(p \text{ value})$  and x axis represents  $\log_2$  fold change. Differentially expressed miRNAs identified with the cut-offs of  $P \leq 0.05$  and  $1 \leq \log_2$  fold change  $\leq -1$ .

### 4.2.3 miRNA target prediction and integrative network construction

The validated and predicted protein-coding gene targets of 104 differentially expressed (DE) miRNAs were collected. miRTarbase and miRwalk databases used to identify validated targets and those miRNA-target pairs that showed an inverse correlation in the expression changes and supported by reporter assays were retained. Additionally, predicted miRNA-target mRNA were found using a combination of the databases TargetScan, miRDB, DIANA-microT-CDS, miRanda and miRmap with thresholds explained in section 2.4.2. Finally, potential DE miRNA-gene pairs that had anti-correlations in their expression changes and were common to two or more prediction databases were extracted. In total, 167 miRNA-target pairs were uncovered with 15 experimentally validated pairs but also 152 bioinformatically predicted pairs (Appendix 4).

#### 4.2.4 Integrative Protein- protein interaction (PPI) and miRNA- mRNA network

To ensure the robustness of protein coding gene identification, the sequences with less than 50 reads that correspond to the specific genes in both metformin treated and untreated RNA sequencing samples were filtered out. A total of 1060 differentially expressed (DE) genes were thus assigned for the following analyses. The PPI network was retrieved using NetworkAnalyst (<http://www.networkanalyst.ca>) and visualized using Cytoscape software (Version 3.4.0) [949]. For PPI generation, IMEx Interactome which is a literature-curated comprehensive database from InnateDB [948] was used and zero order network, which represents direct interactions within the seed proteins, was selected. The whole PPI network was then visualized using Cytoscape and then undirected network analysis was carried out using NetworkAnalyzer, a plug-in of Cytoscape to assess the topological properties of the network. The connectivity degree of the nodes was considered as the central parameter for screening of the nodes. A total of 317 DE genes with degree  $\geq 1$  was selected for visualisation and the following analyses.

Using PPI interaction together with miRNA-gene interactions predicted, a miRNA-based network was assembled (Figure 4-3). The integrated miRNA-based network comprised of 365 nodes (47 miRNAs, 317 mRNAs) and 728 edges (169 miRNA-gene interactions and 559 protein-protein interactions). Overall, this network demonstrates the complex changes in gene/protein interactions. Since, DE miRNAs potentially target multiple and highly connected genes within the integrated network, these miRNAs together with putative/validated target genes constitute a crucial part of the complex of metformin-mediated changes in HCT116 cells.

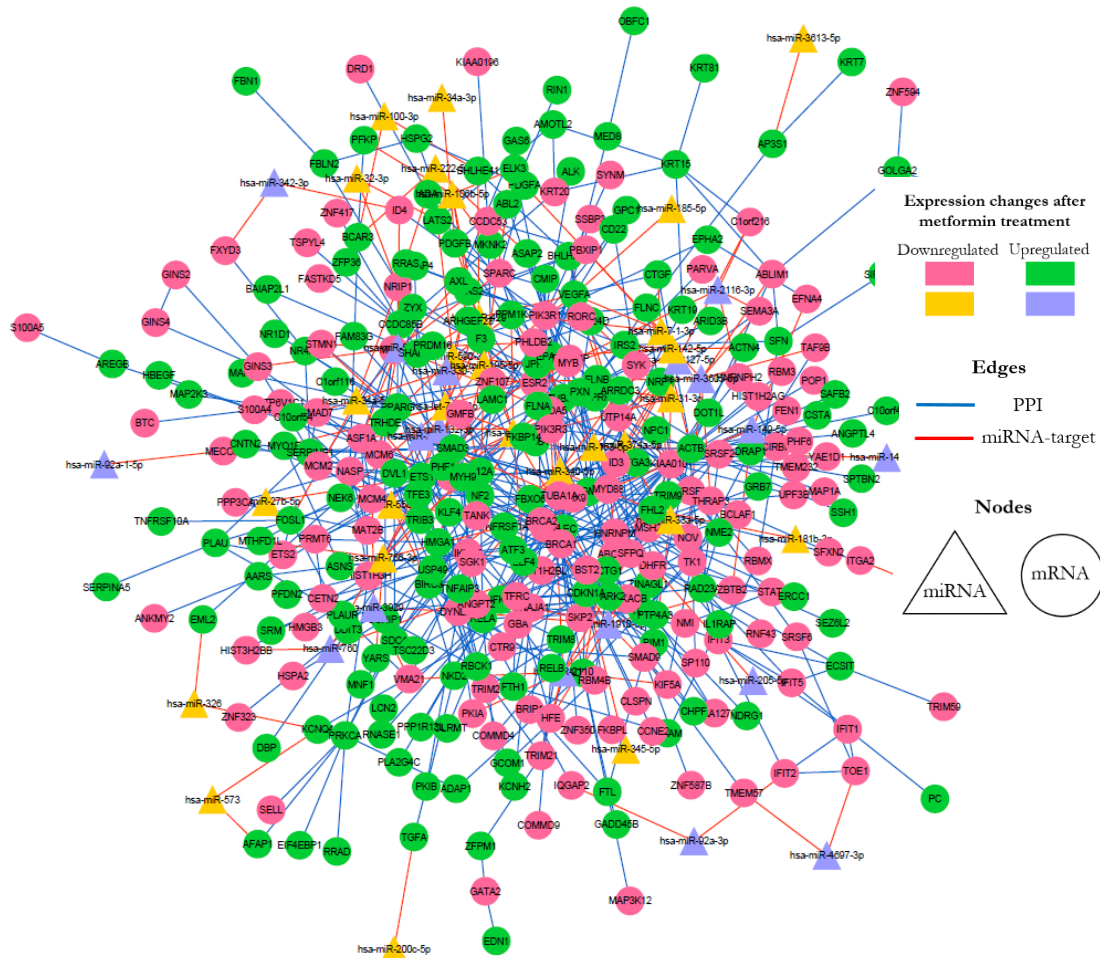


**Figure 4-3: The miRNA-based network affected by metformin treatment of colorectal cancer cells.**

This is an organic layout of the integrated network associated with 2.5 mM metformin treatment of HCT116 cells. PPIs are from InnateDB signalling network and miRNA-target pairs are collated from validated and predicted databases. miRNAs are shown in triangles and genes are the circle nodes. The miRNA-gene interactions are shown as red lines while gene-gene interactions are blue. The pink and orange nodes represent downregulated genes and miRNAs, respectively, while green and purple nodes are upregulated genes and miRNAs, respectively.

#### 4.2.5 Enrichment analysis of GO-terms

Gene ontology (GO) term enrichment analysis was used to characterize the global effect of metformin on the mRNA levels extracted from the PPI network (Appendix 5). Accordingly, DE protein-coding genes with degree  $\geq 1$  were selected for GO analysis. ClueGO (a plug-in of Cytoscape) was used to interrogate the GO terms and to interrogate and visualize the functionally arranged GO terms. Kappa score with a cut-off of 0.4 was applied to group the enriched GO

## CHAPTER 4

terms. Terms with at least 3 genes retrieved and minimum 4% attribution in the term was considered. Enriched GO terms with existing experimental evidence were identified for the categories “Biological Processes” (BPs), “Molecular Functions” (MFs), and “Cellular Compartments” (CC) [988]. GO analysis of DE protein coding genes, revealed 163, 21 and 14 GO terms organised in 15, 11 and 7 groups for BPs, MFs, and CCs, respectively. Three major enriched networks of GO terms related to biological processes were identified. The first group consists of 63 terms related with the ‘negative regulation of biological processes’. The second and third groups, of 21 and 8 terms, are related to the “regulation of macromolecule metabolic process” and “signal transduction”, respectively (Figure 4-4). MF terms related to transcription with the parent term “transcription regulatory region DNA binding” had the highest significance among 11 enriched groups (Figure 4-5). Enriched cellular compartments included groups such as “nuclear chromosome part”, “basal part of cell” and, “actin cytoskeleton”. These groups are shown in Figure 4-6.

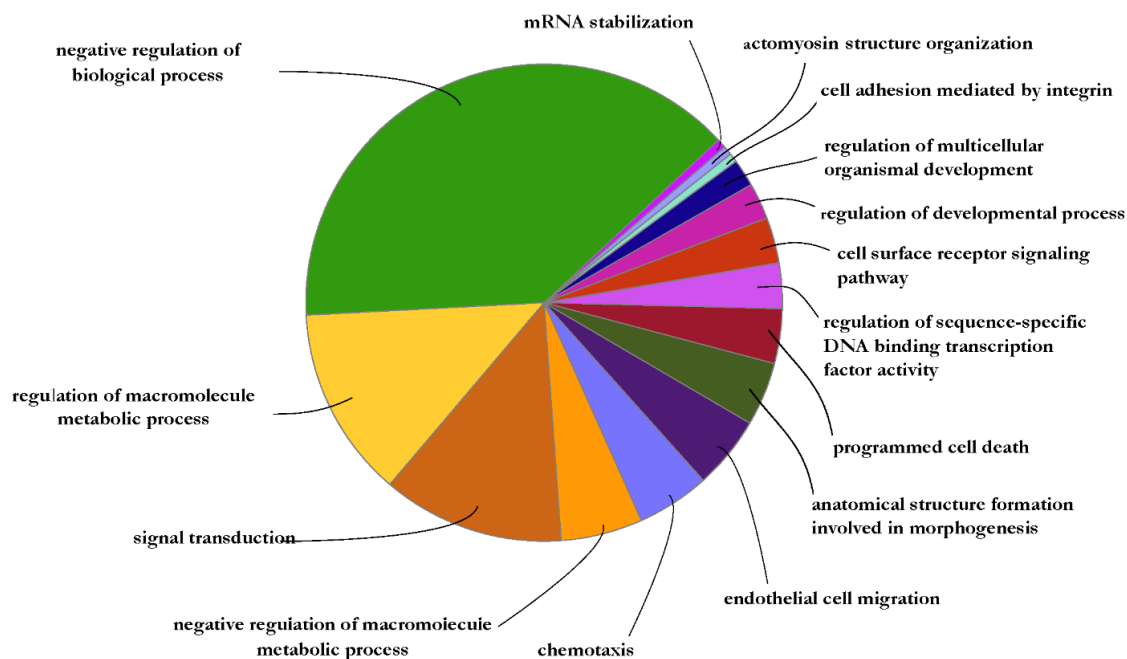


**Figure 4-4: Metformin associated changes in biological processes in HCT116 cells.**

ClueGo analysis of DE genes retrieved from PPI network with degree  $\geq 1$ . Over-represented biological processes were grouped based on kappa statistics ( $\geq 0.04$ ) where only the label of the most significant term per group is shown. The size of each category within a pie chart represents the number of included terms and the terms were all experimentally validated (Term PValue Corrected with Bonferroni step down  $\leq 0.05$ ).

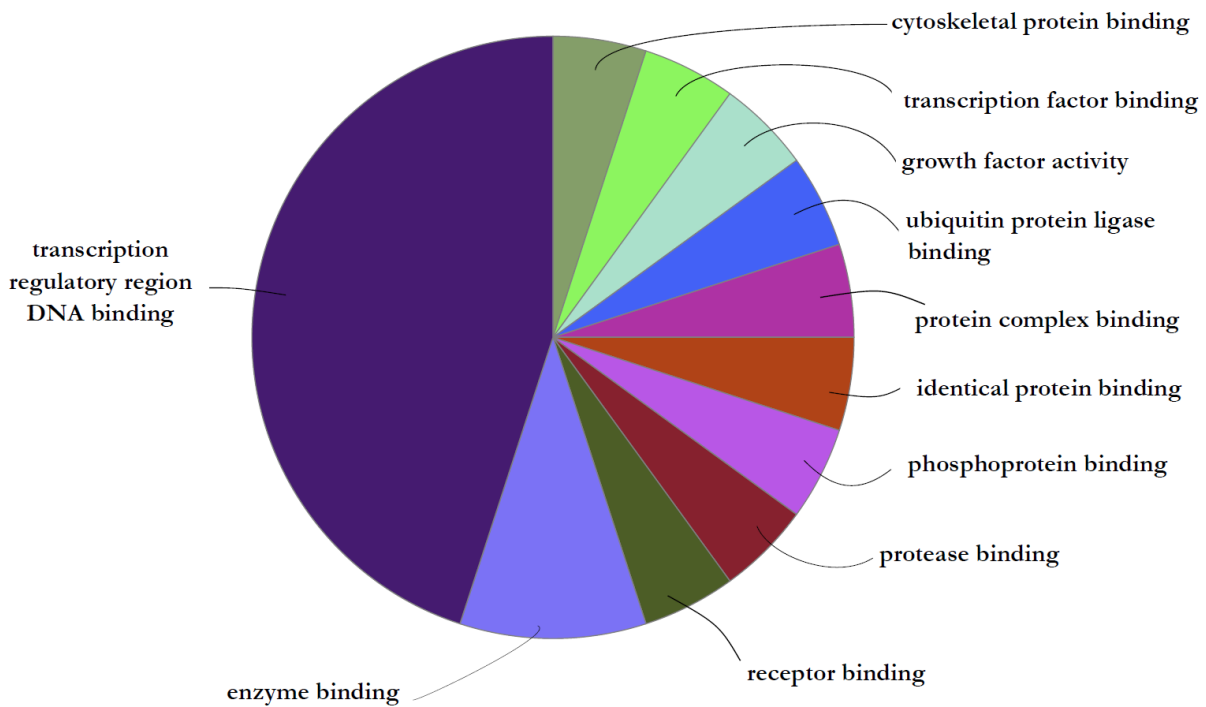


**Figure 4-5: Metformin associated changes in molecular functions in HCT116 cells.**

ClueGo analysis of DE genes retrieved from PPI network with degree  $\geq 1$ . Over-represented molecular functions were grouped based on kappa statistics ( $\geq 0.04$ ) where only the label of the most significant term per group is shown. The size of each category within a pie chart represents the number of included terms and the terms were all experimentally validated (Term PValue Corrected with Bonferroni step down  $\leq 0.05$ ).

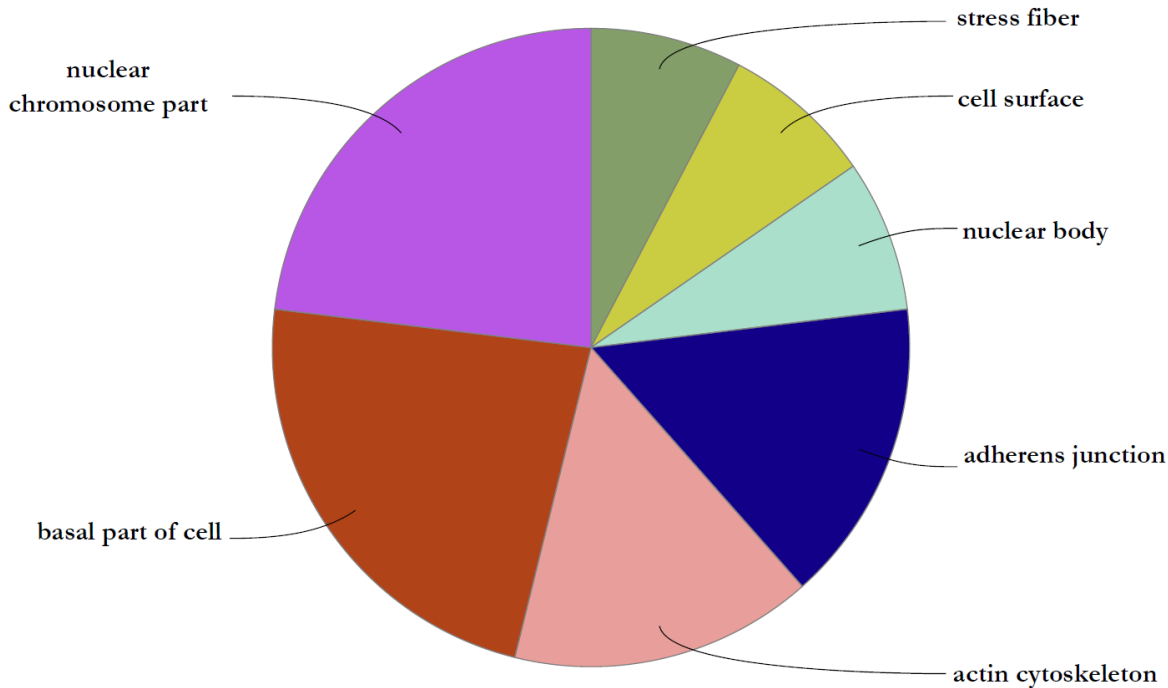


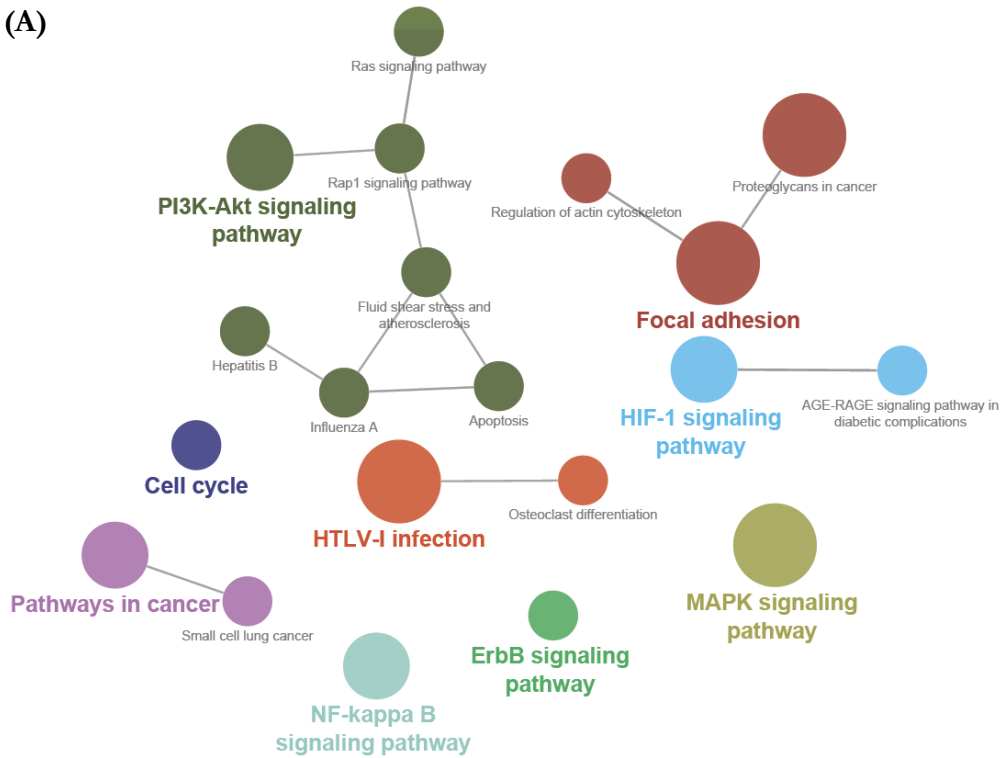
**Figure 4-6: Metformin associated changes in cellular compartments in HCT116 cells.**

ClueGO analysis of DE genes retrieved from PPI network with degree  $\geq 1$ . Over-represented cellular compartments were grouped based on kappa statistics ( $\geq 0.04$ ) where only the label of the most significant term per group is shown. The size of each category within a pie chart represents the number of included terms and the terms were all experimentally validated (Term PValue Corrected with Bonferroni step down  $\leq 0.05$ ).

#### 4.2.6 Global pathway regulation in response to metformin treatment of CRC cells

To examine which biological pathways were altered in HCT116 cells treated with 2.5 mM metformin treatment, the biochemical pathways were extracted from KEGG and pathway analysis was performed for DE genes with degree  $\geq 1$  using ClueGO (Figure 4-7). KEGG pathway analysis revealed 20 statistically enriched pathways organised into 8 groups based of Kappa score including: PI3K-Akt pathway, focal adhesion, pathways in cancer, HTLV-1 infection, HIF-1 signalling pathway, cell cycle, NF-kappa B signalling pathway, Erb signalling pathway, and MAPK signalling pathway. PI3K-Akt signalling pathway had the lowest GO group p value and was the parent term within this group ( $P= 1.0 \times 10^{-8}$ ). Also, as is shown in (Table 4-1) MAPK pathway had the lowest term p value ( $P= 7.4 \times 10^{-7}$ ) with 25 DE genes involved in this pathway.

(A)



(B)

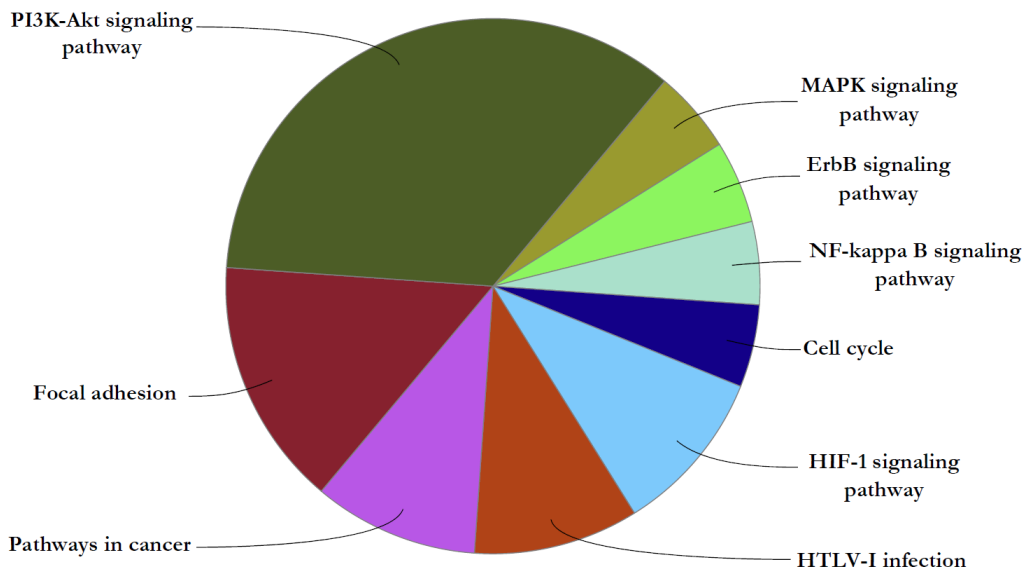


**Figure 4-7: Overrepresented KEGG pathways for DE genes associated with metformin treatment of HCT116 cells.**

Functionally grouped network of enriched categories was generated for all the DE genes with degree  $\geq 1$  by querying the KEGG database, using ClueGO plug-in (A). Pathways are represented as nodes and the node size represents the term's enrichment significance. The node pie chart

represents the KEGG pathway analysis of selected genes (B). Only the most significant term in the group was labelled and the size of each category within a pie chart represents the number of included terms. (Term PValue Corrected with Bonferroni step down  $\leq 0.05$ ).

**Table 4-1: Enriched KEGG pathways overrepresented with metformin treatment of HCT116.**

GO Term	Term PValue Corrected with Bonferroni step down	Group PValue Corrected with Bonferroni step down	GO Groups	% Associated Genes	No. Genes
MAPK signaling pathway	0.00000074	0.000000051	Group0	9.803922	25
Focal adhesion	0.0000036	0.00000011	Group7	10.55276	21
Proteoglycans in cancer	0.0000051	0.00000011	Group7	10.34483	21
HTLV-I infection	0.00025	0.000043	Group5	8.203125	21
HIF-1 signaling pathway	0.00087	0.0001	Group4	12.12121	12
Pathways in cancer	0.00091	0.000045	Group6	6.582278	26
PI3K-Akt signaling pathway	0.0022	0.00000001	Group8	6.725146	23
NF-kappa B signaling pathway	0.0031	0.00011	Group2	11.57895	11
ErbB signaling pathway	0.007	0.00013	Group1	11.62791	10
Ras signaling pathway	0.0074	0.00000001	Group8	7.488987	17
Apoptosis	0.022	0.00000001	Group8	8.695652	12
AGE-RAGE signaling pathway in diabetic complications	0.022	0.0001	Group4	10.10101	10
Fluid shear stress and atherosclerosis	0.023	0.00000001	Group8	8.633094	12
Small cell lung cancer	0.029	0.000045	Group6	10.71429	9
Rap1 signaling pathway	0.032	0.00000001	Group8	7.142857	15
Hepatitis B	0.032	0.00000001	Group8	8.333333	12
Cell cycle	0.032	0.00033	Group3	8.870968	11
Regulation of actin cytoskeleton	0.034	0.00000011	Group7	7.075472	15
Osteoclast differentiation	0.042	0.000043	Group5	8.59375	11
Influenza A	0.047	0.00000001	Group8	7.514451	13

#### 4.2.7 Identification of hub genes, key miRNAs and potential molecular mechanisms of metformin

The association of the miRNAs in overrepresented KEGG pathways was investigated and the genes and miRNAs were mapped to the corresponding pathways. Pathways selected based on the term and group p values corrected with Bonferroni step down. Based on the group p values, PI3K-Akt signalling pathway (GO:0004151) was selected having the lowest group p value and being the

parent term within the group. Also, by comparing the term p values without considering the grouping, MAPK signalling pathway (GO:0004010) was also selected as the most representative term having the lowest term p value.

#### 4.2.8 Expression of putative miRNA-gene pairs within PI3K-Akt pathway following metformin treatment of HCT116 cells

Differentially expressed genes within PI3K-Akt pathways were retained and potential miRNA-target gene pairs were collected (Table 4-2).

**Table 4-2: miRNA-target gene pairs identified within PI3K-Akt pathway.**

miRNA	miRNA basemean	Gene	Gene base mean	Prediction Algorithms/ Validated gene collections
hsa-miR-149-5p	3489.962567	EFNA4	151.1231256	miRmap, TargetScan
hsa-miR-345-5p	1769.185165	CDKN1A	3690.517528	miRTarbase, TargetScan
hsa-miR-34a-3p	39.03989005	PDGFB	223.9736451	miRanda, TargetScan
hsa-miR-940	63.93949325	PDGFB	223.9736451	miRmap, TargetScan
hsa-miR-429	5424.282711	LAMC1	3398.467289	miRmap, miRDB
hsa-miR-429	5424.282711	VEGFA	1460.957388	miRDB, miRTarbase, TargetScan
hsa-miR-374a-5p	509.1246247	VEGFA	1460.957388	DIANA-microTCD, miRanda, miRDB, TargetScan
hsa-miR-195-5p	63.94107141	VEGFA	1460.957388	DIANA-microTCD, miRanda, miRDB, miRTarbase
hsa-miR-185-5p	217.0828786	VEGFA	1460.957388	miRmap, miRDB, miRTarbase
hsa-miR-7-1-3p	330.3205048	VEGFA	1460.957388	miRanda, miRDB
hsa-miR-590-3p	369.0630055	THBS1	980.8838285	DIANA-microT-CD, miRanda
hsa-miR-2110	148.233555	PIK3R3	105.1977775	miRmap, TargetScan
hsa-miR-132-3p	774.6723011	PIK3R3	105.1977775	miRwalk, miRTarbase
hsa-miR-132-3p	774.6723011	MYB	195.5835674	DIANA-microTCD, miRanda
hsa-miR-2116-3p	239.047622	MYB	195.5835674	miRmap, miRanda, TargetScan
hsa-miR-4745-5p	50.08204789	ITGA2	7244.616166	miRmap, TargetScan
hsa-miR-7-1-3p	330.3205048	PDGFA	660.1715656	DIANA-microTCD, miRanda, TargetScan
hsa-miR-940	63.93949325	THBS1	980.8838285	miRmap, TargetScan

Out of 18 miRNA-gene pairs (4 validated and 14 predicted) 13 pairs were selected for further investigation. For the selection, miRNAs and genes with less than 100 reading (average) in sequencing data (see Section 2.2) were filtered out (miR-34a-3p, miR-940, miR-195-5p and miR-4745-5p). Consequently, 8 genes were selected, and the expression changes associated with 2.5 mM metformin treatment were validated using real-time, relative quantitation, RT-PCR (Figure

4-8). The expression levels of 9 miRNAs were validated using Taqman real-time RT-PCR (Figure 4-9). miR-2116-3p was removed from the list as there were no conventional Taqman assays for this miRNA.

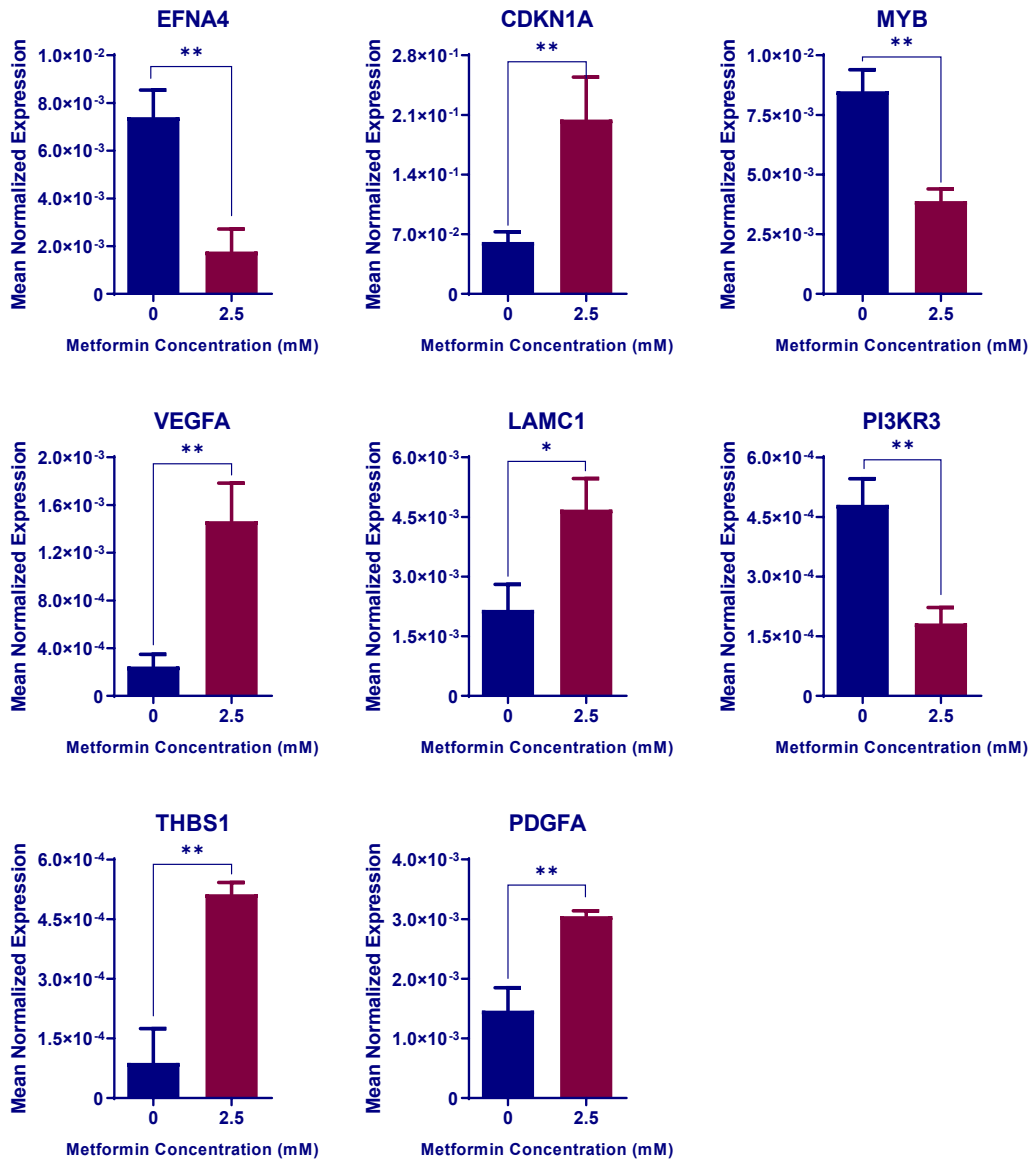


**Figure 4-8. Quantitative real-time PCR analysis of mRNA levels in HCT116 cells for genes identified in PI3K-Akt signalling pathway as being influenced by 2.5 mM metformin treatment.**

Cells were treated with 2.5 mM metformin for 72 hours and compared with cells in control medium. Results are expressed as mean  $\pm$  SD of at least 3 replicates and the expression is normalised to *B2M* expression levels. The statistical significance is indicated with asterisks (\* P  $\leq$  0.05, \*\* P  $\leq$  0.01).

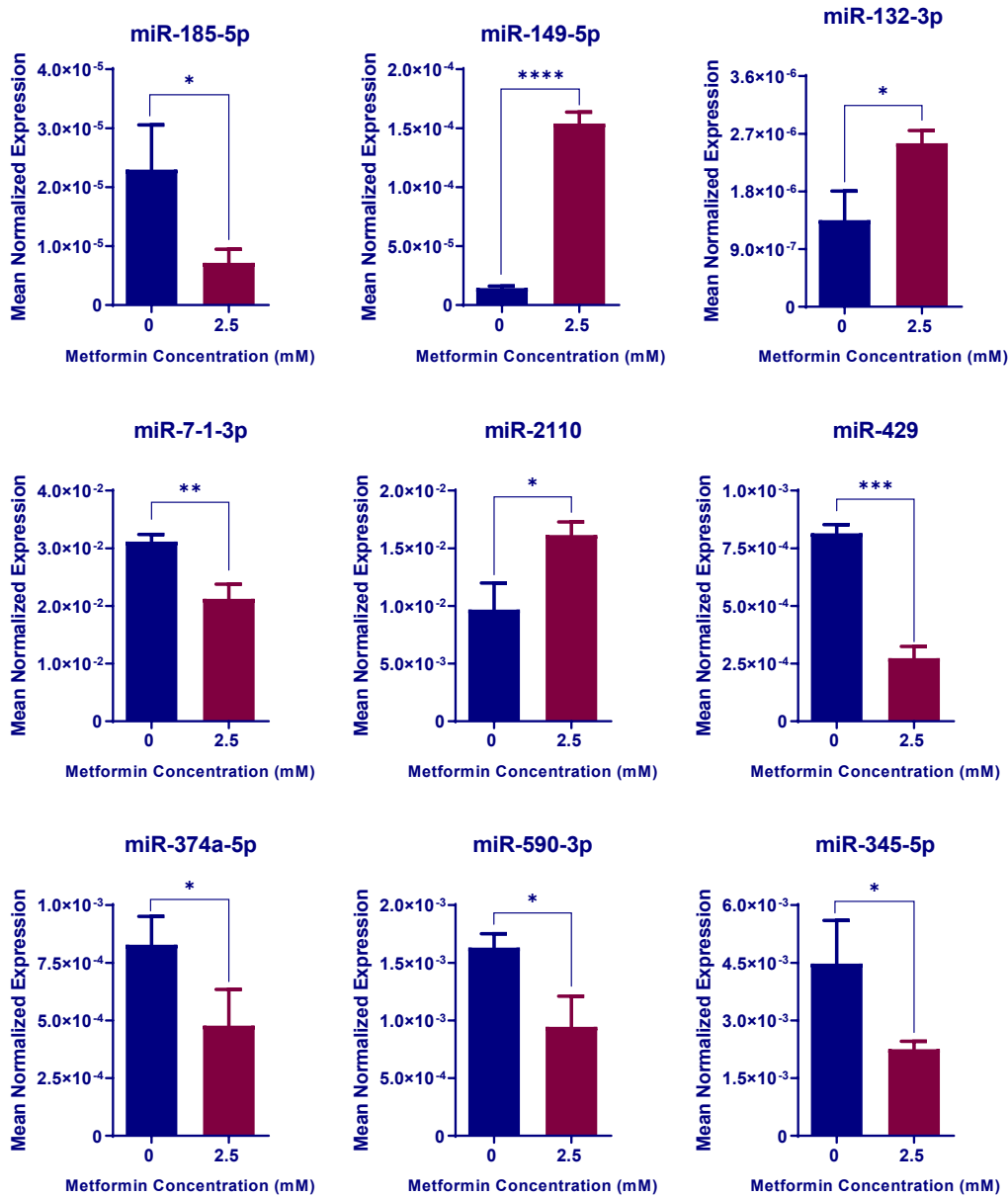


**Figure 4-9: Quantitative real-time PCR analysis of miRNA levels in HCT116 cells for miRNAs identified in PI3K-Akt signalling pathway as being affected by 2.5 mM metformin treatment.**

Cells were treated with 2.5 mM metformin for 72 hours and compared with cells in control medium. Results are expressed as mean  $\pm$  SD of at least 3 replicates and the expression is normalised to miR-16 expression levels. The statistical significance is indicated with asterisks (\*  $P \leq 0.05$ , \*\*  $P \leq 0.01$ , \*\*\*  $P \leq 0.001$ , \*\*\*\*  $P \leq 0.0001$ ).

#### 4.2.9 Validation of anti-correlation between expression levels of miRNAs and potential target mRNAs within PI3K-Akt pathway

The selected miRNA-gene pairs were cross-referenced with the literature and 6 miRNA-gene interactions (4 predicted and 2 validated targets) were selected for further investigation. The miRNA-gene pairs were selected if downregulated miRNAs were described as oncogenic miRNAs and their putative upregulated target genes had a tumour suppressor role in cancer. Vice versa, if a tumour suppressor miRNA was downregulated having a putative oncogenic target gene that was upregulated by metformin treatment was also selected for further investigations. To validate direct or indirect targeting of the genes by the miRNAs, HCT116 cells were reverse-transfected with corresponding miRNA mimics and the gene expression levels were assessed with RT-PCR (Figure 4-10). Among 6 pairs, miR-132-3p and miR-2110 transfection resulted in a significant reduction in *PIK3R3* gene expression ( $P= 0.0073$  and  $0.0006$ , respectively). Also, *THBS1* gene expression was downregulated as a result of miR-590-3p mimic transfection ( $P= 0.0029$ ), while there was no change in *MYB*, *EFNA4* and *CDKN1A* expression levels associated with the transfection of miR-132-3p, miR-149-3p and miR-345-5p mimics, respectively (Figure 4-10).

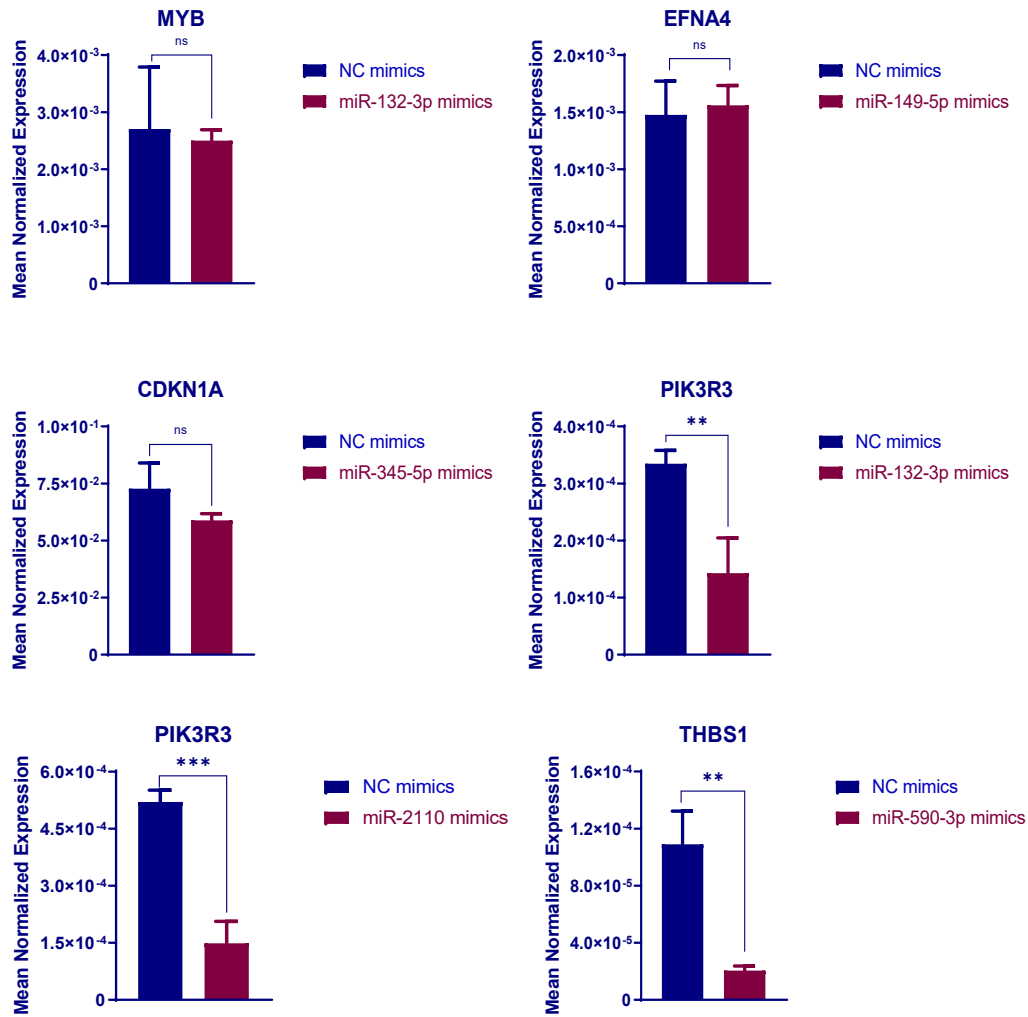


**Figure 4-10: Putative target gene expression in HCT116 cells after transfection with corresponding predicted miRNA.**

Gene expression changes associated with exogenous overexpression of selected miRNA were assessed by real-time RT-PCR. *MYB*, *EFNA4*, *CDKN1A*, *PIK3R3* and *THBS1* mRNA levels were tested in HCT116 cells transfected with miR-132-3p, miR-149-3p, miR-345-5p, miR-132-3p or miR-2110 and miR-590-3p, respectively and compared with NC mimic. Results are expressed as mean  $\pm$  SD of at least 3 replicates and expression levels were normalised to *ACTB* levels. The statistical significance is indicated with asterisk (ns  $P > 0.05$ , \*  $P \leq 0.05$ , \*\*  $P \leq 0.01$ , \*\*\*  $P \leq 0.001$ , \*\*\*\*  $P \leq 0.0001$ ).

#### 4.2.10 Proliferation of colorectal cancer cells following transfection with miR-132-3p, miR-2110 and miR-590-3p mimics

Based on results showed in 4.2.9, only miR-132-3p, miR-2110 and miR-590-3p transfection resulted in a significant reduction in putative target gene expression. Therefore, the effect of miR-132-3p, miR-2110 and miR-590-3p on HCT116 cell proliferation was assessed. Transfection of CRC cells with miR-2110 and miR-132-3p, but not miR-590-3p mimics, showed a suppression effect on HCT116 cell proliferation (Figure 4-11).

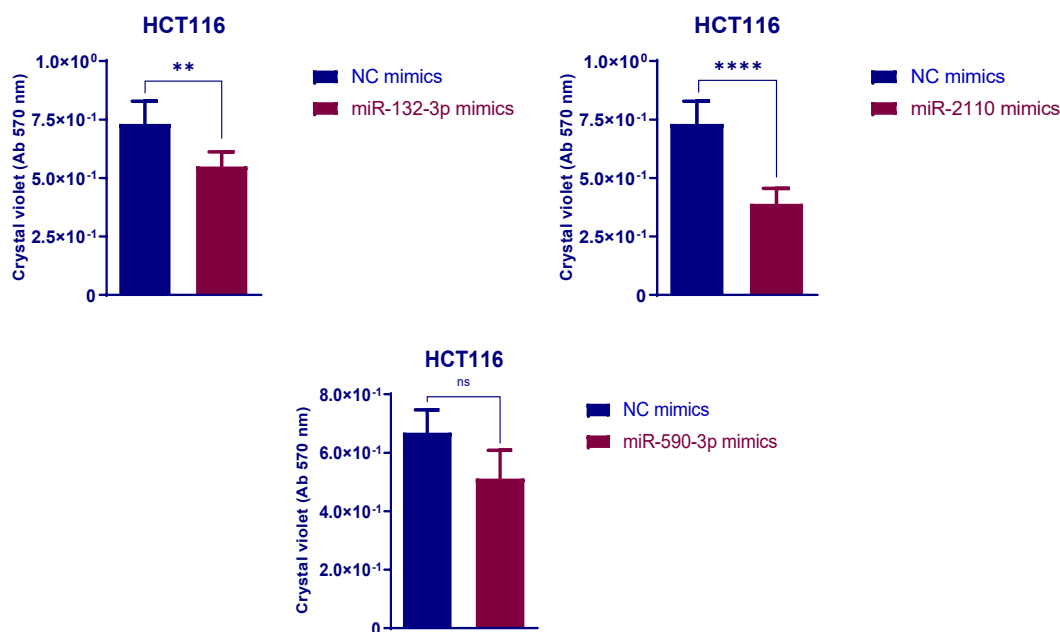


**Figure 4-11: Proliferation of HCT116 cells 96 hours post-transfection with miR-132-3p, miR-2110 and miR-590-3p.**

Quantitative results of crystal violet staining of HCT116 cells showing the effect of miR-132-3p, miR-2110 and miR-590-3p mimics on cell proliferation. Results are expressed as mean  $\pm$  SD of at least 3 replicates and the statistical significance is indicated with asterisks (\*  $P \leq 0.05$ , \*\*  $P \leq 0.01$ , \*\*\*  $P \leq 0.001$ , \*\*\*\*  $P \leq 0.0001$ ).

The effect was also confirmed in RKO, DLD-1, SW480, HT29 and Caco2 cells (Figure 4-12 and Figure 4-13). Altogether, these data suggest that metformin inhibits CRC cell growth partly due to upregulated miR-2110 and miR-132-3p expression levels.

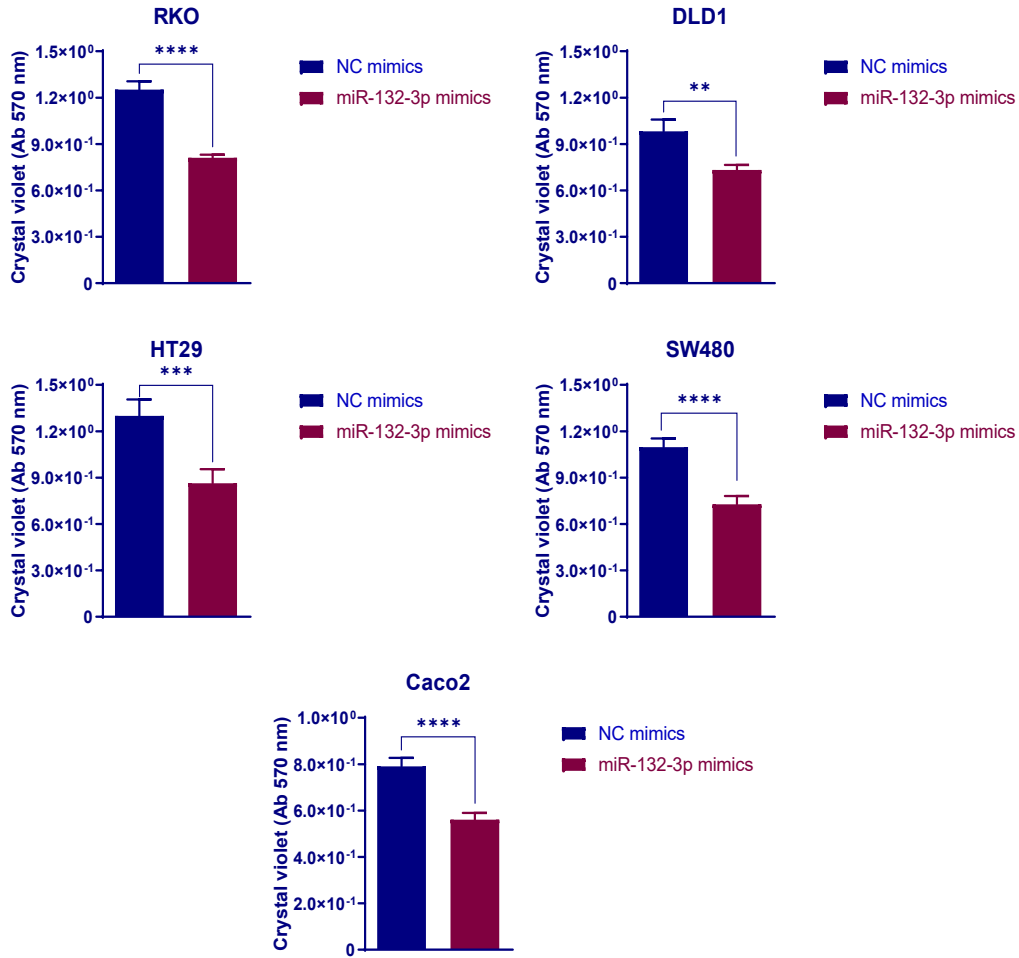


**Figure 4-12: Proliferation of different colorectal cancer cells 96 hours post-transfection with miR-132-3p.**

Quantitative results of crystal violet staining of transfected RKO, SW480, HT29, DLD1 and Caco2 cells confirming the reduction of cell proliferation with miR-132-3p mimic transfection. Results are expressed as mean  $\pm$  SD of at least 5 replicates and the statistical significance is indicated with asterisks (\*\*  $P \leq 0.01$ , \*\*\*  $P \leq 0.001$ , \*\*\*\*  $P \leq 0.0001$ ).

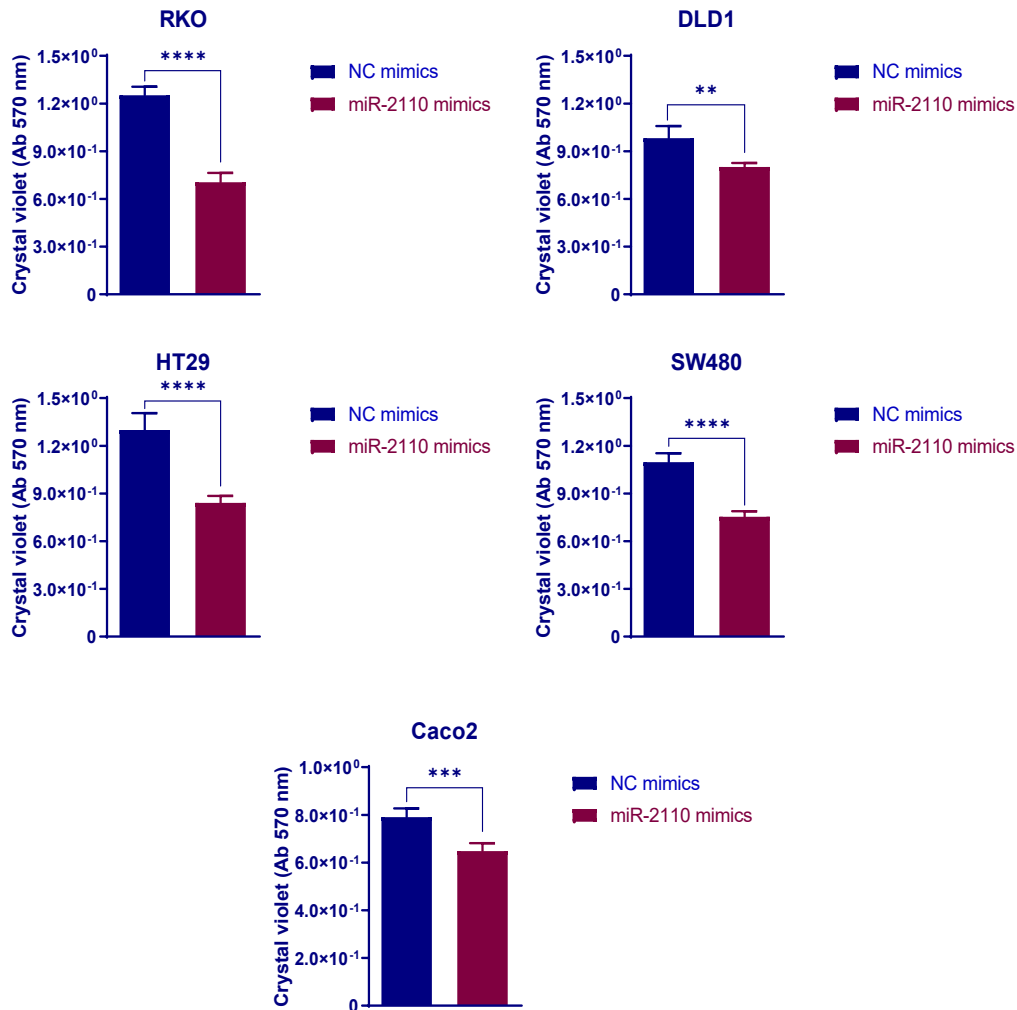


**Figure 4-13: Proliferation of different colorectal cancer cells 96 hours post-transfection with miR-2110.**

Quantitative results of crystal violet staining of transfected RKO, SW480, HT29, DLD1 and Caco2 cells confirming the reduction of cell proliferation with miR-2110 mimic transfection. Results are expressed as mean  $\pm$  SD of at least 5 replicates and the statistical significance is indicated with asterisk (\*\*  $P \leq 0.01$ , \*\*\*  $P \leq 0.001$ , \*\*\*\*  $P \leq 0.0001$ ).

#### 4.2.11 Expression of PIK3R3 protein levels in CRC cells following transfection with miR-132-3p, miR-2110 mimics

As shown in Figure 4-10, *PIK3R3* mRNA levels were downregulated following introduction of miR-2110 and miR-132-3p in HCT116 cells. To confirm the changes in protein levels, HCT116 cell lines were reverse transfected with miR-2110 and miR-132-3p precursors. As shown in Figure 4-10, introduced activity of miR-2110 and miR-132-3p relative to control cells transfected with

NC mimics significantly reduced PIK3R3 protein levels in HCT116 cells (53 %, respectively,  $P < 0.05$ ), Figure 4-14. Together, these results confirm the direct targeting of *PIK3R3* by miR-132-3p as described in [989] and suggest the role of miR-2110 in the regulation of *PIK3R3* in HCT116 cells. However, further experiments were required to confirm the direct targeting of *PIK3R3* by miR-2110.

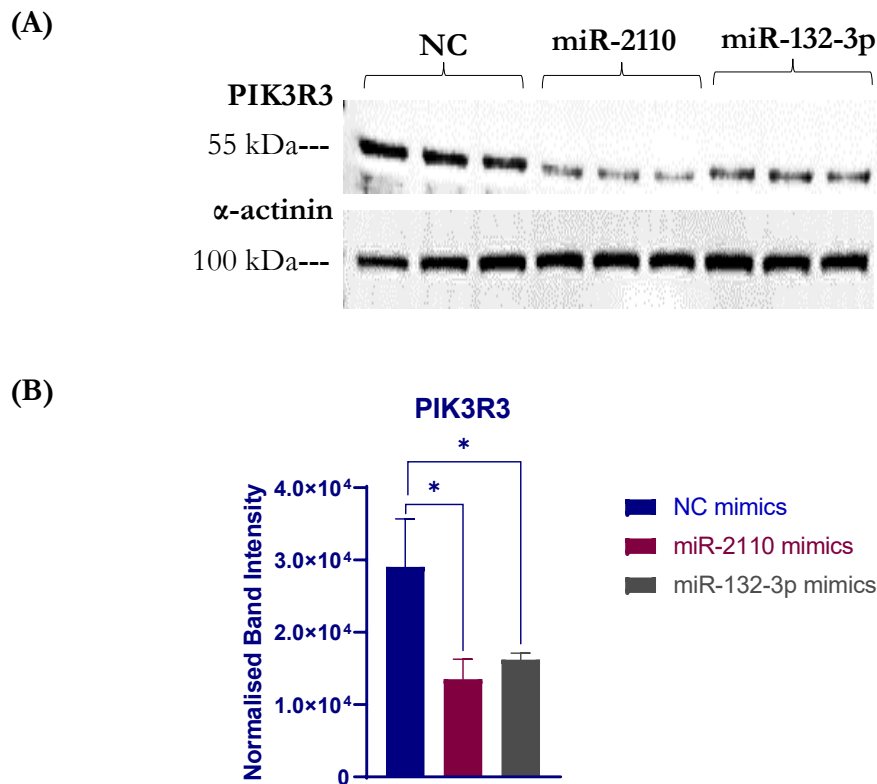


**Figure 4-14. Target gene protein levels in HCT116 cells after transfection with miR-132-3p, miR-2110.**

PIK3R3 protein levels in cells transfected with miR-132-3p, miR-2110 or NC mimics as measured by Western blot analysis 76 hours post-transfection (A). Densitometry analysis of PIK3R3 protein levels normalised to the corresponding  $\alpha$ -actinin protein levels (B). Results are expressed as mean  $\pm$  SD of 3 replicates and the statistical significance is indicated with asterisk ( $*P \leq 0.05$ ).



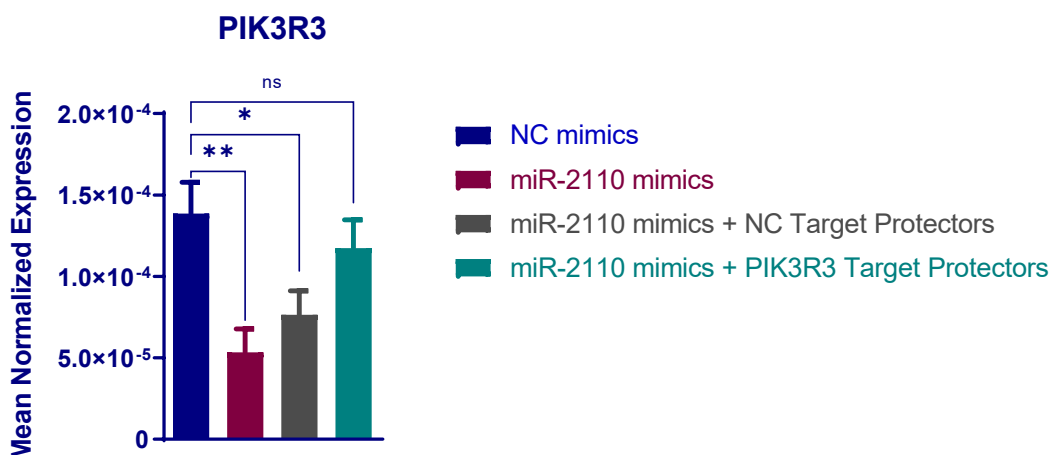


**Figure 4-15. *PIK3R3* expression changes in HCT116 cells after co-transfection with miR-2110 and specific target protectors.**

mRNA levels of miR-2110 target gene *PIK3R3* in HCT116 cells co-transfected with miR-2110 or NC mimics and with NC target protectors or *PIK3R3* target protectors, for 72 hours and normalised to *ACTNB* expression levels. Results are expressed as mean  $\pm$  SD of 3 replicates and the statistical significance is indicated with asterisk (ns  $P > 0.05$ , \*  $P \leq 0.05$ , \*\*  $P \leq 0.01$ ).

#### 4.2.13 Confirmation of *PIK3R3* as a gene that influences proliferation

To confirm that miR-2110 and miR-132-3p target gene, *PIK3R3* exerts biological function in CRC cells, the role of *PIK3R3* gene in regulating cell proliferation of CRC cell lines was examined. An RNA interference approach was used to knock down the activity of *PIK3R3* gene and determine the resultant effect in cell proliferation. Crystal violet assays showed that transfection with *PIK3R3* siRNA significantly decreased growth compared with a negative control siRNA transfection at 72 hours post-transfection in all 6 different colorectal cell lines, Figure 4-16 ( $p$  value  $< 0.0001$  in HCT116, DLD1, RKO, SW480 and HT29 cells and  $p$  value  $< 0.001$  in Caco2 cells). Since reducing *PIK3R3* expression decreased CRC cell proliferation, this supports a role for *PIK3R3* in cancer cell proliferation of CRC cell lines. The transfection efficiency of *PIK3R3* siRNA is shown in Appendix 6. Altogether, this could suggest that metformin exerts an anti-proliferative role in CRC cells partly due to inhibition of *PIK3R3* expression.

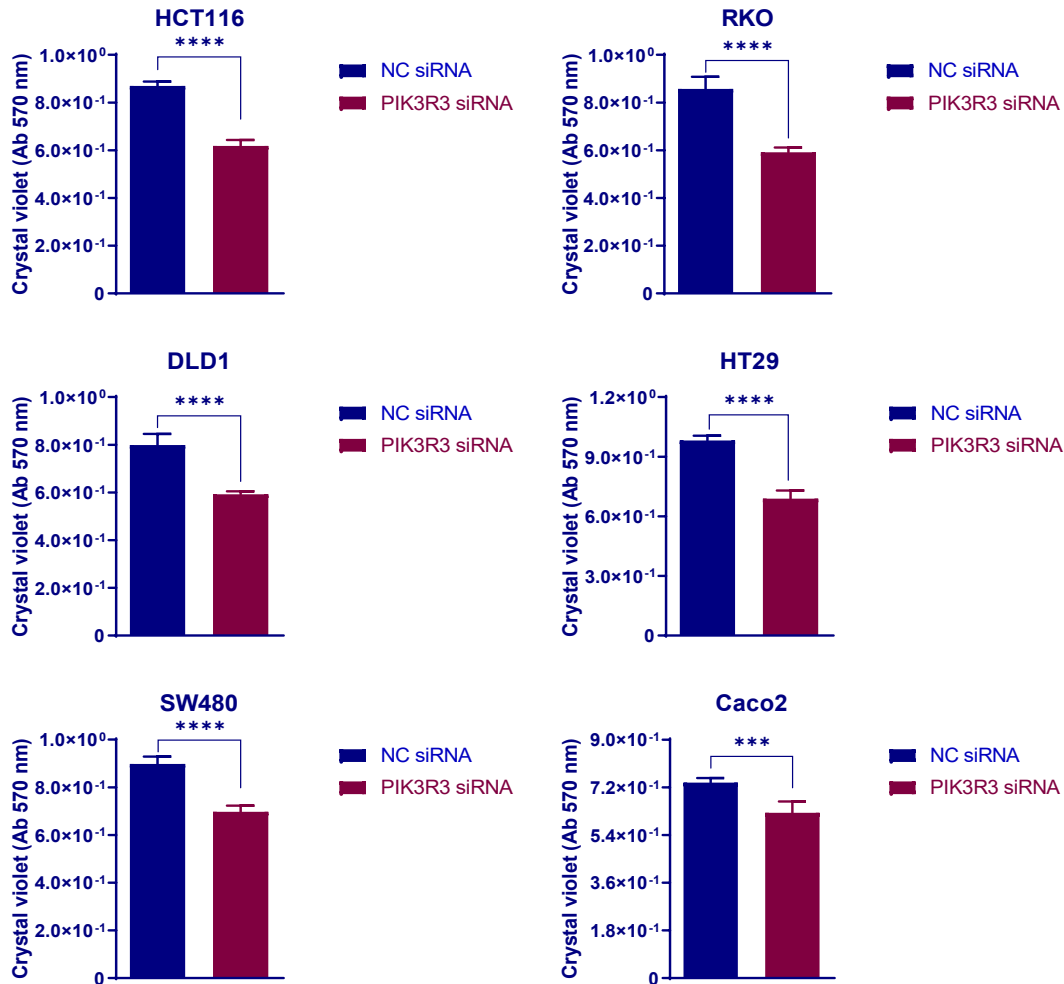


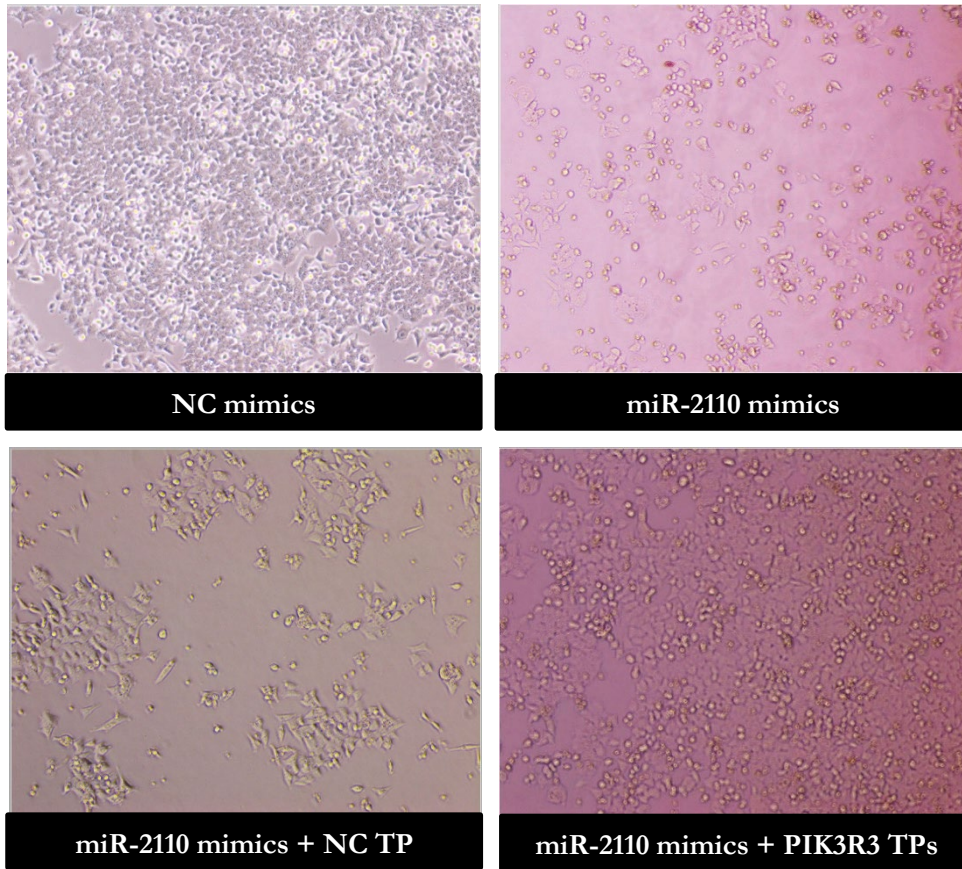
**Figure 4-16: Proliferation of different colorectal cancer cells 96 hours after transfection with PIK3R3 siRNA.**

Quantitative results of crystal violet staining of transfected HCT116, RKO, SW480, HT29, DLD1 and Caco2 cells showing the cell proliferation suppression by PIK3R3 gene knock down. Results are expressed as mean  $\pm$  SD of at least 5 replicates and the statistical significance is indicated with asterisks (\*\*\*)  $P \leq 0.001$ , \*\*\*\*  $P \leq 0.0001$ ).

#### 4.2.14 Confirmation of the role of miR-2110 – PIK3R3 pair in the regulation of CRC cell proliferation

To elucidate the molecular function of miR-2110 in the context of *PIK3R3* gene targeting, cell viability changes associated with the co-transfection of *PIK3R3* target protectors and miR-2110 mimics in HCT116 cells were examined. Cell viability measurements using crystal violet assay demonstrated that the restoration of *PIK3R3* mRNA levels by target protectors results in induced viability of HCT116 cells compared with miR-2110 mimics transfected cells by 90% after 72 hours ( $P= 0.0005$ ), Figure 4-17. Collectively, these results confirmed that miR-2110 binds the recognition sequence of *PIK3R3* mRNA within the 3'-UTR and downregulates *PIK3R3* gene expression to reduce cell proliferation.

(A)



(B)

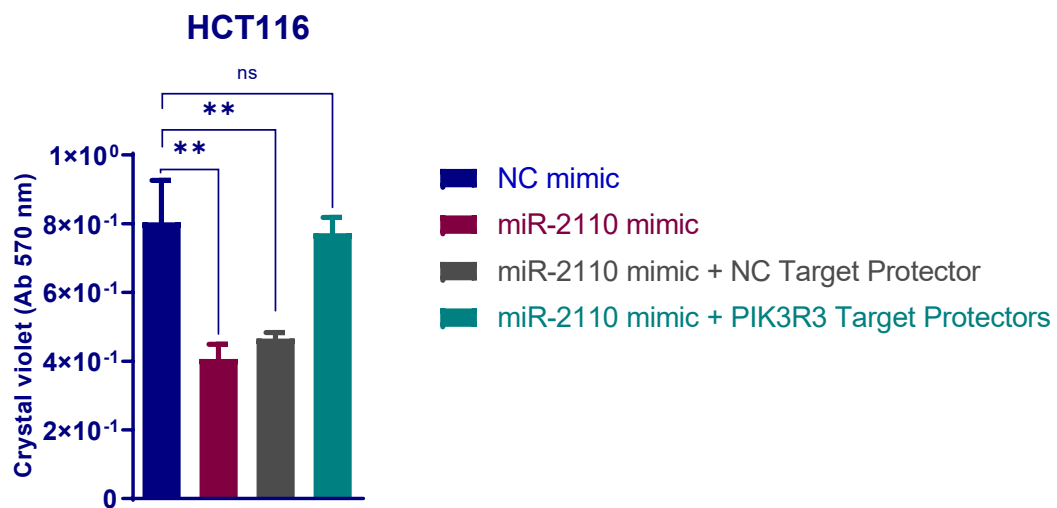


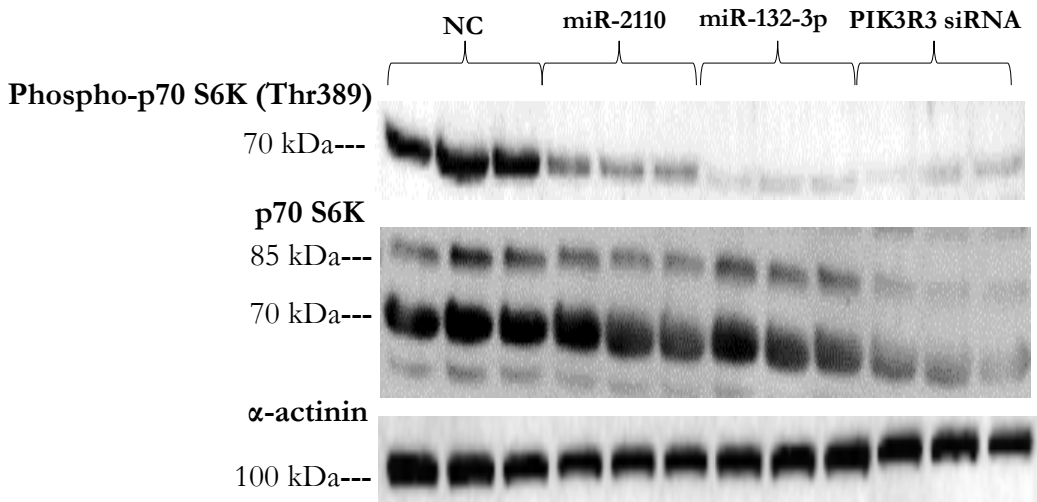
**Figure 4-17. Proliferation of HCT116 cells 72 hours post-transfection with PIK3R3 target protectors and miR-2110 mimics compared with miR-2110 mimics and negative control mimics.**

Representative light microscope images of transfected HCT116 cells. Images were acquired at 10x magnification. TP: Target Protector **(A)**. Cell viability measurements using the Crystal violet assay in HCT116 cells co-transfected with miR-2110 or NC mimics and with negative control target protector or *PIK3R3* target protectors for 72 hours **(B)**. Results are expressed as mean  $\pm$  SD of 3 culture replicates and the statistical significance is indicated with asterisk (ns  $P > 0.05$ , \*\*  $P \leq 0.01$ ).

#### 4.2.15 Effect of miR-132-3p and miR-2110 on PI3K/Akt/ mTOR pathway

Suppression of the PI3K/Akt/mTOR signalling pathway is considered a common cellular response to metformin treatment [990, 991]. p70S6 Kinase is one of the downstream proteins in mTOR pathway that regulates transcription, translation, protein and lipid synthesis, cell growth/size and cell metabolism once phosphorylated and activated [992]. To investigate the role of miR-132-3p and miR-2110 in the cellular response to metformin treatment of colorectal cancer cells, HCT116 cells were transfected with miR-132-3p and miR-2110 mimics and the phosphorylation levels of p70S6 Kinase (Thr389) were assessed. As shown in Figure 4-18, exogenous expression of both miR-132-3p and miR-2110 resulted in a reduced p70 S6 Kinase phosphorylation levels compared to the NC mimics. HCT116 cells transfected with PIK3R3 siRNA showed similar results to miR-132-3p and miR-2110 in suppressing p70S6 Kinase phosphorylation (Figure 4-18). While PIK3R3 siRNA transfection resulted in a slight reduction in total p70S6K protein levels, miR-2110 and miR-132-3p transfection had no significant effect on p70S6K levels. Altogether, these results confirm the role of miR-2110 and miR-132-3p in regulating PI3K-mTOR pathway via downregulating PIK3R3 protein synthesis.

(A)



(B)

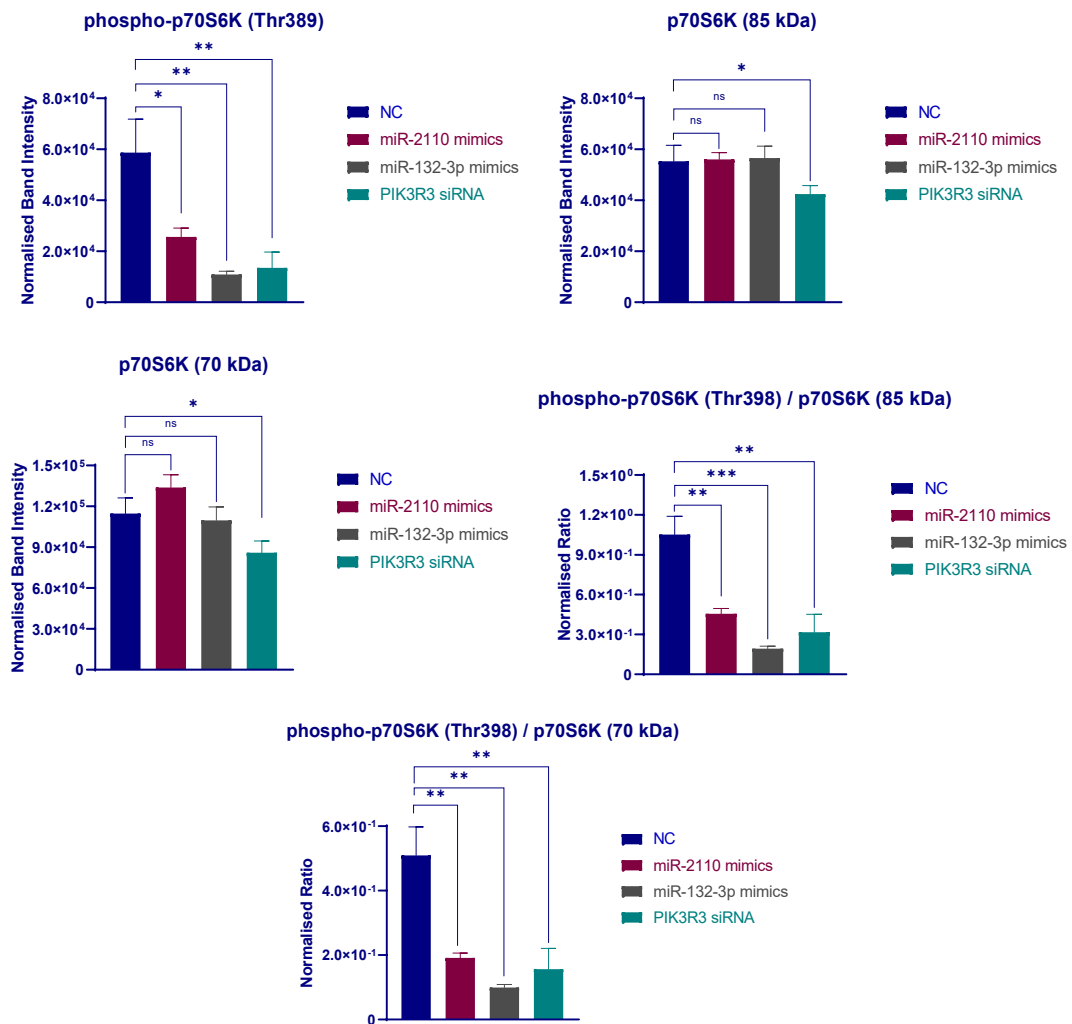


Figure 4-18: Alteration in p70 S6 Kinase phosphorylation levels of HCT116 cells after transfection with miR-132-3p, miR-2110 mimics or *PIK3R3* siRNA compared to NC.

Total p70 S6 Kinase and Phospho-p70 S6 Kinase (Thr389) protein levels in cells transfected with (A) miR-132-3p and miR-2110 mimics and PIK3R3 siRNA as measured by Western blot analysis of three cell culture replicates. Densitometry results were normalised against corresponding  $\alpha$ -actinin protein levels (B). The mean  $\pm$  SD of three cell culture replicates is shown.

#### 4.2.16 Expression of potential miRNA-gene pairs within MAPK pathway following metformin treatment of HCT116 cells

Differentially expressed genes and potential miRNA-gene pairs associated with MAPK pathway were retained from the transcriptome and small RNA sequencing and KEGG pathway analysis data. The miRNA-gene pairs identified from miRNA target prediction tools and from collated validated targets were refined based on being common in  $\geq 2$  prediction algorithms and validated target collections (Table 4-4).

**Table 4-4: miRNA-target gene pairs identified within MAPK pathway.**

miRNA	miRNA baseMean	Gene	Gene baseMean	Prediction Algorithms / Validated gene collections
miR-92a-1-5p	144.35	MECOM	221.96	miRanda, microTCD, TargetScan
miR-7-1-3p	330.32	PDGFA	660.176	microTCD, miRanda, TargetScan
miR-374a-5p	509.13	GADD45A	1093.14	miRanda, miRDB, miRTarBase
miR-222-3p	158962.19	STMN1	13787.24	microTCD, miRanda, TargetScan
miR-589-3p	394.00	STMN1	13787.24	miRanda, TargetScan
miR-766-3p	102.51	TNFRSF1A	893.91	microTCD, miRDB, Targetscan
miR-106b-5p	1597.86	MKNK2	1999.96	miRanda, microTCD, miRDB
miR-34a-3p	39.04	PDGFB	223.97	miRanda, TargetScan
miR-940	63.94	PDGFB	223.97	miRmap, TargetScan
miR-34a-5p	1769.19	RRAS	503.75	microTCD, miRDB

Out of 10 miRNA-gene pairs (1 validated and 9 predicted) 8 pairs were selected for further investigation and 2 miRNA-gene pairs were excluded since the base mean expression for the miRNAs were  $< 100$  (miR-34a-3p and miR-940). miRNA and gene expression changes associated

with 2.5 mM metformin treatment of HCT116 cells were then validated using real-time RT-PCR (Figure 4-19). The expression changes of miR-7-1-3p and miR-374a-5p are shown in Figure 4-9.

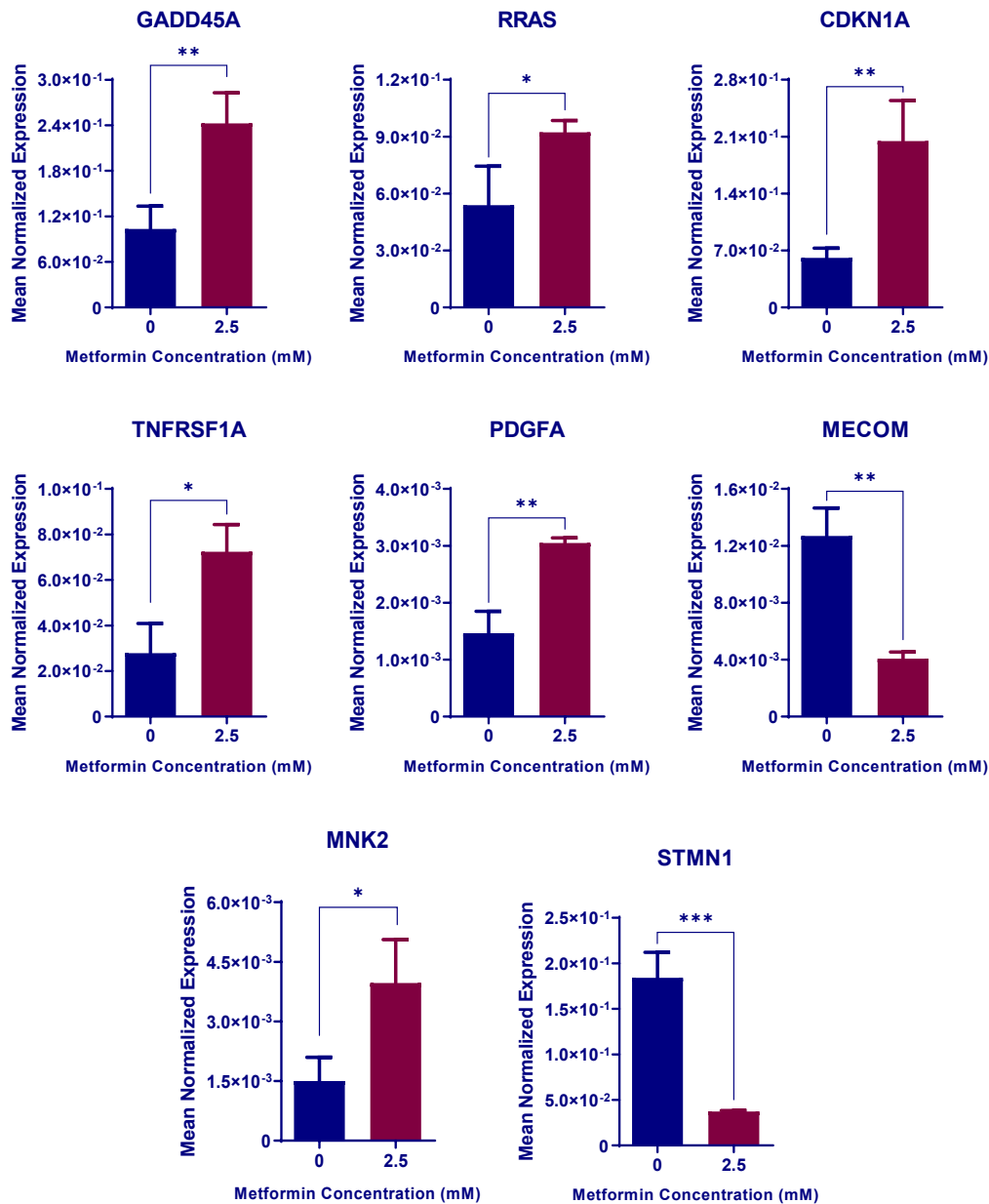


**Figure 4-19: Quantitative real-time PCR results for selected differentially expressed genes associated with metformin treatment of CRC cells within MAPK pathway.**

HCT116 cells treated with 2.5 mM metformin for 72 hours and compared with cells in control medium. Results are expressed as mean ± SD of at least 3 replicates and the expression is normalised to *B2M* expression levels. The statistical significance is indicated with asterisks (\* P ≤ 0.05, \*\* P ≤ 0.01, \*\*\* P ≤ 0.001).

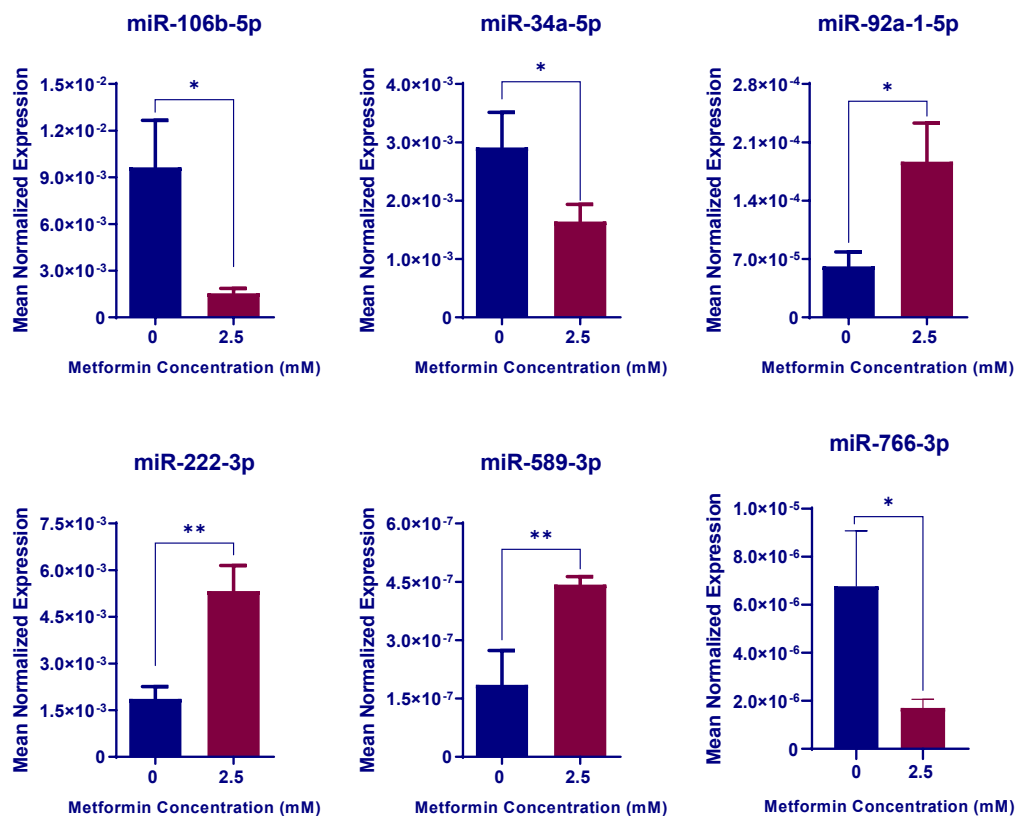


**Figure 4-20: Quantitative real-time PCR results for selected differentially expressed miRNAs associated with metformin treatment of CRC cells within MAPK pathway.**

HCT116 cells treated with 2.5 mM metformin for 72 hours and compared with cells in control medium. Results are expressed as mean  $\pm$  SD of at least 3 replicates and the expression is normalised to miR-16 expression levels. The statistical significance is indicated with asterisks (\*  $P \leq 0.05$ , \*\*  $P \leq 0.01$ , \*\*\*  $P \leq 0.001$ ).

#### 4.2.17 Validation of anti-correlation between expression levels of miRNAs and putative target genes within MAPK pathway

The selected miRNA-gene pairs were cross-referenced with the literature and 4 miRNA-gene interactions (3 predicted and 1 validated targets) were selected for further investigation. According to the literature, selected downregulated and upregulated miRNAs have shown to have oncogenic and tumour suppressive roles, respectively. Whereas, potential upregulated and downregulated target genes had tumour suppressive and oncogenic roles, respectively. To validate direct or indirect targeting of the genes by the miRNAs, HCT116 cells were reverse-transfected with corresponding miRNA mimics and the gene expression levels were assessed by RT-PCR (Figure 4-21).

Among 4 putative/validated miRNA-gene pairs, miR-222-3p and miR-589-3p transfection resulted in downregulated *STMN1* gene expression (by 55 and 75%,  $P= 0.001$  and  $0.0028$ , respectively).

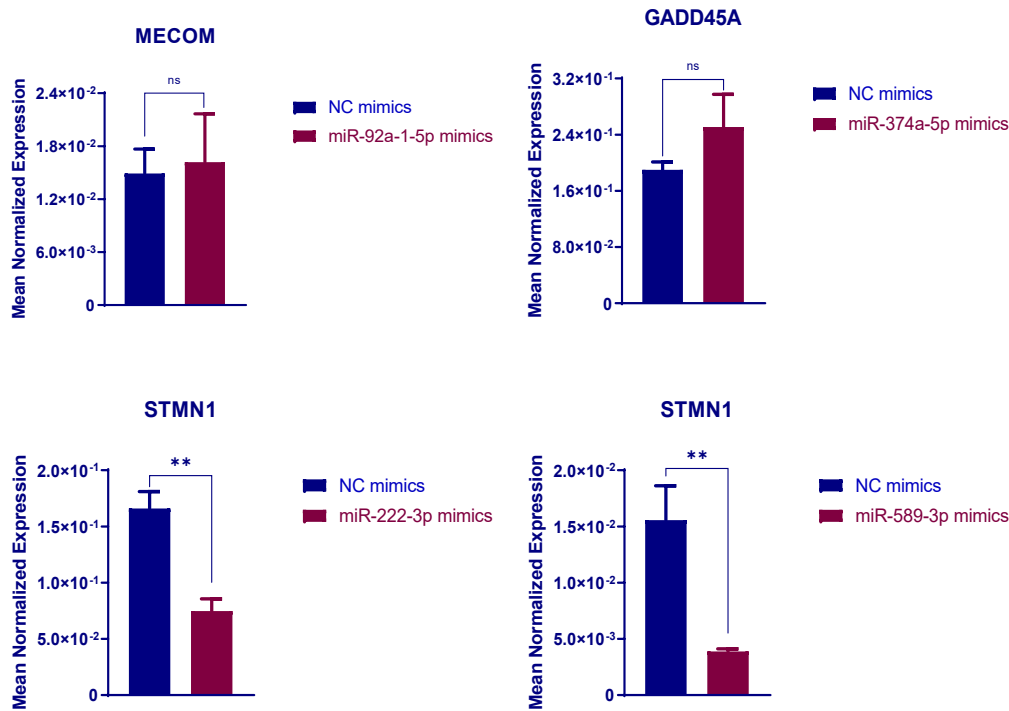


**Figure 4-21: Selected gene expression changes in HCT116 cells 96 hours post-transfection with corresponding miRNA mimics.**

Changes in gene expression levels associated with exogenous expression of selected miRNAs were examined by real-time RT-PCR. *STMN1* and *MECOM* and *GADD45A* expression levels were tested in cells transfected with miR-222-3p and miR-589, miR-92a-1-5p or miR-374a-5p, respectively and compared with NC mimic. Results are expressed as mean  $\pm$  SD of at least 3 replicates and expression levels were normalised to *ACTB* levels. The statistical significance is indicated with asterisks (ns  $P > 0.05$ , \*\*  $P \leq 0.01$ ).

#### 4.2.18 Proliferation of colorectal cancer cells associated with miR-222-3p and miR-589-3p overexpression

To investigate the role of miR-222-3p and miR-589-3p on CRC cell proliferation, the miRNAs were transfected into a CRC cell panel, then viability assayed using crystal violet assay. HCT116, RKO, DLD1, HT29, and Caco2 cell transfection with miR-222-3p or miR-589-3p mimics resulted

in a decrease in cell proliferation as shown by reduction in absorbance of the crystal violet stain (Figure 4-22 and Figure 4-23). Among these cells, HCT116, RKO and HT29 showed lowest cell viability with both overexpressed miRNAs (by 43% and 35% reduction for miR-222-3p and miR-589-3p mimics, respectively) than DLD1, Caco2 and SW480 cells (by 19% and 17% reduction for miR-222-3p and miR-589-3p mimics, respectively). These results confirm the tumour suppressor roles of miR-2110 and miR-132-3p through suppressing cell proliferation.

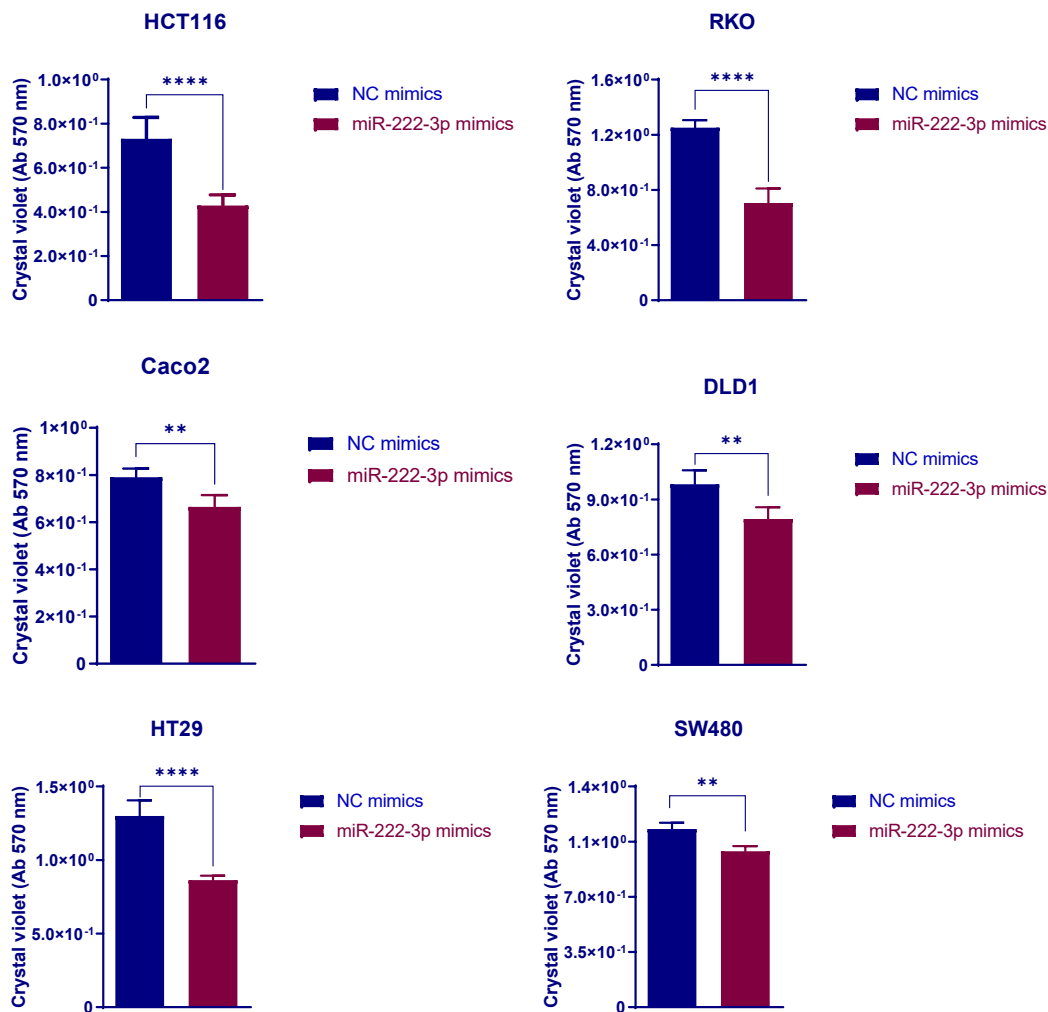


**Figure 4-22: Proliferation of different colorectal cancer cells 96 hours post-transfection with miR-222-3p.**

Quantitative results of crystal violet staining of HCT116, DLD1, RKO, HT29, SW480 and Caco2 cells showing the effect of miR-222-3p mimics on cell proliferation. Results are expressed as mean  $\pm$  SD of at least 3 replicates and the statistical significance is indicated with asterisk (\*\*  $P \leq 0.01$ , \*\*\*\*  $P \leq 0.0001$ ).

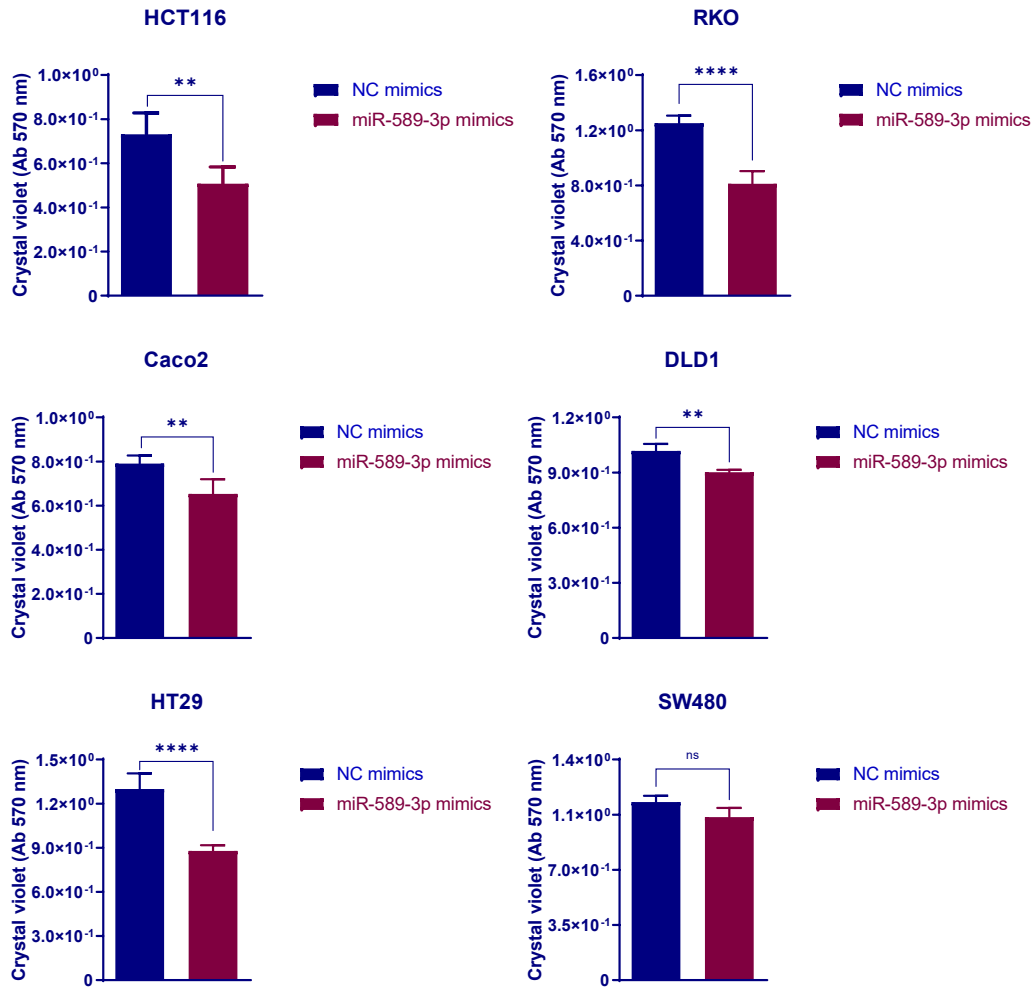


**Figure 4-23: Proliferation of different colorectal cancer cells 96 hours post-transfection with miR-589-3p.**

Quantitative results of crystal violet staining of HCT116, DLD1, RKO, HT29, SW480 and Caco2 cells showing the effect of miR-589-3p mimics on cell proliferation. Results are expressed as mean  $\pm$  SD of at least 3 replicates and the statistical significance is indicated with asterisks (ns  $P > 0.5$ , \*\*  $P \leq 0.01$ , \*\*\*\*  $P \leq 0.0001$ ).

#### 4.2.19 Expression of STMN1 in CRC cells following transfection with miR-222-3p or miR-589-3p mimics

To confirm the mRNA changes associated with miR-222-3p and miR-589-3p overexpression, STMN1 protein levels were assessed in HCT116 cells transfected with miR-222-3p and miR-589-3p mimics. As shown in Figure 4-24, transfection of HCT116 cells with both miRNA mimics led to a significant decrease in STMN1 protein levels relative to control cells transfected with NC mimics. The densitometry analysis revealed 30 and 59 percent reduction in normalised protein

band intensity in miR-222-3p and miR-589-3p transfected cells, respectively. Together, these results suggest roles for both miR-222-3p and miR-589-3p in the regulation of STMN1 in HCT116 cells. However, further experiments were required to confirm the direct targeting of STMN1 these miRNAs.

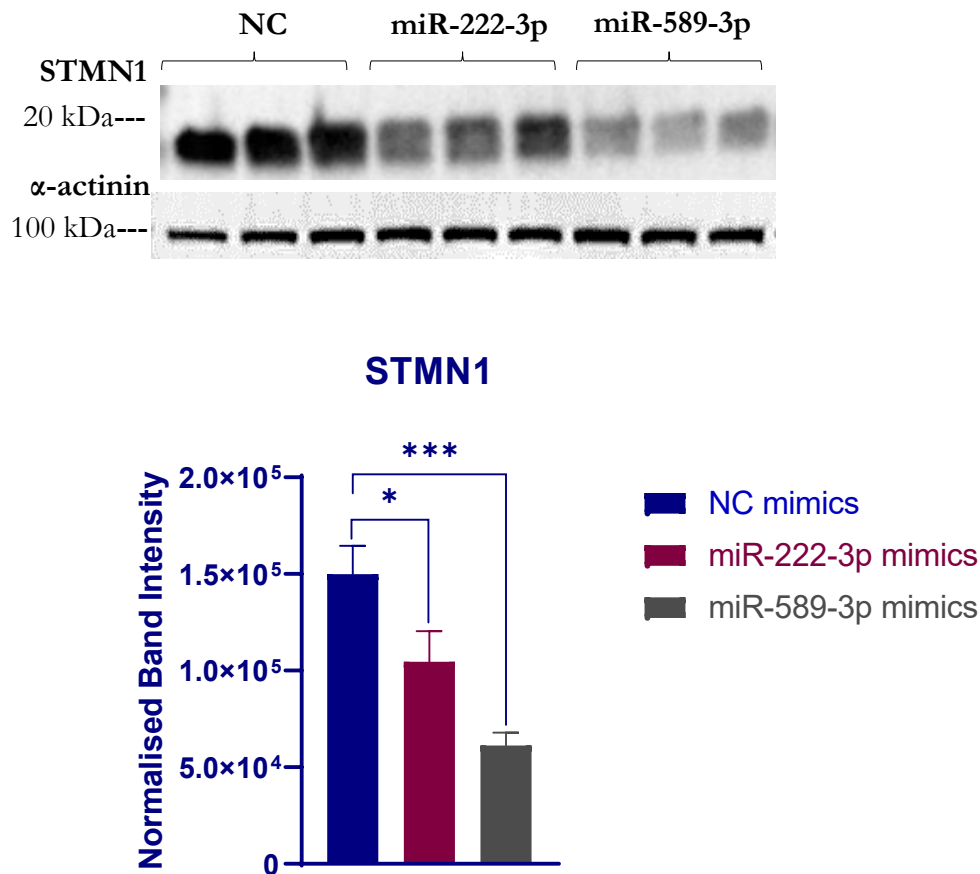


**Figure 4-24: Target gene protein levels in HCT116 cells after transfection with miR-222-3p, miR-589.**

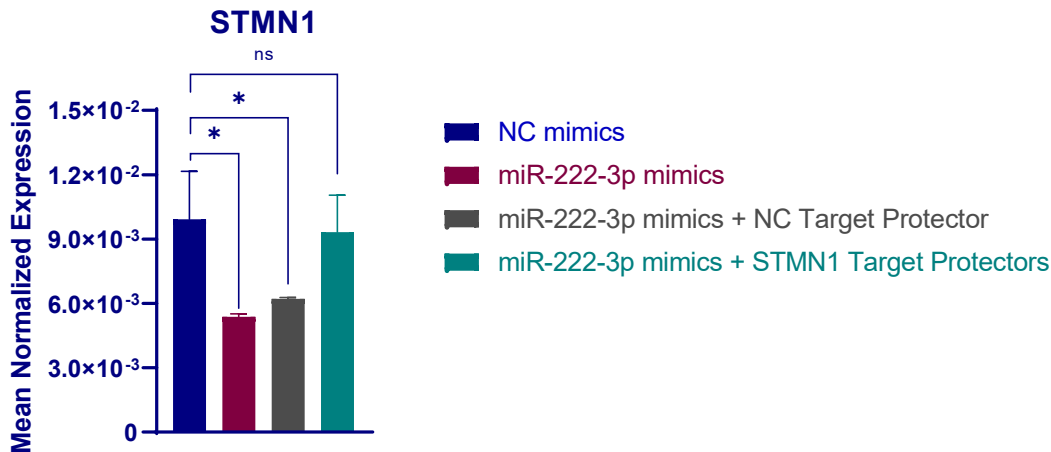
STMN1 protein levels in cells transfected with miR-132-3p, miR-2110 or NC mimics as measured by Western blot analysis 76 hours post-transfection (**A**). Densitometry analysis of PIK3R3 protein levels normalised to the corresponding  $\alpha$ -actinin protein levels (**B**). Results are expressed as mean  $\pm$  SD of 3 replicates and the statistical significance is indicated with asterisk (\*P  $\leq$  0.05, \*\*\* P  $\leq$  0.001).

#### 4.2.20 Validation of STMN1 as a direct target of miR-222-3p and miR-589-3p

STMN1 was predicted to be a direct target of miR-222-3p and miR-589-3p by different target prediction algorithms. (Table 4-4). miR-222-3p and miR-589-3p was identified to have a potential binding site on the 3'UTR of *STMN1* mRNA. The predicted alignments between miRNA seed



(A)



(B)

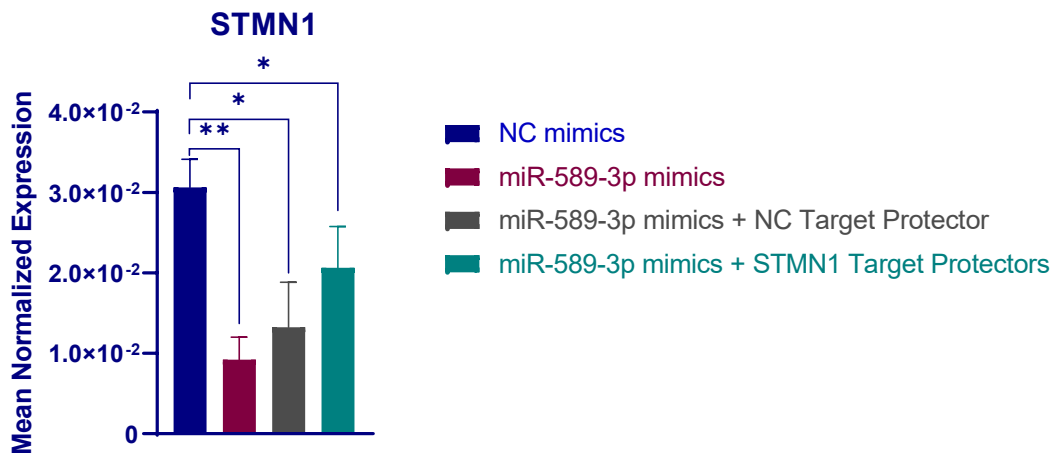


**Figure 4-25: *STMN1* expression changes in HCT116 cells after co-transfection with miR-222-3p or miR-589-3p and specific target protectors.**

mRNA levels of miR-222-3p (A) and miR-589-3p (B) target gene *STMN1* in HCT116 cells co-transfected with miRNA mimics or NC mimics and with NC target protectors or *STMN1* target protectors, for 72 hours and normalised to *ACTNB* expression levels. Results are expressed as mean  $\pm$  SD of 3 replicates and the statistical significance is indicated with asterisks (ns  $P > 0.05$ , \*  $P \leq 0.05$ , \*\*  $P \leq 0.01$ ).

#### 4.2.21 Confirmation of the role of *STMN1* in regulating CRC cell proliferation

As a target of miR-222-3p and miR-589-3p, the effect of *STMN1* knock down on cell proliferation was assessed. *STMN1* expression was dramatically downregulated by transfection cells with specific siRNAs. The knock down efficiency of *STMN1*-specific siRNA is shown in Appendix 6. Following transfection with *STMN1* siRNA, the cell proliferation was investigated using crystal

violet assays. As shown in Figure 4-26, that transfection with *STMN1* siRNA significantly diminished CRC cell growth compared with a negative control siRNA transfection at 72 hours post-transfection in 6 different colorectal cell lines having greatest effect on HCT116 and HT29 cell lines ( $P < 0.0001$ ). The consistent decrease in CRC cell proliferation following *STMN1* knock down confirms the role of *STMN1* as a pro-proliferative gene in CRC cell lines.

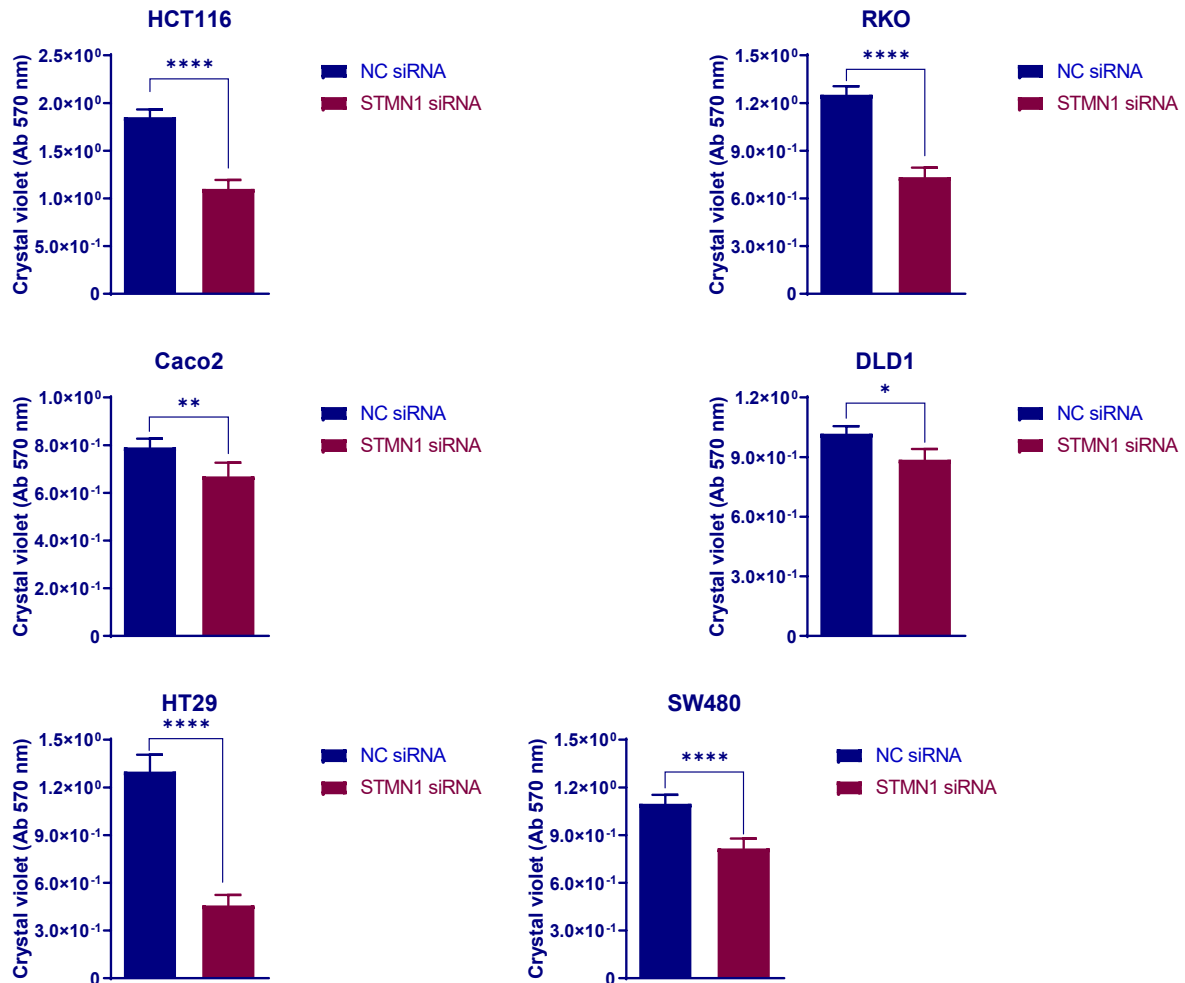


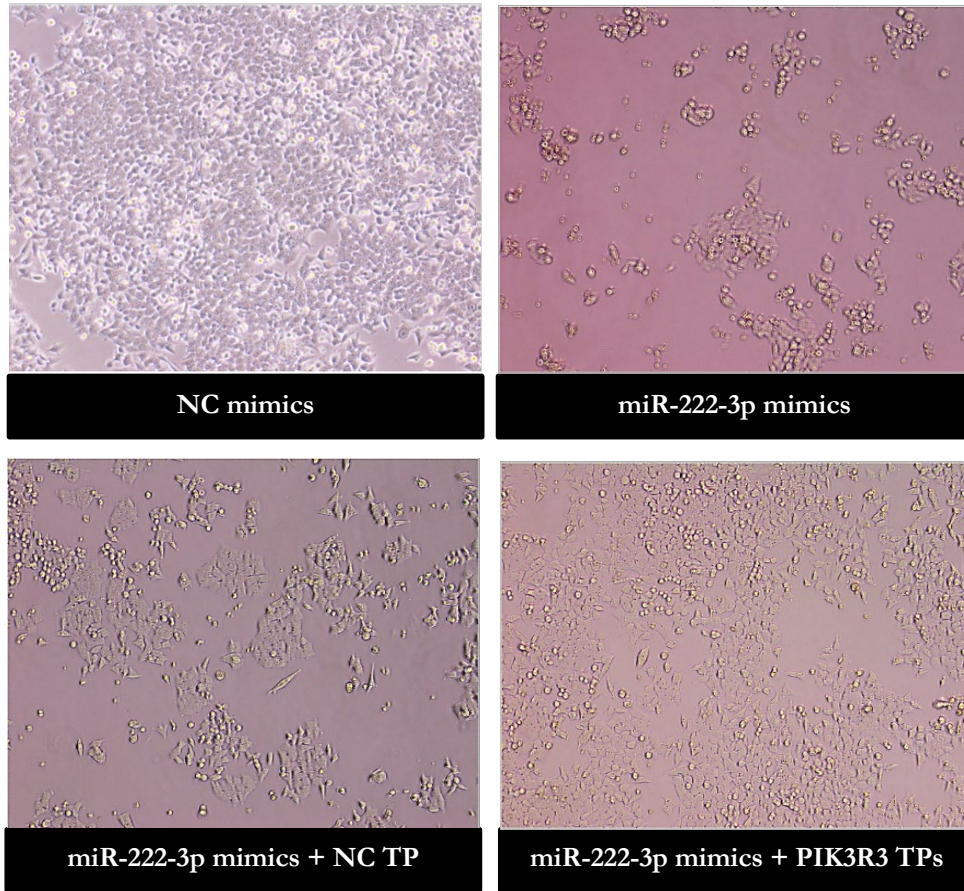
**Figure 4-26: Proliferation of different colorectal cancer cells 96 hours after transfection with *STMN1* siRNA.**

Quantitative results of crystal violet staining of transfected HCT116, RKO, SW480, HT29, DLD1 and Caco2 cells showing the changes in cell proliferation following *STMN1* gene knock down. Results are expressed as mean  $\pm$  SD of at least 3 replicates and the statistical significance is indicated with asterisks (\* $P \leq 0.05$ , \*\*  $P \leq 0.01$ , \*\*\*\*  $P \leq 0.0001$ ).

#### 4.2.22 The biological relevance of *STMN1* suppression by miR-222-3p and miR-589-3p in CRC cells

To investigate the biological outcome of *STMN1* targeting by miR-222-3p and miR-589-3p, cell proliferation was examined following the co-transfection of HCT116 cells with *STMN1* target protectors and miRNA mimics using crystal violet assay 72 hours post-transfection. As shown in Figure 4-27 and Figure 4-28, those cells co-transfected with mimics and corresponding *STMN1* target protectors compared with miR-222-3p or miR-589-3p mimics transfected cells showed significantly higher cell viability as indicated by 24 and 21% increase for miR-222-3p and miR-589-3p associated groups, respectively. Collectively, these results indicate that *STMN1* targeting by miR-222-3p and miR-589-3p contribute to the anti-proliferative effect of miRNA in CRC cell lines.

(A)



(B)

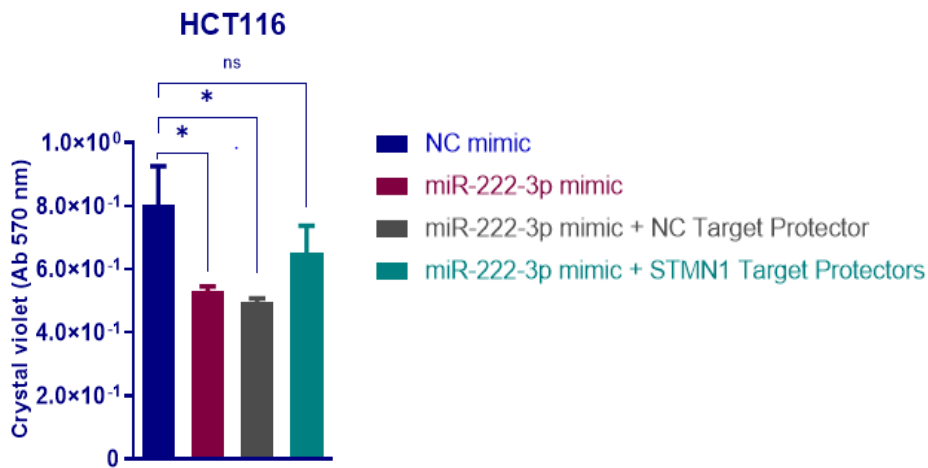
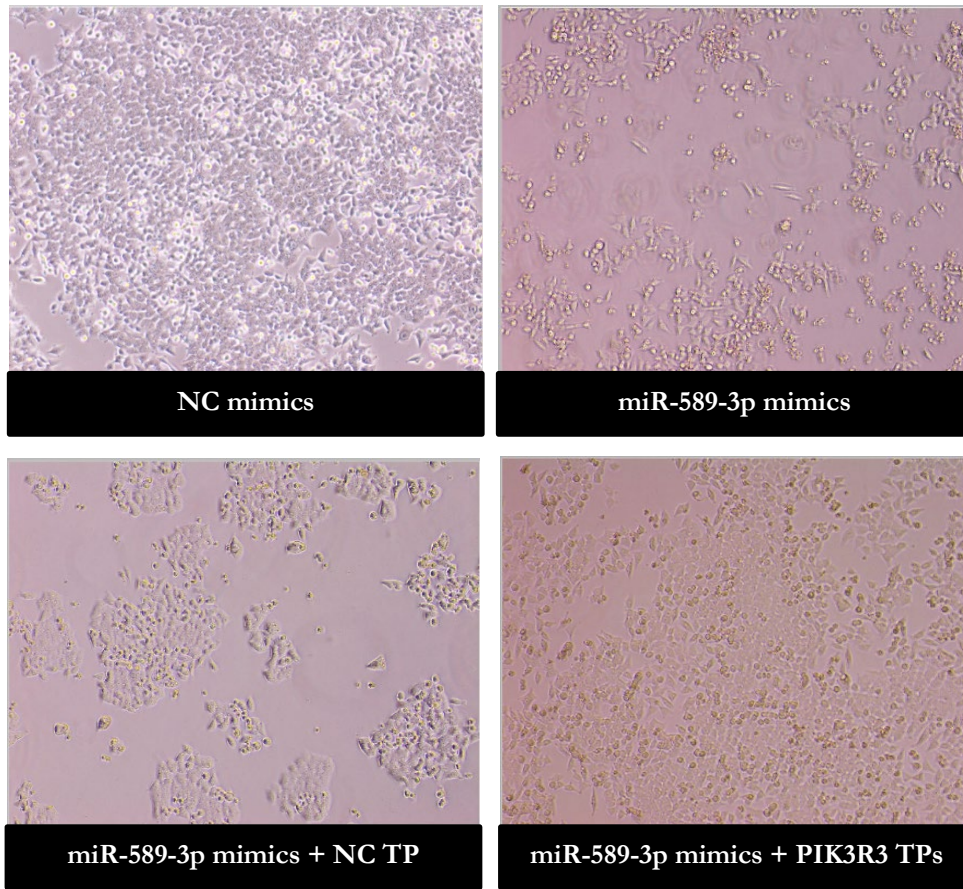


Figure 4-27. Proliferation of HCT116 cells 72 hours post-transfection with *STMN1* target protectors and miR-222-3p mimics compared with miR-2110 mimics and negative control mimics.

## CHAPTER 4

Representative light microscope images of transfected HCT116 cells. Images were acquired at 10x magnification. TP: Target Protector **(A)**. Cell viability measurements using the crystal violet assay in HCT116 cells co-transfected with miR-222-3p or NC mimics and with negative control target protector or *STMN1* target protectors for 72 hours **(B)**. Results are expressed as mean  $\pm$  SD of 3 culture replicates and the statistical significance is indicated with asterisks (ns  $P > 0.05$ , \*\*  $P \leq 0.01$ ).

(A)



(B)

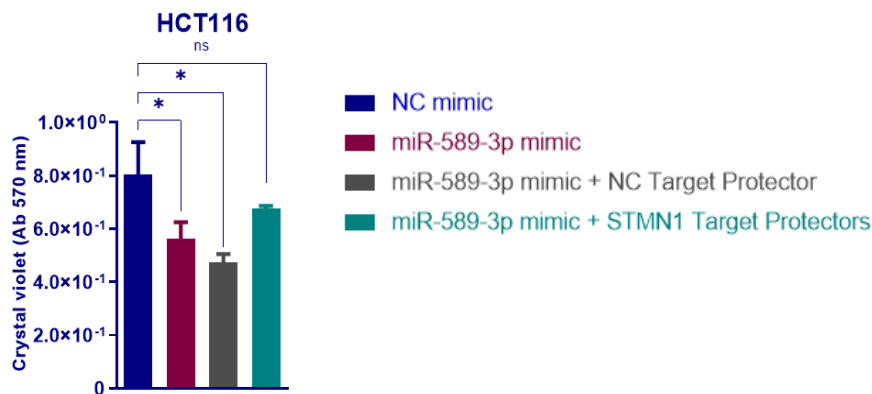


**Figure 4-28. Proliferation of HCT116 cells 72 hours post-transfection with *STMN1* target protectors and miR-589-3p mimics compared with miR-2110 mimics and negative control mimics.**

Representative light microscope images of transfected HCT116 cells. Images were acquired at 10x magnification. TP: Target Protector (A). Cell viability measurements using the Crystal violet assay

in HCT116 cells co-transfected with miR-589- or NC mimics and with negative control target protector or *STMN1* target protectors for 72 hours (**B**). Results are expressed as mean  $\pm$  SD of 3 culture replicates and the statistical significance is indicated with asterisks (ns  $P > 0.05$ , \*\*  $P \leq 0.01$ ).

### 4.3 Discussion

In this chapter, the effect of metformin treatment on transcriptome and miRNA profile changes in different CRC cell line was displayed, through RNA and small RNA sequencing analyses and real-time RT-PCR validation. In HCT116 cells, metformin was shown to alter the expression of 1221 mRNAs and 104 miRNAs. Aberrant expression of mRNAs and miRNAs has been shown to contribute to tumour progression in the gastrointestinal tract, while expression profiles also differ along the gut [42, 43, 993, 994]. While multiple oncogenic miRNA levels decreased in colorectal cell lines, in response to metformin treatment, other miRNAs were shown to increase with metformin treatment. Recent studies on these effects are summarized in 1.7.5. Udhane et al., performed a detailed transcriptome analysis of metformin associated changes and identified 14 DE genes that are involved in intracellular metabolic processes in polycystic ovaries (PCO) [995].

Following systems and integrative analyses, DE genes retrieved from a protein-protein interaction network with degree  $\geq 1$  using ClueGO gene ontology analysis, 163 functional biological processes were identified with significant enrichment scores. “Regulation of macromolecule metabolic process” and “signal transduction” were among the major effector groups in HCT116 cells (Figure 4-4). This is mainly linked to the growth inhibitory effect of metformin as recent cancer metabolism studies confirmed the metabolic shunting of nutrients into macromolecule biosynthesis pathways including proteins, fatty acids, and nucleotides is required for tumorigenesis and sustained proliferative index [3, 7]. Analysis of enriched molecular functions revealed involvement of transcription-related terms to be related to metformin response (Figure 4-5). This is consistent with the effects of metformin on global transcription by regulating histone modifications as well as transcription factors and DNA methylation [996-1000]. Similarly, the featured effect of metformin on “chromosome structure” and “cellular structure”, as revealed by GO analysis of cellular compartments (Figure 4-6), reflects the known targets of this drug in gene expression and cell migration regulation [1001, 1002].

Results on genome-wide scope of the impact of metformin on unique KEGG pathway signatures confirmed the components of PI3K-Akt-related pathways as the major group of molecular targets associated with metformin treatment of HCT116 cells (Figure 4-7). Further validation of the potential miRNA-gene pairs affected by metformin treatment and involved in the PI3K-Akt

pathway, identified *PIK3R3* as a putative target of miR-2110 and miR-132-3p and one of the key regulators of the pathway. miR-2110 and miR-132-3p were significantly upregulated in metformin treated HCT116 cells compared to cells with control medium (Figure 4-9). While several studies have highlighted a key onco-suppressive role for miR-132-3p, there has been little research to date on the role of miR-2110 in cancers. miR-2110 was shown to be rectal cancer-specific and to be associated with tumour development [1003, 1004]. It is a neurite-inducing miRNA and was shown to exert a pro-differentiative and tumour-suppressive role in neuroblastoma [1005]. Similarly, Zhao et al., showed the anti-cancer effect of miR-2110 in inducing neuroblastoma cell differentiation and reducing cell survival through targeting Tsukushi (TSKU) [1006]. Another study on neuroblastoma, showed similar effect of miR-2110 and the anti-correlation of miR-2110 expression with MYCN mRNA levels [1007]. Ectopic expression of miR-132-3p was shown to significantly inhibit CRC cell proliferation and invasion and to be correlated with increased sensitivity to preoperative chemoradiotherapy [1008-1010]. Zheng et al., also showed the inhibitory effect of miR-132-3p on CRC cell invasion and metastasis via direct targeting of ZEB2 [1011]. Downregulation of this miRNA by DNA hypermethylation was shown to be associated with CRC invasion and poor prognosis in colorectal cancer [1009, 1012]. miR-132-3p also suppressed CRC cell proliferation, migration and invasion and induced apoptosis partially via downregulating Derlin-1 or CREB5 mRNA [1013, 1014]. As shown in this chapter, 2.5 mM metformin treatment of HCT116 cells resulted in a significant increase in miR-132-3p and miR-2110 expression levels and a significant reduction in *PIK3R3* expression (Figure 4-8 and Figure 4-9).

The PI3K intracellular signalling pathway plays a critical role in cell apoptosis, proliferation and protein synthesis. Its role in regulation of glucose uptake and metabolism is equally definitive. PI3K dysregulation was reported in several human cancers and several drugs targeting this pathway are currently in clinical trials [302]. An overactivated PI3K-Akt pathway, via genetic mutations and/or gene amplifications, is one of the most common changes associated with tumorigenesis. Activation of PI3K leads to an upregulation of downstream effectors such as AKT and mTOR [1015].

*PI3KR3* encodes a regulatory subunit p55g (so called p55) for PI3 kinases [1016, 1017]. Bearing unique iSH2 and NH2 terminal domains, PI3KR3 binds to the p110 catalytic subunit of PI3K protein and some cell growth key proteins, such as RB1 and PCNA, respectively [1018-1020]. These interactions help PIK3R3 in exerting functions such as promoting tumour cell proliferation, growth, metastasis and angiogenesis [1020-1023].

Liu et al., confirmed direct *PIK3R3* targeting by miR-132-3p in HCC. They also showed that the expression levels of *PIK3R3* were significantly downregulated in HCC tissues and cell lines compared to normal counterparts and had anti-correlation with tumour differentiation, cancer stage and lymph node metastasis. Investigating the molecular target of miR-132-3p, this study confirmed functions such as suppressing cell proliferation, migration, invasion and inhibition of Akt/mTOR signalling pathway: all attributed to *PIK3R3* targeting by this miRNA [989].

In the current chapter, it was shown that ectopic expression of miR-2110 and miR-132-3p resulted in a significant reduction in cell proliferation of the entire CRC cell panel, decreased mRNA and protein levels of *PIK3R3*, as well as decreased mTOR signalling activation, as shown by suppressed p70S6K phosphorylation (Figure 4-12 - Figure 4-19). The functional role of *PIK3R3*, upon metformin treatment, was also confirmed in promoting tumour growth and cell proliferation and suppressing the mTOR pathway following *PIK3R3* knockdown (Figure 4-16).

This study also confirmed *PIK3R3* as a direct target of miR-2110 using target protector assays verifying direct interactions between miR-2110 and *PIK3R3* 3'-UTR. Furthermore, the biological function of this targeting, in this case CRC cell proliferation, was also confirmed (Figure 4-15 and Figure 4-17).

Altogether, these results combined with previous studies, conclude that metformin exerts its anti-cancer properties, partly due to upregulating miRNAs such as miR-2110 and miR-132-3p to directly target genes such as *PIK3R3* and, therefore, regulate signalling pathways such as PI3K-Akt pathway.

On the other hand, KEGG pathway analysis revealed the MAPK signalling pathway to have the highest term significance among 20 terms identified to be associated with metformin treatment of HCT116 cells (Figure 4-7). Further analyses and validation together with literature searches, refined miR-222-3p/miR-589-3p::*STMN1* pairs to be a putative MAPK effector and possible metformin molecular targets.

MAPK proteins are Ser/Thr kinases that relay extracellular signals into a wide range of cellular processes. The MAPK pathway regulates different cellular characteristics such as gene expression, cell cycle, metabolism, motility, cell survival, apoptosis and differentiation [1024].

The hsa-miR-222 encoding gene is located in close proximity of miR-221 on the X chromosome and both are transcribed bicistronically from a single gene cluster [1025]. Both pro- and anti-oncogenic functions have been attributed to miR-222-3p in different cancers, suggesting a

context- dependent and bimodal role for this miRNA [1026-1028] . While upregulation of miR-222-3p was reported in some cancers including glioblastoma, non-small lung cancer, lymphoma, Kaposi sarcoma and hepatocellular cancer, in some cases miR-222-3p was downregulated compared with non-cancer specimens and cells [1025, 1029-1031]. Functioning as an oncogenic miRNA, miR-222-3p was shown to target p27Kip1 and p57 to diminish CDK inhibition. It also induced EMT by noncanonically upregulating *ZEB2* expression [1032-1034]. In contrast, miR-222-3p overexpression in malignant glioblastoma cells increased the cell population in S-phase and induced apoptosis [1035]. Fuse et al., reported a reduced level of miR-222-3p in clinical specimens of prostate cancer compared with non-cancer tissues and a tumour-suppressive function for this miRNA by suppressing cell proliferation, migration and invasion [1036]. In lung cancer cell lines, growth suppression was also shown through intra-S phase arrest and induced apoptosis [1037]. Similarly, phorbol myristate acetate (PMA)-induced over-expression of miR-222-3p in acute myeloid leukemia (AML) resulted in cell-cycle arrest and partial differentiation [1038].

Whilst some research has been carried out into miR-589-5p, there is still very little scientific understanding of the function of miR-589-3p in cancers. Cesarini et al., reported an A-to-I editing within miR-589-3p seed sequence exclusively in normal brain but a significant decrease in editing in glioblastoma cell lines and tissue. They also showed suppressed cell proliferation, migration and invasion once miR-589-3p editing was induced in glioblastoma cells [1039]. Also, miR-589-3p was shown to promote lumbar disc degeneration (LDD) by having a pro-apoptotic role in lipopolysaccharide (LPS) stimulated Nucleus pulposus (NP) cells [1040].

*STMN-1* encodes stathmin1/oncoprotein-18, which is a cytosolic protein and regulates microtubule dynamics during mitotic spindle formation [1041, 1042]. *STMN1* is highly expressed in different types of cancers such as colorectal, gallbladder, breast cancer, hepatocellular carcinoma, sarcoma, and lung and prostatic adenocarcinoma [1043-1050] and is correlated with clinical outcome of patients with cancers such as breast cancer, glioma and hepatocellular carcinoma [1051-1053]. *STMN1* has been found to be associated with MAPK signalling pathway and, thus, to be involved in cell-cycle progression [1054]. Its involvement in tumorigenesis in different types of cancer was also reported. *STMN1* silencing resulted in inhibited cell growth, induced apoptosis and delayed G2/M phase transition in gallbladder cancer cells via regulating the activity of p38 MAPK kinase and p53/p21 signal pathways [1043]. MAPK activation was also shown to upregulate miR-193b, which suppresses *STMN1* in pancreatic cancer and thereby reduces proliferation [1055]. Inhibition of *STMN1* was shown to result in induced apoptosis, arrested cell

growth and invasiveness [1056, 1057]. In colon cancer, *STMN1* phosphorylation by EGFR serves as a rate-limiting step for PI3K/Akt pathway and, thus, involved in metabolism-related carcinogenesis. [1058-1060].

As shown in this chapter, the expression of both miR-222-3p and miR-589-3p was dramatically upregulated by metformin treatment in HCT116 cells and there was a significant reduction in *STMN1* gene expression in treated cells compared with control group. Furthermore, the exogenous expression of miR-222-3p and miR-589-3p had an anti-correlation with CRC cell proliferation and *STMN1* mRNA and protein levels. Target protector assays also confirmed the direct binding and mediated downregulation of *STMN1* expression by these miRNAs. The biological outcome of *STMN1* targeting by miR-222-3p and miR-589-3p was also confirmed where direct *STMN1* targeting was shown to significantly suppress CRC cell proliferation.

In summary, this chapter provide a mechanism of action by which metformin regulates some signalling pathways such as PI3K-Akt and MAPK pathways through direct miRNA inhibition of target expression. In particular, metformin upregulated miR-2110 and miR-132-3p to directly target *PIK3R3* and, consequently, modulate the PI3K-mTOR pathway and suppress CRC cell proliferation. Similarly, *STMN1* was targeted by metformin-mediated upregulation of miR-222-3p and miR-589-3p and its knockdown resulted in cell growth suppression.

These findings provide new insights into the molecular mechanisms of metformin response that determine its anticancer properties in CRC cells. Future studies are needed to further explore the effect of other identified dysregulated miRNA-gene pairs, that regulate signalling and metabolism in CRC cells.

# Chapter 5. Functional High-throughput screening identifies miRNAs that enhance the anti-cancer properties of metformin

---

## 5.1 Introduction

As shown in Chapter 3, CRC cells showed enhanced proliferation when glycolysis was suppressed by LDHA and PKM2 siRNAs as well as 2-DG treatment. This was concomitant with an increased respiration shown by the elevated oxygen consumption rate in CRC cells. On the other hand, inhibition of respiration by oligomycin was followed by an increase in glycolysis, as shown by elevated extracellular acidification rate and lactate production. This, therefore, represents their flexibility in switching to oxidative phosphorylation when glycolysis is suppressed and vice versa to acquire energy and building blocks for their continued proliferation.

Metformin is generally accepted as a respiration suppressor, mainly through targeting complex I within the oxidative phosphorylation chain and, thus, leads to an imbalanced AMP/ATP ratio and metabolic stress [785]. As shown in Chapter 3, metformin treatment resulted in a dramatic reduction in basal and maximal respiration as well as ATP synthesis. Despite various *in vivo* and *in vitro* studies confirming the anti-neoplastic effect of metformin through direct targeting of cancer cells, much uncertainty still exists about the dose-response issues relevant to its clinical applications [1061, 1062]. Furthermore, preclinical studies that identified specific mutations, such as STK11/LKB that dictate cancer cell sensitivity to metformin, support the rationale for using drug combinations to enhance the response of cancer cells to chronic treatment with metformin [1063, 1064].

miRNAs regulate a large variety of cellular processes and, therefore, their aberrant expression can contribute to human diseases, including cancer. Several miRNAs were identified as tumour suppressors where a global decrease in miRNA expression levels correlates with increased grade of neuroplasticity [1065]. The literature contains various reports of miRNAs utilised as a class of cancer therapeutics [1066]. Among several miRNA targets, metabolism-related mRNAs were shown to regulate different tumorigenesis pathways and represent new therapeutic targets [1067]. Furthermore, altered metabolic profiles have been observed in CRC patients [1068, 1069]. As reviewed in Chapter 1, miRNAs are able to rewire multiple metabolic pathways, thereby contributing to the initiation and progression of cancers. However, in the case of CRC, the effect of miRNAs on glucose metabolism and oxidative phosphorylation is largely unknown.

Furthermore, the effect of metabolism-regulating miRNAs on metformin sensitization in CRC is largely unknown. To address this issue, the aim of this chapter was to perform a functional miRNA mimic screen in order to identify miRNAs with the ability of enhancing the anti-cancer properties of metformin and also regulating energy production pathways in CRC cells.

## 5.2 Results

### 5.2.1 Primary High Throughput Screening

An unbiased high throughput functional screen was performed with a library of 2063 synthetic miRNA mimics (Dharmacon, version 19.0) in HCT116 colorectal cancer cells to identify miRNA mimics that can enhance the sensitivity of the cells to the anti-proliferative effect of metformin. The cells in the screen were treated with sub-optimal dose of metformin (2.5 mM) equivalent to an IC<sub>20</sub> and, therefore, 2.5 mM metformin treatment of HCT116 cells resulted in 20% reduction in cell viability without an enhanced effect on apoptosis (Figure 3-4 & Figure 3-7). The procedure is detailed in Chapter 2. Briefly, HCT116 cells were reverse transfected with individual miRNA mimics for 24 hours using a Janus Automated Workstation and BioTek Multi-Mode Washer Dispenser. The cells were then treated with 2.5 mM metformin at 24 hours post-transfection, for 3 days using a BioTek dispenser. The cells were then stained with Hoechst 33342 and Calcein-AM, fixed using formalin and imaged using an Operetta High-Content Imaging System (Figure 5-1). The image analyses were performed using Columbus Image Data Storage and Analysis System and the data were acquired for cell number, cell area and cell roundness. The positive and negative death controls were cells transfected with siPLK1, to block cell division or non-targeting siRNA, respectively (Figure 5-3). All experimental groups were in duplicates and mock control (media alone) used as the liposome transfection control (Figure 5-3). The replicates showed good reproducibility with Spearman  $r = 0.58$  and  $0.71$  for metformin and vehicle treated groups, respectively (Figure 5-2).

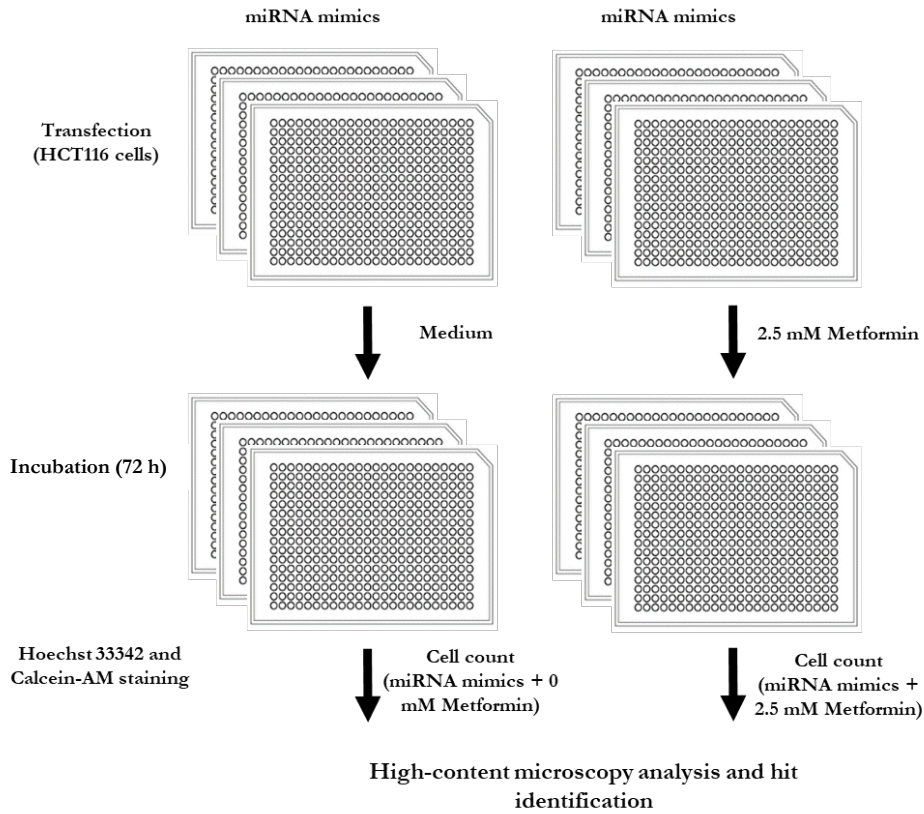


**Figure 5-1: Schematic of high-throughput sensitization screen of miRNA mimics for CRC cell response to metformin treatment.**

Workflow of functional miRNA mimic screen is demonstrated. HCT116 cells were reverse transfected with 25 nM miRNA mimics and following 24 hour incubation, cells were treated with 2.5 mM metformin or control medium for 72 hours. Endpoint high-content image analysis was performed for cells stained with Hoechst 33342 and Calcein-AM 96 hours post-transfection.

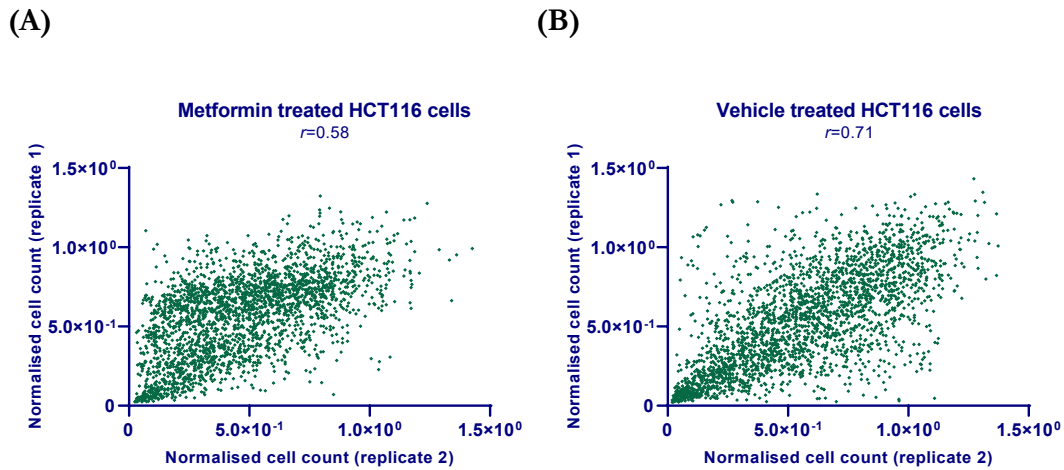


**Figure 5-2: Pairwise correlation between the two independent replicates of the screening.**

Results are based on quantification of normalised cell count in metformin (A) or vehicle treated (B) HCT116 cells 24 hours post-transfection with the library of miRNA mimics and are shown as cell count compared to the control siRNA (siOTP). Spearman rank correlation coefficients are shown.

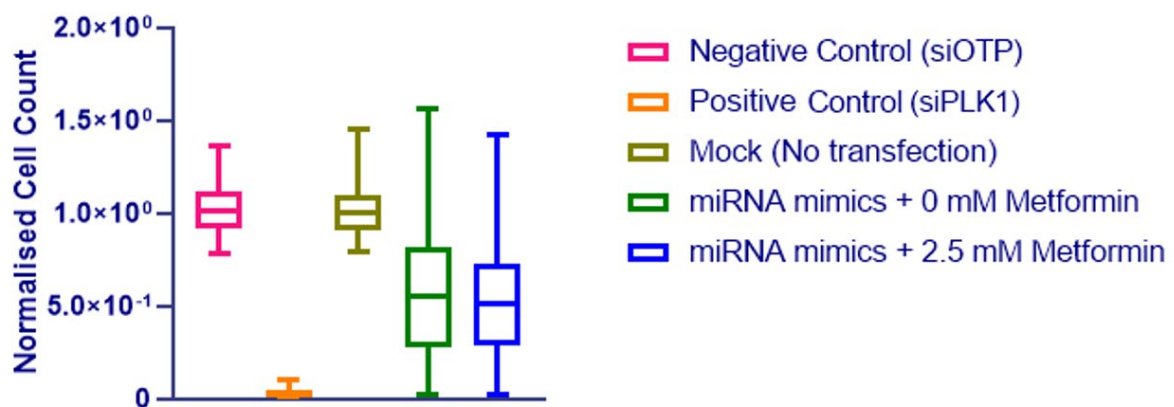


**Figure 5-3: Summary of screen results in HCT116 cells.**

The global overview of the functional high throughput screen of miRNA mimics in combination with 2.5 mM metformin is shown. Negative death control is represented by the viability of cells transfected with negative control (OTP) and positive control is represented by the cells transfected with siRNA targeting PLK1. Mock control also shows the control for transfection.

miRNA mimics were considered to act as a sensitizer if they decreased cell viability by more than 30% with metformin treatment compared with the viability of HCT116 cells transfected with miRNA mimics in control medium. In that case, the viability of metformin treated cells transfected with mimics was  $\leq 70\%$  of the viability of the vehicle treated cells (0 mM metformin) and transfected with non-targeting siRNA (siOTP). This threshold resulted in 176 metformin

sensitising hits among miRNA mimics. The strongest metformin sensitization effect by any of the mimics was an 85% reduction in cell count by hsa-miR-4749-5p mimic (Figure 5-4).

Since this the initial threshold resulted in too many hits, to further refine the list and select the most robust hits, three more rules were applied for the selection: 1) if miRNAs were expressed in HCT116 cells according to earlier small RNA sequencing (Chapter 4) the base mean for the selected miRNAs was more than 30 reads, and/or 2) if the miRNAs are members of the same miRNA family or cluster, and/or 3) if miRNAs were listed in enriched gene ontologies or pathways in the literature, based on the pathway analysis performed using miRNA Pathway Dictionary Database (miRPathDB) [956]. Accordingly, 47 miRNAs mimics were selected. (Figure 5-4).

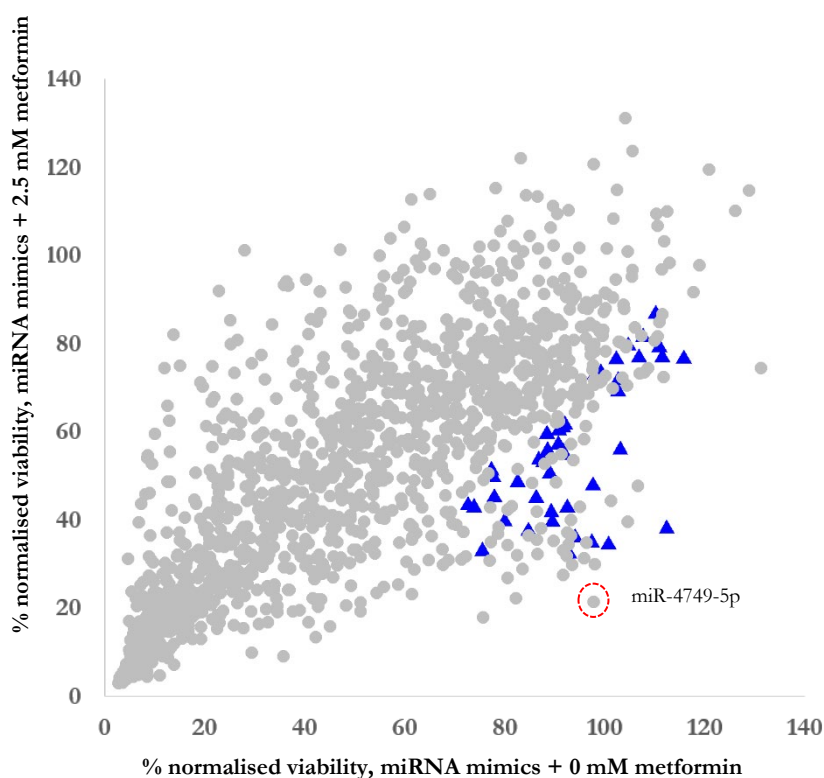


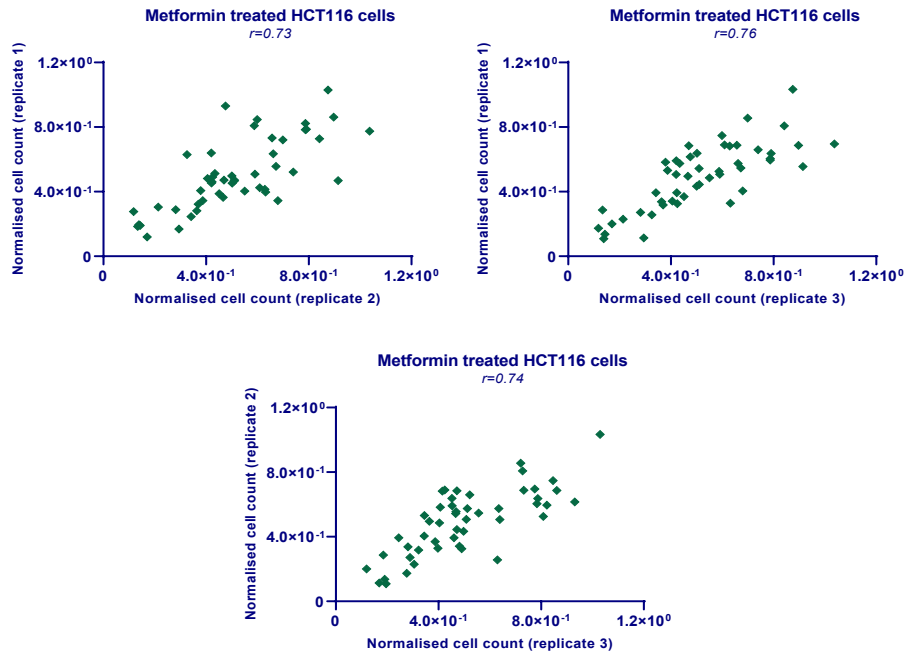
**Figure 5-4: Scatter plot representation of the metformin sensitization screen with a miRNA mimics library.**

Percent viability of HCT116 cells reverse transfected with miRNA mimics and treated with 2.5 mM (y- axis) or 0 mM metformin (x- axis) were shown. The viability values were normalised against siOTP values and miRNAs were cherry picked for a secondary screen (blue triangles).

### 5.2.2 Secondary High Throughput Screening

Selected miRNA mimics that enhanced the sensitivity of HCT116 cells to metformin, were further evaluated in a secondary high throughput screen, with similar workflow but in triplicates. Pairwise correlation of the replicates showed good reproducibility with Spearman  $r = 0.73$ ,  $0.76$  and  $0.74$  for metformin treated and  $0.73$ ,  $0.72$  and  $0.65$  for vehicle treated groups (Figure 5-5).

(A)



(B)

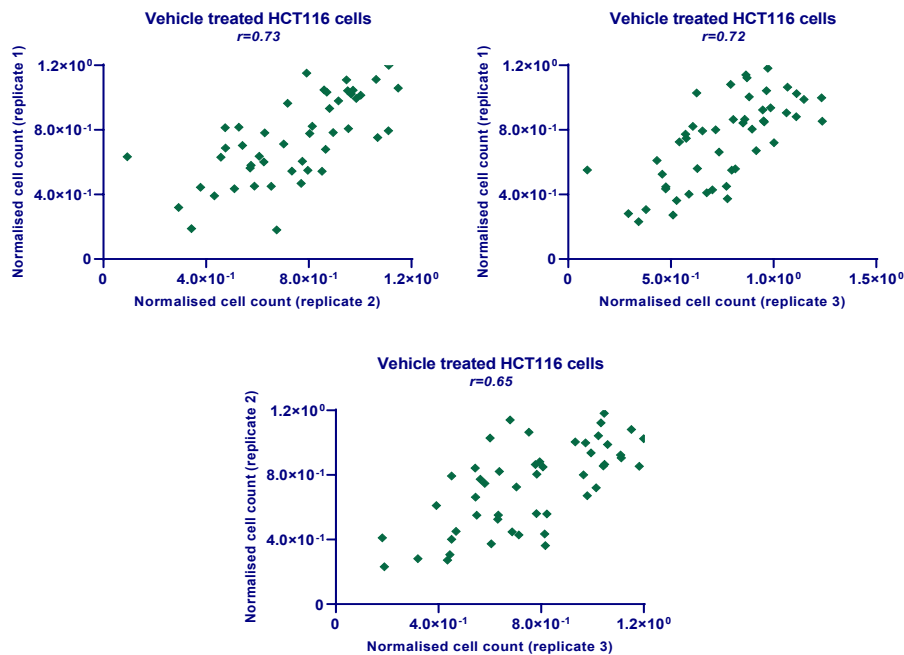


**Figure 5-5: Pairwise correlation between the three independent replicates of the secondary functional screen.**

Results are based on quantification of normalised cell count in metformin (A) or vehicle treated (B) HCT116 cells 24 hours post-transfection with the library of miRNA mimics and are shown as cell count compared to the control siRNA (siOTP). Spearman rank correlation coefficients are shown.

Comparing the effect of combined treatment (miRNA mimic transfection and 2.5 mM metformin treatment) with the effect of metformin treatment or miRNA mimic transfection alone, 12 miRNAs were selected as having a strong synergistic effect ( $CDI < 0.7$ ,  $P < 0.05$ ), Figure 5-6.

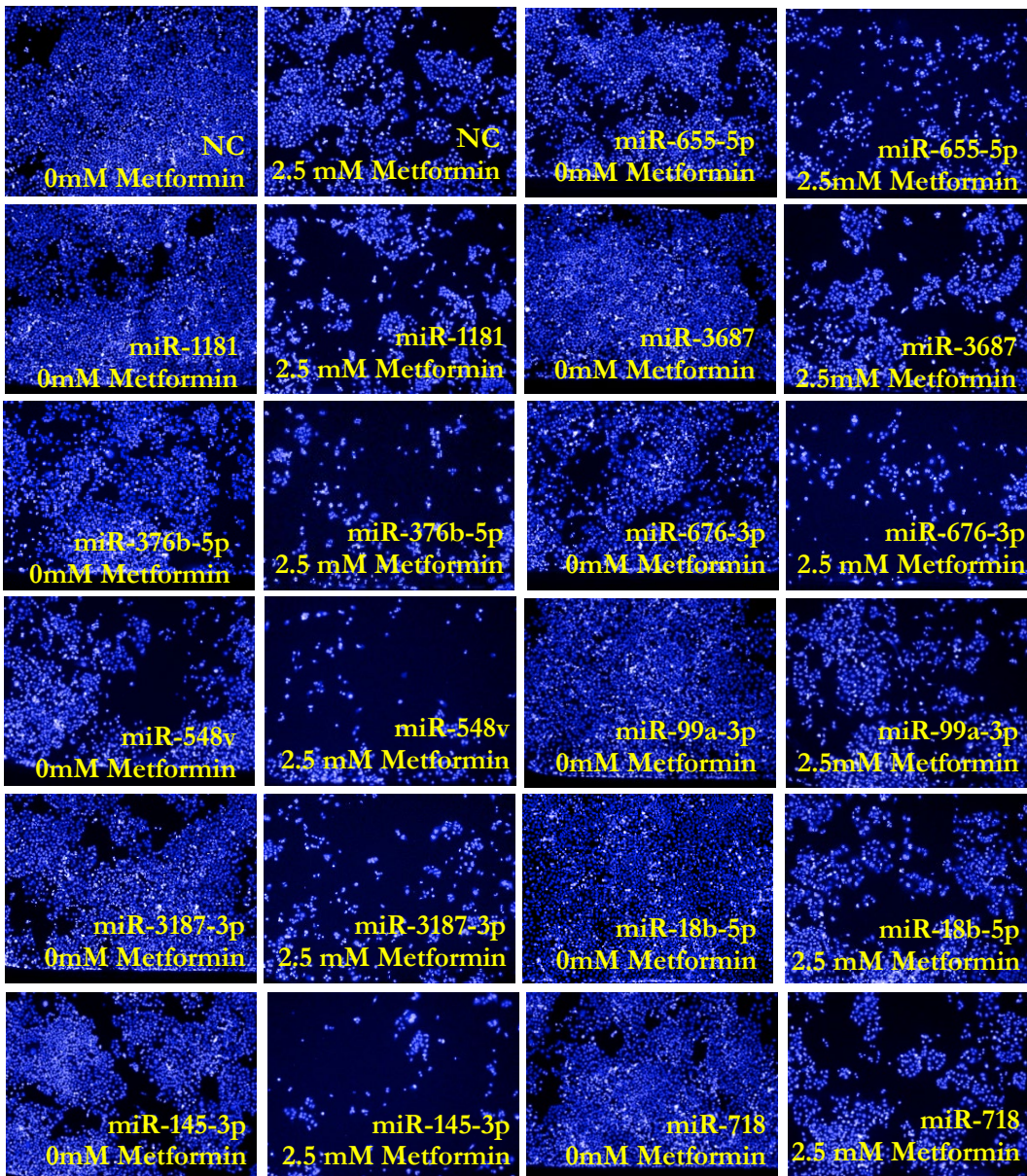


**Figure 5-6: Viability of HCT116 cells transfected with miRNA mimics having strong synergetic effect with 2.5 mM metformin treatment.**

Representative images of HCT116 cells transfected with miRNA mimics, treated with 2.5 mM metformin and compared with 0 mM metformin treatment. Hoechst 33352 staining and image analysis shows viable cells with nucleus shown in blue.

According to the normalised cell count, HCT116 cells treated with metformin and reverse transfected with negative control mimics showed about 30% reduction in viability compared with those counterparts treated with medium ( $P < 0.0001$ , Figure 5-7). While some miRNA mimic transfections in control medium resulted in little to no significant effect on viability of HCT116 cells such as miR-1181, miR-18b-5p, miR-718, miR-3687 and miR-99a-3p, the combination of miRNA mimics and metformin treatment resulted in an enhanced effect on metformin-mediated decrease in CRC cell viability by about 55% compared with cells transfected with NC mimics in control medium ( $P < 0.0001$ ), Figure 5-7. Among other miRNAs that led to a reduction in cell viability in both 2.5 mM metformin treated groups and those in control medium, miR-145-3p and miR-449c-5p had the strongest synergistic effect in combination with metformin reducing cell viability by 85% compared with HCT116 cells transfected with NC in control medium ( $P < 0.0001$ ), Figure 5-7.

CHAPTER 5

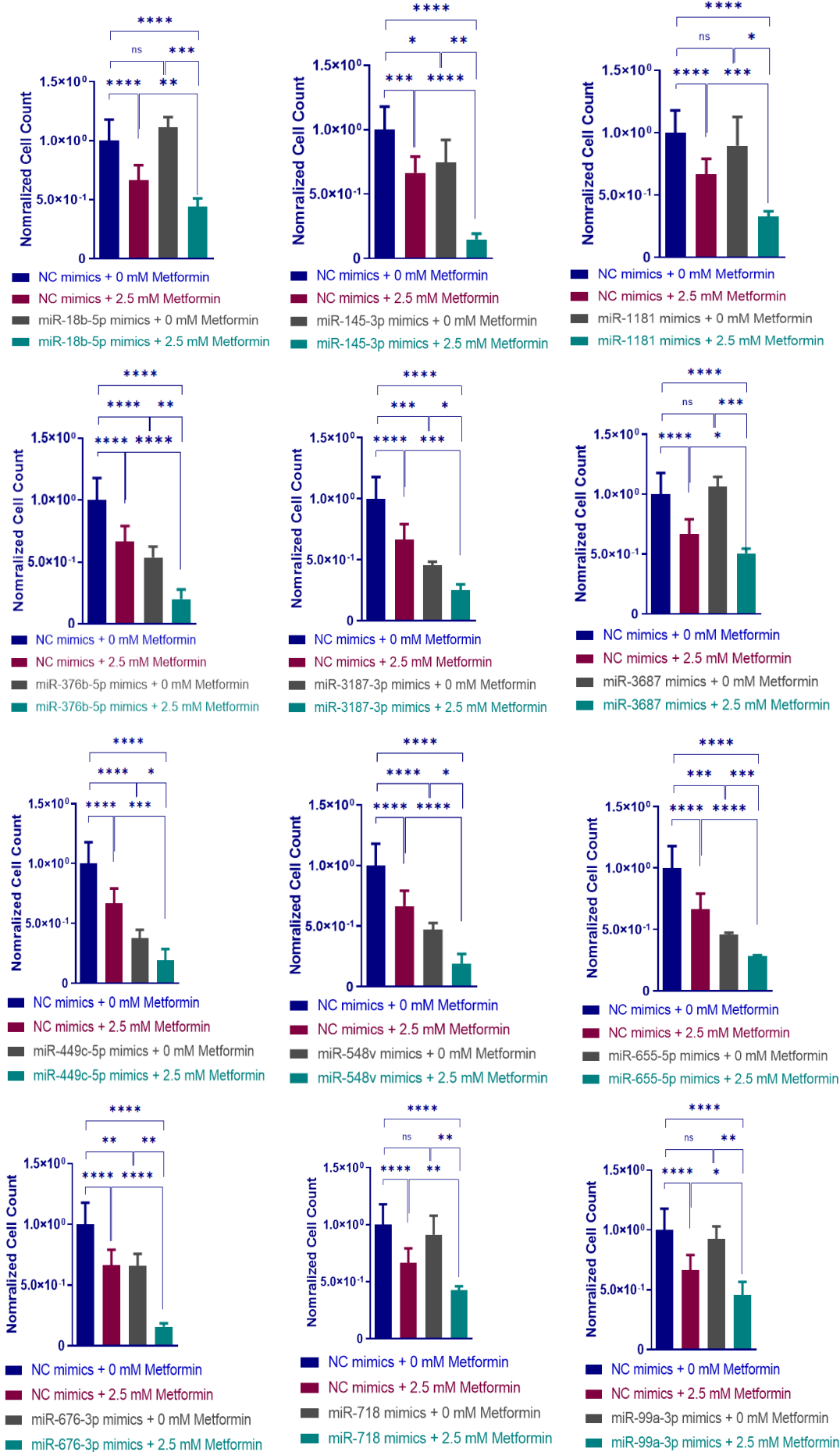


**Figure 5-7: Viability of HCT116 cells transfected with miRNA mimics having strong synergetic effect with 2.5 mM metformin treatment.**

Normalised cell count of HCT116 cells transfected with miRNA mimics, treated with 2.5 mM metformin and compared with 0 mM metformin treatment. Results are expressed as mean  $\pm$  SD of 3 replicates and the statistical significance is indicated with asterisks (ns  $P > 0.05$ , \*  $P \leq 0.05$ , \*\*  $P \leq 0.01$ , \*\*\*  $P \leq 0.001$  and \*\*\*\*  $P \leq 0.0001$ ).

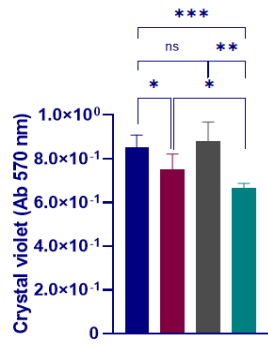
**5.2.3 Real-time Proliferation Validation of secondary screen hits**

A subsequent set of experiments was designed to investigate the anti-proliferative effect of selected miRNAs from the secondary functional screen in combination with metformin. HCT116 cells were transfected with 12 selected miRNAs mimics (miR-145-3p, miR-18b-5p, miR-1181, miR-376b-5p, miR-3187-3p, miR-3687, miR-449c-5p, miR-548v, miR-655-5p, miR-676-3p, miR-718 and miR-99a-3p) or a negative control mimic and on the following day treated with 2.5 mM metformin or control medium for 3 days. Cell proliferation was recorded using the xCELLigence RTCA DP instrument. Also, an endpoint crystal violet assay was used to confirm the cell index measurements (Figure 5-8).

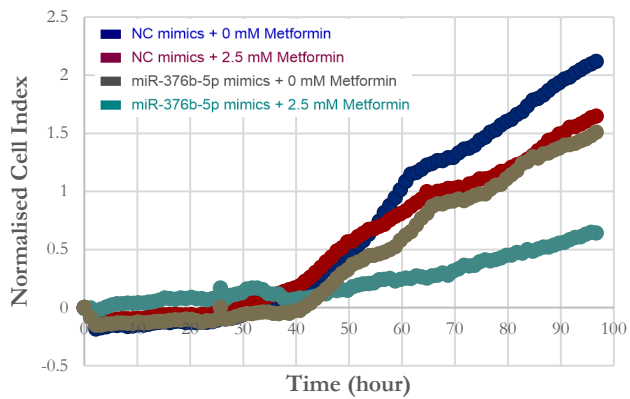
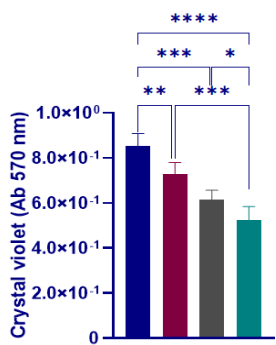
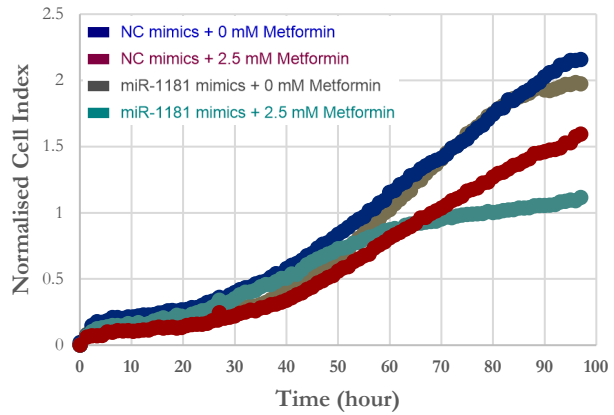
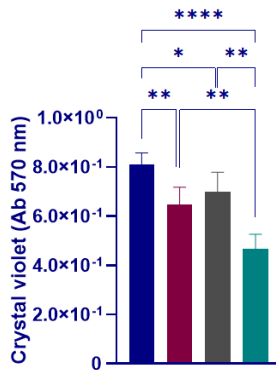
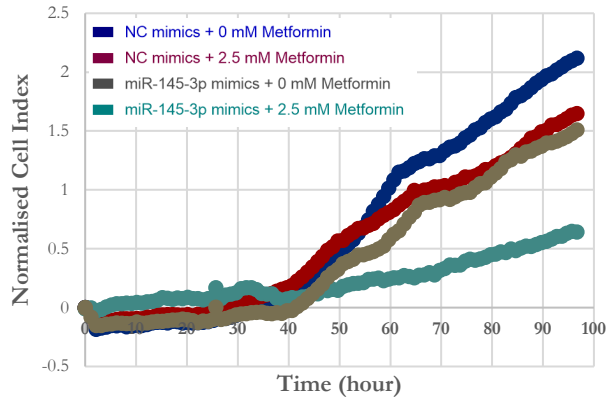
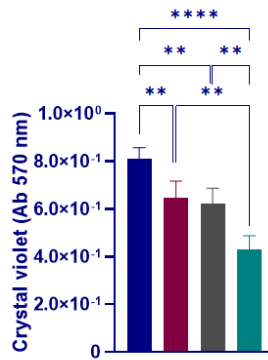
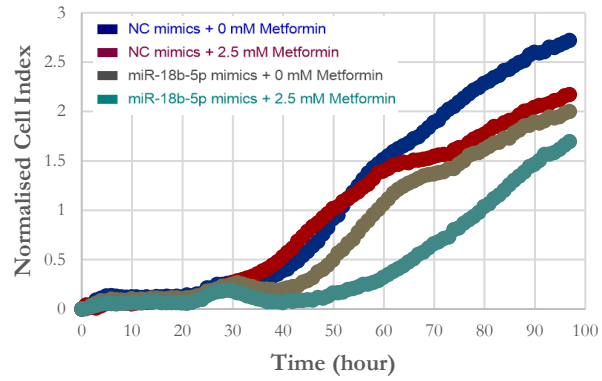
In HCT116 cells, transfection with 8 miRNA mimics enhanced the growth inhibitory effect of metformin as shown by significant reduction in cell viability in cells transfected with mimics and treated with metformin, compared with cells treated with metformin alone or transfected with miRNA mimics alone (Figure 5-8a). These results were consistent with real-time cell index analysis as shown in Figure 5-8b. Among the sensitizing miRNA mimics, in HCT116 cells, transfection of miR-718, miR-145-3p and miR-376b-5p mimics had the most significant effect by reducing the cell index by 76, 70 and 69 %, respectively, in the presence of 2.5 mM metformin.

CHAPTER 5

(A)



(B)



CHAPTER 5

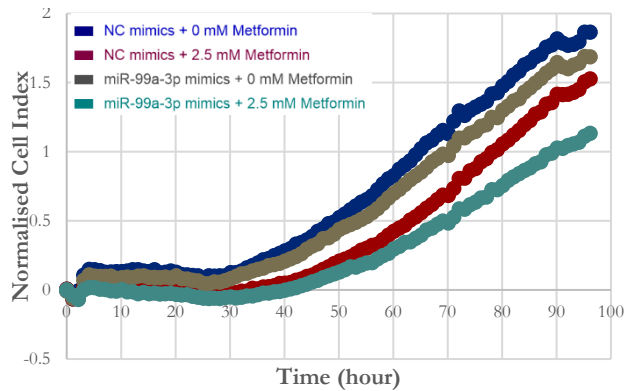
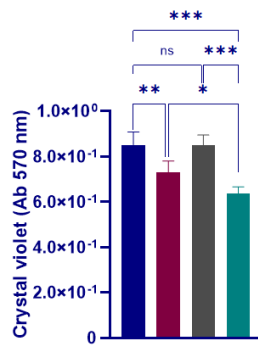
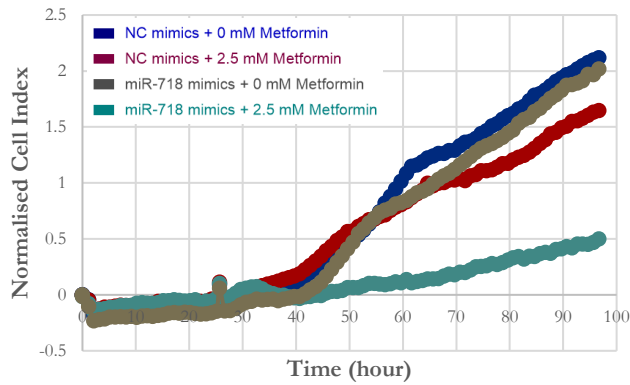
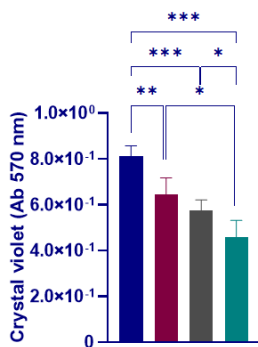
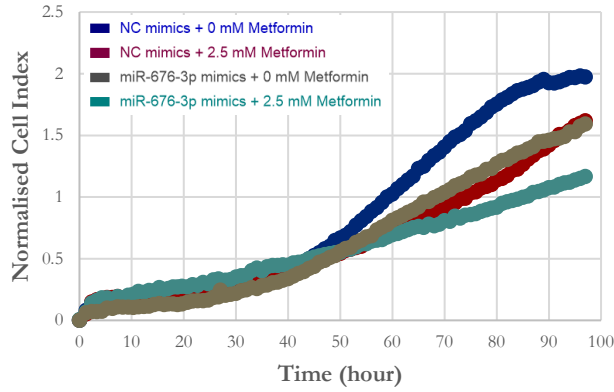
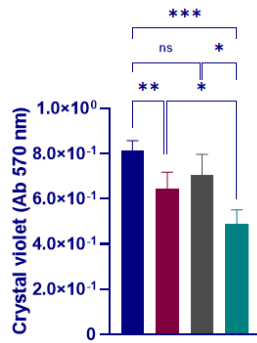
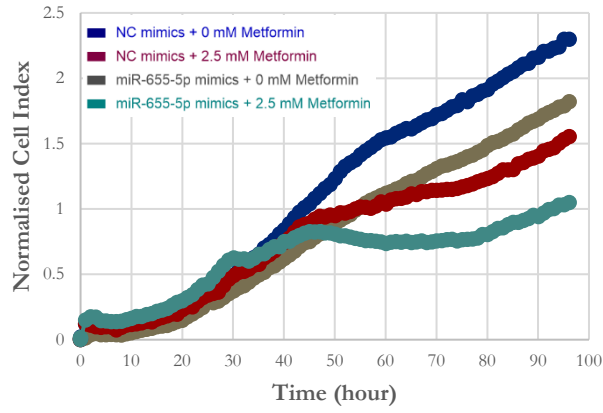
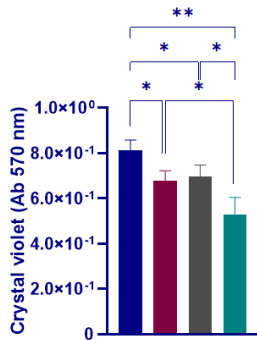


**Figure 5-8. Proliferation of HCT116 96 h post- miRNA mimic transfection and metformin treatment.**

Viability measurements at 96 h using crystal violet assay in HCT116 cells transfected with miRNA mimics or NC and treated with 2.5 mM metformin or control medium 24 hours post-transfection for 72 hours. Results are expressed as mean  $\pm$  SD of at least 3 culture replicates and the statistical significance is indicated with asterisk (ns  $P > 0.05$ , \*  $P \leq 0.05$ , \*\*  $P \leq 0.01$ , \*\*\*  $P \leq 0.001$ , \*\*\*\*  $P \leq 0.0001$ ) **(B)** xCELLigence real-time proliferation graph demonstrating differences in growth kinetics between NC mimics and miRNA treated with control medium or 2.5 mM metformin in HCT116 cells. The average of two replicates is shown. The labels for growth curves in **(B)** correspond to those of the graphs in **(A)**.

### 5.2.4 Changes in glycolytic characteristics of HCT116 cells associated with metformin sensitizing miRNAs

To investigate the ability of the selected sensitizing miRNAs (miR-18b-5p, miR-145-3p, miR-1181, miR-376b-5p, miR-655-5p, miR-676-3p, miR-718 and miR-99a-3p) in regulating cancer glycolysis, Seahorse XFe96 Extracellular Flux Analyzer quantified the generation of lactate as monitored by the consequent extracellular acidification rate (ECAR). Furthermore, sequential compound injections such as glucose and oligomycin and 2-DG allowed calculation of glycolysis, glycolytic capacity and glycolytic reserve (Figure 5-9).

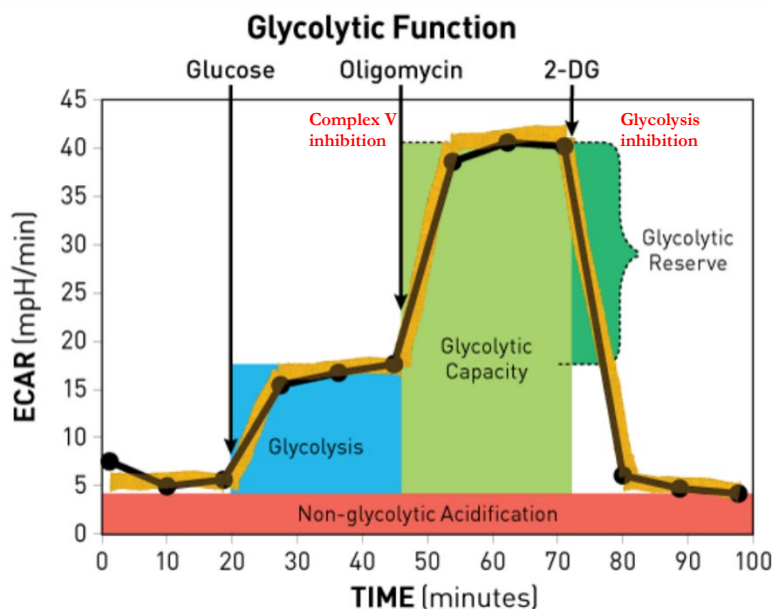


**Figure 5-9: Agilent Seahorse XF Glycolysis Stress Test profile of the key parameters of glycolytic function.**

The extracellular acidification rate (ECAR) measurement by XF Seahorse Bioanalyzer is shown. Sequential compound injections measure glycolysis, glycolytic capacity, and allow calculation of glycolytic reserve and non-glycolytic acidification. (Adapted from [www.agilent.com](http://www.agilent.com)).

## CHAPTER 5

As shown in Chapter 3, metformin treatment results in a significant increase in glycolysis. Similarly, 2.5 mM metformin treatment of HCT116 cells resulted in a significant enhancement of glycolysis as shown by 2.3 fold increase in HCT116 cells transfected with NC mimic and treated with 2.5 mM metformin for 3 days compared with NC mimic transfected cells in control medium ( $P = 0.002$ , Figure 5-10). Among 8 miRNAs tested, transfection with miR-676-3p mimics resulted in a 69% decrease in glycolysis compared with NC mimic transfected HCT116 cells ( $P = 0.0001$ , Figure 5-10). The suppression effect was also significant enough to decrease glycolysis by 79% in cells having combined transfection of miR-676-3p mimics and metformin treatment, compared with cells transfected with NC and treated with 2.5 mM metformin ( $P = 0.0025$ , Figure 5-10). In addition, while transfection of miR-145-3p mimics alone had no significant effect on glycolysis compared with NC mimic transfection in control medium ( $P > 0.05$ ), combination of miR-145-3p mimic transfection and metformin treatment, resulted in a similar effect (16% decrease) on glycolysis compared with metformin treated cells ( $P = 0.037$ , Figure 5-10).

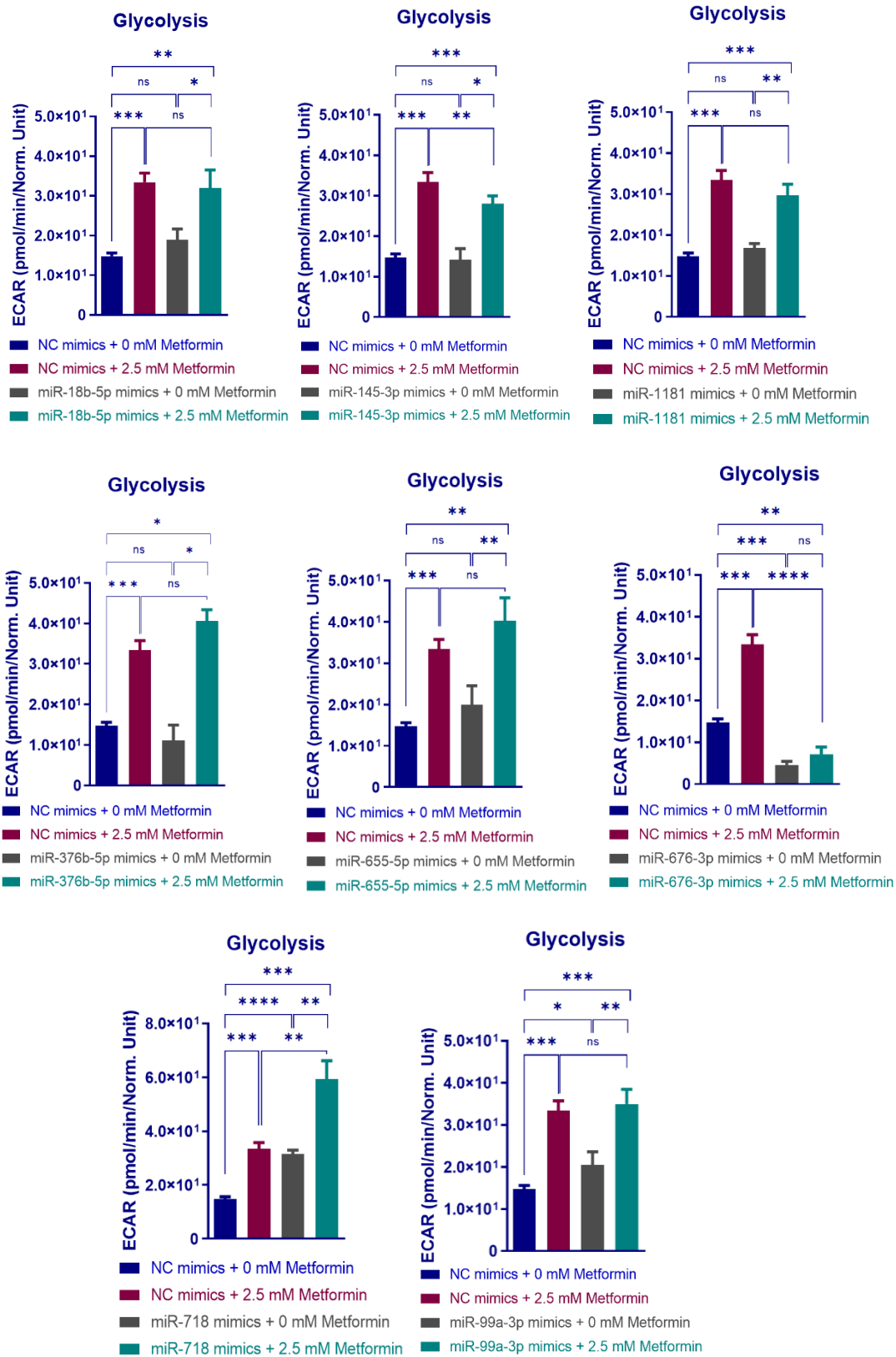


Figure 5-10: Changes in glycolysis associated with miRNA mimic transfections in combination with metformin treatment of HCT116 cells.

## CHAPTER 5

CRC cells were reverse transfected with selected miRNA mimics and treated with 2.5 mM metformin treatment or control medium. Extracellular acidification rate (ECAR) of the cells was determined over a 30-minute period using a Seahorse XF-96 Instrument designed to measure *in vitro* metabolic rates. The ECAR values were normalised to viability of the cells per group determined by crystal violet assay. Results are expressed as mean  $\pm$  SD of 3 culture replicates and the statistical significance is indicated with asterisks (ns  $P > 0.05$ , \*  $P \leq 0.05$ , \*\*  $P \leq 0.01$ , \*\*\*  $P \leq 0.001$ , \*\*\*\*  $P \leq 0.0001$ ). Glycolysis: [(maximum rate measurement before oligomycin injection) – (last rate before glucose injection)].

Although maximal glycolysis, resulting from ATP synthase inhibition, was not affected by metformin treatment of HCT116 cells compared with cells in control medium, combination of metformin treatment with miR-18b-5p and miR-145-3p mimic transfections introduced a significant decrease in glycolytic capacity by 18 and 25% compared with metformin treatment alone ( $P = 0.011$  and  $0.004$ , respectively), Figure 5-11. Transfection with miR-676-3p in control medium showed a dramatic decrease in glycolytic capacity as compared with NC mimic transfection in control medium (by 70%,  $P = 0.0029$ ) and, therefore, combination of miR-676-3p transfection with 2.5 mM metformin treatment represented an enhancement effect by reducing maximal glycolysis compared with metformin treatment alone (by 80 %,  $P = 0.0002$ ), Figure 5-11.

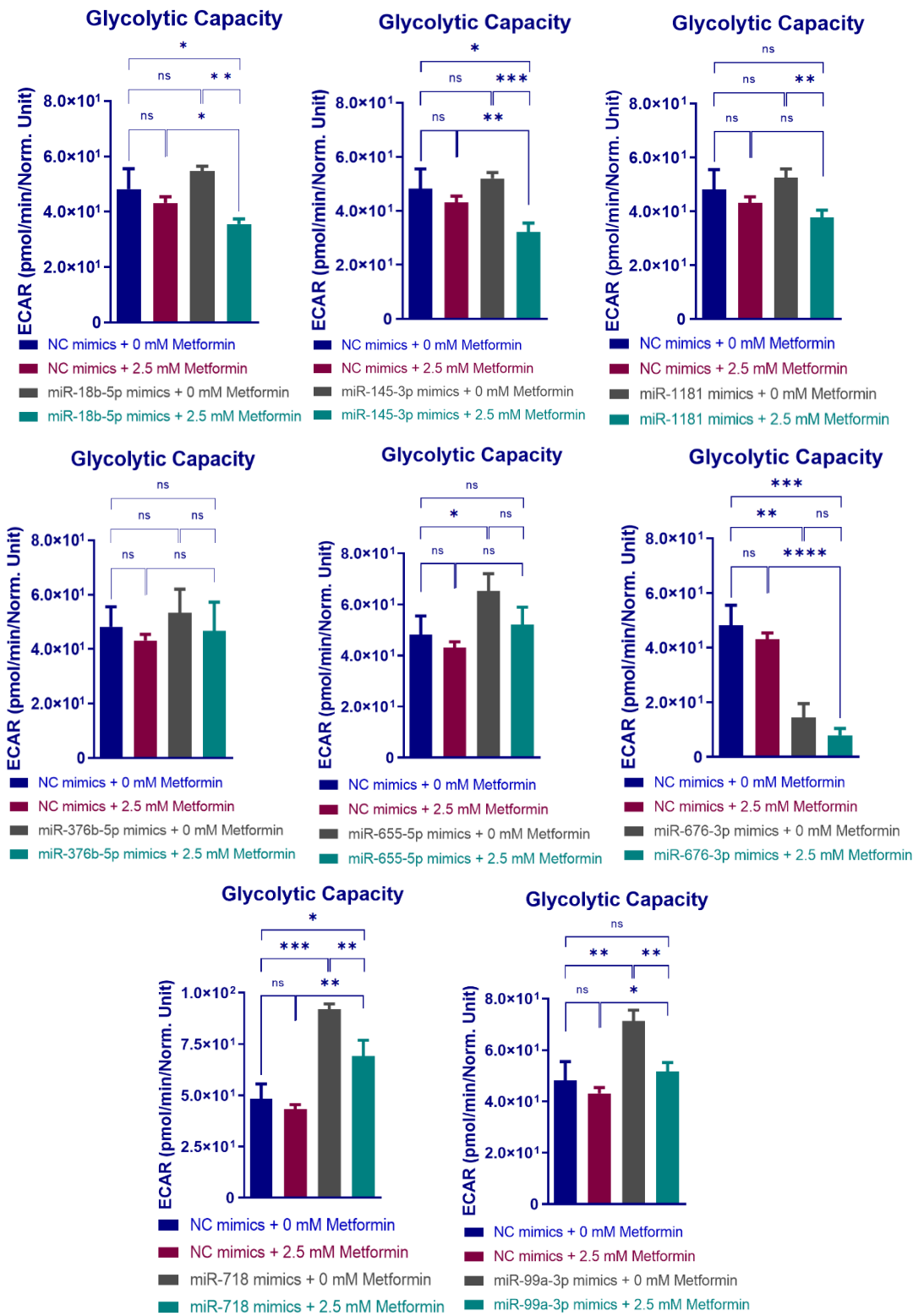


Figure 5-11: Changes in maximum glycolytic capacity of HCT116 cells associated with miRNA mimic transfections in combination with metformin treatment.

## CHAPTER 5

CRC cells were reverse transfected with selected miRNA mimics and treated with 2.5 mM metformin treatment or control medium. Extracellular acidification rate (ECAR) of the cells was determined over a 30-minute period using a Seahorse XF-96 instrument designed to measure *in vitro* metabolic rates. The ECAR values were normalised to viability of the cells per group determined by crystal violet assay. Results are expressed as mean  $\pm$  SD of 3 culture replicates and the statistical significance is indicated with asterisks (ns  $P > 0.05$ , \*  $P \leq 0.05$ , \*\*  $P \leq 0.01$ , \*\*\*  $P \leq 0.001$ , \*\*\*\*  $P \leq 0.0001$ ). Glycolytic capacity: [(maximum rate measurement after oligomycin injection) – (last rate before glucose injection)].

Although the enhancement of metformin on glycolysis was shown in Chapter 3, it resulted in a dramatic decrease in glycolytic reserve (by 3.3 fold,  $P = 0.0005$ ). Investigating the effect of selected sensitizing miRNAs on glycolytic reserve revealed miR-676-3p to have inhibitory effect on glycolytic reserve compared with NC (by 71%,  $P = 0.0028$ ) which led to a 92 % reduction of glycolytic reserve in cells with metformin treatment compared with cells transfected with NC mimics and treated with metformin ( $P < 0.0001$ , Figure 5-12). Moreover, combination of miR-18b-5p and miR-145-3p mimic transfections with metformin treatment resulted in 66 and 57 % fall in glycolytic reserve compared with metformin treatment alone in HCT116 cells ( $P = 0.012$  and 0.0089, respectively). This was in spite of representing no significant effect on glycolytic reserve with miR-145-3p and miR-18b-5p mimic transfections in control medium ( $P > 0.05$ , Figure 5-12).

Altogether, these results showed transfection with miRNA mimics such as miR-676-3p, miR-145-3p and miR-18b-5p, in combination with metformin treatment in HCT116 cells, can diminish the glycolysis enhancement resulting from metformin treatment and to further enhance the metformin mediated reduction of both glycolytic capacity and reserve.

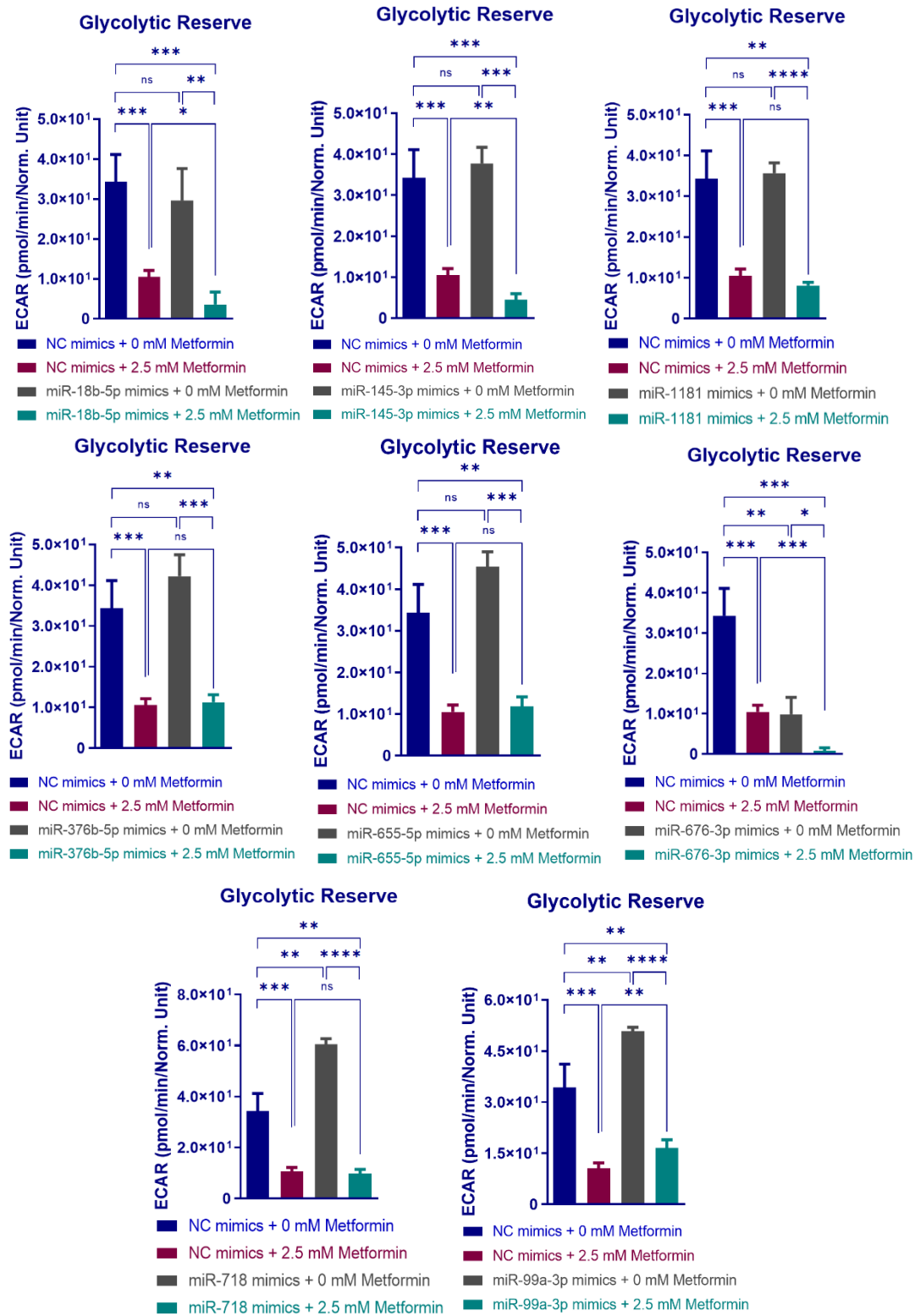


**Figure 5-12: Changes in the glycolytic reserve of HCT116 cells associated with miRNA mimic transfections in combination with metformin treatment.**

CRC cells were reverse transfected with selected miRNA mimics and treated with 2.5 mM metformin treatment or control medium. Extracellular acidification rate (ECAR) of the cells was determined over a 30-minute period using a Seahorse XF-96 instrument designed to measure *in vitro* metabolic rates. The ECAR values were normalised to viability of the cells per group acquired

by crystal violet assay. Results are expressed as mean  $\pm$  SD of 3 culture replicates and the statistical significance is indicated with asterisks (ns  $P > 0.05$ , \*  $P \leq 0.05$ , \*\*  $P \leq 0.01$ , \*\*\*  $P \leq 0.001$ , \*\*\*\*  $P \leq 0.0001$ ). Glycolytic reserve: [(glycolytic capacity) – (glycolysis)].

### 5.2.5 Changes in respiration characteristics of HCT116 cells associated with metformin sensitizing miRNAs

The changes in oxidative phosphorylation of HCT116 cells associated with exogenous miRNA expression in combination with metformin treatment were investigated. Seahorse XFe96 Extracellular Flux Analyzer quantified mitochondrial respiration in which key parameters of mitochondrial function such as basal and maximal respiration, respiratory reserve, ATP synthesis and coupling efficiency were measured by oxygen consumption rate (OCR) and calculated by 3 serial injections of compounds including oligomycin, FCCP, and rotenone/antimycin A (Figure 5-13).

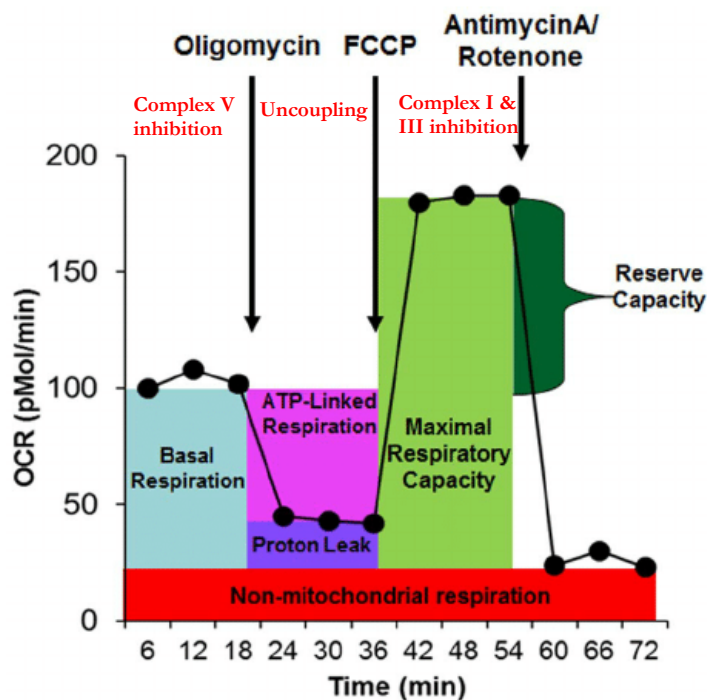


**Figure 5-13:** Agilent Seahorse XF mitochondrial Stress Test profile of the key parameters of respiration.

The oxygen consumption rate (OCR) measurement by XF Seahorse Bioanalyzer is shown. Sequential compound injections enable measurement of basal respiration, ATP-linked respiration and allow calculation of respiratory reserve and proton leak. (Adapted from [www.agilent.com](http://www.agilent.com)).

## CHAPTER 5

Since metformin treatment alone resulted in a dramatic fall in almost all mitochondrial function including basal respiration, maximal respiration, respiratory reserve and ATP synthesis (by 71 %, 66 %, 59 % and 68 % with  $P = 0.0064$ ,  $0.0065$ ,  $0.017$  and  $0.0004$ , respectively) compared with cells in control medium, combining miRNA transfections with metformin treatment had little to no further enhancement effect on some of these parameters. For instance, there was no enhancement in reserved capacity with all 8 mimic transfections investigated in combination with metformin treatments ( $P > 0.05$ , Figure 5-14). Furthermore, only miR-718 mimic transfections led to a 10% reduction in coupling efficiency compared with NC mimic transfections ( $P = 0.0025$ ). When these transfections were combined with metformin treatment there were further 17% and 12% reductions in coupling efficiency compared with NC mimic transfections in control medium or medium with 2.5 mM metformin, respectively ( $P = 0.0007$ ,  $0.002$ , respectively), Figure 5-14.

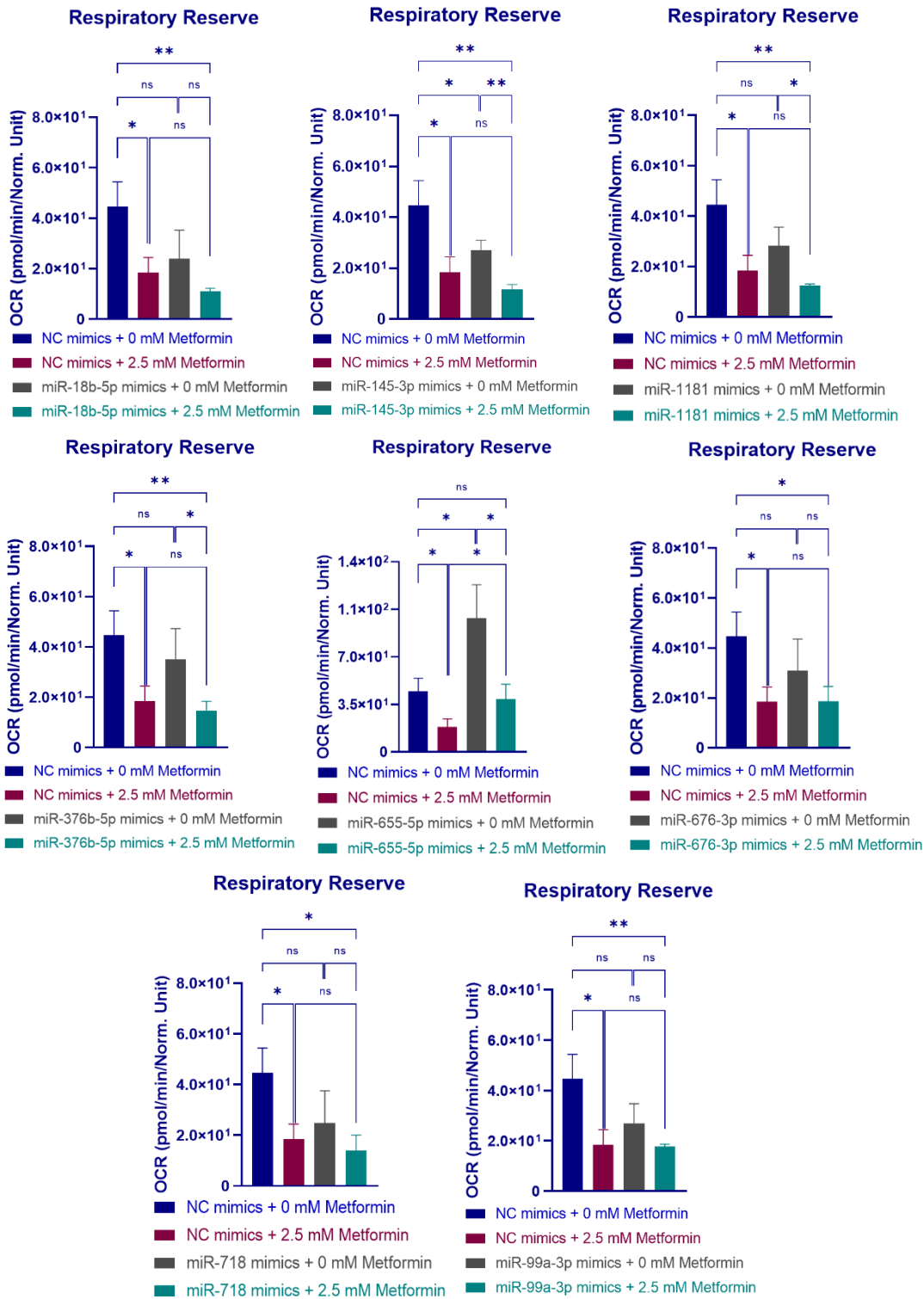


**Figure 5-14: Changes in the reserved respiratory capacity of HCT116 cells associated with miRNA mimic transfections in combination with metformin treatment.**

CRC cells were reverse transfected with selected miRNA mimics and treated with 2.5 mM metformin treatment or control medium. Oxygen consumption rate (OCR) of the cells was determined over a 30-minutes period using Seahorse XF-96 instrument designed to measure *in vitro* metabolic rates. The OCR values were normalised to viability of the corresponding cells



## CHAPTER 5

determined over a 30-minute period using a Seahorse XF-96 instrument designed to measure *in vitro* metabolic rates. The OCR values were normalised to viability of the corresponding cells acquired by crystal violet assay. Results are expressed as mean  $\pm$  SD of 3 culture replicates and the statistical significance is indicated with asterisks (ns  $P > 0.05$ , \*  $P \leq 0.05$ , \*\*  $P \leq 0.01$ ). Coupling efficiency: [(ATP production rate) / (basal respiration)  $\times$  100].

With regard to basal respiration, transfection of miR-376b-5p or miR-718 in combination with metformin treatment resulted in a 82 or 84% reduction in basal respiration compared with NC transfected cells in control medium ( $P = 0.0033$  and  $0.0035$ , respectively), (Figure 5-16). The effect was also significant in comparison with metformin treatment alone as shown by 41 and 46 % reduction in basal respiration in cells transfected with miR-376b-5p and miR-718 and treated with metformin ( $P = 0.02$  and  $0.05$ , respectively), Figure 5-16.

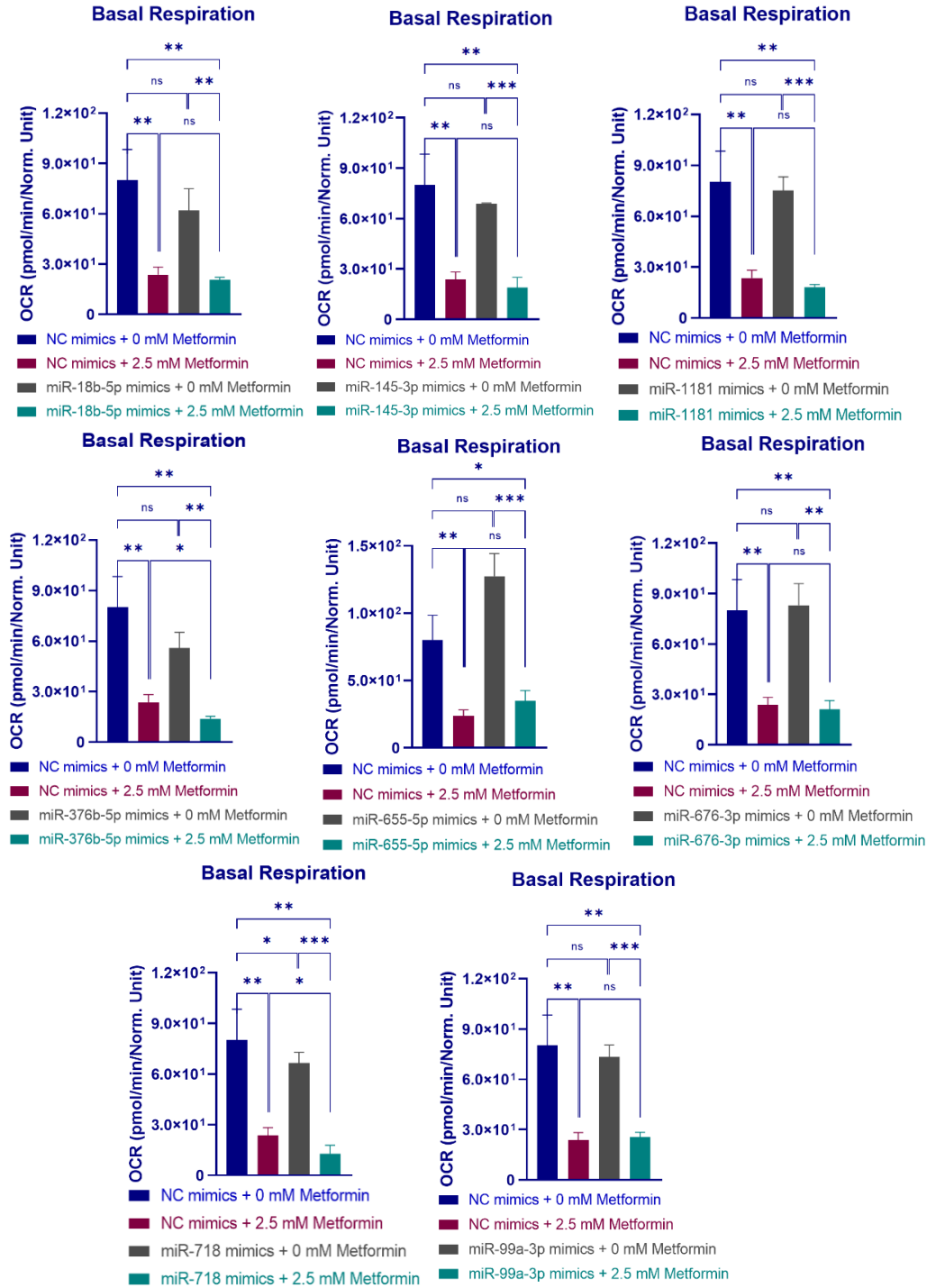


**Figure 5-16: Changes in basal respiration of HCT116 cells associated with miRNA mimic transfections in combination with metformin treatment.**

CRC cells were reverse transfected with selected miRNA mimics and treated with 2.5 mM metformin treatment or control medium. Oxygen consumption rate (OCR) of the cells was determined over a 30-minute time period using a Seahorse XF-96 Instrument designed to measure *in vitro* metabolic rates. The OCR values were normalised to the viability of the corresponding cells acquired by crystal violet assay. Results are expressed as mean  $\pm$  SD of 3 culture replicates and the statistical significance is indicated with asterisk (ns  $P > 0.05$ , \*  $P \leq 0.05$ , \*\*  $P \leq 0.01$ , \*\*\*  $P \leq$

0.001). Basal respiration: [(last rate measurement before oligomycin injection) – (non-mitochondrial respiration rate)].

Considering maximal respiration, resulting from disrupting ATP synthesis by an uncoupler treatment (FCCP), while metformin resulted in a significant reduction in maximal respiration (by 66%,  $P = 0.0065$ ), combination of miR-18b-5p, miR-1181 and miR-376b-5p transfection with metformin treatment led to a further 8.8, 9.3 and 11% decrease in the maximal respiratory capacity of HCT116 cells, respectively, compared with metformin treatment alone ( $P = 0.005, 0.001$  and  $0.01$  respectively, Figure 5-17).

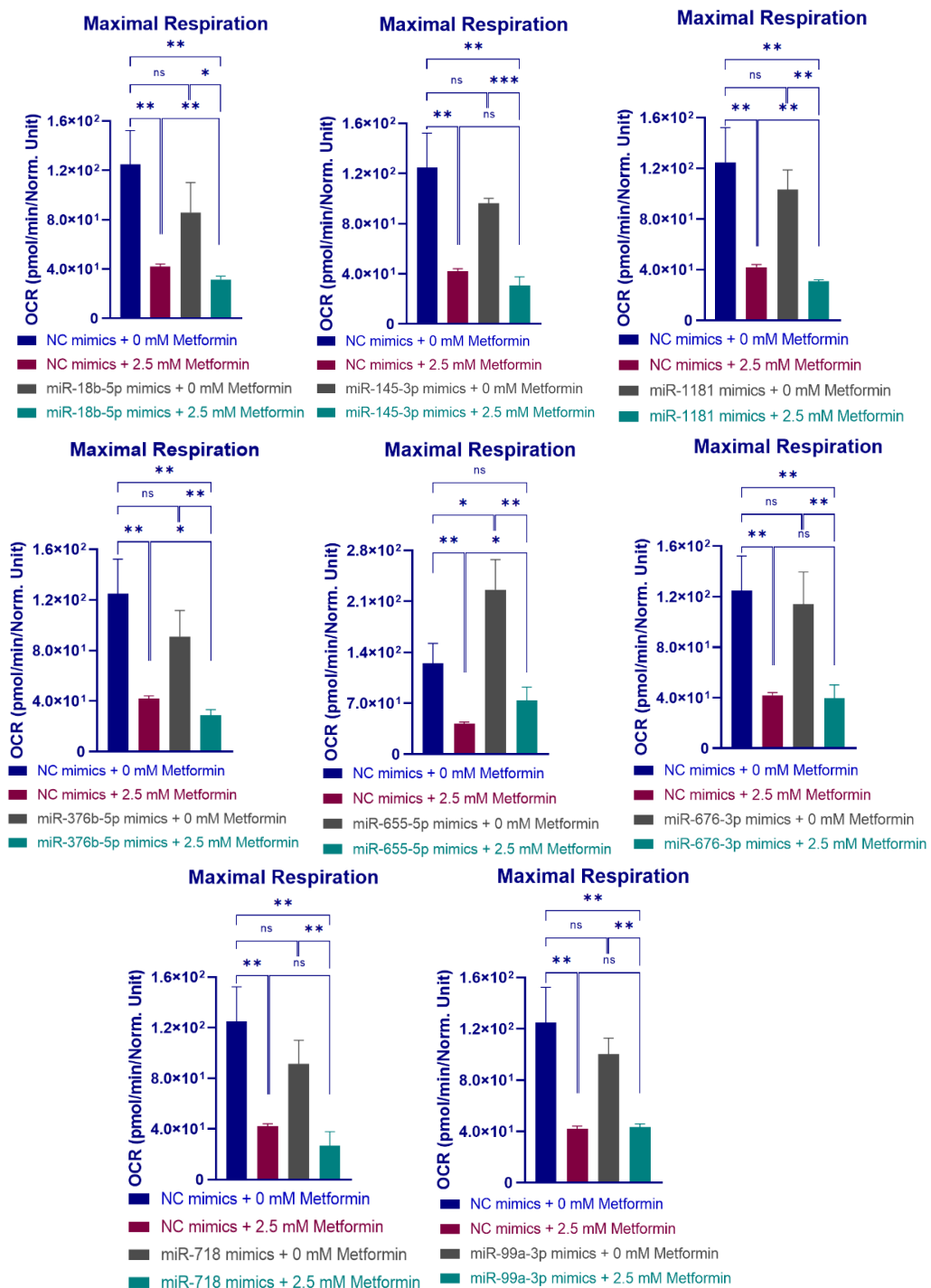


**Figure 5-17: Changes in maximal respiratory capacity of HCT116 cells associated with miRNA mimic transfections in combination with metformin treatment.**

CRC cells were reverse transfected with selected miRNA mimics and treated with 2.5 mM metformin treatment or control medium. Oxygen consumption rate (OCR) of the cells was determined over a 30-minute time period using a Seahorse XF-96 Instrument designed to measure *in vitro* metabolic rates. The OCR values were normalised to viability of the corresponding cells acquired by crystal violet assay. Results are expressed as mean  $\pm$  SD of 3 culture replicates and the statistical significance is indicated with asterisk (ns  $P > 0.05$ , \*  $P \leq 0.05$ , \*\*  $P \leq 0.01$ , \*\*\*  $P \leq 0.001$ ). Maximal respiration: [(maximum rate after FCCP injection) – (non-mitochondrial respiration)]

Also, both miR-376b-5p and miR-718 had similar effects on ATP synthesis, decreasing ATP turnover by 47 and 58% in combination with metformin and compared with HCT116 cells transfected with NC mimics and treated with metformin ( $P = 0.025$  and  $0.028$ , respectively, Figure 5-18). In summary, these results suggest the potential roles of miRNAs such as miR-376b-5p, miR-718, miR-18b and miR-1181 in mitochondrial function by regulating different respiration parameters such as basal and maximal respiration as well as ATP turnover.

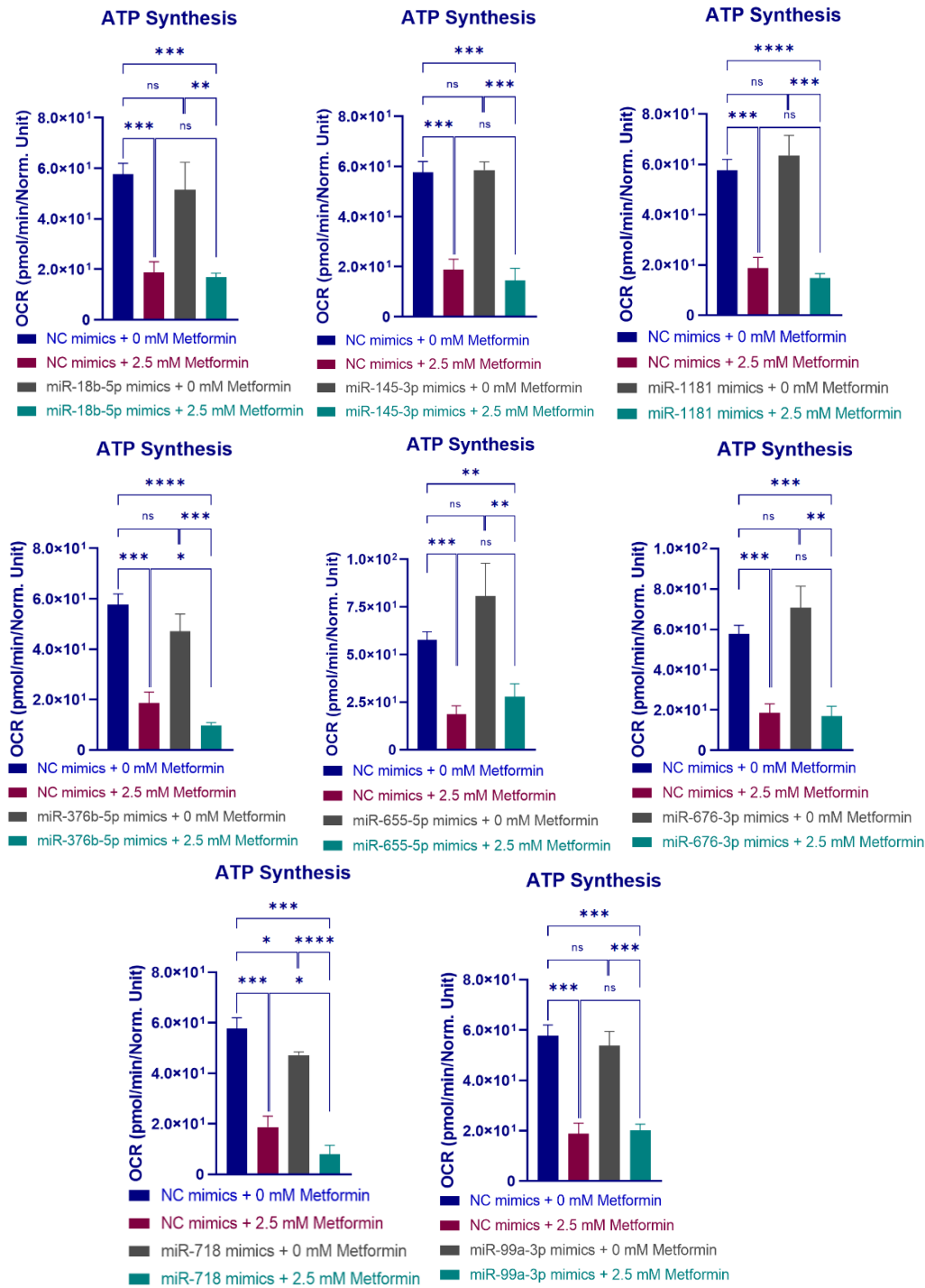


**Figure 5-18: Changes in ATP synthesis of HCT116 cells associated with miRNA mimic transfections in combination with metformin treatment.**

CRC cells were reverse transfected with selected miRNA mimics and treated with 2.5 mM metformin treatment or control medium. Oxygen consumption rate (OCR) of the cells was determined over a 30-minute time period using a Seahorse XF-96 Instrument designed to measure *in vitro* metabolic rates. The OCR values were normalised to viability of the corresponding cells acquired by crystal violet assay. Results are expressed as mean  $\pm$  SD of 3 culture replicates and the statistical significance is indicated with asterisk (ns  $P > 0.05$ , \*  $P \leq 0.05$ , \*\*  $P \leq 0.01$ , \*\*\*  $P \leq 0.001$ )

and \*\*\*\*  $P \leq 0.0001$ ). ATP synthesis [(last rate measurement before oligomycin injection) – (minimum rate after oligomycin injection)].

### 5.2.6 Proliferation of colorectal cancer cells associated with metformin sensitizing miRNA mimics' transfection

To investigate the role of selected miRNAs that regulate colorectal cancer cell metabolism and synergize with metformin treatment on CRC cell proliferation, the miRNAs are exogenously expressed by transfecting a panel of CRC cell lines with miRNA mimics following 2.5 mM metformin treatment and cell viability analysis using crystal violet assay. Among 6 CRC cell lines tested, HCT116, RKO, DLD1 and HT29 cells transfections with miR-18b-5p, miR-145-3p, miR-1181, miR-376b-5p, miR-676-3p and miR-718 mimics resulted in an enhanced sensitivity of the cell to the anti-proliferative effect of metformin (Figure 5-19 - Figure 5-24). However, Caco2 and SW480 cell lines showed very little sensitivity to the effect of these miRNAs. For instance, in Caco2 cells, only miR-18b-5p and miR-145-3p overexpression in combination with metformin showed further 16 and 3 % reduction in viability compared to metformin treatment alone ( $P < 0.0001$  and  $= 0.01$ , respectively), Figure 5-19 and Figure 5-20. Similarly, exogenous expression of miR-18b-5p and miR-676-3p increased sensitivity of SW480 to the anti-neoplastic effect of metformin by decreasing the viability of the cells by 26 and 43 % in combination with metformin ( $P = 0.01$  and  $0.004$ , respectively), Figure 5-19, Figure 5-23.

Comparing the individual miRNA mimic effects on the viability of HCT116, RKO, DLD and HT29 CRC cells, the enhancement effect of miRNA mimics on the sensitivity of the cells to metformin treatment was highest with the exogenous expression of miR-18b-5p, miR-676-3p, miR-1181 and miR-18b-3p in HCT116, RKO, DLD1 and HT29 cells respectively, reducing the viability of the cells by 28, 26, 46 and 30 %, respectively compared with metformin treatment alone ( $P = 0.006$  and  $0.002$  for HCT116 and RKO, respectively and  $P < 0.0001$  for DLD1 and  $P = 0.0005$  for HT29), Figure 5-19, Figure 5-23 and Figure 5-21.

Among the miRNAs tested, miR-676-3p overexpression showed to have the most substantial sensitizing effect in HCT116, RKO, DLD1 and HT29 cell lines as there was more than 38 % reduction in viability by miR-676-3p transfection alone compared with NC transfection in control medium and further 16, 20, 20 and 18% reduction, respectively, in the viability of HCT116, RKO, DLD1 and HT29 cells transfected with miR-676-3p plus 2.5 mM metformin treatment compared with metformin treatment alone ( $P = 0.0003$  and  $0.002$  for HCT116 and RKO, respectively and  $P < 0.0001$  for DLD1 and  $P = 0.004$  for HT29), Figure 5-23. These results confirm the metformin

sensitizing roles of selected miRNAs in different CRC cell lines and also the context-dependent effect on these miRNAs in cell lines with different mutational status.

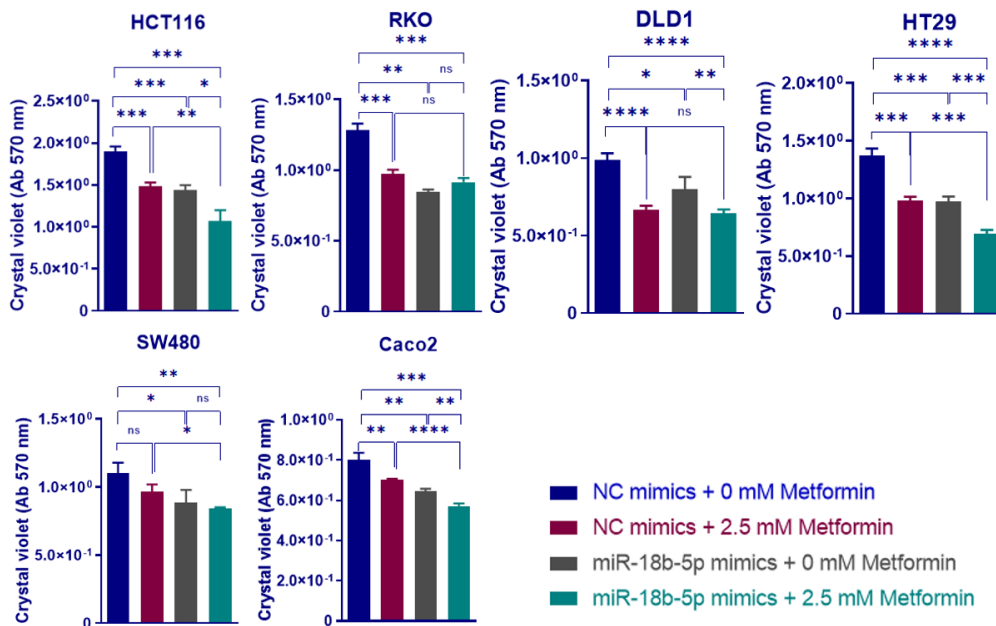


**Figure 5-19: Proliferation of CRC cell lines after transfection with miR-18b-5p miRNAs and treatment with metformin or control medium for 96 hours.**

Viability measurements using crystal violet assays, showing the different effects of miR-18b-5p on proliferation, in the control medium and 2.5 mM metformin-treated HCT116, RKO, DLD1, HT29, SW480 and Caco2 cells. Results are expressed as the mean  $\pm$  SD of 3 culture replicates and the statistical significance is indicated with asterisks (ns  $P > 0.05$ , \*  $P \leq 0.05$ , \*\*  $P \leq 0.01$ , \*\*\*  $P \leq 0.001$  and \*\*\*\*  $P \leq 0.0001$ ).

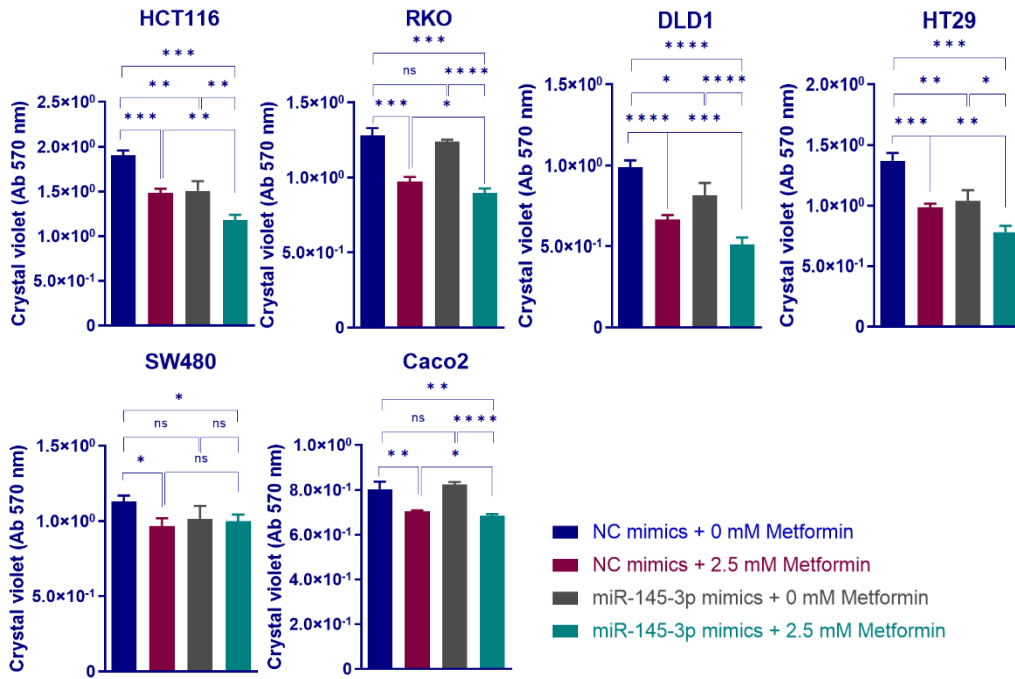


**Figure 5-20: Proliferation of CRC cell lines after transfection with miR-145-3p miRNAs and treatment with metformin or control medium for 96 hours.**

Viability measurements using crystal violet assays showing the different effects of miR-145-3p on proliferation, in the control medium and 2.5 mM metformin-treated HCT116, RKO, DLD1, HT29, SW480 and Caco2 cells. Results are expressed as mean  $\pm$  SD of 3 culture replicates and the statistical significance is indicated with asterisk (ns  $P > 0.05$ , \*  $P \leq 0.05$ , \*\*  $P \leq 0.01$ , \*\*\*  $P \leq 0.001$  and \*\*\*\*  $P \leq 0.0001$ ).

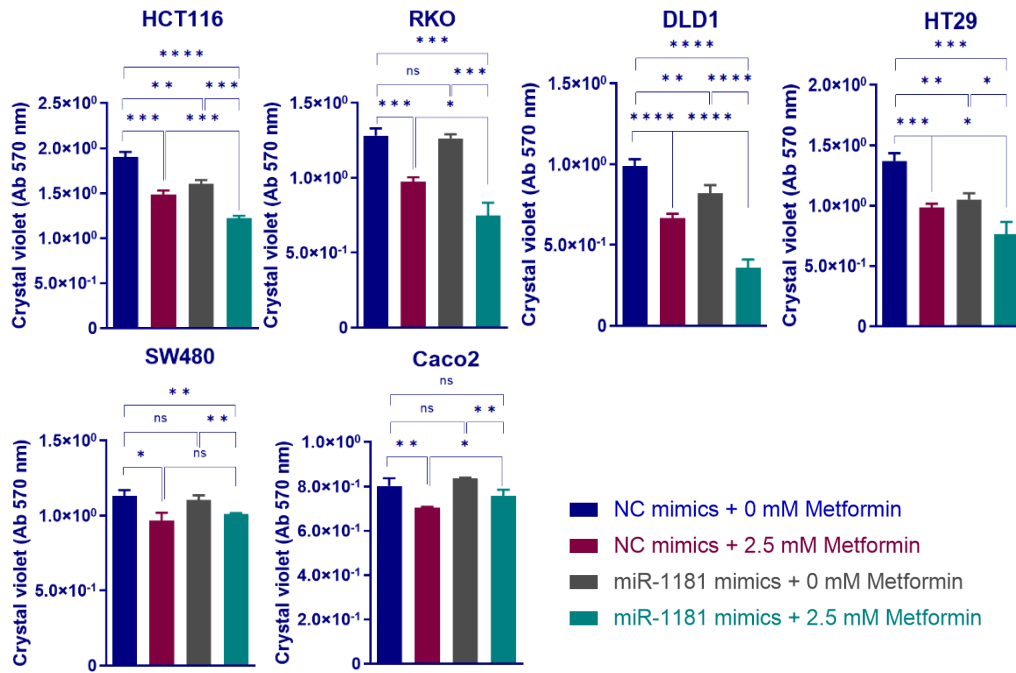


**Figure 5-21: Proliferation of CRC cells after transfection with miR-1181 and treatment with metformin or control medium for 96 hours.**

Viability measurements using crystal violet assay showing the different effects of miR-1181 on proliferation, in the control medium and 2.5 mM metformin-treated HCT116, RKO, DLD1, HT29, SW480 and Caco2 cells. Results are expressed as mean  $\pm$  SD of 3 culture replicates and the statistical significance is indicated with asterisks (ns  $P > 0.05$ , \*  $P \leq 0.05$ , \*\*  $P \leq 0.01$ , \*\*\*  $P \leq 0.001$  and \*\*\*\*  $P \leq 0.0001$ ).

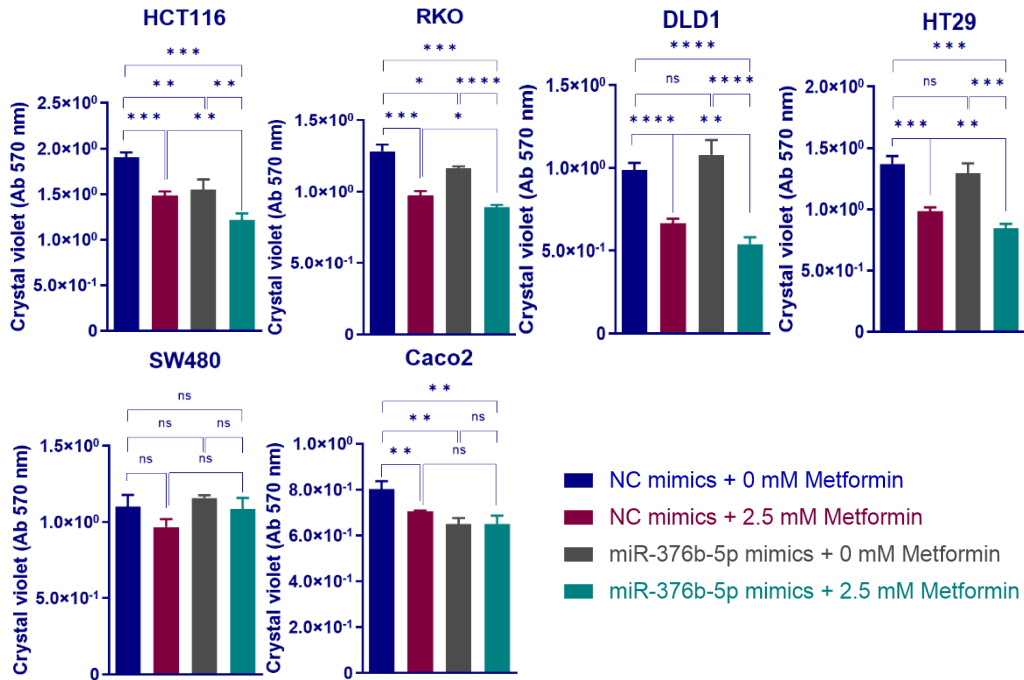


**Figure 5-22: Proliferation of CRC cells after transfection with miR-376b-5p and treatment with metformin or control medium for 96 hours.**

Viability measurements using crystal violet assay showing the different effects of miR-376b-5p on proliferation, in the control medium and 2.5 mM metformin-treated HCT116, RKO, DLD1, HT29, SW480 and Caco2 cells. Results are expressed as mean  $\pm$  SD of 3 culture replicates and the statistical significance is indicated with asterisks (ns  $P > 0.05$ , \*  $P \leq 0.05$ , \*\*  $P \leq 0.01$ , \*\*\*  $P \leq 0.001$  and \*\*\*\*  $P \leq 0.0001$ ).

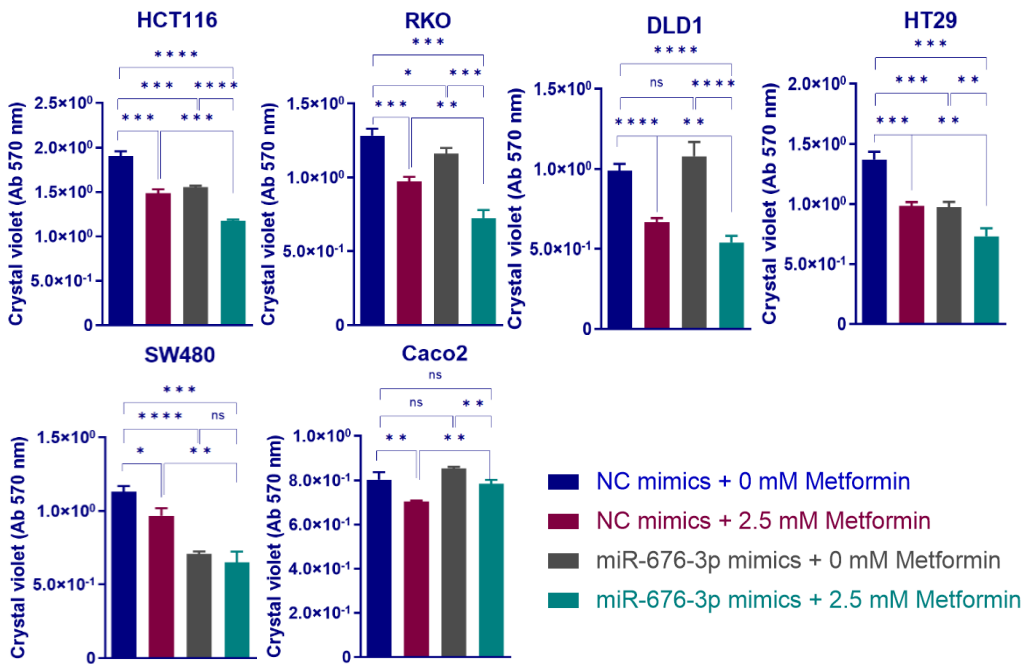


**Figure 5-23: Proliferation of CRC cells after transfection with miR-676-3p and treatment with metformin or control medium for 96 hours.**

Viability measurements using crystal violet assay showing the different effects of miR-676-3p on proliferation, in the control medium and 2.5 mM metformin-treated HCT116, RKO, DLD1, HT29, SW480 and Caco2 cells. Results are expressed as mean  $\pm$  SD of 3 culture replicates and the statistical significance is indicated with asterisks (ns  $P > 0.05$ , \*  $P \leq 0.05$ , \*\*  $P \leq 0.01$ , \*\*\*  $P \leq 0.001$  and \*\*\*\*  $P \leq 0.0001$ ).

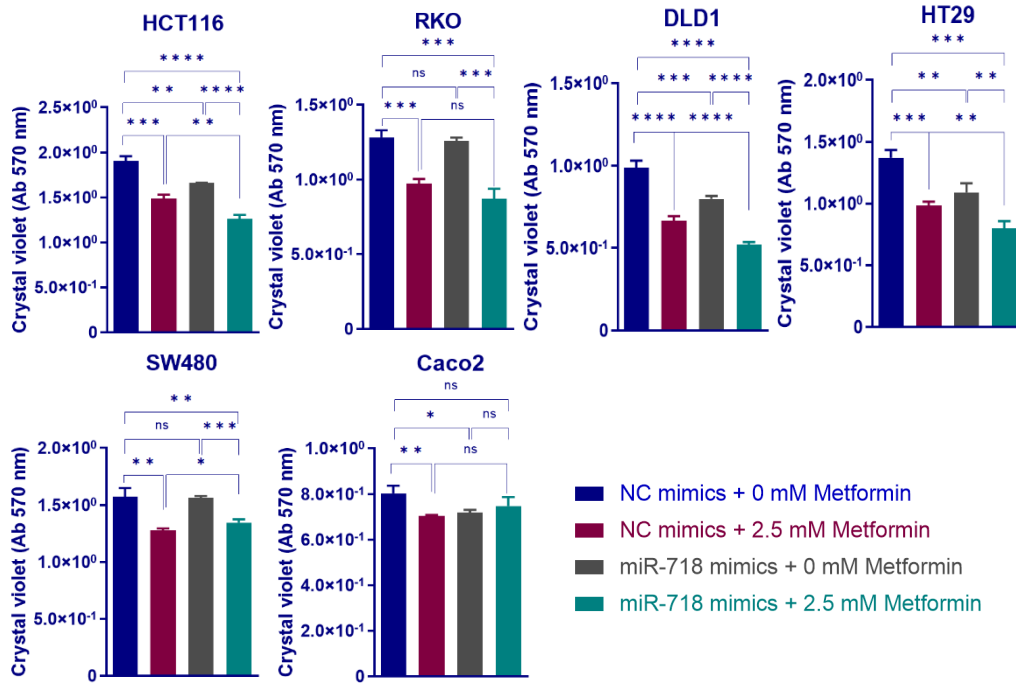


**Figure 5-24: Proliferation of CRC cells after transfection with miR-718 and treatment with metformin or control medium for 96 hours.**

Viability measurements using crystal violet assay showing the different effects of miR-718 on proliferation, in the control medium and 2.5 mM metformin-treated HCT116, RKO, DLD1, HT29, SW480 and Caco2 cells. Results are expressed as mean  $\pm$  SD of 3 culture replicates and the statistical significance is indicated with asterisks (ns  $P > 0.05$ , \*  $P \leq 0.05$ , \*\*  $P \leq 0.01$ , \*\*\*  $P \leq 0.001$  and \*\*\*\*  $P \leq 0.0001$ ).

### 5.2.7 Apoptosis of colorectal cancer cells associated with metformin-sensitizing miRNA mimic transfections

As shown previously in this Chapter, 6 miRNAs including miR-18b-5p, miR-145-3p, miR-1181, miR-376b-5p, miR-676-3p and miR-718 proved to exert a metformin sensitization effect in CRC cells. Among 6 different CRC cells tested, HCT116, RKO, DLD1 and HT29 cell lines were shown to have consistent sensitivity to the above-mentioned miRNA mimic and metformin treatments. To investigate the role of these miRNAs in combination with metformin on CRC cell death, caspase 3/7 activity was assessed as a marker of apoptosis. While transfection of 4 responsive CRC cell lines with miR-18b-3p, miR-145-3p, miR-1181, miR-376b-3p and miR-718 mimics, in combination with metformin treatment, showed no consistent pro-apoptotic function in CRC cell lines, miR-676-3p exerted a pro-apoptotic function via increasing the caspase 3/7 cleavage by 103, 36 and 47% in control medium and 103, 58 and 71% in combination with metformin in HCT116,

DLD1 and HT29 cell lines, respectively ( $P < 0.0001$  and  $= 0.02$  for HCT116,  $P = 0.006$  and  $0.006$  for DLD1 and  $P = 0.001$  and  $< 0.0001$  for HT29, respectively, Figure 5-25 -Figure 5-30). Among 4 cell lines tested for the combinatorial effect of metformin treatment and mimic transfections on programmed cell death, RKO showed the least sensitivity with no significant increase in caspase3/7 activity with the combination of metformin treatment and sensitizing miRNA mimic transfections, while HT29 cell line had the highest sensitivity where a combination of 2.5 mM metformin treatment and miR-18b-5p, miR-1181, miR-376b-5p, miR-676-3p or miR-718 mimics resulted in 46, 87, 42, 123 and 60% increase in caspase 3/7 activity compared with NC mimics in control medium ( $P = 0.0003$ ,  $< 0.0001$ ,  $= 0.0006$ ,  $< 0.0001$  and  $= 0.0008$ , respectively), Figure 5-25 - Figure 5-30. Altogether, these results indicate that except for miR-676-3p, which sensitizes CRC cells to the anti-cancer properties of metformin most probably through increase cell apoptosis, other miRNAs induce the anti-proliferative effect of metformin but do not enhance the cell death in combination with metformin.

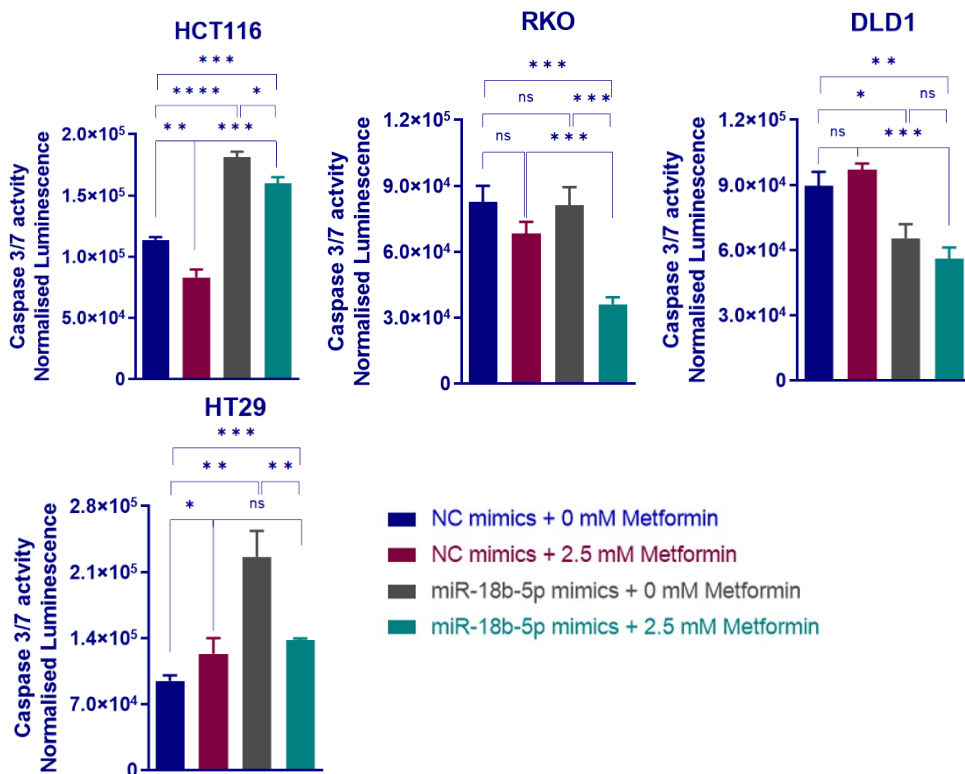


**Figure 5-25: Apoptosis of CRC cell lines after transfection with miR-18b-5p and treatment with metformin or control medium for 96 hours.**

Caspase 3/7 activity luminescent signal measurements in HCT116, DLD1, RKO, and HT29 cells transfected with miR-18b-5p mimics and treated with 2.5 mM metformin for 72 hours, compared

with cells in control medium. Results are expressed as mean  $\pm$  SD of 3 replicates and the statistical significance is indicated with asterisks (ns  $P > 0.05$ , \*  $P \leq 0.05$ , \*\*  $P \leq 0.01$ , \*\*\*  $P \leq 0.001$ , \*\*\*\*  $P \leq 0.0001$ ).

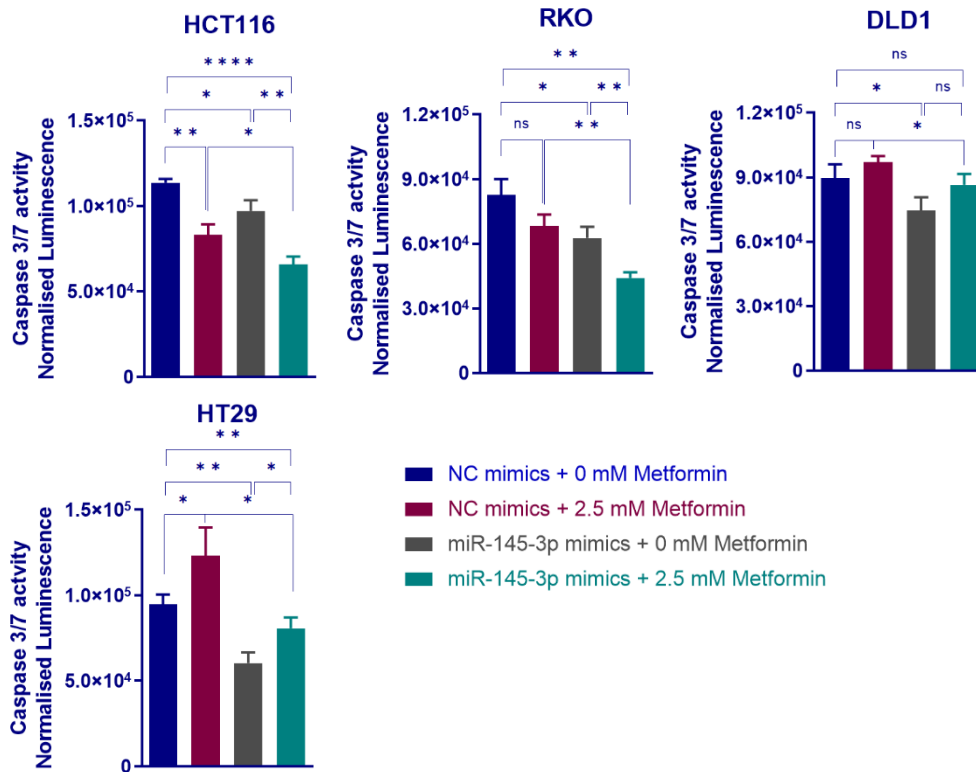


**Figure 5-26: Apoptosis of CRC cell lines after transfection with miR-145-3p and treatment with metformin or control medium for 96 hours.**

Caspase 3/7 activity luminescent signal measurements in HCT116, DLD1, RKO, and HT29 cells transfected with miR-145-3p mimics and treated with 2.5 mM metformin for 72 hours, compared with cells in control medium. Results are expressed as mean  $\pm$  SD of 3 replicates and the statistical significance is indicated with asterisks (ns  $P > 0.05$ , \*  $P \leq 0.05$ , \*\*  $P \leq 0.01$ , \*\*\*  $P \leq 0.001$ , \*\*\*\*  $P \leq 0.0001$ ).

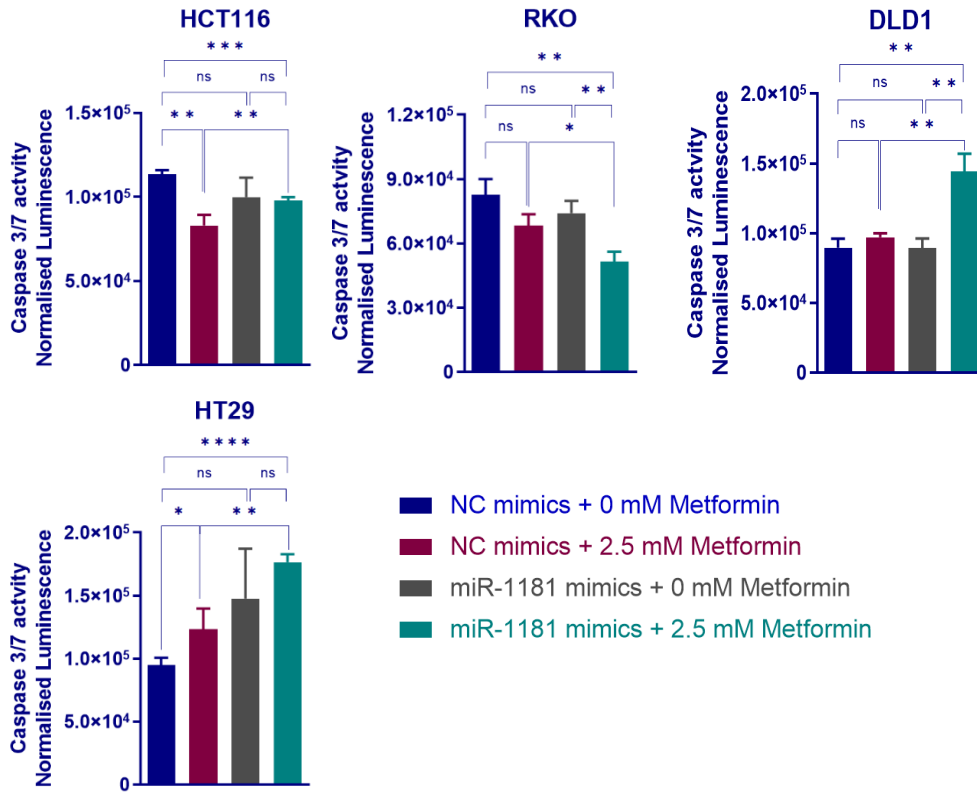


**Figure 5-27: Apoptosis of CRC cell lines after transfection with miR-1181 and treatment with metformin or control medium for 96 hours.**

Caspase 3/7 activity luminescent signal measurements in HCT116, DLD1, RKO, and HT29 cells transfected with miR-1181 mimics and treated with 2.5 mM metformin for 72 hours, compared with cells in control medium. Results are expressed as mean  $\pm$  SD of 3 replicates and the statistical significance is indicated with asterisks (ns  $P > 0.05$ , \*  $P \leq 0.05$ , \*\*  $P \leq 0.01$ , \*\*\*  $P \leq 0.001$ , \*\*\*\*  $P \leq 0.0001$ ).

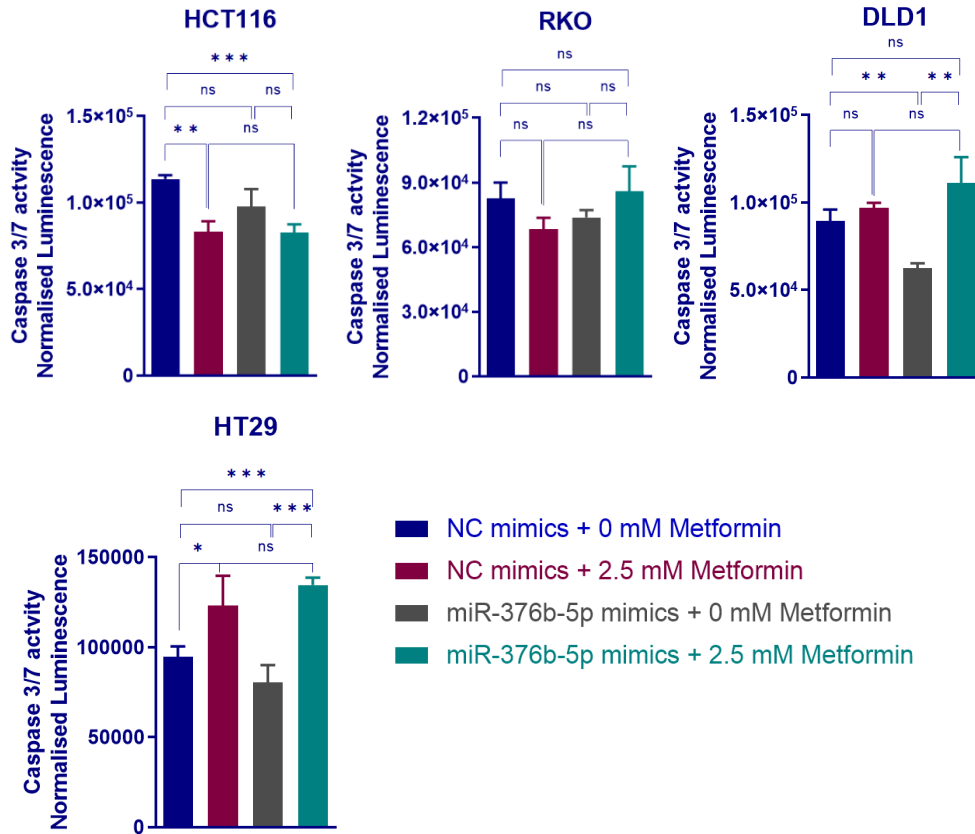


**Figure 5-28: Apoptosis of CRC cell lines after transfection with miR-376b-5p and treatment with metformin or control medium for 96 hours.**

Caspase 3/7 activity luminescent signal measurements in HCT116, DLD1, RKO, and HT29 cells transfected with miR-376b-5p mimics and treated with 2.5 mM metformin for 72 hours, compared with cells in control medium. Results are expressed as mean  $\pm$  SD of 3 replicates and the statistical significance is indicated with asterisks (ns  $P > 0.05$ , \*  $P \leq 0.05$ , \*\*  $P \leq 0.01$ , \*\*\*  $P \leq 0.001$ ).

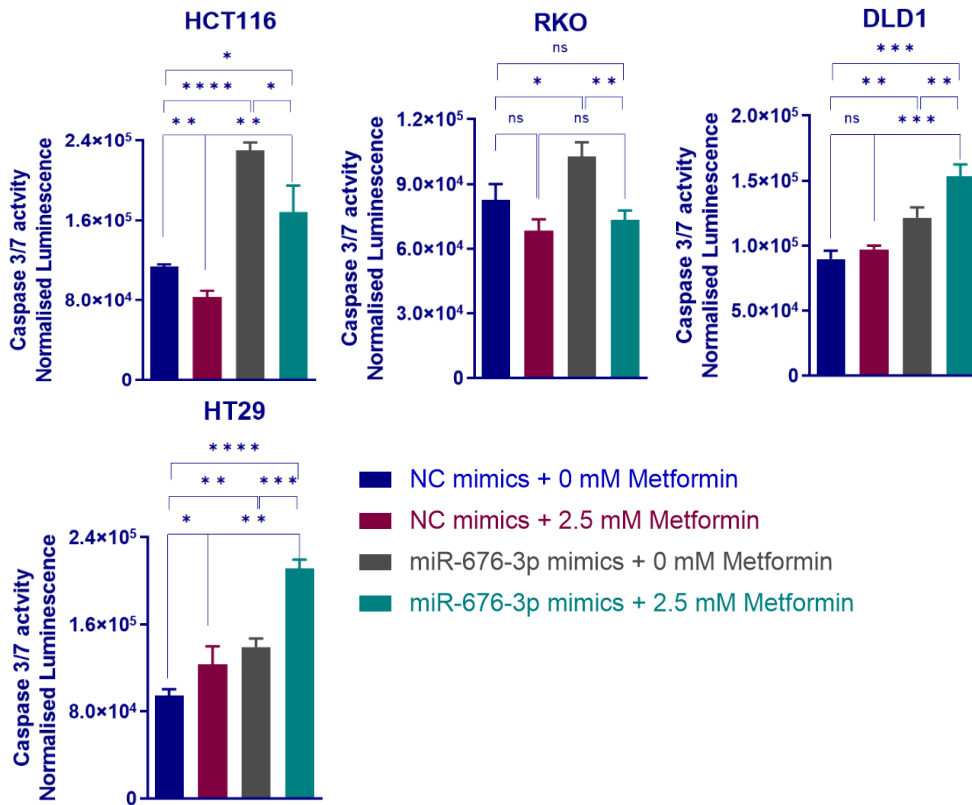


**Figure 5-29: Apoptosis of CRC cell lines after transfection with miR-676-3p and treatment with metformin or control medium for 96 hours.**

Caspase 3/7 activity luminescent signal measurements in HCT116, DLD1, RKO, and HT29 cells transfected with miR-676-3p mimics and treated with 2.5 mM metformin for 72 hours, compared with cells in control medium. Results are expressed as mean  $\pm$  SD of 3 replicates and the statistical significance is indicated with asterisks (ns  $P > 0.05$ , \*  $P \leq 0.05$ , \*\*  $P \leq 0.01$ , \*\*\*  $P \leq 0.001$ , \*\*\*\*  $P \leq 0.0001$ ).

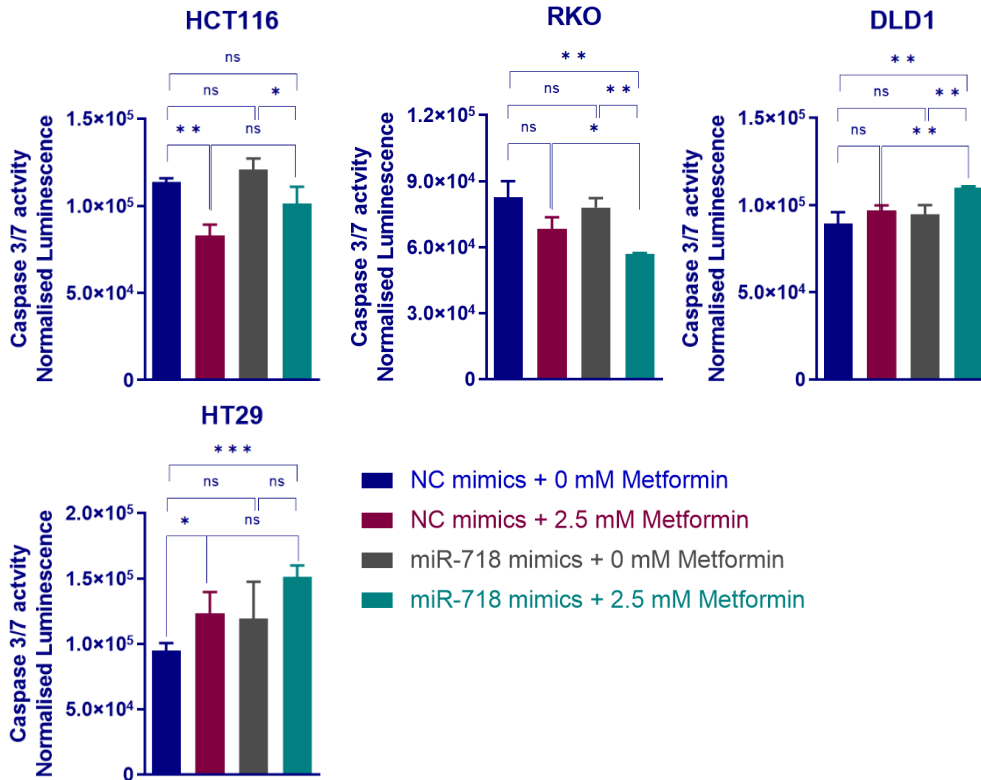


**Figure 5-30: Apoptosis of CRC cell lines after transfection with miR-718 and treatment with metformin or control medium for 96 hours.**

Caspase 3/7 activity luminescent signal measurements in HCT116, DLD1, RKO, and HT29 cells transfected with miR-718 mimics and treated with 2.5 mM metformin for 72 hours, compared with cells in control medium. Results are expressed as mean  $\pm$  SD of 3 replicates and the statistical significance is indicated with asterisks (ns  $P > 0.05$ , \*  $P \leq 0.05$ , \*\*  $P \leq 0.01$ , \*\*\*  $P \leq 0.001$ ).

### 5.3 Discussion

There are two proposed mechanisms of action for metformin. While metformin can act indirectly, where it does not interact with the cancer cells but rather targets the endocrine-metabolic system to influence cancer cell biology. These indirect effects include roles such as gluconeogenesis suppression and reduced systemic glucose and insulin levels [1061]. On the other hand, some direct effects were also shown, where metformin resulted in energy stress in cancer cells [785]. However, it is uncertain that normal systemic levels of metformin are sufficient to induce such responses in cancer cells. Furthermore, the heterogeneity of cancer cells makes it even more complex to investigate the amount of metformin accumulation in the cells, as well as the cancer cells' response to metformin-related metabolic stress [926]. Moreover, metformin treatment leads to a self-limiting accumulation in cancer cells, theoretically, through inhibiting proton pumping, depolarizing the mitochondrial membrane and, therefore, limiting the accumulation of the drug [838]. Chronic inhibition of mTORC1 by drugs such as rapamycin was shown to relieve the negative feedback loop from the S6K-IRS1 axis leading to hyperactivation of mTORC2 and, consequently, Akt activation. Therefore, inhibition of mTORC1, located upstream of S6K in the pathway, prevents the inhibitory feedback on IRS-1 and leads to an increased IGF-1R-mediated proliferation signal. This consequently, limits drug response and may explain the rather underwhelming clinical application of rapamycin in cancer therapy.[927]. Altogether, these results emphasize the need for a combination therapy that can somehow prevent, or delay, the appearance of metformin desensitization and can also increase the sensitivity of cancer cells to the anti-cancer properties of metformin. miRNAs contribute to regulation of the cellular and molecular processes of cancer cells by forming a complex network where one miRNA can target multiple mRNAs and each mRNA could possibly be regulated by multiple miRNAs [1071, 1072]. Given the involvement of miRNAs in key cancer hallmarks, including cellular metabolism, in this chapter, the ability of miRNAs in sensitizing colorectal cancer cells to the anti-proliferative effect of metformin was investigated. To identify miRNAs that regulate CRC cell growth and their response to metformin, a functional high throughput screen of miRNA mimics was performed, followed by a secondary screen and hit validation. Of the 2063 miRNAs tested, the strong synergistic effects of 8 miRNAs, with metformin, were validated in HCT116 and other CRC cell lines ( $CDI < 0.7$ ), (Figure 5-1 - Figure 5-8). Among 8 validated hits, transfection of miR-145-3p, miR-676-3p, miR-655-5p, miR-18b-5p and miR-376b-5p into CRC cells not only repressed tumour cell growth and proliferation, but also potentiated the efficacy of metformin in repressing tumour cell growth (Figure 5-8).

TargetScan prediction of mRNA targets for selected metformin sensitizing miRNAs and ClueGo analysis, revealed regulation of “cellular metabolic processes” (GO:0031323), as the top biological

## CHAPTER 5

process enriched for the putative targets. Together with metformin-regulated genes enriched in the regulation of cellular metabolic processes, a miRNA-based network was constructed showing several inter-connections for differentially expressed coding genes and miRNAs, integrated with those identified as metformin-sensitizing miRNAs in the functional screen (Figure 5-31).



**Figure 5-31: The miRNA-based network: metformin treatment-regulated miRNAs integrated with metformin sensitizing miRNAs and their putative target genes.**

This is a global view of the integrated network associated with 2.5 mM metformin treatment of HCT116 cells and combined with PPI network curated for the potential target genes identified for 6 metformin-sensitizing miRNAs. PPIs are literature-curated from the IMEx Interactome for the genes extracted from the GO term “regulation of cellular metabolic processes”. miRNAs are shown in triangles and genes are the circle nodes. The sensitizing miRNAs and their putative target genes are shown in purple, while downregulated genes and miRNAs are shown in light red and upregulated ones are shown in green. Red lines represent interactions of miRNAs with genes while protein-protein interactions are shown in blue.

To test the anti-cancer roles of the identified sensitizing miRNAs through mechanisms related to cellular metabolism, including cancer cell glycolysis and mitochondrial respiration, the metabolic profile changes associated with metformin treatment and altered miRNA activity were investigated.

Altered energy producing pathways in CRC, including aerobic glycolysis and oxidative phosphorylation, are regulated by cytokines, tumour suppressors, oncogenes and metabolic enzymes (reviewed in Chapter 1). As shown in this chapter, miRNAs such as miR-376b-5p, miR-1181, miR-18b-5p, miR-676-3p, miR-718 and miR-145-3p were also identified as regulators of glycolysis and mitochondrial respiration (Figure 5-10 - Figure 5-18).

Metformin-mediated inhibition of respiration resulted in a compensatory increase in glycolysis but also a dose dependent decrease in glycolytic capacity and reserve (Chapter 3). This may indicate the pleiotropic nature of metformin and suggests direct targeting of molecules involved in regulation of CRC cell glycolysis. In this chapter, investigating different parameters of glycolysis revealed miR-676-3p and miR-376b-5p are suppressors of glycolysis, glycolytic capacity and glycolytic reserve and showed the ability of these miRNAs to hinder the metformin-mediated increase in glycolysis (Figure 5-10 - Figure 5-12). Moreover, the addition of oligomycin, which blocks mitochondrial ATP production, showed that increased miR-676-3p activity in CRC cells enhanced the inhibitory effect of metformin on glycolytic capacity and reserve (Figure 5-12). While some studies showed the diagnostic value of miR-676-3p in cancers such as gastric, prostate and breast cancer, very little is known about the function of this miRNA [1073-1075]. Li et al., demonstrated the inhibitory effect of miR-376b-5p on angiogenesis in middle cerebral artery occlusion by targeting the HIF-1 $\alpha$ -mediated VEGFA signalling pathway [1076]. Low expression of miR-376b-5p was also shown to be correlated with poor prognosis of patients with pancreatic adenocarcinoma [1077]. Also, it has inhibited breast cancer metastasis by targeting HOXD10 [1078].

Moreover, miRNAs such as miR-18b-5p and miR-145-3p were demonstrated to have a suppressor effect on glycolytic properties such as glycolytic rate, glycolytic capacity and glycolytic reserve in combination with metformin whilst exerting no significant effect alone (Figure 5-10 - Figure 5-12). miR-18b-5p was shown to be differentially expressed in certain cancers [1079-1081]. However, there are discrepancies with regard to the functions of this miRNA in cancer, as it can be both a tumour suppressor and oncogenic miRNA. In melanoma cells, this miRNA was downregulated and was shown to directly target the proto-oncogene MDM2 and regulate DNA methylation and, thereby, regulate the p53 signalling pathway to

reduce tumour cell growth and induce cell death [1082]. However, the oncogenic activity of miR-18b-5p was shown in breast cancer cells where miR-18b-5p targets DOCK4, a significant cell division factor mainly involved in the regulation cell adhesion [1083]. miR-145-3p, generally considered the passenger strand of mature miR-145, was shown to be downregulated in different cancer types and is also a known tumour suppressor and regulator of tumour growth, cell death and tumour metastasis [1084-1087]. These results were consistent with the data presented by Qui et al., who conducted a high throughput functional screen of miRNA mimics in CRC cells and identified miRNAs such as miR-143-3p, miR-126-3p and miR-124-3p that can significantly inhibit lactate production [1088].

As a direct target of metformin, mitochondrial function has been shown to be affected by metformin treatment in different cancers [838, 1089, 1090]. Accordingly, as shown in Chapter 3 and in the present chapter, 2.5 mM metformin treatment of CRC cells resulted in a dramatic decrease in mitochondrial parameters, such as basal and maximal respiration (Figure 5-16 - Figure 5-18).

The maximum capacity of HCT116 cell respiration, measured from the baseline in the presence of oligomycin and then FCCP, was lower in cells transfected with miR-18b-5p, miR-1181 or miR-376b-5p and treated with metformin, compared with NC transfected plus metformin cells (Figure 5-17). miR-376b-5p and miR-718 showed the strongest effect on mitochondrial parameters by further enhancing the inhibitory effect of metformin on basal respiration and ATP turnover (Figure 5-16 and Figure 5-18). Hypoxia-inducible miR-1181 is a known tumour suppressor in cancers such as pancreatic, ovarian and prostate cancer and is shown to target *SOX2*, *STAT3* and *HOXA10* to inhibit proliferation, migration and invasion and to promote EMT [1091-1095]. miR-718 was originally identified in 2006 and Leng et al., showed the anti-cancer role of this miRNA, by targeting VEGF, in ovarian cancer [1096, 1097]. The tumour suppressive function of miR-718 was then confirmed in cancers including hepatocellular carcinoma and oesophageal squamous cell carcinoma, as well as thyroid and ovarian cancers; it was shown to inhibit cancer cell proliferation, invasion and regulated innate immune response via targeting VEGF, PDPK1, IRAK1, EGR3 and PTEN [762, 1097-1100]. Similar to the findings in this chapter, miR-718 suppressed cancer cell metabolism and energy production in papillary thyroid cancer through regulating the PI3K/Akt/mTOR pathways [1101].

Also, the investigation of anti-tumour properties of metformin, in combination with miRNAs that regulate CRC cell metabolism, revealed 6 metabolism-regulating miRNAs that enhanced the anti-proliferative effect of metformin. However, the enhancement effect of miRNA mimics on CRC

cell viability is largely due to cellular processes other than apoptosis, which remain to be investigated as only miR-676-3p showed pro-apoptotic activity in HCT116, DLD1 and HT29 cells (Figure 5-29).

Overall, the findings of this chapter demonstrate the capability of miRNAs to enhance the anti-cancer properties of metformin in CRC cells. This chapter has displayed an additional layer of miRNA functions, whereby metformin-sensitizing miRNAs suppressed CRC cell metabolism through the regulation of glycolytic and respiratory parameters in the presence of metformin treatment. Further study is required to elucidate the precise molecular mechanisms of the identified miRNAs in targeting specific genes associated with metabolic regulation of CRC cells. It was also limited in looking at the miRNAs that enhanced the metformin effect. Of course, those that suppressed the metformin effect may reveal more about metformin's mechanism of action. These miRNAs were noted, but not investigated, in this study. Also, this chapter was limited to examining the combinational effect of miRNAs and metformin in CRC cell lines; however *in vivo* investigation of these functions may be beneficial for examining their role in the context of a whole animal complexity.

# Chapter 6. General conclusions

---

## 6.1 Thesis summary

Colorectal cancer (CRC) is the third most prevalent cancer in the world. Metformin has been associated with cancer prevention and selectively represses cancer progression. MicroRNAs are small non-coding RNAs involved in most cellular processes. Although several metabolic effects of metformin treatment have been investigated, detailed analysis of the resultant changes in gene expression is still required. Also, the effect of metformin treatment in combination with anti-cancer miRNAs is yet to be explored.

RNA and small RNA next generation sequencing were performed for CRC cells treated with metformin. Following differential expression analysis, functional enrichment and network analyses, CRC cells were transfected with miRNA mimics to explore the anti-cancer effect of differentially expressed (DE) miRNAs. In addition, high throughput functional screens of a miRNA mimic library, in combination with metformin, were undertaken and a secondary screen was performed to validate the lead miRNAs.

DE miRNAs and genes within specific biological pathways that are affected by metformin treatment were identified. Also, metformin treatment resulted in the downregulation of some pro-proliferative and upregulation of some anti-proliferative miRNAs. Furthermore, miRNAs were shown to sensitize CRC cells to the anti-cancer effect of metformin by enhancing its anti-proliferative effects. Identification of DE miRNAs and their potential target genes, as well as miRNAs that sensitize CRC cells to metformin, provides an advance towards identifying therapeutic interventions and confirms the feasibility of combining metformin with miRNAs to enhance therapeutic efficacy and overcome drug resistance. Future work includes confirmation of the mechanisms of action of newly discovered miRNAs *in vivo* in the context of metformin.

## 6.2 The Warburg effect and interpretations of an established concept

Continuous proliferation of tumour cells demands a consistent energy source as well as macromolecular biosynthesis. In view of that, Otto Warburg demonstrated high levels of glycolysis in cancer cells, both in hypoxia and normoxia, by comparing the glycolytic rate of cancer cells in air and nitrogen. The upregulated glycolysis in cancer cells was later called aerobic glycolysis, or the Warburg effect, which was then considered a universal metabolic hallmark of cancer cells.

Although Warburg's observations in 1920s were correct, his interpretations about the preference of cancer cells for enhanced glycolysis have been challenged. At first glance, aerobic glycolysis seems to serve a disadvantage for cancer cells, since the ATP yield per unit of glucose consumed drops to 2 compared with 36 ATPs generated upon oxidative phosphorylation [3]. However, as glucose is supplied through increased angiogenesis for cancer cells, ATP generation seems to be a lesser priority [778, 1102, 1103]. Moreover, Koppenol and Bounds showed that in spite of reduced ATP generation in cancer cells, surrounding normal cells retain an unchanged capability to produce energy through respiration. As a result, ATP generated from the normal microenvironment provides additional energy for cancer cells [1104].

To support cancer cell proliferation, glycolysis provides several precursors for major types of macromolecules including carbohydrates, proteins, lipids, and the nucleic acids needed to produce a new cell [1105, 1106]. Therefore, the Warburg effect imbues cancer cells with ribose, amino acids, and fatty acid biosynthetic benefits [64, 65, 1107]. High carbon flux into the pentose phosphate pathway, a key anabolic pathway, is in line with this advantage [64, 1108].

Although several decades have been passed since the first report on cancer metabolism and several mechanisms have been proposed for metabolic rewiring, a definitive mechanism underpinning this metabolic shift has remained obscure. Moreover, how individual metabolic pathways converge into an integrated metabolic shift to facilitate tumour phenotype remains to be determined.

Since the ratio of glycolysis to respiration was significantly elevated, Warburg originally hypothesized that cells developing aerobic glycolysis have impaired mitochondrial activity and diminished respiration and, therefore, aerobic glycolysis is an essential adaptation to compensate for the lack of ATP generated through oxidative phosphorylation [1]. However, it was later shown that whilst glucose fermentation accounts for the generation of 40-75% ATP required for tumour cells, almost in all cancer cells mitochondria still function to generate the remaining energy requirements. Mitochondria also contribute to pivotal roles in controlling anaplerotic and cataplerotic pathways within cancer cells [142, 1109-1111].

As outlined in Chapter 3, glycolytic inhibition of CRC cells resulted in a compensatory increase in mitochondrial respiration which led to a slight increase in cell proliferation rate. This was shown by an increase in basal and maximal respiration rate of CRC cells as well as their ATP turnover rate, which reflected the higher proliferation that these cells showed when glycolysis was inhibited by LDHA or PKM2 RNA interference.

Also, an increased rate of glycolysis was observed with mitochondrial complex I inhibition and the resulting suppressed respiration, confirming the ability of cancer cells to switch between glycolysis and oxidative phosphorylation

Therefore, it can be concluded that whilst glycolysis is indeed upregulated in the CRC cells tested, mitochondria remain functional at normal rates. This study also, confirms an OXPHOS-to-glycolysis switch. These findings may be useful for anticancer interventions, not only by taking advantage of upregulated glycolysis, but also necessitating multi-targeting strategies that modulate both energy production pathways as well as other energy pathways, such as lipid metabolism and beta-oxidation.

### 6.3 Anti-neoplastic effects of metformin on colorectal cells

In Chapter 3, the anti-cancer properties of metformin were investigated in CRC cell lines to investigate the changes in CRC cell biology and metabolism in this response. These experiments also aimed to select an appropriate CRC cell model and treatment conditions for the following experiments. Also, an association between the anti-cancer activity of metformin and different driver mutations was explored.

Over the last 50 years, metformin has been prescribed as an anti-diabetic agent to control glucose and insulin levels in type 2 diabetic patients. However, the anti-cancer properties of metformin have become an interest since, over a decade ago, when clinical observations were published suggesting a reduced cancer incidence in patients with diabetes and treated with metformin [790].

There are several studies on colorectal cancer, with more than twenty studies on CRC cell lines investigating the mechanism of action of metformin on tumour formation and its efficacy as a single therapeutic agent or in combination with other drugs commonly used for the prevention or treatment of CRC [1112]. Among the different CRC cell lines tested for the anti-neoplastic properties of metformin, such as HT29, HCT116, COLO205, SW620, DLD1, SW1116, Caco2 and SW480, HCT116 cells with additional modifications, such as derivatives with p53 null status and chemotherapy resistance, were the most used CRC cell lines [859, 876, 879, 881, 883-886, 888, 890]. According to the literature, concentrations higher than 0.5 mM of metformin can exert considerable direct effects on the metabolic events associated with the altered ATP/ADP ratio [1113]. Metformin was shown to affect membrane fluidity and the configuration of membrane proteins, such as glucose transporters, in cancer cells [1114, 1115]. In gut, liver and kidney metformin can accumulate up to 10 mM concentration [1116, 1117].

In this study, metformin treatment markedly suppressed mitochondrial respiration parameters such as basal and maximal respiration. This confers the metformin mediated suppression of oxidative phosphorylation and metabolic stress in CRC cells that were also shown in previous studies [859, 879]. Accordingly, the ATP turnover achieved through mitochondrial respiration was markedly suppressed by metformin treatment of CRC cells. The ATP synthesis measurements also showed a dose dependent decrease in ATP levels in CRC cell lines with *KRAS* and *TP53* mutational status having little to no significant effect on the response.

While metformin had a dose-dependent suppression effect on ATP synthesis, the oxidoreductase activity of mitochondrial complex I, was not in line with the ATP turnover changes attained. Only HCT116 cells showed correlative changes in both ATP synthesis and Complex I activity. While this inconsistency is difficult to explain, it may be related to the uncoupling effect of metformin which can disengage nutrient oxidation from ATP synthesis. Also, another explanation might be the pleiotropic nature of metformin and its effects on glycolytic ATP synthesis. Future experiments on the metformin associated changes in different components of glycolytic and oxidative enzymes could finally shed light on the molecular mechanism of action of metformin in CRC cells. We also confirmed that metformin modulates the mTOR pathway by monitoring the decrease of phosphorylation of p70S6K.

Similar to oligomycin mediated compensatory increases in glycolysis, metformin treatment also resulted in an enhanced glycolytic rate. However, a dose-dependent decrease in glycolytic capacity was also observed with metformin treatment of CRC cells, which is difficult to reconcile with complex I inhibition. The glycolytic capacity is the maximum glycolytic rate that constrains the glycolytic response a cell can have to generate ATP through glycolysis [1118]. This is due to the obligatory link between ATP synthesis and glycolytic carbon flux [1119]. Glycolytic capacity was shown to be a predictor of the sensitivity of cancer cells to anti-tumour drugs such as 2DG [1120, 1121]. Moreover, a reduced glycolytic capacity was also observed in hypoxic cells and a heart failure model [1122, 1123]. Cellular reprogramming and differentiation were also shown to be associated with enhanced glycolytic capacities of stem cells [1124, 1125]. These observations support the anti-tumour and pleiotropic nature of metformin via targeting two major components of metabolic capacity: respiratory and glycolytic, to compromise the metabolic plasticity of CRC cells and impair the matching of energy supply to demand.

A possible limitation of this study involved the extracellular flux analyses. Glycolytic and respiratory parameters are extrapolated by studying changes in extracellular concentrations of dissolved oxygen or protons, respectively. However, a more accurate protocol could be through

flux analyses using tracers to accurately quantify the glycolytic and respiratory rates. Furthermore, given the significance of lipid metabolism in regulating membrane synthesis, energy homeostasis and signalling factors, the role of metformin in regulating lipid metabolism is poorly understood and needs further investigation[1126].

Another limitation of this study could be the supra-pharmacological concentrations of metformin used for the treatment of CRC cell lines. Although the concentration of metformin that was used in this study is still higher than the physiologically achievable plasma levels, metformin was reported to accumulate in tissues to concentrations higher than the blood levels [895, 1127]. In fact, due to the positive charge of metformin, it was shown to achieve a concentration up to 20 mM in mitochondrial matrix [895]. Therefore, the concentrations used in this study (2.5 – 10 mM) might be attained during cancer treatment.

Although the concentrations used were within the range of applied doses of previous studies on CRC cell lines, where the direct anti-complex I activity of metformin emerges, these findings still require confirmation with lower concentrations of metformin

Metformin is reported to suppress CRC cell proliferation, cell migration, cell cycle progression, inflammatory response and to increase the susceptibility of cells to oxidative stress and chemotherapeutic agents [859, 876, 879-889]. Accordingly, investigation of the cellular effects of metformin on CRC cells confirmed a dose-dependent, anti-proliferative, effect. Since the CRC cell lines bearing different driver mutations, such as *KRAS*, *BRAF*, *PIK3CA* and *TP53*, as well as isogenic human colon cancer HCT116 cells with a targeted disruption of *TP53* or *KRAS* rescue, showed consistent decrease in cell viability with increasing doses of metformin treatment, it can be concluded that the anti-proliferative effect of metformin is not dependent on the aforementioned genes. These results are consistent with previous studies showing the anti-proliferative effects of metformin in different CRC models [876, 878, 886].

In contrast to the commonly observed anti-proliferative effect of metformin in cancer cells, there is some controversy regarding the cytotoxicity of this drug. While several studies demonstrated the pro-apoptotic function of metformin in some cells, the protective role of metformin against cell death was also reported and found to be associated with enhanced autophagy [851, 876, 878, 886, 979, 980]. Also, disparate cytotoxic effects were observed depending on the metabolic state of the cells and applied metformin concentration [851, 979]. Testing different CRC cell lines with driver mutations and isogenic cell lines with compromised *TP53* and *KRAS*, in this current study, high concentrations of metformin (10 mM) exerted a pro-apoptotic function. This may be explained by

the functional consequences of different metformin doses, which result in moderate or excessive activation of autophagy and, thus, can exert diverse effects on cell death. However, further experimental investigations are needed to study the effect of metformin with low to high doses on CRC cell autophagy, cell cycle progression and their associations with caspase activation.

While promising results regarding the anti-cancer properties of metformin in CRC cell lines were shown in this study, that are in line with previously published data, they require confirmation using *in vivo* models. Also, the immunotherapy benefits of metformin, that were beyond the scope of this study, could be explored in *in vivo* models [1128]. Further clinical trials are warranted to define the clinical value of combinatorial effects of metformin with other anti-cancer drugs in both cancer prevention and treatment of CRC patients.

#### **6.4 Comprehensive transcriptome and miRNA profile analysis of metformin treatment in CRC cells to uncover regulatory mechanisms**

Metformin regulates cell metabolism and exerts anti-cancer functions via multiple mechanisms [829]. In Chapter 4, large scale quantitative transcriptome and small RNA profiles were presented with the aim of identifying metformin-associated changes at the transcriptional and post-transcriptional levels. Taken together, these observations provide an integrated picture of the metformin - induced signalling pathways, through modulation of key miRNA-target gene pairs.

Integrated analysis of transcriptome and small RNA sequencing datasets indicates that metformin-mediated changes in CRC cells are mediated by dysregulating 1221 gene and 104 miRNAs at a level of significance. Integration of datasets for validated and potential miRNA target genes, with differentially expressed mRNAs and miRNAs, identified networks that are implicated in 198 enriched gene ontologies and 20 pathways.

Canonically, metformin is expected to function as an inhibitor of mitochondrial activity through targeting complex I within respiratory chain [1129, 1130]. However, much uncertainty still exists about cancer cell responses to the metabolic stress caused by the metformin-mediated decrease in mitochondrial oxidative phosphorylation. It was, therefore, postulated that the anti-tumour activity of metformin is not mediated through a limited number of cellular and molecular targets, but rather through an integrative network rewiring [1131]. Nevertheless, the detailed mechanism underlying the effect of the metformin intervention for CRC is not clear. Specifically, whether and how miRNA-gene pairs are involved in the mechanism of action of metformin treatment is poorly understood. Previous studies have demonstrated transcriptome changes associated with

metformin treatment [995, 1132, 1133]. For instance, Udhane et al., identified 14 differentially expressed genes in metformin treated polycystic ovaries (PCO) [995]. Transcriptome profiling of a metformin treated, non-alcoholic, steatohepatitis (NASH) mouse model revealed 792 differentially expressed genes that were implicated in metabolic pathways involving fatty acid and amino acid metabolism and ultimately, resulted in prevented and reversed steatosis and inflammation [1132].

Martin-Montalvo and Mercken et al. conducted a genome-wide microarray analysis on liver and muscle tissues and showed the transcriptome changes in metformin treated groups mimic a calorie restriction profile and, therefore, improve physical performance, insulin sensitivity, and reduce LDL and cholesterol levels [1134]. Also, transcriptome analysis of metformin treated mice with non-alcoholic fatty liver disease (NAFLD) identified genes involved in the steroid biosynthetic process function and the steroid biosynthesis pathway [1135]. While comparison of deep proteomics and transcriptomic analysis of breast cancer cells treated with metformin, showed a relatively low correlation, it was found that metformin modulated glycolysis and other cancer-related pathways by mediating changes in the RNA levels of key proteins, such as SP1 [1131]. This may confirm the post-transcriptional function of metformin in altering cell state.

Therefore, there is still a need to study the gene expression changes after metformin interventions against CRC progression. Furthermore, although the key roles of miRNAs in CRC tumorigenesis have been extensively studied, the associated changes in miRNA expression levels with metformin treatment needs further investigation in CRC cells. For instance, it was shown that metformin exerts anti-tumour cell growth properties by inducing G1 cell cycle arrest following modulation of 51 miRNAs in hepatocellular carcinoma [908]. Among those identified miRNAs, miR-943 was also shown to be downregulated by metformin in our study. miR-943 was shown to be upregulated in cancers such as renal cell carcinoma, thus, could serve as an important miRNA in the mechanism of metformin action and needs further investigation [1136]. Similar studies showed differentially expressed miRNAs as a result of the metformin treatment of pancreatic, gastric, prostate and lung cancer, oesophageal squamous carcinoma and cholangiocarcinoma [899, 901-904, 909, 1127]. In pancreatic cancer cell lines, metformin treatment resulted in unregulated let-7c, miR-192 and miR-26a, which suppressed cell proliferation, invasion and migration and stimulated cell apoptosis via targeting *HMGAI1* [901]. Similarly, metformin inhibited lung cancer cell growth and cell cycle progression by upregulating miR-222 targeting *CDKN1B*, *CDKN1C* and *PTEN* [902]. In chemo-resistant (CR) HCT116 and HT29 CRC cell lines, metformin treatment was associated with significant reduction in miR-21 expression to induce cell death [881].

Moreover, beside the individual miRNA expression changes in different cancers, metformin treatment was also shown to elicit a systematic alteration in miRNA expression by targeting DICER in a breast cancer cell line, diabetic mice and patients [894, 895]. This effect was DICER dependent as metformin treatment of DICER-null breast cancer cell lines did not have any effect on tumour engraftment. Upregulated DICER expression was also reported in cancer cells treated with AICAR, an AMPK activator, suggesting an AMPK-dependent mechanism [895, 1137].

The pathway and gene ontology (GO) analyses of differentially expressed genes in metformin-mediated networks provided an unbiased picture of metformin's effect on signalling pathways as well as functional groups. Investigation of the genome-wide impact of metformin on KEGG pathway signatures confirmed PI3K-Akt-related pathways as the major signalling cascades associated with metformin treatment of CRC cells. These results are in line with those of previous studies showing activated AMPK dependent effects of metformin in different cancers [851, 884, 914, 990]. What is more, the pathway analysis also revealed the MAPK signalling pathway as the most important individual term enriched for metformin-associated DE genes. Since the MAPK pathway regulates different cellular characteristics such as gene expression, cell cycle, metabolism, motility, cell survival, apoptosis and differentiation, this suggests a relatively novel mechanism of action for metformin in cancer cells [1024]. Accordingly, in glioma and lung cancer cells, metformin induced cell death by activating JNK/p38 MAPK [1090, 1138]. Isakovic et al., showed that activation of JNK, located upstream of disrupted mitochondria and associated ROS, was partly involved in metformin-induced cell apoptosis in glioma cells. However, studies showing suppressed JNK, via AMPK inhibitors such as Compound C, and elevated JNK activity, as a mediator of AMPK-initiated apoptotic programs, indicate the possible AMPK-dependent regulation of MAPK [1090, 1139-1141]. For that reason, it can be assumed that activation of AMPK may contribute to the anti-cancer properties of metformin, partly through activating both PI3K and MAPK signalling pathways.

Identification of “regulation of macromolecule metabolic process” and “signal transduction” terms among highly enriched biological processes also suggested a link between the growth inhibitory effect of metformin and the metabolic shunting of nutrients into macromolecule biosynthesis pathways as a hallmark of cancer [3, 7]. Further investigation of enriched molecular functions also revealed involvement of transcription-related terms to be related to metformin response in CRC cells. These data were consistent with previous publications showing the effects of metformin on global transcription by regulating histone modifications, transcription factors and DNA methylation [996-1000]. Similarly, the effect of metformin on “chromosome structure” and

“cellular structure”, as revealed by GO analysis of cellular compartments, further suggested the molecular components of gene expression and cell migration may be the putative targets of metformin, which needs to be confirmed by cellular assays [1001, 1002].

In this study, a framework for a systems biology approach was created that can later also incorporate phosphoproteome changes to derive a comprehensive overview of metformin associated anti-cancer properties in CRC. Therefore, in future studies, deep explorations of the corresponding changes in early protein phosphorylation responses followed by subsequent transcriptional changes combined with identification of key kinases, phosphatases and transcription factors that regulate the response to metformin treatment will also be required. Furthermore, this study administered a prolonged metformin exposure to investigate the epigenetic changes that are most likely associated with chronic adaptation. Future experiments comparing acute with chronic adaptation could reveal further insights into the different metabolic changes associated with prolonged and intense metformin treatment.

In conclusion, the underlying mechanisms of action for metformin in cancers remain unclear. This study, therefore, identified changes in the transcriptome and miRNA profiles of a CRC cell line treated with metformin, as well as molecular interactions that highlight the biochemical mechanisms involved in metformin response of CRC cells. To this end, a miRNA and target-gene based network was created which identified pathways and gene ontologies regulating macromolecule biosynthesis, gene expression and metabolism-related pathways. These data generate a snapshot of the rewiring of the signalling networks and elucidate the potential roles of miRNAs that underlie CRC and metformin intervention.

### **6.5 miR-132-3p and miR-2110 mediate the anti-cancer activity of metformin by inhibiting PIK3R3 expression and the PI3K/Akt pathway**

In this study, we demonstrated that metformin-associated changes are implicated in PI3K-Akt-related pathways. As the predominant pathway, PI3K-Akt pathway was identified as it contained seven DE genes. miRNA target prediction using different algorithms, as well as validated miRNA-gene pair datasets, were used to collate the putative/validated miRNA-gene pairs involved in PI3K-Akt pathway. Further validation of the selected miRNA-gene pairs, dysregulated by metformin treatment and involved in the PI3K-Akt pathway, discovered that *PIK3R3* is a putative or validated target of miR-2110 and miR-132-3p, respectively, and one of the key regulators of the pathway. As shown by transcriptome and small RNA sequencing, as well as subsequent expression

validation, metformin treatment of CRC cells resulted in a significant elevation in miR-2110 and miR-132-3p levels while significantly downregulating *PIK3R3* expression.

While a great deal of evidence suggests that miR-132-3p is a key tumour suppressor miRNA in different cancers, the role of miR-2110 remains to be elucidated. In CRC cells transfection of miR-132-3p resulted in a dramatic decrease in CRC cell proliferation and invasion and was correlated with increased sensitivity of the cells to preoperative chemoradiotherapy [1008-1010]. Ectopic expression of miR-132-3p was also shown to target *ZEB2*, *Derlin-1* and *CREB5* mRNA to suppress CRC cell proliferation, invasion and metastasis and induce cell apoptosis [1011, 1013, 1014]. Vice versa, miR-132-3p downregulation by DNA hypermethylation was associated with increased CRC invasion and poor prognosis in colorectal cancer [1009, 1012]. Consistently, our data also support the anti-proliferative effect of miR-132-3p in a panel of different CRC cell lines.

miR-2110 was discovered while investigating miRNA expression in nasopharyngeal carcinomas (NPC) and normal tissues [1142]. It was downregulated in rectal cancer compared with normal adjacent tissue [1003] and was shown to be a miRNA that induces neurite outgrowth in neuroblastoma and to have anti-correlation with *MYCN* mRNA expression [1005, 1007]. Also, the plasma levels of miR-2110 were shown to be elevated in colorectal cancer patients relative to normal subjects [1143]. In line with these findings, Zhao et al., showed an onco-suppressive role of miR-2110 in neuroblastoma via direct targeting of *TSKU*, which encodes a leucine-rich proteoglycan and regulates cell survival, proliferation and migration [1006]. They also confirmed a correlation between low tumour miR-2110 levels and poor prognosis and survival of neuroblastoma patients [1006, 1144-1146]. Despite studies confirming the onco-suppressive role of miR-132-3p and miR-2110, the role of these miRNAs in CRC is not well known due to limited target gene information. It is expected that this study has identified novel miR-132-3p and miR-2110 target genes in CRC.

*PIK3R3* is a member of the phosphatidylinositol 3-kinase family (PI3K), which has a critical role in cell apoptosis, proliferation and protein synthesis. Its role in regulation of glucose uptake and metabolism is also well established. PI3K dysregulation was reported in several human cancers and small molecule inhibitors are currently in clinical trials [302]. An overactivated PI3K-Akt pathway, caused by genetic mutations and/or gene amplifications, commonly occurs in different forms of tumorigenesis leading to induction of downstream effectors such as AKT and mTOR [1015]. *PI3KR3* encodes a PI3K regulatory subunit p55g and binds to the p110 catalytic subunit of PI3K protein [1016-1020]. The role of *PIK3R3* in promoting tumour cell proliferation, growth,

metastasis and angiogenesis was shown in cancers from liver, ovary, stomach, lung, bowel and breast [1020-1023].

Liu et al., showed an anti-correlation between elevated levels of *PIK3R3* expression and downregulated miR-132-3p expression in hepatocellular carcinoma which was associated the tumour differentiation, TNM stage and lymph node metastasis [989]. They also confirmed the direct targeting of *PIK3R3* by miR-132-3p and demonstrated consequences such as cell proliferation, migration, invasion suppression and inhibition of Akt/mTOR signalling pathway to the *PIK3R3* targeting by this miRNA [989]. Similarly, we showed suppressed p70S6K phosphorylation, which is a downstream effector of the PI3K-Akt pathway, by overexpressed miR-132-3p and miR-2110 and confirmed *PIK3R3* as a direct target of miR-2110 that contributes to the anti-proliferative effect of miR-2110 in CRC cells.

In this study, Target Protectors were used to confirm the direct targeting of *PIK3R3* by miR-2110 that allowed examination of the specific effect that miR-2110 has on PIK3R3 levels. While Target Protectors are broadly applicable interventions, some limitations should be considered for them. While custom designed Target Protectors bind to their complementary sequence on specific miRNA binding sites present on 3'UTR target mRNA, if similar sequences are present elsewhere in the genome, possible off-target effects may occur. Also, since multiple miRNAs can potentially target an individual mRNA with binding sites in a proximity, application of Target Protectors may theoretically interfere with other miRNAs targeting in the vicinity of their binding sequences.

In summary, these results together with previous studies, suggest that metformin exerts its anti-proliferative function in CRC cells, partly due to upregulating miRNAs such as miR-2110 and miR-132-3p, to directly target genes such as *PIK3R3* and, thereby, regulate PI3K-Akt signalling. Future experiments may include an investigation of the identified miRNA-target gene pairs in tissues extracted from CRC patients and treated with metformin (Figure 6-1).

## **6.6 miR-222-3p and miR-589-3p mediate the anti-proliferative activity of metformin by targeting STMN1**

As introduced in Chapter 1, one of the mechanisms by which metformin can regulate gene expression is an epigenetic process. Growing evidence shows that while miRNA expression changes occur following metformin treatment of different disease, it is not known whether metformin-regulated mRNA changes are epigenetic in nature or mediated by the altered miRNA activity. Substantial evidence indicates that miRNAs exert tumour suppressive or oncogenic roles

through targeting oncogenes or tumour suppressor genes, respectively, and a single miRNA can target multiple transcripts.

While this study showed subtle changes in the miRNA expression profile of CRC cells in response to 2.5 mM metformin treatment, even small changes in miRNA expression levels can fine-tune important cellular effects, since a single miRNA can simultaneously target multiple genes and, therefore, multiple pathways [1147].

KEGG pathway analysis of the differentially expressed genes associated with metformin treatment of CRC cells, revealed MAPK signalling pathway to be the most significantly enriched KEGG term among 20 KEGG pathways identified. Investigation and validation of DE genes, as well as predicted or validated miRNA-target gene pairs, identified 317 DE genes and 169 putative/validated mRNA-gene pairs for 47 DE miRNAs, respectively, within the MAPK signalling pathway. Further validation experiments showed that miR-222-3p and miR-589-3p act as onco-suppressive miRNAs since transfection with these miRNAs resulted in a significant reduction in CRC cell viability.

Conflicting evidence exists for the role of miR-222-3p in cancer. A number of studies have shown miR-222-3p to be increased in various cancer types, including glioblastoma, non-small lung cancer, lymphoma, Kaposi sarcoma and hepatocellular cancer; alternatively, some other studies in malignant glioblastoma, lung and prostate cancer have shown downregulated levels of miR-222-3p [1026-1028][1075, 1079-1081]. In an oncogenic role, miR-222-3p was shown to suppress CDK2 by targeting p27Kip1 and p57, both of which are cell cycle proteins. Since upregulated miR-222-3p was found in some poorly differentiated and aggressive cancers, the active role of this miRNA in promoting EMT was shown to involve targeting *ZEB2* [1032-1034]. On the other hand, Medina et al., and Yamashita et al., reported increased S-phase accumulation and induced apoptosis, specifically after transfecting glioblastoma and lung cancer cells with miR-222-3p [1035, 1037]. Furthermore, reduced levels of miR-222-3p in clinical prostate cancer specimens support a tumour suppressive role for this miRNA by inhibiting cell proliferation, migration and invasion [1036]. Similarly, cell-cycle arrest and partial differentiation were observed with phorbol myristate acetate (PMA)-induced over-expression of miR-222-3p in acute myeloid leukemia (AML) [1038].

miR-589-3p is a poorly studied miRNA and, thus, there is still need to conduct research on the functional role of this miRNA in tumorigenesis. Three studies investigated the clinical significance and function of miR-589-3p in lupus nephritis, glioblastoma and lipopolysaccharide

(LPS) stimulated Nucleus pulposus (NP) cells [1039, 1040, 1148]. miR-589-3p was found among circulating miRNAs with differential abundance between Class IV lupus nephritis (LN-IV) and healthy individuals (CTL group) [1148]. A brain exclusive A-to-I editing within the miR-589-3p seed sequence was found, which was significantly decreased in glioblastoma cell lines and tissues and, when induced, it resulted in suppressed cell proliferation, migration and invasion [1039]. miR-589-3p also seems to promote lumbar disc degeneration (LDD) by inducing apoptosis in lipopolysaccharide (LPS) stimulated Nucleus pulposus (NP) cells [1040].

miRNA target prediction analyses identified *STMN1* as a possible target for both miR-222-3p and miR-589-3p. Based on the methods proposed by Kuhn et al., direct targeting of *STMN1* by miR-222-3p and miR-589-3p was confirmed in CRC cells as they fulfilled the four proposed criteria [1149]; in metformin treated CRC cells, miR-222-3p, miR-589 and *STMN1* were co-expressed and *STMN1* expression changes showed anti-correlation with miR-222-3p and miR-589-3p expression levels. Also, transient overexpression of miR-222-3p or miR-589-3p in CRC cells resulted in a significant reduction in RNA and protein levels of *STMN1*. Direct targeting of *STMN1* by miR-222-3p or miR-589-3p was also verified through specific target protectors and finally, the miR-222-3p or miR-589-3p mediated regulation of *STMN1* expression confirmed the biological function of the targeting, in this case CRC cell proliferation, as verified by target protector experiments.

*STMN1*, also called oncoprotein-18, is a cytosolic protein and its overexpression is shown in in cancers including colorectal, gallbladder, breast, liver, lung and prostatic adenocarcinomas and sarcoma [1043-1050]. Regulation of microtubule dynamics during mitotic spindle formation is proposed as the main molecular function of *STMN1*. Protein levels of this cytosolic gene was shown to predict the effectiveness of microtubule mediated therapeutics such as paclitaxel and disease recurrence [1041, 1042]. At the cellular level, *STMN1* regulates cell cycle progression. Reduced *STMN1* inhibited cell growth, induced apoptosis and delayed G2/M phase transformation in GBC cells by regulating the activity of p38 MAPK kinase and p53/p21 signal pathways [1043, 1054]. Activated MAPK was shown to suppress *STMN1* expression by inducing the miRNAs that target it, such as miR-193b, which resulted in suppressed pancreatic cancer cell proliferation [1055]. Similarly, inhibition of *STMN1* was shown to result in induced apoptosis, arrested cell growth and invasiveness [1056, 1057]. The metabolic influence on colon carcinogenesis was shown with *STMN1* phosphorylation by EGF which serves as a rate-limiting event for PI3K/Akt signalling [1058-1060].

In our study, transfection of miR-222-3p or miR-589-3p, leading to knock down of *STMN1*, inhibited cell proliferation in CRC cell lines, similar to the phenotype observed with metformin treatment of CRC cells. This provides evidence regarding a possible mechanism of action of metformin, through upregulating miR-222-3p and miR-589-3p and, thus, downregulating *STMN1* expression to inhibit CRC cell proliferation.

A limitation of this study was that a large amount of each mimic was transfected into CRC cells, which may not reflect the physiological levels of these miRNAs in colorectal cells. However, as exaggerated functional outcomes of these miRNAs compared with metformin responses, this may indicate a function of metformin-mediated aberrant miRNA activity in CRC cells.

Altogether these findings depict the close interplay between miRNAs that exert a profound impact on the proteins associated with metformin activity in CRC cells. Future studies include the investigation of cell cycle changes associated with metformin treatment of CRC cells, as well as *STMN1* inhibition by miR-222-3p and miR-589-3p (Figure 6-1). Also, experiments are needed to further explore the effect of the identified dysregulated miRNA-target gene pairs in regulating MAPK signalling pathway components and other CRC cellular processes, such as associated changes in microtubule dynamics.

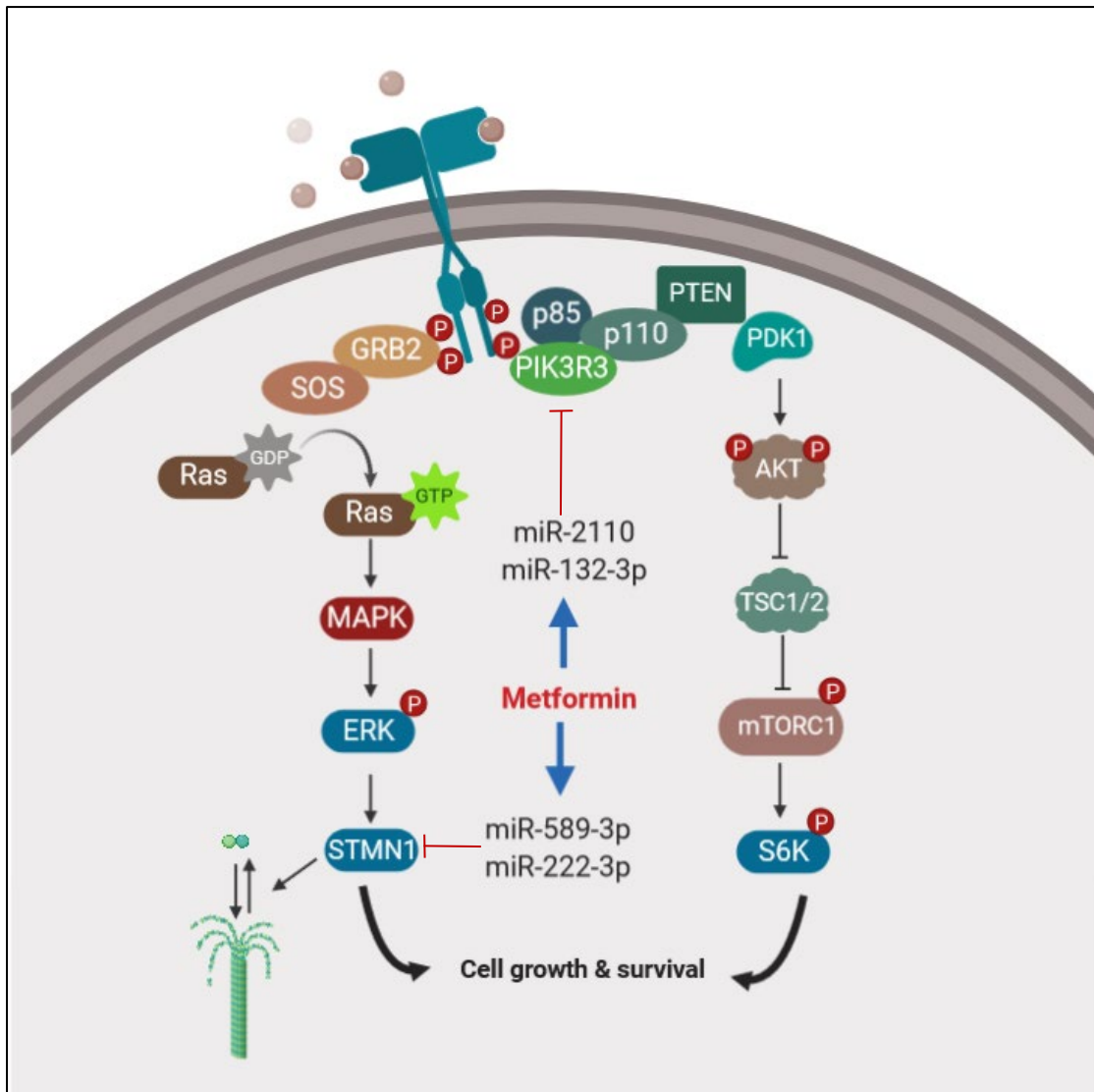


**Figure 6-1: Proposed molecular model for mechanism of action of metformin in CRC cells.**

Metformin suppresses CRC cell growth via regulating PIK3-Akt and MAPK signalling pathway. It exerts this function via the upregulation of tumour suppression miRNAs including miR-2110 and miR-132-3p as well as miR-589-3p and miR-222-3p to downregulate PIK3R3 and STMN1 expression, respectively (The figure is adapted from [www.biorender.com](http://www.biorender.com) )

### 6.7 Functional screening identifies miRNAs that modulate the sensitivity of CRC cells to metformin

The incidence and mortality of CRC have decreased over the past decades due to the improved diagnostic tools that help in early diagnosis and effective treatment of CRC patients. Nonetheless, the disease remains a major public health issue, as one of the leading causes of cancer mortality worldwide. Apart from potentially curative colectomy, chemotherapy and radiochemotherapy may be applied at advanced stages in CRC. However, these therapies are not highly efficient in cases

with poor prognosis at a relatively high efficacy. Therefore, there is still a strong demand for novel curative approaches to CRC.

While there is mounting preclinical and clinical evidence for the anti-cancer properties of metformin, consensus on its beneficial properties and mechanism of action is lacking. Recent epidemiological studies have also reported conflicting conclusions regarding the cancer-protective effect of metformin [1150]. Indirect effects of metformin on cancer cells occur through modulation of the endocrine metabolic system to suppress gluconeogenesis and control glucose and insulin levels. On the other hand, direct interactions between cancer cells and metformin were also shown where metformin treatment resulted in an energetic stress. However, as with most chemotherapeutic agents for CRC, metformin doses are not optimised for cancer prevention and treatment. Lowering the administered doses of metformin could potentially alleviate the deleterious effects on normal cells in the intestinal crypts and bone marrow [1151]. Therefore, it is clinically important to identify metformin enhancing agents to decrease doses without reducing their effectiveness, as well as to avoid or overcome drug resistance. Accordingly, an accumulating number of studies demonstrate the effectiveness of metformin, in combination with chemotherapeutic drugs, in minimizing the possible side effects and maximizing the efficacy in tumour regression [1152, 1153]. The genetic heterogeneity of CRC tumours adds another layer of complexity when determining how much metformin accumulates in cancer cells. For instance, Cai et al., demonstrated a wide heterogeneity in cation transporter expression among various breast cancer cell lines, especially OCT3 and PMAT, which defined the optimal doses of metformin for an anti-cancer response in breast cancer cells [1154]. *In vitro* and *in vivo* studies confirmed the effectiveness of metformin combined with 5-FU and vitamin D in CRC treatment [877, 1155]. Two phase II clinical trials are also investigating the effectiveness of metformin in combination with irinotecan and 5-FU in refractory colorectal cancer therapy [1156, 1157].

miRNAs are frequently altered in cancers owing to genomic and epigenetic events, as well as biogenesis defects [1158, 1159]. Given their involvement in vital cellular processes, it is expected that miRNAs play profound roles in cancer biology. This involvement was first demonstrated by the loss of miR-15a/16 in chronic lymphocytic leukemia (CLL) [1160]. Subsequent studies demonstrated the aberrant expression of specific miRNAs in tumours with different tissues of origin and further confirmed that miRNAs can act as tumour suppressors or oncogenes [1161]. Since the global downregulation of miRNA expression was observed in tumours, and miRNAs contribute to cancer cell metabolism, an attractive therapeutic avenue may include restoring the levels of deficient miRNA species [994]. To date, miRNA replacement therapy, using

predominantly synthetic double-stranded miRNA mimics with a delivery agent, has been reported in preclinical tumour models [1162, 1163]. Moreover, a clinical trial investigated the restoration of miR-16 expression in mesothelioma and represented feasibility of miRNA replacement therapy for cancer patients [1164].

In this study, the ability of miRNAs to sensitize CRC cells to the anti-proliferative effect of metformin was investigated using a functional high throughput screen of synthetic miRNA mimics. Among 2063 miRNA mimics tested, 46 were selected from the primary screen and then further refined to 8 miRNAs following secondary screens and validation experiments that showed enhancement of the metformin anti-proliferative effect in CRC cell lines. These miRNAs included miR-18b-5p, miR-145-3p, miR-1181, miR-376b-5p, miR-665-5p, miR-676-3p, miR-718 and miR-99a-3p. Some of these miRNAs, such as miR-145-3p, miR-676-3p, miR-655-5p, miR-18b-5p and miR-376b-5p not only repressed tumour cell growth and proliferation by themselves, but also synergistically enhanced the efficacy of metformin in repressing tumour cell growth.

We also studied the roles of metformin sensitizing miRNAs in regulating CRC cell metabolism. As shown previously, metformin treatment of CRC cells, resulted in suppressed mitochondrial respiration and a compensatory increase in glycolysis [838, 1089, 1090]. However, in this study, glycolytic capacity and glycolytic reserve were decreased with metformin treatment of CRC cells. This may suggest the pleiotropic nature of metformin and demonstrate the glycolytic-related genes to be putative molecular targets of metformin in CRC cells. As a direct target of metformin, mitochondrial function is affected by metformin treatment in different cancers [838, 1089, 1090]. Accordingly, 2.5 mM metformin treatment of CRC cells resulted in a dramatic decrease in mitochondrial functions, including basal and maximal respiration as well as ATP synthesis.

As reviewed in Chapter 1, the energy producing pathways such as aerobic glycolysis and oxidative phosphorylation are tightly regulated by cytokines, tumour suppressors, oncogenes and enzymes associated with glucose metabolism. We also confirmed novel roles for selected miRNAs such as miR-376b-5p, miR-1181, miR-18b-5p, miR-676-3p, miR-718 and miR-145-3p in regulating glycolysis or mitochondrial respiration to potentiate the anti-proliferative effects of metformin.

Transfection with miR-376b-5p alone revealed an inhibitory effect on glycolytic parameters including basal and maximal glycolysis and glycolytic reserve. Also, combination of miR-376b-5p transfection and metformin treatment had the strongest effect on mitochondrial function by further enhancing the inhibitory effect of metformin on basal and maximal respiration and ATP turnover.

Li et al., demonstrated the anti-angiogenic nature of miR-376b-5p in middle cerebral artery occlusion, through its activity on the HIF1 $\alpha$ -mediated VEGFA signalling pathway [1076]. Low expression of miR-376b-5p was also shown to be correlated with poor prognosis of patients with pancreatic adenocarcinoma [1077]. miR-376b-5p was also shown to inhibit breast cancer cell metastasis by targeting *HOXD10* [1078].

Experiments with miR-376b-5p showed that the significant changes in glycolytic parameters were large enough to hinder the metformin-mediated increase in CRC cell glycolysis. Due to the anti-respiratory functions of miR-376b-5p, it appears that combining this microRNA activity with metformin treatment is able to suppress both energy producing pathways in CRC cells, resulting in reduced cell viability.

While some studies highlighted the diagnostic value of miR-676-3p in cancers such as gastric, prostate and breast cancer [refs 1071-1073 here], very little is known about the metabolic and anti-cancer function of this miRNA [1073-1075]. Here we showed the anti-cancer effect of metformin-sensitizing miR-676-3p to be a suppressor of glycolysis, glycolytic capacity and glycolytic reserve. This hindered the metformin-mediated increase in CRC cell glycolysis and enhanced the inhibitory effect of metformin on glycolytic reserve and capacity.

Similarly, both miR-18b-5p and miR-145-3p were shown to suppress glycolytic properties such as glycolytic rate, glycolytic capacity and glycolytic reserve in combination with metformin, whilst exerting no significant effect alone.

miR-18b-5p was shown to be differentially expressed in certain cancers such as rectal and breast cancer [1079-1081]. However, there are discrepancies with regard to the function of this miRNA in cancer, as it can be both a tumour suppressor or oncogenic miRNA depending on the cellular context and target genes present. In melanoma cells, downregulated miR-18b-5p was shown to directly target the proto-oncogene MDM2 and regulate DNA methylation and, thereby, regulate the p53 signalling pathway to reduce tumour cell growth and induce cell death [1082].

miR-145-3p was also shown to be downregulated in different cancers and is also a known tumour suppressor and regulator of tumour growth, cell death and tumour metastasis [1084-1087]. In line with our findings, Qui et al., also showed an anti-glycolytic function for miR-145-3p in CRC cells, after conducting a high throughput functional screen of miRNA mimics [1088].

Furthermore, we showed an enhancement role for miR-1181, through further suppressing maximal respiration in CRC cells when combined with metformin treatment. miR-1181 is a hypoxia-inducible miRNA and its tumour suppressive roles were shown in pancreatic, ovarian and prostate cancers by targeting *SOX2*, *STAT3* and *HOXA10* where it inhibited proliferation, migration and invasion and promoted EMT [1091-1095].

miR-718 was another miRNA identified in our study and showed strongest effect on mitochondrial parameters by further enhancing the inhibitory effect of metformin on basal respiration and ATP turnover. miR-718 was originally identified in 2006 and Leng et al., showed the anti-cancer role of this miRNA via targeting of *VEGF* transcripts in ovarian cancer [1096, 1097]. The anti-oncogenic and tumour suppressive function of miR-718 was then confirmed in other cancers including hepatocellular and oesophageal squamous cell carcinoma, as well as thyroid and ovarian cancers where it inhibited cancer cell proliferation, invasion and regulated the innate immune response by inhibiting *VEGF*, *PDPK1*, *IRAK1*, *EGR3* and *PTEN* expression [762, 1097-1100]. In agreement with our findings, Wang et al., showed miR-718 mediated suppression of metabolism and energy production in papillary thyroid cancer through regulating the *PI3K/Akt/mTOR* pathway [1101].

Since the sub-lethal dose of metformin (2.5 mM) used on CRC cells did not lead to a pro-apoptotic state, we further investigated the anti-tumour properties of metformin combined with the various metabolism regulating miRNA mimics. While six selected miRNAs enhanced the anti-proliferative effect of metformin by further decreasing the viability of CRC cell lines, only miR-676-3p showed pro-apoptotic activity in HCT116, DLD1 and HT29 cells, both alone and in combination with metformin, which suggests the involvement of other cellular events, such as cell cycle regulation, in inducing the CRC cell response to metformin.

In conclusion, these findings confirm the ability of metformin to not only play a monotherapy role in cancer treatment, but also in combination with miRNAs for treating cancer. Since CRC cells retain the ability to switch to aerobic glycolysis when respiration is suppressed by metformin treatment, a combination of glycolytic inhibitors with metformin may provide better therapeutic interventions. Accordingly, Lea et al., confirmed that 1 mM metformin treatment had an anti-growth effect when combined with 10 mM 2-DG in SW1116, HT29 and Caco2 CRC cells [884]. Furthermore, we demonstrate the capability of miRNAs to enhance the anti-cancer properties of metformin in CRC cells. We also confirmed an additional capacity of miRNA function whereby metformin-sensitizing miRNAs suppressed CRC cell metabolism through the regulation of glycolytic and respiratory parameters in the presence of metformin. Further study is required to

elucidate the precise molecular targets of the identified miRNAs associated with metabolic regulation of CRC cells.

This study was limited to examining the combinational effect of miRNAs and metformin in CRC cell lines; however *in vivo* investigation of these functions may be beneficial for examining their role in a higher organismal complexity. It is also important to note that, in most previous studies including ours, supra-pharmacological concentrations of metformin were used, which are well above the plasma concentrations reported in systemic circulation. It is therefore proposed that results obtained from *in vitro* and *in vivo* models cannot be directly extrapolated to safety, nor efficacy, in clinical trials. However, it has been reported that metformin accumulates in tissues at concentrations significantly higher than those obtained in the portal vein [1116], indicating that these therapeutically active concentrations may be achieved during cancer treatment. Also, as explained before, sub-lethal doses were selected for most experiments, with a focus on chronic metformin treatments to minimise the cytotoxicity of metformin in our *in vitro* model. In addition, further exploration of our high throughput miRNA screen data on specific miRNAs that inhibited the metformin response might provide additional insights into the role of metformin in CRC cells.

## 6.8 Systems biology approach for metformin-associated networks

In conclusion, we aimed to determine the metabolic requirements of CRC cells and the roles of miRNAs in this context. We showed that CRC cells contain functional mitochondria, especially since they exhibit elevated proliferation in the presence of glycolytic inhibitors. Also, we investigated the effect of metformin as a drug that inhibits mitochondrial respiration in CRC cells. In this study, we confirmed some of the anti-cancer properties of metformin in CRC cells, as well as its role in regulating CRC cell metabolism. However, despite previous reports, no pro-apoptotic activity from metformin treatment was observed, at concentrations below 10 mM, in CRC cells. Therefore, to further explain the anti-proliferative role of metformin, future studies should include the specific role in regulating cell cycle progression.

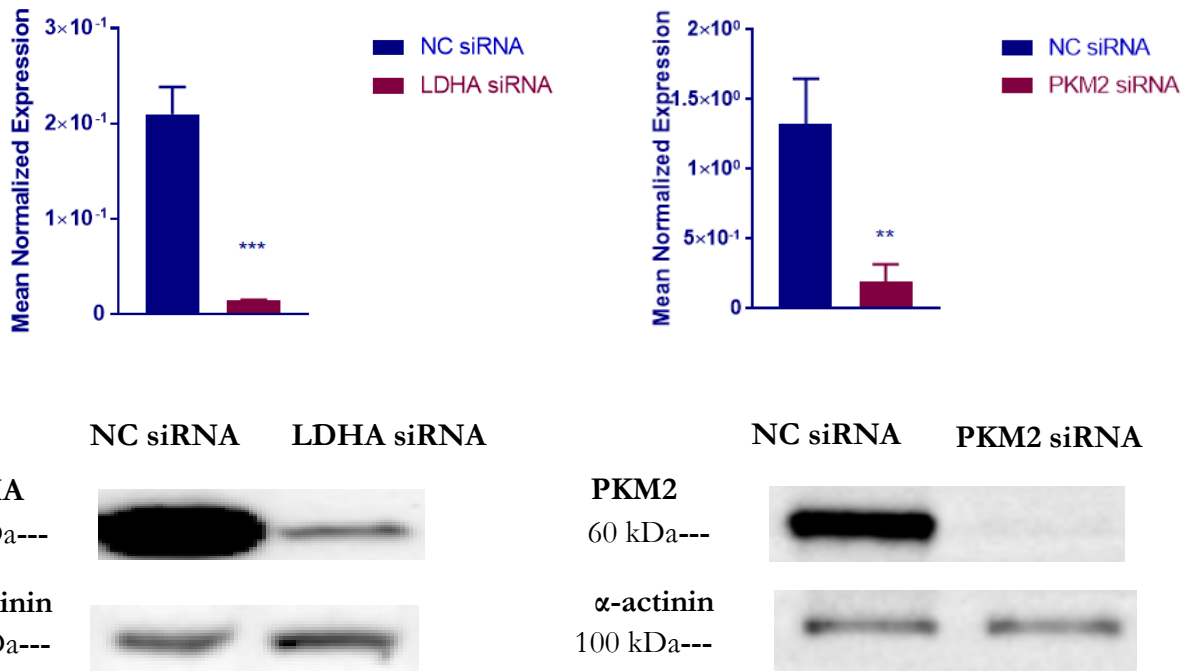
Given that extensive rewiring of cell signalling networks resulted from metformin treatment of CRC cells, here we showed that an increase in some tumour suppressive miRNAs, such as miR-132-3p, miR-2110, miR-222-3p and miR-589-3p and increases in target gene expression, including *PIK3R3* and *STMM1*, may explain some of the anti-cancer effects of metformin in CRC cells. These genes and miRNAs were mapped into pathways such as PI3K-Akt and MAPK signalling pathways that were shown to dictate various cellular characteristics of cancer cells. While this study mainly focused on the specific effects of these miRNA-target gene pairs on CRC cell proliferation,

future work to assess their specific roles in modulating the associated signalling pathways may strengthen the tumour-suppressive role of the identified miRNAs. Expression levels of the selected miRNAs, in comparison to the expression of identified target genes, in CRC tissue samples and adjacent normal tissues could also be explored using the public TCGA database [1165].

Given the profound effect of metformin on cell metabolism, we entertained the possibility that miRNAs can enhance the anti-proliferative effect of metformin in CRC cells, possibly through modulating CRC cell glycolysis and/or oxidative phosphorylation. We identified 6 miRNAs that sensitize CRC cells to the anti-proliferative effect of metformin. The roles of these miRNAs in regulating CRC cell metabolism were also confirmed. Characterizing the roles of these miRNAs, using *in vivo* models to confirm the anti-cancer properties observed in this study, represents one area for further study. Also, a functional high throughput screen of miRNA inhibitors could further assist in stratifying the anti-neoplastic roles of these miRNAs. Moreover, there was not a significant number of overlaps between miRNAs that were differentially expressed in metformin treated CRC cells with miRNAs that sensitize CRC cells to metformin effect. The only overlaps were miR-205-5p and miR-2116-3p that were upregulated by metformin treatment and had a metformin sensitizing effect on CRC cells. This may suggest the inadequacy of metformin as a monotherapy and the need for a combination modality as the cornerstone of cancer therapy. miR-2116-3p and miR-205-5p were upregulated with metformin treatment and had additive and synergistic effects with metformin in HCT116 cells (Fold change = 2.1 and 1.2, CDI= 1.05 and 0.82 for miR-2116-3p and miR-205-5p, respectively). miR-205-5p is not a highly abundant miRNA in colon tissues and our PCR data analyses were unable to detect this miRNA in HCT116 cells (data not presented). However, miR-2116-3p could be an miRNA of interest to investigate further and characterize its function in mediating the CRC cell response to metformin treatment. Furthermore, there was no overlap between downregulated miRNAs in our small RNA sequencing data and those that had antagonistic effect on the CRC cell response in our secondary high throughput screening data. This may also suggest the inefficiency of miRNAs to counteract the profound effects of metformin treatment in CRC cells. However, to confirm this hypothesis, there is a need to reanalyze our primary functional screening data and to perform a secondary screen investigating the counteracting CRC responses to metformin and specific miRNAs. Altogether, miRNAs that were regulated by metformin treatment, as well as those with metformin-sensitizing potential (Figure 5-31), are useful tools to gauge the effectiveness of metformin treatment and to provide clues to the molecular basis of the anti-cancer effects of metformin, particularly in the context of cellular metabolism.

# Appendices

## Appendix 1. RNAi efficiencies of LDHA and PKM2 siRNAs



### Quantitative real-time PCR analysis of mRNA levels and western blot analysis of protein levels in HCT116 cells transfected with LDHA and PKM2 siRNAs.

Cells were transfected with LDHA, PKM2 or NC siRNA and the RNA and protein levels were measured by RT-PCR and western blot analysis, respectively. The mRNA expression is normalised to *B2M* expression and  $\alpha$ -actinin protein levels were considered as a loading control. The statistical significance is indicated with asterisks (\*\*  $P \leq 0.01$  and \*\*\*  $P \leq 0.001$ ).

APPENDICES

**Appendix 2. Differentially expressed protein-coding genes associated with 2.5 mM metformin treatment of HCT116 cells and compared with control medium.**

Gene_name	baseMean	log2FoldChange	padj
ATOH8	46.9721	-3.3	6.99E-16
ID4	32.09625	-2.2	5.15E-07
SDPR	30.35188	-1.9	2.02E-05
SAMD15	40.74267	-2.3	4.86E-08
DHRS2	48.52145	-2.4	4.73E-10
TSNAXIP1	32.26793	-1.8	5.4E-05
ELF5	51.86407	-2.5	9.14E-11
STC1	40.20684	-2.0	3.46E-06
CXCR4	38.75304	-1.9	3.39E-06
ACTRT3	40.84459	-2.0	2.09E-06
TMEM232	33.23936	-1.6	0.000327
SEPP1	63.29062	-2.4	3.93E-11
STS	39.78733	-1.6	7.16E-05
GATM	46.92703	-1.9	3.62E-06
LRRIQ3	40.4575	-1.7	7.19E-05
PNMA2	57.79638	-2.1	9.56E-09
CCDC148	40.16384	-1.5	0.00033
ZBBX	43.78319	-1.6	0.000102
AFAP1L2	47.03575	-1.7	2.08E-05
ZNF280A	54.54237	-1.9	6.67E-07
PIH1D2	40.66023	-1.4	0.001079
ANKRD62	36.54516	-1.1	0.011513
TTLL6	38.76561	-1.2	0.003465
HLA-DOA	44.93363	-1.5	0.000178
VMAC	37.68329	-1.2	0.006119
BHMG1	37.72456	-1.2	0.006339
ZCCHC12	65.01823	-2.1	8.79E-09
FSIP1	37.57779	-1.1	0.013252
KRT222	39.64999	-1.2	0.005234
ESR2	39.20556	-1.1	0.007889
HFM1	42.02311	-1.2	0.00501
DFNB59	45.86076	-1.4	0.000659
RIMKLB	52.08478	-1.6	3.47E-05
RORC	37.34252	-1.0	0.034869
TSPAN7	40.70687	-1.1	0.016574
DNAJC28	55.46849	-1.7	8.87E-06
RCBTB2	117.5555	-2.8	9.16E-21
KRBA2	38.3681	-1.0	0.025165
SPARCL1	71.85689	-2.0	3.25E-08
RAB36	44.39158	-1.2	0.004744
C1orf228	42.08695	-1.0	0.016675
STON1	49.31538	-1.3	0.001339
C14orf169	55.84286	-1.5	7.19E-05
SH2D1B	61.1691	-1.6	1.23E-05
ZNF396	66.56534	-1.7	1.24E-06

APPENDICES

ZNF747	43.84986	-1.0	0.019388
CCT6B	48.19521	-1.1	0.006566
HSPA2	49.43904	-1.2	0.00218
SLC6A20	43.10893	-1.0	0.025689
KLF8	45.53423	-1.0	0.014823
ZNF350	47.83456	-1.1	0.006118
KRT20	52.03926	-1.3	0.001088
DCDC1	56.98713	-1.4	0.000178
CALML4	45.38021	-1.0	0.015794
NRGN	49.6182	-1.1	0.005189
FMO5	52.39763	-1.2	0.002583
LHX2	60.74284	-1.4	0.000185
PRF1	63.86236	-1.5	7.88E-05
ZBED6CL	68.28731	-1.6	3.91E-06
CSPG5	48.70709	-1.0	0.011871
KLRC4	55.99752	-1.3	0.000843
SPTSSB	84.48642	-2.0	2.85E-09
SERTAD4	87.79239	-2.0	3.45E-10
ATRNL1	49.22317	-1.0	0.016559
ZC3H12B	51.01846	-1.1	0.008435
ZMAT1	51.46806	-1.1	0.008603
SLC9A9	51.27612	-1.0	0.009782
TTPA	52.82349	-1.1	0.005457
IDNK	53.54612	-1.1	0.00622
NOV	73.69105	-1.7	9.49E-07
SLC2A9	53.24632	-1.1	0.006739
SKIDA1	56.50251	-1.2	0.002196
ZNF132	64.60248	-1.3	0.00029
ZNF688	52.61385	-1.0	0.010503
IKZF2	64.68144	-1.4	0.000137
ZNF425	74.4798	-1.6	3.98E-06
KLRC4-KLRK1	72.99033	-1.5	2E-05
FSTL5	92.22415	-1.9	2.84E-09
AMDHD1	81.3703	-1.7	6.44E-07
SP110	59.91525	-1.1	0.003996
TTC30A	105.6978	-2.1	1.41E-11
APOBEC3G	109.284	-2.1	1.23E-11
APITD1	63.90661	-1.1	0.002955
ANK1	71.60223	-1.3	0.00013
ASB9	73.42557	-1.4	5.45E-05
NME5	75.06034	-1.4	5.79E-05
AKAP3	106.6308	-2.0	4.73E-11
MRAP2	70.56532	-1.2	0.000668
TSPAN10	63.96122	-1.1	0.003242
TNFRSF19	78.755	-1.4	2.71E-05
LRRIQ1	80.65308	-1.5	1.09E-05
ZNF214	105.701	-2.0	5.6E-10
S100A5	66.65207	-1.1	0.001873
STXBP5L	73.30117	-1.3	0.000208
SYK	103.9221	-1.9	2.18E-10

APPENDICES

NCAM1	89.3237	-1.6	2.95E-07
FOXP2	63.44357	-1.0	0.008302
C1QL3	87.60643	-1.5	2.08E-06
PPM1N	104.8	-1.8	2.81E-09
LBHD1	68.32126	-1.0	0.00388
SLC46A3	72.91404	-1.2	0.000934
PCDHAC1	76.72875	-1.3	0.000181
CTSO	79.85594	-1.3	0.000104
SDR16C5	65.75873	-1.0	0.010675
LFNG	88.81964	-1.5	3.09E-06
SELL	83.29203	-1.4	3.48E-05
CNPY4	81.3889	-1.3	0.00011
AMDHD2	78.04689	-1.2	0.001724
SMAD9	99.23549	-1.6	2.39E-07
NAT1	116.1777	-1.8	4.09E-09
RASGRF1	76.03037	-1.0	0.003093
FAAP24	73.61168	-1.0	0.007179
SAMD11	93.10092	-1.4	1.05E-05
FBLN2	24.2003	2.3	8.11E-07
INSL3	30.96152	1.1	0.020986
CHN2	81.06286	-1.2	0.00058
MAP1A	82.98662	-1.2	0.00042
CLDN2	129.3531	-2.0	5.51E-12
FSD1	189.9112	-2.6	3.84E-24
SIDT1	24.64466	2.0	7.84E-06
RRAD	32.36977	1.0	0.041669
DNAH6	110.8135	-1.7	2.5E-08
ZBED1	76.64138	-1.0	0.003986
MDH1B	154.6599	-2.2	1.37E-16
KCNQ4	33.52213	1.0	0.02482
PADI3	94.29835	-1.3	3.87E-05
DZANK1	107.8819	-1.5	6.12E-07
KLRC3	88.31337	-1.1	0.000721
BST2	96.01079	-1.3	6.75E-05
DRD1	96.8035	-1.3	4.83E-05
ISPD	213.1295	-2.6	4.38E-26
RAPGEF4	32.03715	1.4	0.001218
SPTLC3	34.08453	1.2	0.013655
NEURL1	35.41767	1.2	0.006637
GPR137C	93.62706	-1.1	0.000401
KLHL32	96.31834	-1.2	0.000302
HYAL3	95.26738	-1.2	0.000786
PIK3R3	105.1978	-1.3	9.35E-06
ZNF287	27.79207	2.6	6.95E-09
NEK11	89.4476	-1.0	0.002524
SLC9A2	107.0372	-1.3	2.46E-05
SERPINA10	37.05194	1.0	0.024694
TMEM170B	122.3554	-1.6	1.54E-07
SLC38A7	101.351	-1.2	0.000709
NOG	33.94789	1.7	0.000139

APPENDICES

ABHD1	39.44653	1.0	0.029538
MEX3B	96.26117	-1.1	0.000992
EFNA4	151.1231	-1.9	9.8E-13
WFDC3	38.35175	1.1	0.015137
LIMD2	93.85204	-1.0	0.003191
C9orf116	109.4855	-1.3	0.000121
PHF24	34.0414	1.8	1.68E-05
GATSL3	41.11985	1.0	0.022067
KIF17	38.68063	1.3	0.003272
GCOM1	40.9299	1.0	0.017319
TAGAP	41.31508	1.0	0.020082
MMP11	96.65565	-1.0	0.002882
KLK5	40.54163	1.2	0.005985
RIBC2	119.7132	-1.4	1.77E-06
ALAS2	34.50324	1.7	0.000155
CASC10	113.5726	-1.3	1.61E-05
PARK2	40.88006	1.2	0.004506
IKBKE	113.5559	-1.2	0.000102
CDHR5	38.31177	1.4	0.001924
ATL1	101.5271	-1.0	0.001288
SNX31	36.81204	1.8	1.37E-05
NLRP14	43.00983	1.1	0.010948
SMAD7	104.7201	-1.1	0.000772
BHLHE41	41.52745	1.3	0.001281
ABC7- 42404400C24.1	45.38344	1.0	0.020082
WDR63	106.0887	-1.0	0.00125
ABCA8	32.40796	2.7	7.46E-10
MUM1L1	219.2351	-2.3	9.67E-21
GPR182	38.72528	1.8	1.53E-05
ALK	42.34952	1.3	0.002209
RGL1	132.989	-1.4	1.01E-06
KRT81	41.47281	1.7	3.18E-05
ZBTB8B	113.8561	-1.0	0.001047
RAB15	113.6783	-1.1	0.001286
C1QTNF7	39.16735	1.7	0.000111
ACBD7	116.8658	-1.1	0.000546
HOMER2	123.2041	-1.2	3.28E-05
SLC3A1	49.37297	1.0	0.012936
KCNJ14	48.45283	1.2	0.004353
FAT4	121.0436	-1.1	0.000114
FAM132A	41.20316	2.1	3.43E-07
WNT7B	43.03391	1.7	6.3E-05
RAET1L	50.93223	1.0	0.015576
NAV2	46.39597	1.4	0.000323
ZSCAN5A	120.7406	-1.0	0.000415
ASIC4	46.40819	1.5	0.000331
CEP19	150.2333	-1.4	2.33E-07
TMED7-TICAM2	47.65665	1.5	0.000202
CNTN2	49.35693	1.3	0.001229
MAGEB17	49.95116	1.1	0.005629

## APPENDICES

GPM6B	117.3947	-1.0	0.001374
TXK	147.5801	-1.4	1.29E-06
SLC10A5	124.3872	-1.1	0.000294
GPR15	132.0326	-1.2	4.82E-05
CCDC107	51.17822	1.1	0.005919
PRSS37	49.79727	1.1	0.019598
PCDHAC2	128.2504	-1.1	0.000359
PRMT6	145.7917	-1.4	4.91E-07
DRAXIN	131.7276	-1.1	5.4E-05
FXYD3	137.0109	-1.2	4.07E-05
MMP28	56.65961	1.0	0.015049
AC026449.1	52.57876	1.2	0.001584
PBLD	148.1269	-1.3	8.89E-07
DNAJC12	125.8737	-1.0	0.000684
KIF5A	130.8106	-1.1	0.00027
METTL7A	242.9712	-2.2	2.78E-21
CDH17	46.01141	1.9	5.59E-06
IGSF9	152.6905	-1.4	6.82E-07
UNC79	48.24872	1.9	2.47E-06
ZNF136	149.247	-1.3	5.39E-06
LCMT2	160.4389	-1.4	1.48E-07
JOSD2	128.2295	-1.0	0.006282
ACCS	140.1864	-1.1	3.79E-05
CYB561D1	139.8391	-1.1	5E-05
AXIN2	178.9824	-1.6	4.25E-10
CCDC121	133.9158	-1.0	0.000395
ZNF738	151.6623	-1.3	1.08E-05
NFASC	49.12376	1.9	2.06E-06
SLC28A2	57.02088	1.1	0.008162
PRDM16	58.51278	1.1	0.003541
RBM46	50.76006	1.9	1.54E-06
C10orf55	52.894	1.7	1.22E-05
GGT1	60.79016	1.0	0.017847
RHOBTB2	131.6768	-1.0	0.001479
FAM179B	145.2754	-1.1	3.4E-05
BTC	200.8492	-1.7	7.73E-13
TNFSF13B	53.34811	1.5	0.000179
RDH16	50.9463	1.8	1.2E-05
SRXN1	64.53328	1.0	0.009608
PLEKHA4	144.8202	-1.1	9.35E-05
ELAC1	183.1137	-1.5	1.05E-09
MICALCL	55.75294	1.6	1.63E-05
RAPGEF3	57.56828	1.4	0.00031
PSKH1	144.2424	-1.0	0.00049
GATS	139.6396	-1.0	0.000632
ARL6	184.2863	-1.5	4.22E-09
PMEPA1	61.92076	1.3	0.000336
BANK1	145.091	-1.0	0.000539
IFIT3	168.8407	-1.3	1.04E-06
RMDN2	157.5378	-1.1	7.8E-05

## APPENDICES

NMI	155.4713	-1.0	0.000169
CEMIP	155.0994	-1.1	0.000104
SLC2A6	156.6606	-1.1	8.69E-05
SUN3	65.01531	1.3	0.000431
PKIA	163.8426	-1.1	0.000133
AK9	173.8057	-1.3	1.88E-06
RNASE1	57.92022	1.7	2.67E-05
MYOM1	71.82375	1.0	0.008381
MORN2	154.1649	-1.0	0.000352
METTL7B	216.7657	-1.6	2.32E-12
FAM111B	419.678	-2.7	2.38E-43
KIAA0825	157.5765	-1.0	0.000155
ZNF572	229.3073	-1.7	1.4E-11
DTX4	172.2298	-1.2	5.49E-06
HYI	69.10893	1.2	0.000748
DMGDH	66.37348	1.3	0.000357
GPR3	65.05543	1.6	2.04E-05
TMCC2	70.62149	1.1	0.002903
FKBP7	178.7278	-1.2	1.25E-06
MYB	195.5836	-1.4	3.25E-08
C1S	69.79735	1.2	0.000514
ZNF675	169.461	-1.1	4.54E-05
ZBED1	169.7526	-1.1	9.22E-05
EDN1	65.00069	1.6	5.21E-06
ENTPD2	72.93737	1.1	0.002624
KRCC1	299.658	-2.1	6.7E-22
CEP162	311.9547	-2.2	1.52E-23
KRT86	58.00447	2.5	2.86E-11
ZNF493	171.85	-1.1	5.75E-05
PPP1R32	71.40876	1.3	0.00014
GPRASP2	201.5325	-1.4	1.71E-08
C14orf79	176.1024	-1.1	7.67E-05
GALNT9	78.52007	1.0	0.005729
SGK1	175.7404	-1.1	3.55E-05
ZFPM1	80.20309	1.0	0.006221
ABCA1	236.2064	-1.6	7.59E-13
CFAP43	208.0568	-1.3	8.72E-08
MYZAP	76.53331	1.2	0.00035
ANKRD20A2	69.39443	1.6	8.01E-06
PLA2G4C	79.95908	1.1	0.001717
SSBP3	188.5736	-1.1	4.94E-06
NME1-NME2	76.17179	1.2	0.000981
DHFRL1	192.1827	-1.2	2.37E-06
IQCJ-SCHIP1	74.88509	1.3	0.000353
POU6F1	76.18147	1.3	0.000137
NUAK2	78.02043	1.3	0.000302
CREB5	82.06211	1.0	0.002979
TCTA	180.5376	-1.0	0.000272
KLF15	70.25509	1.9	4.18E-08
WDR31	195.3177	-1.1	5.05E-06

APPENDICES

KLRD1	76.98137	1.3	0.000743
SAMD9	793.3134	-3.4	1.36E-79
RBM44	72.65304	1.8	8.3E-07
RMI2	193.5227	-1.0	6.08E-05
ZNF75A	226.6405	-1.3	5.08E-09
HMCN1	416.6665	-2.4	4.87E-34
C22orf46	273.7236	-1.7	4.14E-15
ANGPTL1	85.58027	1.0	0.01437
RP11-11N7.5	87.90242	1.0	0.001612
HIST1H2BL	643.6692	-3.1	3.38E-55
ZNF585B	188.9274	-1.0	0.000244
FGL2	81.0152	1.2	0.002815
ZNF596	207.0021	-1.1	5.72E-06
TSPYL4	208.1899	-1.1	6.85E-06
NDRG4	235.9265	-1.4	1.49E-08
CPEB2	85.63337	1.2	0.00052
FKBPL	222.4466	-1.2	1.85E-07
RGS4	462.8084	-2.5	1.75E-34
AP4S1	227.5283	-1.3	3.71E-07
ANGPTL4	93.33311	1.0	0.002414
POTEI	94.69164	1.0	0.002566
PAPL	88.82315	1.3	0.0001
VWA1	249.7606	-1.4	4.21E-08
LONRF2	297.1007	-1.7	4.97E-14
HIST1H2BM	885.5106	-3.4	3.03E-67
CGNL1	206.5731	-1.0	2.39E-05
NIPSNAP3A	261.4171	-1.4	5E-11
DDR2	90.68355	1.3	0.000159
APOBEC3F	210.9779	-1.0	2.71E-05
HIST1H4H	490.5946	-2.5	1.58E-32
MEX3A	220.2171	-1.1	1E-05
SETMAR	286.4021	-1.5	1E-11
ZNF792	214.9111	-1.0	4.25E-05
ZNF469	96.36904	1.3	7.66E-05
MECOM	221.958	-1.0	2.07E-05
CMTM3	227.3606	-1.0	1.68E-05
ZNF341	102.3193	1.1	0.000471
ZNF112	281.7779	-1.4	1.95E-11
ZNF816	222.5971	-1.0	8.85E-05
BDH2	259.1089	-1.3	9.71E-09
SAMD3	98.84997	1.2	0.000297
CFAP58	97.63931	1.4	2.05E-05
ZNF860	227.341	-1.0	4.27E-05
C11orf95	317.9762	-1.6	2.35E-15
FRZB	91.41418	1.6	1.6E-05
FAIM	348.0076	-1.8	2.72E-19
KRT23	383.791	-2.0	1.31E-20
MSRB1	234.3034	-1.0	3.02E-05
ZNF552	275.5278	-1.4	2.92E-10
WIPF3	99.62052	1.3	5.16E-05

## APPENDICES

BBS12	229.1186	-1.0	6.37E-05
ATP6V1E2	252.4356	-1.1	8.74E-07
TRIM9	110.9082	1.0	0.001315
ARRDC4	489.9332	-2.3	1.75E-34
ELMOD1	114.0538	1.0	0.001797
IQGAP2	261.1676	-1.2	8.69E-08
FAM200A	313.201	-1.5	6.4E-12
MYD88	333.6199	-1.6	2.92E-14
GATA2	284.1651	-1.3	1.08E-09
CILP2	115.8772	1.0	0.004429
PDE2A	108.2159	1.3	1.51E-05
CPT2	244.1302	-1.0	3.26E-05
PGBD2	284.6247	-1.3	2.77E-09
GUCA1B	102.1288	1.6	1.12E-07
CLN6	272.5626	-1.2	2.84E-07
ALG1	285.4984	-1.2	5.18E-08
CCNE2	424.8075	-2.0	5.19E-25
FOXD1	112.4218	1.2	7.62E-05
GTF3C6	324.3074	-1.4	3.76E-10
IFIT2	327.1998	-1.5	6.78E-13
MLKL	250.1495	-1.0	2.47E-05
LMLN	267.361	-1.1	1.15E-06
MOCS3	280.2828	-1.2	3.04E-08
SLC37A2	108.5684	1.5	1.43E-06
MSS51	116.8556	1.1	0.000948
APH1B	275.3657	-1.1	6.61E-07
EFCAB11	276.0549	-1.1	3.03E-07
AC011043.1	253.7217	-1.0	2.11E-05
COMMD9	381.6269	-1.7	4.4E-19
ZSCAN16	262.7369	-1.0	1.31E-05
GBA	312.7152	-1.3	1.24E-10
BEST1	114.9516	1.3	1.06E-05
PPM1J	121.5797	1.1	0.000264
ZNF417	276.5252	-1.1	5.51E-07
TMSB15A	408.5582	-1.8	4.13E-19
TRIML2	338.5087	-1.5	7.96E-13
TEX9	353.1551	-1.6	7.02E-14
ARSD	269.1717	-1.0	1.21E-05
KCNQ1	128.8844	1.0	0.001139
DFNB31	121.9724	1.3	1.37E-05
ITPKA	121.4137	1.2	8.72E-05
TNXB	124.8189	1.0	0.001488
KRT7	122.4911	1.4	7.86E-06
CREB3L4	321.014	-1.3	5.59E-10
ZNF594	459.0687	-1.9	6.29E-23
IL6R	118.2677	1.6	1.38E-07
VGf	120.6351	1.5	1.52E-07
VPS33A	310.5986	-1.2	2.16E-08
CTGF	110.3387	2.1	1.14E-12
CHURC1	508.7106	-2.0	1.62E-28

APPENDICES

ADAM20	107.4104	1.3	0.008297
HINT2	301.6574	-1.1	3.25E-06
BORCS7	409.2822	-1.6	3.09E-16
TNFAIP3	130.5247	1.3	2.55E-06
ZNF559	391.8598	-1.5	9.03E-15
TRMO	319.5461	-1.1	9.65E-08
GINS3	375.9824	-1.4	9.5E-14
ZNF225	319.2837	-1.1	1.38E-07
NFIX	146.8576	1.0	0.000598
CCDC53	298.835	-1.0	6.41E-06
MGLL	136.3694	1.3	3E-06
HOMEZ	308.3102	-1.0	2.25E-06
TSPAN18	149.973	1.0	0.000462
PIGM	318.3438	-1.0	6.73E-07
ANKRD20A1	136.6392	1.3	7.02E-06
DYRK3	308.7869	-1.0	3.89E-06
NKD2	137.7136	1.3	9.72E-06
ZNF708	433.2134	-1.6	5.85E-18
ZNF480	485.0079	-1.8	6.56E-24
FAM122A	316.1113	-1.0	2.06E-06
SLC16A6	371.7871	-1.3	7.41E-11
ADAP1	150.228	1.0	0.000595
TOE1	327.5339	-1.1	4.67E-07
ZNF100	331.8575	-1.1	1.11E-07
ANKRD20A3	127.8682	1.7	4.22E-09
FAM173B	321.6428	-1.0	1.83E-06
IFI6	338.4478	-1.1	9E-08
PAM16	137.052	1.5	4.98E-08
C1orf116	153.4133	1.1	0.000134
IQCG	327.5062	-1.0	1.14E-06
SAMD13	350.9636	-1.1	7.36E-08
SUOX	355.8278	-1.1	8.77E-08
PEX11B	361.2118	-1.2	1.07E-08
TEX261	363.7026	-1.2	2.34E-08
ZNF525	413.8453	-1.4	2.25E-14
PXDC1	157.2054	1.1	7.58E-05
RASSF2	438.177	-1.5	1.26E-16
RILPL2	352.9556	-1.1	3.92E-08
KLRC2	358.3072	-1.1	1.4E-07
ADAMTS16	134.1447	1.9	7.85E-12
NCOA5	525.5352	-1.8	1.27E-23
FBN1	136.7387	1.8	8.75E-10
CD24	423.5784	-1.4	2.26E-12
SH2D5	147.3992	1.5	5.64E-08
CHRNA1	157.1255	1.2	1.42E-05
STYK1	377.0208	-1.1	2.78E-08
HR	373.2914	-1.2	3.01E-08
C12orf4	393.8428	-1.3	4.81E-10
WNT7A	118.9927	3.6	7.09E-28
CASP6	400.6185	-1.3	4.21E-11

## APPENDICES

PSD4	365.29	-1.1	1.96E-07
FPGT	412.4261	-1.3	1.19E-10
CSTA	171.1975	1.0	0.000122
IFIT1	414.1152	-1.3	4.58E-11
SPARC	953.4847	-2.7	4.23E-61
N4BP3	174.1324	1.0	0.000311
ARID3B	154.9823	1.5	1.64E-08
PPP1R13L	168.6122	1.1	2.68E-05
CA13	353.7272	-1.0	5.14E-06
ANKRD20A4	155.0125	1.4	3.77E-07
CHAC1	171.1772	1.0	0.000794
EID3	155.7652	1.4	1.2E-06
ERICH5	361.6943	-1.0	1.84E-06
SYNM	402.1271	-1.2	3.22E-09
PIK3AP1	478.5117	-1.5	1.7E-16
TOX2	160.4714	1.4	2.87E-08
ADAMTS17	168.8675	1.1	8.21E-05
HFE	370.885	-1.0	7.6E-07
TMEM158	152.1783	1.8	4.3E-11
CD22	152.2792	1.7	1.5E-10
ZBED8	461.797	-1.4	7.68E-15
WDR72	552.1757	-1.7	6.2E-21
FAM161A	410.155	-1.1	8.69E-08
YAE1D1	417.1698	-1.2	3.45E-10
PTP4A3	167.0829	1.4	1.13E-07
SHANK2	180.2981	1.0	4.86E-05
TRIM21	396.3435	-1.1	4.79E-08
PHTF1	420.473	-1.2	4.05E-09
MBNL3	564.6074	-1.7	1.58E-20
ANGPT2	535.8642	-1.6	2.83E-13
ZNF224	395.548	-1.0	3.77E-07
DYNC2H1	438.2311	-1.3	2.51E-09
ZBTB2	414.9853	-1.1	1.98E-08
LMF1	183.7054	1.1	8.35E-05
ZNF283	395.8471	-1.0	1.26E-06
CLCF1	191.0876	1.0	0.000107
ZNF629	399.3001	-1.0	1.07E-06
CFAP44	503.7659	-1.5	1.05E-13
KCNH2	173.5141	1.4	8.82E-08
SFXN2	415.1282	-1.1	2.11E-08
FAR2	409.2741	-1.0	9.34E-08
EFCAB7	409.8063	-1.0	4.56E-07
SPC25	420.0067	-1.1	9.7E-08
EVI5L	194.7766	1.0	3.35E-05
ZNF117	496.447	-1.4	1.6E-12
NRP1	166.4913	2.0	1.1E-13
TMEM98	511.0302	-1.4	9.29E-14
C1RL	434.8425	-1.1	4.76E-08
ZNF181	448.0431	-1.1	1.67E-08
DLGAP4	208.139	1.0	9.35E-05

APPENDICES

ZFP14	509.6933	-1.3	2.14E-12
IL15RA	188.7406	1.5	7.64E-09
ZNF620	479.237	-1.2	4.94E-11
GINS4	432.6684	-1.0	2.63E-07
C1orf216	513.8243	-1.3	2.54E-13
ZNF268	562.5426	-1.5	1.55E-16
ZNF765	496.9495	-1.2	5.34E-12
PBXIP1	539.7971	-1.4	2.23E-13
SPRY1	182.5239	1.8	1.11E-12
OSGIN1	211.9205	1.0	0.000217
ZBTB26	447.3249	-1.0	1.19E-06
ZSCAN31	518.8286	-1.3	2.33E-12
ARID3A	216.4227	1.1	1.9E-05
RBBP9	618.9114	-1.6	3.02E-21
FAHD1	459.1772	-1.0	3.01E-08
PRICKLE1	184.5349	1.9	2.83E-13
NT5M	192.6374	1.6	5.97E-10
KRTAP2-3	159.1892	3.4	1.47E-31
TMC7	215.0456	1.1	4.94E-06
GFOD1	221.4223	1.0	4.8E-05
IFT81	594.3284	-1.5	1.74E-15
MMRN2	204.7491	1.4	3.94E-09
MFSD1	500.213	-1.1	3.94E-09
ZNF587B	495.1835	-1.1	1.09E-09
SUSD3	221.1596	1.1	2.83E-06
NR4A1	216.2668	1.3	1.51E-05
RELB	222.5258	1.1	1.43E-06
IL12A	182.4039	2.4	2.19E-20
ZNF512	665.7281	-1.6	3.67E-20
ZBTB18	226.7783	1.1	1.56E-06
KIAA0101	677.7849	-1.6	1.08E-21
DDIT4L	1630.809	-3.1	9.5E-100
ELF4	229.5084	1.0	1.76E-05
ZNF551	509.0068	-1.1	1.94E-08
IFT22	522.6217	-1.1	6.99E-10
COL9A3	484.2637	-1.0	3.96E-07
MTURN	523.9755	-1.1	2.52E-10
TMEM52	240.0258	1.0	8.91E-05
CMIP	235.0567	1.0	1.81E-05
POLR3F	515.53	-1.1	2.42E-08
PDGFB	223.9736	1.3	1.14E-08
TTC26	516.2781	-1.1	2.5E-08
DIXDC1	537.0876	-1.1	2.4E-10
PLD6	230.283	1.3	4.31E-08
CA5B	244.2979	1.0	8.42E-06
ZNF180	567.7392	-1.2	8.43E-11
MAP3K12	496.1287	-1.0	4.35E-07
CACNB4	243.9819	1.0	3.46E-05
MCEE	237.5621	1.2	2.89E-07
CHMP4B	524.7487	-1.0	9.77E-09

APPENDICES

LZTFL1	737.363	-1.7	1.6E-20
LVRN	208.7527	1.9	9.93E-15
TMEM74B	254.7755	1.0	3.01E-05
TMEM19	578.6783	-1.2	1.96E-11
ZNF107	627.902	-1.4	1.37E-14
ZNF776	614.9707	-1.3	2.11E-12
HBEGF	248.1156	1.2	1.48E-07
SEZ6L2	257.7301	1.0	6.57E-05
TXNDC15	632.8452	-1.3	1.35E-13
TIMM17B	256.9687	1.0	5.42E-05
UPF3B	575.9541	-1.1	1.83E-08
SEMA6A	260.3248	1.0	4.19E-05
ATP6V0D1	612.8995	-1.2	4.51E-11
HKDC1	212.3265	2.3	2.03E-21
IRS2	233.1101	1.6	1.47E-12
GDAP1	762.0093	-1.6	1.47E-21
ZNF302	769.9448	-1.6	1.83E-19
PARP9	569.451	-1.1	2.32E-09
DNAJC15	660.0634	-1.3	1.63E-14
RHOF	262.769	1.1	4.38E-05
ULBP2	265.316	1.2	2.14E-06
FASTKD5	659.1679	-1.3	4.91E-15
DOCK6	263.8366	1.1	3.99E-07
HIST1H3E	557.8385	-1.0	5.64E-08
GABPB2	566.1723	-1.0	8.72E-08
XRCC2	791.1631	-1.6	1.73E-23
PTPRH	281.3009	1.0	6.19E-05
HYLS1	623.6803	-1.2	3.17E-11
SRM	276.1848	1.0	6.54E-05
TMEM57	630.5675	-1.2	1.1E-10
OVGP1	261.6134	1.3	1.56E-08
BTBD11	252.8561	1.5	2.72E-11
SAP30L	591.1647	-1.1	5.94E-09
IL1RAP	260.074	1.3	2.13E-09
TMEM40	261.6365	1.4	2.04E-09
PKD2	685.81	-1.3	4.83E-15
NXT2	591.3728	-1.0	2.78E-09
NPAS2	272.6745	1.1	1.65E-07
DNASE1L1	285.4263	1.0	0.000119
POGLUT1	808.9352	-1.6	3.23E-23
ARID5B	740.565	-1.4	4.96E-19
LAMA2	605.061	-1.1	1.07E-07
ITPRIP	285.9284	1.0	1.31E-06
TPK1	286.2628	1.1	3.28E-07
FAM210B	625.9008	-1.1	2.1E-09
PEAR1	283.2376	1.2	4.61E-08
SAMD5	881.194	-1.7	3.2E-22
KRT80	289.9038	1.1	1.75E-07
MID2	269.9013	1.5	1.35E-11
PKIB	281.8369	1.3	1.98E-09

APPENDICES

MEF2D	281.6026	1.4	4.92E-11
PLEKHB1	639.6914	-1.0	1.3E-08
HAS3	300.322	1.1	1.69E-07
ZP3	306.0772	1.1	6.73E-07
LCN2	302.4202	1.2	1.06E-08
KCNG1	303.3797	1.2	3.11E-07
RBM4B	696.7943	-1.1	4.24E-11
DOT1L	321.3181	1.0	5.21E-06
C6orf1	285	1.6	1.3E-13
ZYX	308.9868	1.2	1.96E-06
SPTBN2	319.8901	1.1	7.63E-07
TAF9B	708.7209	-1.1	5.64E-10
HOXB7	805.699	-1.3	1.06E-15
C1orf131	914.4495	-1.6	3.8E-24
FIBCD1	328.7191	1.0	1.33E-05
POPDC3	310.2778	1.4	1.58E-10
ZNF780B	778.8151	-1.2	9.38E-11
NR1D1	306.6459	1.4	1.6E-10
PPARGC1B	299.5613	1.6	1.26E-13
TRHDE	293.0112	1.7	8.37E-16
ANTXR2	335.1494	1.0	4.02E-06
HIST1H3A	1289.104	-2.1	3.15E-30
B4GALT6	329.0831	1.1	3.99E-07
ZNF780A	1016.8	-1.7	6.28E-23
SESN2	334.7834	1.1	1.17E-07
CETN2	715.3161	-1.0	2.61E-08
BCL9L	325.9927	1.3	5.96E-08
CCDC82	762.1968	-1.1	2.51E-09
PHF23	834.019	-1.3	2.05E-15
IFT88	745.0919	-1.0	1.83E-08
ZBED2	1066.758	-1.7	1.15E-30
TBC1D2	346.9296	1.1	7.46E-08
DCLK1	339.0862	1.3	2.52E-10
LYRM2	1048.266	-1.7	8.18E-28
SLC35F3	349.6792	1.1	3.81E-08
RIN1	355.3546	1.1	9.54E-08
LATS2	366.8708	1.0	2.57E-06
MAP2K3	350.7698	1.1	1.97E-07
PC	352.0036	1.2	7.95E-07
IFT80	849.7914	-1.2	9.98E-11
GINS2	1054.269	-1.6	1.22E-26
DPM3	373.5316	1.0	6.96E-06
GCNT3	322.5273	1.8	1.31E-18
C15orf61	368.0333	1.1	2.72E-08
ZNF189	846.7638	-1.1	1.07E-12
SYNE3	312.7153	2.1	3.12E-23
ARG2	368.3632	1.2	1.15E-09
ECSIT	386.6814	1.0	6.37E-06
RPGRIP1L	920.046	-1.3	2.13E-15
ICAM5	336.397	1.7	4.24E-17

APPENDICES

TFE3	396.109	1.0	1.38E-06
MEGF6	393.0541	1.0	2.55E-05
HSPB11	910.2258	-1.2	2.23E-14
WWC3	374.7813	1.3	6.93E-11
CTIF	391.4723	1.2	8.16E-10
SRSF8	1087.825	-1.5	7.75E-24
EPM2AIP1	912.7302	-1.2	2.46E-10
DHFR	1653.904	-2.2	4.81E-48
PARVA	842.3138	-1.0	2.57E-09
SGCB	954.9348	-1.2	3.04E-13
QPCTL	398.8618	1.2	3.5E-07
LIPG	409.8159	1.1	2.64E-08
IGSF8	418.2883	1.0	6.5E-06
STK40	422.7129	1.0	3.22E-07
STAT6	952.767	-1.2	7.63E-14
C5orf51	910.2814	-1.1	2.51E-11
TLE1	436.7335	1.0	1.2E-07
GRAMD1B	426.9309	1.1	3.76E-08
ZNF84	986.4617	-1.2	6.1E-13
COMMD4	1008.868	-1.2	5.69E-13
ANKRD22	359.0392	2.2	1.41E-28
HES4	414.455	1.4	1.06E-12
JAG2	445.708	1.0	8.24E-06
ETV1	1027.307	-1.2	3.93E-13
CCBL1	411.4696	1.5	1.02E-11
ABLIM3	455.7846	1.1	9.54E-08
ARL14EPL	463.1142	1.0	5.81E-07
MAFF	428.446	1.4	7.34E-13
ZNF436	980.8312	-1.1	9.97E-12
C10orf54	443.1476	1.3	4.09E-11
ZNF333	459.5543	1.1	5.08E-09
MARCKSL1	1091.769	-1.2	1.98E-14
CHML	1557.77	-1.9	3.84E-30
PROSER2	437.0619	1.5	1.02E-14
FBXO6	454.3843	1.3	5.49E-11
UTP14A	1195.094	-1.4	1.2E-20
KLF4	386.0305	2.5	6.28E-36
ARTN	379.1917	2.7	3.66E-40
DARS2	1069.106	-1.1	1.65E-12
ANKRD29	408.1463	2.1	3.84E-24
LRRCC1	1078.694	-1.1	8.22E-10
HSPG2	478.2468	1.1	1.08E-07
TTLL7	1162.596	-1.2	4.7E-11
LEPROT	1313.062	-1.5	2.49E-20
RRAS	503.7524	1.1	1.64E-07
FAM20A	458.7425	1.5	9.13E-13
TMEM14A	1085.995	-1.1	2.57E-12
KIF1BP	1112.052	-1.1	2.79E-10
CIPC	1087.414	-1.0	8.21E-11
LURAP1L	408.7347	2.7	6.97E-40

## APPENDICES

ITGB8	1224.513	-1.3	5.72E-16
ERN1	491.0308	1.3	1.24E-13
LINC00116	493.8729	1.3	9.48E-10
ZNF516	517.1825	1.1	5.64E-08
LEMD1	521.7851	1.1	7.11E-09
CLSPN	1084.645	-1.0	8.62E-10
RNF19B	530.2549	1.1	2.08E-09
PDLIM3	498.7135	1.4	6.13E-14
GALNT5	493.633	1.5	3.09E-13
GEN1	1188.771	-1.1	8.93E-12
ABI3BP	426.0774	1.7	1.79E-05
IFIT5	1229.49	-1.2	3.75E-15
HIST1H3J	2583.661	-2.5	1.45E-47
TRAK2	1341.022	-1.4	8.08E-21
TRMT1L	1160.269	-1.1	5.67E-12
GAD1	544.2007	1.1	5.95E-10
ESCO2	1444.017	-1.5	2.55E-20
ETS1	468.3031	2.1	2.75E-27
EP400	555.1942	1.0	3.94E-06
SYDE2	512.9865	1.5	3.71E-16
TTC7A	575.3877	1.0	3.71E-08
VSNL1	1165.097	-1.0	3.82E-11
ADA	577.4002	1.0	3.91E-07
SEMA7A	480.0328	2.0	1.3E-26
SIPA1L3	512.947	1.5	9.48E-17
DNAJC22	1183.85	-1.0	1.23E-11
ZFP62	1236.619	-1.1	3.47E-12
ZNF714	1182.374	-1.0	1.12E-09
JPH1	575.4063	1.0	7.43E-09
GAS6	551.2352	1.2	1.17E-09
ANKRD33B	532.4843	1.5	1.67E-17
MICAL2	567.6499	1.2	1.14E-11
HIST1H2BF	1520.846	-1.4	1.16E-15
DCLRE1A	1244.501	-1.0	6.04E-10
USP49	596.8091	1.0	1.91E-08
FAM111A	2148.566	-2.0	4.54E-41
ZNF12	1592.708	-1.5	3.14E-24
NDUFS7	578.4148	1.2	1.03E-08
RNF43	1462.064	-1.3	5.49E-20
TRIM59	1279.841	-1.0	1.06E-10
RGS5	3594.092	-2.8	2.11E-79
BNIP1	617.78	1.0	8.62E-09
KLHL42	1445.315	-1.2	2.38E-15
SLC12A4	631.7455	1.0	3.35E-07
PRKCA	552.8132	1.6	1.15E-20
PHF1	621.6154	1.0	2.09E-08
SERPINA5	608.796	1.2	2.72E-11
ASF1A	1365.683	-1.1	2.23E-11
PIM1	534.8893	2.0	1.4E-24
ST3GAL1	597.408	1.3	6.47E-14

APPENDICES

ADI1	1337.638	-1.0	1.2E-11
PLPP3	618.217	1.2	9.5E-12
ZBTB1	1461.188	-1.2	7.59E-15
AVPI1	600.8422	1.3	3.84E-10
SKP2	1479.487	-1.2	1.56E-16
POP1	1435.687	-1.1	2.4E-15
EFHD2	652.0039	1.1	2.88E-09
ZNF195	1396.143	-1.1	5.19E-13
SYNJ2BP	1764.14	-1.5	7.83E-22
PRDM10	630.212	1.2	3.51E-12
HIST3H2BB	1492.35	-1.2	2.72E-12
PTER	1345.856	-1.0	1.31E-10
TM2D2	1398.194	-1.0	2.25E-12
THSD4	601.8959	1.5	8.66E-19
MKX	1834.789	-1.6	3.23E-27
BRCA2	1432.498	-1.1	4.58E-11
SBNO2	594.4359	1.6	4.98E-19
SEMA4B	632.4659	1.3	4.17E-13
SES3	1456.945	-1.1	3.53E-11
C19orf33	597.8128	1.4	0.000315
TP53INP1	1576.211	-1.2	5.69E-13
HIST1H2AB	1783.713	-1.5	3.61E-18
PPM1K	631.9297	1.4	4.96E-16
ALS2CL	623.7792	1.4	1.27E-15
KIAA0196	2013.042	-1.7	3.6E-34
SLC16A14	635.5637	1.4	4.81E-17
ID3	2492.167	-2.1	2.49E-45
TRIM16L	682.9443	1.1	4.65E-11
RELA	709.7392	1.0	3.17E-08
FAM83G	691.0294	1.1	2.02E-08
PER1	592.3661	1.9	3.39E-20
LOXL2	668.9717	1.2	1.19E-11
COL13A1	585.2131	2.1	3.6E-34
ETS2	1462.069	-1.0	1.37E-11
SLC25A46	1632.825	-1.2	1.24E-15
PDGFA	660.1716	1.5	1.98E-18
ZNF33B	1965.911	-1.5	2.08E-23
IFFO2	597.6823	2.2	1.77E-35
SMG9	699.3952	1.2	3.58E-13
PLK3	661.0982	1.5	8.93E-21
KIAA1143	1837.97	-1.4	3.51E-21
ATF3	647.243	1.7	1.45E-22
ACADM	1517.964	-1.0	1.06E-10
ODF2L	1553.588	-1.0	1.95E-08
AFAP1	769.2534	1.0	1.37E-08
LPCAT4	733.7635	1.2	1.3E-13
CYP4F11	775.7863	1.0	1.8E-09
CTU2	773.6584	1.0	5.11E-07
ARHGEF28	769.4234	1.1	3.01E-10
SPPL2A	1644.988	-1.1	4.03E-12

APPENDICES

ID2	2638.048	-1.9	2.43E-46
STK38L	1594.654	-1.0	6.9E-09
BRIP1	1713.331	-1.1	9.97E-13
IGFBP6	790.6405	1.0	3.83E-08
ARFGEF3	696.6789	1.6	5.53E-22
TRIM8	753.9787	1.2	1.1E-13
TMEM200A	713.1594	1.5	3.22E-19
TGM2	796.7303	1.0	7.57E-08
ANKMY2	1622.021	-1.0	4.96E-12
PDE4B	4481.502	-2.8	2.1E-110
GADD45B	711.1339	1.6	1.4E-19
CDC42EP1	792.8252	1.1	6.71E-08
PCMTD2	1765.322	-1.1	8.59E-14
RREB1	747.5356	1.3	1.18E-14
ADAM19	757.258	1.3	6.76E-16
DHRS3	815.9385	1.0	8.93E-09
DENND3	746.8001	1.4	1.26E-16
C11orf68	700.5895	1.8	2.16E-24
SAMD4A	772.0653	1.3	2.52E-16
SREK1IP1	1668.17	-1.0	7.38E-11
POLRMT	809.6695	1.2	1.05E-10
ZFP36	687.8062	2.1	1.07E-31
BRCA1	1770.562	-1.0	1.57E-13
FLNC	782.1872	1.3	1.99E-11
GEM	862.4542	1.0	3.64E-09
HIST1H4A	1847.104	-1.1	8.98E-10
MAEA	1844.183	-1.1	6.6E-13
ZNF37A	1765.334	-1.0	1.13E-10
KIFC3	787.7909	1.4	5.83E-17
PIK3C3	1726.137	-1.0	2.9E-11
BMP4	2328.848	-1.6	3.1E-27
EIF4EBP2	1893.183	-1.2	1.77E-15
CALB2	652.8907	2.8	1.85E-56
ASAP2	856.5111	1.0	1.5E-10
MCM5	1759.64	-1.0	5.59E-08
HK2	768.7622	1.6	4.71E-24
ENC1	1799.97	-1.0	6.62E-13
CHTF8	1870.74	-1.1	1.51E-12
FLYWCH1	798.5693	1.4	1.08E-13
SEMA3A	1924.514	-1.1	5.22E-14
RAD23A	874.1151	1.1	3.18E-11
TMEM67	1894.422	-1.1	1.22E-12
PIK3R1	1900.873	-1.1	9.25E-14
GRB7	872.6722	1.2	6.4E-12
NOL6	898.5322	1.1	8.8E-09
TNFRSF1A	893.9051	1.1	4.09E-11
TSC22D3	855.2761	1.3	1.97E-14
PHLDA2	855.2509	1.4	5.18E-18
PTPRU	892.4061	1.2	1.93E-09
DGKD	897.3384	1.2	5.31E-11

## APPENDICES

ZWINT	1947.131	-1.0	3.54E-13
FOSL1	736.508	2.6	6.71E-53
FEN1	2587.535	-1.5	1.27E-26
ABCA2	966.17	1.0	1.89E-07
HNRNPM	2845.279	-1.7	2.84E-40
PHKA1	971.441	1.0	1.18E-09
PTPRM	948.657	1.1	1.13E-11
SESTD1	2193.176	-1.2	6.27E-15
BIRC3	891.4717	1.5	9.52E-18
BHLHE40	895.7223	1.5	9.52E-20
KIAA1671	969.4134	1.1	2.52E-11
HNRNPH2	2421.801	-1.3	8.49E-23
MRFAP1L1	2085.887	-1.0	5.54E-13
UPP1	837.7632	2.1	1.58E-32
SFT2D2	2502.399	-1.3	6.28E-23
GJB3	844.9668	2.4	2.94E-44
NEK6	1071.774	1.0	2.75E-09
CRABP2	2189.824	-1.0	3.91E-12
TARDBP	2288.238	-1.1	2.86E-15
THBS1	980.8838	1.5	2.46E-18
KRT15	852.8576	2.5	6.22E-40
EPAS1	1042.453	1.3	2.6E-16
VMA21	2815.884	-1.4	1.33E-22
IRF2BP2	1001.857	1.5	3.66E-22
PRSS3	979.8061	1.6	3.11E-21
DBP	1037.843	1.3	2.56E-17
ZC3H6	1133.306	1.0	8.56E-11
PITPNC1	1100.77	1.1	5.17E-14
GADD45A	1093.135	1.2	2.61E-14
FKBP14	1116.06	1.1	3.45E-10
MCM2	2289.59	-1.0	4.92E-09
FGF19	1120.14	1.1	1.98E-13
NRIP1	2375.091	-1.0	9.38E-12
NFKB2	1139.954	1.1	8.21E-11
HPCAL1	1061.439	1.5	6.14E-17
MED8	1180.453	1.0	2.6E-09
PXN	1184.172	1.0	2.79E-09
FAM122B	2807.466	-1.3	2.1E-19
AMOTL2	1195.388	1.0	1.9E-09
ELK3	1190.751	1.0	1.94E-10
MT1E	2882.447	-1.3	1.08E-13
UNC13A	1088.763	1.5	9.48E-20
TANK	2396.114	-1.0	1.7E-10
GPC1	1162.606	1.2	4.41E-11
BDNF	4192.892	-2.0	3.2E-54
ELMOD2	2784.119	-1.2	2.59E-15
AMN1	1142.435	1.4	5.13E-20
CIRBP	2875.503	-1.3	6.26E-19
SERTAD2	1084.33	1.6	4.26E-25
MYO18A	1245.664	1.0	4.3E-09

APPENDICES

BNIP3L	2544.098	-1.0	8.97E-12
ATP6V1C1	3173.261	-1.4	9.39E-23
MSH2	2816.571	-1.1	1.05E-15
ZNF704	2836.294	-1.2	1.04E-16
TRIB3	1178.482	1.5	2.84E-22
L3MBTL3	2887.817	-1.2	6.57E-16
TUBA1A	3020.522	-1.2	2.11E-14
CCDC85B	1152.975	1.9	2.21E-32
DYNLL1	2847.892	-1.1	1.13E-15
LAMB3	1169.943	1.8	2.96E-29
SLC7A1	1305.927	1.2	5.23E-14
SEC24D	1288.779	1.4	2.54E-22
HIST1H2AI	3553.43	-1.4	9.48E-17
PPARG	1233.211	1.8	2.54E-32
CDR2	1396.307	1.1	1.17E-14
DENND5B	3072.135	-1.1	6.17E-14
MAN1A1	4290.687	-1.7	1.99E-31
EHD4	1459.663	1.0	2.57E-11
UQCC2	1473.963	1.0	2.92E-10
CLMN	1407.996	1.2	5.72E-16
VEGFA	1460.957	1.1	1.67E-14
GPAT3	1279.998	1.9	6.82E-36
HMGB3	3131.983	-1.0	7.15E-13
MAT2B	3076.774	-1.0	1.04E-12
FXVD5	1503.07	1.1	2.6E-13
SFN	1480.763	1.2	8.37E-12
SAFB2	1567.625	1.0	6.94E-11
FTH1	1558.141	1.0	1.23E-11
TNFRSF10A	1572.065	1.0	1.41E-10
PHF6	3691.983	-1.3	6.59E-20
SERPINE1	1156.708	3.5	4.15E-98
RBCK1	1505.28	1.2	4.69E-16
PVR	1518.065	1.2	3.07E-15
ACSS2	1560.164	1.1	6.12E-15
GOLGA2	1596.272	1.1	4.23E-13
DDIT4	1514.885	1.3	1.55E-18
ZNF518B	3509.815	-1.1	6.29E-16
TUBE1	1639.225	1.1	1.24E-12
TK1	3489.457	-1.0	2.71E-07
EML2	1500.472	1.7	3.67E-26
BAIAP2L1	1698.029	1.1	8.26E-15
DRAP1	1668.791	1.2	5.7E-15
MCM6	3678.824	-1.1	1.77E-16
SOX4	4847.933	-1.6	1.25E-34
TINAGL1	1761.863	1.0	3.64E-12
SMAD3	1559.089	1.7	5.62E-32
MYO1E	1808.108	1.0	1.59E-11
MORC4	3603.901	-1.0	2.31E-12
EIF4EBP1	1805.538	1.1	1.18E-11
LAMC2	1706.906	1.5	1.44E-24

APPENDICES

NPC1	1845.342	1.1	1.22E-14
ARHGEF2	1702.354	1.5	1.81E-23
STC2	1521.697	2.3	2.07E-57
NAV3	1653.629	1.7	1.91E-30
SSH1	1799.319	1.2	5.9E-18
RBM3	4118.45	-1.1	1.71E-16
FGD6	1799.825	1.4	1.21E-21
CPA4	1411.892	3.8	3.8E-123
INPP4B	3962.255	-1.0	1.46E-11
RHOBTB3	4099.791	-1.0	3.3E-12
CTR9	4354.253	-1.1	5.3E-18
MLPH	1785.154	1.5	4.12E-29
BCAR3	1650.351	2.2	1.7E-55
NDUFS8	2052.698	1.0	5.64E-08
SRSF2	4475.598	-1.1	1.47E-15
ARRDC3	1935.93	1.4	2.4E-20
MKNK2	1999.964	1.2	5.89E-13
THRAP3	4530.026	-1.1	9.16E-18
DVL1	2089.373	1.0	2.16E-09
NASP	4601.705	-1.1	2.79E-18
PLAUR	1944.543	1.5	2.92E-23
HIST1H3H	4724.299	-1.1	7.86E-10
AXL	1941.414	1.6	7.72E-28
PFDN2	2026.272	1.4	4.82E-18
KIF18A	4577.871	-1.0	2.4E-14
CHPF	2167.793	1.1	9.15E-10
SLC9A7	2235.674	1.0	1.17E-11
OBFC1	2297.646	1.1	4.24E-15
ABL2	2105.246	1.7	5.01E-38
GMFB	4922.926	-1.0	6.34E-11
ITPR3	2428.393	1.0	1.52E-11
ANKRD36C	5382.207	-1.0	0.003427
ERCC1	2491.559	1.0	1.42E-08
TNFRSF12A	2297.9	1.4	1.06E-20
NDRG1	2408.073	1.4	2.5E-21
DDIT3	1874.432	3.7	6.4E-134
NF2	2521.766	1.2	4.78E-16
PYGB	2459.782	1.4	3.13E-18
TGFA	2704.764	1.0	3.39E-13
SRSF6	7217.133	-1.5	4.99E-29
MCM4	6129.118	-1.1	7.41E-17
LIF	2504.247	1.6	3.96E-27
CAPRIN2	2758.681	1.2	3.06E-13
NT5E	2784.338	1.2	2.17E-20
MTHFD1L	2971.858	1.0	1.47E-12
PPP3CA	6318.501	-1.1	2.16E-15
TRIM2	5942.154	-1.0	9.45E-13
DUSP6	6445.081	-1.0	1.76E-14
F3	2609.415	2.1	1.78E-43
FHL2	2837.923	1.6	1.09E-30

APPENDICES

PTPRF	3197.795	1.1	9.81E-13
EHF	6709.511	-1.0	5.63E-14
CLIP4	3200.079	1.2	3.11E-16
ABCC2	10529.99	-1.8	3.37E-48
LAMC1	3398.467	1.1	7.26E-15
ITGA2	7244.616	-1.1	1.22E-14
YOD1	3139.139	1.5	2.16E-24
SRSF3	9018.447	-1.5	5.26E-29
PFKP	3523.071	1.0	1.76E-10
CPOX	8295.012	-1.3	8.24E-23
DNAJA1	8209.597	-1.3	3.13E-23
RBMX	8168.178	-1.3	2.81E-21
SFPQ	7674.197	-1.1	1.25E-16
AGPAT5	8979.604	-1.4	6.59E-28
PAQR5	3205.361	1.7	1.79E-40
GAN	3712.053	1.0	7.97E-15
BCLAF1	7920.202	-1.1	1.56E-13
CDKN1A	3690.518	1.3	2.33E-20
SLC7A5	3661.787	1.3	1E-14
TMED4	3981.964	1.0	4.47E-12
EMP1	3280.412	2.0	6.1E-52
SDC4	3950.541	1.0	3.77E-13
MSMO1	3852.832	1.1	1.07E-12
ABLIM1	8976.699	-1.0	1.54E-15
TFRC	8983.463	-1.0	2.16E-15
CDCP1	4298.425	1.2	1.36E-21
PLEC	4468.576	1.1	5.55E-13
CD55	4071.437	1.8	2.84E-40
SLC4A7	4574.223	1.1	1.22E-15
FLNB	4699.945	1.1	3.14E-14
PSD3	4883.374	1.0	3.85E-13
PLAU	3954.397	2.3	3.64E-59
DHX9	10818.75	-1.1	4.35E-19
S100A4	11908.42	-1.3	1.06E-26
ITGB4	4679.186	1.5	5.64E-21
PRKACB	13229.7	-1.4	3.88E-26
AREG	5389.849	1.0	1.87E-13
ITGA3	5205.212	1.3	2.83E-20
YARS	5752.507	1.1	1.35E-18
STMN1	13787.24	-1.1	5.83E-17
ARHGAP18	15294.21	-1.3	1.49E-22
CTNNAL1	6577.904	1.0	6.19E-13
EPHA2	5756.49	2.1	3.7E-37
MYH9	7121.807	1.1	3.25E-15
AARS	6856.461	1.4	8.63E-26
ACTN4	7086.065	1.2	3.75E-13
ASNS	7815.144	1.1	2.02E-18
GDF15	6528.496	2.1	9.89E-69
PHLDB2	25206.2	-1.7	1.78E-36
DUSP5	7113.058	2.6	9.06E-92

## APPENDICES

FLNA	8869.419	1.1	2.5E-11
GPRC5A	8977.003	1.4	8.15E-28
AP3S1	10357.91	1.0	5.02E-12
CYB5B	25733.19	-1.2	9.82E-23
ATG12	10971.04	1.5	8.67E-27
KRT19	13455.47	1.1	1.48E-16
ALDH1A3	14211.48	1.5	3.49E-32
HMGA1	14205.19	1.7	3.31E-28
DCBLD2	42850.52	-1.3	5.6E-26
KITLG	56064.37	-1.7	5.78E-39
ACTB	19413.07	1.1	5.57E-17
TXNRD1	22255.61	1.1	1.02E-18
ASPH	23626.54	1.2	1.96E-20
FTL	32730.5	1.3	7.13E-22
ACTG1	88557.5	1.2	1.81E-19

APPENDICES

Appendix 3. Differentially expressed miRNAs associated with 2.5 mM metformin treatment of HCT116 cells and compared with control medium.

miRNA ID	baseMean	log2FoldChange	padj
hsa-miR-208a-3p	73.3136819	5.82723	1.06E-09
hsa-miR-3929	38.61256622	4.53944	2.76E-14
hsa-miR-4745-5p	50.08204789	2.10424	0.000695
hsa-miR-505-5p	52.03702462	1.78444	0.002752
hsa-miR-4697-3p	62.5133586	2.01915	4.04E-06
hsa-miR-6777-3p	55.18537861	1.74001	0.002464
hsa-miR-3605-5p	89.65928108	2.44312	7.21E-06
hsa-miR-205-5p	59.8077181	1.22811	0.00221
hsa-miR-556-3p	31.38624413	-1.64359	0.021145
hsa-miR-590-5p	30.79298553	-1.77153	0.00756
hsa-miR-3127-5p	73.49032637	1.35624	0.003219
hsa-miR-4521	32.20065365	-3.04475	5.47E-05
hsa-miR-153-5p	38.85975351	-1.03091	0.035757
hsa-miR-34a-3p	39.03989005	-1.29475	0.023571
hsa-miR-760	83.48021373	1.14324	0.009027
hsa-miR-937-3p	171.5681013	2.39981	0.000137
hsa-miR-181b-3p	51.4406631	-1.32179	0.008122
hsa-miR-200c-5p	52.94658636	-1.80796	0.002993
hsa-miR-2110	148.233555	1.69629	3.21E-05
hsa-miR-195-5p	63.94107141	-1.06542	0.010257
hsa-miR-92a-1-5p	144.3451494	1.44668	0.00987
hsa-miR-3605-3p	270.5497657	2.72002	4.76E-08
hsa-miR-573	66.80857659	-1.48428	0.012844
hsa-miR-10399-5p	61.03026655	-2.01691	0.022256
hsa-miR-940	63.93949325	-1.60369	0.000542
hsa-miR-2116-3p	239.047622	2.13005	4.09E-05
hsa-miR-328-3p	152.9984195	0.95395	0.011753
hsa-miR-3613-5p	80.54619371	-1.88519	0.003957
hsa-miR-33a-5p	88.29136726	-1.24428	0.002825
hsa-let-7a-2-3p	99.83078343	-1.13423	0.005802
hsa-miR-766-3p	102.5086198	-1.53796	0.017428
hsa-miR-1247-3p	217.2930922	1.29304	0.027556
hsa-miR-653-5p	111.8150325	-1.26225	0.001066
hsa-miR-142-5p	126.2221281	-1.32279	0.000813
hsa-miR-4746-5p	243.326927	1.06466	0.007982
hsa-miR-1255a	275.0093848	1.35442	0.002451
hsa-miR-1247-5p	284.5341227	1.36378	0.000903
hsa-miR-326	143.0115037	-1.15424	0.001776
hsa-miR-26a-2-3p	127.1739664	-1.72075	1.28E-05
hsa-miR-32-3p	135.9986887	-1.70072	0.000667
hsa-miR-589-3p	393.99799	1.64094	4.45E-09
hsa-miR-330-3p	318.8988635	0.95983	0.001748

APPENDICES

hsa-miR-27b-5p	188.1973769	-1.02853	0.001147
hsa-miR-15b-3p	176.8092461	-1.37977	0.032711
hsa-miR-548e-3p	200.0625367	-0.95306	0.01193
hsa-miR-185-5p	217.0828786	-1.07920	0.051289
hsa-miR-1910-5p	1559.816902	3.07735	8.85E-06
hsa-miR-26b-3p	623.2633894	1.22660	0.008106
hsa-miR-7-1-3p	330.3205048	-1.04282	0.005812
hsa-miR-590-3p	369.0630055	-1.07910	0.049151
hsa-miR-222-5p	376.8965146	-1.10616	0.001789
hsa-miR-1468-5p	767.4817277	1.05943	0.005627
hsa-miR-132-3p	774.6723011	0.94739	0.008842
hsa-miR-374a-5p	509.1246247	-1.13161	0.012742
hsa-miR-342-3p	1217.363382	1.04540	0.028227
hsa-miR-671-3p	1461.694644	1.22974	0.003889
hsa-miR-744-5p	4402.888443	2.73273	7.43E-06
hsa-miR-31-3p	1074.742732	-1.83449	0.000187
hsa-miR-877-5p	6264.572689	3.10131	3.89E-05
hsa-miR-106b-5p	1597.856413	-1.01234	0.004034
hsa-miR-34a-5p	1769.185165	-1.27267	0.019499
hsa-miR-149-5p	3489.962567	1.20604	0.002663
hsa-miR-374a-3p	1842.556676	-1.19731	0.008495
hsa-miR-340-5p	3419.485341	-1.11461	0.00365
hsa-miR-345-5p	4666.596616	-1.19411	0.000124
hsa-miR-100-3p	5020.647696	-1.36659	0.000205
hsa-miR-429	5424.282711	-1.20078	0.002644
hsa-miR-92a-3p	28256.4432	1.33214	3.90E-07
hsa-miR-222-3p	158962.1942	1.13135	0.000223

APPENDICES

**Appendix 4. Predicted and validated miRNA-mRNA targets showing anticorrelation in expression changes associated with 2.5 mM metformin treatment of CRC cells.**

<b>miRNA</b>	<b>Target gene</b>
hsa-let-7a-2-3p	MYO1E
hsa-let-7a-2-3p	NEK6
hsa-let-7a-2-3p	FKBP14
hsa-let-7a-2-3p	NPAS2
hsa-let-7a-2-3p	IRS2
hsa-let-7a-2-3p	TRHDE
hsa-miR-100-3p	BHLHE41
hsa-miR-100-3p	BCAR3
hsa-miR-106b-5p	PFKP
hsa-miR-106b-5p	ELK3
hsa-miR-106b-5p	NPAS2
hsa-miR-106b-5p	MKNK2
hsa-miR-106b-5p	F3
hsa-miR-132-3p	MYB
hsa-miR-132-3p	PIK3R3
hsa-miR-132-3p	ASF1A
hsa-miR-132-3p	GMFB
hsa-miR-142-5p	TRIM9
hsa-miR-142-5p	ACTN4
hsa-miR-142-5p	EPAS1
hsa-miR-142-5p	ARRDC3
hsa-miR-142-5p	IRS2
hsa-miR-1468-5p	SRSF2
hsa-miR-149-5p	EFNA4
hsa-miR-149-5p	MYD88
hsa-miR-149-5p	ZBTB2
hsa-miR-153-5p	USP49
hsa-miR-153-5p	ACTB
hsa-miR-153-5p	PPM1K
hsa-miR-153-5p	NRP1
hsa-miR-181b-3p	FHL2
hsa-miR-185-5p	VEGFA
hsa-miR-1910-5p	DHFR
hsa-miR-1910-5p	CXCR4
hsa-miR-1910-5p	DNAJA1
hsa-miR-1910-5p	ZBTB2
hsa-miR-1910-5p	KIF5A
hsa-miR-1910-5p	DYNLL1
hsa-miR-1910-5p	HFE
hsa-miR-195-5p	DVL1
hsa-miR-195-5p	VEGFA
hsa-miR-195-5p	NF2
hsa-miR-195-5p	ABL2

## APPENDICES

hsa-miR-195-5p	HMGA1
hsa-miR-200c-5p	TGFA
hsa-miR-205-5p	DHFR
hsa-miR-2110	DHFR
hsa-miR-2110	VMA21
hsa-miR-2110	PIK3R3
hsa-miR-2110	SFPQ
hsa-miR-2110	PKIA
hsa-miR-2110	KIF5A
hsa-miR-2110	TRIM21
hsa-miR-2110	HFE
hsa-miR-2116-3p	MYB
hsa-miR-2116-3p	C1orf216
hsa-miR-2116-3p	HNRNPH2
hsa-miR-2116-3p	SEMA3A
hsa-miR-222-3p	TUBA1A
hsa-miR-222-3p	STMN1
hsa-miR-222-5p	ASAP2
hsa-miR-222-5p	NRIP1
hsa-miR-222-5p	BCAR3
hsa-miR-27b-5p	ETS1
hsa-miR-3127-5p	ID3
hsa-miR-3127-5p	MYD88
hsa-miR-3127-5p	UTP14A
hsa-miR-3127-5p	C1orf216
hsa-miR-31-3p	FKBP14
hsa-miR-31-3p	ARRDC3
hsa-miR-31-3p	SEC24D
hsa-miR-32-3p	LATS2
hsa-miR-32-3p	NRIP1
hsa-miR-326	KCNQ4
hsa-miR-326	EML2
hsa-miR-330-3p	TARDBP
hsa-miR-330-3p	SMAD7
hsa-miR-33a-5p	NPC1
hsa-miR-33a-5p	PIM1
hsa-miR-33a-5p	NRP1
hsa-miR-340-5p	JPH1
hsa-miR-340-5p	EPAS1
hsa-miR-340-5p	TNFAIP3
hsa-miR-340-5p	ARRDC3
hsa-miR-340-5p	FHL2
hsa-miR-342-3p	ID4
hsa-miR-342-3p	FXD3
hsa-miR-345-5p	CDKN1A
hsa-miR-34a-3p	PDGFB

## APPENDICES

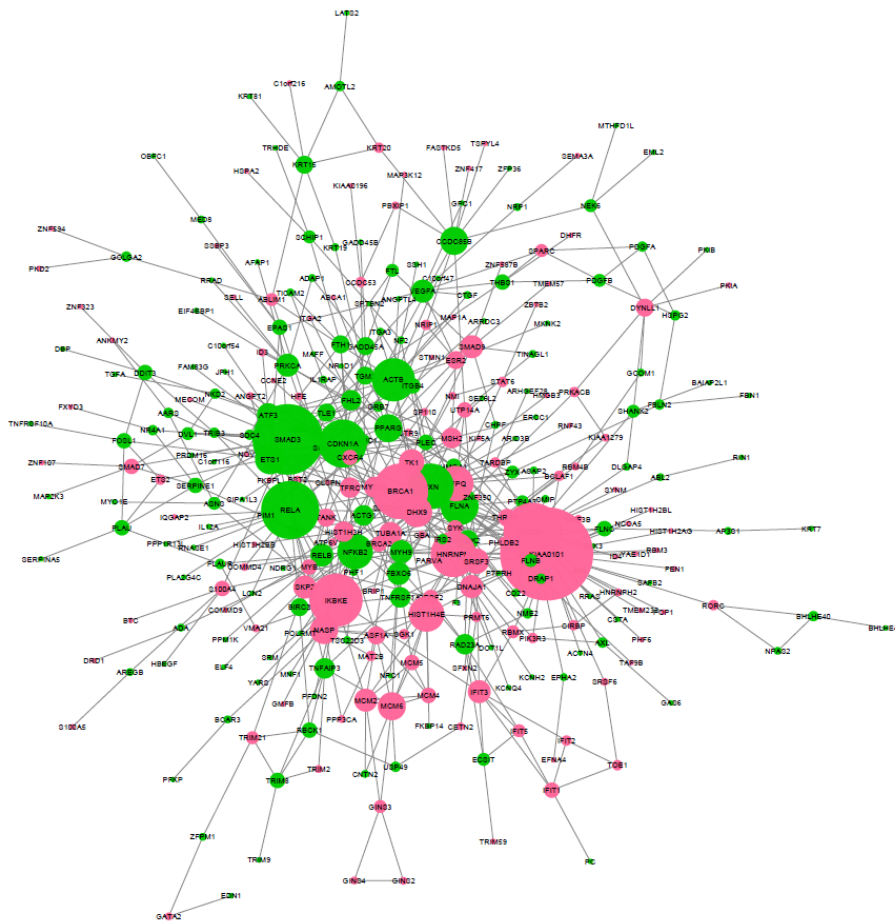
hsa-miR-34a-5p	RRAS
hsa-miR-34a-5p	AXL
hsa-miR-34a-5p	KLF4
hsa-miR-34a-5p	FOSL1
hsa-miR-3605-5p	NOV
hsa-miR-3605-5p	PBXIP1
hsa-miR-3605-5p	ZNF107
hsa-miR-3605-5p	THRAP3
hsa-miR-3605-5p	SEMA3A
hsa-miR-3605-5p	TAF9B
hsa-miR-3605-5p	ABLIM1
hsa-miR-3613-5p	AP3S1
hsa-miR-374a-5p	VEGFA
hsa-miR-374a-5p	RAD23A
hsa-miR-374a-5p	GADD45A
hsa-miR-374a-5p	ARRDC3
hsa-miR-374a-5p	BHLHE40
hsa-miR-374a-5p	NRP1
hsa-miR-3929	VMA21
hsa-miR-3929	MCM4
hsa-miR-3929	DYNLL1
hsa-miR-429	LAMC1
hsa-miR-429	VEGFA
hsa-miR-429	PRDM16
hsa-miR-429	BHLHE41
hsa-miR-429	ETS1
hsa-miR-4521	C10orf47
hsa-miR-4697-3p	TMEM57
hsa-miR-4697-3p	TOE1
hsa-miR-4745-5p	ITGA2
hsa-miR-556-3p	BIRC3
hsa-miR-556-3p	F3
hsa-miR-556-3p	KLF4
hsa-miR-573	AFAP1
hsa-miR-573	KCNQ4
hsa-miR-589-3p	SPARC
hsa-miR-589-3p	ID4
hsa-miR-589-3p	NCOA5
hsa-miR-589-3p	PHLDB2
hsa-miR-589-3p	GINS3
hsa-miR-589-3p	STMN1
hsa-miR-589-3p	ASF1A
hsa-miR-589-3p	MCM6
hsa-miR-590-3p	LATS2
hsa-miR-590-3p	PHF1
hsa-miR-590-3p	JPH1

## APPENDICES

hsa-miR-590-3p	NPAS2
hsa-miR-590-3p	PPM1K
hsa-miR-590-3p	THBS1
hsa-miR-590-3p	TRHDE
hsa-miR-590-3p	ETS1
hsa-miR-590-3p	IL12A
hsa-miR-7-1-3p	ACTB
hsa-miR-7-1-3p	VEGFA
hsa-miR-7-1-3p	PPM1K
hsa-miR-7-1-3p	PDGFA
hsa-miR-7-1-3p	CTGF
hsa-miR-760	HIST1H2BL
hsa-miR-760	HIST3H2BB
hsa-miR-760	HIST1H3H
hsa-miR-766-3p	MTHFD1L
hsa-miR-766-3p	TFE3
hsa-miR-766-3p	TNFRSF1A
hsa-miR-766-3p	MYH9
hsa-miR-766-3p	YARS
hsa-miR-766-3p	ETS1
hsa-miR-92a-1-5p	MECOM
hsa-miR-92a-3p	IFIT2
hsa-miR-92a-3p	IQGAP2
hsa-miR-940	TFE3
hsa-miR-940	PTPRH
hsa-miR-940	ELF4
hsa-miR-940	ARHGEF28
hsa-miR-940	NF2
hsa-miR-940	PARK2
hsa-miR-940	PDGFB
hsa-miR-940	PPM1K
hsa-miR-940	THBS1
hsa-miR-940	TRIB3
hsa-miR-940	ETS1

## APPENDICES

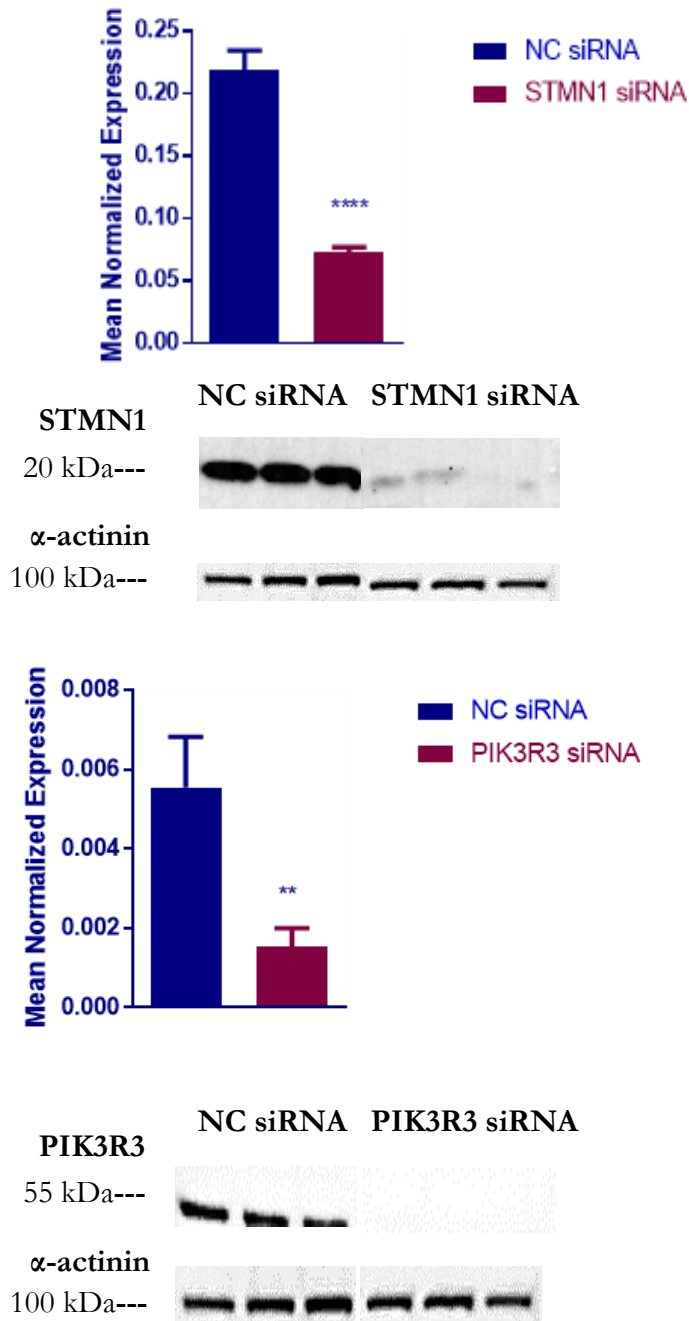
### Appendix 5. Protein-protein interaction network associated with 2.5 mM metformin treatment of HCT116 cells.



#### The Protein-Protein interaction network affected by metformin treatment of colorectal cancer cells.

This is zero-ordered network associated with 2.5 mM metformin treatment of HCT116 cells. PPIs are from InnateDB signalling network. The pink nodes represent downregulated genes while green nodes are upregulated genes.

## Appendix 6. RNAi efficiencies of STMN1 and PIK3R3 siRNAs



**Quantitative real-time PCR analysis of mRNA levels and western blot analysis of protein levels in HCT116 cells transfected with STMN1 and PIK3R3 siRNAs.**

Cells were transfected with STMN1, PIK3R3 or NC siRNA and the RNA and protein levels were measured by RT-PCR and western blot analysis, respectively. The mRNA expression is normalised to *B2M* expression and  $\alpha$ -actinin protein levels were considered as a loading control. The statistical significance is indicated with asterisks (\*\*  $P \leq 0.01$  and \*\*\*  $P \leq 0.001$ ).

# References

---

1. Warburg, O., *On respiratory impairment in cancer cells*. Science, 1956. **124**(3215): p. 269-70.
2. Zhang, H., et al., *Increased expression of microRNA-148a in osteosarcoma promotes cancer cell growth by targeting PTEN*. Oncol Lett, 2016. **12**(5): p. 3208-3214.
3. Vander Heiden, M.G., L.C. Cantley, and C.B. Thompson, *Understanding the Warburg effect: the metabolic requirements of cell proliferation*. Science, 2009. **324**(5930): p. 1029-33.
4. Rossignol, R., et al., *Energy substrate modulates mitochondrial structure and oxidative capacity in cancer cells*. Cancer Res, 2004. **64**(3): p. 985-93.
5. Zheng, L., et al., *Fumarate induces redox-dependent senescence by modifying glutathione metabolism*. Nat Commun, 2015. **6**: p. 6001.
6. Bardella, C., P.J. Pollard, and I. Tomlinson, *SDH mutations in cancer*. Biochim Biophys Acta, 2011. **1807**(11): p. 1432-43.
7. Cairns, R.A., I.S. Harris, and T.W. Mak, *Regulation of cancer cell metabolism*. Nat Rev Cancer, 2011. **11**(2): p. 85-95.
8. Varmus, H., et al., *Oncogenes come of age*. Cold Spring Harb Symp Quant Biol, 2005. **70**: p. 1-9.
9. Singh, P.K., et al., *Regulation of Aerobic Glycolysis by microRNAs in Cancer*. Mol Cell Pharmacol, 2011. **3**(3): p. 125-134.
10. Ruby, J.G., C.H. Jan, and D.P. Bartel, *Intronic microRNA precursors that bypass Drosha processing*. Nature, 2007. **448**(7149): p. 83-6.
11. Ha, M. and V.N. Kim, *Regulation of microRNA biogenesis*. Nat Rev Mol Cell Biol, 2014. **15**(8): p. 509-24.
12. Valinezhad Orang, A., R. Safaralizadeh, and M. Kazemzadeh-Bavili, *Mechanisms of miRNA-Mediated Gene Regulation from Common Downregulation to mRNA-Specific Upregulation*. Int J Genomics, 2014. **2014**: p. 970607.
13. Lin, S. and R.I.J.N.r.c. Gregory, *MicroRNA biogenesis pathways in cancer*. 2015. **15**(6): p. 321.
14. AIHW, *Cancer incidence projections: Australia, 2011 to 2020. Cancer Series no. 66. Cat. no. CAN 62*. 2012, Canberra: Australian Institute of Health and Welfare.
15. IARC. *Globocan 2008 Colorectal Cancer Incidence, Mortality and Prevalence Worldwide in 2008*. International Agency for Research on Cancer. 2012; Available from: <http://globocan.iarc.fr/>.
16. WCRF, *Food, Nutrition, Physical Activity and the Prevention of Cancer: a Global Perspective*. 2007, Washington DC: World Cancer Research Fund / American Institute for Cancer Research.
17. Toyota, M., et al., *CpG island methylator phenotype in colorectal cancer*. Proc Natl Acad Sci U S A, 1999. **96**(15): p. 8681-6.
18. Esteller, M., et al., *A gene hypermethylation profile of human cancer*. Cancer Res, 2001. **61**(8): p. 3225-9.
19. Zhu, P., et al., *Induction of HDAC2 expression upon loss of APC in colorectal tumorigenesis*. Cancer Cell, 2004. **5**(5): p. 455-63.
20. Enroth, S., et al., *Cancer associated epigenetic transitions identified by genome-wide histone methylation binding profiles in human colorectal cancer samples and paired normal mucosa*. BMC Cancer, 2011. **11**: p. 450.
21. Boyle, P. and J.S. Langman, *ABC of colorectal cancer: Epidemiology*. Bmj, 2000. **321**(7264): p. 805-8.
22. Roder, D., et al., *Colorectal cancer treatment and survival: the experience of major public hospitals in south Australia over three decades*. Asian Pac J Cancer Prev, 2015. **16**(6): p. 2431-40.

## REFERENCES

23. FC, D.A.S., et al., *Update on Hereditary Colorectal Cancer*. Anticancer Res, 2016. **36**(9): p. 4399-405.
24. Peters, U., S. Bien, and N. Zubair, *Genetic architecture of colorectal cancer*. Gut, 2015. **64**(10): p. 1623-36.
25. National Health and Medical Research Council. Clinical Practice Guidelines for the Prevention, E.D.a.M.o.C.C.C.A., 1999.
26. Crea, F., et al., *Epigenetics and chemoresistance in colorectal cancer: an opportunity for treatment tailoring and novel therapeutic strategies*. Drug Resist Updat, 2011. **14**(6): p. 280-96.
27. Cunningham, D., et al., *Colorectal cancer*. Lancet, 2010. **375**(9719): p. 1030-47.
28. Kohne, C.-H. and H.-J. Lenz, *Chemotherapy with targeted agents for the treatment of metastatic colorectal cancer*. Oncologist, 2009. **14**(5): p. 478-88.
29. Fearnhead, N.S., J.L. Wilding, and W.F. Bodmer, *Genetics of colorectal cancer: hereditary aspects and overview of colorectal tumorigenesis*. Br Med Bull, 2002. **64**: p. 27-43.
30. Al-Sohaily, S., et al., *Molecular pathways in colorectal cancer*. J Gastroenterol Hepatol, 2012. **27**(9): p. 1423-31.
31. Fearon, E.R. and B. Vogelstein, *A genetic model for colorectal tumorigenesis*. Cell, 1990. **61**(5): p. 759-67.
32. Tariq, K. and K. Ghias, *Colorectal cancer carcinogenesis: a review of mechanisms*. Cancer Biol Med, 2016. **13**(1): p. 120-35.
33. Kinzler, K.W., et al., *Identification of FAP locus genes from chromosome 5q21*. Science, 1991. **253**(5020): p. 661-5.
34. Fishel, R., et al., *The human mutator gene homolog MSH2 and its association with hereditary nonpolyposis colon cancer*. Cell, 1993. **75**(5): p. 1027-38.
35. Bronner, C.E., et al., *Mutation in the DNA mismatch repair gene homologue hMLH1 is associated with hereditary non-polyposis colon cancer*. Nature, 1994. **368**(6468): p. 258-61.
36. Papadopoulos, N., et al., *Mutation of a mutL homolog in hereditary colon cancer*. Science, 1994. **263**(5153): p. 1625-9.
37. Migliore, L., et al., *Genetics, cytogenetics, and epigenetics of colorectal cancer*. J Biomed Biotechnol, 2011. **2011**: p. 792362.
38. Pavicic, W., et al., *Promoter-specific alterations of APC are a rare cause for mutation-negative familial adenomatous polyposis*. Genes Chromosomes Cancer, 2014. **53**(10): p. 857-64.
39. Segui, N., et al., *Longer telomeres are associated with cancer risk in MMR-proficient hereditary non-polyposis colorectal cancer*. PLoS One, 2014. **9**(2): p. e86063.
40. Werner, R.J., A.D. Kelly, and J.J. Issa, *Epigenetics and Precision Oncology*. Cancer J, 2017. **23**(5): p. 262-269.
41. Duthie, S.J., *Folate and cancer: how DNA damage, repair and methylation impact on colon carcinogenesis*. J Inherit Metab Dis, 2011. **34**(1): p. 101-9.
42. Michael, M.Z., et al., *Reduced accumulation of specific microRNAs in colorectal neoplasia*. Mol Cancer Res, 2003. **1**(12): p. 882-91.
43. Cummins, J.M., et al., *The colorectal microRNAome*. Proc Natl Acad Sci U S A, 2006. **103**(10): p. 3687-92.
44. Slaby, O., et al., *Altered expression of miR-21, miR-31, miR-143 and miR-145 is related to clinicopathologic features of colorectal cancer*. Oncology, 2007. **72**(5-6): p. 397-402.
45. Brown, D.G., et al., *Metabolomics and metabolic pathway networks from human colorectal cancers, adjacent mucosa, and stool*. Cancer Metab, 2016. **4**: p. 11.
46. Schmidt, C.W., *Metabolomics: what's happening downstream of DNA*. Environ Health Perspect, 2004. **112**(7): p. A410-5.
47. Chan, E.C., et al., *Metabolic profiling of human colorectal cancer using high-resolution magic angle spinning nuclear magnetic resonance (HR-MAS NMR) spectroscopy and gas chromatography mass spectrometry (GC/MS)*. J Proteome Res, 2009. **8**(1): p. 352-61.

## REFERENCES

48. Qiu, Y., et al., *A distinct metabolic signature of human colorectal cancer with prognostic potential*. Clin Cancer Res, 2014. **20**(8): p. 2136-46.
49. Yamane, L.S., et al., *KRAS and BRAF mutations and MSI status in precursor lesions of colorectal cancer detected by colonoscopy*. Oncol Rep, 2014. **32**(4): p. 1419-26.
50. Williams, M.D., et al., *Metabolomics of colorectal cancer: past and current analytical platforms*. Anal Bioanal Chem, 2013. **405**(15): p. 5013-30.
51. Donohoe, D.R., et al., *The Warburg effect dictates the mechanism of butyrate-mediated histone acetylation and cell proliferation*. Mol Cell, 2012. **48**(4): p. 612-26.
52. Assfalg, M., et al., *Evidence of different metabolic phenotypes in humans*. Proc Natl Acad Sci U S A, 2008. **105**(5): p. 1420-4.
53. Montrose, D.C., et al., *Metabolic profiling, a noninvasive approach for the detection of experimental colorectal neoplasia*. Cancer Prev Res (Phila), 2012. **5**(12): p. 1358-67.
54. Fraga, M.F., et al., *Epigenetic differences arise during the lifetime of monozygotic twins*. Proc Natl Acad Sci U S A, 2005. **102**(30): p. 10604-9.
55. Power, D.G., E. Glogowski, and S.M. Lipkin, *Clinical genetics of hereditary colorectal cancer*. Hematol Oncol Clin North Am, 2010. **24**(5): p. 837-59.
56. Mathers, J.C., G. Strathdee, and C.L. Relton, *Induction of epigenetic alterations by dietary and other environmental factors*. Adv Genet, 2010. **71**: p. 3-39.
57. Campbell, P.T., et al., *Prospective study reveals associations between colorectal cancer and type 2 diabetes mellitus or insulin use in men*. Gastroenterology, 2010. **139**(4): p. 1138-46.
58. Cavicchia, P.P., et al., *Racial disparities in colorectal cancer incidence by type 2 diabetes mellitus status*. Cancer Causes Control, 2013. **24**(2): p. 277-85.
59. Tabak, A.G., et al., *Trajectories of glycaemia, insulin sensitivity, and insulin secretion before diagnosis of type 2 diabetes: an analysis from the Whitehall II study*. Lancet, 2009. **373**(9682): p. 2215-21.
60. Giovannucci, E., *Insulin and colon cancer*. Cancer Causes Control, 1995. **6**(2): p. 164-79.
61. Vigneri, P., et al., *Diabetes and cancer*. Endocr Relat Cancer, 2009. **16**(4): p. 1103-23.
62. Bauer, D.E., et al., *Cytokine stimulation of aerobic glycolysis in hematopoietic cells exceeds proliferative demand*. FASEB J, 2004. **18**(11): p. 1303-5.
63. Ramanathan, A., C. Wang, and S.L. Schreiber, *Perturbational profiling of a cell-line model of tumorigenesis by using metabolic measurements*. Proc Natl Acad Sci U S A, 2005. **102**(17): p. 5992-7.
64. Tong, X., F. Zhao, and C.B. Thompson, *The molecular determinants of de novo nucleotide biosynthesis in cancer cells*. Curr Opin Genet Dev, 2009. **19**(1): p. 32-7.
65. Menendez, J.A. and R. Lupu, *Fatty acid synthase and the lipogenic phenotype in cancer pathogenesis*. Nat Rev Cancer, 2007. **7**(10): p. 763-77.
66. Horie, T., et al., *MicroRNA-133 regulates the expression of GLUT4 by targeting KLF15 and is involved in metabolic control in cardiac myocytes*. Biochem Biophys Res Commun, 2009. **389**(2): p. 315-20.
67. Jiang, S., et al., *A novel miR-155/miR-143 cascade controls glycolysis by regulating hexokinase 2 in breast cancer cells*. EMBO J, 2012. **31**(8): p. 1985-98.
68. Yao, M., et al., *Dicer mediating the expression of miR-143 and miR-155 regulates hexokinase II associated cellular response to hypoxia*. Am J Physiol Lung Cell Mol Physiol, 2014. **307**(11): p. L829-37.
69. Taniguchi, K., et al., *Organ-specific PTB1-associated microRNAs determine expression of pyruvate kinase isoforms*. Sci Rep, 2015. **5**: p. 8647.
70. Sun, Y., et al., *miR-124, miR-137 and miR-340 regulate colorectal cancer growth via inhibition of the Warburg effect*. Oncol Rep, 2012. **28**(4): p. 1346-52.
71. Taniguchi, K., et al., *MicroRNA-124 inhibits cancer cell growth through PTB1/PKM1/PKM2 feedback cascade in colorectal cancer*. Cancer Lett, 2015.

## REFERENCES

72. Sugiyama, T., et al., *MiR-133b inhibits growth of human gastric cancer cells by silencing pyruvate kinase muscle-splicer polypyrimidine tract-binding protein 1*. *Cancer Sci*, 2016. **107**(12): p. 1767-1775.
73. Taniguchi, K., et al., *PTBP1-associated microRNA-1 and -133b suppress the Warburg effect in colorectal tumors*. *Oncotarget*, 2016. **7**(14): p. 18940-52.
74. Yamasaki, T., et al., *Tumor-suppressive microRNA-1291 directly regulates glucose transporter 1 in renal cell carcinoma*. *Cancer Sci*, 2013. **104**(11): p. 1411-9.
75. Chow, T.F., et al., *The miR-17-92 cluster is over expressed in and has an oncogenic effect on renal cell carcinoma*. *J Urol*, 2010. **183**(2): p. 743-51.
76. Nie, S., et al., *miR-495 Mediates Metabolic Shift in Glioma Cells via Targeting Glut1*. *J Craniofac Surg*, 2015. **26**(2): p. e155-8.
77. Chen, B., et al., *miR-22 as a prognostic factor targets glucose transporter protein type 1 in breast cancer*. *Cancer Lett*, 2015. **356**(2 Pt B): p. 410-7.
78. Qu, W., et al., *miR-132 mediates a metabolic shift in prostate cancer cells by targeting Glut1*. *FEBS Open Bio*, 2016. **6**(7): p. 735-41.
79. King, B.C., et al., *CD46 Activation Regulates miR-150-Mediated Control of GLUT1 Expression and Cytokine Secretion in Human CD4+ T Cells*. *J Immunol*, 2016. **196**(4): p. 1636-45.
80. Li, P., et al., *MicroRNA-218 Increases the Sensitivity of Bladder Cancer to Cisplatin by Targeting Glut1*. *Cell Physiol Biochem*, 2017. **41**(3): p. 921-932.
81. Xu, P., et al., *MicroRNA-340 Mediates Metabolic Shift in Oral Squamous Cell Carcinoma by Targeting Glucose Transporter-1*. *J Oral Maxillofac Surg*, 2016. **74**(4): p. 844-50.
82. Guo, H., et al., *miRNA-451 inhibits glioma cell proliferation and invasion by downregulating glucose transporter 1*. *Tumour Biol*, 2016. **37**(10): p. 13751-13761.
83. Trakooljul, N., J.A. Hicks, and H.C. Liu, *Identification of target genes and pathways associated with chicken microRNA miR-143*. *Anim Genet*, 2010. **41**(4): p. 357-64.
84. Fei, X., et al., *MicroRNA-195-5p suppresses glucose uptake and proliferation of human bladder cancer T24 cells by regulating GLUT3 expression*. *FEBS Lett*, 2012. **586**(4): p. 392-7.
85. Dai, D.W., et al., *Decreased miR-106a inhibits glioma cell glucose uptake and proliferation by targeting SLC2A3 in GBM*. *BMC Cancer*, 2013. **13**: p. 478.
86. Lu, H., R.J. Buchan, and S.A. Cook, *MicroRNA-223 regulates Glut4 expression and cardiomyocyte glucose metabolism*. *Cardiovasc Res*, 2010. **86**(3): p. 410-20.
87. Karolina, D.S., et al., *MicroRNA 144 impairs insulin signaling by inhibiting the expression of insulin receptor substrate 1 in type 2 diabetes mellitus*. *PLoS One*, 2011. **6**(8): p. e22839.
88. Chen, Y.H., et al., *miRNA-93 inhibits GLUT4 and is overexpressed in adipose tissue of polycystic ovary syndrome patients and women with insulin resistance*. *Diabetes*, 2013. **62**(7): p. 2278-86.
89. Zhou, T., et al., *Regulation of Insulin Resistance by Multiple MiRNAs via Targeting the GLUT4 Signalling Pathway*. *Cell Physiol Biochem*, 2016. **38**(5): p. 2063-78.
90. Peschiaroli, A., et al., *miR-143 regulates hexokinase 2 expression in cancer cells*. *Oncogene*, 2013. **32**(6): p. 797-802.
91. Kim, H.R., et al., *p53 regulates glucose metabolism by miR-34a*. *Biochem Biophys Res Commun*, 2013. **437**(2): p. 225-31.
92. Zhao, S., et al., *miR-143 inhibits glycolysis and depletes stemness of glioblastoma stem-like cells*. *Cancer Lett*, 2013. **333**(2): p. 253-60.
93. Jiang, J.X., et al., *Overexpression of microRNA-125b sensitizes human hepatocellular carcinoma cells to 5-fluorouracil through inhibition of glycolysis by targeting hexokinase II*. *Mol Med Rep*, 2014. **10**(2): p. 995-1002.
94. Song, J., et al., *Long non-coding RNA PVT1 promotes glycolysis and tumor progression by regulating miR-497/HK2 axis in osteosarcoma*. *Biochem Biophys Res Commun*, 2017. **490**(2): p. 217-224.

## REFERENCES

95. Li, W., et al., *Astragalín Reduces Hexokinase 2 through Increasing miR-125b to Inhibit the Proliferation of Hepatocellular Carcinoma Cells in Vitro and in Vivo*. *J Agric Food Chem*, 2017. **65**(29): p. 5961-5972.
96. Tao, T., et al., *Involvement of EZH2 in aerobic glycolysis of prostate cancer through miR-181b/HK2 axis*. *Oncol Rep*, 2017. **37**(3): p. 1430-1436.
97. Zhu, W., et al., *MicroRNA-98 Suppress Warburg Effect by Targeting HK2 in Colon Cancer Cells*. *Dig Dis Sci*, 2017. **62**(3): p. 660-668.
98. Li, L.Q., et al., *MicroRNA-181b inhibits glycolysis in gastric cancer cells via targeting hexokinase 2 gene*. *Cancer Biomark*, 2016. **17**(1): p. 75-81.
99. Qin, Y., et al., *miR-4458 suppresses glycolysis and lactate production by directly targeting hexokinase2 in colon cancer cells*. *Biochem Biophys Res Commun*, 2016. **469**(1): p. 37-43.
100. Lan, H., et al., *[miR-181c inhibits glycolysis by targeting hexokinase 2 in cancer-associated fibroblasts]*. *Nan Fang Yi Ke Da Xue Xue Bao*, 2015. **35**(11): p. 1619-23.
101. Zhou, P., W.G. Chen, and X.W. Li, *MicroRNA-143 acts as a tumor suppressor by targeting hexokinase 2 in human prostate cancer*. *Am J Cancer Res*, 2015. **5**(6): p. 2056-63.
102. Guo, W., et al., *MiR-199a-5p is negatively associated with malignancies and regulates glycolysis and lactate production by targeting hexokinase 2 in liver cancer*. *Hepatology*, 2015. **62**(4): p. 1132-44.
103. Rengaraj, D., et al., *Regulation of glucose phosphate isomerase by the 3'UTR-specific miRNAs miR-302b and miR-17-5p in chicken primordial germ cells*. *Biol Reprod*, 2013. **89**(2): p. 33.
104. Ahmad, A., et al., *Phosphoglucose isomerase/ autocrine motility factor mediates epithelial-mesenchymal transition regulated by miR-200 in breast cancer cells*. *Cancer Res*, 2011. **71**(9): p. 3400-9.
105. Park, Y.Y., et al., *Tat-activating regulatory DNA-binding protein regulates glycolysis in hepatocellular carcinoma by regulating the platelet isoform of phosphofructokinase through microRNA 520*. *Hepatology*, 2013. **58**(1): p. 182-91.
106. Tang, H., et al., *Oxidative stress-responsive microRNA-320 regulates glycolysis in diverse biological systems*. *FASEB J*, 2012. **26**(11): p. 4710-21.
107. White, N.M., et al., *Dysregulation of kallikrein-related peptidases in renal cell carcinoma: potential targets of miRNAs*. *Biol Chem*, 2010. **391**(4): p. 411-23.
108. Du, J.Y., et al., *miR-26b inhibits proliferation, migration, invasion and apoptosis induction via the downregulation of 6-phosphofructo-2-kinase/fructose-2,6-bisphosphatase-3 driven glycolysis in osteosarcoma cells*. *Oncol Rep*, 2015. **33**(4): p. 1890-8.
109. Seliger, B., et al., *Linkage of microRNA and proteome-based profiling data sets: a perspective for the prioritization of candidate biomarkers in renal cell carcinoma?* *J Proteome Res*, 2011. **10**(1): p. 191-9.
110. Ge, X., et al., *Overexpression of miR-206 suppresses glycolysis, proliferation and migration in breast cancer cells via PFKFB3 targeting*. *Biochem Biophys Res Commun*, 2015. **463**(4): p. 1115-21.
111. Savarimuthu Francis, S.M., et al., *MicroRNA-34c is associated with emphysema severity and modulates SERPINE1 expression*. *BMC Genomics*, 2014. **15**: p. 88.
112. Calin, G.A., et al., *MiR-15a and miR-16-1 cluster functions in human leukemia*. *Proc Natl Acad Sci U S A*, 2008. **105**(13): p. 5166-71.
113. Boesch-Saadatmandi, C., et al., *Effect of quercetin on inflammatory gene expression in mice liver in vivo - role of redox factor 1, miRNA-122 and miRNA-125b*. *Pharmacol Res*, 2012. **65**(5): p. 523-30.
114. Nana-Sinkam, S.P. and C.M. Croce, *MicroRNA regulation of tumorigenesis, cancer progression and interpatient heterogeneity: towards clinical use*. *Genome Biol*, 2014. **15**(9): p. 445.
115. Sikand, K., et al., *Housekeeping gene selection advisory: glyceraldehyde-3-phosphate dehydrogenase (GAPDH) and beta-actin are targets of miR-644a*. *PLoS One*, 2012. **7**(10): p. e47510.
116. White, N.M., et al., *Identification and validation of dysregulated metabolic pathways in metastatic renal cell carcinoma*. *Tumour Biol*, 2014. **35**(3): p. 1833-46.
117. Ichimi, T., et al., *Identification of novel microRNA targets based on microRNA signatures in bladder cancer*. *Int J Cancer*, 2009. **125**(2): p. 345-52.

## REFERENCES

118. Li, Y., et al., *Epigenetic deregulation of miR-29a and miR-1256 by isoflavone contributes to the inhibition of prostate cancer cell growth and invasion*. Epigenetics, 2012. **7**(8): p. 940-9.
119. Muniyappa, M.K., et al., *MiRNA-29a regulates the expression of numerous proteins and reduces the invasiveness and proliferation of human carcinoma cell lines*. Eur J Cancer, 2009. **45**(17): p. 3104-18.
120. Taguchi, A., et al., *Identification of hypoxia-inducible factor-1 alpha as a novel target for miR-17-92 microRNA cluster*. Cancer Res, 2008. **68**(14): p. 5540-5.
121. Leder, A., et al., *Micron-sized iron oxide-containing particles for microRNA-targeted manipulation and MRI-based tracking of transplanted cells*. Biomaterials, 2015. **51**: p. 129-37.
122. Ramirez, C.M., et al., *MicroRNA 33 regulates glucose metabolism*. Mol Cell Biol, 2013. **33**(15): p. 2891-902.
123. Wong, T.S., et al., *Identification of pyruvate kinase type M2 as potential oncoprotein in squamous cell carcinoma of tongue through microRNA profiling*. Int J Cancer, 2008. **123**(2): p. 251-7.
124. Kefas, B., et al., *Pyruvate kinase M2 is a target of the tumor-suppressive microRNA-326 and regulates the survival of glioma cells*. Neuro Oncol, 2010. **12**(11): p. 1102-12.
125. Li, W., et al., *Insulin promotes glucose consumption via regulation of miR-99a/mTOR/PKM2 pathway*. PLoS One, 2013. **8**(6): p. e64924.
126. Tao, T., et al., *Loss of SNAIL inhibits cellular growth and metabolism through the miR-128-mediated RPS6KB1/HIF-1alpha/PKM2 signaling pathway in prostate cancer cells*. Tumour Biol, 2014. **35**(9): p. 8543-50.
127. Kinoshita, T., et al., *Tumor suppressive microRNA-375 regulates lactate dehydrogenase B in maxillary sinus squamous cell carcinoma*. Int J Oncol, 2012. **40**(1): p. 185-93.
128. Li, D.F., et al., *Induction of microRNA-24 by HIF-1 protects against ischemic injury in rat cardiomyocytes*. Physiol Res, 2012. **61**(6): p. 555-65.
129. Saumet, A., et al., *Estrogen and retinoic acid antagonistically regulate several microRNA genes to control aerobic glycolysis in breast cancer cells*. Mol Biosyst, 2012. **8**(12): p. 3242-53.
130. Kaller, M., et al., *Genome-wide characterization of miR-34a induced changes in protein and mRNA expression by a combined pulsed SILAC and microarray analysis*. Mol Cell Proteomics, 2011. **10**(8): p. M111 010462.
131. Wang, J., et al., *Lactate dehydrogenase A negatively regulated by miRNAs promotes aerobic glycolysis and is increased in colorectal cancer*. Oncotarget, 2015. **6**(23): p. 19456-68.
132. Zhang, Y., G. Liu, and X. Gao, *Attenuation of miR-34a protects cardiomyocytes against hypoxic stress through maintenance of glycolysis*. Biosci Rep, 2017.
133. Li, L., et al., *miR-30a-5p suppresses breast tumor growth and metastasis through inhibition of LDHA-mediated Warburg effect*. Cancer Lett, 2017. **400**: p. 89-98.
134. Han, R.L., et al., *miR-383 inhibits ovarian cancer cell proliferation, invasion and aerobic glycolysis by targeting LDHA*. Neoplasma, 2017. **64**(2): p. 244-252.
135. Zhang, R., et al., *HPV E6/p53 mediated down-regulation of miR-34a inhibits Warburg effect through targeting LDHA in cervical cancer*. Am J Cancer Res, 2016. **6**(2): p. 312-20.
136. Mi, Y., et al., *miR-410 enhanced hESC-derived pancreatic endoderm transplant to alleviate gestational diabetes mellitus*. J Mol Endocrinol, 2015. **55**(3): p. 219-29.
137. Chen, Y., X. Wang, and X. Shao, *A Combination of Human Embryonic Stem Cell-Derived Pancreatic Endoderm Transplant with LDHA-Repressing miRNA Can Attenuate High-Fat Diet Induced Type II Diabetes in Mice*. J Diabetes Res, 2015. **2015**: p. 796912.
138. Pullen, T.J., et al., *miR-29a and miR-29b contribute to pancreatic beta-cell-specific silencing of monocarboxylate transporter 1 (Mct1)*. Mol Cell Biol, 2011. **31**(15): p. 3182-94.
139. Li, K.K., et al., *miR-124 is frequently down-regulated in medulloblastoma and is a negative regulator of SLC16A1*. Hum Pathol, 2009. **40**(9): p. 1234-43.
140. Liang, D., et al., *Embryonic stem cell-derived pancreatic endoderm transplant with MCT1-suppressing miR-495 attenuates type II diabetes in mice*. Endocr J, 2015. **62**(10): p. 907-20.

## REFERENCES

141. Zu, X.L. and M. Guppy, *Cancer metabolism: facts, fantasy, and fiction*. Biochem Biophys Res Commun, 2004. **313**(3): p. 459-65.
142. Mathupala, S.P., Y.H. Ko, and P.L. Pedersen, *The pivotal roles of mitochondria in cancer: Warburg and beyond and encouraging prospects for effective therapies*. Biochim Biophys Acta, 2010. **1797**(6-7): p. 1225-30.
143. Ward, P.S., et al., *The common feature of leukemia-associated IDH1 and IDH2 mutations is a neomorphic enzyme activity converting alpha-ketoglutarate to 2-hydroxyglutarate*. Cancer Cell, 2010. **17**(3): p. 225-34.
144. Janeway, K.A., et al., *Defects in succinate dehydrogenase in gastrointestinal stromal tumors lacking KIT and PDGFRA mutations*. Proc Natl Acad Sci U S A, 2011. **108**(1): p. 314-8.
145. Linehan, W.M. and T.A. Rouault, *Molecular pathways: Fumarate hydratase-deficient kidney cancer--targeting the Warburg effect in cancer*. Clin Cancer Res, 2013. **19**(13): p. 3345-52.
146. Moreadith, R.W. and A.L. Lehninger, *The pathways of glutamate and glutamine oxidation by tumor cell mitochondria. Role of mitochondrial NAD(P)<sup>+</sup>-dependent malic enzyme*. J Biol Chem, 1984. **259**(10): p. 6215-21.
147. Chowdhury, R., et al., *The oncometabolite 2-hydroxyglutarate inhibits histone lysine demethylases*. EMBO Rep, 2011. **12**(5): p. 463-9.
148. Li, P., et al., *Control of mitochondrial activity by miRNAs*. J Cell Biochem, 2012. **113**(4): p. 1104-10.
149. Ilaria, D., et al., *Antioxidant Mechanisms and ROS-Related MicroRNAs in Cancer Stem Cells*. Oxid Med Cell Longev, 2015. **2015**.
150. Tanaka, H., et al., *MicroRNA-183 upregulates HIF-1alpha by targeting isocitrate dehydrogenase 2 (IDH2) in glioma cells*. J Neurooncol, 2013. **111**(3): p. 273-83.
151. Puissegur, M.P., et al., *miR-210 is overexpressed in late stages of lung cancer and mediates mitochondrial alterations associated with modulation of HIF-1 activity*. Cell Death Differ, 2011. **18**(3): p. 465-78.
152. Shi, Q. and G.E. Gibson, *Up-regulation of the mitochondrial malate dehydrogenase by oxidative stress is mediated by miR-743a*. J Neurochem, 2011. **118**(3): p. 440-8.
153. Aschrafi, A., et al., *MicroRNA-338 regulates local cytochrome c oxidase IV mRNA levels and oxidative phosphorylation in the axons of sympathetic neurons*. J Neurosci, 2008. **28**(47): p. 12581-90.
154. Jung, K.A., S. Lee, and M.K. Kwak, *NFE2L2/NRF2 Activity Is Linked to Mitochondria and AMP-Activated Protein Kinase Signaling in Cancers Through miR-181c/Mitochondria-Encoded Cytochrome c Oxidase Regulation*. Antioxid Redox Signal, 2017.
155. Saenz-de-Santa-Maria, I., et al., *Clinically relevant HIF-1alpha-dependent metabolic reprogramming in oropharyngeal squamous cell carcinomas includes coordinated activation of CAIX and the miR-210/ISCU signaling axis, but not MCT1 and MCT4 upregulation*. Oncotarget, 2017. **8**(8): p. 13730-13746.
156. Gao, P., et al., *c-Myc suppression of miR-23a/b enhances mitochondrial glutaminase expression and glutamine metabolism*. Nature, 2009. **458**(7239): p. 762-5.
157. Rodriguez-Enriquez, S., et al., *Multisite control of the Crabtree effect in ascites hepatoma cells*. Eur J Biochem, 2001. **268**(8): p. 2512-9.
158. Semenza, G.L., *Hypoxia-inducible factors: mediators of cancer progression and targets for cancer therapy*. Trends Pharmacol Sci, 2012. **33**(4): p. 207-14.
159. Mahon, P.C., K. Hirota, and G.L. Semenza, *FIH-1: a novel protein that interacts with HIF-1alpha and VHL to mediate repression of HIF-1 transcriptional activity*. Genes Dev, 2001. **15**(20): p. 2675-86.
160. Kulshreshtha, R., et al., *A microRNA signature of hypoxia*. Mol Cell Biol, 2007. **27**(5): p. 1859-67.
161. Keith, B., R.S. Johnson, and M.C. Simon, *HIF1alpha and HIF2alpha: sibling rivalry in hypoxic tumour growth and progression*. Nat Rev Cancer, 2012. **12**(1): p. 9-22.

## REFERENCES

162. Zundel, W., et al., *Loss of PTEN facilitates HIF-1-mediated gene expression*. *Genes Dev*, 2000. **14**(4): p. 391-6.
163. Wiesener, M.S., et al., *Constitutive activation of hypoxia-inducible genes related to overexpression of hypoxia-inducible factor-1 alpha in clear cell renal carcinomas*. *Cancer Res*, 2001. **61**(13): p. 5215-22.
164. Shackelford, D.B., et al., *mTOR and HIF-1alpha-mediated tumor metabolism in an LKB1 mouse model of Peutz-Jeghers syndrome*. *Proc Natl Acad Sci U S A*, 2009. **106**(27): p. 11137-42.
165. Bernardi, R., et al., *PML inhibits HIF-1alpha translation and neoangiogenesis through repression of mTOR*. *Nature*, 2006. **442**(7104): p. 779-85.
166. Brugarolas, J., et al., *Regulation of mTOR function in response to hypoxia by REDD1 and the TSC1/TSC2 tumor suppressor complex*. *Genes Dev*, 2004. **18**(23): p. 2893-904.
167. Lim, J.H., et al., *Ras-dependent induction of HIF-1alpha785 via the Raf/MEK/ERK pathway: a novel mechanism of Ras-mediated tumor promotion*. *Oncogene*, 2004. **23**(58): p. 9427-31.
168. Jiang, B.H., et al., *V-SRC induces expression of hypoxia-inducible factor 1 (HIF-1) and transcription of genes encoding vascular endothelial growth factor and enolase 1: involvement of HIF-1 in tumor progression*. *Cancer Res*, 1997. **57**(23): p. 5328-35.
169. Courtney, R., et al., *Cancer metabolism and the Warburg effect: the role of HIF-1 and PI3K*. *Mol Biol Rep*, 2015. **42**(4): p. 841-51.
170. Laughner, E., et al., *HER2 (neu) signaling increases the rate of hypoxia-inducible factor 1 alpha (HIF-1alpha) synthesis: novel mechanism for HIF-1-mediated vascular endothelial growth factor expression*. *Mol Cell Biol*, 2001. **21**(12): p. 3995-4004.
171. Luo, W., et al., *Pyruvate kinase M2 is a PHD3-stimulated coactivator for hypoxia-inducible factor 1*. *Cell*, 2011. **145**(5): p. 732-44.
172. Kaelin, W.G., Jr. and P.J. Ratcliffe, *Oxygen sensing by metazoans: the central role of the HIF hydroxylase pathway*. *Mol Cell*, 2008. **30**(4): p. 393-402.
173. Gustafsson, M.V., et al., *Hypoxia requires notch signaling to maintain the undifferentiated cell state*. *Dev Cell*, 2005. **9**(5): p. 617-28.
174. Kaidi, A., A.C. Williams, and C. Paraskeva, *Interaction between beta-catenin and HIF-1 promotes cellular adaptation to hypoxia*. *Nat Cell Biol*, 2007. **9**(2): p. 210-7.
175. Yeung, S.J., J. Pan, and M.H. Lee, *Roles of p53, MYC and HIF-1 in regulating glycolysis - the seventh hallmark of cancer*. *Cell Mol Life Sci*, 2008. **65**(24): p. 3981-99.
176. Fukuda, R., et al., *HIF-1 regulates cytochrome oxidase subunits to optimize efficiency of respiration in hypoxic cells*. *Cell*, 2007. **129**(1): p. 111-22.
177. Sutendra, G., et al., *Mitochondrial activation by inhibition of PDKII suppresses HIF1a signaling and angiogenesis in cancer*. *Oncogene*, 2013. **32**(13): p. 1638-50.
178. Majmundar, A.J., W.J. Wong, and M.C. Simon, *Hypoxia-inducible factors and the response to hypoxic stress*. *Mol Cell*, 2010. **40**(2): p. 294-309.
179. Zhao, F., et al., *Imatinib resistance associated with BCR-ABL upregulation is dependent on HIF-1alpha-induced metabolic reprogramming*. *Oncogene*, 2010. **29**(20): p. 2962-72.
180. Nallamshetty, S., S.Y. Chan, and J. Loscalzo, *Hypoxia: a master regulator of microRNA biogenesis and activity*. *Free Radic Biol Med*, 2013. **64**: p. 20-30.
181. Azzouzi, H.E., et al., *HypoxamiRs: regulators of cardiac hypoxia and energy metabolism*. *Trends Endocrinol Metab*, 2015. **26**(9): p. 502-8.
182. Yan, H.L., et al., *Repression of the miR-17-92 cluster by p53 has an important function in hypoxia-induced apoptosis*. *EMBO J*, 2009. **28**(18): p. 2719-32.
183. Lei, Z., et al., *Regulation of HIF-1alpha and VEGF by miR-20b tunes tumor cells to adapt to the alteration of oxygen concentration*. *PLoS One*, 2009. **4**(10): p. e7629.
184. Hebert, C., et al., *High mobility group A2 is a target for miRNA-98 in head and neck squamous cell carcinoma*. *Mol Cancer*, 2007. **6**: p. 5.
185. He, M., et al., *HIF-1alpha downregulates miR-17/20a directly targeting p21 and STAT3: a role in myeloid leukemic cell differentiation*. *Cell Death Differ*, 2013. **20**(3): p. 408-18.

## REFERENCES

186. Li, C., et al., *Peroxisome proliferator-activated receptor-alpha-mediated transcription of miR-199a2 attenuates endothelin-1 expression via hypoxia-inducible factor-1alpha*. J Biol Chem, 2014. **289**(52): p. 36031-47.
187. Li, J.Y., et al., *Differential distribution of miR-20a and miR-20b may underly metastatic heterogeneity of breast cancers*. Asian Pac J Cancer Prev, 2012. **13**(5): p. 1901-6.
188. Ma, L., J. Teruya-Feldstein, and R.A. Weinberg, *Tumour invasion and metastasis initiated by microRNA-10b in breast cancer*. Nature, 2007. **449**(7163): p. 682-8.
189. Wu, C., et al., *Hypoxia potentiates microRNA-mediated gene silencing through posttranslational modification of Argonaute2*. Mol Cell Biol, 2011. **31**(23): p. 4760-74.
190. Chakravarthi, B.V., et al., *The miR-124-prolyl hydroxylase P4HA1-MMP1 axis plays a critical role in prostate cancer progression*. Oncotarget, 2014. **5**(16): p. 6654-69.
191. Aakula, A., et al., *MicroRNA-135b regulates ERalpha, AR and HIF1AN and affects breast and prostate cancer cell growth*. Mol Oncol, 2015.
192. Leung, A.K., et al., *Poly(ADP-ribose) regulates stress responses and microRNA activity in the cytoplasm*. Mol Cell, 2011. **42**(4): p. 489-99.
193. Liu, Y.P., et al., *Mechanistic insights on the Dicer-independent AGO2-mediated processing of AgosbRNAs*. RNA Biol, 2015. **12**(1): p. 92-100.
194. Chen, T., et al., *MicroRNA-31 contributes to colorectal cancer development by targeting factor inhibiting HIF-1alpha (FIH-1)*. Cancer Biol Ther, 2014. **15**(5): p. 516-23.
195. Yuan, Q., et al., *Upregulation of miR-184 enhances the malignant biological behavior of human glioma cell line A172 by targeting FIH-1*. Cell Physiol Biochem, 2014. **34**(4): p. 1125-36.
196. Peng, H., et al., *MicroRNA-31 targets FIH-1 to positively regulate corneal epithelial glycogen metabolism*. FASEB J, 2012. **26**(8): p. 3140-7.
197. Ghosh, A.K., et al., *Aberrant regulation of pVHL levels by microRNA promotes the HIF/VEGF axis in CLL B cells*. Blood, 2009. **113**(22): p. 5568-74.
198. Yue, J., et al., *MicroRNA-206 is involved in hypoxia-induced pulmonary hypertension through targeting of the HIF-1alpha/Fhl-1 pathway*. Lab Invest, 2013. **93**(7): p. 748-59.
199. Liu, L.Z., et al., *MiR-21 induced angiogenesis through AKT and ERK activation and HIF-1alpha expression*. PLoS One, 2011. **6**(4): p. e19139.
200. Yamakuchi, M., et al., *P53-induced microRNA-107 inhibits HIF-1 and tumor angiogenesis*. Proc Natl Acad Sci U S A, 2010. **107**(14): p. 6334-9.
201. Meng, S., et al., *MicroRNA 107 partly inhibits endothelial progenitor cells differentiation via HIF-1beta*. PLoS One, 2012. **7**(7): p. e40323.
202. Ho, J.J., et al., *Functional importance of Dicer protein in the adaptive cellular response to hypoxia*. J Biol Chem, 2012. **287**(34): p. 29003-20.
203. Kelly, T.J., et al., *A hypoxia-induced positive feedback loop promotes hypoxia-inducible factor 1alpha stability through miR-210 suppression of glycerol-3-phosphate dehydrogenase 1-like*. Mol Cell Biol, 2011. **31**(13): p. 2696-706.
204. Johnson, R.F. and N.D. Perkins, *Nuclear factor-kappaB, p53, and mitochondria: regulation of cellular metabolism and the Warburg effect*. Trends Biochem Sci, 2012. **37**(8): p. 317-24.
205. Ghosh, G., et al., *Hypoxia-induced microRNA-424 expression in human endothelial cells regulates HIF-alpha isoforms and promotes angiogenesis*. J Clin Invest, 2010. **120**(11): p. 4141-54.
206. Sun, G., et al., *Over-expression of microRNA-494 up-regulates hypoxia-inducible factor-1 alpha expression via PI3K/ Akt pathway and protects against hypoxia-induced apoptosis*. J Biomed Sci, 2013. **20**: p. 100.
207. Velagapudi, S.P., et al., *Approved Anti-cancer Drugs Target Oncogenic Non-coding RNAs*. Cell Chem Biol, 2018. **25**(9): p. 1086-1094.e7.
208. Bertozzi, D., et al., *The natural inhibitor of DNA topoisomerase I, camptothecin, modulates HIF-1alpha activity by changing miR expression patterns in human cancer cells*. Mol Cancer Ther, 2014. **13**(1): p. 239-48.

## REFERENCES

209. Poitz, D.M., et al., *Regulation of the Hif-system by micro-RNA 17 and 20a - role during monocyte-to-macrophage differentiation*. Mol Immunol, 2013. **56**(4): p. 442-51.
210. Lin, S.C., et al., *Hypoxia-induced microRNA-20a expression increases ERK phosphorylation and angiogenic gene expression in endometriotic stromal cells*. J Clin Endocrinol Metab, 2012. **97**(8): p. E1515-23.
211. Kang, S.G., et al., *Hypoxia-inducible factor-1alpha inhibition by a pyrrolopyrazine metabolite of oltipraz as a consequence of microRNAs 199a-5p and 20a induction*. Carcinogenesis, 2012. **33**(3): p. 661-9.
212. Cascio, S., et al., *miR-20b modulates VEGF expression by targeting HIF-1 alpha and STAT3 in MCF-7 breast cancer cells*. J Cell Physiol, 2010. **224**(1): p. 242-9.
213. Xue, T.M., et al., *Clinicopathological Significance of MicroRNA-20b Expression in Hepatocellular Carcinoma and Regulation of HIF-1alpha and VEGF Effect on Cell Biological Behaviour*. Dis Markers, 2015. **2015**: p. 325176.
214. Bartoszewska, S., et al., *The hypoxia-inducible miR-429 regulates hypoxia-inducible factor-1alpha expression in human endothelial cells through a negative feedback loop*. FASEB J, 2015. **29**(4): p. 1467-79.
215. Hua, Z., et al., *MiRNA-directed regulation of VEGF and other angiogenic factors under hypoxia*. PLoS One, 2006. **1**: p. e116.
216. Sen, D. and G.R. Jayandharan, *MicroRNA-15b Modulates Molecular Mediators of Blood Induced Arthropathy in Hemophilia Mice*. Int J Mol Sci, 2016. **17**(4): p. 492.
217. Akhtar, S., et al., *Endothelial Hypoxia-Inducible Factor-1alpha Promotes Atherosclerosis and Monocyte Recruitment by Upregulating MicroRNA-19a*. Hypertension, 2015. **66**(6): p. 1220-6.
218. Han, M., et al., *MiR-21 regulates epithelial-mesenchymal transition phenotype and hypoxia-inducible factor-1alpha expression in third-sphere forming breast cancer stem cell-like cells*. Cancer Sci, 2012. **103**(6): p. 1058-64.
219. White, N.M., et al., *Galectin-1 has potential prognostic significance and is implicated in clear cell renal cell carcinoma progression through the HIF/ mTOR signaling axis*. Br J Cancer, 2014. **110**(5): p. 1250-9.
220. Yamakuchi, M., et al., *MicroRNA-22 regulates hypoxia signaling in colon cancer cells*. PLoS One, 2011. **6**(5): p. e20291.
221. Calin, G.A. and C.M. Croce, *MicroRNA signatures in human cancers*. Nat Rev Cancer, 2006. **6**(11): p. 857-66.
222. Peng, H., et al., *microRNA-31/factor-inhibiting hypoxia-inducible factor 1 nexus regulates keratinocyte differentiation*. Proc Natl Acad Sci U S A, 2012. **109**(35): p. 14030-4.
223. Peng, H., et al., *FIH-1/c-kit signaling: a novel contributor to corneal epithelial glycogen metabolism*. Invest Ophthalmol Vis Sci, 2013. **54**(4): p. 2781-6.
224. Zhou, J., et al., *miR-33a functions as a tumor suppressor in melanoma by targeting HIF-1alpha*. Cancer Biol Ther, 2015: p. 0.
225. Umez, T., et al., *Exosomal miR-135b shed from hypoxic multiple myeloma cells enhances angiogenesis by targeting factor-inhibiting HIF-1*. Blood, 2014. **124**(25): p. 3748-57.
226. Song, T., et al., *MiR-138 suppresses expression of hypoxia-inducible factor 1alpha (HIF-1alpha) in clear cell renal cell carcinoma 786-O cells*. Asian Pac J Cancer Prev, 2011. **12**(5): p. 1307-11.
227. Yeh, Y.M., et al., *MicroRNA-138 suppresses ovarian cancer cell invasion and metastasis by targeting SOX4 and HIF-1alpha*. Int J Cancer, 2013. **133**(4): p. 867-78.
228. Liu, L., et al., *MiR-186 inhibited aerobic glycolysis in gastric cancer via HIF-1alpha regulation*. Oncogenesis, 2017. **6**(4): p. e318.
229. Bai, R., et al., *MicroRNA-195 induced apoptosis in hypoxic chondrocytes by targeting hypoxia-inducible factor 1 alpha*. Eur Rev Med Pharmacol Sci, 2015. **19**(4): p. 545-51.
230. Joshi, H.P., et al., *Dynamin 2 along with microRNA-199a reciprocally regulate hypoxia-inducible factors and ovarian cancer metastasis*. Proc Natl Acad Sci U S A, 2014. **111**(14): p. 5331-6.

## REFERENCES

231. He, J., et al., *Chronic arsenic exposure and angiogenesis in human bronchial epithelial cells via the ROS/miR-199a-5p/HIF-1alpha/COX-2 pathway*. Environ Health Perspect, 2014. **122**(3): p. 255-61.
232. Guillaume, M., et al., *miR204/RUNX2 axis regulates HIF-1a activation in pulmonary arterial hypertension*. FASEB J, 2013. **27**: p. 1140.20.
233. Merlo, A., et al., *Identification of a signaling axis HIF-1alpha/microRNA-210/ISCU independent of SDH mutation that defines a subgroup of head and neck paragangliomas*. J Clin Endocrinol Metab, 2012. **97**(11): p. E2194-200.
234. Biswas, S., et al., *Hypoxia inducible microRNA 210 attenuates keratinocyte proliferation and impairs closure in a murine model of ischemic wounds*. Proc Natl Acad Sci U S A, 2010. **107**(15): p. 6976-81.
235. Camps, C., et al., *hsa-miR-210 Is induced by hypoxia and is an independent prognostic factor in breast cancer*. Clin Cancer Res, 2008. **14**(5): p. 1340-8.
236. Dal Monte, M., et al., *Antiangiogenic role of miR-361 in human umbilical vein endothelial cells: functional interaction with the peptide somatostatin*. Naunyn Schmiedebergs Arch Pharmacol, 2013. **386**(1): p. 15-27.
237. Chen, D., et al., *MiR-373 drives the epithelial-to-mesenchymal transition and metastasis via the miR-373-TXNIP-HIF1alpha-TWIST signaling axis in breast cancer*. Oncotarget, 2015. **6**(32): p. 32701-12.
238. Cha, S.T., et al., *MicroRNA-519c suppresses hypoxia-inducible factor-1alpha expression and tumor angiogenesis*. Cancer Res, 2010. **70**(7): p. 2675-85.
239. Soga, T., *Cancer metabolism: key players in metabolic reprogramming*. Cancer Sci, 2013. **104**(3): p. 275-81.
240. Baldus, S.E., et al., *Prevalence and heterogeneity of KRAS, BRAF, and PIK3CA mutations in primary colorectal adenocarcinomas and their corresponding metastases*. Clin Cancer Res, 2010. **16**(3): p. 790-9.
241. Neuzil, J., J. Rohlena, and L.F. Dong, *K-Ras and mitochondria: dangerous liaisons*. Cell Res, 2012. **22**(2): p. 285-7.
242. Lu, W., et al., *Novel role of NOX in supporting aerobic glycolysis in cancer cells with mitochondrial dysfunction and as a potential target for cancer therapy*. PLoS Biol, 2012. **10**(5): p. e1001326.
243. Wang, P., et al., *Identification of NDUFAF1 in mediating K-Ras induced mitochondrial dysfunction by a proteomic screening approach*. Oncotarget, 2015. **6**(6): p. 3947-62.
244. Li, Z.H., et al., *A let-7 binding site polymorphism rs712 in the KRAS 3' UTR is associated with an increased risk of gastric cancer*. Tumour Biol, 2013. **34**(5): p. 3159-63.
245. Pan, X.M., et al., *A let-7 KRAS rs712 polymorphism increases colorectal cancer risk*. Tumour Biol, 2014. **35**(1): p. 831-5.
246. Jin, H., et al., *Association between a functional polymorphism rs712 within let-7-binding site and risk of papillary thyroid cancer*. Med Oncol, 2014. **31**(10): p. 221.
247. Chin, L.J., et al., *A SNP in a let-7 microRNA complementary site in the KRAS 3' untranslated region increases non-small cell lung cancer risk*. Cancer Res, 2008. **68**(20): p. 8535-40.
248. Kim, R.K., et al., *Activation of KRAS promotes the mesenchymal features of basal-type breast cancer*. Exp Mol Med, 2015. **47**: p. e137.
249. Kopp, F., E. Wagner, and A. Roidl, *The proto-oncogene KRAS is targeted by miR-200c*. Oncotarget, 2014. **5**(1): p. 185-95.
250. Hara, T., et al., *Selective targeting of KRAS-mutant cells by miR-126 through repression of multiple genes essential for the survival of KRAS-mutant cells*. Oncotarget, 2014. **5**(17): p. 7635-50.
251. Jin, X., et al., *Deregulation of the MiR-193b-KRAS Axis Contributes to Impaired Cell Growth in Pancreatic Cancer*. PLoS One, 2015. **10**(4): p. e0125515.
252. Hiraki, M., et al., *Concurrent Targeting of KRAS and AKT by MiR-4689 Is a Novel Treatment Against Mutant KRAS Colorectal Cancer*. Mol Ther Nucleic Acids, 2015. **4**: p. e231.

## REFERENCES

253. Jiao, L.R., et al., *MicroRNAs targeting oncogenes are down-regulated in pancreatic malignant transformation from benign tumors*. PLoS One, 2012. **7**(2): p. e32068.
254. Khodayari, N., et al., *EphrinA1 inhibits malignant mesothelioma tumor growth via let-7 microRNA-mediated repression of the RAS oncogene*. Cancer Gene Ther, 2011. **18**(11): p. 806-16.
255. Tanaka, M., et al., *EVI1 oncogene promotes KRAS pathway through suppression of microRNA-96 in pancreatic carcinogenesis*. Oncogene, 2014. **33**(19): p. 2454-63.
256. Zhang, Y., et al., *Multiple receptor tyrosine kinases converge on microRNA-134 to control KRAS, STAT5B, and glioblastoma*. Cell Death Differ, 2014. **21**(5): p. 720-34.
257. Iliopoulos, D., A. Rotem, and K. Struhl, *Inhibition of miR-193a expression by Max and RXRalpha activates K-Ras and PLA1 to mediate distinct aspects of cellular transformation*. Cancer Res, 2011. **71**(15): p. 5144-53.
258. Chung, H.J. and D. Levens, *c-myc expression: keep the noise down!* Mol Cells, 2005. **20**(2): p. 157-66.
259. Shim, H., et al., *c-Myc transactivation of LDH-A: implications for tumor metabolism and growth*. Proc Natl Acad Sci U S A, 1997. **94**(13): p. 6658-63.
260. Kim, J., J.H. Lee, and V.R. Iyer, *Global identification of Myc target genes reveals its direct role in mitochondrial biogenesis and its E-box usage in vivo*. PLoS One, 2008. **3**(3): p. e1798.
261. Li, F., et al., *Myc stimulates nuclearly encoded mitochondrial genes and mitochondrial biogenesis*. Mol Cell Biol, 2005. **25**(14): p. 6225-34.
262. Miller, D.M., et al., *c-Myc and cancer metabolism*. Clin Cancer Res, 2012. **18**(20): p. 5546-53.
263. Fan, Y., K.G. Dickman, and W.X. Zong, *Akt and c-Myc differentially activate cellular metabolic programs and prime cells to bioenergetic inhibition*. J Biol Chem, 2010. **285**(10): p. 7324-33.
264. Chen, X., Y. Qian, and S. Wu, *The Warburg effect: Evolving interpretations of an established concept*. Free Radic Biol Med, 2015. **79C**: p. 253-263.
265. Anastasiou, D., et al., *Inhibition of pyruvate kinase M2 by reactive oxygen species contributes to cellular antioxidant responses*. Science, 2011. **334**(6060): p. 1278-83.
266. Kim, J.W., et al., *Hypoxia-inducible factor 1 and dysregulated c-Myc cooperatively induce vascular endothelial growth factor and metabolic switches hexokinase 2 and pyruvate dehydrogenase kinase 1*. Mol Cell Biol, 2007. **27**(21): p. 7381-93.
267. Subramanian, A. and D.M. Miller, *Structural analysis of alpha-enolase. Mapping the functional domains involved in down-regulation of the c-myc protooncogene*. J Biol Chem, 2000. **275**(8): p. 5958-65.
268. Xu, N., et al., *MicroRNA-33b suppresses migration and invasion by targeting c-Myc in osteosarcoma cells*. PLoS One, 2014. **9**(12): p. e115300.
269. Sun, S., et al., *Downregulation of microRNA-155 accelerates cell growth and invasion by targeting c-myc in human gastric carcinoma cells*. Oncol Rep, 2014. **32**(3): p. 951-6.
270. Lin, F., et al., *Decrease expression of microRNA-744 promotes cell proliferation by targeting c-Myc in human hepatocellular carcinoma*. Cancer Cell Int, 2014. **14**: p. 58.
271. Yamamura, S., et al., *MicroRNA-34a modulates c-Myc transcriptional complexes to suppress malignancy in human prostate cancer cells*. PLoS One, 2012. **7**(1): p. e29722.
272. Li, Y., et al., *MicroRNA-130a associates with ribosomal protein L11 to suppress c-Myc expression in response to UV irradiation*. Oncotarget, 2015. **6**(2): p. 1101-14.
273. Yang, X., et al., *Inhibition of c-Myc by let-7b mimic reverses multidrug resistance in gastric cancer cells*. Oncol Rep, 2015. **33**(4): p. 1723-30.
274. Ting, Y., et al., *Differentiation-associated miR-22 represses Max expression and inhibits cell cycle progression*. Biochem Biophys Res Commun, 2010. **394**(3): p. 606-11.
275. Wang, F., et al., *miR-145 inhibits proliferation and invasion of esophageal squamous cell carcinoma in part by targeting c-Myc*. Onkologie, 2013. **36**(12): p. 754-8.

## REFERENCES

276. Lal, A., et al., *miR-24 Inhibits cell proliferation by targeting E2F2, MYC, and other cell-cycle genes via binding to "seedless" 3'UTR microRNA recognition elements.* Mol Cell, 2009. **35**(5): p. 610-25.
277. Liao, J.M. and H. Lu, *Autoregulatory suppression of c-Myc by miR-185-3p.* J Biol Chem, 2011. **286**(39): p. 33901-9.
278. Han, H., et al., *A c-Myc-MicroRNA functional feedback loop affects hepatocarcinogenesis.* Hepatology, 2013. **57**(6): p. 2378-89.
279. Xu, H., et al., *Liver-enriched transcription factors regulate microRNA-122 that targets CUTL1 during liver development.* Hepatology, 2010. **52**(4): p. 1431-42.
280. Coulouarn, C., et al., *Loss of miR-122 expression in liver cancer correlates with suppression of the hepatic phenotype and gain of metastatic properties.* Oncogene, 2009. **28**(40): p. 3526-36.
281. Wang, B., et al., *Reciprocal regulation of microRNA-122 and c-Myc in hepatocellular cancer: role of E2F1 and transcription factor dimerization partner 2.* Hepatology, 2014. **59**(2): p. 555-66.
282. O'Donnell, K.A., et al., *c-Myc-regulated microRNAs modulate E2F1 expression.* Nature, 2005. **435**(7043): p. 839-43.
283. Nadiminty, N., et al., *MicroRNA let-7c suppresses androgen receptor expression and activity via regulation of Myc expression in prostate cancer cells.* J Biol Chem, 2012. **287**(2): p. 1527-37.
284. Chang, T.C., et al., *Lin-28B transactivation is necessary for Myc-mediated let-7 repression and proliferation.* Proc Natl Acad Sci U S A, 2009. **106**(9): p. 3384-9.
285. Sampson, V.B., et al., *MicroRNA let-7a down-regulates MYC and reverts MYC-induced growth in Burkitt lymphoma cells.* Cancer Res, 2007. **67**(20): p. 9762-70.
286. He, L., et al., *A microRNA polycistron as a potential human oncogene.* Nature, 2005. **435**(7043): p. 828-33.
287. Bui, T.V. and J.T. Mendell, *Myc: Maestro of MicroRNAs.* Genes Cancer, 2010. **1**(6): p. 568-575.
288. Land, H., L.F. Parada, and R.A. Weinberg, *Tumorigenic conversion of primary embryo fibroblasts requires at least two cooperating oncogenes.* Nature, 1983. **304**(5927): p. 596-602.
289. Xu, X., et al., *miR-34a induces cellular senescence via modulation of telomerase activity in human hepatocellular carcinoma by targeting FoxM1/c-Myc pathway.* Oncotarget, 2015. **6**(6): p. 3988-4004.
290. Sachdeva, M., et al., *p53 represses c-Myc through induction of the tumor suppressor miR-145.* Proc Natl Acad Sci U S A, 2009. **106**(9): p. 3207-12.
291. Qian, J., et al., *The full-length transcripts and promoter analysis of intergenic microRNAs in Drosophila melanogaster.* Genomics, 2011. **97**(5): p. 294-303.
292. Schulte, J.H., et al., *MYCN regulates oncogenic MicroRNAs in neuroblastoma.* Int J Cancer, 2008. **122**(3): p. 699-704.
293. Aceto, N., et al., *Tyrosine phosphatase SHP2 promotes breast cancer progression and maintains tumor-initiating cells via activation of key transcription factors and a positive feedback signaling loop.* Nat Med, 2012. **18**(4): p. 529-37.
294. Chang, T.C., et al., *Widespread microRNA repression by Myc contributes to tumorigenesis.* Nat Genet, 2008. **40**(1): p. 43-50.
295. Sander, S., et al., *MYC stimulates EZH2 expression by repression of its negative regulator miR-26a.* Blood, 2008. **112**(10): p. 4202-12.
296. Koh, C.M., et al., *Myc enforces overexpression of EZH2 in early prostatic neoplasia via transcriptional and post-transcriptional mechanisms.* Oncotarget, 2011. **2**(9): p. 669-83.
297. Rothschild, S.I., et al., *MicroRNA-29b is involved in the Src-ID1 signaling pathway and is dysregulated in human lung adenocarcinoma.* Oncogene, 2012. **31**(38): p. 4221-32.
298. Lin, C.H., et al., *Myc-regulated microRNAs attenuate embryonic stem cell differentiation.* Embo j, 2009. **28**(20): p. 3157-70.
299. Zhang, L., et al., *microRNA-141 is involved in a nasopharyngeal carcinoma-related genes network.* Carcinogenesis, 2010. **31**(4): p. 559-66.

## REFERENCES

300. Khew-Goodall, Y. and G.J. Goodall, *Myc-modulated miR-9 makes more metastases*. Nat Cell Biol, 2010. **12**(3): p. 209-11.
301. Ma, L., et al., *miR-9, a MYC/MYCN-activated microRNA, regulates E-cadherin and cancer metastasis*. Nat Cell Biol, 2010. **12**(3): p. 247-56.
302. Greenwell, I.B., et al., *Clinical use of PI3K inhibitors in B-cell lymphoid malignancies: today and tomorrow*. Expert Rev Anticancer Ther, 2017. **17**(3): p. 271-279.
303. Staal, S.P., *Molecular cloning of the akt oncogene and its human homologues AKT1 and AKT2: amplification of AKT1 in a primary human gastric adenocarcinoma*. Proc Natl Acad Sci U S A, 1987. **84**(14): p. 5034-7.
304. Bellacosa, A., et al., *Molecular alterations of the AKT2 oncogene in ovarian and breast carcinomas*. Int J Cancer, 1995. **64**(4): p. 280-5.
305. Elstrom, R.L., et al., *Akt stimulates aerobic glycolysis in cancer cells*. Cancer Res, 2004. **64**(11): p. 3892-9.
306. Rathmell, J.C., et al., *Akt-directed glucose metabolism can prevent Bax conformation change and promote growth factor-independent survival*. Mol Cell Biol, 2003. **23**(20): p. 7315-28.
307. Roberts, D.J., et al., *Akt phosphorylates HK-II at Thr-473 and increases mitochondrial HK-II association to protect cardiomyocytes*. J Biol Chem, 2013. **288**(33): p. 23798-806.
308. Deprez, J., et al., *Phosphorylation and activation of heart 6-phosphofructo-2-kinase by protein kinase B and other protein kinases of the insulin signaling cascades*. J Biol Chem, 1997. **272**(28): p. 17269-75.
309. Zhang, W., et al., *FoxO1 regulates multiple metabolic pathways in the liver: effects on gluconeogenic, glycolytic, and lipogenic gene expression*. J Biol Chem, 2006. **281**(15): p. 10105-17.
310. Inoki, K., et al., *TSC2 is phosphorylated and inhibited by Akt and suppresses mTOR signalling*. Nat Cell Biol, 2002. **4**(9): p. 648-57.
311. Robey, R.B. and N. Hay, *Is Akt the "Warburg kinase"?-Akt-energy metabolism interactions and oncogenesis*. Semin Cancer Biol, 2009. **19**(1): p. 25-31.
312. Guo, C., et al., *The noncoding RNA, miR-126, suppresses the growth of neoplastic cells by targeting phosphatidylinositol 3-kinase signaling and is frequently lost in colon cancers*. Genes Chromosomes Cancer, 2008. **47**(11): p. 939-46.
313. Zhang, G.M., et al., *MicroRNA-302a Suppresses Tumor Cell Proliferation by Inhibiting AKT in Prostate Cancer*. PLoS One, 2015. **10**(4): p. e0124410.
314. Yan, B., et al., *Micro-ribonucleic acid 29b inhibits cell proliferation and invasion and enhances cell apoptosis and chemotherapy effects of cisplatin via targeting of DNMT3b and AKT3 in prostate cancer*. Onco Targets Ther, 2015. **8**: p. 557-65.
315. Noguchi, S., et al., *MicroRNA-143 functions as a tumor suppressor in human bladder cancer T24 cells*. Cancer Lett, 2011. **307**(2): p. 211-20.
316. Que, T., et al., *Decreased miRNA-637 is an unfavorable prognosis marker and promotes glioma cell growth, migration and invasion via direct targeting Akt1*. Oncogene, 2015. **0**.
317. Rathod, S.S., et al., *Tumor suppressive miRNA-34a suppresses cell proliferation and tumor growth of glioma stem cells by targeting Akt and Wnt signaling pathways*. FEBS Open Bio, 2014. **4**: p. 485-95.
318. Sarbassov, D.D., et al., *Phosphorylation and regulation of Akt/PKB by the rictor-mTOR complex*. Science, 2005. **307**(5712): p. 1098-101.
319. Iorio, M.V., et al., *microRNA-205 regulates HER3 in human breast cancer*. Cancer Res, 2009. **69**(6): p. 2195-200.
320. Hamano, R., et al., *Overexpression of miR-200c induces chemoresistance in esophageal cancers mediated through activation of the Akt signaling pathway*. Clin Cancer Res, 2011. **17**(9): p. 3029-38.
321. Al-Khalaf, H.H. and A. Aboussekhra, *MicroRNA-141 and microRNA-146b-5p inhibit the prometastatic mesenchymal characteristics through the RNA-binding protein AUF1 targeting the*

## REFERENCES

- transcription factor ZEB1 and the protein kinase AKT*. J Biol Chem, 2014. **289**(45): p. 31433-47.
322. Alessi, D.R., et al., *Characterization of a 3-phosphoinositide-dependent protein kinase which phosphorylates and activates protein kinase Balpha*. Curr Biol, 1997. **7**(4): p. 261-9.
323. Liao, Y. and M.C. Hung, *Physiological regulation of Akt activity and stability*. Am J Transl Res, 2010. **2**(1): p. 19-42.
324. Yuan, Y., et al., *Suppression of AKT expression by miR-153 produced anti-tumor activity in lung cancer*. Int J Cancer, 2015. **136**(6): p. 1333-40.
325. Wu, Z., et al., *Upregulation of miR-153 promotes cell proliferation via downregulation of the PTEN tumor suppressor gene in human prostate cancer*. Prostate, 2013. **73**(6): p. 596-604.
326. Zhou, X., et al., *MicroRNA-7 inhibits tumor metastasis and reverses epithelial-mesenchymal transition through AKT/ERK1/2 inactivation by targeting EGFR in epithelial ovarian cancer*. PLoS One, 2014. **9**(5): p. e96718.
327. Kefas, B., et al., *microRNA-7 inhibits the epidermal growth factor receptor and the Akt pathway and is down-regulated in glioblastoma*. Cancer Res, 2008. **68**(10): p. 3566-72.
328. Giles, K.M., et al., *MicroRNA regulation of growth factor receptor signaling in human cancer cells*. Methods Mol Biol, 2011. **676**: p. 147-63.
329. Cully, M., et al., *Beyond PTEN mutations: the PI3K pathway as an integrator of multiple inputs during tumorigenesis*. Nat Rev Cancer, 2006. **6**(3): p. 184-92.
330. Tumaneng, K., et al., *YAP mediates crosstalk between the Hippo and PI(3)K-TOR pathways by suppressing PTEN via miR-29*. Nat Cell Biol, 2012. **14**(12): p. 1322-9.
331. Huse, J.T., et al., *The PTEN-regulating microRNA miR-26a is amplified in high-grade glioma and facilitates gliomagenesis in vivo*. Genes Dev, 2009. **23**(11): p. 1327-37.
332. Small, E.M., et al., *Regulation of PI3-kinase/ Akt signaling by muscle-enriched microRNA-486*. Proc Natl Acad Sci U S A, 2010. **107**(9): p. 4218-23.
333. Li, Y.n., et al., *Sirt2 suppresses glioma cell growth through targeting NF- $\kappa$ B-miR-21 axis*. Biochemical and biophysical research communications, 2013. **441**(3): p. 661-667.
334. Palumbo, T., et al., *Functional screen analysis reveals miR-26b and miR-128 as central regulators of pituitary somatotroph tumor growth through activation of the PTEN-AKT pathway*. Oncogene, 2013. **32**(13): p. 1651-9.
335. Fornari, F., et al., *In hepatocellular carcinoma miR-519d is up-regulated by p53 and DNA hypomethylation and targets CDKN1A/p21, PTEN, AKT3 and TIMP2*. J Pathol, 2012. **227**(3): p. 275-85.
336. Yan, S.Y., et al., *MiR-32 induces cell proliferation, migration, and invasion in hepatocellular carcinoma by targeting PTEN*. Tumour Biol, 2015.
337. Zou, H., et al., *MicroRNA-29A/PTEN pathway modulates neurite outgrowth in PC12 cells*. Neuroscience, 2015. **291**: p. 289-300.
338. Kato, M., et al., *TGF-beta activates Akt kinase through a microRNA-dependent amplifying circuit targeting PTEN*. Nat Cell Biol, 2009. **11**(7): p. 881-9.
339. Fu, X., et al., *Involvement of microRNA-93, a new regulator of PTEN/ Akt signaling pathway, in regulation of chemotherapeutic drug cisplatin chemosensitivity in ovarian cancer cells*. FEBS Lett, 2012. **586**(9): p. 1279-86.
340. Yang, H., et al., *MicroRNA expression profiling in human ovarian cancer: miR-214 induces cell survival and cisplatin resistance by targeting PTEN*. Cancer Res, 2008. **68**(2): p. 425-33.
341. Xue, M., et al., *HIV-1 Nef and KSHV oncogene K1 synergistically promote angiogenesis by inducing cellular miR-718 to regulate the PTEN/ AKT/ mTOR signaling pathway*. Nucleic Acids Res, 2014. **42**(15): p. 9862-79.
342. Xie, Q., et al., *MicroRNA-221 targeting PI3-K/ Akt signaling axis induces cell proliferation and BCNU resistance in human glioblastoma*. Neuropathology, 2014. **34**(5): p. 455-64.
343. Wang, X., et al., *MicroRNA-494 targeting both proapoptotic and antiapoptotic proteins protects against ischemia/ reperfusion-induced cardiac injury*. Circulation, 2010. **122**(13): p. 1308-18.

## REFERENCES

344. Liu, L., et al., *Overexpressed miR-494 down-regulates PTEN gene expression in cells transformed by anti-benzo(a)pyrene-trans-7,8-dihydrodiol-9,10-epoxide*. Life Sci, 2010. **86**(5-6): p. 192-8.
345. Cioffi, J.A., et al., *MicroRNA-21 overexpression contributes to vestibular schwannoma cell proliferation and survival*. Otol Neurotol, 2010. **31**(9): p. 1455-62.
346. Qadir, X.V., et al., *miR-185 inhibits hepatocellular carcinoma growth by targeting the DNMT1/PTEN/Akt pathway*. Am J Pathol, 2014. **184**(8): p. 2355-64.
347. Glass, C. and D.K. Singla, *ES cells overexpressing microRNA-1 attenuate apoptosis in the injured myocardium*. Mol Cell Biochem, 2011. **357**(1-2): p. 135-41.
348. Sachdeva, M., et al., *MicroRNA-101-mediated Akt activation and estrogen-independent growth*. Oncogene, 2011. **30**(7): p. 822-31.
349. Zhu, G., et al., *Downregulated microRNA-32 expression induced by high glucose inhibits cell cycle progression via PTEN upregulation and Akt inactivation in bone marrow-derived mesenchymal stem cells*. Biochem Biophys Res Commun, 2013. **433**(4): p. 526-31.
350. Roccaro, A.M., et al., *microRNA expression in the biology, prognosis, and therapy of Waldenstrom macroglobulinemia*. Blood, 2009. **113**(18): p. 4391-402.
351. Kaper, F., N. Dornhoefer, and A.J. Giaccia, *Mutations in the PI3K/PTEN/TSC2 pathway contribute to mammalian target of rapamycin activity and increased translation under hypoxic conditions*. Cancer Res, 2006. **66**(3): p. 1561-9.
352. Moon, K.S., et al., *Cystic vestibular schwannomas: a possible role of matrix metalloproteinase-2 in cyst development and unfavorable surgical outcome*. J Neurosurg, 2007. **106**(5): p. 866-71.
353. Liu, Y., et al., *MicroRNA-494 is required for the accumulation and functions of tumor-expanded myeloid-derived suppressor cells via targeting of PTEN*. J Immunol, 2012. **188**(11): p. 5500-10.
354. Bai, H., et al., *Involvement of miR-21 in resistance to daunorubicin by regulating PTEN expression in the leukaemia K562 cell line*. FEBS Lett, 2011. **585**(2): p. 402-8.
355. Zhang, L., et al., *Microenvironment-induced PTEN loss by exosomal microRNA primes brain metastasis outgrowth*. Nature, 2015. **527**(7576): p. 100-104.
356. Guertin, D.A. and D.M. Sabatini, *Defining the role of mTOR in cancer*. Cancer Cell, 2007. **12**(1): p. 9-22.
357. Yecies, J.L. and B.D. Manning, *mTOR links oncogenic signaling to tumor cell metabolism*. J Mol Med (Berl), 2011. **89**(3): p. 221-8.
358. Brugarolas, J.B., et al., *TSC2 regulates VEGF through mTOR-dependent and -independent pathways*. Cancer Cell, 2003. **4**(2): p. 147-58.
359. Hay, N. and N. Sonenberg, *Upstream and downstream of mTOR*. Genes Dev, 2004. **18**(16): p. 1926-45.
360. Sun, Q., et al., *Mammalian target of rapamycin up-regulation of pyruvate kinase isoenzyme type M2 is critical for aerobic glycolysis and tumor growth*. Proc Natl Acad Sci U S A, 2011. **108**(10): p. 4129-34.
361. Zha, X., et al., *Lactate dehydrogenase B is critical for hyperactive mTOR-mediated tumorigenesis*. Cancer Res, 2011. **71**(1): p. 13-8.
362. Buller, C.L., et al., *A GSK-3/TSC2/mTOR pathway regulates glucose uptake and GLUT1 glucose transporter expression*. Am J Physiol Cell Physiol, 2008. **295**(3): p. C836-43.
363. Thomas, G.V., et al., *Hypoxia-inducible factor determines sensitivity to inhibitors of mTOR in kidney cancer*. Nat Med, 2006. **12**(1): p. 122-7.
364. Land, S.C. and A.R. Tee, *Hypoxia-inducible factor 1alpha is regulated by the mammalian target of rapamycin (mTOR) via an mTOR signaling motif*. J Biol Chem, 2007. **282**(28): p. 20534-43.
365. Sofer, A., et al., *Regulation of mTOR and cell growth in response to energy stress by REDD1*. Mol Cell Biol, 2005. **25**(14): p. 5834-45.
366. Li, Y., et al., *Bnip3 mediates the hypoxia-induced inhibition on mammalian target of rapamycin by interacting with Rheb*. J Biol Chem, 2007. **282**(49): p. 35803-13.

## REFERENCES

367. Connolly, E., et al., *Hypoxia inhibits protein synthesis through a 4E-BP1 and elongation factor 2 kinase pathway controlled by mTOR and uncoupled in breast cancer cells*. *Mol Cell Biol*, 2006. **26**(10): p. 3955-65.
368. Obre, E. and R. Rossignol, *Emerging concepts in bioenergetics and cancer research: metabolic flexibility, coupling, symbiosis, switch, oxidative tumors, metabolic remodeling, signaling and bioenergetic therapy*. *Int J Biochem Cell Biol*, 2015. **59**: p. 167-81.
369. Vadlakonda, L., et al., *The Paradox of Akt-mTOR Interactions*. *Front Oncol*, 2013. **3**: p. 165.
370. Sano, H., et al., *Rab10, a target of the AS160 Rab GAP, is required for insulin-stimulated translocation of GLUT4 to the adipocyte plasma membrane*. *Cell Metab*, 2007. **5**(4): p. 293-303.
371. Humphrey, S.J. and D.E. James, *Uncaging akt*. *Sci Signal*, 2012. **5**(223): p. pe20.
372. Kumar, A., et al., *Fat cell-specific ablation of rictor in mice impairs insulin-regulated fat cell and whole-body glucose and lipid metabolism*. *Diabetes*, 2010. **59**(6): p. 1397-406.
373. Wang, L., et al., *miR-99a and -99b inhibit cervical cancer cell proliferation and invasion by targeting mTOR signaling pathway*. *Med Oncol*, 2014. **31**(5): p. 934.
374. Torres, A., et al., *Deregulation of miR-100, miR-99a and miR-199b in tissues and plasma coexists with increased expression of mTOR kinase in endometrioid endometrial carcinoma*. *BMC Cancer*, 2012. **12**: p. 369.
375. Xu, C., et al., *miRNA-100 inhibits human bladder urothelial carcinogenesis by directly targeting mTOR*. *Mol Cancer Ther*, 2013. **12**(2): p. 207-19.
376. Sun, J., et al., *MicroRNA-99a/100 promotes apoptosis by targeting mTOR in human esophageal squamous cell carcinoma*. *Med Oncol*, 2013. **30**(1): p. 411.
377. Grundmann, S., et al., *MicroRNA-100 regulates neovascularization by suppression of mammalian target of rapamycin in endothelial and vascular smooth muscle cells*. *Circulation*, 2011. **123**(9): p. 999-1009.
378. Fang, Y., et al., *MicroRNA-7 inhibits tumor growth and metastasis by targeting the phosphoinositide 3-kinase/Akt pathway in hepatocellular carcinoma*. *Hepatology*, 2012. **55**(6): p. 1852-62.
379. Webster, R.J., et al., *Regulation of epidermal growth factor receptor signaling in human cancer cells by microRNA-7*. *J Biol Chem*, 2009. **284**(9): p. 5731-41.
380. Lin, S., et al., *Effect of microRNA-101 on proliferation and apoptosis of human osteosarcoma cells by targeting mTOR*. *J Huazhong Univ Sci Technolog Med Sci*, 2014. **34**(6): p. 889-95.
381. Chen, K., et al., *MicroRNA-101 mediates the suppressive effect of laminar shear stress on mTOR expression in vascular endothelial cells*. *Biochem Biophys Res Commun*, 2012. **427**(1): p. 138-42.
382. Liu, P. and M.J. Wilson, *miR-520c and miR-373 upregulate MMP9 expression by targeting mTOR and SIRT1, and activate the Ras/Raf/MEK/Erk signaling pathway and NF-kappaB factor in human fibrosarcoma cells*. *J Cell Physiol*, 2012. **227**(2): p. 867-76.
383. Vaksman, O., et al., *miRNA profiling along tumour progression in ovarian carcinoma*. *J Cell Mol Med*, 2011. **15**(7): p. 1593-602.
384. Du, J., et al., *MicroRNA-451 regulates stemness of side population cells via PI3K/Akt/mTOR signaling pathway in multiple myeloma*. *Oncotarget*, 2015.
385. Feng, Z. and A.J. Levine, *The regulation of energy metabolism and the IGF-1/mTOR pathways by the p53 protein*. *Trends Cell Biol*, 2010. **20**(7): p. 427-34.
386. Matoba, S., et al., *p53 regulates mitochondrial respiration*. *Science*, 2006. **312**(5780): p. 1650-3.
387. Kulawiec, M., V. Ayyasamy, and K.K. Singh, *p53 regulates mtDNA copy number and mitochekpoint pathway*. *J Carcinog*, 2009. **8**: p. 8.
388. Bourdon, A., et al., *Mutation of RRM2B, encoding p53-controlled ribonucleotide reductase (p53R2), causes severe mitochondrial DNA depletion*. *Nat Genet*, 2007. **39**(6): p. 776-80.
389. Liu, Y., et al., *Proline oxidase, a p53-induced gene, targets COX-2/PGE2 signaling to induce apoptosis and inhibit tumor growth in colorectal cancers*. *Oncogene*, 2008. **27**(53): p. 6729-37.
390. Suzuki, S., et al., *Phosphate-activated glutaminase (GLS2), a p53-inducible regulator of glutamine metabolism and reactive oxygen species*. *Proc Natl Acad Sci U S A*, 2010. **107**(16): p. 7461-6.

## REFERENCES

391. Chen, W., et al., *Direct interaction between Nrf2 and p21(Cip1/WAF1) upregulates the Nrf2-mediated antioxidant response.* Mol Cell, 2009. **34**(6): p. 663-73.
392. Ma, W., et al., *A pivotal role for p53: balancing aerobic respiration and glycolysis.* J Bioenerg Biomembr, 2007. **39**(3): p. 243-6.
393. Stambolic, V., et al., *Regulation of PTEN transcription by p53.* Mol Cell, 2001. **8**(2): p. 317-25.
394. Almeida, R., et al., *OCT-1 is over-expressed in intestinal metaplasia and intestinal gastric carcinomas and binds to, but does not transactivate, CDX2 in gastric cells.* J Pathol, 2005. **207**(4): p. 396-401.
395. Jiang, F., et al., *miR-222 regulates the cell biological behavior of oral squamous cell carcinoma by targeting PUMA.* Oncol Rep, 2014. **31**(3): p. 1255-62.
396. Li, J., et al., *miR-30 regulates mitochondrial fission through targeting p53 and the dynamin-related protein-1 pathway.* PLoS Genet, 2010. **6**(1): p. e1000795.
397. Bensaad, K., et al., *TIGAR, a p53-inducible regulator of glycolysis and apoptosis.* Cell, 2006. **126**(1): p. 107-20.
398. Green, D.R. and J.E. Chipuk, *p53 and metabolism: Inside the TIGAR.* Cell, 2006. **126**(1): p. 30-2.
399. Chen, S., et al., *MiR-144 inhibits proliferation and induces apoptosis and autophagy in lung cancer cells by targeting TIGAR.* Cell Physiol Biochem, 2015. **35**(3): p. 997-1007.
400. Chen, L., et al., *Proteolytic cleavage of the mdm2 oncoprotein during apoptosis.* J Biol Chem, 1997. **272**(36): p. 22966-73.
401. Ishimura, A., et al., *Jmjd2c histone demethylase enhances the expression of Mdm2 oncogene.* Biochem Biophys Res Commun, 2009. **389**(2): p. 366-71.
402. Xiao, J., et al., *miR-605 joins p53 network to form a p53:miR-605:Mdm2 positive feedback loop in response to stress.* EMBO J, 2011. **30**(3): p. 524-32.
403. Fortunato, O., et al., *Mir-660 is downregulated in lung cancer patients and its replacement inhibits lung tumorigenesis by targeting MDM2-p53 interaction.* Cell Death Dis, 2014. **5**: p. e1564.
404. Ren, Z.J., et al., *Mir-509-5p joins the Mdm2/p53 feedback loop and regulates cancer cell growth.* Cell Death Dis, 2014. **5**: p. e1387.
405. Avasarala, S., et al., *hsa-miR29b, a critical downstream target of non-canonical Wnt signaling, plays an anti-proliferative role in non-small cell lung cancer cells via targeting MDM2 expression.* Biol Open, 2013. **2**(7): p. 675-85.
406. Zhang, J., et al., *Loss of microRNA-143/145 disturbs cellular growth and apoptosis of human epithelial cancers by impairing the MDM2-p53 feedback loop.* Oncogene, 2013. **32**(1): p. 61-9.
407. Braun, C.J., et al., *p53-Responsive micrnas 192 and 215 are capable of inducing cell cycle arrest.* Cancer Res, 2008. **68**(24): p. 10094-104.
408. Suzuki, H.I., et al., *Modulation of microRNA processing by p53.* Nature, 2009. **460**(7254): p. 529-33.
409. Hu, W., et al., *Negative regulation of tumor suppressor p53 by microRNA miR-504.* Mol Cell, 2010. **38**(5): p. 689-99.
410. Wei, Q., et al., *MiR-17-5p targets TP53INP1 and regulates cell proliferation and apoptosis of cervical cancer cells.* IUBMB Life, 2012. **64**(8): p. 697-704.
411. Bommer, G.T., et al., *p53-mediated activation of miRNA34 candidate tumor-suppressor genes.* Curr Biol, 2007. **17**(15): p. 1298-307.
412. Raver-Shapira, N., et al., *Transcriptional activation of miR-34a contributes to p53-mediated apoptosis.* Mol Cell, 2007. **26**(5): p. 731-43.
413. Ma, S., et al., *miR-130b Promotes CD133(+) liver tumor-initiating cell growth and self-renewal via tumor protein 53-induced nuclear protein 1.* Cell Stem Cell, 2010. **7**(6): p. 694-707.
414. Gironella, M., et al., *Tumor protein 53-induced nuclear protein 1 expression is repressed by miR-155, and its restoration inhibits pancreatic tumor development.* Proc Natl Acad Sci U S A, 2007. **104**(41): p. 16170-5.
415. Jiang, F., et al., *MiR-125b promotes proliferation and migration of type II endometrial carcinoma cells through targeting TP53INP1 tumor suppressor in vitro and in vivo.* BMC Cancer, 2011. **11**: p. 425.

## REFERENCES

416. Saleh, A.D., et al., *Cellular stress induced alterations in microRNA let-7a and let-7b expression are dependent on p53*. PLoS One, 2011. **6**(10): p. e24429.
417. Ugalde, A.P., et al., *Aging and chronic DNA damage response activate a regulatory pathway involving miR-29 and p53*. Embo j, 2011. **30**(11): p. 2219-32.
418. Chang, C.J., et al., *p53 regulates epithelial-mesenchymal transition and stem cell properties through modulating miRNAs*. Nat Cell Biol, 2011. **13**(3): p. 317-23.
419. Kim, T., et al., *p53 regulates epithelial-mesenchymal transition through microRNAs targeting ZEB1 and ZEB2*. J Exp Med, 2011. **208**(5): p. 875-83.
420. He, L., et al., *A microRNA component of the p53 tumour suppressor network*. Nature, 2007. **447**(7148): p. 1130-4.
421. Georges, S.A., et al., *Coordinated regulation of cell cycle transcripts by p53-Inducible microRNAs, miR-192 and miR-215*. Cancer Res, 2008. **68**(24): p. 10105-12.
422. Nalls, D., et al., *Targeting epigenetic regulation of miR-34a for treatment of pancreatic cancer by inhibition of pancreatic cancer stem cells*. PLoS One, 2011. **6**(8): p. e24099.
423. Fujita, Y., et al., *Effects of miR-34a on cell growth and chemoresistance in prostate cancer PC3 cells*. Biochem Biophys Res Commun, 2008. **377**(1): p. 114-9.
424. Corney, D.C., et al., *MicroRNA-34b and MicroRNA-34c are targets of p53 and cooperate in control of cell proliferation and adhesion-independent growth*. Cancer Res, 2007. **67**(18): p. 8433-8.
425. Xiao, J., et al., *miR-605 joins p53 network to form a p53:miR-605:Mdm2 positive feedback loop in response to stress*. Embo j, 2011. **30**(3): p. 524-32.
426. Pichiorri, F., et al., *Downregulation of p53-inducible microRNAs 192, 194, and 215 impairs the p53/MDM2 autoregulatory loop in multiple myeloma development*. Cancer Cell, 2010. **18**(4): p. 367-81.
427. Bohlig, L., M. Friedrich, and K. Engeland, *p53 activates the PANK1/miRNA-107 gene leading to downregulation of CDK6 and p130 cell cycle proteins*. Nucleic Acids Res, 2011. **39**(2): p. 440-53.
428. Lavu, S., et al., *Sirtuins--novel therapeutic targets to treat age-associated diseases*. Nat Rev Drug Discov, 2008. **7**(10): p. 841-53.
429. Tanno, M., et al., *Nucleocytoplasmic shuttling of the NAD<sup>+</sup>-dependent histone deacetylase SIRT1*. J Biol Chem, 2007. **282**(9): p. 6823-32.
430. Canto, C., et al., *AMPK regulates energy expenditure by modulating NAD<sup>+</sup> metabolism and SIRT1 activity*. Nature, 2009. **458**(7241): p. 1056-60.
431. Rodgers, J.T., et al., *Nutrient control of glucose homeostasis through a complex of PGC-1alpha and SIRT1*. Nature, 2005. **434**(7029): p. 113-8.
432. Brunet, A., et al., *Stress-dependent regulation of FOXO transcription factors by the SIRT1 deacetylase*. Science, 2004. **303**(5666): p. 2011-5.
433. Jager, S., et al., *AMP-activated protein kinase (AMPK) action in skeletal muscle via direct phosphorylation of PGC-1alpha*. Proc Natl Acad Sci U S A, 2007. **104**(29): p. 12017-22.
434. Nemoto, S., M.M. Fergusson, and T. Finkel, *Nutrient availability regulates SIRT1 through a forkhead-dependent pathway*. Science, 2004. **306**(5704): p. 2105-8.
435. Xiong, S., et al., *FoxO1 mediates an autofeedback loop regulating SIRT1 expression*. J Biol Chem, 2011. **286**(7): p. 5289-99.
436. Chen, W.Y., et al., *Tumor suppressor HIC1 directly regulates SIRT1 to modulate p53-dependent DNA-damage responses*. Cell, 2005. **123**(3): p. 437-48.
437. Ferber, E.C., et al., *FOXO3a regulates reactive oxygen metabolism by inhibiting mitochondrial gene expression*. Cell Death Differ, 2012. **19**(6): p. 968-79.
438. Zhang, P., et al., *Tumor suppressor p53 cooperates with SIRT6 to regulate gluconeogenesis by promoting FoxO1 nuclear exclusion*. Proc Natl Acad Sci U S A, 2014. **111**(29): p. 10684-9.
439. Van Meter, M., et al., *SIRT6 represses LINE1 retrotransposons by ribosylating KAP1 but this repression fails with stress and age*. Nat Commun, 2014. **5**: p. 5011.

## REFERENCES

440. Masri, S., et al., *Partitioning circadian transcription by SIRT6 leads to segregated control of cellular metabolism*. Cell, 2014. **158**(3): p. 659-72.
441. Lerrer, B. and H.Y. Cohen, *The guardian: metabolic and tumour-suppressive effects of SIRT6*. Embo j, 2013. **32**(1): p. 7-8.
442. Yin, X., et al., *Overexpression of SIRT6 in the hippocampal CA1 impairs the formation of long-term contextual fear memory*. Sci Rep, 2016. **6**: p. 18982.
443. Mao, Z., et al., *SIRT6 promotes DNA repair under stress by activating PARP1*. Science, 2011. **332**(6036): p. 1443-6.
444. Zhong, L., et al., *The histone deacetylase Sirt6 regulates glucose homeostasis via Hif1alpha*. Cell, 2010. **140**(2): p. 280-93.
445. Zwaans, B.M. and D.B. Lombard, *Interplay between sirtuins, MYC and hypoxia-inducible factor in cancer-associated metabolic reprogramming*. Dis Model Mech, 2014. **7**(9): p. 1023-32.
446. Mostoslavsky, R., et al., *Genomic instability and aging-like phenotype in the absence of mammalian SIRT6*. Cell, 2006. **124**(2): p. 315-29.
447. Mikawa, T., et al., *Dysregulated glycolysis as an oncogenic event*. Cell Mol Life Sci, 2015.
448. Barber, M.F., et al., *SIRT7 links H3K18 deacetylation to maintenance of oncogenic transformation*. Nature, 2012. **487**(7405): p. 114-8.
449. Ford, E., et al., *Mammalian Sir2 homolog SIRT7 is an activator of RNA polymerase I transcription*. Genes Dev, 2006. **20**(9): p. 1075-80.
450. Vakhrusheva, O., et al., *Sirt7 increases stress resistance of cardiomyocytes and prevents apoptosis and inflammatory cardiomyopathy in mice*. Circ Res, 2008. **102**(6): p. 703-10.
451. Lee, J., et al., *A pathway involving farnesoid X receptor and small heterodimer partner positively regulates hepatic sirtuin 1 levels via microRNA-34a inhibition*. J Biol Chem, 2010. **285**(17): p. 12604-11.
452. Yamakuchi, M., M. Ferlito, and C.J. Lowenstein, *miR-34a repression of SIRT1 regulates apoptosis*. Proc Natl Acad Sci U S A, 2008. **105**(36): p. 13421-6.
453. Choi, S.E., et al., *Elevated microRNA-34a in obesity reduces NAD+ levels and SIRT1 activity by directly targeting NAMPT*. Aging Cell, 2013. **12**(6): p. 1062-72.
454. Xu, D., et al., *miR-22 represses cancer progression by inducing cellular senescence*. J Cell Biol, 2011. **193**(2): p. 409-24.
455. Shi, Y., et al., *MicroRNA-204 inhibits proliferation, migration, invasion and epithelial-mesenchymal transition in osteosarcoma cells via targeting Sirtuin 1*. Oncol Rep, 2015. **34**(1): p. 399-406.
456. Eades, G., et al., *miR-200a regulates SIRT1 expression and epithelial to mesenchymal transition (EMT)-like transformation in mammary epithelial cells*. J Biol Chem, 2011. **286**(29): p. 25992-6002.
457. Zhou, B., et al., *Downregulation of miR-181a upregulates sirtuin-1 (SIRT1) and improves hepatic insulin sensitivity*. Diabetologia, 2012. **55**(7): p. 2032-43.
458. Lovis, P., et al., *Alterations in microRNA expression contribute to fatty acid-induced pancreatic beta-cell dysfunction*. Diabetes, 2008. **57**(10): p. 2728-36.
459. Ramachandran, D., et al., *Sirt1 and mir-9 expression is regulated during glucose-stimulated insulin secretion in pancreatic beta-islets*. Febs j, 2011. **278**(7): p. 1167-74.
460. Pramanik, D., et al., *Restitution of tumor suppressor microRNAs using a systemic nanovector inhibits pancreatic cancer growth in mice*. Mol Cancer Ther, 2011. **10**(8): p. 1470-80.
461. Menghini, R., et al., *MicroRNA 217 modulates endothelial cell senescence via silent information regulator 1*. Circulation, 2009. **120**(15): p. 1524-32.
462. Li, N., et al., *Increased expression of miR-34a and miR-93 in rat liver during aging, and their impact on the expression of Mgst1 and Sirt1*. Mech Ageing Dev, 2011. **132**(3): p. 75-85.
463. Saunders, L.R., et al., *miRNAs regulate SIRT1 expression during mouse embryonic stem cell differentiation and in adult mouse tissues*. Aging (Albany NY), 2010. **2**(7): p. 415-31.
464. Zovoilis, A., et al., *microRNA-34c is a novel target to treat dementias*. Embo j, 2011. **30**(20): p. 4299-308.

## REFERENCES

465. Strum, J.C., et al., *MicroRNA 132 regulates nutritional stress-induced chemokine production through repression of SirT1*. Mol Endocrinol, 2009. **23**(11): p. 1876-84.
466. Zhu, H., et al., *MicroRNA-195 promotes palmitate-induced apoptosis in cardiomyocytes by down-regulating Sirt1*. Cardiovasc Res, 2011. **92**(1): p. 75-84.
467. Bou Kheir, T., et al., *miR-449 inhibits cell proliferation and is down-regulated in gastric cancer*. Mol Cancer, 2011. **10**: p. 29.
468. Davalos, A., et al., *miR-33a/b contribute to the regulation of fatty acid metabolism and insulin signaling*. Proc Natl Acad Sci U S A, 2011. **108**(22): p. 9232-7.
469. Najafi-Shoushtari, S.H., et al., *MicroRNA-33 and the SREBP host genes cooperate to control cholesterol homeostasis*. Science, 2010. **328**(5985): p. 1566-9.
470. Rayner, K.J., et al., *MiR-33 contributes to the regulation of cholesterol homeostasis*. Science, 2010. **328**(5985): p. 1570-3.
471. Sharma, A., et al., *The role of SIRT6 protein in aging and reprogramming of human induced pluripotent stem cells*. J Biol Chem, 2013. **288**(25): p. 18439-47.
472. Kim, J.K., et al., *Sirtuin7 oncogenic potential in human hepatocellular carcinoma and its regulation by the tumor suppressors MiR-125a-5p and MiR-125b*. Hepatology, 2013. **57**(3): p. 1055-67.
473. North, B.J., et al., *SIRT2 induces the checkpoint kinase BubR1 to increase lifespan*. Embo j, 2014. **33**(13): p. 1438-53.
474. Wang, F., et al., *SIRT2 deacetylates FOXO3a in response to oxidative stress and caloric restriction*. Aging Cell, 2007. **6**(4): p. 505-14.
475. Wang, F., et al., *Deacetylation of FOXO3 by SIRT1 or SIRT2 leads to Skp2-mediated FOXO3 ubiquitination and degradation*. Oncogene, 2012. **31**(12): p. 1546-57.
476. Black, J.C., et al., *The SIRT2 deacetylase regulates autoacetylation of p300*. Mol Cell, 2008. **32**(3): p. 449-55.
477. Rothgiesser, K.M., et al., *SIRT2 regulates NF-kappaB dependent gene expression through deacetylation of p65 Lys310*. J Cell Sci, 2010. **123**(Pt 24): p. 4251-8.
478. Kim, H.S., et al., *SIRT2 maintains genome integrity and suppresses tumorigenesis through regulating APC/C activity*. Cancer Cell, 2011. **20**(4): p. 487-99.
479. Jiang, W., et al., *Acetylation regulates gluconeogenesis by promoting PEPCK1 degradation via recruiting the UBR5 ubiquitin ligase*. Mol Cell, 2011. **43**(1): p. 33-44.
480. Xu, Y., et al., *Oxidative stress activates SIRT2 to deacetylate and stimulate phosphoglycerate mutase*. Cancer Res, 2014. **74**(13): p. 3630-42.
481. Wang, J.Y., et al., *Acupuncture may exert its therapeutic effect through microRNA-339/Sirt2/NFkappaB/FOXO1 axis*. Biomed Res Int, 2015. **2015**: p. 249013.
482. Crocco, P., et al., *Polymorphisms Falling Within Putative miRNA Target Sites in the 3'UTR Region of SIRT2 and DRD2 Genes Are Correlated With Human Longevity*. J Gerontol A Biol Sci Med Sci, 2016. **71**(5): p. 586-92.
483. Medina, P.P., M. Nolde, and F.J. Slack, *OncomiR addiction in an in vivo model of microRNA-21-induced pre-B-cell lymphoma*. Nature, 2010. **467**(7311): p. 86-90.
484. Vatrinet, R., et al., *Targeting respiratory complex I to prevent the Warburg effect*. Int J Biochem Cell Biol, 2015.
485. He, W., et al., *Mitochondrial sirtuins: regulators of protein acylation and metabolism*. Trends Endocrinol Metab, 2012. **23**(9): p. 467-76.
486. Schlicker, C., et al., *Substrates and regulation mechanisms for the human mitochondrial sirtuins Sirt3 and Sirt5*. J Mol Biol, 2008. **382**(3): p. 790-801.
487. Someya, S., et al., *Sirt3 mediates reduction of oxidative damage and prevention of age-related hearing loss under caloric restriction*. Cell, 2010. **143**(5): p. 802-12.
488. Jing, E., et al., *Sirtuin-3 (Sirt3) regulates skeletal muscle metabolism and insulin signaling via altered mitochondrial oxidation and reactive oxygen species production*. Proc Natl Acad Sci U S A, 2011. **108**(35): p. 14608-13.

## REFERENCES

489. Finley, L.W., et al., *SIRT3 opposes reprogramming of cancer cell metabolism through HIF1alpha destabilization*. *Cancer Cell*, 2011. **19**(3): p. 416-28.
490. Pellegrini, L., et al., *SIRT3 protects from hypoxia and staurosporine-mediated cell death by maintaining mitochondrial membrane potential and intracellular pH*. *Cell Death Differ*, 2012. **19**(11): p. 1815-25.
491. Sundaresan, N.R., et al., *Sirt3 blocks the cardiac hypertrophic response by augmenting Foxo3a-dependent antioxidant defense mechanisms in mice*. *J Clin Invest*, 2009. **119**(9): p. 2758-71.
492. Chen, Y., et al., *Tumour suppressor SIRT3 deacetylates and activates manganese superoxide dismutase to scavenge ROS*. *EMBO Rep*, 2011. **12**(6): p. 534-41.
493. Finley, L.W., et al., *Succinate dehydrogenase is a direct target of sirtuin 3 deacetylase activity*. *PLoS One*, 2011. **6**(8): p. e23295.
494. Ahn, B.H., et al., *A role for the mitochondrial deacetylase Sirt3 in regulating energy homeostasis*. *Proc Natl Acad Sci U S A*, 2008. **105**(38): p. 14447-52.
495. Nasrin, N., et al., *SIRT4 regulates fatty acid oxidation and mitochondrial gene expression in liver and muscle cells*. *J Biol Chem*, 2010. **285**(42): p. 31995-2002.
496. Zhang, X., et al., *miR-195 Regulates Myocardial SIRT3 Expression and Mitochondrial Enzyme Acetylation*. 2015, Am Heart Assoc.
497. Hodzic, M., Y. Naaldijk, and A. Stolzing, *Regulating aging in adult stem cells with microRNA*. *Z Gerontol Geriatr*, 2013. **46**(7): p. 629-34.
498. Poulsen, R.C., et al., *Cell differentiation versus cell death: extracellular glucose is a key determinant of cell fate following oxidative stress exposure*. *Cell Death Dis*, 2014. **5**: p. e1074.
499. Liang, D., et al., *Genetic variants in MicroRNA biosynthesis pathways and binding sites modify ovarian cancer risk, survival, and treatment response*. *Cancer Res*, 2010. **70**(23): p. 9765-76.
500. Slaby, O., et al., *Identification of microRNAs regulated by isothiocyanates and association of polymorphisms inside their target sites with risk of sporadic colorectal cancer*. *Nutr Cancer*, 2013. **65**(2): p. 247-54.
501. Johnson, S.M., et al., *RAS is regulated by the let-7 microRNA family*. *Cell*, 2005. **120**(5): p. 635-47.
502. Wang, X.R., et al., *Overexpressed let-7a inhibits glioma cell malignancy by directly targeting K-ras, independently of PTEN*. *Neuro Oncol*, 2013. **15**(11): p. 1491-501.
503. De Ruyck, K., et al., *A let-7 microRNA polymorphism in the KRAS 3'-UTR is prognostic in oropharyngeal cancer*. *Cancer Epidemiol*, 2014. **38**(5): p. 591-8.
504. Wang, Y., et al., *Lin28B facilitates the progression and metastasis of pancreatic ductal adenocarcinoma*. *Oncotarget*, 2017. **8**(36): p. 60414-60428.
505. Bhat-Nakshatri, P., et al., *Estradiol-regulated microRNAs control estradiol response in breast cancer cells*. *Nucleic Acids Res*, 2009. **37**(14): p. 4850-61.
506. Luan, W., et al., *PKM2 promotes glucose metabolism and cell growth in gliomas through a mechanism involving a let-7a/c-Myc/hnRNP A1 feedback loop*. *Oncotarget*, 2015. **6**(15): p. 13006-18.
507. Lu, L., et al., *Feedback circuitry via let-7c between lncRNA CCAT1 and c-Myc is involved in cigarette smoke extract-induced malignant transformation of HBE cells*. *Oncotarget*, 2017. **8**(12): p. 19285-19297.
508. Zhang, W.F., et al., *MicroRNA let-7g inhibited hypoxia-induced proliferation of PASMCs via G0/G1 cell cycle arrest by targeting c-myc*. *Life Sci*, 2017. **170**: p. 9-15.
509. Chen, X., et al., *miR-1, regulated by LMP1, suppresses tumour growth and metastasis by targeting K-ras in nasopharyngeal carcinoma*. *Int J Exp Pathol*, 2015. **96**(6): p. 427-32.
510. Koshizuka, K., et al., *Dual-receptor (EGFR and c-MET) inhibition by tumor-suppressive miR-1 and miR-206 in head and neck squamous cell carcinoma*. *J Hum Genet*, 2017. **62**(1): p. 113-121.
511. Chen, T., et al., *Insulin ameliorates miR-1-induced injury in H9c2 cells under oxidative stress via Akt activation*. *Mol Cell Biochem*, 2012. **369**(1-2): p. 167-74.
512. Zhang, B., et al., *MicroRNA 100 sensitizes luminal A breast cancer cells to paclitaxel treatment in part by targeting mTOR*. *Oncotarget*, 2016. **7**(5): p. 5702-14.

## REFERENCES

513. Tao, J., et al., *Distinct anti-oncogenic effect of various microRNAs in different mouse models of liver cancer*. *Oncotarget*, 2015. **6**(9): p. 6977-88.
514. Xu, X., C. Liu, and J. Bao, *Hypoxia-induced hsa-miR-101 promotes glycolysis by targeting TIGAR mRNA in clear cell renal cell carcinoma*. *Mol Med Rep*, 2017. **15**(3): p. 1373-1378.
515. Huang, S., et al., *miR-101 Enhances Cisplatin-Induced DNA Damage Through Decreasing Nicotinamide Adenine Dinucleotide Phosphate Levels by Directly Repressing Tp53-Induced Glycolysis and Apoptosis Regulator Expression in Prostate Cancer Cells*. *DNA Cell Biol*, 2017. **36**(4): p. 303-310.
516. Edatt, L., et al., *MicroRNA106a regulates matrix metalloprotease 9 in a sirtuin-1 dependent mechanism*. *J Cell Physiol*, 2018. **233**(1): p. 238-248.
517. Zhou, K., et al., *MicroRNA-106b promotes pituitary tumor cell proliferation and invasion through PI3K/AKT signaling pathway by targeting PTEN*. *Tumour Biol*, 2016. **37**(10): p. 13469-13477.
518. Li, N., et al., *MiR-106b and miR-93 regulate cell progression by suppression of PTEN via PI3K/Akt pathway in breast cancer*. *Cell Death Dis*, 2017. **8**(5): p. e2796.
519. Wang, P., et al., *MicroRNA-107-5p suppresses non-small cell lung cancer by directly targeting oncogene epidermal growth factor receptor*. *Oncotarget*, 2017. **8**(34): p. 57012-57023.
520. Bahena-Ocampo, I., et al., *miR-10b expression in breast cancer stem cells supports self-renewal through negative PTEN regulation and sustained AKT activation*. *EMBO Rep*, 2016. **17**(5): p. 648-58.
521. Zhang, B., et al., *MicroRNA-122a Regulates Zonulin by Targeting EGFR in Intestinal Epithelial Dysfunction*. *Cell Physiol Biochem*, 2017. **42**(2): p. 848-858.
522. Heyn, J., et al., *miR-124a and miR-155 enhance differentiation of regulatory T cells in patients with neuropathic pain*. *J Neuroinflammation*, 2016. **13**(1): p. 248.
523. Coppola, N., et al., *Lowered expression of microRNA-125a-5p in human hepatocellular carcinoma and up-regulation of its oncogenic targets sirtuin-7, matrix metalloproteinase-11, and c-Raf*. *Oncotarget*, 2017. **8**(15): p. 25289-25299.
524. Qin, Y., et al., *MicroRNA-125b inhibits lens epithelial cell apoptosis by targeting p53 in age-related cataract*. *Biochim Biophys Acta*, 2014. **1842**(12 Pt A): p. 2439-47.
525. Gordon, M.W., et al., *Regulation of p53-targeting microRNAs by polycyclic aromatic hydrocarbons: Implications in the etiology of multiple myeloma*. *Mol Carcinog*, 2014.
526. Le, M.T., et al., *Conserved regulation of p53 network dosage by microRNA-125b occurs through evolving miRNA-target gene pairs*. *PLoS Genet*, 2011. **7**(9): p. e1002242.
527. Le, M.T., et al., *MicroRNA-125b is a novel negative regulator of p53*. *Genes Dev*, 2009. **23**(7): p. 862-76.
528. Zhao, Y., X. Li, and S. Zhu, *rs78378222 polymorphism in the 3'-untranslated region of TP53 contributes to development of age-associated cataracts by modifying microRNA-125b-induced apoptosis of lens epithelial cells*. *Mol Med Rep*, 2016. **14**(3): p. 2305-10.
529. Han, J., et al., *Downregulation of MicroRNA-126 Contributes to Tumorigenesis of Squamous Tongue Cell Carcinoma via Targeting KRAS*. *Med Sci Monit*, 2016. **22**: p. 522-9.
530. Li, Y., et al., *MiR-126 Regulates the ERK Pathway via Targeting KRAS to Inhibit the Glioma Cell Proliferation and Invasion*. *Mol Neurobiol*, 2017. **54**(1): p. 137-145.
531. Tian, S., et al., *MicroRNA-1285 inhibits the expression of p53 by directly targeting its 3' untranslated region*. *Biochem Biophys Res Commun*, 2010. **396**(2): p. 435-9.
532. Liu, K., et al., *Down-Regulation of MiR-1294 is Related to Dismal Prognosis of Patients with Esophageal Squamous Cell Carcinoma through Elevating C-MYC Expression*. *Cell Physiol Biochem*, 2015. **36**(1): p. 100-10.
533. Liu, C., et al., *MicroRNA-1297 contributes to tumor growth of human breast cancer by targeting PTEN/PI3K/AKT signaling*. *Oncol Rep*, 2017. **38**(4): p. 2435-2443.
534. Chen, J., et al., *MicroRNA-130a promotes the metastasis and epithelial-mesenchymal transition of osteosarcoma by targeting PTEN*. *Oncol Rep*, 2016. **35**(6): p. 3285-92.

## REFERENCES

535. Lv, M., et al., *Genome-Wide Screen of miRNAs and Targeting mRNAs Reveals the Negatively Regulatory Effect of miR-130b-3p on PTEN by PI3K and Integrin beta1 Signaling Pathways in Bladder Carcinoma*. *Int J Mol Sci*, 2016. **18**(1).
536. Ye, L., et al., *MiR-130 exerts tumor suppressive function on the tumorigenesis of human non-small cell lung cancer by targeting PTEN*. *Am J Transl Res*, 2017. **9**(4): p. 1856-1865.
537. Li, Y., et al., *MicroRNA-132 cause apoptosis of glioma cells through blockade of the SREBP-1c metabolic pathway related to SIRT1*. *Biomed Pharmacother*, 2016. **78**: p. 177-84.
538. Gong, K., et al., *MiR-132 regulates osteogenic differentiation via downregulating Sirtuin1 in a peroxisome proliferator-activated receptor beta/delta-dependent manner*. *Biochem Biophys Res Commun*, 2016. **478**(1): p. 260-267.
539. Zhang, L., et al., *Upregulated miR-132 in Lgr5+ gastric cancer stem cell-like cells contributes to cisplatin-resistance via SIRT1/CREB/ABCG2 signaling pathway*. *Mol Carcinog*, 2017. **56**(9): p. 2022-2034.
540. Xiong, Y., et al., *Activation of sirtuin 1 by catalpol-induced down-regulation of microRNA-132 attenuates endoplasmic reticulum stress in colitis*. *Pharmacol Res*, 2017. **123**: p. 73-82.
541. Wei, W., et al., *LncRNA XIST Promotes Pancreatic Cancer Proliferation Through miR-133a/EGFR*. *J Cell Biochem*, 2017. **118**(10): p. 3349-3358.
542. Liu, X. and G. Li, *MicroRNA-133b inhibits proliferation and invasion of ovarian cancer cells through Akt and Erk1/2 inactivation by targeting epidermal growth factor receptor*. *Int J Clin Exp Pathol*, 2015. **8**(9): p. 10605-14.
543. Liu, Y., et al., *miR-134 Functions as a Tumor Suppressor in Cell Proliferation and Epithelial-to-Mesenchymal Transition by Targeting KRAS in Renal Cell Carcinoma Cells*. *DNA Cell Biol*, 2015.
544. Qin, Q., et al., *miR-134 inhibits non-small cell lung cancer growth by targeting the epidermal growth factor receptor*. *J Cell Mol Med*, 2016. **20**(10): p. 1974-83.
545. El-Daly, S.M., et al., *miRs-134 and -370 function as tumor suppressors in colorectal cancer by independently suppressing EGFR and PI3K signalling*. *Sci Rep*, 2016. **6**: p. 24720.
546. Yamada, Y., et al., *Tumor-suppressive microRNA-135a inhibits cancer cell proliferation by targeting the c-MYC oncogene in renal cell carcinoma*. *Cancer Sci*, 2013. **104**(3): p. 304-12.
547. Xu, B., et al., *hsa-miR-135a-1 inhibits prostate cancer cell growth and migration by targeting EGFR*. *Tumour Biol*, 2016. **37**(10): p. 14141-14151.
548. Zhang, Z., et al., *MicroRNA-137 inhibits growth of glioblastoma through EGFR suppression*. *Am J Transl Res*, 2017. **9**(3): p. 1492-1499.
549. Luo, Y., et al., *microRNA-137 is downregulated in thyroid cancer and inhibits proliferation and invasion by targeting EGFR*. *Tumour Biol*, 2016. **37**(6): p. 7749-55.
550. Xu, J., et al., *MiR-138 promotes smooth muscle cells proliferation and migration in db/db mice through down-regulation of SIRT1*. *Biochem Biophys Res Commun*, 2015. **463**(4): p. 1159-64.
551. Wang, B., et al., *MiR-138-5p promotes TNF-alpha-induced apoptosis in human intervertebral disc degeneration by targeting SIRT1 through PTEN/PI3K/Akt signaling*. *Exp Cell Res*, 2016. **345**(2): p. 199-205.
552. Tian, S., et al., *miR-138-5p suppresses autophagy in pancreatic cancer by targeting SIRT1*. *Oncotarget*, 2017. **8**(7): p. 11071-11082.
553. Yuan, Z., et al., *Suppressive effect of microRNA-138 on the proliferation and invasion of osteosarcoma cells via targeting SIRT1*. *Exp Ther Med*, 2017. **13**(6): p. 3417-3423.
554. Jin, Y.Y., et al., *Involvement of microRNA-141-3p in 5-fluorouracil and oxaliplatin chemo-resistance in esophageal cancer cells via regulation of PTEN*. *Mol Cell Biochem*, 2016. **422**(1-2): p. 161-170.
555. Neveu, P., et al., *MicroRNA profiling reveals two distinct p53-related human pluripotent stem cell states*. *Cell Stem Cell*, 2010. **7**(6): p. 671-81.
556. Zhou, X., et al., *MicroRNA-141-3p promotes glioma cell growth and temozolomide resistance by directly targeting p53*. *Oncotarget*, 2017. **8**(41): p. 71080-71094.

## REFERENCES

557. Yang, Y., et al., *MicroRNA-141 Targets Sirt1 and Inhibits Autophagy to Reduce HBV Replication*. Cell Physiol Biochem, 2017. **41**(1): p. 310-322.
558. Bai, X., et al., *MicroRNA-142-5p induces cancer stem cell-like properties of cutaneous squamous cell carcinoma via inhibiting PTEN*. J Cell Biochem, 2017.
559. Pekow, J., et al., *Tumor suppressors miR-143 and miR-145 and predicted target proteins API5, ERK5, K-RAS, and IRS-1 are differentially expressed in proximal and distal colon*. Am J Physiol Gastrointest Liver Physiol, 2015. **308**(3): p. G179-87.
560. Chen, X., et al., *Role of miR-143 targeting KRAS in colorectal tumorigenesis*. Oncogene, 2009. **28**(10): p. 1385-92.
561. Pichler, M., et al., *Down-regulation of KRAS-interacting miRNA-143 predicts poor prognosis but not response to EGFR-targeted agents in colorectal cancer*. Br J Cancer, 2012. **106**(11): p. 1826-32.
562. Zhang, L., et al., *MiRNA-143 mediates the proliferative signaling pathway of FSH and regulates estradiol production*. J Endocrinol, 2017. **234**(1): p. 1-14.
563. Zhang, H.B., et al., *miR-143 suppresses the proliferation of NSCLC cells by inhibiting the epidermal growth factor receptor*. Exp Ther Med, 2016. **12**(3): p. 1795-1802.
564. Xiao, J., et al., *miR-144 may regulate the proliferation, migration and invasion of trophoblastic cells through targeting PTEN in preeclampsia*. Biomed Pharmacother, 2017. **94**: p. 341-353.
565. Huo, F., et al., *MicroRNA-144-3p inhibits proliferation and induces apoptosis of human salivary adenoid carcinoma cells via targeting of mTOR*. Biotechnol Lett, 2016. **38**(3): p. 409-16.
566. Xiang, C., S.P. Cui, and Y. Ke, *MiR-144 inhibits cell proliferation of renal cell carcinoma by targeting MTOR*. J Huazhong Univ Sci Technolog Med Sci, 2016. **36**(2): p. 186-92.
567. Wang, Z., et al., *Hemoglobin enhances miRNA-144 expression and autophagic activation mediated inflammation of microglia via mTOR pathway*. Sci Rep, 2017. **7**(1): p. 11861.
568. Zhang, W., et al., *MicroRNA-145 function as a cell growth repressor by directly targeting c-Myc in human ovarian cancer*. Technol Cancer Res Treat, 2014. **13**(2): p. 161-8.
569. Shao, Y., et al., *MiR-145 inhibits oral squamous cell carcinoma (OSCC) cell growth by targeting c-Myc and Cdk6*. Cancer Cell Int, 2013. **13**(1): p. 51.
570. Masui, K., et al., *mTOR complex 2 controls glycolytic metabolism in glioblastoma through FoxO acetylation and upregulation of c-Myc*. Cell Metab, 2013. **18**(5): p. 726-39.
571. Cao, H., et al., *miR-148a suppresses human renal cell carcinoma malignancy by targeting AKT2*. Oncol Rep, 2017. **37**(1): p. 147-154.
572. Zhang, J.G., et al., *MiR-148b suppresses cell proliferation and invasion in hepatocellular carcinoma by targeting WNT1/beta-catenin pathway*. Sci Rep, 2015. **5**: p. 8087.
573. Zhang, Y., et al., *Comprehensive analysis of microRNA-regulated protein interaction network reveals the tumor suppressive role of microRNA-149 in human hepatocellular carcinoma via targeting AKT-mTOR pathway*. Mol Cancer, 2014. **13**: p. 253.
574. Lin, R.J., Y.C. Lin, and A.L. Yu, *miR-149\* induces apoptosis by inhibiting Akt1 and E2F1 in human cancer cells*. Mol Carcinog, 2010. **49**(8): p. 719-27.
575. Ghasemi, A., S. Fallah, and M. Ansari, *MicroRNA-149 is epigenetically silenced tumor-suppressive microRNA, involved in cell proliferation and downregulation of AKT1 and cyclin D1 in human glioblastoma multiforme*. Biochem Cell Biol, 2016. **94**(6): p. 569-576.
576. Zhang, N., X. Wei, and L. Xu, *miR-150 promotes the proliferation of lung cancer cells by targeting P53*. FEBS Lett, 2013. **587**(15): p. 2346-51.
577. Wang, S., et al., *MicroRNA 152 regulates hepatic glycogenesis by targeting PTEN*. Febs j, 2016. **283**(10): p. 1935-46.
578. Gu, S., et al., *miR-152 induces human dental pulp stem cell senescence by inhibiting SIRT7 expression*. FEBS Lett, 2016. **590**(8): p. 1123-31.
579. Forzati, F., et al., *miR-155 is positively regulated by CBX7 in mouse embryonic fibroblasts and colon carcinomas, and targets the KRAS oncogene*. BMC Cancer, 2017. **17**(1): p. 170.
580. Fu, X., et al., *MicroRNA-155-5p promotes hepatocellular carcinoma progression by suppressing PTEN through the PI3K/Akt pathway*. Cancer Sci, 2017. **108**(4): p. 620-631.

## REFERENCES

581. Yamanaka, Y., et al., *Aberrant overexpression of microRNAs activate AKT signaling via down-regulation of tumor suppressors in natural killer-cell lymphoma/leukemia*. *Blood*, 2009. **114**(15): p. 3265-75.
582. Yang, J., et al., *MiR-15a/16 deficiency enhances anti-tumor immunity of glioma-infiltrating CD8+ T cells through targeting mTOR*. *Int J Cancer*, 2017. **141**(10): p. 2082-2092.
583. Roccaro, A.M., et al., *MicroRNAs 15a and 16 regulate tumor proliferation in multiple myeloma*. *Blood*, 2009. **113**(26): p. 6669-80.
584. Zhu, L.P., et al., *MiR-15b-5p Regulates Collateral Artery Formation by Targeting AKT3 (Protein Kinase B-3)*. *Arterioscler Thromb Vasc Biol*, 2017. **37**(5): p. 957-968.
585. Lang, A., et al., *MicroRNA-15b regulates mitochondrial ROS production and the senescence-associated secretory phenotype through sirtuin 4/SIRT4*. *Aging (Albany NY)*, 2016. **8**(3): p. 484-505.
586. Samaraweera, L., B.A. Spengler, and R.A. Ross, *Reciprocal antagonistic regulation of N-myc mRNA by miR17 and the neuronal-specific RNA-binding protein HuD*. *Oncol Rep*, 2017. **38**(1): p. 545-550.
587. Tsang, W.P. and T.T. Kwok, *The miR-18a\* microRNA functions as a potential tumor suppressor by targeting on K-Ras*. *Carcinogenesis*, 2009. **30**(6): p. 953-9.
588. Rodriguez-Aguayo, C., et al., *Regulation of hnRNP A1 by microRNAs controls the miR-18a-K-RAS axis in chemotherapy-resistant ovarian cancer*. *Cell Discov*, 2017. **3**: p. 17029.
589. Zhang, X., et al., *STAT1 Inhibits MiR-181a Expression to Suppress Colorectal Cancer Cell Proliferation Through PTEN/Akt*. *J Cell Biochem*, 2017. **118**(10): p. 3435-3443.
590. Jiang, C., et al., *Triptolide inhibits the growth of osteosarcoma by regulating microRNA-181a via targeting PTEN gene in vivo and vitro*. *Tumour Biol*, 2017. **39**(4): p. 1010428317697556.
591. Shin, K.H., et al., *miR-181a shows tumor suppressive effect against oral squamous cell carcinoma cells by downregulating K-ras*. *Biochem Biophys Res Commun*, 2011. **404**(4): p. 896-902.
592. Wang, X.F., et al., *MiR-181d acts as a tumor suppressor in glioma by targeting K-ras and Bcl-2*. *J Cancer Res Clin Oncol*, 2012. **138**(4): p. 573-84.
593. Neu, J., et al., *miR-181a decelerates proliferation in cutaneous squamous cell carcinoma by targeting the proto-oncogene KRAS*. *PLoS One*, 2017. **12**(9): p. e0185028.
594. Huang, X., et al., *Targeting the RAS/MAPK pathway with miR-181a in acute myeloid leukemia*. *Oncotarget*, 2016. **7**(37): p. 59273-59286.
595. Chen, Y., et al., *MiR-181b modulates chemosensitivity of glioblastoma multiforme cells to temozolomide by targeting the epidermal growth factor receptor*. *J Neurooncol*, 2017. **133**(3): p. 477-485.
596. Zheng, J., et al., *Hepatic stellate cell is activated by microRNA-181b via PTEN/Akt pathway*. *Mol Cell Biochem*, 2015. **398**(1-2): p. 1-9.
597. Wang, Y., et al., *MiR-181b regulates steatosis in nonalcoholic fatty liver disease via targeting SIRT1*. *Biochem Biophys Res Commun*, 2017. **493**(1): p. 227-232.
598. Zhang, C., et al., *microRNA-1827 represses MDM2 to positively regulate tumor suppressor p53 and suppress tumorigenesis*. *Oncotarget*, 2016. **7**(8): p. 8783-96.
599. Xie, X., et al., *MicroRNA-183 Suppresses Neuropathic Pain and Expression of AMPA Receptors by Targeting mTOR/VEGF Signaling Pathway*. *Cell Physiol Biochem*, 2017. **41**(1): p. 181-192.
600. Liu, Z., et al., *Candidate tumour suppressor CCDC19 regulates miR-184 direct targeting of C-Myc thereby suppressing cell growth in non-small cell lung cancers*. *J Cell Mol Med*, 2014. **18**(8): p. 1667-79.
601. Zhen, Y., et al., *Tumor suppressor PDCD4 modulates miR-184-mediated direct suppression of C-MYC and BCL2 blocking cell growth and survival in nasopharyngeal carcinoma*. *Cell Death Dis*, 2013. **4**: p. e872.
602. Zhou, L., et al., *MicroRNA-185 induces potent autophagy via AKT signaling in hepatocellular carcinoma*. *Tumour Biol*, 2017. **39**(2): p. 1010428317694313.

## REFERENCES

603. Tsitoura, E., et al., *MiR-185/ AKT and miR-29a/ collagen 1a pathways are activated in IPF BAL cells*. *Oncotarget*, 2016. **7**(46): p. 74569-74581.
604. Li, S., et al., *MiR-185 acts as a tumor suppressor by targeting AKT1 in non-small cell lung cancer cells*. *Int J Clin Exp Pathol*, 2015. **8**(9): p. 11854-62.
605. Liu, L., et al., *Downregulation of miR-193a-3p inhibits cell growth and migration in renal cell carcinoma by targeting PTEN*. *Tumour Biol*, 2017. **39**(6): p. 1010428317711951.
606. Gastaldi, C., et al., *miR-193b/ 365a cluster controls progression of epidermal squamous cell carcinoma*. *Carcinogenesis*, 2014. **35**(5): p. 1110-20.
607. Seviour, E.G., et al., *Targeting KRas-dependent tumour growth, circulating tumour cells and metastasis in vivo by clinically significant miR-193a-3p*. *Oncogene*, 2017. **36**(10): p. 1339-1350.
608. Li, C., et al., *Downregulation of MicroRNA-193b-3p Promotes Autophagy and Cell Survival by Targeting TSC1/ mTOR Signaling in NSC-34 Cells*. *Front Mol Neurosci*, 2017. **10**: p. 160.
609. Wang, S.H., et al., *Long noncoding RNA H19 contributes to gallbladder cancer cell proliferation by modulated miR-194-5p targeting AKT2*. *Tumour Biol*, 2016. **37**(7): p. 9721-30.
610. Fiori, M.E., et al., *Antitumor effect of miR-197 targeting in p53 wild-type lung cancer*. *Cell Death Differ*, 2014. **21**(5): p. 774-82.
611. Li, Z., et al., *MicroRNA-199a induces differentiation of induced pluripotent stem cells into endothelial cells by targeting sirtuin 1*. *Mol Med Rep*, 2015. **12**(3): p. 3711-7.
612. Lin, N., et al., *microRNA-199a-5p mediates high glucose-induced reactive oxygen species production and apoptosis in INS-1 pancreatic beta-cells by targeting SIRT1*. *Eur Rev Med Pharmacol Sci*, 2017. **21**(5): p. 1091-1098.
613. Cao, Y., et al., *MicroRNA-dependent regulation of PTEN after arsenic trioxide treatment in bladder cancer cell line T24*. *Tumour Biol*, 2011. **32**(1): p. 179-88.
614. Zhao, D., et al., *MiR-19a regulates the cell growth and apoptosis of osteosarcoma stem cells by targeting PTEN*. *Tumour Biol*, 2017. **39**(5): p. 1010428317705341.
615. Zhang, X., et al., *MicroRNA-19a functions as an oncogene by regulating PTEN/ AKT/ pAKT pathway in myeloma*. *Leuk Lymphoma*, 2017. **58**(4): p. 932-940.
616. Fan, Y., et al., *miR-19b promotes tumor growth and metastasis via targeting TP53*. *RNA*, 2014. **20**(6): p. 765-72.
617. Huang, C., et al., *XLAP BIR domain suppresses miR-200a expression and subsequently promotes EGFR protein translation and anchorage-independent growth of bladder cancer cell*. *J Hematol Oncol*, 2017. **10**(1): p. 6.
618. Becker, L.E., et al., *The role of miR-200a in mammalian epithelial cell transformation*. *Carcinogenesis*, 2015. **36**(1): p. 2-12.
619. Uhlmann, S., et al., *miR-200bc/ 429 cluster targets PLCgamma1 and differentially regulates proliferation and EGF-driven invasion than miR-200a/ 141 in breast cancer*. *Oncogene*, 2010. **29**(30): p. 4297-306.
620. Song, C., et al., *miR-200c inhibits breast cancer proliferation by targeting KRAS*. *Oncotarget*, 2015. **6**(33): p. 34968-78.
621. Chen, P., et al., *MiR-200c is a cMyc-activated miRNA that promotes nasopharyngeal carcinoma by downregulating PTEN*. *Oncotarget*, 2017. **8**(3): p. 5206-5218.
622. Li, Y., et al., *MiR-200a acts as an oncogene in colorectal carcinoma by targeting PTEN*. *Exp Mol Pathol*, 2016. **101**(3): p. 308-313.
623. Yang, J.J., et al., *miR-200a controls hepatic stellate cell activation and fibrosis via SIRT1/ Notch1 signal pathway*. *Inflamm Res*, 2017. **66**(4): p. 341-352.
624. Cha, Y., et al., *Metabolic control of primed human pluripotent stem cell fate and function by the miR-200c-SIRT2 axis*. *Nat Cell Biol*, 2017. **19**(5): p. 445-456.
625. Wu, Y.H., et al., *A novel fine tuning scheme of miR-200c in modulating lung cell redox homeostasis*. *Free Radic Res*, 2017. **51**(6): p. 591-603.
626. Fu, H., et al., *MiRNA-200a induce cell apoptosis in renal cell carcinoma by directly targeting SIRT1*. *Mol Cell Biochem*, 2017.

## REFERENCES

627. Lohcharoenkal, W., et al., *MicroRNA-203 Inversely Correlates with Differentiation Grade, Targets c-MYC, and Functions as a Tumor Suppressor in cSCC*. *J Invest Dermatol*, 2016. **136**(12): p. 2485-2494.
628. Niu, B., et al., *miR-204 Regulates the Proliferation of Dairy Goat Spermatogonial Stem Cells via Targeting to Sirt1*. *Rejuvenation Res*, 2016. **19**(2): p. 120-30.
629. Jiang, G., et al., *miR-204-5p targeting SIRT1 regulates hepatocellular carcinoma progression*. *Cell Biochem Funct*, 2016. **34**(7): p. 505-510.
630. Li, J., et al., *Upregulation of MiR-205 transcriptionally suppresses SMAD4 and PTEN and contributes to human ovarian cancer progression*. *Sci Rep*, 2017. **7**: p. 41330.
631. Ren, J., et al., *MicroRNA-206 suppresses gastric cancer cell growth and metastasis*. *Cell Biosci*, 2014. **4**: p. 26.
632. Keklikoglou, I., et al., *MicroRNA-206 functions as a pleiotropic modulator of cell proliferation, invasion and lymphangiogenesis in pancreatic adenocarcinoma by targeting ANXA2 and KRAS genes*. *Oncogene*, 2014.
633. Lin, F., et al., *MiR-206 functions as a tumor suppressor and directly targets K-Ras in human oral squamous cell carcinoma*. *Onco Targets Ther*, 2014. **7**: p. 1583-91.
634. Wang, D., et al., *MicroRNA-20a participates in the aerobic exercise-based prevention of coronary artery disease by targeting PTEN*. *Biomed Pharmacother*, 2017. **95**: p. 756-763.
635. Qin, B., et al., *MiR-20b targets AKT3 and modulates vascular endothelial growth factor-mediated changes in diabetic retinopathy*. *Acta Biochim Biophys Sin (Shanghai)*, 2016. **48**(8): p. 732-40.
636. Wang, X., et al., *microRNA-20b contributes to high glucose-induced podocyte apoptosis by targeting SIRT7*. *Mol Med Rep*, 2017. **16**(4): p. 5667-5674.
637. Hatley, M.E., et al., *Modulation of K-Ras-dependent lung tumorigenesis by MicroRNA-21*. *Cancer Cell*, 2010. **18**(3): p. 282-93.
638. Zhang, J., et al., *Abnormal Expression of miR-21 and miR-95 in Cancer Stem-Like Cells is Associated with Radioreistance of Lung Cancer*. *Cancer Invest*, 2015.
639. Dey, N., et al., *MicroRNA-21 orchestrates high glucose-induced signals to TOR complex 1, resulting in renal cell pathology in diabetes*. *J Biol Chem*, 2011. **286**(29): p. 25586-603.
640. Liu, C., et al., *MicroRNA-21 acts as an oncomir through multiple targets in human hepatocellular carcinoma*. *J Hepatol*, 2010. **53**(1): p. 98-107.
641. Zhou, X., et al., *Downregulation of miR-21 inhibits EGFR pathway and suppresses the growth of human glioblastoma cells independent of PTEN status*. *Lab Invest*, 2010. **90**(2): p. 144-55.
642. Tao, J., et al., *microRNA-21 modulates cell proliferation and sensitivity to doxorubicin in bladder cancer cells*. *Oncol Rep*, 2011. **25**(6): p. 1721-9.
643. Zhang, Z., et al., *MicroRNA miR-210 modulates cellular response to hypoxia through the MYC antagonist MNT*. *Cell Cycle*, 2009. **8**(17): p. 2756-68.
644. Ramalinga, M., et al., *MicroRNA-212 negatively regulates starvation induced autophagy in prostate cancer cells by inhibiting SIRT1 and is a modulator of angiogenesis and cellular senescence*. *Oncotarget*, 2015. **6**(33): p. 34446-57.
645. Li, Q.Q., et al., *Sulforaphane inhibits cancer stem-like cell properties and cisplatin resistance through miR-214-mediated downregulation of c-MYC in non-small cell lung cancer*. *Oncotarget*, 2017. **8**(7): p. 12067-12080.
646. Wang, F., et al., *MicroRNA-214 acts as a potential oncogene in breast cancer by targeting the PTEN-PI3K/Akt signaling pathway*. *Int J Mol Med*, 2016. **37**(5): p. 1421-8.
647. Xu, C.X., et al., *MicroRNA miR-214 regulates ovarian cancer cell stemness by targeting p53/Nanog*. *J Biol Chem*, 2012. **287**(42): p. 34970-8.
648. Wang, F., et al., *microRNA-214 enhances the invasion ability of breast cancer cells by targeting p53*. *Int J Mol Med*, 2015. **35**(5): p. 1395-402.
649. Zhang, J., et al., *Transforming growth factor (TGF)-beta-induced microRNA-216a promotes acute pancreatitis via Akt and TGF-beta pathway in mice*. *Dig Dis Sci*, 2015. **60**(1): p. 127-35.

## REFERENCES

650. Liu, H., et al., *MicroRNA-216a promotes the metastasis and epithelial-mesenchymal transition of ovarian cancer by suppressing the PTEN/AKT pathway*. *Onco Targets Ther*, 2017. **10**: p. 2701-2709.
651. Deng, M., et al., *miR-216b suppresses tumor growth and invasion by targeting KRAS in nasopharyngeal carcinoma*. *J Cell Sci*, 2011. **124**(Pt 17): p. 2997-3005.
652. Zhao, W.G., et al., *The miR-217 microRNA functions as a potential tumor suppressor in pancreatic ductal adenocarcinoma by targeting KRAS*. *Carcinogenesis*, 2010. **31**(10): p. 1726-33.
653. Guo, J., et al., *MicroRNA-217 functions as a tumour suppressor gene and correlates with cell resistance to cisplatin in lung cancer*. *Mol Cells*, 2014. **37**(9): p. 664-71.
654. Sun, J., et al., *Repression of miR-217 protects against high glucose-induced podocyte injury and insulin resistance by restoring PTEN-mediated autophagy pathway*. *Biochem Biophys Res Commun*, 2017. **483**(1): p. 318-324.
655. Zhu, K., et al., *Tumor-suppressive miR-218-5p inhibits cancer cell proliferation and migration via EGFR in non-small cell lung cancer*. *Oncotarget*, 2016. **7**(19): p. 28075-85.
656. Guan, B., et al., *Tumor-suppressive microRNA-218 inhibits tumor angiogenesis via targeting the mTOR component RICTOR in prostate cancer*. *Oncotarget*, 2017. **8**(5): p. 8162-8172.
657. Bar, N. and R. Dikstein, *miR-22 forms a regulatory loop in PTEN/AKT pathway and modulates signaling kinetics*. *PLoS One*, 2010. **5**(5): p. e10859.
658. Fan, W., et al., *MicroRNA-22 is downregulated in clear cell renal cell carcinoma, and inhibits cell growth, migration and invasion by targeting PTEN*. *Mol Med Rep*, 2016. **13**(6): p. 4800-6.
659. Zhang, S., et al., *MicroRNA-22 functions as a tumor suppressor by targeting SIRT1 in renal cell carcinoma*. *Oncol Rep*, 2016. **35**(1): p. 559-67.
660. Chen, H., et al., *miR-22 inhibits the proliferation, motility, and invasion of human glioblastoma cells by directly targeting SIRT1*. *Tumour Biol*, 2016. **37**(5): p. 6761-8.
661. Du, J.K., et al., *Upregulation of microRNA-22 contributes to myocardial ischemia-reperfusion injury by interfering with the mitochondrial function*. *Free Radic Biol Med*, 2016. **96**: p. 406-17.
662. Zhang, C., et al., *MicroRNA-221 and -222 regulate radiation sensitivity by targeting the PTEN pathway*. *Int J Radiat Oncol Biol Phys*, 2011. **80**(1): p. 240-8.
663. Amankwatia, E.B., et al., *MicroRNA-224 is associated with colorectal cancer progression and response to 5-fluorouracil-based chemotherapy by KRAS-dependent and -independent mechanisms*. *Br J Cancer*, 2015. **112**(9): p. 1480-90.
664. Zhang, Y., et al., *MicroRNA-224 aggravates tumor growth and progression by targeting mTOR in gastric cancer*. *Int J Oncol*, 2016. **49**(3): p. 1068-80.
665. Wang, S., W. He, and C. Wang, *MiR-23a Regulates the Vasculogenesis of Coronary Artery Disease by Targeting Epidermal Growth Factor Receptor*. *Cardiovasc Ther*, 2016. **34**(4): p. 199-208.
666. Zhao, S., et al., *miR-23b-3p induces the cellular metabolic memory of high glucose in diabetic retinopathy through a SIRT1-dependent signalling pathway*. *Diabetologia*, 2016. **59**(3): p. 644-54.
667. Lee, S.H., et al., *A feedback loop comprising PRMT7 and miR-24-2 interplays with Oct4, Nanog, Klf4 and c-Myc to regulate stemness*. *Nucleic Acids Res*, 2016. **44**(22): p. 10603-10618.
668. Chen, L., et al., *MicroRNA-24 increases hepatocellular carcinoma cell metastasis and invasion by targeting p53: miR-24 targeted p53*. *Biomed Pharmacother*, 2016. **84**: p. 1113-1118.
669. Li, H., et al., *MicroRNA-25 inhibits high glucose-induced apoptosis in renal tubular epithelial cells via PTEN/AKT pathway*. *Biomed Pharmacother*, 2017. **96**: p. 471-479.
670. Kumar, M., et al., *Negative regulation of the tumor suppressor p53 gene by microRNAs*. *Oncogene*, 2011. **30**(7): p. 843-53.
671. Zhu, L., et al., *microRNA-27a functions as a tumor suppressor in esophageal squamous cell carcinoma by targeting KRAS*. *Oncol Rep*, 2014. **31**(1): p. 280-6.
672. Maqbool, R., S.N. Lone, and M. Ul Hussain, *Post-transcriptional regulation of the tumor suppressor p53 by a novel miR-27a, with implications during hypoxia and tumorigenesis*. *Biochem J*, 2016. **473**(20): p. 3597-3610.

## REFERENCES

673. Chen, S., et al., *MicroRNA-27b reverses docetaxel resistance of non-small cell lung carcinoma cells via targeting epithelial growth factor receptor*. Mol Med Rep, 2016. **14**(1): p. 949-54.
674. Wang, J., et al., *MiR-29a Regulates Radiosensitivity in Human Intestinal Cells by Targeting PTEN Gene*. Radiat Res, 2016. **186**(3): p. 292-301.
675. Zhang, H., et al., *MicroRNA-29s could target AKT2 to inhibit gastric cancer cells invasion ability*. Med Oncol, 2015. **32**(1): p. 342.
676. Li, Y., et al., *MiRNA-29b suppresses tumor growth through simultaneously inhibiting angiogenesis and tumorigenesis by targeting Akt3*. Cancer Lett, 2017. **397**: p. 111-119.
677. Bhardwaj, A., et al., *Regulation of miRNA-29c and its downstream pathways in preneoplastic progression of triple-negative breast cancer*. Oncotarget, 2017. **8**(12): p. 19645-19660.
678. He, J., et al., *miR-300 regulates cellular radiosensitivity through targeting p53 and apaf1 in human lung cancer cells*. Cell Cycle, 2017. **16**(20): p. 1943-1953.
679. Wang, L. and P. Yu, *miR-300 promotes proliferation and EMT-mediated colorectal cancer migration and invasion by targeting p53*. Oncol Rep, 2016. **36**(6): p. 3225-3232.
680. Xia, X., et al., *Downregulation of miR-301a-3p sensitizes pancreatic cancer cells to gemcitabine treatment via PTEN*. Am J Transl Res, 2017. **9**(4): p. 1886-1895.
681. Cui, L., et al., *Expression of MicroRNA-301a and its Functional Roles in Malignant Melanoma*. Cell Physiol Biochem, 2016. **40**(1-2): p. 230-244.
682. Liao, W.T., et al., *MicroRNA-30b functions as a tumour suppressor in human colorectal cancer by targeting KRAS, PIK3CD and BCL2*. J Pathol, 2014. **232**(4): p. 415-27.
683. Tanic, M., et al., *Deregulated miRNAs in hereditary breast cancer revealed a role for miR-30c in regulating KRAS oncogene*. PLoS One, 2012. **7**(6): p. e38847.
684. Nakayama, T., M. Funakoshi-Tago, and H. Tamura, *Coffee reduces KRAS expression in Caco-2 human colon carcinoma cells via regulation of miRNAs*. Oncol Lett, 2017. **14**(1): p. 1109-1114.
685. Creighton, C.J., et al., *Molecular profiling uncovers a p53-associated role for microRNA-31 in inhibiting the proliferation of serous ovarian carcinomas and other cancers*. Cancer Res, 2010. **70**(5): p. 1906-15.
686. Lankenau, M.A., et al., *MicroRNA-3151 inactivates TP53 in BRAF-mutated human malignancies*. Proc Natl Acad Sci U S A, 2015. **112**(49): p. E6744-51.
687. Xie, F., et al., *miRNA-320a inhibits tumor proliferation and invasion by targeting c-Myc in human hepatocellular carcinoma*. Onco Targets Ther, 2017. **10**: p. 885-894.
688. Herrera-Merchan, A., et al., *miR-33-mediated downregulation of p53 controls hematopoietic stem cell self-renewal*. Cell Cycle, 2010. **9**(16): p. 3277-85.
689. Cai, Y., et al., *Upregulation of microRNA337 promotes the proliferation of endometrial carcinoma cells via targeting PTEN*. Mol Med Rep, 2016. **13**(6): p. 4827-34.
690. Han, J., et al., *miR-338-3p confers 5-fluorouracil resistance in p53 mutant colon cancer cells by targeting the mammalian target of rapamycin*. Exp Cell Res, 2017.
691. Jansson, M.D., et al., *miR-339-5p regulates the p53 tumor-suppressor pathway by targeting MDM2*. Oncogene, 2015. **34**(15): p. 1908-18.
692. Huang, K., et al., *MicroRNA-340 inhibits prostate cancer cell proliferation and metastasis by targeting the MDM2-p53 pathway*. Oncol Rep, 2016. **35**(2): p. 887-95.
693. Yamamura, S., et al., *MicroRNA-34a suppresses malignant transformation by targeting c-Myc transcriptional complexes in human renal cell carcinoma*. Carcinogenesis, 2012. **33**(2): p. 294-300.
694. Li, Y.L., et al., *MicroRNA-34a/EGFR axis plays pivotal roles in lung tumorigenesis*. Oncogenesis, 2017. **6**(8): p. e372.
695. Akao, Y., et al., *Dysregulation of microRNA-34a expression causes drug-resistance to 5-FU in human colon cancer DLD-1 cells*. Cancer Lett, 2011. **300**(2): p. 197-204.
696. Wang, G., et al., *miR-34a-5p Inhibition Alleviates Intestinal Ischemia/Reperfusion-Induced Reactive Oxygen Species Accumulation and Apoptosis via Activation of SIRT1 Signaling*. Antioxid Redox Signal, 2016. **24**(17): p. 961-73.

## REFERENCES

697. Castro, R.E., et al., *miR-34a/SIRT1/p53 is suppressed by ursodeoxycholic acid in the rat liver and activated by disease severity in human non-alcoholic fatty liver disease*. J Hepatol, 2013. **58**(1): p. 119-25.
698. Chen, Y., et al., *MicroRNA 363 mediated positive regulation of c-myc translation affect prostate cancer development and progress*. Neoplasia, 2015. **62**(2): p. 191-8.
699. Li, D. and L. Li, *MicroRNA3666 inhibits breast cancer cell proliferation by targeting sirtuin 7*. Mol Med Rep, 2017.
700. Xu, J., et al., *The miR-367-3p Increases Sorafenib Chemotherapy Efficacy to Suppress Hepatocellular Carcinoma Metastasis through Altering the Androgen Receptor Signals*. EBioMedicine, 2016. **12**: p. 55-67.
701. Ning, T., et al., *miR-370 regulates cell proliferation and migration by targeting EGFR in gastric cancer*. Oncol Rep, 2017. **38**(1): p. 384-392.
702. Zeng, Y., et al., *Upregulation of microRNA-370 promotes cell apoptosis and inhibits proliferation by targeting PTEN in human gastric cancer*. Int J Oncol, 2016. **49**(4): p. 1589-99.
703. Wu, D., et al., *MicroRNA-379-5p plays a tumor-suppressive role in human bladder cancer growth and metastasis by directly targeting MDM2*. Oncol Rep, 2017. **37**(6): p. 3502-3508.
704. Peng, F., et al., *Isoliquiritigenin modulates miR-374a/PTEN/Akt axis to suppress breast cancer tumorigenesis and metastasis*. Sci Rep, 2017. **7**(1): p. 9022.
705. Peng, J., et al., *MiR-377 promotes white adipose tissue inflammation and decreases insulin sensitivity in obesity via suppression of sirtuin-1 (SIRT1)*. Oncotarget, 2017. **8**(41): p. 70550-70563.
706. Feng, M., et al., *Myc/miR-378/TOB2/cyclin D1 functional module regulates oncogenic transformation*. Oncogene, 2011. **30**(19): p. 2242-51.
707. Swarbrick, A., et al., *miR-380-5p represses p53 to control cellular survival and is associated with poor outcome in MYCN-amplified neuroblastoma*. Nat Med, 2010. **16**(10): p. 1134-40.
708. Wang, Y.X., et al., *MiR-384 inhibits human colorectal cancer metastasis by targeting KRAS and CDC42*. Oncotarget, 2016. **7**(51): p. 84826-84838.
709. Zhang, G., et al., *miR-409-3p suppresses breast cancer cell growth and invasion by targeting Akt1*. Biochem Biophys Res Commun, 2016. **469**(2): p. 189-95.
710. Cheng, Y., et al., *MicroRNA-421 induces hepatic mitochondrial dysfunction in non-alcoholic fatty liver disease mice by inhibiting sirtuin 3*. Biochem Biophys Res Commun, 2016. **474**(1): p. 57-63.
711. Sun, T., et al., *miR-429 modulates the expression of c-myc in human gastric carcinoma cells*. Eur J Cancer, 2011. **47**(17): p. 2552-9.
712. Yao, Y., et al., *MiR-449a exerts tumor-suppressive functions in human glioblastoma by targeting Myc-associated zinc-finger protein*. Mol Oncol, 2015. **9**(3): p. 640-56.
713. Li, Q., et al., *DNA Methylation Mediated Downregulation of miR-449c Controls Osteosarcoma Cell Cycle Progression by Directly Targeting Oncogene c-Myc*. Int J Biol Sci, 2017. **13**(8): p. 1038-1050.
714. Mao, A., et al., *MicroRNA-449a enhances radiosensitivity by downregulation of c-Myc in prostate cancer cells*. Sci Rep, 2016. **6**: p. 27346.
715. Chen, D., et al., *MicroRNA-451 induces epithelial-mesenchymal transition in docetaxel-resistant lung adenocarcinoma cells by targeting proto-oncogene c-Myc*. Eur J Cancer, 2014. **50**(17): p. 3050-67.
716. Wang, R., et al., *Acquisition of radioresistance in docetaxel-resistant human lung adenocarcinoma cells is linked with dysregulation of miR-451/c-Myc-survivin/rad-51 signaling*. Oncotarget, 2014. **5**(15): p. 6113-29.
717. Zeng, Z., et al., *Down-regulation of microRNA-451a facilitates the activation and proliferation of CD4+ T cells by targeting Myc in patients with dilated cardiomyopathy*. J Biol Chem, 2017. **292**(14): p. 6004-6013.
718. Wang, J., et al., *miR-451 suppresses bladder cancer cell migration and invasion via directly targeting c-Myc*. Oncol Rep, 2016. **36**(4): p. 2049-58.
719. Bian, H.B., et al., *Upregulation of microRNA-451 increases cisplatin sensitivity of non-small cell lung cancer cell line (A549)*. J Exp Clin Cancer Res, 2011. **30**: p. 20.

## REFERENCES

720. Nan, Y., et al., *MiRNA-451 plays a role as tumor suppressor in human glioma cells*. Brain Res, 2010. **1359**: p. 14-21.
721. Song, L., et al., *MiR-451 is decreased in hypertrophic cardiomyopathy and regulates autophagy by targeting TSC1*. J Cell Mol Med, 2014. **18**(11): p. 2266-74.
722. Zhang, S., et al., *miR-98 regulates cisplatin-induced A549 cell death by inhibiting TP53 pathway*. Biomed Pharmacother, 2011. **65**(6): p. 436-42.
723. Nip, H., et al., *Oncogenic microRNA-4534 regulates PTEN pathway in prostate cancer*. Oncotarget, 2016. **7**(42): p. 68371-68384.
724. Zhu, D.Y., et al., *MiR-454 promotes the progression of human non-small cell lung cancer and directly targets PTEN*. Biomed Pharmacother, 2016. **81**: p. 79-85.
725. Borzi, C., et al., *mir-660-p53-mir-486 Network: A New Key Regulatory Pathway in Lung Tumorigenesis*. Int J Mol Sci, 2017. **18**(1).
726. Shi, X.F., et al., *Exosomal miR-486 regulates hypoxia-induced erythroid differentiation of erythroleukemia cells through targeting Sirt1*. Exp Cell Res, 2017. **351**(1): p. 74-81.
727. Guo, R., et al., *MicroRNA miR-491-5p targeting both TP53 and Bcl-XL induces cell apoptosis in SW1990 pancreatic cancer cells through mitochondria mediated pathway*. Molecules, 2012. **17**(12): p. 14733-47.
728. Jiang, J., et al., *MicroRNA-492 expression promotes the progression of hepatic cancer by targeting PTEN*. Cancer Cell Int, 2014. **14**(1): p. 95.
729. Yuan, J., K. Wang, and M. Xi, *MiR-494 Inhibits Epithelial Ovarian Cancer Growth by Targeting c-Myc*. Med Sci Monit, 2016. **22**: p. 617-24.
730. He, W., et al., *miR-494 acts as an anti-oncogene in gastric carcinoma by targeting c-myc*. J Gastroenterol Hepatol, 2014. **29**(7): p. 1427-34.
731. Yang, Y.K., et al., *MicroRNA494 promotes cervical cancer proliferation through the regulation of PTEN*. Oncol Rep, 2015. **33**(5): p. 2393-401.
732. Liu, Y., et al., *Ectopic expression of miR-494 inhibited the proliferation, invasion and chemoresistance of pancreatic cancer by regulating SIRT1 and c-Myc*. Gene Ther, 2015. **22**(9): p. 729-38.
733. Yang, A., et al., *microRNA-494 is a potential prognostic marker and inhibits cellular proliferation, migration and invasion by targeting SIRT1 in epithelial ovarian cancer*. Oncol Lett, 2017. **14**(3): p. 3177-3184.
734. Li, J.Z., et al., *MicroRNA-495 Regulates Migration and Invasion in Prostate Cancer Cells Via Targeting Akt and mTOR Signaling*. Cancer Invest, 2016. **34**(4): p. 181-8.
735. Rubie, C., et al., *microRNA-496 - A new, potentially aging-relevant regulator of mTOR*. Cell Cycle, 2016. **15**(8): p. 1108-16.
736. Kwak, S.Y., et al., *miR-5003-3p promotes epithelial-mesenchymal transition in breast cancer cells through Snail stabilization and direct targeting of E-cadherin*. J Mol Cell Biol, 2016.
737. Zhang, R., et al., *A Novel Role for MiR-520a-3p in Regulating EGFR Expression in Colorectal Cancer*. Cell Physiol Biochem, 2017. **42**(4): p. 1559-1574.
738. Cao, X., et al., *miRNA504 inhibits p53dependent vascular smooth muscle cell apoptosis and may prevent aneurysm formation*. Mol Med Rep, 2017. **16**(3): p. 2570-2578.
739. Hou, C., et al., *MicroRNA509 acts as a tumor suppressor in tongue squamous cell carcinoma by targeting epidermal growth factor receptor*. Mol Med Rep, 2017.
740. Tian, X.M., et al., *Inhibition of invasion and migration of prostate cancer cells by miRNA-509-5p via targeting MDM2*. Genet Mol Res, 2017. **16**(1).
741. Zhang, F. and Z. Wu, *Significantly altered expression of miR-511-3p and its target AKT3 has negative prognostic value in human prostate cancer*. Biochimie, 2017. **140**: p. 66-72.
742. Li, S., et al., *MiR-520b/e Regulates Proliferation and Migration by Simultaneously Targeting EGFR in Gastric Cancer*. Cell Physiol Biochem, 2016. **40**(6): p. 1303-1315.
743. Griesing, S., et al., *Thyroid transcription factor-1-regulated microRNA-532-5p targets KRAS and MKL2 oncogenes and induces apoptosis in lung adenocarcinoma cells*. Cancer Sci, 2017. **108**(7): p. 1394-1404.

## REFERENCES

744. Hu, X., et al., *Down-regulation of the miR-543 alleviates insulin resistance through targeting the SIRT1*. *Biochem Biophys Res Commun*, 2015. **468**(4): p. 781-7.
745. Li, J., et al., *miR-543 promotes gastric cancer cell proliferation by targeting SIRT1*. *Biochem Biophys Res Commun*, 2016. **469**(1): p. 15-21.
746. Huang, X. and S. Lu, *MicroR-545 mediates colorectal cancer cells proliferation through up-regulating epidermal growth factor receptor expression in HOTAIR long non-coding RNA dependent*. *Mol Cell Biochem*, 2017. **431**(1-2): p. 45-54.
747. Liu, C., et al., *microRNA-548l is involved in the migration and invasion of non-small cell lung cancer by targeting the AKT1 signaling pathway*. *J Cancer Res Clin Oncol*, 2015. **141**(3): p. 431-41.
748. Qian, K., et al., *MicroRNA-561 inhibits gastric cancer cell proliferation and invasion by downregulating c-Myc expression*. *Am J Transl Res*, 2016. **8**(9): p. 3802-3811.
749. Fattore, L., et al., *miR-579-3p controls melanoma progression and resistance to target therapy*. *Proc Natl Acad Sci U S A*, 2016. **113**(34): p. E5005-13.
750. Zhang, P., et al., *miR-600 inhibits cell proliferation, migration and invasion by targeting p53 in mutant p53-expressing human colorectal cancer cell lines*. *Oncol Lett*, 2017. **13**(3): p. 1789-1796.
751. Cao, W., et al., *Identification of miR-601 as a novel regulator in the development of pancreatic cancer*. *Biochem Biophys Res Commun*, 2017. **483**(1): p. 638-644.
752. Yan, Y., et al., *MicroRNA-610 is downregulated in glioma cells, and inhibits proliferation and motility by directly targeting MDM2*. *Mol Med Rep*, 2016. **14**(3): p. 2657-64.
753. Fu, X., et al., *MicroRNA-613 inhibited ovarian cancer cell proliferation and invasion by regulating KRAS*. *Tumour Biol*, 2016. **37**(5): p. 6477-83.
754. Sun, Y., et al., *MiRNA-615-5p Functions as a Tumor Suppressor in Pancreatic Ductal Adenocarcinoma by Targeting AKT2*. *PLoS One*, 2015. **10**(4): p. e0119783.
755. Han, Z., et al., *MicroRNA-622 functions as a tumor suppressor by targeting K-Ras and enhancing the anticarcinogenic effect of resveratrol*. *Carcinogenesis*, 2012. **33**(1): p. 131-9.
756. Fang, Y., et al., *MiR-622 inhibited colorectal cancer occurrence and metastasis by suppressing K-Ras*. *Mol Carcinog*, 2016. **55**(9): p. 1369-77.
757. Chen, W.S., et al., *Bostrycin inhibits proliferation of human lung carcinoma A549 cells via downregulation of the PI3K/ Akt pathway*. *J Exp Clin Cancer Res*, 2011. **30**: p. 17.
758. Kong, Q., et al., *MiR-641 Functions as a Tumor Suppressor by Targeting MDM2 in Human Lung Cancer*. *Oncol Res*, 2017.
759. Xu, X., et al., *MiR-650 inhibits proliferation, migration and invasion of rheumatoid arthritis synovial fibroblasts by targeting AKT2*. *Biomed Pharmacother*, 2017. **88**: p. 535-541.
760. Qin, K., X. Zhong, and D. Wang, *MicroRNA-7-5p regulates human alveolar epithelial sodium channels by targeting the mTORC2/SGK-1 signaling pathway*. *Exp Lung Res*, 2016. **42**(5): p. 237-44.
761. Xu, N., et al., *miR-7 Increases Cisplatin Sensitivity of Gastric Cancer Cells Through Suppressing mTOR*. *Technol Cancer Res Treat*, 2017: p. 1533034617717863.
762. Kalantari, P., et al., *miR-718 represses proinflammatory cytokine production through targeting phosphatase and tensin homolog (PTEN)*. *J Biol Chem*, 2017. **292**(14): p. 5634-5644.
763. Jiang, D., et al., *MiR-758-3p suppresses proliferation, migration and invasion of hepatocellular carcinoma cells via targeting MDM2 and mTOR*. *Biomed Pharmacother*, 2017. **96**: p. 535-544.
764. Wang, Q., L.A. Selth, and D.F. Callen, *MiR-766 induces p53 accumulation and G2/M arrest by directly targeting MDM4*. *Oncotarget*, 2017. **8**(18): p. 29914-29924.
765. Subramani, A., et al., *The brain microenvironment negatively regulates miRNA-768-3p to promote K-ras expression and lung cancer metastasis*. *Sci Rep*, 2013. **3**: p. 2392.
766. El Bezawy, R., et al., *miR-875-5p counteracts epithelial-to-mesenchymal transition and enhances radiation response in prostate cancer through repression of the EGFR-ZEB1 axis*. *Cancer Lett*, 2017. **395**: p. 53-62.
767. Qi, F., et al., *MiR-9a-5p regulates proliferation and migration of hepatic stellate cells under pressure through inhibition of Sirt1*. *World J Gastroenterol*, 2015. **21**(34): p. 9900-15.

## REFERENCES

768. Ao, R., et al., *Altered microRNA-9 Expression Level is Directly Correlated with Pathogenesis of Nonalcoholic Fatty Liver Disease by Targeting Onecut2 and SIRT1*. *Med Sci Monit*, 2016. **22**: p. 3804-3819.
769. Zhou, L., et al., *A minicircuitry comprised of microRNA-9 and SIRT1 contributes to leukemogenesis in t(8;21) acute myeloid leukemia*. *Eur Rev Med Pharmacol Sci*, 2017. **21**(4): p. 786-794.
770. Ke, T.W., et al., *MiR-92a Promotes Cell Metastasis of Colorectal Cancer Through PTEN-Mediated PI3K/AKT Pathway*. *Ann Surg Oncol*, 2014.
771. Zhang, H., et al., *MicroRNA-92a promotes metastasis of nasopharyngeal carcinoma by targeting the PTEN/AKT pathway*. *Onco Targets Ther*, 2016. **9**: p. 3579-88.
772. Lu, C., et al., *MicroRNA-92a promotes epithelial-mesenchymal transition through activation of PTEN/PI3K/AKT signaling pathway in non-small cell lung cancer metastasis*. *Int J Oncol*, 2017. **51**(1): p. 235-244.
773. Tang, Q., et al., *MicroRNA-93 suppress colorectal cancer development via Wnt/beta-catenin pathway downregulating*. *Tumour Biol*, 2015. **36**(3): p. 1701-10.
774. Ke, Z.P., et al., *MicroRNA-93 inhibits ischemia-reperfusion induced cardiomyocyte apoptosis by targeting PTEN*. *Oncotarget*, 2016. **7**(20): p. 28796-805.
775. Yu, S., et al., *miRNA-96 suppresses KRAS and functions as a tumor suppressor gene in pancreatic cancer*. *Cancer Res*, 2010. **70**(14): p. 6015-25.
776. Ress, A.L., et al., *MiR-96-5p influences cellular growth and is associated with poor survival in colorectal cancer patients*. *Mol Carcinog*, 2014.
777. Sun, X. and C. Zhang, *MicroRNA-96 promotes myocardial hypertrophy by targeting mTOR*. *Int J Clin Exp Pathol*, 2015. **8**(11): p. 14500-6.
778. Chen, Z., et al., *The Warburg effect and its cancer therapeutic implications*. *J Bioenerg Biomembr*, 2007. **39**(3): p. 267-74.
779. Jang, M., S.S. Kim, and J. Lee, *Cancer cell metabolism: implications for therapeutic targets*. *Exp Mol Med*, 2013. **45**: p. e45.
780. Saridaki, Z., et al., *A let-7 microRNA-binding site polymorphism in KRAS predicts improved outcome in patients with metastatic colorectal cancer treated with salvage cetuximab/panitumumab monotherapy*. *Clin Cancer Res*, 2014. **20**(17): p. 4499-4510.
781. Witters, L.A., *The blooming of the French lilac*. *J Clin Invest*, 2001. **108**(8): p. 1105-7.
782. Werner, E.A. and J. Bell, *CCXIV.—The preparation of methylguanidine, and of  $\beta\beta$ -dimethylguanidine by the interaction of dicyanodiamide, and methylammonium and dimethylammonium chlorides respectively*. *Journal of the Chemical Society, Transactions*, 1922. **121**: p. 1790-1794.
783. Nattrass, M. and K.G. Alberti, *Biguanides*. *Diabetologia*, 1978. **14**(2): p. 71-4.
784. Group, U.P.D.S., *Effect of intensive blood-glucose control with metformin on complications in overweight patients with type 2 diabetes (UKPDS 34)*. *The Lancet*, 1998. **352**(9131): p. 854-865.
785. El-Mir, M.Y., et al., *Dimethylbiguanide inhibits cell respiration via an indirect effect targeted on the respiratory chain complex I*. *J Biol Chem*, 2000. **275**(1): p. 223-8.
786. Landi, S.N., et al., *Association of Long-term Child Growth and Developmental Outcomes With Metformin vs Insulin Treatment for Gestational Diabetes*. *JAMA Pediatr*, 2018.
787. Kozka, I.J. and G.D. Holman, *Metformin blocks downregulation of cell surface GLUT4 caused by chronic insulin treatment of rat adipocytes*. *Diabetes*, 1993. **42**(8): p. 1159-65.
788. Sasson, S., et al., *Regulation by metformin of the hexose transport system in vascular endothelial and smooth muscle cells*. *Br J Pharmacol*, 1996. **117**(6): p. 1318-24.
789. Artani, M., M.F. Iftikhar, and S. Khan, *Effects of Metformin on Symptoms of Polycystic Ovarian Syndrome Among Women of Reproductive Age*. *Cureus*, 2018. **10**(8): p. e3203.
790. Evans, J.M., et al., *Metformin and reduced risk of cancer in diabetic patients*. *Bmj*, 2005. **330**(7503): p. 1304-5.
791. Bowker, S.L., et al., *Increased cancer-related mortality for patients with type 2 diabetes who use sulfonylureas or insulin: Response to Farooki and Schneider*. *Diabetes Care*, 2006. **29**(8): p. 1990-1.

## REFERENCES

792. Libby, G., et al., *New users of metformin are at low risk of incident cancer: a cohort study among people with type 2 diabetes*. *Diabetes Care*, 2009. **32**(9): p. 1620-5.
793. Li, D., et al., *Antidiabetic therapies affect risk of pancreatic cancer*. *Gastroenterology*, 2009. **137**(2): p. 482-8.
794. Currie, C.J., C.D. Poole, and E.A. Gale, *The influence of glucose-lowering therapies on cancer risk in type 2 diabetes*. *Diabetologia*, 2009. **52**(9): p. 1766-77.
795. Jiralerspong, S., et al., *Metformin and pathologic complete responses to neoadjuvant chemotherapy in diabetic patients with breast cancer*. *J Clin Oncol*, 2009. **27**(20): p. 3297-302.
796. Wright, J.L. and J.L. Stanford, *Metformin use and prostate cancer in Caucasian men: results from a population-based case-control study*. *Cancer Causes Control*, 2009. **20**(9): p. 1617-22.
797. Donadon, V., et al., *Glycated hemoglobin and antidiabetic strategies as risk factors for hepatocellular carcinoma*. *World J Gastroenterol*, 2010. **16**(24): p. 3025-32.
798. Donadon, V., et al., *Metformin and reduced risk of hepatocellular carcinoma in diabetic patients with chronic liver disease*. *Liver Int*, 2010. **30**(5): p. 750-8.
799. Landman, G.W., et al., *Metformin associated with lower cancer mortality in type 2 diabetes: ZODIAC-16*. *Diabetes Care*, 2010. **33**(2): p. 322-6.
800. Decensi, A., et al., *Metformin and cancer risk in diabetic patients: a systematic review and meta-analysis*. *Cancer Prev Res (Phila)*, 2010. **3**(11): p. 1451-61.
801. Bodmer, M., et al., *Long-term metformin use is associated with decreased risk of breast cancer*. *Diabetes Care*, 2010. **33**(6): p. 1304-8.
802. Hosono, K., et al., *Metformin suppresses colorectal aberrant crypt foci in a short-term clinical trial*. *Cancer Prev Res (Phila)*, 2010. **3**(9): p. 1077-83.
803. Azoulay, L., et al., *Metformin and the incidence of prostate cancer in patients with type 2 diabetes*. *Cancer Epidemiol Biomarkers Prev*, 2011. **20**(2): p. 337-44.
804. He, X.X., et al., *Thiazolidinediones and metformin associated with improved survival of diabetic prostate cancer patients*. *Ann Oncol*, 2011. **22**(12): p. 2640-5.
805. Sadeghi, N., et al., *Metformin use is associated with better survival of diabetic patients with pancreatic cancer*. *Clin Cancer Res*, 2012. **18**(10): p. 2905-12.
806. Noto, H., et al., *Cancer risk in diabetic patients treated with metformin: a systematic review and meta-analysis*. *PLoS One*, 2012. **7**(3): p. e33411.
807. Smiechowski, B., et al., *The use of metformin and colorectal cancer incidence in patients with type II diabetes mellitus*. *Cancer Epidemiol Biomarkers Prev*, 2013. **22**(10): p. 1877-83.
808. Cardel, M., et al., *Long-term use of metformin and colorectal cancer risk in type II diabetics: a population-based case-control study*. *Cancer Med*, 2014. **3**(5): p. 1458-66.
809. Sehdev, A., et al., *Metformin for primary colorectal cancer prevention in patients with diabetes: a case-control study in a US population*. *Cancer*, 2015. **121**(7): p. 1071-8.
810. Tseng, C.H., *Metformin reduces ovarian cancer risk in Taiwanese women with type 2 diabetes mellitus*. *Diabetes Metab Res Rev*, 2015. **31**(6): p. 619-26.
811. Tseng, C.H., *Use of metformin and risk of kidney cancer in patients with type 2 diabetes*. *Eur J Cancer*, 2016. **52**: p. 19-25.
812. Tseng, C.H., *Metformin may reduce oral cancer risk in patients with type 2 diabetes*. *Oncotarget*, 2016. **7**(2): p. 2000-8.
813. Heidari, F., et al., *Metformin for the Prevention of Bladder Cancer Recurrence: Is it Effective?* *Nephrourol Mon*, 2016. **8**(3): p. e30261.
814. Tseng, C.H., *Metformin reduces gastric cancer risk in patients with type 2 diabetes mellitus*. *Aging (Albany NY)*, 2016. **8**(8): p. 1636-49.
815. Jung, Y.S., et al., *Metformin use and the risk of colorectal adenoma: A systematic review and meta-analysis*. *J Gastroenterol Hepatol*, 2017. **32**(5): p. 957-965.
816. Tseng, C.H., *Metformin and lung cancer risk in patients with type 2 diabetes mellitus*. *Oncotarget*, 2017. **8**(25): p. 41132-41142.

## REFERENCES

817. Campbell, J.M., et al., *Metformin reduces all-cause mortality and diseases of ageing independent of its effect on diabetes control: A systematic review and meta-analysis*. *Ageing Res Rev*, 2017. **40**: p. 31-44.
818. Bradley, M.C., et al., *A Cohort Study of Metformin and Colorectal Cancer Risk among Patients with Diabetes Mellitus*. *Cancer Epidemiol Biomarkers Prev*, 2018. **27**(5): p. 525-530.
819. Cho, Y.Y., et al., *Protective Effect of Metformin Against Thyroid Cancer Development: A Population-Based Study in Korea*. *Thyroid*, 2018. **28**(7): p. 864-870.
820. Murff, H.J., et al., *Metformin use and incidence cancer risk: evidence for a selective protective effect against liver cancer*. *Cancer Causes Control*, 2018. **29**(9): p. 823-832.
821. Ye, J.H., et al., *Association Between Metformin and Sulfonylurea Monotherapies and Cancer Incidence: A Real-World Cohort Study in Shanghai, China*. *Diabetes Ther*, 2019. **10**(1): p. 245-258.
822. Bonanni, B., et al., *Dual effect of metformin on breast cancer proliferation in a randomized presurgical trial*. *J Clin Oncol*, 2012. **30**(21): p. 2593-600.
823. Spratt, D.E., et al., *Metformin and prostate cancer: reduced development of castration-resistant disease and prostate cancer mortality*. *Eur Urol*, 2013. **63**(4): p. 709-16.
824. Febbraro, T., E. Lengyel, and I.L. Romero, *Old drug, new trick: repurposing metformin for gynecologic cancers?* *Gynecol Oncol*, 2014. **135**(3): p. 614-21.
825. Shackelford, D.B., et al., *LKB1 inactivation dictates therapeutic response of non-small cell lung cancer to the metabolism drug phenformin*. *Cancer Cell*, 2013. **23**(2): p. 143-58.
826. Algire, C., et al., *Metformin blocks the stimulative effect of a high-energy diet on colon carcinoma growth in vivo and is associated with reduced expression of fatty acid synthase*. *Endocr Relat Cancer*, 2010. **17**(2): p. 351-60.
827. Karnevi, E., et al., *Metformin-mediated growth inhibition involves suppression of the IGF-I receptor signalling pathway in human pancreatic cancer cells*. *BMC Cancer*, 2013. **13**: p. 235.
828. Spiller, H.A. and T.S. Sawyer, *Toxicology of oral antidiabetic medications*. *Am J Health Syst Pharm*, 2006. **63**(10): p. 929-38.
829. Gong, L., et al., *Metformin pathways: pharmacokinetics and pharmacodynamics*. *Pharmacogenet Genomics*, 2012. **22**(11): p. 820-7.
830. Zhou, M., L. Xia, and J. Wang, *Metformin transport by a newly cloned proton-stimulated organic cation transporter (plasma membrane monoamine transporter) expressed in human intestine*. *Drug Metab Dispos*, 2007. **35**(10): p. 1956-62.
831. Graham, G.G., et al., *Clinical pharmacokinetics of metformin*. *Clin Pharmacokinet*, 2011. **50**(2): p. 81-98.
832. Muller, J., et al., *Drug specificity and intestinal membrane localization of human organic cation transporters (OCT)*. *Biochem Pharmacol*, 2005. **70**(12): p. 1851-60.
833. Takane, H., et al., *Polymorphism in human organic cation transporters and metformin action*. *Pharmacogenomics*, 2008. **9**(4): p. 415-22.
834. Tsuda, M., et al., *Involvement of human multidrug and toxin extrusion 1 in the drug interaction between cimetidine and metformin in renal epithelial cells*. *J Pharmacol Exp Ther*, 2009. **329**(1): p. 185-91.
835. Sato, T., et al., *Transcellular transport of organic cations in double-transfected MDCK cells expressing human organic cation transporters hOCT1/hMATE1 and hOCT2/hMATE1*. *Biochem Pharmacol*, 2008. **76**(7): p. 894-903.
836. Tanihara, Y., et al., *Substrate specificity of MATE1 and MATE2-K, human multidrug and toxin extrusions/H(+)-organic cation antiporters*. *Biochem Pharmacol*, 2007. **74**(2): p. 359-71.
837. Ben Sahra, I., et al., *The antidiabetic drug metformin exerts an antitumoral effect in vitro and in vivo through a decrease of cyclin D1 level*. *Oncogene*, 2008. **27**(25): p. 3576-86.
838. Owen, M.R., E. Doran, and A.P. Halestrap, *Evidence that metformin exerts its anti-diabetic effects through inhibition of complex 1 of the mitochondrial respiratory chain*. *Biochem J*, 2000. **348 Pt 3**: p. 607-14.

## REFERENCES

839. Zhou, G., et al., *Role of AMP-activated protein kinase in mechanism of metformin action*. J Clin Invest, 2001. **108**(8): p. 1167-74.
840. Hinke, S.A., et al., *Methyl succinate antagonises biguanide-induced AMPK-activation and death of pancreatic beta-cells through restoration of mitochondrial electron transfer*. Br J Pharmacol, 2007. **150**(8): p. 1031-43.
841. Shaw, R.J., et al., *The kinase LKB1 mediates glucose homeostasis in liver and therapeutic effects of metformin*. Science, 2005. **310**(5754): p. 1642-6.
842. Hardie, D.G., *AMP-activated/SNF1 protein kinases: conserved guardians of cellular energy*. Nat Rev Mol Cell Biol, 2007. **8**(10): p. 774-85.
843. Vazquez-Martin, A., et al., *Mitotic kinase dynamics of the active form of AMPK (phospho-AMPK $\alpha$ Thr172) in human cancer cells*. Cell Cycle, 2009. **8**(5): p. 788-91.
844. Cazzaniga, M., et al., *Is it time to test metformin in breast cancer clinical trials?* Cancer Epidemiol Biomarkers Prev, 2009. **18**(3): p. 701-5.
845. Clemmons, D.R., et al., *Role of the integrin  $\alpha V\beta 3$  in mediating increased smooth muscle cell responsiveness to IGF-I in response to hyperglycemic stress*. Growth Horm IGF Res, 2007. **17**(4): p. 265-70.
846. Malaguarnera, R., et al., *Metformin inhibits androgen-induced IGF-IR up-regulation in prostate cancer cells by disrupting membrane-initiated androgen signaling*. Endocrinology, 2014. **155**(4): p. 1207-21.
847. Zakikhani, M., et al., *Metformin and rapamycin have distinct effects on the AKT pathway and proliferation in breast cancer cells*. Breast Cancer Res Treat, 2010. **123**(1): p. 271-9.
848. Ning, J. and D.R. Clemmons, *AMP-activated protein kinase inhibits IGF-I signaling and protein synthesis in vascular smooth muscle cells via stimulation of insulin receptor substrate 1 S794 and tuberous sclerosis 2 S1345 phosphorylation*. Mol Endocrinol, 2010. **24**(6): p. 1218-29.
849. Kisfalvi, K., et al., *Metformin disrupts crosstalk between G protein-coupled receptor and insulin receptor signaling systems and inhibits pancreatic cancer growth*. Cancer Res, 2009. **69**(16): p. 6539-45.
850. Klubo-Gwiedzinska, J., et al., *Metformin inhibits growth and decreases resistance to anoikis in medullary thyroid cancer cells*. Endocr Relat Cancer, 2012. **19**(3): p. 447-56.
851. Shi, W.Y., et al., *Therapeutic metformin/AMPK activation blocked lymphoma cell growth via inhibition of mTOR pathway and induction of autophagy*. Cell Death Dis, 2012. **3**: p. e275.
852. Kim, H.G., et al., *Metformin inhibits P-glycoprotein expression via the NF- $\kappa$ B pathway and CRE transcriptional activity through AMPK activation*. Br J Pharmacol, 2011. **162**(5): p. 1096-108.
853. Morgillo, F., et al., *Synergistic effects of metformin treatment in combination with gefitinib, a selective EGFR tyrosine kinase inhibitor, in LKB1 wild-type NSCLC cell lines*. Clin Cancer Res, 2013. **19**(13): p. 3508-19.
854. Rocha, G.Z., et al., *Metformin amplifies chemotherapy-induced AMPK activation and antitumoral growth*. Clin Cancer Res, 2011. **17**(12): p. 3993-4005.
855. Checkley, L.A., et al., *Metformin inhibits skin tumor promotion in overweight and obese mice*. Cancer Prev Res (Phila), 2014. **7**(1): p. 54-64.
856. Vakana, E., et al., *Antileukemic effects of AMPK activators on BCR-ABL-expressing cells*. Blood, 2011. **118**(24): p. 6399-402.
857. Gwinn, D.M., et al., *AMPK phosphorylation of raptor mediates a metabolic checkpoint*. Mol Cell, 2008. **30**(2): p. 214-26.
858. Inoki, K., T. Zhu, and K.L. Guan, *TSC2 mediates cellular energy response to control cell growth and survival*. Cell, 2003. **115**(5): p. 577-90.
859. Muaddi, H., et al., *Contributions of AMPK and p53 dependent signaling to radiation response in the presence of metformin*. Radiother Oncol, 2013. **108**(3): p. 446-50.
860. Ben Sahra, I., et al., *Metformin, independent of AMPK, induces mTOR inhibition and cell-cycle arrest through REDD1*. Cancer Res, 2011. **71**(13): p. 4366-72.

## REFERENCES

861. Arai, M., et al., *Metformin, an antidiabetic agent, suppresses the production of tumor necrosis factor and tissue factor by inhibiting early growth response factor-1 expression in human monocytes in vitro*. J Pharmacol Exp Ther, 2010. **334**(1): p. 206-13.
862. Gou, S., et al., *Low concentrations of metformin selectively inhibit CD133(+) cell proliferation in pancreatic cancer and have anticancer action*. PLoS One, 2013. **8**(5): p. e63969.
863. Memmott, R.M., et al., *Metformin prevents tobacco carcinogen--induced lung tumorigenesis*. Cancer Prev Res (Phila), 2010. **3**(9): p. 1066-76.
864. Pollak, M., *Insulin and insulin-like growth factor signalling in neoplasia*. Nat Rev Cancer, 2008. **8**(12): p. 915-28.
865. Sharma, A., et al., *Targeting mitogen-activated protein kinase/extracellular signal-regulated kinase kinase in the mutant (V600E) B-Raf signaling cascade effectively inhibits melanoma lung metastases*. Cancer Res, 2006. **66**(16): p. 8200-9.
866. Kyriakis, J.M. and J. Avruch, *Mammalian mitogen-activated protein kinase signal transduction pathways activated by stress and inflammation*. Physiol Rev, 2001. **81**(2): p. 807-69.
867. McCubrey, J.A., et al., *Roles of the Raf/MEK/ERK pathway in cell growth, malignant transformation and drug resistance*. Biochim Biophys Acta, 2007. **1773**(8): p. 1263-84.
868. Panka, D.J., M.B. Atkins, and J.W. Mier, *Targeting the mitogen-activated protein kinase pathway in the treatment of malignant melanoma*. Clin Cancer Res, 2006. **12**(7 Pt 2): p. 2371s-2375s.
869. Chaudhary, S.C., et al., *Metformin, an antidiabetic agent reduces growth of cutaneous squamous cell carcinoma by targeting mTOR signaling pathway*. Photochem Photobiol, 2012. **88**(5): p. 1149-56.
870. Vazquez-Martin, A., et al., *The antidiabetic drug metformin: a pharmaceutical AMPK activator to overcome breast cancer resistance to HER2 inhibitors while decreasing risk of cardiomyopathy*. Ann Oncol, 2009. **20**(3): p. 592-5.
871. Vazquez-Martin, A., et al., *The anti-diabetic drug metformin suppresses self-renewal and proliferation of trastuzumab-resistant tumor-initiating breast cancer stem cells*. Breast Cancer Res Treat, 2011. **126**(2): p. 355-64.
872. Thompson, A.M., *Molecular pathways: preclinical models and clinical trials with metformin in breast cancer*. Clin Cancer Res, 2014. **20**(10): p. 2508-15.
873. Lee, M.S., et al., *Type 2 diabetes increases and metformin reduces total, colorectal, liver and pancreatic cancer incidences in Taiwanese: a representative population prospective cohort study of 800,000 individuals*. BMC Cancer, 2011. **11**: p. 20.
874. Tseng, C.H., *Diabetes but not insulin is associated with higher colon cancer mortality*. World J Gastroenterol, 2012. **18**(31): p. 4182-90.
875. Cho, Y.H., et al., *Does metformin affect the incidence of colonic polyps and adenomas in patients with type 2 diabetes mellitus?* Intest Res, 2014. **12**(2): p. 139-45.
876. Buzzai, M., et al., *Systemic treatment with the antidiabetic drug metformin selectively impairs p53-deficient tumor cell growth*. Cancer Res, 2007. **67**(14): p. 6745-52.
877. Li, W., et al., *Combined use of vitamin D3 and metformin exhibits synergistic chemopreventive effects on colorectal neoplasia in rats and mice*. Cancer Prev Res (Phila), 2015. **8**(2): p. 139-48.
878. Feng, Y.H., et al., *MicroRNA-21-mediated regulation of Sprouty2 protein expression enhances the cytotoxic effect of 5-fluorouracil and metformin in colon cancer cells*. Int J Mol Med, 2012. **29**(5): p. 920-6.
879. Zannella, V.E., et al., *Reprogramming metabolism with metformin improves tumor oxygenation and radiotherapy response*. Clin Cancer Res, 2013. **19**(24): p. 6741-50.
880. He, G., et al., *AMP-activated protein kinase induces p53 by phosphorylating MDMX and inhibiting its activity*. Mol Cell Biol, 2014. **34**(2): p. 148-57.
881. Nangia-Makker, P., et al., *Metformin: a potential therapeutic agent for recurrent colon cancer*. PLoS One, 2014. **9**(1): p. e84369.

## REFERENCES

882. Do, M.T., et al., *Metformin induces microRNA-34a to downregulate the Sirt1/Pgc-1alpha/Nrf2 pathway, leading to increased susceptibility of wild-type p53 cancer cells to oxidative stress and therapeutic agents*. Free Radic Biol Med, 2014. **74**: p. 21-34.
883. Lea, M.A., et al., *Addition of 2-deoxyglucose enhances growth inhibition but reverses acidification in colon cancer cells treated with phenformin*. Anticancer Res, 2011. **31**(2): p. 421-6.
884. Lea, M.A., et al., *Growth inhibition of colon cancer cells by compounds affecting AMPK activity*. World J Gastrointest Oncol, 2014. **6**(7): p. 244-52.
885. Richard, S.M. and V.L. Martinez Marignac, *Sensitization to oxaliplatin in HCT116 and HT29 cell lines by metformin and ribavirin and differences in response to mitochondrial glutaminase inhibition*. J Cancer Res Ther, 2015. **11**(2): p. 336-40.
886. Montales, M.T., et al., *Metformin and soybean-derived bioactive molecules attenuate the expansion of stem cell-like epithelial subpopulation and confer apoptotic sensitivity in human colon cancer cells*. Genes Nutr, 2015. **10**(6): p. 49.
887. Jeong, Y.K., et al., *Metformin Radiosensitizes p53-Deficient Colorectal Cancer Cells through Induction of G2/M Arrest and Inhibition of DNA Repair Proteins*. PLoS One, 2015. **10**(11): p. e0143596.
888. Saber, M.M., et al., *Combination of metformin and 5-aminosalicylic acid cooperates to decrease proliferation and induce apoptosis in colorectal cancer cell lines*. BMC Cancer, 2016. **16**: p. 126.
889. Jia, Y., et al., *Metformin prevents DMH-induced colorectal cancer in diabetic rats by reversing the warburg effect*. Cancer Med, 2015. **4**(11): p. 1730-41.
890. Tsai, C.C., et al., *Increase in apoptosis by combination of metformin with silibinin in human colorectal cancer cells*. World J Gastroenterol, 2015. **21**(14): p. 4169-77.
891. Cho, S.Y., et al., *Activation of AMP-Activated Protein Kinase alpha and Extracellular Signal-Regulated Kinase Mediates CB-PIC-Induced Apoptosis in Hypoxic SW620 Colorectal Cancer Cells*. Evid Based Complement Alternat Med, 2013. **2013**: p. 974313.
892. Zhou, X.Z., et al., *Effects of metformin on proliferation of human colon carcinoma cell line SW-480*. Nan Fang Yi Ke Da Xue Xue Bao, 2010. **30**(8): p. 1935-8, 1942.
893. Zakikhani, M., et al., *The effects of adiponectin and metformin on prostate and colon neoplasia involve activation of AMP-activated protein kinase*. Cancer Prev Res (Phila), 2008. **1**(5): p. 369-75.
894. Noren Hooten, N., et al., *Metformin-mediated increase in DICER1 regulates microRNA expression and cellular senescence*. Aging Cell, 2016. **15**(3): p. 572-81.
895. Blandino, G., et al., *Metformin elicits anticancer effects through the sequential modulation of DICER and c-MYC*. Nat Commun, 2012. **3**: p. 865.
896. Karimi, L., et al., *miRNA-143 replacement therapy harnesses the proliferation and migration of colorectal cancer cells in vitro*. J Cell Physiol, 2019.
897. van Zandwijk, N., et al., *Safety and activity of microRNA-loaded minicells in patients with recurrent malignant pleural mesothelioma: a first-in-man, phase 1, open-label, dose-escalation study*. Lancet Oncol, 2017. **18**(10): p. 1386-1396.
898. Oliveras-Ferraros, C., et al., *Micro(mi)RNA expression profile of breast cancer epithelial cells treated with the anti-diabetic drug metformin: induction of the tumor suppressor miRNA let-7a and suppression of the TGFbeta-induced oncomiR miRNA-181a*. Cell Cycle, 2011. **10**(7): p. 1144-51.
899. Kato, K., et al., *The antidiabetic drug metformin inhibits gastric cancer cell proliferation in vitro and in vivo*. Mol Cancer Ther, 2012. **11**(3): p. 549-60.
900. Bao, B., et al., *Metformin inhibits cell proliferation, migration and invasion by attenuating CSC function mediated by deregulating miRNAs in pancreatic cancer cells*. Cancer Prev Res (Phila), 2012. **5**(3): p. 355-64.
901. Li, W., et al., *Metformin alters the expression profiles of microRNAs in human pancreatic cancer cells*. Diabetes Res Clin Pract, 2012. **96**(2): p. 187-95.
902. Wang, Y., et al., *Metformin inhibits lung cancer cells proliferation through repressing microRNA-222*. Biotechnol Lett, 2013. **35**(12): p. 2013-9.

## REFERENCES

903. Kobayashi, M., et al., *Antitumor effect of metformin in esophageal cancer: in vitro study*. Int J Oncol, 2013. **42**(2): p. 517-24.
904. Avci, C.B., et al., *Therapeutic potential of an anti-diabetic drug, metformin: alteration of miRNA expression in prostate cancer cells*. Asian Pac J Cancer Prev, 2013. **14**(2): p. 765-8.
905. Zhang, J., et al., *Metformin inhibits epithelial-mesenchymal transition in prostate cancer cells: involvement of the tumor suppressor miR30a and its target gene SOX4*. Biochem Biophys Res Commun, 2014. **452**(3): p. 746-52.
906. Yang, F.Q., et al., *Metformin inhibits cell growth by upregulating microRNA-26a in renal cancer cells*. Int J Clin Exp Med, 2014. **7**(10): p. 3289-96.
907. Wahdan-Alaswad, R.S., et al., *Metformin-induced killing of triple-negative breast cancer cells is mediated by reduction in fatty acid synthase via miRNA-193b*. Horm Cancer, 2014. **5**(6): p. 374-89.
908. Miyoshi, H., et al., *Effect of the anti-diabetic drug metformin in hepatocellular carcinoma in vitro and in vivo*. Int J Oncol, 2014. **45**(1): p. 322-32.
909. Jiang, X., et al., *Metformin inhibits tumor growth by regulating multiple miRNAs in human cholangiocarcinoma*. Oncotarget, 2015. **6**(5): p. 3178-94.
910. Cifarelli, V., et al., *Metformin and Rapamycin Reduce Pancreatic Cancer Growth in Obese Prediabetic Mice by Distinct MicroRNA-Regulated Mechanisms*. Diabetes, 2015. **64**(5): p. 1632-42.
911. Tanaka, R., et al., *Metformin Causes G1-Phase Arrest via Down-Regulation of MiR-221 and Enhances TRAIL Sensitivity through DR5 Up-Regulation in Pancreatic Cancer Cells*. PLoS One, 2015. **10**(5): p. e0125779.
912. Cabello, P., et al., *The Antitumor Effect of Metformin Is Mediated by miR-26a in Breast Cancer*. Int J Mol Sci, 2016. **17**(8).
913. Kato, K., et al., *The anti-diabetic drug metformin inhibits pancreatic cancer cell proliferation in vitro and in vivo: Study of the microRNAs associated with the antitumor effect of metformin*. Oncol Rep, 2016. **35**(3): p. 1582-92.
914. Sun, Y., et al., *Metformin induces apoptosis of human hepatocellular carcinoma HepG2 cells by activating an AMPK/p53/miR-23a/FOXA1 pathway*. Onco Targets Ther, 2016. **9**: p. 2845-53.
915. Zhao, W., et al., *miR-27a-mediated antiproliferative effects of metformin on the breast cancer cell line MCF-7*. Oncol Rep, 2016. **36**(6): p. 3691-3699.
916. Sun, R., et al., *The effect and mechanism of action of metformin on in vitro FaDu cell proliferation*. J Int Med Res, 2016. **44**(5): p. 1049-1054.
917. Wang, F., et al., *Metformin induces apoptosis by microRNA-26a-mediated downregulation of myeloid cell leukaemia-1 in human oral cancer cells*. Mol Med Rep, 2016. **13**(6): p. 4671-6.
918. Kalogirou, C., et al., *Metformin-Derived Growth Inhibition in Renal Cell Carcinoma Depends on miR-21-Mediated PTEN Expression*. Urol Int, 2016. **96**(1): p. 106-15.
919. Zhong, T., et al., *Metformin alters DNA methylation genome-wide via the H19/SAHH axis*. Oncogene, 2017. **36**(17): p. 2345-2354.
920. Zhang, J., et al., *Metformin Inhibits Tumorigenesis and Tumor Growth of Breast Cancer Cells by Upregulating miR-200c but Downregulating AKT2 Expression*. J Cancer, 2017. **8**(10): p. 1849-1864.
921. Pulito, C., et al., *Metformin-induced ablation of microRNA 21-5p releases Sestrin-1 and CAB39L antitumoral activities*. Cell Discov, 2017. **3**: p. 17022.
922. Chiyo, T., et al., *Therapeutic potential of the antidiabetic drug metformin in small bowel adenocarcinoma*. Int J Oncol, 2017. **50**(6): p. 2145-2153.
923. Xie, W., et al., *Metformin Induces Growth Inhibition and Cell Cycle Arrest by Upregulating MicroRNA34a in Renal Cancer Cells*. Med Sci Monit, 2017. **23**: p. 29-37.

## REFERENCES

924. Wang, Y., Z. Wu, and L. Hu, *The regulatory effects of metformin on the [SNAIL/miR-34]:[ZEB/miR-200] system in the epithelial-mesenchymal transition(EMT) for colorectal cancer(CRC)*. Eur J Pharmacol, 2018. **834**: p. 45-53.
925. Li, Y., et al., *Crucial microRNAs and genes in metformin's anti-pancreatic cancer effect explored by microRNA-mRNA integrated analysis*. Invest New Drugs, 2018. **36**(1): p. 20-27.
926. Algire, C., et al., *Diet and tumor LKB1 expression interact to determine sensitivity to anti-neoplastic effects of metformin in vivo*. Oncogene, 2011. **30**(10): p. 1174-82.
927. Harrington, L.S., et al., *The TSC1-2 tumor suppressor controls insulin-PI3K signaling via regulation of IRS proteins*. J Cell Biol, 2004. **166**(2): p. 213-23.
928. Zhou, K., et al., *Heritability of variation in glycaemic response to metformin: a genome-wide complex trait analysis*. Lancet Diabetes Endocrinol, 2014. **2**(6): p. 481-7.
929. Fischer, H.P., *Towards quantitative biology: integration of biological information to elucidate disease pathways and to guide drug discovery*. Biotechnol Annu Rev, 2005. **11**: p. 1-68.
930. Fendt, S.M., et al., *Metformin decreases glucose oxidation and increases the dependency of prostate cancer cells on reductive glutamine metabolism*. Cancer Res, 2013. **73**(14): p. 4429-38.
931. Brattain, M.G., et al., *Heterogeneity of human colon carcinoma*. Cancer Metastasis Rev, 1984. **3**(3): p. 177-91.
932. Kyriazis, A.P., et al., *Growth patterns and metastatic behavior of human tumors growing in athymic mice*. Cancer Res, 1978. **38**(10): p. 3186-90.
933. Knutsen, T., et al., *Definitive molecular cytogenetic characterization of 15 colorectal cancer cell lines*. Genes Chromosomes Cancer, 2010. **49**(3): p. 204-23.
934. von Kleist, S., et al., *Immunohistology of the antigenic pattern of a continuous cell line from a human colon tumor*. J Natl Cancer Inst, 1975. **55**(3): p. 555-60.
935. van Kuppeveld, F.J., et al., *Genus- and species-specific identification of mycoplasmas by 16S rRNA amplification*. Appl Environ Microbiol, 1992. **58**(8): p. 2606-15.
936. Muller, P.Y., et al., *Processing of gene expression data generated by quantitative real-time RT-PCR*. Biotechniques, 2002. **32**(6): p. 1372-4, 1376, 1378-9.
937. Dobin, A., et al., *STAR: ultrafast universal RNA-seq aligner*. Bioinformatics, 2013. **29**(1): p. 15-21.
938. Li, H., et al., *The Sequence Alignment/Map format and SAMtools*. Bioinformatics, 2009. **25**(16): p. 2078-9.
939. Anders, S., P.T. Pyl, and W. Huber, *HTSeq--a Python framework to work with high-throughput sequencing data*. Bioinformatics, 2015. **31**(2): p. 166-9.
940. Love, M.I., W. Huber, and S. Anders, *Moderated estimation of fold change and dispersion for RNA-seq data with DESeq2*. Genome Biol, 2014. **15**(12): p. 550.
941. Hsu, S.D., et al., *miRTarBase: a database curates experimentally validated microRNA-target interactions*. Nucleic Acids Res, 2011. **39**(Database issue): p. D163-9.
942. Xiao, F., et al., *miRecords: an integrated resource for microRNA-target interactions*. Nucleic Acids Res, 2009. **37**(Database issue): p. D105-10.
943. Agarwal, V., et al., *Predicting effective microRNA target sites in mammalian mRNAs*. Elife, 2015. **4**.
944. Vejnar, C.E. and E.M. Zdobnov, *MiRmap: comprehensive prediction of microRNA target repression strength*. Nucleic Acids Res, 2012. **40**(22): p. 11673-83.
945. Wong, N. and X. Wang, *miRDB: an online resource for microRNA target prediction and functional annotations*. Nucleic Acids Res, 2015. **43**(Database issue): p. D146-52.
946. Paraskevopoulou, M.D., et al., *DIANA-microT web server v5.0: service integration into miRNA functional analysis workflows*. Nucleic Acids Res, 2013. **41**(Web Server issue): p. W169-73.
947. John, B., et al., *Human MicroRNA targets*. PLoS Biol, 2004. **2**(11): p. e363.
948. Breuer, K., et al., *InnateDB: systems biology of innate immunity and beyond--recent updates and continuing curation*. Nucleic Acids Res, 2013. **41**(Database issue): p. D1228-33.

## REFERENCES

949. Shannon, P., et al., *Cytoscape: a software environment for integrated models of biomolecular interaction networks*. Genome Res, 2003. **13**(11): p. 2498-504.
950. Assenov, Y., et al., *Computing topological parameters of biological networks*. Bioinformatics, 2008. **24**(2): p. 282-4.
951. Bindea, G., et al., *ClueGO: a Cytoscape plug-in to decipher functionally grouped gene ontology and pathway annotation networks*. Bioinformatics, 2009. **25**(8): p. 1091-3.
952. Slenter, D.N., et al., *WikiPathways: a multifaceted pathway database bridging metabolomics to other omics research*. Nucleic Acids Res, 2018. **46**(D1): p. D661-d667.
953. Kutmon, M., et al., *PathVisio 3: an extendable pathway analysis toolbox*. PLoS Comput Biol, 2015. **11**(2): p. e1004085.
954. Massey, A.J., *Multiparametric Cell Cycle Analysis Using the Operetta High-Content Imager and Harmony Software with PhenoLOGIC*. PLoS One, 2015. **10**(7): p. e0134306.
955. Birmingham, A., et al., *Statistical methods for analysis of high-throughput RNA interference screens*. Nat Methods, 2009. **6**(8): p. 569-75.
956. Backes, C., et al., *miRPathDB: a new dictionary on microRNAs and target pathways*. Nucleic Acids Res, 2017. **45**(D1): p. D90-d96.
957. Yan, F., et al., *Synergistic hepatoprotective effect of Schisandrae lignans with Astragalus polysaccharides on chronic liver injury in rats*. Phytomedicine, 2009. **16**(9): p. 805-13.
958. Jafary, F., et al., *Novel Peptide Inhibitors for Lactate Dehydrogenase A (LDHA): A Survey to Inhibit LDHA Activity via Disruption of Protein-Protein Interaction*. Sci Rep, 2019. **9**(1): p. 4686.
959. Feoktistova, M., P. Gesserick, and M.J.C.S.H.P. Leverkus, *Crystal violet assay for determining viability of cultured cells*. 2016. **2016**(4): p. pdb. prot087379.
960. Kasznicki, J., A. Sliwinska, and J. Drzewoski, *Metformin in cancer prevention and therapy*. Ann Transl Med, 2014. **2**(6): p. 57.
961. Warburg, O., *On the origin of cancer cells*. Science, 1956. **123**(3191): p. 309-14.
962. Semenza, G.L., et al., *'The metabolism of tumours': 70 years later*. Novartis Found Symp, 2001. **240**: p. 251-60; discussion 260-4.
963. Miao, P., et al., *Lactate dehydrogenase A in cancer: a promising target for diagnosis and therapy*. IUBMB Life, 2013. **65**(11): p. 904-10.
964. Kim, E.Y., et al., *A Novel Lactate Dehydrogenase Inhibitor, 1-(Phenylseleno)-4-(Trifluoromethyl) Benzene, Suppresses Tumor Growth through Apoptotic Cell Death*. Sci Rep, 2019. **9**(1): p. 3969.
965. Das, C.K., et al., *Lactate dehydrogenase A regulates autophagy and tamoxifen resistance in breast cancer*. Biochim Biophys Acta Mol Cell Res, 2019. **1866**(6): p. 1004-1018.
966. He, L., et al., *[Effect of LDHA Knockdown by siRNA on Migration and Invasion of ErbB2 Overexpressing Breast Cancer Cell Line]*. Sichuan Da Xue Xue Bao Yi Xue Ban, 2019. **50**(1): p. 55-60.
967. Beltinger, C., *LDHA and LDHB are dispensable for aerobic glycolysis in neuroblastoma cells while promoting their aggressiveness*. J Biol Chem, 2019. **294**(1): p. 66.
968. Pathria, G., et al., *Targeting the Warburg effect via LDHA inhibition engages ATF4 signaling for cancer cell survival*. Embo j, 2018. **37**(20).
969. Le, A., et al., *Inhibition of lactate dehydrogenase A induces oxidative stress and inhibits tumor progression*. Proc Natl Acad Sci U S A, 2010. **107**(5): p. 2037-42.
970. Qiu, H., et al., *JQ1 suppresses tumor growth through downregulating LDHA in ovarian cancer*. Oncotarget, 2015.
971. Tamada, M., M. Suematsu, and H. Saya, *Pyruvate kinase M2: multiple faces for conferring benefits on cancer cells*. Clin Cancer Res, 2012. **18**(20): p. 5554-61.
972. Hitosugi, T., et al., *Tyrosine phosphorylation inhibits PKM2 to promote the Warburg effect and tumor growth*. Sci Signal, 2009. **2**(97): p. ra73.

## REFERENCES

973. Zhou, Z., et al., *Depletion of PKM2 leads to impaired glycolysis and cell death in 2-demethoxy-2,3-ethylenediamino hypocrelin B-photoinduced A549 cells*. J Photochem Photobiol B, 2014. **134**: p. 1-8.
974. Li, S., et al., *Dihydroartemisinin represses esophageal cancer glycolysis by down-regulating pyruvate kinase M2*. Eur J Pharmacol, 2019. **854**: p. 232-239.
975. Guo, C., et al., *Tumor pyruvate kinase M2: A promising molecular target of gastrointestinal cancer*. Chin J Cancer Res, 2018. **30**(6): p. 669-676.
976. Cheong, H., et al., *Therapeutic targets in cancer cell metabolism and autophagy*. Nature biotechnology, 2012. **30**(7): p. 671.
977. Fogal, V., et al., *Mitochondrial p32 protein is a critical regulator of tumor metabolism via maintenance of oxidative phosphorylation*. Mol Cell Biol, 2010. **30**(6): p. 1303-18.
978. Weinberg, F., et al., *Mitochondrial metabolism and ROS generation are essential for Kras-mediated tumorigenicity*. Proc Natl Acad Sci U S A, 2010. **107**(19): p. 8788-93.
979. Park, I.J., et al., *Cryptotanshinone induces G1 cell cycle arrest and autophagic cell death by activating the AMP-activated protein kinase signal pathway in HepG2 hepatoma*. Apoptosis, 2014. **19**(4): p. 615-28.
980. Chen, D., et al., *Metformin protects against apoptosis and senescence in nucleus pulposus cells and ameliorates disc degeneration in vivo*. Cell Death Dis, 2016. **7**(10): p. e2441.
981. Foretz, M., et al., *Metformin inhibits hepatic gluconeogenesis in mice independently of the LKB1/AMPK pathway via a decrease in hepatic energy state*. J Clin Invest, 2010. **120**(7): p. 2355-69.
982. Kalender, A., et al., *Metformin, independent of AMPK, inhibits mTORC1 in a rag GTPase-dependent manner*. Cell Metab, 2010. **11**(5): p. 390-401.
983. Pierotti, M.A., et al., *Targeting metabolism for cancer treatment and prevention: metformin, an old drug with multi-faceted effects*. Oncogene, 2013. **32**(12): p. 1475-87.
984. Hirsch, H.A., D. Iliopoulos, and K. Struhl, *Metformin inhibits the inflammatory response associated with cellular transformation and cancer stem cell growth*. Proc Natl Acad Sci U S A, 2013. **110**(3): p. 972-7.
985. Hirsch, H.A., et al., *Metformin selectively targets cancer stem cells, and acts together with chemotherapy to block tumor growth and prolong remission*. Cancer Res, 2009. **69**(19): p. 7507-11.
986. Tomimoto, A., et al., *Metformin suppresses intestinal polyp growth in ApcMin/+ mice*. Cancer Sci, 2008. **99**(11): p. 2136-41.
987. Thent, Z.C., et al., *Is Metformin a Therapeutic Paradigm for Colorectal Cancer: Insight into the Molecular Pathway?* Curr Drug Targets, 2017. **18**(6): p. 734-750.
988. Rezaei Tavirani, M., S. Rezaei Tavirani, and F. Tajik Rostami, *Biochemical pathway analysis of gastric atrophy*. Gastroenterol Hepatol Bed Bench, 2018. **11**(2): p. 118-124.
989. Liu, K., et al., *MiR-132 inhibits cell proliferation, invasion and migration of hepatocellular carcinoma by targeting PIK3R3*. Int J Oncol, 2015. **47**(4): p. 1585-93.
990. Musi, N., et al., *Metformin increases AMP-activated protein kinase activity in skeletal muscle of subjects with type 2 diabetes*. Diabetes, 2002. **51**(7): p. 2074-81.
991. Petroulakis, E., et al., *mTOR signaling: implications for cancer and anticancer therapy*. Br J Cancer, 2006. **94**(2): p. 195-9.
992. Magnuson, B., B. Ekim, and D.C. Fingar, *Regulation and function of ribosomal protein S6 kinase (S6K) within mTOR signalling networks*. Biochem J, 2012. **441**(1): p. 1-21.
993. Slattery, M.L., et al., *MicroRNAs and colon and rectal cancer: differential expression by tumor location and subtype*. Genes Chromosomes Cancer, 2011. **50**(3): p. 196-206.
994. Lu, J., et al., *MicroRNA expression profiles classify human cancers*. Nature, 2005. **435**(7043): p. 834-8.
995. Udhane, S.S., et al., *Combined transcriptome and metabolome analyses of metformin effects reveal novel links between metabolic networks in steroidogenic systems*. Sci Rep, 2017. **7**(1): p. 8652.

## REFERENCES

996. Marin, T.L., et al., *AMPK promotes mitochondrial biogenesis and function by phosphorylating the epigenetic factors DNMT1, RBBP7, and HAT1*. *Sci Signal*, 2017. **10**(464).
997. Zhang, Y., et al., *AMP-activated protein kinase suppresses endothelial cell inflammation through phosphorylation of transcriptional coactivator p300*. *Arterioscler Thromb Vasc Biol*, 2011. **31**(12): p. 2897-908.
998. McGee, S.L., et al., *AMP-activated protein kinase regulates GLUT4 transcription by phosphorylating histone deacetylase 5*. *Diabetes*, 2008. **57**(4): p. 860-7.
999. White-Al Habeeb, N.M., et al., *Metformin Elicits Antitumor Effects and Downregulates the Histone Methyltransferase Multiple Myeloma SET Domain (MMSET) in Prostate Cancer Cells*. *Prostate*, 2016. **76**(16): p. 1507-1518.
1000. He, L., et al., *Metformin and insulin suppress hepatic gluconeogenesis through phosphorylation of CREB binding protein*. *Cell*, 2009. **137**(4): p. 635-46.
1001. Tseng, H.W., S.C. Li, and K.W. Tsai, *Metformin Treatment Suppresses Melanoma Cell Growth and Motility Through Modulation of microRNA Expression*. *Cancers (Basel)*, 2019. **11**(2).
1002. Chen, Y., et al., *Molecular mechanism of LKB1 in the invasion and metastasis of colorectal cancer*. *Oncol Rep*, 2019. **41**(2): p. 1035-1044.
1003. Gaedcke, J., et al., *The rectal cancer microRNAome--microRNA expression in rectal cancer and matched normal mucosa*. *Clin Cancer Res*, 2012. **18**(18): p. 4919-30.
1004. Falzone, L., et al., *Integrated analysis of colorectal cancer microRNA datasets: identification of microRNAs associated with tumor development*. *Aging (Albany NY)*, 2018. **10**(5): p. 1000-1014.
1005. Zhao, Z., et al., *A high-content morphological screen identifies novel microRNAs that regulate neuroblastoma cell differentiation*. *Oncotarget*, 2014. **5**(9): p. 2499-512.
1006. Zhao, Z., et al., *microRNA-2110 functions as an onco-suppressor in neuroblastoma by directly targeting Tsukushi*. *PLoS One*, 2018. **13**(12): p. e0208777.
1007. Zhao, Z., et al., *A combined gene expression and functional study reveals the crosstalk between N-Myc and differentiation-inducing microRNAs in neuroblastoma cells*. *Oncotarget*, 2016. **7**(48): p. 79372-79387.
1008. Salendo, J., et al., *Identification of a microRNA expression signature for chemoradiosensitivity of colorectal cancer cells, involving miRNAs-320a, -224, -132 and let7g*. *Radiother Oncol*, 2013. **108**(3): p. 451-7.
1009. Mokitani, Y., et al., *Down-Regulation of microRNA-132 is Associated with Poor Prognosis of Colorectal Cancer*. *Ann Surg Oncol*, 2016. **23**(Suppl 5): p. 599-608.
1010. Song, H., et al., *Long non-coding RNA XIST functions as an oncogene in human colorectal cancer by targeting miR-132-3p*. *J buon*, 2017. **22**(3): p. 696-703.
1011. Zheng, Y.B., et al., *miR-132 inhibits colorectal cancer invasion and metastasis via directly targeting ZEB2*. *World J Gastroenterol*, 2014. **20**(21): p. 6515-22.
1012. Qin, J., et al., *Downregulation of microRNA-132 by DNA hypermethylation is associated with cell invasion in colorectal cancer*. *Onco Targets Ther*, 2015. **8**: p. 3639-48.
1013. Liu, Z., et al., *Long non-coding RNA MLAT promotes growth and metastasis of colorectal cancer cells through regulation of miR-132/Derlin-1 pathway*. *Cancer Cell Int*, 2018. **18**: p. 59.
1014. Zhang, M., et al., *LncRNA SNHG5 affects cell proliferation, metastasis and migration of colorectal cancer through regulating miR-132-3p/ CREB5*. *Cancer Biol Ther*, 2019. **20**(4): p. 524-536.
1015. Thorpe, L.M., H. Yuzugullu, and J.J. Zhao, *PI3K in cancer: divergent roles of isoforms, modes of activation and therapeutic targeting*. *Nat Rev Cancer*, 2015. **15**(1): p. 7-24.
1016. Foukas, L.C., et al., *Activity of any class IA PI3K isoform can sustain cell proliferation and survival*. *Proc Natl Acad Sci U S A*, 2010. **107**(25): p. 11381-6.
1017. Backer, J.M., *The regulation of class IA PI 3-kinases by inter-subunit interactions*. *Curr Top Microbiol Immunol*, 2010. **346**: p. 87-114.
1018. Pons, S., et al., *The structure and function of p55PIK reveal a new regulatory subunit for phosphatidylinositol 3-kinase*. *Mol Cell Biol*, 1995. **15**(8): p. 4453-65.

## REFERENCES

1019. Xia, X., et al., *The N-terminal 24 amino acids of the p53 gamma regulatory subunit of phosphoinositide 3-kinase binds Rb and induces cell cycle arrest*. Mol Cell Biol, 2003. **23**(5): p. 1717-25.
1020. Miura, M., et al., *Roles of XPG and XPF/ERCC1 endonucleases in UV-induced immunostaining of PCNA in fibroblasts*. Exp Cell Res, 1996. **226**(1): p. 126-32.
1021. Hutton, R.D., et al., *PCNA stimulates catalysis by structure-specific nucleases using two distinct mechanisms: substrate targeting and catalytic step*. Nucleic Acids Res, 2008. **36**(21): p. 6720-7.
1022. Hu, J., et al., *A peptide inhibitor derived from p53/PIK3R3 phosphatidylinositol 3-kinase regulatory subunit: a novel cancer therapy*. Mol Cancer Ther, 2008. **7**(12): p. 3719-28.
1023. Zhang, L., et al., *Integrative genomic analysis of phosphatidylinositol 3'-kinase family identifies PIK3R3 as a potential therapeutic target in epithelial ovarian cancer*. Clin Cancer Res, 2007. **13**(18 Pt 1): p. 5314-21.
1024. Dhillon, A.S., et al., *MAP kinase signalling pathways in cancer*. Oncogene, 2007. **26**(22): p. 3279-90.
1025. Galardi, S., et al., *miR-221 and miR-222 expression affects the proliferation potential of human prostate carcinoma cell lines by targeting p27Kip1*. J Biol Chem, 2007. **282**(32): p. 23716-24.
1026. Felli, N., et al., *MicroRNAs 221 and 222 inhibit normal erythropoiesis and erythroleukemic cell growth via kit receptor down-modulation*. Proc Natl Acad Sci U S A, 2005. **102**(50): p. 18081-6.
1027. Ciafre, S.A., et al., *Extensive modulation of a set of microRNAs in primary glioblastoma*. Biochem Biophys Res Commun, 2005. **334**(4): p. 1351-8.
1028. Stinson, S., et al., *TRPS1 targeting by miR-221/222 promotes the epithelial-to-mesenchymal transition in breast cancer*. Sci Signal, 2011. **4**(177): p. ra41.
1029. Kobayashi, M., et al., *MicroRNA expression profiling in canine prostate cancer*. J Vet Med Sci, 2017. **79**(4): p. 719-725.
1030. Shah, M.Y. and G.A. Calin, *MicroRNAs miR-221 and miR-222: a new level of regulation in aggressive breast cancer*. Genome Med, 2011. **3**(8): p. 56.
1031. O'Hara, A.J., et al., *Tumor suppressor microRNAs are underrepresented in primary effusion lymphoma and Kaposi sarcoma*. Blood, 2009. **113**(23): p. 5938-41.
1032. Howe, E.N., D.R. Cochrane, and J.K. Richer, *The miR-200 and miR-221/222 microRNA families: opposing effects on epithelial identity*. J Mammary Gland Biol Neoplasia, 2012. **17**(1): p. 65-77.
1033. Fornari, F., et al., *MiR-221 controls CDKN1C/p57 and CDKN1B/p27 expression in human hepatocellular carcinoma*. Oncogene, 2008. **27**(43): p. 5651-61.
1034. Kim, Y.K., et al., *Functional links between clustered microRNAs: suppression of cell-cycle inhibitors by microRNA clusters in gastric cancer*. Nucleic Acids Res, 2009. **37**(5): p. 1672-81.
1035. Medina, R., et al., *MicroRNAs 221 and 222 bypass quiescence and compromise cell survival*. Cancer Res, 2008. **68**(8): p. 2773-80.
1036. Fuse, M., et al., *Tumor suppressive microRNAs (miR-222 and miR-31) regulate molecular pathways based on microRNA expression signature in prostate cancer*. J Hum Genet, 2012. **57**(11): p. 691-9.
1037. Yamashita, R., et al., *Growth inhibitory effects of miR-221 and miR-222 in non-small cell lung cancer cells*. Cancer Med, 2015. **4**(4): p. 551-64.
1038. Forrest, A.R., et al., *Induction of microRNAs, mir-155, mir-222, mir-424 and mir-503, promotes monocytic differentiation through combinatorial regulation*. Leukemia, 2010. **24**(2): p. 460-6.
1039. Cesarini, V., et al., *ADAR2/miR-589-3p axis controls glioblastoma cell migration/invasion*. Nucleic Acids Res, 2018. **46**(4): p. 2045-2059.
1040. Lu, A., Z. Wang, and S. Wang, *Role of miR-589-3p in human lumbar disc degeneration and its potential mechanism*. Exp Ther Med, 2018. **15**(2): p. 1616-1621.
1041. Niethammer, P., P. Bastiaens, and E. Karsenti, *Stathmin-tubulin interaction gradients in motile and mitotic cells*. Science, 2004. **303**(5665): p. 1862-6.

## REFERENCES

1042. Borghese, L., et al., *Systematic analysis of the transcriptional switch inducing migration of border cells*. Dev Cell, 2006. **10**(4): p. 497-508.
1043. Wang, J., et al., *Downregulation of stathmin 1 in human gallbladder carcinoma inhibits tumor growth in vitro and in vivo*. Sci Rep, 2016. **6**: p. 28833.
1044. Belletti, B., et al., *Stathmin activity influences sarcoma cell shape, motility, and metastatic potential*. Mol Biol Cell, 2008. **19**(5): p. 2003-13.
1045. Bieche, I., et al., *Overexpression of the stathmin gene in a subset of human breast cancer*. Br J Cancer, 1998. **78**(6): p. 701-9.
1046. Singer, S., et al., *Protumorigenic overexpression of stathmin/Op18 by gain-of-function mutation in p53 in human hepatocarcinogenesis*. Hepatology, 2007. **46**(3): p. 759-68.
1047. Chen, G., et al., *Overexpression of oncoprotein 18 correlates with poor differentiation in lung adenocarcinomas*. Mol Cell Proteomics, 2003. **2**(2): p. 107-16.
1048. Friedrich, B., et al., *Differentiation-stage specific expression of oncoprotein 18 in human and rat prostatic adenocarcinoma*. Prostate, 1995. **27**(2): p. 102-9.
1049. Abal, M., et al., *APC inactivation associates with abnormal mitosis completion and concomitant BUB1B/MAD2L1 up-regulation*. Gastroenterology, 2007. **132**(7): p. 2448-58.
1050. Liu, Z., et al., *PUMA overexpression induces reactive oxygen species generation and proteasome-mediated stathmin degradation in colorectal cancer cells*. Cancer Res, 2005. **65**(5): p. 1647-54.
1051. Golouh, R., et al., *The prognostic value of Stathmin-1, S100A2, and SYK proteins in ER-positive primary breast cancer patients treated with adjuvant tamoxifen monotherapy: an immunohistochemical study*. Breast Cancer Res Treat, 2008. **110**(2): p. 317-26.
1052. Ngo, T.T., et al., *The 1p-encoded protein stathmin and resistance of malignant gliomas to nitrosoureas*. J Natl Cancer Inst, 2007. **99**(8): p. 639-52.
1053. Yuan, R.H., et al., *Stathmin overexpression cooperates with p53 mutation and osteopontin overexpression, and is associated with tumour progression, early recurrence, and poor prognosis in hepatocellular carcinoma*. J Pathol, 2006. **209**(4): p. 549-58.
1054. Marklund, U., et al., *Serine 25 of oncoprotein 18 is a major cytosolic target for the mitogen-activated protein kinase*. J Biol Chem, 1993. **268**(20): p. 15039-47.
1055. Ikeda, Y., et al., *MicroRNAs associated with mitogen-activated protein kinase in human pancreatic cancer*. Mol Cancer Res, 2012. **10**(2): p. 259-69.
1056. Baldassarre, G., et al., *p27(Kip1)-stathmin interaction influences sarcoma cell migration and invasion*. Cancer Cell, 2005. **7**(1): p. 51-63.
1057. Xiao, B., et al., *Transcriptome sequencing of the naked mole rat (Heterocephalus glaber) and identification of hypoxia tolerance genes*. Biol Open, 2017. **6**(12): p. 1904-1912.
1058. Saal, L.H., et al., *Poor prognosis in carcinoma is associated with a gene expression signature of aberrant PTEN tumor suppressor pathway activity*. Proc Natl Acad Sci U S A, 2007. **104**(18): p. 7564-9.
1059. Manning, B.D. and L.C. Cantley, *AKT/PKB signaling: navigating downstream*. Cell, 2007. **129**(7): p. 1261-74.
1060. Engelman, J.A., J. Luo, and L.C. Cantley, *The evolution of phosphatidylinositol 3-kinases as regulators of growth and metabolism*. Nat Rev Genet, 2006. **7**(8): p. 606-19.
1061. Pollak, M.N., *Investigating metformin for cancer prevention and treatment: the end of the beginning*. Cancer Discov, 2012. **2**(9): p. 778-90.
1062. Viollet, B., et al., *Cellular and molecular mechanisms of metformin: an overview*. Clin Sci (Lond), 2012. **122**(6): p. 253-70.
1063. Huang, X., et al., *Important role of the LKB1-AMPK pathway in suppressing tumorigenesis in PTEN-deficient mice*. Biochem J, 2008. **412**(2): p. 211-21.
1064. Birsoy, K., et al., *Metabolic determinants of cancer cell sensitivity to glucose limitation and biguanides*. Nature, 2014. **508**(7494): p. 108-12.
1065. Dvinge, H., et al., *The shaping and functional consequences of the microRNA landscape in breast cancer*. Nature, 2013. **497**(7449): p. 378-82.

## REFERENCES

1066. Ling, H., M. Fabbri, and G.A. Calin, *MicroRNAs and other non-coding RNAs as targets for anticancer drug development*. Nat Rev Drug Discov, 2013. **12**(11): p. 847-65.
1067. Orang, A.V., et al., *Micromanaging aerobic respiration and glycolysis in cancer cells*. Mol Metab, 2019. **23**: p. 98-126.
1068. Guo, S.T., et al., *MicroRNA-497 targets insulin-like growth factor 1 receptor and has a tumour suppressive role in human colorectal cancer*. Oncogene, 2013. **32**(15): p. 1910-20.
1069. Ma, K., et al., *Loss of miR-638 in vitro promotes cell invasion and a mesenchymal-like transition by influencing SOX2 expression in colorectal carcinoma cells*. Mol Cancer, 2014. **13**: p. 118.
1070. Crose, L.E. and C.M. Linardic, *Receptor tyrosine kinases as therapeutic targets in rhabdomyosarcoma*. Sarcoma, 2011. **2011**: p. 756982.
1071. Lim, L.P., et al., *Microarray analysis shows that some microRNAs downregulate large numbers of target mRNAs*. Nature, 2005. **433**(7027): p. 769-73.
1072. Farh, K.K., et al., *The widespread impact of mammalian MicroRNAs on mRNA repression and evolution*. Science, 2005. **310**(5755): p. 1817-21.
1073. Li, F., et al., *Differential microRNA expression in signet-ring cell carcinoma compared with tubular adenocarcinoma of human gastric cancer*. 2015. **14**(1): p. 739-47.
1074. Li, J.-Y., et al., *Differential distribution of microRNAs in breast cancer grouped by clinicopathological subtypes*. 2013. **14**(5): p. 3197-3203.
1075. Bertoli, G., C. Cava, and I.J.I.o.m.s. Castiglioni, *MicroRNAs as biomarkers for diagnosis, prognosis and theranostics in prostate cancer*. 2016. **17**(3): p. 421.
1076. Li, L.J., et al., *miR-376b-5p regulates angiogenesis in cerebral ischemia*. Mol Med Rep, 2014. **10**(1): p. 527-35.
1077. Liang, L., et al., *Prognostic microRNAs and their potential molecular mechanism in pancreatic cancer: A study based on The Cancer Genome Atlas and bioinformatics investigation*. Mol Med Rep, 2018. **17**(1): p. 939-951.
1078. An, N., et al., *MicroRNA-376b promotes breast cancer metastasis by targeting Hoxd10 directly*. Exp Ther Med, 2017. **13**(1): p. 79-84.
1079. Bjork, J.K., et al., *miR-18, a member of Oncomir-1, targets heat shock transcription factor 2 in spermatogenesis*. Development, 2010. **137**(19): p. 3177-84.
1080. Azizian, A., et al., *Preoperative prediction of lymph node status by circulating mir-18b and mir-20a during chemoradiotherapy in patients with rectal cancer*. 2015. **39**(9): p. 2329-2335.
1081. Fonseca-Sánchez, M.A., et al., *microRNA-18b is upregulated in breast cancer and modulates genes involved in cell migration*. 2013. **30**(5): p. 2399-2410.
1082. Dar, A.A., et al., *The role of miR-18b in MDM2-p53 pathway signaling and melanoma progression*. 2013. **105**(6): p. 433-442.
1083. Wang, Y.Y., et al., *Long noncoding RNA AC073284.4 suppresses epithelial-mesenchymal transition by sponging miR-18b-5p in paclitaxel-resistant breast cancer cells*. J Cell Physiol, 2019.
1084. Cui, S.Y., et al., *Micro RNA-145: a potent tumour suppressor that regulates multiple cellular pathways*. 2014. **18**(10): p. 1913-1926.
1085. Letelier, P., et al., *miR-1 and miR-145 act as tumor suppressor microRNAs in gallbladder cancer*. 2014. **7**(5): p. 1849.
1086. Goto, Y., et al., *Impact of novel miR-145-3p regulatory networks on survival in patients with castration-resistant prostate cancer*. 2017. **117**(3): p. 409.
1087. Matakai, H., et al., *Dual-strand tumor-suppressor microRNA-145 (miR-145-5p and miR-145-3p) coordinately targeted MTDH in lung squamous cell carcinoma*. 2016. **7**(44): p. 72084.
1088. Qiu, Z., et al., *MicroRNA-124 reduces the pentose phosphate pathway and proliferation by targeting PRPS1 and RPLA mRNAs in human colorectal cancer cells*. 2015. **149**(6): p. 1587-1598. e11.
1089. Sharma, P. and S. Kumar, *Metformin inhibits human breast cancer cell growth by promoting apoptosis via a ROS-independent pathway involving mitochondrial dysfunction: pivotal role of superoxide dismutase (SOD)*. Cell Oncol (Dordr), 2018. **41**(6): p. 637-650.

## REFERENCES

1090. Isakovic, A., et al., *Dual antiglioma action of metformin: cell cycle arrest and mitochondria-dependent apoptosis*. Cell Mol Life Sci, 2007. **64**(10): p. 1290-302.
1091. Jiang, J., et al., *MiR-1181 inhibits stem cell-like phenotypes and suppresses SOX2 and STAT3 in human pancreatic cancer*. Cancer Lett, 2015. **356**(2 Pt B): p. 962-70.
1092. Wang, J., et al., *miR-1181 inhibits invasion and proliferation via STAT3 in pancreatic cancer*. World J Gastroenterol, 2017. **23**(9): p. 1594-1601.
1093. Zhang, H.Y., et al., *Activation of ARK5/miR-1181/HOXA10 axis promotes epithelial-mesenchymal transition in ovarian cancer*. Oncol Rep, 2015. **34**(3): p. 1193-202.
1094. Qian, Z., et al., *miR-4632 mediates PDGF-BB-induced proliferation and antiapoptosis of human pulmonary artery smooth muscle cells via targeting cJUN*. Am J Physiol Cell Physiol, 2017. **313**(4): p. C380-c391.
1095. Qian, Z., et al., *PDGFBB promotes proliferation and migration via regulating miR-1181/STAT3 axis in human pulmonary arterial smooth muscle cells*. Am J Physiol Lung Cell Mol Physiol, 2018. **315**(6): p. L965-l976.
1096. Griffiths-Jones, S., et al., *miRBase: microRNA sequences, targets and gene nomenclature*. Nucleic Acids Res, 2006. **34**(Database issue): p. D140-4.
1097. Leng, R., L. Zha, and L. Tang, *MiR-718 represses VEGF and inhibits ovarian cancer cell progression*. FEBS Lett, 2014. **588**(12): p. 2078-86.
1098. Sugimachi, K., et al., *Identification of a bona fide microRNA biomarker in serum exosomes that predicts hepatocellular carcinoma recurrence after liver transplantation*. Br J Cancer, 2015. **112**(3): p. 532-8.
1099. Wang, Z.D., et al., *Involvement of microRNA-718, a new regulator of EGR3, in regulation of malignant phenotype of HCC cells*. J Zhejiang Univ Sci B, 2017. **18**(1): p. 27-36.
1100. Sun, L., et al., *Predictive value of plasma miRNA-718 for esophageal squamous cell carcinoma*. Cancer Biomark, 2016. **16**(2): p. 265-73.
1101. Wang, X. and M. Qi, *miR-718 is involved in malignancy of papillary thyroid cancer through repression of PDPK1*. Pathol Res Pract, 2018. **214**(11): p. 1787-1793.
1102. Gatenby, R.A. and R.J. Gillies, *Why do cancers have high aerobic glycolysis?* Nat Rev Cancer, 2004. **4**(11): p. 891-9.
1103. Gillies, R.J., I. Robey, and R.A. Gatenby, *Causes and consequences of increased glucose metabolism of cancers*. J Nucl Med, 2008. **49 Suppl 2**: p. 24S-42S.
1104. Koppenol, W.H., P.L. Bounds, and C.V. Dang, *Otto Warburg's contributions to current concepts of cancer metabolism*. Nat Rev Cancer, 2011. **11**(5): p. 325-37.
1105. Ying, H., et al., *Oncogenic Kras maintains pancreatic tumors through regulation of anabolic glucose metabolism*. Cell, 2012. **149**(3): p. 656-70.
1106. Hitosugi, T., et al., *Phosphoglycerate mutase 1 coordinates glycolysis and biosynthesis to promote tumor growth*. Cancer Cell, 2012. **22**(5): p. 585-600.
1107. Locasale, J.W., et al., *Phosphoglycerate dehydrogenase diverts glycolytic flux and contributes to oncogenesis*. Nat Genet, 2011. **43**(9): p. 869-74.
1108. Newsholme, E.A., B. Crabtree, and M.S. Ardawi, *The role of high rates of glycolysis and glutamine utilization in rapidly dividing cells*. Biosci Rep, 1985. **5**(5): p. 393-400.
1109. Wu, M., et al., *Multiparameter metabolic analysis reveals a close link between attenuated mitochondrial bioenergetic function and enhanced glycolysis dependency in human tumor cells*. Am J Physiol Cell Physiol, 2007. **292**(1): p. C125-36.
1110. Mathupala, S.P., Y.H. Ko, and P.L. Pedersen, *Hexokinase II: cancer's double-edged sword acting as both facilitator and gatekeeper of malignancy when bound to mitochondria*. Oncogene, 2006. **25**(34): p. 4777-86.
1111. Zornig, M., et al., *Apoptosis regulators and their role in tumorigenesis*. Biochim Biophys Acta, 2001. **1551**(2): p. F1-37.
1112. Kobiela, J., et al., *Metformin and Colorectal Cancer - A Systematic Review*. Exp Clin Endocrinol Diabetes, 2018.

## REFERENCES

1113. Wiernsperger, N.F., *Membrane physiology as a basis for the cellular effects of metformin in insulin resistance and diabetes*. *Diabetes Metab*, 1999. **25**(2): p. 110-27.
1114. Freisleben, H.J., et al., *Interaction of glucose and metformin with isolated red cell membrane*. *Arzneimittelforschung*, 1996. **46**(8): p. 773-8.
1115. Muller, S., et al., *Action of metformin on erythrocyte membrane fluidity in vitro and in vivo*. *Eur J Pharmacol*, 1997. **337**(1): p. 103-10.
1116. Wilcock, C. and C.J. Bailey, *Accumulation of metformin by tissues of the normal and diabetic mouse*. *Xenobiotica*, 1994. **24**(1): p. 49-57.
1117. Cuber, J., et al., *Metabolic and drug distribution studies do not support direct inhibitory effects of metformin on intestinal glucose absorption*. 1994. **20**(6): p. 532-539.
1118. Mookerjee, S.A., D.G. Nicholls, and M.D. Brand, *Determining Maximum Glycolytic Capacity Using Extracellular Flux Measurements*. *PLoS One*, 2016. **11**(3): p. e0152016.
1119. Epstein, T., et al., *Separation of metabolic supply and demand: aerobic glycolysis as a normal physiological response to fluctuating energetic demands in the membrane*. *Cancer Metab*, 2014. **2**: p. 7.
1120. Issaq, S.H., B.A. Teicher, and A. Monks, *Bioenergetic properties of human sarcoma cells help define sensitivity to metabolic inhibitors*. *Cell Cycle*, 2014. **13**(7): p. 1152-61.
1121. Kumagai, S., R. Narasaki, and K. Hasumi, *Glucose-dependent active ATP depletion by koniginic acid kills high-glycolytic cells*. *Biochem Biophys Res Commun*, 2008. **365**(2): p. 362-8.
1122. Das, K.C., *Hyperoxia decreases glycolytic capacity, glycolytic reserve and oxidative phosphorylation in MLE-12 cells and inhibits complex I and II function, but not complex IV in isolated mouse lung mitochondria*. *PLoS One*, 2013. **8**(9): p. e73358.
1123. Phillips, D., et al., *Mice over-expressing the myocardial creatine transporter develop progressive heart failure and show decreased glycolytic capacity*. 2010. **48**(4): p. 582-590.
1124. Chung, S., et al., *Glycolytic network restructuring integral to the energetics of embryonic stem cell cardiac differentiation*. *J Mol Cell Cardiol*, 2010. **48**(4): p. 725-34.
1125. Folmes, C.D., et al., *Somatic oxidative bioenergetics transitions into pluripotency-dependent glycolysis to facilitate nuclear reprogramming*. *Cell Metab*, 2011. **14**(2): p. 264-71.
1126. Santos, C.R. and A. Schulze, *Lipid metabolism in cancer*. *Febs j*, 2012. **279**(15): p. 2610-23.
1127. Fujimori, T., et al., *Antitumor effect of metformin on cholangiocarcinoma: In vitro and in vivo studies*. *Oncol Rep*, 2015. **34**(6): p. 2987-96.
1128. Han, Y., et al., *Metformin reverses PARP inhibitors-induced epithelial-mesenchymal transition and PD-L1 upregulation in triple-negative breast cancer*. *Am J Cancer Res*, 2019. **9**(4): p. 800-815.
1129. Greco, S., C. Storelli, and S. Marsigliante, *Protein kinase C (PKC)-delta/ -epsilon mediate the PKC/ Akt-dependent phosphorylation of extracellular signal-regulated kinases 1 and 2 in MCF-7 cells stimulated by bradykinin*. *J Endocrinol*, 2006. **188**(1): p. 79-89.
1130. Porat, S., et al., *Control of pancreatic beta cell regeneration by glucose metabolism*. *Cell Metab*, 2011. **13**(4): p. 440-449.
1131. Sacco, F., et al., *Deep Proteomics of Breast Cancer Cells Reveals that Metformin Rewires Signaling Networks Away from a Pro-growth State*. *Cell Syst*, 2016. **2**(3): p. 159-71.
1132. Kita, Y., et al., *Metformin prevents and reverses inflammation in a non-diabetic mouse model of nonalcoholic steatohepatitis*. *PLoS One*, 2012. **7**(9): p. e43056.
1133. Salomaki, H., et al., *Prenatal metformin exposure in mice programs the metabolic phenotype of the offspring during a high fat diet at adulthood*. *PLoS One*, 2013. **8**(2): p. e56594.
1134. Martin-Montalvo, A., et al., *Metformin improves healthspan and lifespan in mice*. *Nat Commun*, 2013. **4**: p. 2192.
1135. Guo, J., et al., *Metformin-Induced Changes of the Coding Transcriptome and Non-Coding RNAs in the Livers of Non-Alcoholic Fatty Liver Disease Mice*. *Cell Physiol Biochem*, 2018. **45**(4): p. 1487-1505.
1136. Yi, Z., et al., *Differential expression of miRNA patterns in renal cell carcinoma and nontumorous tissues*. *J Cancer Res Clin Oncol*, 2010. **136**(6): p. 855-62.

## REFERENCES

1137. Pulito, C., et al., *microRNAs and cancer metabolism reprogramming: the paradigm of metformin*. 2014. **2**(6).
1138. Wu, N., et al., *Metformin induces apoptosis of lung cancer cells through activating JNK/p38 MAPK pathway and GADD153*. *Neoplasma*, 2011. **58**(6): p. 482-90.
1139. Kefas, B.A., et al., *Metformin-induced stimulation of AMP-activated protein kinase in beta-cells impairs their glucose responsiveness and can lead to apoptosis*. *Biochem Pharmacol*, 2004. **68**(3): p. 409-16.
1140. Kefas, B.A., et al., *AMP-activated protein kinase can induce apoptosis of insulin-producing MIN6 cells through stimulation of c-Jun-N-terminal kinase*. *J Mol Endocrinol*, 2003. **30**(2): p. 151-61.
1141. Graf, D., et al., *Inhibition of taurothiocholate 3-sulfate-induced apoptosis by cyclic AMP in rat hepatocytes involves protein kinase A-dependent and -independent mechanisms*. *Arch Biochem Biophys*, 2003. **415**(1): p. 34-42.
1142. Zhu, J.Y., et al., *Identification of novel Epstein-Barr virus microRNA genes from nasopharyngeal carcinomas*. *J Virol*, 2009. **83**(7): p. 3333-41.
1143. Ferracin, M., et al., *Absolute quantification of cell-free microRNAs in cancer patients*. *Oncotarget*, 2015. **6**(16): p. 14545-55.
1144. Schaefer, L. and R.V. Iozzo, *Biological functions of the small leucine-rich proteoglycans: from genetics to signal transduction*. *J Biol Chem*, 2008. **283**(31): p. 21305-9.
1145. Merline, R., R.M. Schaefer, and L. Schaefer, *The matricellular functions of small leucine-rich proteoglycans (SLRPs)*. *J Cell Commun Signal*, 2009. **3**(3-4): p. 323-35.
1146. Henke, A., et al., *Stromal expression of decorin, Semaphorin6D, SPARC, Sprouty1 and Tsukushi in developing prostate and decreased levels of decorin in prostate cancer*. *PLoS One*, 2012. **7**(8): p. e42516.
1147. Hendrickson, D.G., et al., *Concordant regulation of translation and mRNA abundance for hundreds of targets of a human microRNA*. *PLoS Biol*, 2009. **7**(11): p. e1000238.
1148. Navarro-Quiroz, E., et al., *Profiling analysis of circulating microRNA in peripheral blood of patients with class IV lupus nephritis*. *PLoS One*, 2017. **12**(11): p. e0187973.
1149. Kuhn, D.E., et al., *Experimental validation of miRNA targets*. *Methods*, 2008. **44**(1): p. 47-54.
1150. Kowall, B., et al., *No reduced risk of overall, colorectal, lung, breast, and prostate cancer with metformin therapy in diabetic patients: database analyses from Germany and the UK*. *Pharmacoepidemiol Drug Saf*, 2015. **24**(8): p. 865-74.
1151. Drews, R.E. and L.N. Shulman, *Update in hematology and oncology*. *Ann Intern Med*, 2010. **152**(10): p. 655-62.
1152. Iliopoulos, D., H.A. Hirsch, and K. Struhl, *Metformin decreases the dose of chemotherapy for prolonging tumor remission in mouse xenografts involving multiple cancer cell types*. *Cancer Res*, 2011. **71**(9): p. 3196-201.
1153. Hanna, R.K., et al., *Metformin potentiates the effects of paclitaxel in endometrial cancer cells through inhibition of cell proliferation and modulation of the mTOR pathway*. *Gynecol Oncol*, 2012. **125**(2): p. 458-69.
1154. Cai, H., et al., *Cation-selective transporters are critical to the AMPK-mediated antiproliferative effects of metformin in human breast cancer cells*. *Int J Cancer*, 2016. **138**(9): p. 2281-92.
1155. Zhang, Y., et al., *Effects of metformin on CD133+ colorectal cancer cells in diabetic patients*. *PLoS One*, 2013. **8**(11): p. e81264.
1156. Bragagnoli, A., et al., *Final results of a phase II of metformin plus irinotecan for refractory colorectal cancer*. 2018, American Society of Clinical Oncology.
1157. Miranda, V.C., et al., *A phase II trial of metformin and fluorouracil (MetFU) for patients (pts) with metastatic colorectal cancer (mCRC) refractory to standard treatment*. 2014, American Society of Clinical Oncology.
1158. Bartel, D.P., *MicroRNAs: genomics, biogenesis, mechanism, and function*. *Cell*, 2004. **116**(2): p. 281-97.

## REFERENCES

1159. Rupaimoole, R., et al., *miRNA Deregulation in Cancer Cells and the Tumor Microenvironment*. *Cancer Discov*, 2016. **6**(3): p. 235-46.
1160. Aqeilan, R.I., G.A. Calin, and C.M. Croce, *miR-15a and miR-16-1 in cancer: discovery, function and future perspectives*. *Cell Death Differ*, 2010. **17**(2): p. 215-20.
1161. Reinhart, B.J., et al., *The 21-nucleotide let-7 RNA regulates developmental timing in *Caenorhabditis elegans**. *Nature*, 2000. **403**(6772): p. 901-6.
1162. Henry, J.C., A.C. Azevedo-Pouly, and T.D. Schmittgen, *MicroRNA replacement therapy for cancer*. *Pharm Res*, 2011. **28**(12): p. 3030-42.
1163. Rupaimoole, R. and F.J. Slack, *MicroRNA therapeutics: towards a new era for the management of cancer and other diseases*. *Nat Rev Drug Discov*, 2017. **16**(3): p. 203-222.
1164. Reid, G., et al., *Clinical development of TargomiRs, a miRNA mimic-based treatment for patients with recurrent thoracic cancer*. *Epigenomics*, 2016. **8**(8): p. 1079-85.
1165. Tomczak, K., P. Czerwińska, and M. Wiznerowicz, *The Cancer Genome Atlas (TCGA): an immeasurable source of knowledge*. *Contemporary oncology*, 2015. **19**(1A): p. A68.